The evolution of Maldivian coral reef rim islands

Holly Kate East

Submitted by H. K. East to the University of Exeter as a thesis
for the degree of Doctor of Philosophy in Geography in April 2017

Abstract

The first detailed investigation of Maldivian rim island development and reef-to-island connectivity is presented. Study sites were selected on windward and leeward rim aspects of Huvadhu Atoll, and analyses were undertaken at a millennial, contemporary and near-future temporal scales. At millennial temporal scales, contrasting models of island development were presented for the windward and leeward sites. Marked between-site differences were found in the timings of island initiation (2,800-2,000 cal. yr. B.P. and 4,200-3,600 cal. yr. B.P. at the windward and leeward sites respectively). Hence, sea-level does not represent the sole control upon island formation. The period of island initiation and heightened mobility occurred during the mid-Holocene sea-level highstand. Future sea-level rise may thus reactivate the process regime responsible for reef island initiation, potentially inducing further island building and/or heightened island mobilisation. Contemporary analyses highlighted the homogeneity of the sediment reservoir across marine, beach and island sediments. Specifically, sand-grade coral was dominant across all samples within both sites (>50%). The most likely source of sand-grade coral is excavator parrotfish, which was consistent with ecological survey-based estimates of sediment production (excavator parrotfish accounted for 72.8% and 68.2% of sediment production at the windward and leeward sites). The highest sediment production rates were found within the lagoonward environments (59.4% and 75.4% at the windward and leeward sites), which is consistent with the more recent lateral lagoonward mode of island building. With regard to near-future analyses, the apparent recent areal expansion of seagrass beds demonstrated the capacity of ecological changes to cause shifts in sediment production budgets (contributing an additional ~243 tonnes yr^{-1} of sediment on the leeward rim platform). In addition, significant increases in benthic sediment mobility were found at both study sites under sea-level rise scenarios. Increases in mobility were markedly larger in magnitude at the leeward site than at the windward site. A challenge for the adaptive capacity of atoll nations is thus to acknowledge this atoll-scale diversity in future management strategies.

Acknowledgements

Firstly, I would like to thank to Prof. Chris Perry for his supervision. I have very much appreciated our meetings and hearing your thoughts over the course of this work. I am so grateful that you gave me this fantastic opportunity and also the chance to develop my lecturing skills. Thank you to Prof. Paul Kench for his supervision, the thought-provoking discussions on island development, and for hosting my research visit in Auckland.

For facilitating fieldwork, I am very thankful to Mohamed Aslam (LaMer) for his fantastic and generous support. Particular thanks are owed to your family for very kindly hosting our stay on Fares-Maathodaa. I am grateful to both Abraham Didis for the boat hire, particularly to the first Abraham Didi for teaching me great digging and sledge hammering techniques. We were extremely lucky to have Hiroki Ogawa to accompany our first days in the field, which was a great boost – your GPR assistance was really appreciated. A big thanks also to Christine Liang for her substantial GPR guidance, for hosting my Auckland visit and for being The Best field buddy! I was so happy to have your company in our interesting challenges and encounters!!

For additional academic support, Dr. Eddie Beetham is thanked for his wave modelling expertise, which vastly strengthened Chapter 7. At Exeter, thank you to the lab technicians, and Dr. Diane Fraser for such great guidance with python. Many thanks also to the Exeter Reef Team for conversations that informed several of the ideas within this thesis.

This project was funded by a NERC studentship. I am very grateful to the NERC Radiocarbon Facility for funding radiocarbon dates, and to Dr. Paulline Gulliver for her expertise in this field. Many thanks to the Digital Globe Foundation for providing high resolution satellite imagery, which strengthened and facilitated many aspects of the project. In addition, for enabling me to present at international conferences, I am really very thankful for the grants received from the Quaternary Research Association, British Society for Geomorphology, Cullercoats Educational Trust, and Santander.

I am super grateful to my Exeter friends, particularly Sarah, Katie, Lilo, Dom, Gary and Charles for providing heaps of fun times, strong chat and support. A big thanks to Jamie for his great support over the last few months – I'm looking forward to our future adventures! Finally, an enormous thanks to my family – Mum, Dad and Andrew – for always supporting and encouraging me in everything I do.

"With every drop of water you drink, every breath you take,
you're connected to the sea. No matter where on Earth you live."
Sylvia Earle, Oceanographer, First female Chief Scientist of NOAA.

Contents

The evolution of Maldivian coral reef rim islands 1

Abstract 2

Acknowledgements 3

List of Figures 12

List of Tables 23

List of frequently used abbreviations and symbols 27

Chapter 1: Introduction 29

1.1 Introduction 29

1.2 Literature Review 30

1.2.1 Reef islands: distribution and types 30

1.2.2 Controls on reef island formation 35

1.2.2.1 Sea level – reef – reef island interactions 35

1.2.2.2 Sediment Dynamics 37

1.2.3 Models of reef island development 47

1.2.4 Conceptual models of reef island morphodynamics 48

1.2.5 Reef island dynamics: from decadal to event temporal scales 49

1.3 Research Rationale 51

1.3.1 Study site selection 52

1.4 Aims and Objectives 53

1.5 Thesis Structure 54

Chapter 2: Study Site and Atoll-Scale Differences in Wave Forcing 58

2.1 Introduction 58

2.2 The Maldives Archipelago 58

2.2.1 Geological evolution of the Maldivian Archipelago 59

2.2.2 Contemporary Process regime 62

2.2.3 Characteristics of the Maldives 63

2.3 Huvadhu Atoll 64
2.4 Atoll-scale differences in wave forcing 68
2.4.1 Methodology 68
2.4.1.1 WaveWatch III Hindcast Data 68
2.4.1.2 Wave Exposure Modelling 69
Wind fetch model 69
Wave energy model 71
2.4.2 Results 72
2.4.2.1 WaveWatch III Hindcast Data 72
2.4.3 Discussion 78
2.4.3.1 Oceanward Atoll Margins 78
2.4.3.2 Lagoonward Rim Margins 81
2.4.4 Conclusion 81
Chapter 3 Island Development 83
3.1 Introduction 83
3.2 Methodology 84
3.3 Results 88
3.3.1 Reef island morphology 88
3.3.2 Reef island sedimentology and stratigraphy 96
Facies 1: Organically enriched carbonate sand 103
Facies 2: Matrix-supported coral-rich sand 103
Facies 3: Clast-supported coral-rich sand 104
Oceanward-lagoonward gradient in reef island sedimentology 105
3.3.3 Reef island chronologies 106
3.3.4 Volumetric sediment storage 109
3.3.4 GPR traces 110
3.4 Discussion 119

3.4.1 Reef island morphology: topography and planform surveys 119
3.4.2 Reef island sedimentology and stratigraphy 120
3.4.3 Reef island chronologies 124
3.4.3.1 Island initiation 124
3.4.3.2 Models of reef island development 127
3.5 Conclusions 134
Chapter 4: Eco-geomorphic zonations and sediment storage 136
4.1 Introduction 136
4.2 Methodology 137
4.2.1 Study Site 137
4.2.2 Eco-geomorphic Zonation 138
4.2.3 Marine Benthic Surveys 140
4.2.4 Marine Benthic and Beach Sedimentology 141
4.2.5 Volumetric Sediment Storage 142
4.2.6 Statistical Analyses 143
4.3 Results 143
4.3.1 Eco-geomorphic Zonation 143
4.3.1.1 Windward Site Zonation: 149
4.3.1.2 Leeward Site Zonation: 151
4.3.2 Marine Benthic Sedimentology 153
4.3.2.1 Windward Site 158
4.3.2.2 Leeward Site 159
4.3.2.3 Spatial Variability in Marine Benthic Sedimentology 161
4.3.3 Beach Sedimentology 171
4.3.4 Marine – Beach – Island Sedimentology 174
4.3.5 Methodological Comparison: Sieving versus Settling 176
4.3.6 Volumetric Sediment Storage 177

4.4 Discussion 181
4.4.1 Eco-geomorphic Zonation 181
4.4.2 Marine Benthic Sedimentology 182
4.4.2.1 Physical Processes 182
4.4.2.2 Biological Processes 184
4.4.3 From Source to Sink: Delineation of Zones of Sediment Deposition and Transport 186
4.4.4 Marine – Beach – Island Sedimentary Connectivity 187
4.4.5 Inter- and Intra-Regional Comparisons of Marine Benthic Sedimentology 189
4.5 Conclusions 191
Chapter 5: Sediment Production 193
5.1 Introduction 193
5.2 Methodology 195
5.3 Results 199
5.3.1 Windward site 199
5.3.2 Leeward site 200
5.4 Discussion 207
5.4.1 Sediment generation 207
5.4.2 Methodological considerations 210
5.4.3 Linking sediment production to sediment storage 213
5.4.4 Linking ecological and geomorphic temporal scales 214
5.5 Conclusion 216
Chapter 6: The distribution of Maldivian seagrass meadows and implications for sediment production 217
6.1 Introduction 217
6.2 Methodology 222
6.2.1 Archipelago-scale: Seagrass-urbanisation association 222

6.2.2 Atoll-scale: Shifts in seagrass areal extent between 2006 and 2015, Huvadhu Atoll 223
6.2.3 Platform-scale: Implications of seagrass expansion for sediment productivity 226
6.2.3.1 Seagrass density and epiphytic calcium carbonate production 226
6.2.3.2 Benthic Sedimentology 227
6.2.3.3 Sediment productivity 227
6.3 Results 228
6.3.1 Archipelago-scale: Seagrass-urbanisation association 228
6.3.2 Atoll-scale: Shifts in seagrass areal extent between 2006 and 2015, Huvadhu Atoll 231
6.3.3 Platform-scale: Implications of seagrass expansion for sediment productivity 235
6.3.3.1 Seagrass density and epiphytic calcium carbonate production 235
6.3.3.2 Benthic Sedimentology 241
6.3.3.3 Sediment Productivity 242
6.4 Discussion 247
6.4.1 Archipelago-scale: Seagrass-urbanisation association 247
6.4.2 Atoll-scale: Shifts in seagrass areal extent between 2006 and 2015, Huvadhu Atoll 253
6.4.3 Platform-scale: Implications of seagrass expansion for sediment productivity 255
6.4.3.1 Seagrass density and epiphytic calcium carbonate production 255
6.4.3.2 Benthic Sedimentology 256
6.4.3.3 Sediment Productivity 258
6.5 Conclusion 260
Chapter 7: Sediment transport 262
7.1 Introduction 262

7.2 Methodology 263
7.2.1 Bathymetry 263
7.2.2 Wave processes 264
7.2.2.1 Approach 264
7.2.2.2 Model inputs 264
7.2.2.3 Model outputs 266
7.2.3 Sediment Potential Mobility 267
7.3 Results 268
7.3.1 Bathymetric modelling 268
7.3.2 Wave processes 272
7.3.2.1 Contemporary wave processes 272
7.3.2.2 Sea-level rise projections 282
7.3.3 Sediment Potential Mobility 285
7.3.3.1 Contemporary process regime 285
7.3.3.2 Sea-level rise projections 286
7.4 Discussion 296
7.4.1 Wave processes 296
7.4.1.1 Contemporary process regime 296
7.4.1.2 Sea-level rise projections 298
7.4.2 Sediment Potential Mobility 300
7.4.3 Geomorphic implications 303
7.4.4 Methodological considerations and further work 307
7.5 Conclusion 311
Chapter 8: Conclusion 313
8.1 Research Rationale 313
8.2 Key Findings 314

Q. 1) What are the key controls upon, and modes of, Maldivian reef rim island development? 314

Q. 2) To what extent does variability exist in reef island development at the scale of an individual atoll? 317

Q. 3) Can a sediment budget be constructed linking sediment production to both island and marine benthic sediment storage? 319

Q. 4) What is the degree of contemporary reef-to-island connectivity? 324

Q. 5) What are the implications of research findings for the future of Maldivian reef rim island systems and their management under conditions of environmental change? 328

Q. 6) Does an integrated methodology provide an effective means of understanding reef rim island systems? 331

8.3 Limitations and Further Work 332

References 335

List of Figures

Figure 1.1 - Global Distribution of reefs (blue dots) and reef islands (red dots), according to UNEP-WCMC, ReefBase (2012) distribution data.

Figure 1.1 - Schematic planform and cross-sectional diagrams of a theoretical atoll. Reef island types and geomorphic structures are labelled.

Figure 1.2 - Interpreted regional sea-level histories and timings of reef island development (from Perry et al., 2011).

Figure 1.3 – Examples of breakdown pathways and associated grain size distributions for *Halimeda* and coral (from Scoffin, 1992). Hence, a bimodality is evident where breakdown occurs in a step-like manner.

Figure 1.4 – Reef island evolution models indicated by isochrons of deposition (in Woodroffe et al., 1999).

Figure 1.6 – Space-time diagram illustrating the theoretical framework within which this thesis is situated. Adapted from Cowell and Thom (1994) and Perry et al. (2008).

Figure 1.7 – Overall thesis structure illustrating key linkages between data chapters. Dashed grey boxes represent the temporal scale to which each chapter primarily relates.

Figure 2.1 - Location of the Maldives within the Indian Ocean (A), of Huvadhu Atoll within the Maldives (B), and of the leeward (i.e. north-eastern) and windward (i.e. south-western) study sites (C). Predominant swell and wind wave directions provided within C.

Figure 2.2 – The Maldives Archipelago; imagery from ESRI (2017).

Figure 2.3 – Huvadhu Atoll and the locations of the windward and leeward study sites. Imagery source: ESRI (2017).

Figure 2.4 – Examples of rim types A, B, C and D from Huvadhu Atoll (Google Earth imagery, 2013).

Figure 2.5 – Node locations selected for WaveWatch III hindcast analyses

Figure 2.6 – Comparison of WaveWatch III output values for T_O at the north-eastern and south-western study sites (n = 279,768 for each parameter at each site). Linear regression line is plotted in green (R^2 = 0.855; y = 0.864x + 1.003). For ease of comparison y = x is plotted in blue.

Figure 2.7 – Comparison of WaveWatch III output values for H_s at the north-eastern and south-western study sites (n = 279,768 for each parameter at each site). Linear regression line is plotted in green (R^2 = 0.854; y = 0.747x + 0.196). For ease of comparison y = x is plotted in blue.

Figure 2.8 – Wind rose showing wind speed (m s^{-1}) and direction generated using 2014 wind data from Kaadedhdhoo Airport (0.49°N, 73.00°E; n = 2643).

Figure 2.9 – Wave exposure model of Huvadhu Atoll (J m^{-3}; A). The cross-atoll transect (red line within A) intersects both the south-western and north-eastern study sites and the associated wave exposure values (n = 8780) are plotted within B.

Figure 2.10 – Location of the south-western (A) and north-eastern (B) study sites within Huvadhu Atoll alongside the Mandlier's (2008) windward (W.) and leeward (L.) study sites. Mean swell direction from Young (1999). Figure adapted from Mandlier (2008).

Figure 2.11 – Illustration of terminology used throughout the thesis to refer study sites (A), and the oceanward and lagoonward marine environments within the leeward (B) and windward (C) sites. (Imagery source: ESRI, 2017). N.B. within the Chapter 3, Baavanadhoo island will also be incorporated into the leeward site analyses.

Figure 3.1 – Islands within the windward (left) and leeward (right) study sites.

Figure 3.2 – Five-point abrasive scale adapted from Pandolphi and Greenstein, 1997; Lescinsky et al., 2012 (image from Lescinsky et al., 2012)

Figure 3.3 – Topographic cross-sections, planform surveys, core logs, and median radiometric dates from Mainadhoo, windward site.

Figure 3.4 – Topographic cross-sections, planform surveys, core logs, and median radiometric dates from Boduhini and Kudahini, windward site.

Figure 3.5 – Examples of geomorphic features at the windward study site: lagoonward island coast of Mainadhoo (A); oceanward island coast of Mainadhoo, near the

western transect (B); oceanward coast of Mainadhoo, near the central transect (C); rubble ridge on the oceanward island coast of Mainadhoo, western transect (D); conglomerate platform off Boduhini (E) and Kudahini (F).

Figure 3.6 – Topographic cross-sections, planform surveys, core logs, and median radiometric dates from Galamadhoo, leeward site.

Figure 3.7 – Topographic cross-sections, planform surveys, core logs, and median radiometric dates from Galamadhoo, leeward site.

Figure 3.8 – Examples of geomorphic features at the leeward study site: northern sand spit (A); stranded beachrock off the south coast of Galamadhoo (B and E); lagoonward-dipping beachrock on the lagoonward coast of Baavanadhoo (C); and flatter beachrock on the oceanward coast of Baavanadhoo (D).

Figure 3.9 – Windward site facies: images (white bar = 1 mm), grain size distributions and compositional data.

Figure 3.10 – Leeward site facies: images (white bar = 1 mm), grain size distributions and compositional data.

Figure 3.11 - Ternary plots of grain size data from each island sediment sample recovered from the windward and leeward sites

Figure 3.12 – Examples of coral clasts > 1 cm recovered from each facies

Figure 3.13 – Relationship between grain size and distance from the oceanward reef crest at windward (black) and leeward (red) sites. Regression for individual sample grain size vs. distance from reef crest: windward site, $P = <0.001$, $R^2 = 0.203$; leeward site, $P = 0.008$, $R^2 = 0.16$).

Figure 3.14 – GPR lagoonward-oceanward trace from the central transect of Baavanadhoo, leeward site.

Figure 3.15 – Locations of GPR traces obtained from Mainadhoo, windward site.

Figure 3.16 – GPR trace A, obtained from the western transect of Mainadhoo, perpendicular to the lagoonward coast.

Figure 3.17 – GPR west-east trace B, obtained perpendicular to the western transect of Mainadhoo, parallel to the lagoonward coast.

Figure 3.18 – GPR lagoonward-oceanward trace C, obtained from the central transect of Mainadhoo, perpendicular to the lagoonward coast.

Figure 3.19 – GPR west-east trace D, obtained perpendicular to the central transect of Mainadhoo, parallel to the lagoonward coast.

Figure 3.20 – GPR lagoonward-oceanward trace E, obtained from central transect of Mainadhoo, perpendicular to the oceanward coast.

Figure 3.21 – Timings of island formation at the windward site (A), leeward site (B), and South Maalhosmadulu atoll interior islands (Kench et al., 2005), in relation to the sea-level curve for the region given in Kench et al. (2009b)

Figure 3.22 – Conceptual model of reef rim island development, windward site. Note that vertical exageration is substantial for the pupose of illustration.

Figure 3.23 – Conceptual model of reef rim island development, leeward site. Note that vertical exageration is substantial for the pupose of illustration.

Figure 4.1 – Quickbird and WorldView-2 imagery of the windward (left) and leeward (right) study sites.

Figure 4.2 – Windward site sampling design. Locations of benthic surveys (left), sediment samples (centre), and ground-truth points (right).

Figure 4.3 – Leeward site sampling design. Locations of benthic surveys (left), sediment samples (centre), and ground-truth points (right).

Figure 4.4 – Windward site classification of eco-geomorphic zones generated from Quickbird imagery (spatial reslution = 0.6 m).

Figure 4.5 – Leeward site classification of eco-geomorphic zones generated from WorldView-2 imagery (spatial reslution = 0.46 m).

Figure 4.6 – Benthic characteristics and images of each windward site eco-geomorphic zone whereby A = oceanward reef crest, B = rubble, C = oceanward patch, D = lagoonward patch, E = lagoonward sand. Benthic classes: rubble (R), sand (S), limestone pavement (LP), seagrass (SG), live coral (LC), dead coral (DC), and CCA.

Figure 4.7 – Benthic characteristics and images of each leeward site eco-geomorphic zone whereby A = lagoonward reef crest, B = lagoonward patch, C = oceanward patch, D = dense seagrass, E = oceanward sparser seagrass, and F = oceanward reef crest. Benthic classes: rubble (R), sand (S), limestone pavement (LP), seagrass (SG), live coral (LC), dead coral (DC), and CCA.

Figure 4.8 – Rubble tongues and the intervening oceanward patch zone at low tide, windward site.

Figure 4.9 – Ternary plots of sediment texture within each eco-geomorphic zone at both the windward (upper) and leeward (lower) sites.

Figure 4.10 – Windward site grain size distributions, median grain sizes, composition, and images (white bar = 1 mm) from each eco-geomorphic zone, top and toe of beach samples, and island facies 2A (i.e. uppermost facies).

Figure 4.11 – Leeward site grain size distributions, median grain sizes, composition, and images (white bar = 1 mm) from each eco-geomorphic zone, top and toe of beach samples, and island facies 2A (i.e. uppermost facies).

Figure 4.12 – Block kriging results of textural characteristics of windward site sediment samples.

Figure 4.13 – Block kriging results of textural characteristics of leeward site sediment samples.

Figure 4.14 – Block kriging results of windward site sediment composition.

Figure 4.15 – Block kriging results of leeward site sediment composition.

Figure 4.16 – Windward site correlation matrix showing significant relationships (only those where $P < 0.05$ are included) between sediment textural characteristics, composition, sediment depths, and distance from the oceanward reef crest. Colour intensity and circle size are proportional to the correlation coefficients.

Figure 4.17 – Leeward site correlation matrix showing significant relationships (only those where $P < 0.05$ are displayed) between sediment textural characteristics, composition, sediment depths, and distance from the oceanward reef crest. Colour intensity and circle size are proportional to the correlation coefficients.

Figure 4.18 – Windward site nMDS plot including sediment tectural and compositional data from each eco-geomorphic zone (lp = lagoonward patch, ls = lagoonward sand, r = rubble, op = oceanward patch, orc = oceanward reef crest), island facies (I2A, I2B, I3A, I3B), and beach samples (LT = lagoonward toe, Ltp = lagoonward top, OT = oceanward toe, Otp = oceanward top).

Figure 4.19 – Leeward site nMDS plot including sediment tectural and compositional data from each eco-geomorphic zone (lrc = lagoonward reef crest, lp = lagoonward patch, os = oceanward sand, dsg = dense seagrass, oss = oceanward sparser seagrass, orc = oceanward reef crest), island facies (I2A, I2B, I3A, I3B), and beach samples (LT = lagoonward toe, Ltp = lagoonward top, OT = oceanward toe, Otp = oceanward top).

Figure 4.20 – Comparison of mean grain size (Φ) calculated using settling- (i.e. RSA) and sieve-derived approaches. For eae of comparison, the plotted line in plot B is y = x.

Figure 4.21 – Block kriging results of windward site benthic sediment storage.

Figure 4.22 – Block kriging results of leeward site benthic sediment storage.

Figure 5.1 – Relative contributions of sediment producers within each of the eco-geomorphic zones and overall at the windward (A) and leeward (B) study sites.

Figure 5.2 – Spatial variability (i.e. between zones) in average rates of sediment production (G) at the windward (left) and leeward (right) sites.

Figure 6.1 – The transition from nutrient- to light-limitation and the associated impacts upon seagrass and macroalgal biomass in shallow coastal marine ecosystems (adapted from Harlin, 1993; also in Burkholder et al., 2007)

Figure 6.2 – Location of change detection reef platform sites: (1) inhabited interior; (2) northerly leeward platform incorporating a geographic barrier; (3) resort; (4) southerly leeward rim platform; and (5) windward rim.

Figure 6.3 – Reflectance spectra of benthic cover types for wavelengths between 400 and 1000 nm., i.e. spectral signatures are notably distinct.

Figure 6.4 – The eight most populated areas in the Maldives (white bars = 1 km): (1) Hulamale (included instead of Male), (2) Fuvahmulah, (3) Hithadhoo, (4) Thinadhoo, (5) Naifaru, (6) Feydhoo, Addu Atoll.

Figure 6.5 - 2006 (QuickBird-2) and 2015 (WorldView-2) imagery of the interior platform (Devvadhoo island); 6.6% (0.1 ha) increase in seagrass areal extent.

Figure 6.6 - 2006 (QuickBird-2) and 2015 (WorldView-2 and -3) imagery of the northerly leeward platform (left: Dhaandhoo island; right: Vodamulaa island); 37.6% (42 ha) increase in seagrass areal extent, 91.5% of which occurred within the inhabited side of the small channel (i.e. geographic barrier). Land has evidently been reclaimed off the island's western coast; this area was excluded from the change detection analysis.

Figure 6.7 - 2006 (QuickBird-2) and 2015 (WorldView-2) imagery of the resort platform (Mahadhdhoo island); 29.2% (7 ha) increase in seagrass areal extent, 1 ha of seagrass appears to have been removed artificially.

Figure 6.8 - 2006 (QuickBird-2) and 2015 (WorldView-2) imagery of the southerly leeward rim platform; 72.3% (240 ha) increase in seagrass areal extent.

Figure 6.9 – 2006 (QuickBird-2) and 2015 (WorldView-2) imagery of the windward rim platform; 37.9% (159 ha) increase in seagrass areal extent.

Figure 6.10 – *Thallassia hemprichii* bed within the 'dense seagrass' zone off the oceanward coast of Galamadhoo island.

Figure 6.11 – Blade densities within each eco-geomorphic zone whereby OS = oceanward sand, DSG = dense seagrass, OSS = oceanward sparser seagrass, and ORC = oceanward reef crest.

Figure 6.12 – Epiphytic $CaCO_3$ production within each eco-geomorphic zone whereby OS = oceanward sand, DSG = dense seagrass, OSS = oceanward sparser seagrass, and ORC = oceanward reef crest.

Figure 6.13 – Relationship between blade density and epiphytic $CaCO_3$ production.

Figure 6.14 – Semi-quantitative assessments of seagrass epiphyte composition within each eco-geomorphic zone whereby OS = oceanward sand, DSG = dense seagrass, OSS = oceanward sparser seagrass, and ORC = oceanward reef crest.

Figure 6.15 – Binocular microscope images of examples of typical seagrass epiphytes (white bar = 1 mm): CCA (A, C), serp ulids (A, C), bryozoans (B), and foraminifera (C - *Marginopora vertebralis*; D - *Calcarina spengleri*).

Figure 6.16 – Thin section images of cross-sections through blocks of dried seagrass blades embedded in resin. Thin (<75 µm) monostromatic layers of encrusting CCA are evident.

Figure 6.17 – Percentage of foraminifera found within benthic sediment from each eco-geomorphic zone whereby OS = oceanward sand, DSG = dense seagrass, OSS = oceanward sparser seagrass, and ORC = oceanward reef crest.

Figure 6.18 – Relationship between epibiont carbonate production (g $CaCO_3$ $m^{-1}yr^{-1}$) and the percentage of foraminifera found within benthic sediment samples.

Figure 6.19 – Classifications of geomorphic zones in the marine environment off the oceanward coast of Galamadhoo generated from QuickBird-2 (2006) and WorldView-2 (2015) imagery. OS = oceanward sand, DSG = dense seagrass, OSS = oceanward sparser seagrass, and ORC = oceanward reef crest.

Figure 6.20 – Platform-scale classifications of eco-geomorphic zones generated from QuickBird-2 (2006) and WorldView-2 (2015).

Figure 6.21 – Dense seagrass beds are evident in Google Earth (2015) imagery adjacent to the non-fishing village sites of Miller and Sluka's (1999a) study, Laamu Atoll.

Figure 7.1 – Experimentally-derived threshold entrainment relationship digitsed from Kench and McLean (1996). This relationship was used to calculate the threshold sediment settling velocity (chi) associated with the model-derived velocities extracted from each sample location.

Figure 7.2 – Windward site validation plots of the relation between echosounder-derived (i.e. measured) and model-derived water depths relative to MSL.

Figure 7.3 – Leeward site validation plots of the relation between echosounder-derived (i.e. measured) and model-derived water depths relative to MSL.

Figure 7.4 – Windward site bathymetric model derived from Quickbird imagery.

Figure 7.5 – 3-dimensional perspective view of windward site bathymetric model (vertical exaggeration = x2).

Figure 7.6 – Leeward site bathymetric model derived from WorldVIew-2 imagery.

Figure 7.7 – 3-dimensional perspective view of windward site bathymetric model (vertical exaggeration = x5).

Figure 7.8 – Windward site wave setup (i.e. mean water level, m) where SLR = 0.0 m (A), 0.5 m (B) and 1.0 m (C).

Figure 7.9 – Leeward site wave setup (i.e. mean water level, m) where SLR = 0.0 m (A), 0.5 m (B) and 1.0 m (C).

Figure 7.10 – Root mean square wave height (H_{rms}, m) across the windward site where SLR = 0.0 m (A), 0.5 m (B), and 1.0 m (C).

Figure 7.11 – Root mean square wave height (H_{rms}, m) across the leeward site where SLR = 0.0 m (A), 0.5 m (B), and 1.0 m (C).

Figure 7.12 – Mean wave velocity (V_{mean}, m s^{-1}) across the windward site where SLR = 0.0 m (A), 0.5 m (B), and 1.0 m (C).

Figure 7.13 – Mean wave velocity (V_{mean}, m s^{-1}) across the leeward site where SLR = 0.0 m (A), 0.5 m (B), and 1.0 m (C).

Figure 7.14 – Maximum wave velocity (V_{max}, m s^{-1}) across the windward site where SLR = 0.0 m (A), 0.5 m (B), and 1.0 m (C).

Figure 7.15 – Maximum wave velocity (V_{max}, m s^{-1}) across the leeward site where SLR = 0.0 m (A), 0.5 m (B), and 1.0 m (C). To allow visualisation of trends, note the scale differs to that in Figure 7.15.

Figure 7.16 – Wave processes along oceanward-lagoonward cross-rim transects at the windward site under 0.0 m, 0.5 m and 1.0 m SLR.

Figure 7.17 – Wave processes along oceanward-lagoonward transects at the leeward site under 0.0 m, 0.5 m and 1.0 m SLR.

Figure 7.18 – The potential mobility (PM) of windward site sediment samples with both mean (V_{mean}) and maximum (V_{max}) velocities under scenarios of 0.0 m, 0.5 m and 1.0

m SLR where LP = lagoonward patch, LS = lagoonward sand, OP = oceanward patch, R = rubble, and ORC = oceanward reef crest.

Figure 7.19 – Windward site block kriging results of sediment potential mobility (PM, %) with both mean (V_{mean}) and maximum (V_{max}) velocities under scenarios of 0.0 m, 0.5 m and 1.0 m SLR.

Figure 7.20 – Windward site average grain size distributions of sediment from each eco-geomorphic zone (derived via settling techniques) and average mobilised fractions under V_{mean} and V_{max} where SLR = 0.0 m, 0.5 m and 1.0 m. Note that average values are presented, but there is substantial variability within each zone (Figure 7.20).

Figure 7.21 –The potential mobility (PM) of leeward site sediment samples with both mean (V_{mean}) and maximum (V_{max}) velocities under scenarios of 0.0 m, 0.5 m and 1.0 m SLR where LRC = lagoonward reef crest, LP = lagoonward patch, OS = oceanward sand, DSG = dense seagrass, OSS = oceanward sparser seagrass, and ORC = oceanward reef crest. Note that axes scales differ to those within Figure 7.19.

Figure 7.22 – Leeward site block kriging results of sediment potential mobility (PM, %) with both mean (V_{mean}) and maximum (V_{max}) velocities under scenarios of 0.0 m, 0.5 m and 1.0 m SLR.

Figure 7.23 – Leeward site average grain size distributions of sediment from each eco-geomorphic zone (derived via settling techniques) and the mobilised fractions under V_{mean} and V_{max} where SLR = 0.0 m, 0.5 m and 1.0 m.

Figure 7.24 – Relationships between benthic sedimentology and contemporary mean velocities (SLR = 0).

Figure 7.25 – Conceptual model of potential rim reef island morphological response to shifts in sediment potential mobility. For illustrative purposes, cross-sectional diagrams are substantially vertically exaggerated.

Figure 8.1 – Conceptual model characterising the predominant island building processes within modes A and B. Models were informed by datasets from Chapters 3, 4, 5 and 7. Note that for illustrative purposes, vertical (and fish) exaggeration is substantial.

Figure 8.2 – Leeward site sediment budget diagram linking rim system inputs, outputs and storage. Arrow size is approximately proportional to the associated value. Dashed lines represent unquantified processes. Data from Chapters 3 (Galamadhoo island storage), 4 (marine benthic storage) and 5 (inputs).

Figure 8.3 – Windward site sediment budget diagram linking rim system inputs, outputs and storage. Arrow size is approximately proportional to the associated value. Dashed lines represent unquantified processes. Data from Chapters 3 (Mainadhoo, Boduhini and Kudahini island storage), 4 (marine benthic storage) and 5 (inputs).

Figure 8.4 – Conceptual model of cross-rim trends at the windward site. This incorporates datasets from Chapters 3, 4, 5 and 7.

Figure 8.5 – Conceptual model of cross-rim trends at the leeward site. This incorporates datasets from Chapters 3, 4, 5 and 7.

Figure 8.6 – Illustration of the integrated approach employed within this thesis in order to improve understanding of the evolution of reef island systems and, in turn, their potential vulnerability to future change.

List of Tables

Table 1.1 – Marine environmental parameters influencing the spatial distribution of reef-building corals. Values in brackets relate to non-reef-building corals. [a] = weekly data; [b] = monthly average; [c] = overall averages (1900-1999); [d] = overall averages (1972-1978). *Table source:* Kench et al. (2009a). *Data source:* Kleypas et al. (1999).

Table 1.2 - Terminology used to describe reef islands and their geomorphic settings.

Table 3.1 - Textural data for each facies from both windward and leeward sites, interquartile ranges (quartile 1 – quartile 3 in italics)

Table 3.2 – Compositional data for each facies from both windward and leeward sites, interquartile ranges (quartile 1 – quartile 3) in italics.

Table 3.3 – Identification of coral clasts (with longest axes >1 cm) within facies 3 at the windward and leeward sites. Proportion of unidentifiable coral clasts is given as a proportion of total clast weight. Compositional data is provided as a proportion of the weight of identifiable clasts.

Table 3.4 – Radiometric dates from the windward and leeward study sites and their associated error terms. *C = Consolidated underlying substrate; **CP = Conglomerate platform.

Table 4.1 - Error matrix detailing the correspondence of the marine classification and ground truth data within each of the eco-geomorphic zones at the windward site where LP = lagoonward patch, LS = lagoonward sand, OP = oceanward patch, R = rubble, and ORC = oceanward reef crest.

Table 4.2 - Error matrix detailing the correspondence of the marine classification and ground truth data within each of the eco-geomorphic zones at the leeward site where LRC = lagoonward reef crest, LP = lagoonward patch, OS = oceanward sand, DSG = dense seagrass, OSS = oceanward sparser seagrass, and ORC = oceanward reef crest.

Table 4.3 – Benthic cover, rugosity, depth (relative to MSL) and areal extent of eco-gomorphic zones at the windward site.

Table 4.4 – Benthic cover, rugosity, depth (relative to MSL) and areal extent of eco-geomorphic zones at the leeward site.

Table 4.5 – Textural characteristics of sediment samples recovered from each eco-geomorphic zone. Interquartile ranges in italics (*IQR1 – IQR3*).

Table 4.6 – Concentrations (%) of skeletal constituents within sediment samples recovered from each eco-geomorphic zone. Interquartile ranges in italics (*IQR1 – IQR3*).

Table 4.7 – Windward site correlation matrix of sediment textural characteristics, composition, sediment depths, and distance from the oceanward reef crest. Correlation coefficients and P values are in the upper right and lower left portions of the table respectively. Significant P values (<0.05) are in bold.

Table 4.8 – Leeward site correlation matrix of sediment textural characteristics, composition, sediment depths, and distance from the oceanward reef crest. Correlation coefficients and P values are in the upper right and lower left portions of the table respectively. Significant P values (<0.05) are in bold.

Table 4.9 – Textural characteristics of top and toe of beach sediment samples from both the windward and leeward study sites. Interquartile ranges in italics (*IQR1 – IQR3*).

Table 4.10 – Concentrations (%) of skeletal constituents within top and toe of beach sediment samples from both the windward and leeward study sites. Interquartile ranges in italics (*IQR1 – IQR3*).

Table 4.11 – Estimates of sediment storage within each of the windward site eco-geomorphic zones.

Table 4.12 – Estimates of sediment storage within each of the leeward site eco-geomorphic zones.

Table 5.1 – Abundances and sediment production rates (G = kg $CaCO_3$ m^{-2} yr^{-1}) associated with direct sediment producers and endolithic sponges at the windward study site.

Table 5.2 – Abundances and sediment production rates (G = kg $CaCO_3$ m^{-2} yr^{-1}) associated with direct sediment producers and endolithic sponges at the leeward study site.

Table 5.3 – Windward site parrotfish abundances and substrate erosion/sediment generation rates (G = kg $CaCO_3$ m^{-2} yr^{-1}) grouped by functional group and body size category.

Table 5.4 – Leeward site parrotfish abundances and substrate erosion/sediment generation rates (G = kg $CaCO_3$ m^{-2} yr^{-1}) grouped by functional group and body size category.

Table 5.5 – Windward site urchin abundances and substrate erosion/sediment generation rates (G = kg $CaCO_3$ m^{-2} yr^{-1}) grouped by species and size category.

Table 5.6 – Leeward site urchin abundances and substrate erosion/sediment generation rates (G = kg $CaCO_3$ m^{-2} yr^{-1}) grouped by species and size category.

Table 5.7 – Rates (G = kg $CaCO_3$ m^{-2} yr^{-1}) and the proportional contributions (per m^2) of new sediment production associated with each of the key sediment producers at the windward site.

Table 5.8 – Rates (G = kg $CaCO_3$ m^{-2} yr^{-1}) and the proportional contributions (per m^2) of new sediment production associated with each of the key sediment producers at the leeward site.

Table 5.9 – Total new sediment production within each zone at the windward site (kg yr^{-1}, i.e. following multiplication by the areal extent of each eco-geomorphic zone), and proportional contributions both within each zone and by each of the key sediment producers.

Table 5.10 – Total new sediment production within each zone at the leeward site (kg yr^{-1}, i.e. following multiplication by the areal extent of each eco-geomorphic zone), and proportional contributions both within each zone and by each of the key sediment producers.

Table 6.1 – Sources of imagery and acquisition dates.

Table 6.2 – Seagrass presence (P) – absence (A) counts of reef platforms grouped by Atoll, land use (uninhabited, inhabited, other human influence, resort), and accommodation space (where island occupy > or < 75% of the reef platform).

Table 6.3 – Change in seagrass areal extent between 2006 and 2015 on 5 rim platforms within Huvadhu Atoll.

Table 6.4 – Survey stations, blade densities and estimates of $CaCO_3$ production.

Table 6.5 – Zonal change matrix (ha) derived by subtracting the 2006 and 2015 classifications of the marine environment off the oceanward coast of Galamadhoo.

Table 6.6 – Estimations of sediment production by seagrass epiphytes in 2006 and 2015.

Table 6.7 – Zonal change matric (ha) derived by subtracting the 2006 and 2015 classifications of the leeward rim platform.

Table 6.8 – Estimations of sediment production by seagrass epiphytes in 2006 and 2015.

Table 7.1 – Wave data employed as model inputs from the oceanward and lagoonward margins for both the windward and leeward study sites. H_s = significant wave height (m), T_s = significant wave period (s).

Table 7.2 – Depths of each eco-geomorphic zone relative to MSL as derived from bathymetric models.

Table 7.3 – Windward site V_{mean}, V_{max}, H_{rms} and setup within each of eco-geomorphic zones where SLR = 0.0, 0.5 and 1.0. Note that marked spatial variability exists within each zone.

Table 7.4 – Leeward site V_{mean}, V_{max}, H_{rms} and setup within each of eco-geomorphic zones where SLR = 0.0, 0.5 and 1.0. Note that marked spatial variability exists within each zone.

Table 7.5 – Potential Mobility (PM, % – mean ± 1 S.D., ranges in italics) of sediment from each eco-geomorphic zone at the windward site.

Table 7.6 – Potential Mobility (PM, % – mean ± 1 S.D., ranges in italics) of sediment from each eco-geomorphic zone at the leeward site.

List of frequently used abbreviations and symbols

cal. yr. B.P.	Calibrated years Before Present
CCA	Crustose coralline algae
G	kg $CaCO_3$ m^{-2} yr^{-1}
GPR	Ground penetrating radar
H_{rms}	Root mean square wave height
H_s	Significant wave height
MSL	Mean sea level
PM	Potential mobility
SD	Sediment depth
SLR	Sea level rise
T_o	Dominant wave period
T_s	Significant wave period
V_{max}	Maximum velocity
V_{mean}	Mean velocity

To Hilary, Ian, Andrew, Vera and Florence

Chapter 1: Introduction

1.1 Introduction

Coral reef islands are low-lying (typically <3 m above mean sea level, MSL) accumulations of wave deposited bioclastic sediment (McLean and Woodroffe, 1994). They are of high ecological and socioeconomic significance as they provide habitats for many threatened and endemic species (Roy and Connell, 1991; Fuentes et al., 2011). Reef islands also offer the only habitable land in atoll nations, including the Maldives, Kiribati and the Marshall Islands where they support populations of 345,023, 102,351 and 52,634 respectively (World Bank, 2013).

As a function of their low elevations, relatively small size (typically 0.01 – 2.5 km^2), largely unconsolidated structures, and reliance upon locally generated sediment, reef islands are regarded among the most vulnerable environments to climate change, particularly to sea level rise (Roy and Connell, 1991; Kench and Cowell, 2001; Kench and Brander, 2006b). This view was endorsed by the IPCC 4th Assessment (Parry et al., 2007) and reef island nations have thus been flagged among the first potential environmental refugees of climate change (e.g. Farbotco, 2010). Potential geomorphic impacts of environmental change include shoreline erosion, saline intrusion, and flooding. Each of these potential impacts have projected consequences for island size, shoreline reworking, island (re)mobilisation, contamination of fresh groundwater and waterlogging of low-lying areas (McLean, 2011). However, perceptions of vulnerability are often underpinned by the overly simplistic assumption that reef islands are geomorphically passive landforms that will erode and inundate incrementally with sea-level rise (e.g. Kench et al., 2009a). However, there is a growing body of research highlighting that reef islands are in fact dynamic, rather than passive, landforms (e.g. Kench and Brander, 2006b; Webb and Kench, 2010; Kench et al., 2015; Duvat and Pillet, 2017). Reef islands may therefore exhibit a range of responses to environmental change, which may occur as a function of the interactions between reef growth, the prevailing process regime, and rates and types of sediment production. Integrated, eco-morphodynamic approaches, which incorporate both ecological and morphological processes, are thus needed to improve understanding of reef island

dynamics and their potential resilience to environmental change (Woodroffe, 2008; Kench et al., 2009a; Perry et al., 2011).

This Chapter will: (1) review existing reef island and reef sediment literature in order to situate this thesis in the context of previous work; (2) draw out questions that arise from the literature review; (3) outline the rationale for this thesis; (4) state the aims and objectives; and (5) outline the overall thesis structure.

1.2 Literature Review

This review will discuss: (1) the distribution and types of reef islands; (2) the key controls upon reef island development and evolution, specifically sea-level and sediment dynamics; (3) models of reef island development; (4) conceptual models of island morphodynamics; and (6) reef island dynamics at a range of temporal scales.

1.2.1 Reef islands: distribution and types

Reef islands are widely distributed across the tropical and subtropical regions from Bermuda (*c*. 32°N) to the southern Great Barrier Reef (*c*. 29°S). They are, by definition, underpinned by reef structures that have evolved near sea level or sea level constrained surfaces on which the sub-aerial accumulation of sediments can occur. At the global scale, their distribution is similarly constrained (as it is for reefs) by a suite of marine environmental parameters, including sea surface temperature, salinity, depth of light penetration and nutrient levels (Kleypas et al., 1999; Table 1.1) and these conditions then determine the areas in which reefs occur (). However, at the local scale, differences in the nature and timing of reef island formation have occurred as a function of factors including sea level-reef growth interactions, prevailing process regimes, and sediment production. Hence, the distribution of reefs and reef islands is not entirely synonymous ().

As reef islands exist in a range of geomorphic settings, a range of island types can be identified (**Table** 1.2). Within atoll settings, islands may be divided into two key types: (1) *interior islands* form upon reef platforms within atoll lagoons; whereas (2) *rim islands* form on atoll rim platforms, around the atoll perimeter. Further divisions may be drawn between reef platforms themselves. For example, in the Maldives, reef interior platforms are locally termed ‘faros’ and exhibit varying degrees of sediment infilling on a continuum from unfilled to those that are entirely infilled (Kench et al.,

2005). Divisions between rim platforms may be drawn on the basis of their continuity, i.e. between discontinuous and continuous (Table 1.2, Figure 1.2).

Reef islands can also be broadly divided on the basis of their composition. *Motu* are islands composed of coarse material, including rubble and shingle, which are located in areas of frequent storm activity. They typically receive a net input of material during storms, which is then redistributed during fair weather periods. In contrast, cays are islands that are primarily associated with sand-size sediments and experience infrequent storms. Cays are more vulnerable to erosion during storm events and recover during subsequent fair weather periods (Stoddart and Steers, 1977; Bayliss-Smith, 1988).

		Environmental limits	
Environmental parameter	'Optimal' levels	Lower	Upper
Temperature (°C)[a]	21.0–29.5	16.0 (13.9)	34.4 (32.1)
Salinity (PSU)[b]	34.3–35.3	23.3 (20.7)	41.8 (No data)
Nitrate (μmol L^{-1})[c]	< 2.0	0.00	3.34 (up to 5.61)
Phosphate (μmol L^{-1})[c]	< 0.2	0.00	0.40 (up to 0.54)
Aragonite saturation state (Ω-arag)[d]	~ 3.83	3.28 (3.06)	No data
Depth of light penetration (m)	~ 50	<10	~ 90

Table 1.1 – Marine environmental parameters influencing the spatial distribution of reef-building corals. Values in brackets relate to non-reef-building corals. [a] = weekly data; [b] = monthly average; [c] = overall averages (1900-1999); [d] = overall averages (1972-1978). *Table source:* Kench et al. (2009a). *Data source:* Kleypas et al. (1999).

Term	*Definition*
Atoll rim islands	Islands that form on platforms that comprise the atoll rim (i.e. around the atoll perimeter).
Interior islands	Islands that atop interior reef platforms within atoll lagoons.
Continuous rim	Where an atoll rim is characterised by continuous reefs that restrict lagoon-ocean exchange.
Discontinuous rim	Where there are gaps in the reefs that form the atoll rim, allowing increased lagoon-ocean exchange.
Faro	Maldivian term used to describe interior reef platforms within atoll lagoons.
Motu	Reef islands dominated by coarse material, including rubble and shingle, which are located in areas of frequent storm activity.
Cays	Reef islands that are dominated by sand-size sediments and experience infrequent storms.
Unvegetated reef islands	Unvegetated reef islands are typically highly mobile, relatively small in size (<50-100 m along their longest axes) and do not possess beachrock outcrops.
Vegetated reef islands	Such reef islands are typically more stable than their unvegetated counterparts and, as such, may possess beachrock as their comparative stability can allow cementation to occur. Vegetated islands can be <1000 m along their longest axes, and their elevation is typically 1-3 m above the level of high tide (Stoddart and Steers, 1977).
Hoa	Polynesian term for the shallow passages between islands and/or the deeper passages between discontinuous sections of an atoll rim.
Tairua	Polynesian term which refers to a closed pond which may form if the spits of neighbouring islands join to close the *hoa*.
Mangrove cays	Formed by the colonisation of shoal areas by mangrove species which promote sedimentation.
Low wooded islands	Reef platforms which possess: (i) a shingle ridge close to the windward platform edge; (ii) a sand cay toward the leeward side of the platform; and (iii) an area between the two of open water which may, in cases, be colonised by mangroves (Stoddart and Steers, 1977).

Table 1.2 - Terminology used to describe reef islands and their geomorphic settings.

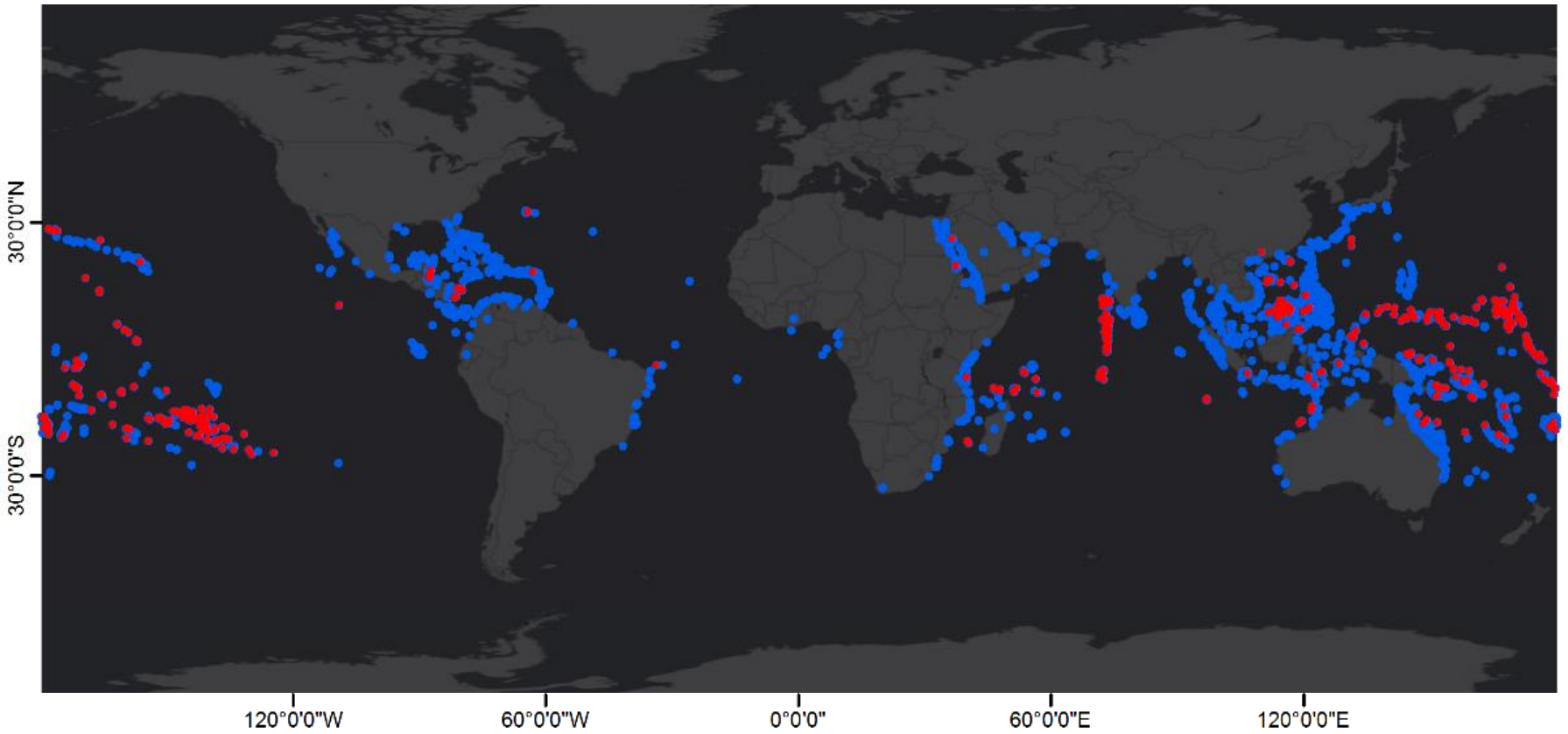

Figure 1.1 - Global Distribution of reefs (blue dots) and reef islands (red dots), according to UNEP-WCMC**, ReefBase (2012) distribution data.**

Figure 1.2 - Schematic planform and cross-sectional diagrams of a theoretical atoll. Reef island types and geomorphic structures are labelled.

1.2.2 Controls on reef island formation

As outlined above, reef island types, formation and structure are reflective of a hierarchy of controls, in particular, sea level – reef – reef island interactions and sediment dynamics, which will thus be discussed in turn.

1.2.2.1 Sea level – reef – reef island interactions

A fundamental prerequisite for reef island formation is the development of reef structures that may provide suitable foundations for reef island formation. Reef islands have typically formed during the late Holocene on top of sea level-constrained or near-constrained reef platforms. Sea level-reef growth, and in turn sea level-reef island, interactions are therefore important controls on reef island formation.

The significant regional variations that have occurred in Holocene sea level dynamics are of great importance for reef islands (**Figure 1.**). In the Pacific, there is evidence that rapid sea level rise occurred between 10,000 and 6,000 yr. B.P. (years Before Present). For instance, in a meta-analysis of data from the central Great Barrier Reef, Larcombe et al. (1995) postulate that sea levels rose from -45 m AHD (Australian Height Datum) at *c*. 10,500 yr. B.P. to -2 m at *c*. 6,000 yr. B.P. (*c.* 9.56 mm yr^{-1}). Modern sea levels were then attained *c*. 6,500 yr. B.P. following a 1 to 1.5 m highstand *c*. 6,000 yr. B.P. (Larcombe et al., 1995; Lewis et al., 2008). In the western Indian Ocean, there is evidence of rapid sea level rise of *c*. 6 mm yr^{-1} between 10,000 and 7,500 yr. B.P., followed by a gradual rises of *c*. 1.1 mm yr^{-1} and 1 to 1.5 mm yr^{-1} in the post-glacial period. Modern sea levels were then attained approximately 3,000 to 2,500 yr. B.P. with no highstand (Camoin et al., 2004).

Within the central Indian Ocean, Gischler et al. (2008) examined Rasdhoo Atoll (central Maldives) and suggested that high rates of sea-level rise occurred (~15 m kyr^{-1}) from 8,500–7,500 yr. B.P.. This was followed by a decrease to ~2 m kyr^{-1} between 7,500 and 6000 yr. B.P., and a subsequent slow increase (~0.25 m kyr^{-1}) since 6,000 yr. B.P. to present MSL. However, Gischler et al. highlight that it was 'unclear' whether a highstand occurred in the late Holocene. More recently, evidence of a highstand has been presented by Kench et al. (2009b) using data from South Maalhosmadulu Atoll (central Maldives). Kench et al. outline evidence of a rapid rise (~7 mm yr^{-1}) between 8,100 and 6,500 yr. B.P., followed by slower rise (<1 mm yr^{-1}), with contemporary sea levels attained 4,000 yr. B.P.. Subsequently, they suggest a

highstand occurred whereby sea levels continued to rise to at least 0.5 ± 0.1 m above present until ~2,100 cal. yr. B.P., after which it fell to its current level (Kench et al., 2009b). In contrast, in the Caribbean, rapid sea level rise (~5.2 mm yr^{-1}) occurred between 10,600 and 7,700 yr. B.P.. Sea levels have subsequently risen steadily throughout the Holocene at c. 1.47 mm yr^{-1} between 7,700 and 2,000 yr. B.P., and subsequently ~0.93 mm yr^{-1} until modern sea levels were attained *c*. 380 yr. B.P. with no highstand (Toscano and Macintyre, 2003).

The Pacific and Caribbean regions are evidently the two end-members in terms of variable sea level histories, which is reflected in associated morphological differences in their reef systems. Pacific systems are commonly characterised by broad expansive reef flats that developed as contemporary sea levels were attained *c*. 6,500 yr. B.P.. Conversely, Caribbean reef flats are somewhat restricted and reef crests are typically narrow reflecting the fact that modern sea levels were only reached relatively recently meaning reefs have had less time to sustain modes of catch-up reef growth (Neumann and Macintyre, 1985). In turn, there are associated implications for the development of the substrates underlying reef islands. Reef flats or infilled lagoons are required to be at least near-emergent (and hence sea level constrained) to allow for subaerial accumulation of sediment. Sea level histories and local reef growth are thus key to the timing of Holocene reef island formation (Perry et al., 2011). Indeed, the development of reef islands in the Pacific has led to the suggestion that the mid-Holocene sea level highstand and subsequent gradual fall in sea level are necessary precursors to reef island formation (e.g. Schofield, 1977; Dickinson, 1999). Such studies implicate sea level as the primary control upon reef island morphology (Kench et al., 2009a), which suggests reef islands may be rendered especially vulnerable to projections of future sea-level rise. However, the Caribbean region did not experience a mid-Holocene sea level highstand (Toscano and Macintyre, 2003) and there is evidence that Maldivian islands formed as sea level was in the final stages of rise (Kench et al., 2005). Hence, the presence and development of both Caribbean and Maldivian reef islands offer support for the notion that this is not an inherent prerequisite for island initiation (Perry et al., 2011).

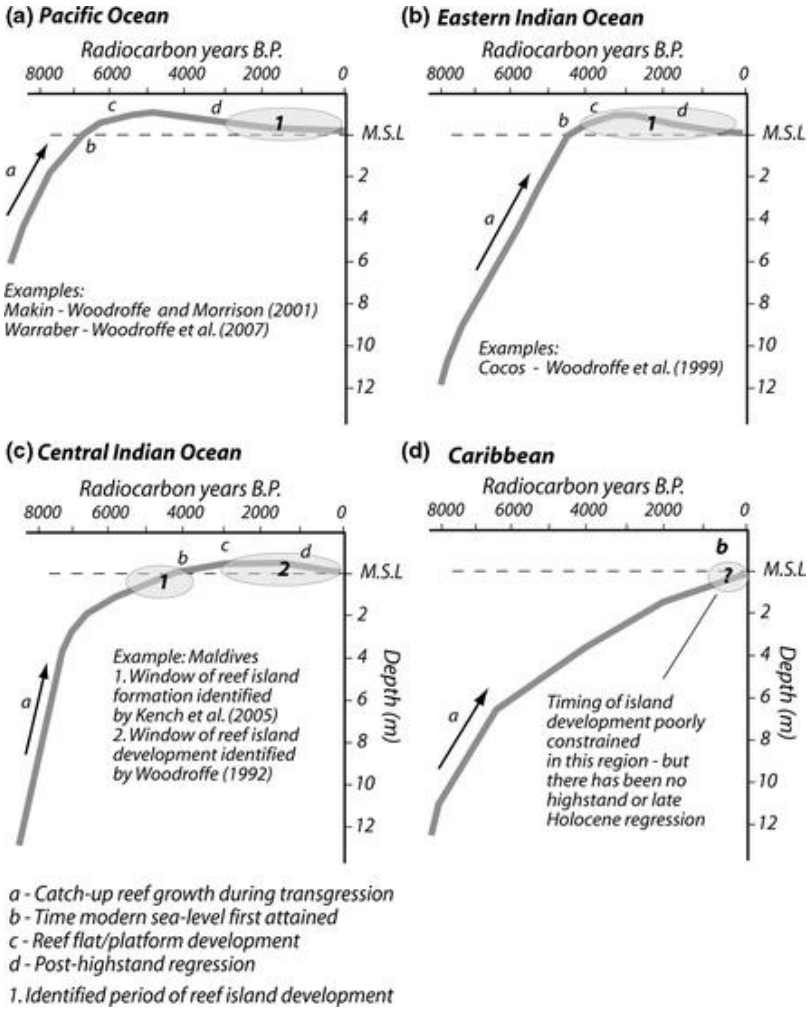

Figure 1.3 – Interpreted regional sea-level histories and timings of reef island development (from Perry et al., 2011).

1.2.2.2 Sediment Dynamics

In addition to the critical interactions between reef growth and sea level, which control the development of the foundations for reef island formation, sediment dynamics represent a further key control upon reef island systems and their development. In turn, studies of reefal sedimentology can provide key insights into the controls on reef systems. This is because sedimentary facies characteristics are an expression of the key biological and physical processes that control coral reef systems (Kench, 2011a; Hamylton et al., 2016). Indeed, a central tenet of coastal geomorphology is the intrinsic inter-relationship between process and form (Cowell and Thom, 1994). Coastal morphodynamics are therefore the product of the mutual process-form co-adjustment. This paradigm permeates much of coral reef research whereby the characteristics of reef systems and sedimentology have been examined in order to infer the controls

upon them (e.g. Done, 1983; Glynn, 1990; Blanchon et al., 1997; Kench and McLean, 1996; Hamylton et al., 2016).

Understanding reef sedimentology is also critical for assessing reef island vulnerabilities and future trajectories. This is because, in atoll settings, islands are formed entirely of biogenic sediment produced by organisms in the adjacent marine environments. Reef island development necessitates transport and subsequent deposition of this material at focal points. It is often assumed that reefs yield a quasi-continuous supply of sediment to reef islands. However, shifts in either sediment transport or production, for instance due to shifts in the process regime or ecology, can cause reef island sediment supply to be 'turned-on' or 'turned-off' regulating episodes of reef island construction (Hart and Kench, 2007; Perry et al., 2011). The production, transport and storage of reefal sediments are thus fundamental requirements for reef island formation, maintenance and ongoing morphological stability (Cowell and Kench, 2001). The key pathways of sediment production and transport are discussed as additional prerequisites for reef island formation.

Sediment Production

As reef islands are entirely composed of biogenically generated sediment derived from the adjacent carbonate producing reef communities, there are inherent linkages between reef ecology and sediment production. Reef islands are typically composed of the following dominant sediment constituents: coral, foraminifera, molluscs, *Halimeda* and coralline algae. These derive from two predominant sediment production pathways: (1) *indirect production* due to physical erosion and bioerosion of the reef framework; and (2) *direct production* via post-mortem deposition of the skeletal remains of infaunal and epifaunal calcareous taxa (Perry et al., 2011). Sediment properties are largely inherited from their parent material (Kench, 2011a; Maiklem, 1968). The parent material is also a primary control upon sediment breakdown and, in turn, the properties of degraded sediment. Consequently, reef sediments may possess bimodal grain-size distributions as described by the Sorby principle (Sorby, 1879; Folk and Robles, 1964; Figure 1.4). Sediment breakdown is of great significance to reef islands as not all grades of material, particularly fine-graded sediment, are thought to be suitable for reef island building (e.g. Morgan and Kench, 2016a).

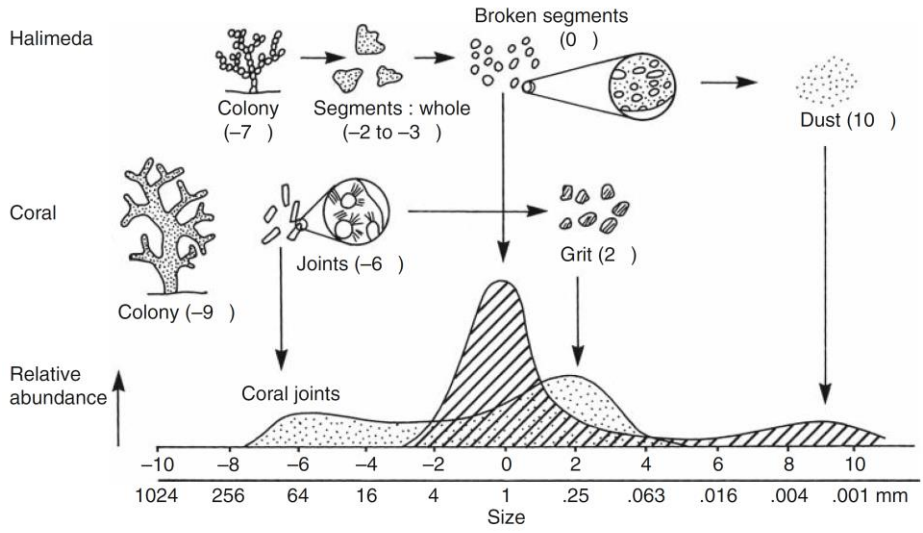

Figure 1.4 – Examples of breakdown pathways and associated grain size distributions for *Halimeda* and coral (from Scoffin, 1992). Hence, a bimodality is evident where breakdown occurs in a step-like manner.

As the building blocks of reef island development, each of the dominant sediment constituents that may contribute to island formation will be discussed in turn:

Coral

Coral skeletal carbonate is released into the reef and/or reef flat sediment reservoir via either the processes of physical or biological erosion. Physical erosion occurs episodically as a result of storms, cyclones and tsunami, and is a function of the hydrodynamic energy exceeding the strength of the coral (Madin, 2005). Sensitivity to physical erosion is a function of growth form as massive corals typically have a higher resistance than branched, tabulate and arborescent forms (Done, 1992; Madin and Connolly, 2006; Kench, 2011a). Large pulses of sediment are therefore often associated with the breakdown of branched species into coral sticks (Scoffin, 1993). Such pulses can attain significant volumes, for instance 1.4 x 10^6 m^3 of sediment was estimated to have been deposited on the reef flat off Funafuti, Tuvalu following cyclone Bebe in 1972 (Maragos et al., 1973; Kench, 2011a). This sediment was in the form of coral rubble, which is often rapidly deposited onto shorelines or reef flats. Coral may also break down, initially into joints of *c*. 64 mm, which in turn may be physically degraded to produce fine grit of *c*. 250 µm (Scoffin, 1987; Figure 1.4). While rubble-sized material may be generated relatively rapidly by low-frequency high-magnitude

events (i.e. at event temporal scales), coral abrasion is likely to be a more gradual process given its high durability (Ford and Kench, 2012)

Primary coral framework may also be broken down and released as sediment through biological erosion, i.e. *bioerosion*. Bioerosion is facilitated by various species of fish, echinoids, and endolithic forms of sponges, worms and bivalves (Spencer, 1992). Both parrotfish and surgeonfish have calcified mouthparts, while echinoids have calcified feeding apparatus. They are therefore able to remove coral during feeding and subsequently excrete finer, predominantly sand-grade coral fragments (Perry et al., 2011; Perry, 2012). Indeed, Morgan and Kench (2016a) examined the properties of sediment produced by parrotfish on Vabbinfaru reef platform, Maldives and found sediment grain size to be predominantly (94%) between 0 and 2 ϕ (i.e. sand-grade). Prior parrotfish studies, have found rates of sediment production to be as high as ~44.6 kg m^{-2} yr^{-1} in back reef environments on the Great Barrier Reef (Hoey and Bellwood, 2008).

Diadema (a genus of sea urchins) faecal pellets may also comprise coral fragments (Scoffin, 1987). Endolithic organisms may also degrade the reef framework through boring. Macroborers, including groups of sponges, worms and bivalves, create holes of >1 mm diameter within dead coral skeletons through using physical and/or chemical processes. Microborers, such as types of fungi, chlorophytes and cyanobacteria, excavate the reef framework on a microscopic scale (Perry, 1998). Sediment produced by boring is released predominantly by sponges, while the majority of borers either dissolve the substrate or produce a carbonate paste that lines boreholes (Perry, 2012). In terms of size fractions, evidence suggests *Cliona* sponge boring produces coral chips of < 63 μm (Scoffin, 1987).

Physical erosion (associated with low-frequency high-magnitude events), and erosion by parrotfish are likely to represent significant sources of rubble- and sand-sized sediment (respectively) for potential reef island building. In contrast, it is thought that sediment produced by boring is of too fine a grade to be of importance to reef island building. Indeed, in Tarawa, Kiribati, Schofield (1977) demonstrated that coral rubble is a major island constituent (i.e. largest percentage of reef island constituents – Yamano et al., 2005). In contrast, examples of coral sand-dominated islands include islands in the Maldives (Woodroffe, 1992) and Mamanuca Island, Fiji (mean 28.7-

48.3% - McKoy et al., 2010). Parrotfish have previously been highlighted as the most likely source of sand-sized coral within Maldivian interior reef island sediments (Perry et al., 2015; Morgan and Kench, 2016a).

Foraminifera

Foraminifera are single-celled protists that typically secrete a shell (test), which may possess one or more chambers. Benthic foraminifera are particularly abundant in lagoonal reef environments. They may live epifaunally, epiphytically, infaunally, or attached to a substrate. Some varieties may attach to seagrass or encrust rocky surfaces, but the majority reside on the loose sea bed (Scoffin, 1987). Living foraminifera form a key component in reef carbonate budgets as they produce $CaCO_3$ with growth and they may be incorporated into the reef framework upon death. Yamano et al. (2000) calculated $CaCO_3$ production by foraminifera on Green Island Reef, Australia, to be between 210 and 480 g m^{-2} yr^{-1}. Alternatively, the skeletal remains of foraminifera may be directly incorporated into the sediment reservoir upon death and thus they also represent a key component of reef sediment budgets (e.g. Harney and Fletcher, 2003). Controls on rates of sediment production therefore include species life cycle, turnover and abundance (Kench, 2011a). For instance, in Kailua Bay, Hawaii, rates of sediment production by benthic foraminifera have been estimated as 0.01-0.14 kg m^{-2} yr^{-1} (Harney and Fletcher, 2003). Sediment size distributions are species dependent, for instance, genera *Peneroplis* and *Quinqueloculina* disarticulate into ~0.5-2 mm discoidal and <~0.5 mm spindle shaped tests respectively (Perry et al., 2011).

Foraminifera have been widely identified as a major sedimentary constituent in reef islands across the Pacific, including at Kapingamara (McKee et al., 1959); Eniwetok, Rongelap and Rongerik in the Marshall Islands (Emery et al., 1954; Todd, 1960); Makin (Woodroffe and Morrison, 2001) and Butaritari (Schofield, 1977) in Kiribati; and Green (Yamano et al., 2000) and Raine (43% - Dawson and Smithers, 2010) Islands on the Great Barrier Reef. Foraminifera were also found to be a major island constituent in the Indian Ocean on Cocos Keeling (Woodroffe et al., 1999).

Molluscs

Molluscs represent the largest marine phylum and the most diverse group of coral reef organisms (Paulay, 1997). The most common groups are gastropods (e.g. snails, chitons), bivalves (e.g. clams, mussels, scallops) and cephalopods (squid, cuttlefish, octopus). As with foraminifera, their skeletal remains are directly incorporated into the sediment reservoir upon death. Sediment size distributions are dependent upon species and life phase, though often gravel-sized material may be >10 mm.

Although molluscs have not been documented as major reef island constituents, they have been identified as minor constituents on islands in both the Pacific and Caribbean (Yamano et al., 2005). For instance, in the Pacific, they have been found on Kapingamara (McKee et al., 1959), Rongelap, in the Marshall Islands (Emery et al., 1954; Todd, 1960), Warraber Island in the Torres Strait (Woodroffe et al., 2007), Butaritari in Kiribati (Schofield, 1977), and Green (Yamano et al., 2000) and Raine (25% - Dawson and Smithers, 2010) Islands on the Great Barrier Reef.

Halimeda

Halimeda is a genus of macroalgae consisting of disjointed calcified segments composed of fused aragonite needles. In reef environments, it is often abundant where herbivorous fish exert high grazing pressure (Drew, 2011). Segments have a characteristic lobed, cylindrical or disc-shaped morphology, and an external surface covered with minute pits (utricles). *Halimeda* thalli grow by producing new segments that develop from tufts of medullary filaments which become organised into a soft uncalcified segment overnight. By the following morning, the segment will typically have begun to calcify. The degree of calcification is a function of species, segment age (older, lower segments are more calcified that those at the growing tip), levels of irradiance and water depth (Drew, 2011). Upon death, segments separate from each other to contribute to the sediment reservoir (Scoffin, 1987). *Halimeda* will first break into flakes of 2-8 mm diameter (depending on the species), and subsequently, with abrasion, disarticulate into smaller segments and, eventually, into micron-sized aragonite crystallites of *c*. 0.001 mm (Folk and Robles, 1964; Figure 1.4).

Halimeda has been noted as a minor reef island constituent on South Maalhosmadulu atoll, Maldives, but its importance has been highlighted in its contribution to the early stages of faro infilling and thus the foundations for interior reef island development

(Kench et al., 2005). In the Pacific, *Halimeda* was found as a major constituent on Mamanuca Island, Fiji (McKoy et al., 2010), and as a minor constituent on Funafuti (24% - Collen and Garton, 2004) and Suwarrow, Cook Islands (Tudhope et al., 1985). Most typically, *Halimeda* is particularly prevalent in the Caribbean and has been noted as the major constituent on Alacran Reef (Folk and Robles, 1964), Turneffe Island, Lighthouse Reef and Glover's Reef (Stoddart, 1962b).

Coralline Algae

A wide range of calcifying algae have been identified as sediment contributors, including *Amphiroa* spp., *Penicillus* spp. and *Rhipocephalus* spp. (e.g. Neumann and Land, 1975). Approximately 10% of species are calcified and secrete calcium carbonate in the forms of either aragonite or calcite. This precipitation occurs either at the cell surface during CO_2 extraction from water during photosynthesis, or intracellularly by metabolic processes (Scoffin, 1987). Coralline algae may be divided by morphological form into species that are geniculate (articulate) or non-geniculate (non-articulated). Geniculate species are those with branching morphologies, attached to the substrate by crustose or calcified root-like holdfasts. Conversely, non-geniculate corallines are encrusting species that may grow on rock, coral, other algae, seagrasses or shells (Johansen, 1969). Non-geniculate corallines are realised as sediment via bioerosion, while geniculate species disarticulate. Disarticulation may produce mud-grade (<63 μm) carbonate, while bioerosion may be associated with more sand-sized grades of material. Crustose coralline algae (CCA) has been found as a minor reef island constituent in the Caribbean (Hogsty Reef – Milliman, 1967), Pacific (e.g. Funafuti, 23% – Collen and Garton, 2004) and Indian Ocean (e.g. South Maalhosmadulu atoll, Maldives – Kench et al., 2005).

Relationship between reef ecology and sediment production

As detailed above, sediment is produced by organisms in carbonate-producing reef communities. There is thus an inherent relationship between reef ecology, sediment production and sediment storage. Spatial variability in sediment assemblages (texture and composition) are therefore, in part, a function of reef ecology. At the global scale, *Halimeda* represents the dominant sand-grade island sediment constituent in the Caribbean, while benthic foraminifera are of greater significance in the Pacific. More specifically, *Baculogypsina* and *Calcarina* are dominant in the western Pacific, while

Amphistegina is common throughout the Pacific (Murray, 1991; Langer and Hottinger, 1999; Yamano, 2005). Global variability is likely a result of different sea level histories, which have produced shallow reef crests and lagoons in the Caribbean favouring *Halimeda* production; whilst the wide, tidally emergent reef flats in the Indo-Pacific favour benthic foraminifera production (Kench et al., 2009a). At the local scale, variability in the importance of sediment constituents has also been noted, for instance, at Warraber Island (Torres Strait) gastropods represented a key long-term constituent and were sourced from sites proximal to the island, while coral and foraminifera were sourced from sites further from the reef island (Woodroffe et al., 2007).

Temporal variability in sedimentology may be attributed to shifts in sediment production with ecological changes, such as shifts in reef species composition and abundance, or changes in the rates at which ecological processes act (Perry et al., 2011). Shifts in reef growth are typically marked by transitions in the relative dominance of sediment constituents (Kench, 2011a). For instance, in south-western Japan, corals and coralline algae were found to be the major sediment constituent when vertical reef growth was dominant. However, reef flat formation was marked by a significant increase in the relative abundance of benthic foraminifera (Yamano et al., 2001). Similarly, Kench et al. (2005) found that reef island development on Maldivian faros is initially associated with the accumulation of *Halimeda* dominated sediments. However, an increased proportion of coral and coralline algae sediments has been noted with subsequent reef flat development (Kench et al., 2005).

Comparative analyses of sediment stored within islands and the adjacent marine environments can aid understanding of the degree of coupling with the contemporary process regime. Where the sedimentary characteristics of an island and its surrounding sediment production zones are dissimilar, it is likely uncoupled from the contemporary process regime. In contrast, comparable reef island and reef platform sedimentary characteristics are indicative of an actively accreting island (McKoy et al., 2010). Strong reef flat-reef island connectivity has been inferred in the Mamanuca Islands, Fiji (McKoy et al., 2010), Kiribati (Woodroffe and Morrison, 20010), the Marshall Islands (Fujita et al., 2009), the Maldives (Morgan and Kench, 2016b), and Tuvalu (Collen and Garton, 2004). However, disparities between constituents in a reef island and on the surrounding sediment production zones may exist due to factors

including variations in framework accommodation space (e.g. Hart and Kench, 2007), and in the transportability of the material (e.g. Hart, 2009). There is also a common view that reef islands are disproportionately dependent upon a limited number of sediment producer groups (Kench, 2011a; Perry et al., 2015; Morgan and Kench, 2016a). Although this perspective is founded upon a paucity of work (e.g. Yamano et al., 2000; McKoy et al., 2010), it would suggest that shifts in sediment supply may be of fundamental importance to reef island geomorphic resilience. A better understanding of island composition and surrounding sediment production is key to improve the reconciliation of reef island futures.

Future sea level change will also likely be associated with shifts in reef ecology and, in turn, key sediment constituents as a function of changing species abundance and sediment producing processes. Such changes may become critical for island stability depending on reef island make-up (i.e. sediment composition and texture). Islands dominated by a single sediment constituent may be rendered most vulnerable to future change (Perry et al., 2011). Indeed, modelling studies have suggested such sedimentological adjustments may be of greater significance to reef islands than sea level rise *per se*. Kench and Cowell (2003) found a reduction in sediment supply on the reef flat resulted in a two-fold increase in the rate of reef island shoreline change with 0.5 and 0.9 m increases in sea level. Hence, focusing perceptions of reef island vulnerability solely upon sea level is an oversimplification of the complex interactions between a range of factors including accommodation space, wave energy and sediment supply, in addition to changes in sea level (Kench et al., 2009a).

Sediment Transport

Following sediment production, reef island formation and maintenance necessitate sediment transport to nodal points of accumulation (e.g. Stoddart and Steers, 1977). Wave-driven hydrodynamic processes on reef platform surfaces are thus a primary control upon island location, evolution and contemporary stability (Samosorn and Woodroffe, 2008; Mandlier and Kench, 2012). Reef islands represent one of several possible sediment destinations, including reincorporation into the reef framework (Perry and Hepburn, 2008); storage on reef platform surfaces (e.g. Hamylton et al., 2016); atoll lagoonal infilling (e.g. Purdy and Gischler, 2005); or contributions to other sedimentary landforms, such as sand aprons (Kench, 2011a). Hence, any shifts in

sediment flux may alter reef island sediment supply and also the geomorphology of broader reef island platform systems.

Hydrodynamic processes are the primary physical control upon sediment transport. Currents in reef environments are the product of tides, winds and breaking waves at the reef edge (Yamano, 2005). Spatio-temporal gradients are associated with the entrainment and transport of sediment (Kench, 2011a) as greater wave energies can move across reef flats with increasing water depths (Brander et al., 2004). Kench and Brander (2006a) quantify the temporal window within which sediment entrainment may occur on reefs in the 'reef energy window index', which is a function of depth, reef width and incident wave conditions. Hence, shorter periods of sediment transport are associated with shallow water depths over wide reefs (Kench, 2011a). Similarly, Mandlier and Kench (2012) showed the propagation behaviour of incident waves to be a function of water depths and reef platform shape. In turn, reef island formation and morphology are impacted by hydrodynamic processes. For instance, Gourlay (1988) suggested reef platform shape, size and orientation determine wave diffraction and thus coral cay stability.

While hydrodynamic processes mobilise sediment, transport potential is a product of sediment properties, including grain shape, grade (size) and density. Analyses of clastic sediments employ grain size as the primary control on entrainment, but such approaches are of limited value in reef environments (Scoffin, 1992) as reefal deposits are more complex. Grain size is also a poor indicator of settling velocity due to the heterogeneous microarchitectures of reef sediment constituents (Maiklem, 1968; Braithwaite, 1973). Particles of comparable size may settle at markedly different rates rendering calculations of sediment transport somewhat problematic (Kench and McLean, 1996). Indeed, determining true 'particle size' is difficult as there is great variation in grain shape. Furthermore, unlike in terrigenous environments, size is a poor indicator of weight. For instance, gastropods possess internal chambers, and both *Halimeda* and coral have networks of internal canals, which lower grain densities (Folk and Robles, 1964). Each form is therefore associated with a different settling style, for instance, straight falling, spiralling, spinning or erratic tumbling (Braitwaite, 1973; Allen, 1984), and a characteristic settling threshold (Maiklem, 1968; Scoffin, 1992; Kench and McLean, 1996).

1.2.3 Models of reef island development

Previous studies have informed understanding of the controls upon reef island building: sea level-reef island interactions, sediment production and transport, and reef ecology. The processes and the sediments involved inherently change as islands develop and, consequently, different models of reef island development have been postulated, which are underpinned by regional-scale differences in sea-level histories (Figure 1.3). Of these, the two most widely referred to are (1) the post-highstand sea level fall model, and (2) the lagoon infill model. The former is based on studies of Pacific reef islands and suggests that islands formed at the end of, or post, the mid-Holocene regional sea-level highstand. This is regarded as the traditional model of reef island development (Yamano et al., 2005) and comprises a series of sequential stages. As Pacific sea levels have been at or slightly higher than contemporary sea levels for the past 6,000 years, reefs completed vertical growth and became constrained by the stable, or slightly falling, sea levels. As a result, lateral reef growth became dominant producing broad reef flats, which provide a substrate for island building as sea level subsequently fell to present levels in the late Holocene (McLean and Woodroffe, 1994; Kench et al., 2009b). Examples of islands built in this period include the Mamanuca Islands, Fiji (McKoy et al., 2010), Tuvalu (McLean and Hosking, 1991), Kiribati (Woodroffe and Morrison, 2001), Cocos Keeling (western Indian Ocean, Woodroffe et al., 1999), and Warraber, Yam and Hammond Islands, Torres Strait (Woodroffe et al., 2000).

An alternative, lagoon infill, model has been proposed based on studies of interior islands within South Maalhosmadulu Atoll, northern-central Maldives (Indian Ocean; Kench et al., 2005), a region with a different sea level history. This model differs from the post-highstand sea-level fall model as the underlying substrate for reef islands was unconsolidated lagoon infilling sediments, rather than emergent reef platforms. Reef island development likely occurred when reefs were 2.5-1 m below contemporary sea level. Vertical reef growth was found to dominate during the mid-Holocene (prior to 6,000 yr. B.P.). Between 5,500 and 4,000 yr. B.P., sedimentation on the central reef platform constrained reef growth. The period 5,200 to 4000 yr. B.P. was marked by rapid lateral island building. Since 4000 yr. B.P., islands have essentially become relict with minimal modification, except seasonal shifts in beach position and stabalisation of the island core through internal and peripheral lithification of island sediments

(Kench et al., 2005). Perry et al. (2013) provided further evidence for this model through chronostratigraphic data from a series of partially to fully filled faro from South Maalhosmadulu Atoll, Maldives, and found size thresholds to exist in reef island development. A relationship was found between faro size, evolutionary state and island development.

Kench et al. (2009a) suggest the Maldivian model may have similarities with Caribbean reef island development as reef islands have developed during the late Holocene with continual rising sea level (Toscano and Macintyre, 2003). Hence, Maldivian and Caribbean reef islands highlight the fact that there is no single model of reef island development and initiation. Rather, island formation has evidently occurred both under rising and falling sea levels and over different underlying substrate types. By using the past as an analogue for the future, such research into the timing of reef island development with respect to past environmental change, is key to improving projections of reef island trajectories under conditions of future environmental change.

1.2.4 Conceptual models of reef island morphodynamics

Following reef island initiation, multiple styles of island evolution have been inferred. Indeed, Woodroffe et al. (1999) identified 27 chrono-sequences (Figure 1.5). The *central core* scenario occurs where island deposition commenced at the centre and has since accreted on both the oceanward and lagoonward shores. The *oceanward accretion* model describes sediment addition primarily to the oceanward shore, whereas *lagoonward accretion* refers to sediment addition largely on the lagoonward shore. Rather than lateral accretion, an alternative to the preceding scenarios may occur where the dominant mode of accretion is *vertical*. The *rollover* model represents the erosion of the oceanward shore and the subsequent deposition of the material on the lagoonward shore. *Overwash* is a similar process to rollover, except the sediment transported lagoonward is typically new, rather than eroded material. Each of these six models may occur in association with patterns of either *episodic*, *decelerating*, *accelerating* or *regular* accretion, hence describing 24 reef island chrono-sequences. Further alternatives are the island was deposited in a *single episode* or represents the *erosional remnant* of a once larger island. The final model describes situations in which the *longshore* transport of sediment is dominant, meaning island age varies along the shoreline. Woodroffe et al.'s (1999) models have been investigated through

radiocarbon dating of island sediments. However, such studies are limited due to difficulties (both practical and financial) in developing and interpreting temporally constrained accretionary histories. Gradual oceanward accretion was inferred on West Island, Cocos Keeling (Woodroffe et al., 1999) and on Makin, Kiribati (Woodroffe and Morrison, 2001). Accretion from a central core was suggested on Majuro Atoll, Marshall Islands (Kayanne et al., 2011) and on Bewick Island, Great Barrier Reef (Kench et al., 2012). However, the majority of islands likely develop through a combination of several evolution scenarios. For instance, both horizontal and vertical accretion in both lagoonward and oceanward directions were found in the Mamanuca Islands, Fiji (McKoy et al., 2010).

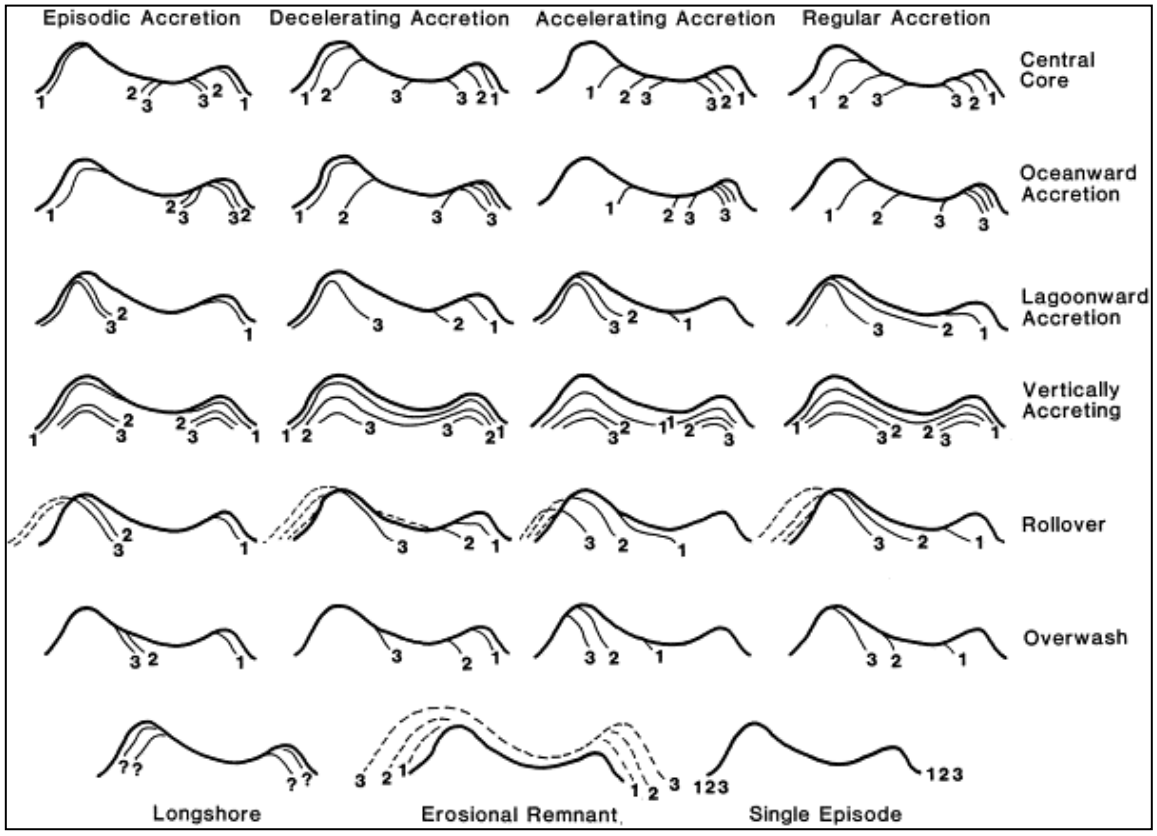

Figure 1.5 – Reef island evolution models indicated by isochrons of deposition (in Woodroffe et al., 1999).

1.2.5 Reef island dynamics: from decadal to event temporal scales

Superimposed upon variable styles of overall island evolution, are shorter term episodic shifts in sediment production and transport that may cause island reworking. At decadal temporal scales, in a change detection analysis of 27 atoll islands in the Central Pacific, Webb and Kench (2010) found that over the preceding 20 to 60 years

86% of the islands remained stable or expanded in area despite rising sea levels. 12 of the islands increased in area by more than 3%, 6 of which increased by more than 10%. Moreover, such net change values were found to mask larger gross changes in island planform with lagoonward migration found in 65% of cases. For instance, on Fualifeke in Funafutinet, southern migration of the eastern part of the island indicated over 30% of island materials were reworked over 19 years (Webb and Kench, 2010). There is an increasing body of decadal-scale GIS analyses of reef island shoreline change, which is emphasising their mobile and dynamic nature (e.g. Ford, 2011; Yates et al., 2013; Mann and Westphal, 2014; Ford and Kench, 2015).

Drivers of decadal scale change may include shifts in oceanographic conditions that can result in changes in wave energy and direction. For instance, the Pacific Decadal Oscillation (PDO) has been related to longshore transport of sediment on Kihei, Maui causing shoreline movements of ±100 m (Rooney and Fletcher, 2005). Similarly, the El Niño-Southern Oscillation (ENSO) has been found to impact upon both carbonate budgets (e.g. Panama, Eakin, 1996) and patterns of shoreline erosion and accretion (e.g. Kiribati, Solomon and Forbes, 1999).

Reef island dynamism has also been highlighted as seasonal temporal scales. For instance, Kench and Brander (2006a) found cyclic shifts in beach position on Baa Atoll, Maldives, associated with monsoonally-forced changes in wind and wave processes. On 13 islands, 20,000 m^3 of sediment movement was found, though net annual change to island area was minimal. A key control on the magnitude of change was the shape of the reef platform, and hence wave refraction processes, with the greatest changes associated with circular reefs.

Low-frequency high-magnitude events, such as storms, tsunami (e.g. Kench et al., 2006), and earthquakes (e.g. Aronson et al., 2012), can have a significant impact upon reef islands. In particular, storms can have profound erosional and depositional effects. For instance, in 1972 Cyclone Bebe resulted in the deposition of an estimated 1.4×10^6 m^3 of rubble in Tuvalu producing a 10% increase in land area (Maragos et al., 1973). In contrast, Stoddart (1962a) documented the disappearance of reef islands following Hurricane Hattie in Belize in 1961. Accretion may occur as storms rip sediment from the reef front and deliver it to an existing reef island (Woodroffe, 2002). Hence, reef island response to storm events is a function of the texture of island

sediment and storm frequency (Bayliss-Smith, 1988; McLean, 2011). Thresholds have been suggested to exist in storm recovery where wind speeds exceed 200 km hr^{-1} as reef systems are likely to take *c*. 50 years to recover. In comparison, where wind speeds are 120-150 km hr^{-1} a reef may entirely recover within a decade (Stoddart, 1985; Scoffin, 1993; Woodroffe, 2002).

1.3 Research Rationale

Despite their high ecological and socioeconomic significance, our knowledge of reef island systems and their likely resilience to future environmental change is limited. Across the entire body of reef island literature, several data and knowledge gaps are evident from the preceding literature review. Firstly, despite the integrated nature of reef island systems (e.g. Perry et al., 2011), there is currently no study of a reef island system that integrates reef island chronostratigraphy, with datasets on marine sediment storage, production and transport. Indeed, there is an absence of any standardised integrated approach for investigating reef island vulnerabilities. Hence, this thesis will provide the first such integrated study of a reef island system, and thus propose an approach for understanding the controls upon, and in turn vulnerabilities of, reef island systems.

A second gap in the existing literature is the minimal understanding of atoll-scale variability in reef island systems. Indeed, models of reef island development have primarily focused upon regional scale differences (e.g. Perry et al., 2011), specifically between the Pacific post-highstand sea level fall model (e.g. McLean and Hosking, 1991; Woodroffe et al., 1999; Woodroffe et al., 2000; Woodroffe and Morrison, 2001; McKoy et al., 2010), and the Maldivian lagoon infill model (Kench et al., 2005; Perry et al., 2013). There is minimal understanding of atoll-scale variability in reef island systems, such as at different points around atoll rims, or between rim and interior island settings. For example, does atoll-scale variability exist in terms of the models, modes and timings of reef island development; marine benthic sedimentology (composition and texture); rates of contemporary sediment production; and the potential mobility of marine benthic sediments under the contemporary process regime?

A third knowledge gap is the global paucity of studies directly examining reef island geomorphic futures (notable exceptions are Kench and Cowell, 2001a; 2001b). This

thesis therefore also seeks to advance our limited understanding of aspects of potential future change: (1) the potential for shifts in reef ecology to impact upon rates of sediment production; and (2) the impact that sea-level rise scenarios may have upon benthic sediment mobility.

1.3.1 Study site selection

The Maldives Archipelago was selected as a field setting for this study. This is because the majority of island studies have been focused upon the Pacific region (e.g. McLean and Hosking, 1991; Woodroffe et al., 1999; Woodroffe et al., 2000; Woodroffe and Morrison, 2001; McKoy et al., 2010; Kench et al., 2014; McLean and Kench, 2015). In contrast, far less work has been undertaken within the central Indian Ocean, a region with a very different sea-level history (section 1.2.2.1). This is despite the fact that the Maldives is the most populated of the atoll nation in the world (World Bank, 2013).

There has been a recent (even over the course of this PhD) increase in our knowledge of the Maldives, but this has been limited to interior island settings (i.e. islands formed upon platforms within atoll lagoons, Figure 1.2). Within these settings, detailed datasets have been developed in the northern-central part of the archipelago relating to island development (Kench et al., 2005; Perry et al., 2013), marine benthic sedimentology (Perry et al., 2015; Morgan and Kench, 2016b), and sediment production (Perry et al., 2015; Morgan and Kench, 2016a). In contrast, there is an absence of any detailed datasets from the rim islands of the Maldives. This is likely due to the more challenging working conditions presented by atoll rim environments, which experience markedly higher wave exposure (from oceanward swell), frequently possess conglomerate outcrops (which provide extensive obstacles), and often seem to be more densely vegetated than their leeward counterparts (personal field observation). However, it is the rim, as oppose to interior, islands that are of greater physical and socioeconomic significance: the rim islands dominate spatially (accounting for 82.43% of the land area; Andréfouët et al., 2006), host the majority of the nation's population (88.93%), and thus support a large proportion of the nation's infrastructure (all regional administrative capitals, hospitals, designated 'safe islands' and 57% of resorts are on rim islands). To advance our understanding of these systems, Maldivian rim islands were thus identified as the focus of this thesis.

Specifically, Huvadhu Atoll was selected as the majority of preceding detailed work on Maldivian reef islands has been restricted to the Northern-Central part of the Archipelago (e.g. Kench et al., 2005; Perry et al., 2013; Morgan, 2014; Perry et al., 2015; Morgan and Kench, 2016a, 2016b). Notable exceptions are Stoddart (1966) and Woodroffe (1992). Within Huvadhu Atoll, two study sites were selected in order to improve understanding of local-scale variability in reef island systems. Sites were thus chosen on windward and leeward rim aspects to represent end-members in the contemporary process regime (Chapter 2).

1.4 Aims and Objectives

The primary aim of this thesis is to provide the first study of a reef island system that integrates reef island chronostratigraphy, with datasets on sediment production, transport and storage in the adjacent marine environments. This thesis thus presents an integrated approach for understanding the controls upon, and in turn the future vulnerability of, reef island systems. Such an approach will inherently transcend across a range of cascading temporal scales (millennial, contemporary and towards the future). This is a method that could be replicated in other reef island settings worldwide. To this end, a secondary research aim is to undertake the first detailed investigation of Maldivian rim island evolution, specifically reef island development and reef-to-island connectivity.

To undertake an integrated reef island study and to improve our understanding of Maldivian rim island systems, two contrasting (windward and leeward) environments were selected on the rim of Huvadhu Atoll (Chapter 2). Within these settings, key research objectives were:

i. To establish the topography and accretionary histories (sedimentary structure and chronologies) of reef rim islands.
ii. To determine the contemporary spatial extent, distribution and characteristics of the adjacent marine eco-geomorphic zones.
iii. To quantify the physical properties (texture and composition) of contemporary sediment assemblages and estimate volumes of sediment storage within each of the eco-geomorphic zones.

iv. To generate first-order estimates of contemporary sediment production within each eco-geomorphic zone and, in turn, to investigate the relative importance of the suite of different sediment producing organisms.
v. To investigate the distribution of Maldivian seagrass beds as a means of examining the potential for ecological change to cause shifts in sediment production regimes.
vi. To characterise the contemporary process regime in order to quantify the potential mobility of benthic sediments.
vii. To estimate the impact of future sea-level rise scenarios upon the potential mobility of benthic sediments.

Through fulfilling the above objectives, this thesis seeks to contribute to our understanding of the following six broad research questions in relation to windward and leeward settings on Huvadhu Atoll rim:

Q. 1) What are the key controls upon, and modes of, Maldivian reef rim island development?

Q. 2) To what extent does variability exist in reef island development (geomorphology and chronostratigraphy) at the scale of an individual atoll?

Q. 3) Can a sediment budget be constructed linking sediment production to both island and marine benthic sediment storage?

Q. 4) What is the degree of contemporary reef-to-island connectivity?

Q. 5) What are the implications of research findings for the future of Maldivian reef rim island systems and their management under conditions of environmental change?

Q. 6) Does an integrated methodology provide an effective means of understanding reef rim island systems?

1.5 Thesis Structure

Just as the processes that control reef systems exist at cascading temporal scales (Kench et al., 2009a), in an attempt to characterise these controls, the integrated approach presented in this thesis also transcends a range of temporal scales: from millennial timescales (Chapter 3), to the contemporary (i.e. ecological; Chapters 4 and 5); and, in light of contemporary phenomena, towards the future (Chapters 6 and 7).

Hence, the structure of this thesis is situated the framework provided by the space-time diagram in presented in Figure 1.6. In turn, given the intrinsic linkages that exist in reef island environments across space and time, the components of these environments ought not to be considered in isolation, but rather as one integrated system. In turn, the Chapters of this thesis ought also to be examined in combination as there are intrinsic linkages between them (Figure 1.7).

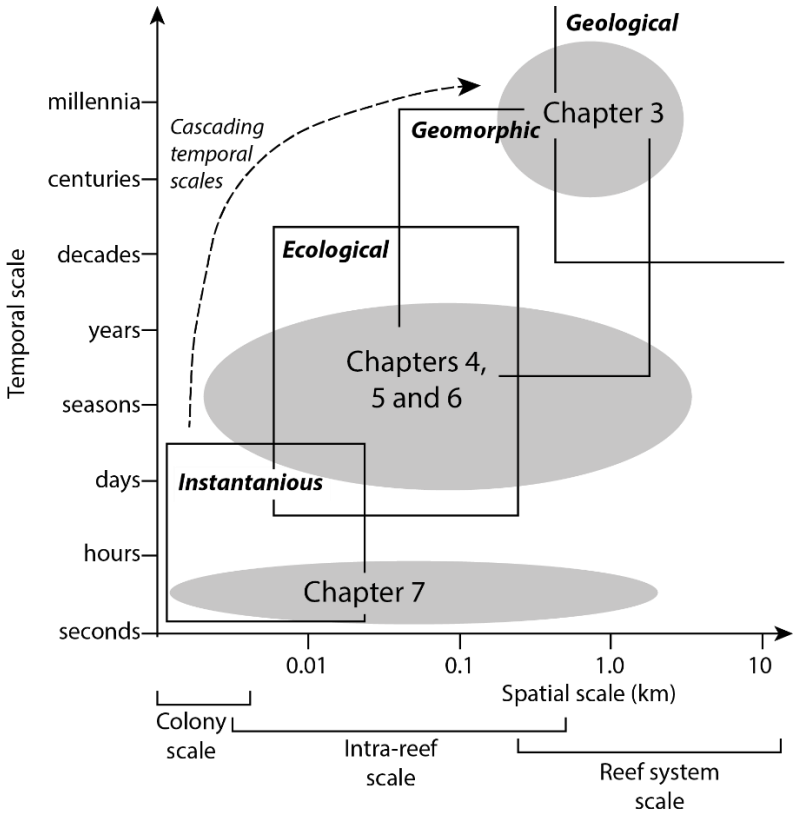

Figure 1.6 – Space-time diagram illustrating the theoretical framework within which this thesis is situated. Adapted from Cowell and Thom (1994) and Perry et al. (2008).

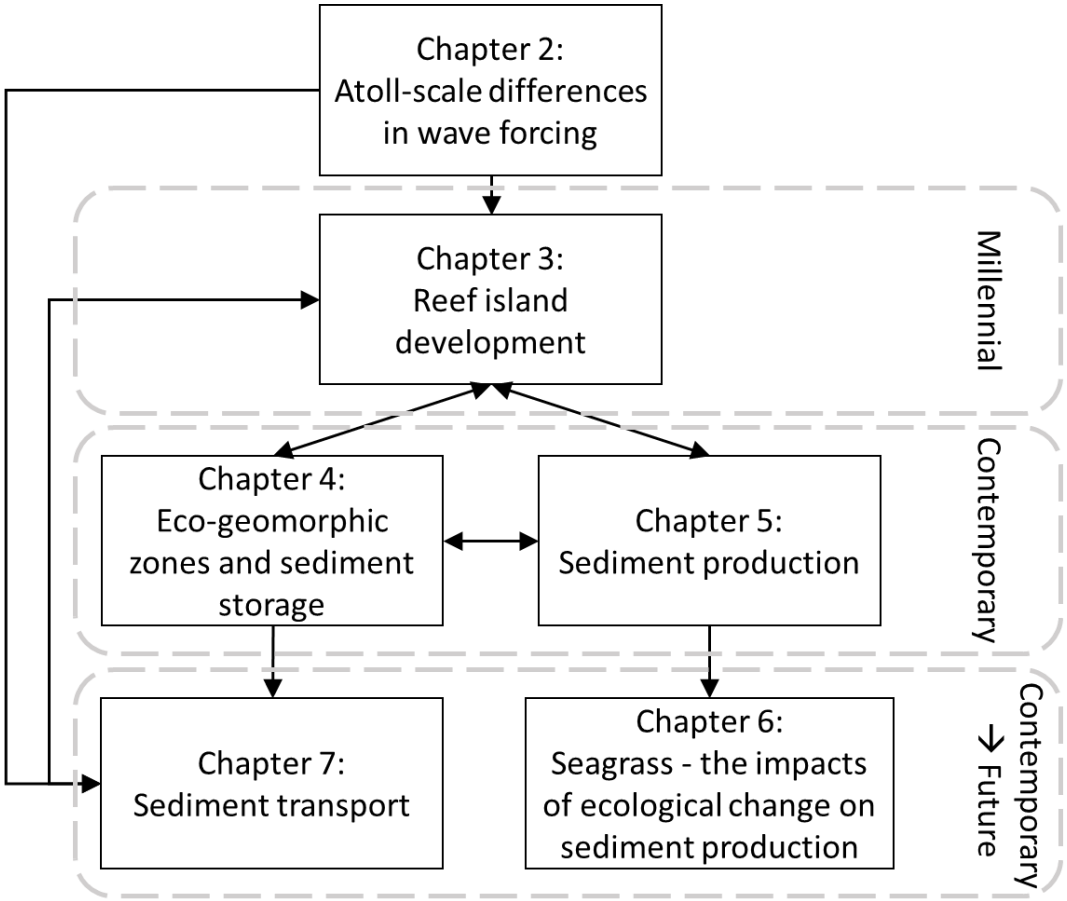

Figure 1.7– Overall thesis structure illustrating key linkages between data Chapters. Dashed grey boxes represent the temporal scale to which each Chapter primarily relates.

Chapter 1 – Introduction

This Chapter seeks to situate this thesis within the broader coral reef system literature. The overall aims and objectives are presented alongside an outline of the thesis structure.

Chapter 2 – Study site and atoll-scale differences in wave forcing

Chapter 2 provides a review of the Maldives Archipelago and outlines the rationale behind study site selection. In particular, the Chapter investigates the contemporary process regime at the oceanward and lagoonward margins of each study site in order to test the assumption that the sites may be termed ‘windward’ and ‘leeward’.

Chapter 3 – Island development

Chapter 3 comprises a series of reef island datasets: planform surveys, topographic cross-sections, sedimentological data (texture, composition and spatial distribution),

AMS radiocarbon dates, and GPR traces. In combination, these data allow elucidation of the likely modes and timings of rim reef island development.

Chapter 4 – Eco-geomorphic zonations and sediment storage

This Chapter quantifies the spatial distribution and benthic characteristics of the marine eco-geomorphic zones. Within each zone, analyses were undertaken of sediment textural and compositional properties. In addition, spatial variability in the depths and volumes of sediment storage were examined. Benthic sedimentary data were discussed alongside that from beach and island samples as a means of investigating the degree of reef-to-island connectivity.

Chapter 5 – Sediment production

Chapter 5 comprises ecological survey data of the suite of sediment producing organisms within each of the eco-geomorphic zones. This data is employed to generate first order estimates of sediment production rates within each zone. The relative importance of each of the sediment producers is then examined. In turn, the relationship between reef ecology, sediment production and sediment storage is discussed.

Chapter 6 - The distribution of Maldivian seagrass meadows and implications for sediment production

Chapter 6 discusses the spatial distribution of Maldivian seagrass beds and evidence for recent shifts in their aerial extent. This provides a means of examining the potential for ecological change to cause shifts in contemporary sediment production regimes.

Chapter 7 – Sediment transport

This Chapter characterises the contemporary process regime and, in turn, quantifies the potential mobility of benthic sediments. The impact of sea-level rise upon sediment potential mobility is also examined. Parallels are drawn between the findings of this Chapter and those from Chapter 3 which discussed the influence of the mid-Holocene sea-level highstand (Kench et al., 2009b) upon reef island development and dynamics.

Chapter 8 – Conclusion

To conclude, key findings are discussed in relation to the broad questions posed within Chapter 1 (section 1.4).

Chapter 2: Study Site and Atoll-Scale Differences in Wave Forcing

2.1 Introduction

This Chapter introduces the study site and, to this end, it comprises several components: (1) an introduction to the Maldives Archipelago, including a review of its geological history and process regime; (2) an introduction to Huvadhu Atoll and the premise behind study site selection therein; and (3) an investigation into the contemporary process regime at the oceanward and lagoonward margins of the study sites.

2.2 The Maldives Archipelago

The Maldives Archipelago comprises a double linear chain of 22 atolls located 700 km southwest of Sri Lanka (Figure 2.1A). The Archipelago forms the central section of the Laccadives-Chagos ridge spanning from Ihavandhippolhu in the north (6°57'N) to Centurion Bank in the south (07°39'S).

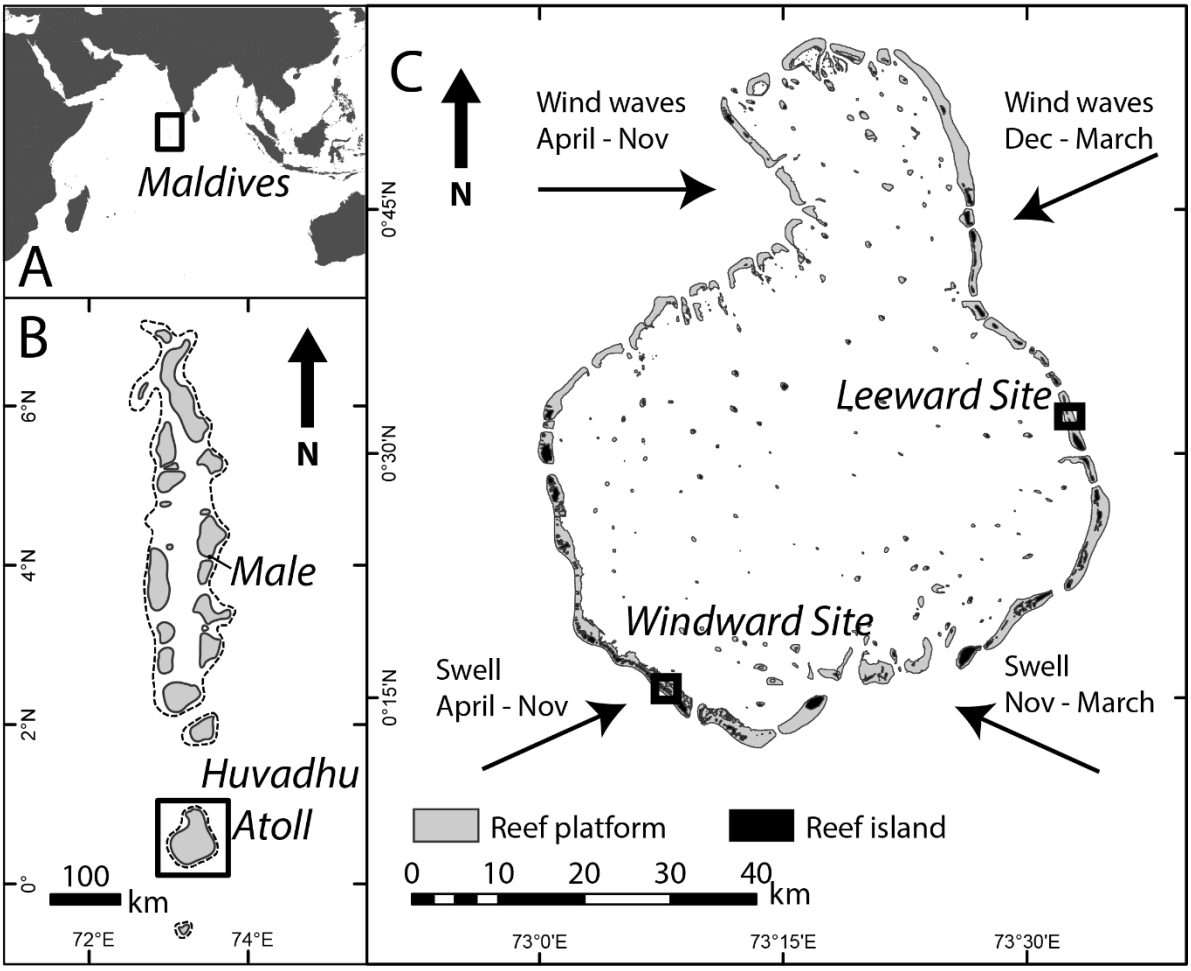

Figure 2.1 - Location of the Maldives within the Indian Ocean (A), of Huvadhu Atoll within the Maldives (B), and of the leeward (i.e. north-eastern) and windward (i.e. south-western) study sites (C). Predominant swell and wind wave directions provided within C.

2.2.1 Geological evolution of the Maldivian Archipelago

The development of the Indian Ocean sea floor commenced with the break-up of Gondwanaland over 160 million years ago. During the late Jurassic, at the time of the magnetic anomaly M25, India, Madagascar and Antarctica broke from the African continent (Parson and Evans, 2005). The Indian sub-continent then broke from Madagascar in the late Cretaceous and then from the Seychelles micro-continent at the end of the Cretaceous (Norton and Sclater, 1979; Courtillot et al., 1988; White and McKenzie, 1989). Nair et al. (2013) suggest that the Laccadive Ridge rifted from India with Madagascar during the Cretaceous, while the Maldivian and Chagossian sections of the ridge are thought to be oceanic in origin (Pushcharovsky, 1996; 2011).

The development of atolls is traditionally described by Darwinian subsidence theory (1842) whereby reefs are classified in a temporal evolutionary sequence: fringing reefs, barrier reefs and atolls. Darwin postulated that transitions between stages occur with the subsidence of volcanic foundations over geological timescales at rates of 0.01-0.1 mm yr^{-1}. The development of the Maldives differs from this conventional theory. Rather, the Maldives Archipelago is underlain by an Eocene volcanic basement with a potassium/argon date of *c*. 55 Myr.. This volcanic ridge is thought to have been a part of the Réunion hotspot trace (Duncan and Hargraves, 1990). Tectonic movements then caused the northerly migration of the basalts to their current position. Indeed, a systematic south-north increase in the ages of basalts recovered along the hotspot track has been found with Réunion being the youngest at 2 Myr, Mauritius at 1-7 Myr, Mascarene Plateau at 31-45 Myr, Chagos at 49 Myr, the Maldives at 55 Myr and the Deccan basalts at 67 Myr (Duncan and Hargraves, 1990).

Accumulation of calcium carbonate during the Tertiary was controlled by periods of progradation and aggradation with fluctuations in sea level (Purdy and Bertram, 1993; Kench, 2011b). During the Quaternary, vertical accretion has been the dominant mode of reef development. This is a result of high amplitude Pliocene-Pleistocene oscillations in sea level which produced alternate periods of exposure and submergence. The Holocene is the most recent period of submergence and thus vertical reef growth above the karstified remnants has ensued to fill the accommodation space (Woodroffe, 1992; Kench, 2012). Drill cores from South Maalhosmadulu and Ari Atolls show Holocene reef growth began with Pleistocene sea level rise *c*. 8,100 yr. B.P.. Between 8,100 and 6,500 yr. B.P., vertical reef growth was at rates of *c*. 7 mm yr^{-1}, before decreasing to 1 mm yr^{-1} (Gischler et al., 2008; Kench et al., 2009b; Kench, 2011b).

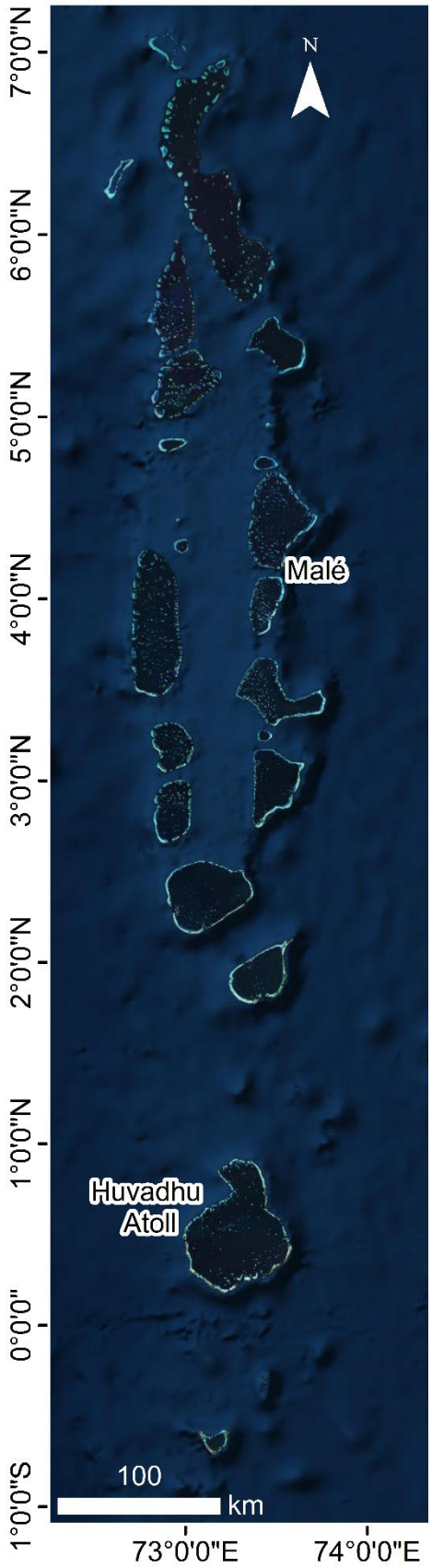

Figure 2.2 – The Maldives Archipelago; imagery from ESRI (2017).

2.2.2 Contemporary Process regime

The contemporary wind and wave climate of the Maldives is strongly influenced by two monsoon periods. Between December and March, the *iruvai* monsoon is associated with winds that are predominantly from the northeast-east (*c*. 45-90°) with a mean speed of 4.9 m s^{-1}. In contrast, the *hulangu* monsoon occurs between April and November with west to northwest winds (*c*. 225-315°) and mean speeds of 5.1 m s^{-1}. Between monsoons there is a period associated with variable wind speeds, for instance in March mean wind speed falls to 3.5 m s^{-1} (Kench and Brander, 2006). Limited information exists concerning the deepwater wave climate (Figure 2.1C). However, global data for the region (Young, 1999) suggests that swell is from the south to southeast between November and March, and from the south-southwest between April and November (Kench, 2012; Figure 2.1C).

For each Maldivian reef platform, incident wave energy is a function of monsoonally-forced wind-waves, boundary oceanic swell, and local sheltering factors (Kench et al., 2006). Such parameters have key implications for reef island geomorphology (e.g. Kench and Brander, 2006b). For example, an east-west gradient in reef island development is evident across South Maalhosmadulu Atoll. On the atoll's western rim, high wave energy transports sediment across the platform and thus island development only occurs on the broadest sections of the reef flat. In contrast, islands occupy most of the available reef platforms on the eastern rim where wave energy is lower (Kench et al., 2006; McLean, 2011).

In terms of event scale dynamics, although erosive impacts of past storm activity have been documented (e.g. Gardiner, 1903; Gibb, 1987), the Maldives are located in close proximity to (i.e. straddling) the equator outside the main storm belt and thus rarely experience severe storms or cyclones (although they do occur rarely). As a result, Maldivian reef islands are thought to be predominantly composed of sand-sized sediment (Woodroffe, 2008). The Archipelago has also been subject to the impacts of tsunami. For instance, the 2004 Sumatran tsunami had erosional and depositional effects on Maldivian reef islands, though the net long-term effect was of island accretion (Kench et al., 2006c).

2.2.3 Characteristics of the Maldives

The Maldives Archipelago is comprised of 16 atolls, 5 oceanic faros (ring-shaped reefs exposed to open ocean), and 4 oceanic platform reefs (reefs without lagoons which are exposed open ocean; Figure 2.2). This incorporates 2,041 individual reef structures (larger than 0.01 km^2) which have a total area of 4,494 km^2, and 1,190 reef islands with a total area of 227.45 km^2 (Naseer and Hatcher, 2004). This ecological and geomorphic diversity forms a key component of the Maldivian economy as reef island tourism provides 60% of foreign exchange earnings, 10% of employment and 20% of gross national product (Buckley and Ralf, 2003).

The atolls of the Maldives are among the largest in the world (Woodroffe, 1992). They may be broadly divided into those that are 'closed' and others which are 'open'. Closed atolls consist of a near continuous rim with limited lagoon-ocean connectivity. Conversely, open atolls represent the majority of Maldivian atolls, which possess a reef rim with multiple dissections and thus high lagoon-ocean connectivity. A further key feature of open atolls is the presence of faros, the annular-shaped reefs within the atoll lagoon. A north-south gradient in atoll morphology exists across the Archipelago with more open atolls of moderate depth (40-50 m) to the north. In contrast, southern atolls are typically more closed, deeper (70-80 m), and host a higher proportion of peripheral reef rim islands. Morphological variability may be attributed to parameters that control reef growth, sediment production and transport, and reef island evolution. Indeed, there are associated oceanographic and climate gradients. In particular, annual rainfall increases from north to south causing the greater solutional deepening of the southern lagoons during Quaternary glacial periods (Purdy and Winterer, 2001). Furthermore, monsoonal oscillations increase in intensity to the north of the Archipelago producing a northerly reduction in wave energy levels, which impacts upon contemporary island evolution (Woodroffe, 1992; Kench, 2011b).

Initial broad scale descriptive work on the ecology and geomorphology of the Archipelago was undertaken by the expeditions of Moresby (1835-1838), Gardiner (1899-1900), Agassiz (1901-1902) and Sewell (1933-1934). Until 2005, subsequent work was relatively sparse, rendering the Maldives one of the least known groups of atolls (Kench, 2011b). There has been a recent increase in the development of datasets obtained from the Archipelago, relating to models of island development

(Kench et al., 2005; Perry et al., 2013), sediment storage (Perry et al., 2015; Morgan and Kench, 2016b), and sediment production (Perry and Morgan, 2017; Perry et al., 2015, 2016; Morgan and Kench, 2016a). However, such detailed datasets have been solely obtained from interior islands (i.e. those formed upon platforms within the atoll lagoon) and thus our knowledge of rim island systems is far more limited.

The Maldives are regarded as one of the most vulnerable countries to the impacts of climate change with the lowest mean elevation (1.5 m above mean sea level, MSL) and the lowest natural highpoint (2.4 m above MSL; Brown, 2005). Superimposed upon this is a population of 345,023 (World Bank, 2013), the largest of any atoll nation. By comparison, the second most populous atoll country is Kiribati with 102,351 inhabitants (World Bank, 2013). The issues are further compounded by the spread of the population across some 199 inhabited islands (van Alphen et al., 2007).

2.3 Huvadhu Atoll

At the atoll-scale, the focus of this thesis is Huvadhu Atoll, which is located south of the Suvadiva Channel, forming the second most southerly Maldivian atoll (Figure 2.1B, 2.3). It is the largest atoll in the Maldives and 10th largest atoll in the world with an area of 3297 km^2, a perimeter of 261.4 km (Nasseer and Hatcher, 2004), and dimensions of 80 km (north-south) by 60 km (east-west). Maximum lagoon depth is 80 m, the connection of which to the open ocean is facilitated by 38 deep inter-rim passages (width = 110 to 3350 m). The ratio of passage with to reef platform lengths, i.e. the aperture, is 0.14 (Naseer, 2003). At a maximum, tidal range is approximately 1.1 m. The atoll has a total land area of 33.2 km^2, which comprises 228 islands (Andréfouët et al., 2006). A recent study of shoreline change in Huvadhu Atoll highlighted the dynamic nature of reef island shorelines, whereby change was found on all 184 of the studied islands over the 40 year period. Islands with predominant erosional responses (45%) typically had a small areal extent (<10 ha), whereas larger islands were dominated by accretion (Aslam and Kench, 2017).

The majority of land area on Huvadhu is attributable to the 180 rim islands (totalling 30.2 km^2 of land area), in contrast to 48 interior platform islands (totalling 3 km^2 of land area; Andréfouët et al., 2006). Huvadhu atoll is divided into two administrative districts, Gaafu Dhaalu and Gaaf Alif, with capitals (Thinadhoo and Vilingili respectively) both sited on rim islands. Of the atoll's 21 inhabited islands, only 1 is an interior platform

atoll with 1,005 inhabitants of the total atoll population of 30,601. Of the atoll's 9 resorts, 6 are sited on rim islands (Godfrey, 2004). Hence, the significance of rim reef islands within Huvadhu is evident both spatially (comprising 90.4% of the land area) and socioeconomically (hosting 96.7% of the atoll's population), as is consistent with the trend across the Maldives (section 1.3).

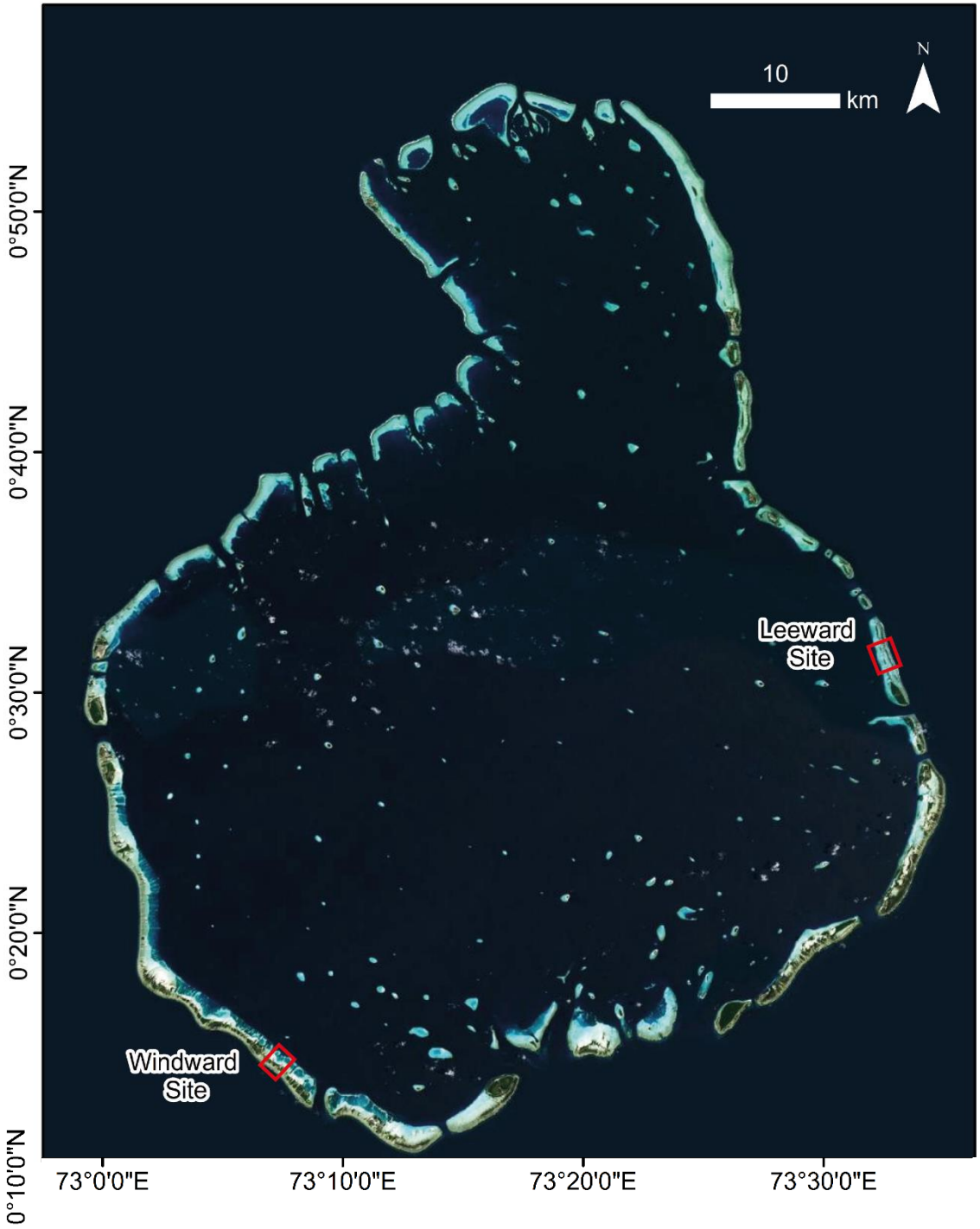

Figure 2.3 – Huvadhu Atoll and the locations of the windward and leeward study sites. Imagery source: ESRI (2017).

Geomorphically, the rim of Huvadhu is demonstrative of the diversity of atoll rim and island morphology. Four rim types can be identified with: (A) no vegetated land area; (B) discontinuous rim with elongate islands whose longest axis runs parallel to the rim; (C) continuous rim with a large proportion of islands whose longest axes is perpendicular to the atoll rim; and (D) relatively discontinuous sections of rim host to more morphologically complex groups of islands with a range of morphologies (Figure 1.2). Type A is generally representative of the northwest of the atoll, B of the northeast, C of the southwest, and D of the southeast. This study will focus upon sites representative of the two end-member rim types that possess vegetated land area: B and C (Figure 2.4). Similar divisions may be drawn throughout the Archipelago and are similarly spatially distributed. Hence, although generalisations ought to be made with caution, it is anticipated that findings will also be of relevance to other Maldivian atolls.

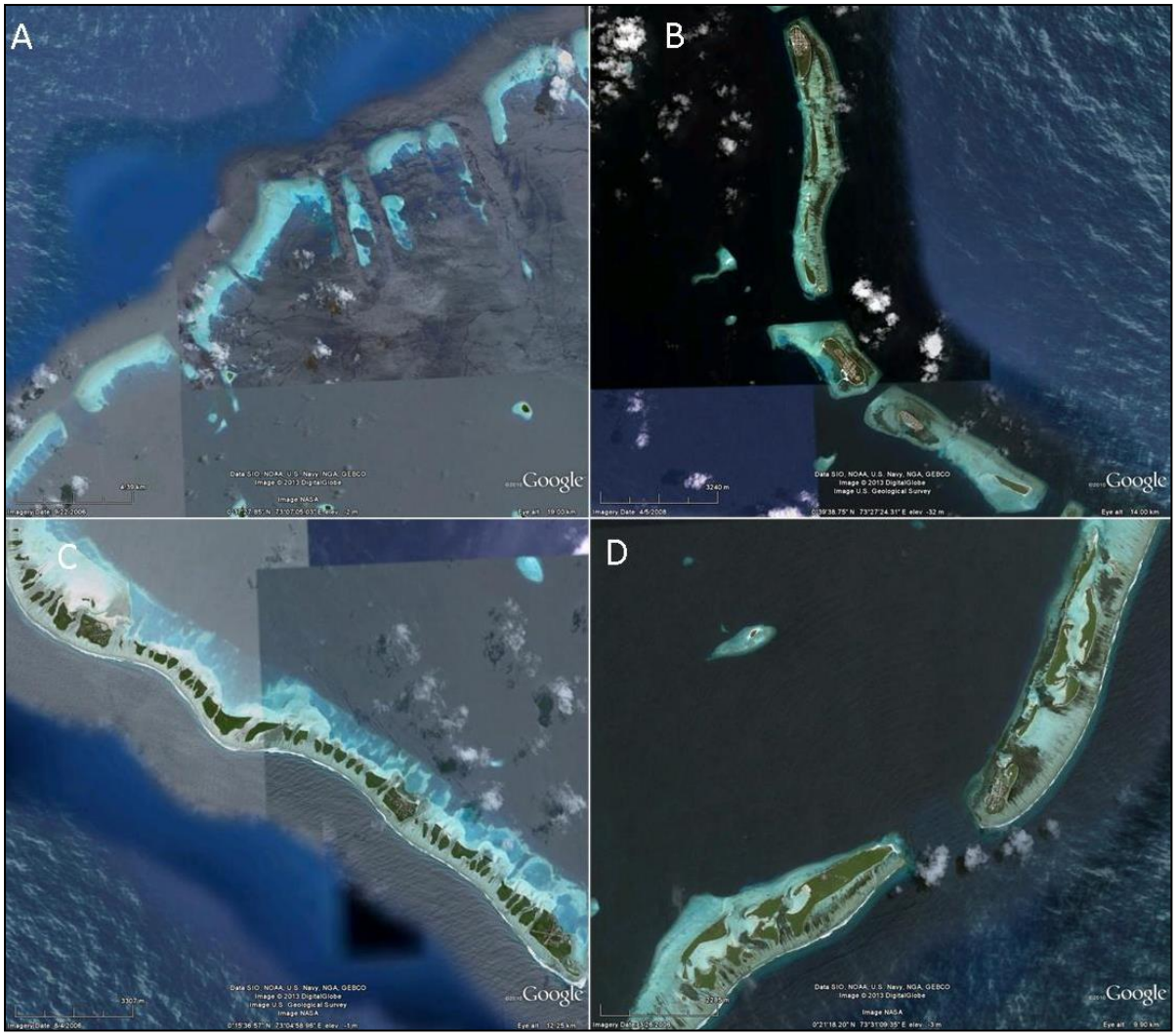

Figure 2.4 - Examples of rim types A, B, C and D from Huvadhu Atoll (Google Earth imagery, 2013).

The north-eastern and south-western study sites likely represent geomorphic end-members as a product of differences in the process regime. Indeed, wave energy is one of the primary controls upon coral reef geomorphology and ecology (e.g. Roberts, 1974; Done, 1982, 1983; Dollar, 1982; Storlazzi et al., 2005; Yamano et al., 2003; Kench and Brander, 2006a). Rim and reef island diversity is therefore likely, at least partially, attributable to relative differences in incident wave energy around the atoll rim (e.g. Kench et al., 2006). Satellite altimetry wave climate data derived from the period 1986 – 1999 showed that incident swell within the southern Maldives (at 0°N, 73°E) was from predominantly southern directions (Young, 1999). During the northeast (*iruvai*, December – March) monsoon oceanic swell arrived from the southeast, whereas during the longer southwest (*hulangu*, April – November) monsoon, swell arrived from southerly to south-westerly directions (Young, 1999). It

may thus be assumed that the south-western and north-eastern sites represent windward and leeward atoll rim settings respectively. However, there is an absence of any published data which investigates the contemporary process regime within and around Huvadhu Atoll. The aim of the remainder of this Chapter is thus to characterise the relative differences in the contemporary process regime at the north-eastern and south-western study sites.

2.4 Atoll-scale differences in wave forcing

The premise of this work is to test the assumption that the north-eastern and south-western sites represent windward and leeward rim environments. Specifically, two approaches will be employed in order to characterise the relative between-site differences in the contemporary process regime:

i) WaveWatch III 30 year hindcast modelling;
ii) Wave exposure modelling.

2.4.1 Methodology

2.4.1.1 WaveWatch III Hindcast Data

WaveWatch III (WW III) is a spectral, phase averaged wave model developed at the National Center for Environmental Prediction (NCEP; Tolman, 2009). WaveWatch III model hindcasts (Durrant et al., 2013) were used to estimate deep water significant wave height (H_s) and dominant wave period (T_o) for the period 1979 to 2009. Hindcast data is available via CSIRO (https://data.csiro.au/dap/landingpage?pid=csiro%3A6616; Durrant et al., 2013) on a global 0.4° x 0.4° global grid. Data was obtained (via a Matlab script) from ~20 km off the oceanward reef crest at both the south-western and north-eastern sites (specifically, 0.087823 N, 72.9769 E and 0.578801 N, 73.710562 E respectively; Figure 2.5). Locations were selected ~20 km offshore in order to negate bathymetric artefacts which are a known challenge for the WaveWatch III model (Ford, pers. comm., 2014). Paired t-tests were undertaken to determine whether values were significantly different between study sites.

2.4.1.2 Wave Exposure Modelling

Fetch-based models have been applied widely alongside linear wave theory to generate spatially explicit estimations of wave exposure (e.g. Ekebom et al., 2003; Harborne et al., 2006; Lima et al., 2007; Chollett and Mumby, 2012; Graham et al., 2015). The protocol applied in reef environments by Chollett and Mumby (2012) and Graham et al. (2015) was followed, with slight modifications, to generate estimations of wave exposure across Huvadhu Atoll. This involved running a wind fetch model, which subsequently served as an input to a wave energy model.

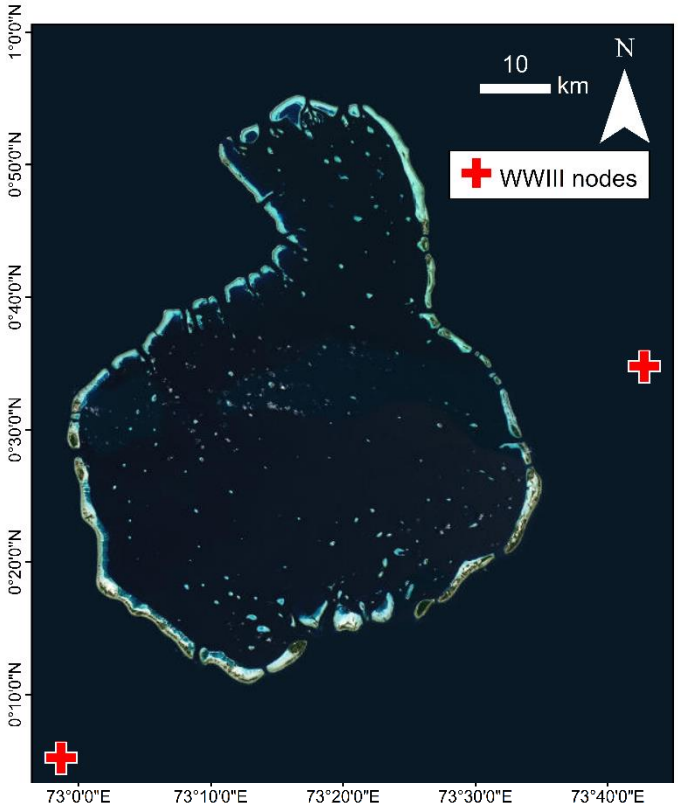

Figure 2.5 – Node locations selected for WaveWatch III hindcast analyses

Wind fetch model

Fetch is the distance over open ocean that wind can travel in a specific direction unobstructed by land or reefs to generate waves (Ekebom et al., 2003). The premise of fetch-based modelling is that larger wind-generated waves develop with increased fetch lengths and wind velocities. Fetches were calculated using the USGS (Rohweder et al., 2012) adaptation of the scripts developed by Finlayson (2005), which follows the procedure recommended by the Shoreline Protection Manual (U.S. Army Corps of

Engineers, 1984). This model is freely available to download via the USGS webpage: umesc.usgs.gov/management/dss/wind_fetch_wave_models_2012update.html.

A binary raster was generated representing the distribution of land and reef crests (land and reef crests = 1, water = 0; 3 m^2 spatial resolution). This incorporated the GPS planform surveys of both the windward and leeward study sites (section 3.3.1) and, for the remainder of the atoll, the maps produced by the Millennium Coral Reef Mapping Project (MCRMP, 30 m spatial resolution – Andréfouët et al., 2006, freely available at imars.marine.usf.edu/MC/products.html).

Fetch lengths were calculated for 16 compass directions (every 22.5°) whereby each length represents the arithmetic mean of 5 radials spread at 3° increments around the desired wind direction. Increasing the arc beyond a single radial produces a more realistic output as wind data are rounded (in this instance to the nearest 22.5°) and the direction will vary within the intervals between measurements. In addition, although fetch-based models have been formulated in island environments (Ekebom et al., 2003), they do not account for wave refraction. Enlarging the arc therefore produces more realistic predictions of island shadow zones are produced (Rohweder et al., 2012). The Shoreline Protection Manual (USACE, 1984) recommends the use of 9 radials at 3° increments, however this creates a 24° arc and as this study employs measurements every 22.5°, radials from adjacent directions would overlap. This study therefore uses an ‘SPM-restricted’ approach with 5 radials to avoid introducing bias into the calculations.

A modification to the USGS script was also made in order to include a spatial offset in the calculations. In GIS fetch-based models, a trade-off is typically made between spatial extent (i.e. area of the input raster) and spatial resolution (i.e. pixel dimensions) to ensure the model is not over computationally intensive both in terms of hard disk space and the operating time. This poses a particular issue in (1) island environments as if the raster resolution becomes too coarse, thin islands or sections of the atoll rim are lost; (2) areas exposed to open ocean as the distance required for maximal wave conditions to be reached is 650 km (under gale-force wave conditions based on the equations of Denny, 1988; Hill et al., 2010), which computationally is an unrealistically large spatial extent (i.e. <1300 x 1300 km). Often in previous applications of fetch-based models, the maximum fetch lengths are not mentioned (e.g. Chollett and

Mumby, 2012) or the maximum length is substantially shorter than 650 km (e.g. 5 km - Hamylton, 2011; 0.5 km – Siljander et al., 2015). The script was therefore modified so that a spatial offset was included in the text file for each compass direction. The distances from the edge of this input raster to the nearest land (<650 km) were measured in each direction and included in the input text file. This meant that the spatial extent of the input raster could be limited to the study site (i.e. Huvadhu Atoll), as oppose to an area of 1300 x 1300 km. The model could thus run with a spatial resolution of 3 m^2 while incorporating large fetch lengths.

Wave energy model

The fetch model outputs were then converted into wave energies using linear wave theory following the equations of Chollett and Mumby (2012). Wind data were used as an additional input for the model. Wind measurements for 2014 were acquired from Kaadedhdhoo Airport (0.49°N, 73.00°E; n = 2643; wunderground.com) and used to calculate both the percentage likelihood of wind coming from each of the 16 compass directions, and also the mean wind velocities from each direction. Ideally, a longer time period would have been used, however this was unfeasible due to practical issues of data acquisition. The year 2014 was thus selected as it was a non-El Niño and La Niña year and thus likely reflects somewhat typical conditions. However, it ought to be borne in mind that results may thus be sensitive to the time period selected.

Wave energies were modelled for each of the 16 compass directions in turn. A distinction was made between 'fetch-limited' and 'fully-developed' seas as with a long fetch and given wind speed, there is a fixed limit to which wave height, period and energy can grow. At this transition point, seas are 'fully-developed', whereby wind energy input to waves is balanced by wind energy dissipation with wave breaking and turbulence (Ekebom et al., 2003). In order to draw this distinction, for each of the 16 directions, the non-dimensional fetch (ξ) was calculated:

$$\xi = \frac{gF}{U_{10}^2} < 38{,}590$$

Where g = gravitational acceleration (9.81 m s^{-2}), F = fetch (m), U_{10} = wind speed at an elevation of 10 m in ms^{-1}. Pixels were classed as fetch-limited if the non-dimensional fetch was below the threshold value of 38,590 m (Resio et al., 2003; Chollett and Mumby, 2012).

For each compass direction, wave period and amplitude were then calculated for fetch-limited seas using the equations:

$$H_{m0} = 0.00082\ U_{10}^{1.1}\ F^{0.45}$$
$$T_p = 0.087\ U_{10}^{0.46}\ F^{0.27}$$

where H_{m0} = significant wave height, and T_p = wave period at the peak of the spectrum. For fully-developed seas, H_{m0} and T_p were calculated as:

$$H_{m0} = 0.034\ U_{10}^{2}$$
$$T_p = 0.81\ U_{10}$$

The wave energy (*WE*, in J) was then calculated using the equation:

$$WE = \frac{1}{16}\ \rho g H_{m0}^{2}$$

where ρ = the density of seawater (1030 kg m^{-3}).

The calculations of *WE* in each compass direction were then used to calculate the apparent wave energy (WE_p) at a given point *p*:

$$WE_p = \sum_{i=1}^{n} (t_i WE_i)$$

where t_i = annual probability of wind coming from direction *i*, WE_i = wave energy in the direction of line *i*, and *n* = number of compass directions (n = 16). Following Chollett and Mumby (2012), WE_p is given in J m^{-3}. However, as in all other prior applications of the approach (e.g. Graham et al., 2015; Perry et al., 2015), WE_p ought to be considered as a relative, rather than an absolute, measure of wave energy.

2.4.2 Results

2.4.2.1 WaveWatch III Hindcast Data

The WaveWatch III hindcast outputs returned mean T_O values of 10.0 ± 1.55 s and 9.65 ± 1.45 s at the south-western and north-eastern sites respectively (n = 279,768 for each site; Figure 2.6). This places T_O within the swell range (8 – 20s; Brander et al., 2004) at both sites. T_O at the south-western site was significantly longer than that at the north-eastern site (P = <0.0005; paired t-test). Plotting T_O at the north-eastern site against that at the south-western site shows, as anticipated, a tight relation

between T_O at each site (R^2 = 0.855; Figure 2.6). The linear regression line is slightly below y = x, indicating that T_O was slightly shorter in the northeast than in the southwest at any given point in time. Indeed, linear regression analysis showed the gradient to be 0.864 (y = 0.864x + 1.003).

Average H_s values at the south-western site (1.55 ± 0.43 m) exceeded those from the north-eastern site (1.35 ± 0.35 m; Figure 2.7). Indeed, H_s was significantly larger at the south-western site than the north-eastern site (P = <0.0005; paired t-test). Plotting H_s at the north-eastern site against that at the south-western site shows a comparably strong relation between H_s at each site (R^2 = 0.855; Figure 2.7) to that associated with T_O (Figure 2.6). The linear regression line is below y = x, showing that H_s was smaller in the north-east than in the south-west at any given point in time. The between-site difference was slightly more pronounced than that found for T_O and, indeed, linear regression analysis showed the gradient to be 0.747 (y= 0.864x + 1.003).

The 15th – 17th May Fares-Maathoda (southwest Huvadhu atoll) overwash event (Aslam and Le Bere, 2007) was identified within the output data with larger than average values returned for H_s (2.49 m and 1.88 m at the south-western and north-eastern sites respectively) and T_O (15.53 s and 13.95 s respectively). Hence, values were larger at the south-western site where H_s attained maximum heights of 2.88 m during the May 2007 event, which lends confidence to the model results. Assuming occasions where H_s >2.5 m represent high magnitude events, 15 isolated events (n = 296) occurred at the north-eastern site and 149 events (n = 5,332) at the south-western site. Over the 30 year period, H_s attained maximum values of 3.82 m and 3.02 m in the south-west and north-east respectively.

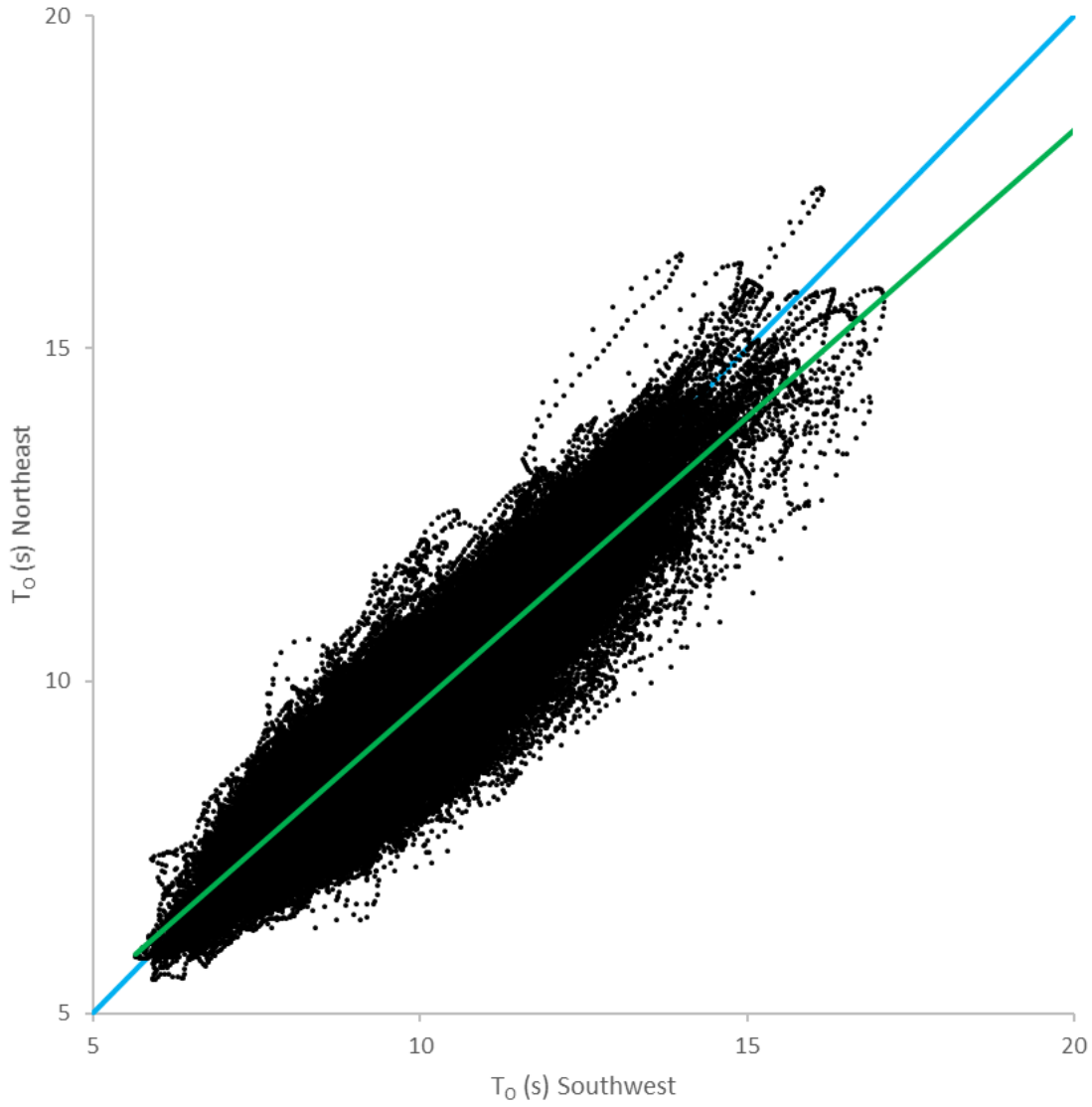

Figure 2.6 – Comparison of WaveWatch III output values for T_O at the north-eastern and south-western study sites (n = 279,768 for each parameter at each site). Linear regression line is plotted in green (R^2 = 0.855; y = 0.864x + 1.003). For ease of comparison y = x is plotted in blue.

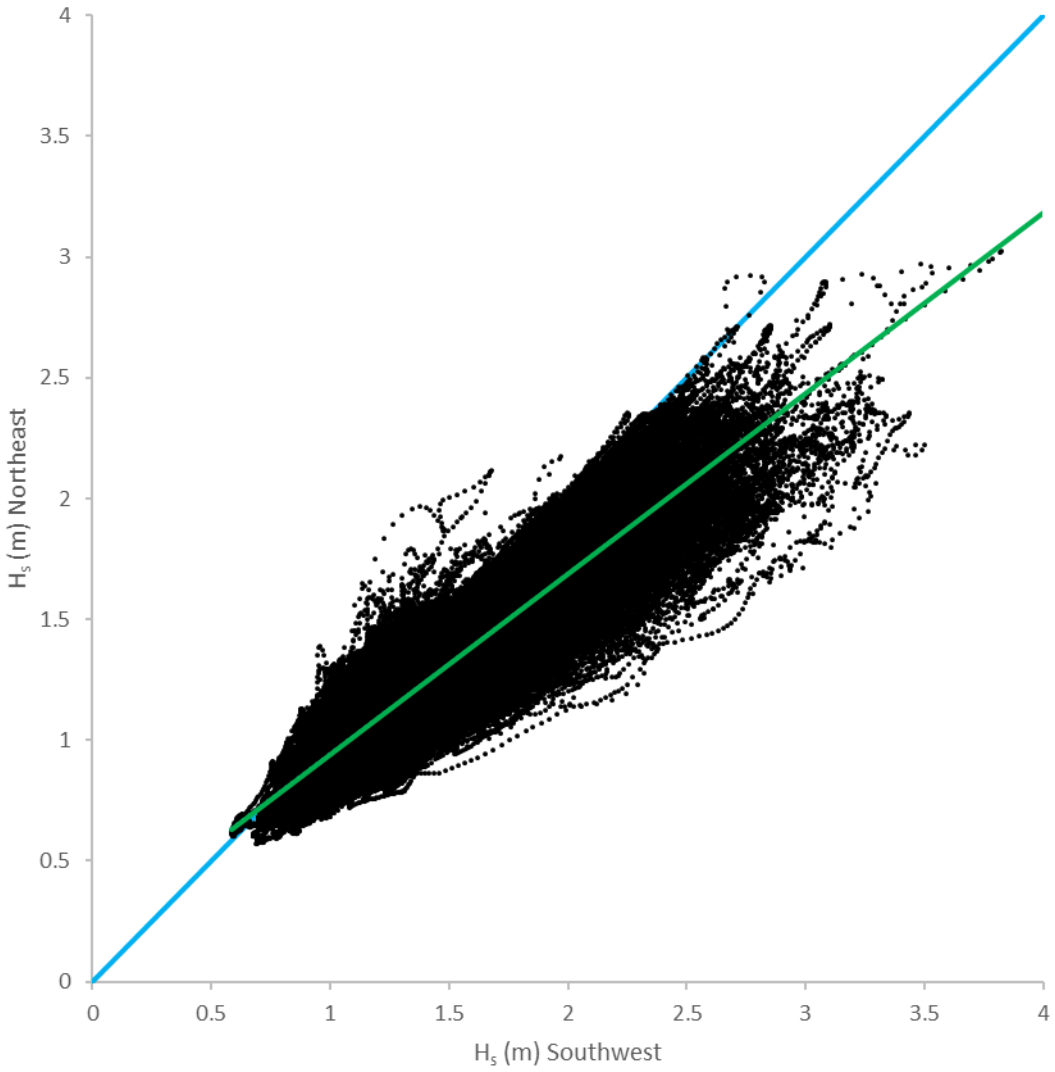

Figure 2.7 – Comparison of WaveWatch III output values for H_s at the north-eastern and south-western study sites (n = 279,768 for each parameter at each site). Linear regression line is plotted in green (R^2 = 0.854; y = 0.747x + 0.196). For ease of comparison y = x is plotted in blue.

2.4.2.2 Wave Exposure Modelling

The annual wind climate of Huvadhu Atoll was dominated by westerly winds (41.9% from direction between 247.5˚ and 292.5˚) with mean velocities of 3.99 m s^{-1} (Figure 2.8). Oceanward wave exposures (i.e. outside of Huvadhu atoll) were thus highest (<124.35 J m^{-3}) off Huvadhu's western margin, whilst the most sheltered locations were in the lee of the westerly and south-westerly atoll rim platforms (>0 J m^{-3}; Figure 2.5). Within the atoll lagon, a cross-atoll gradient was evident with wave expore

increasing from the west-southwest (<0 J m^{-3}) towards the east-northeast (<~95 J m^{-3}). Albeit stepped (as an artefect of the model), such overall cross-atoll trends are represented in Figure 2.9B.

Specifically, oceanward wave exposure was ~94.72 ± 0.09 J m^{-3} and 12.93 ± 0.01 J m^{-3} at the south-western and north-eastern sites respectively. At the lagoonward margin of the study sites, wave exposure was 18.92 ± 0.04 J m^{-3} and 110.95 ± 3.26 J m^{-3} at the south-western and north-eastern sites respectively.

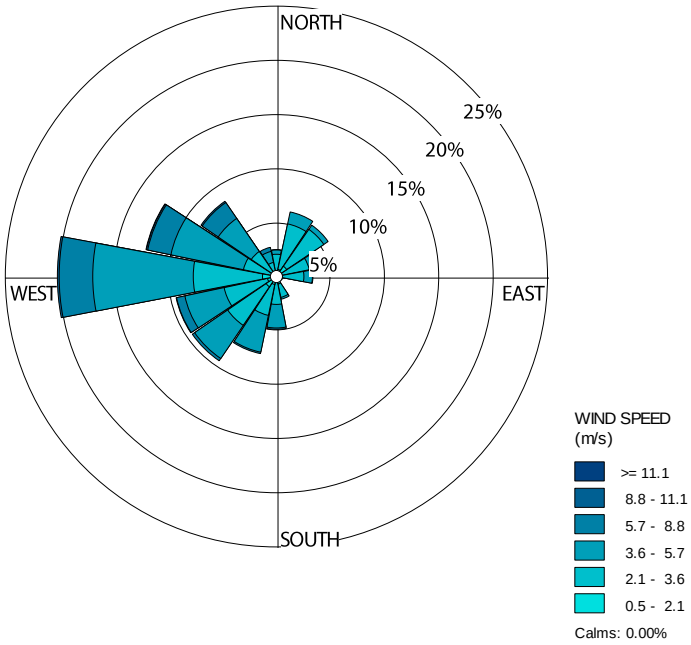

Figure 2.8 – Wind rose showing wind speed (m s^{-1}) and direction generated using 2014 wind data from Kaadedhdhoo Airport (0.49°N, 73.00°E; n = 2643).

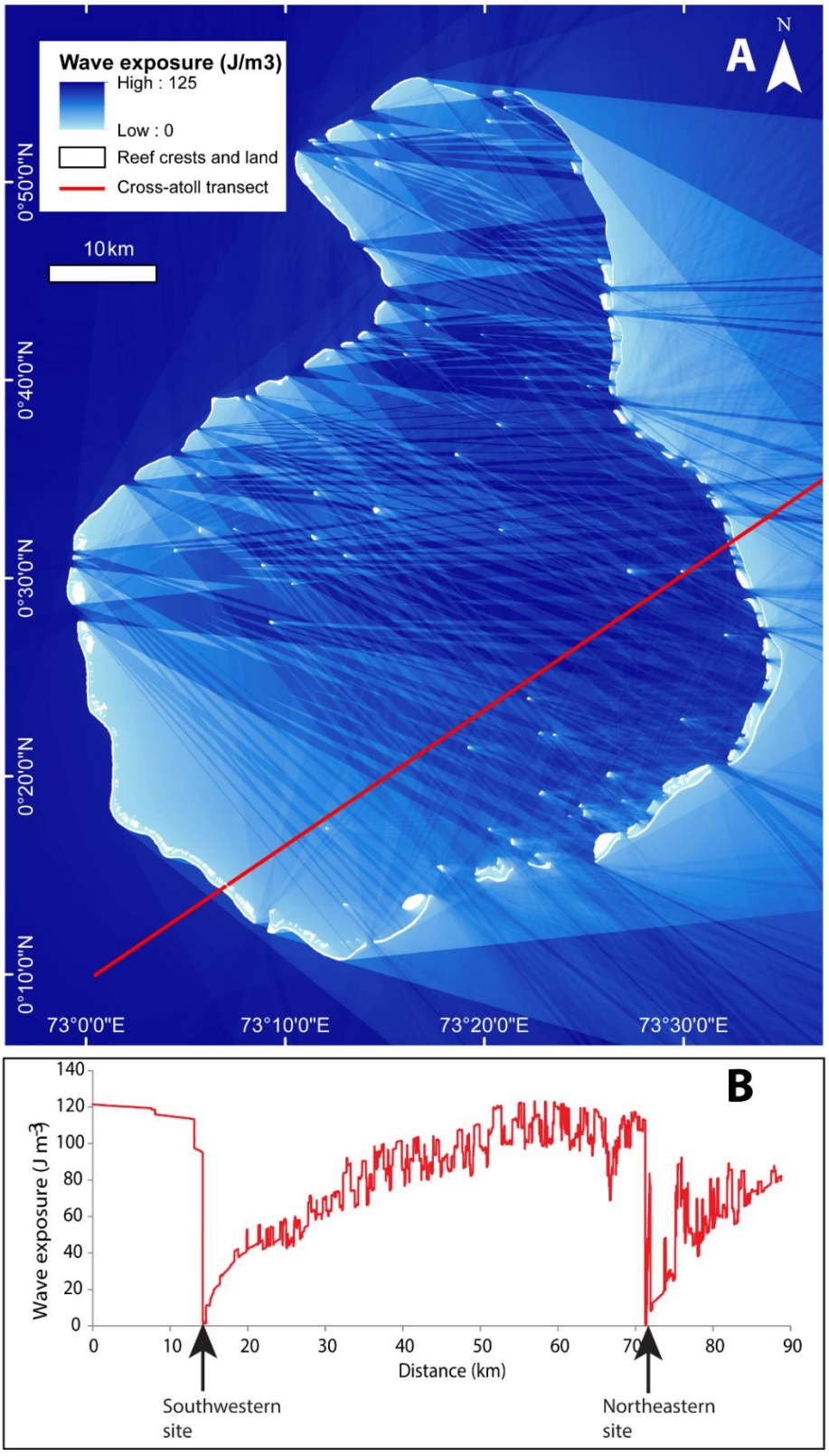

Figure 2.9 – Wave exposure model of Huvadhu Atoll (J m^{-3}; A). The cross-atoll transect (red line within A) intersects both the south-western and north-eastern study sites and the associated wave exposure values (n = 8780) are plotted within B.

2.4.3 Discussion

Two approaches are presented in order to quantify relative differences in the contemporary process regime at the south-western and north-eastern study sites. There is a key distinction in the hydrodynamic environment between the oceanward and lagoonward rim margins. Indeed, the oceanward margins are the recipients of oceanward swell wave energy. In contrast, the lagoonward margins are characterised by the greater significance of wind-driven waves, which are locally generated as winds blow from windward to leeward directions across the atoll lagoon. In light of this distinction, the wave climates of the oceanward and lagoonward atoll rim margins will be discussed in turn.

2.4.3.1 Oceanward Atoll Margins

The two approaches provide consistent evidence that, at the oceanward atoll margin, wave energy is markedly greater at the south-western site than the north-eastern site. This is consistent with field data from an unpublished MSc thesis (Mandlier, 2008), which comprised wave measurements from 3 sites across Huvadhu Atoll. Mandlier sought to examine cross-atoll gradients in wave energy and therefore selected sites on a windward (south-western) rim, central interior, and leeward (north-eastern) rim platforms. The windward and leeward sites were thus in close proximity to the south-western and north-eastern sites within this thesis (~8 km and ~20 km respectively). Likewise, platform aspects, relative to incident wave energy, were also similar to those of this study (Figure 2.10). Hence, it is likely that wave conditions would also be comparable to the study sites within this thesis. Measurements were obtained during an 8-day experiment undertaken between 8th and 16th November 2007 over 16 successive high tidal stages. Significant periods were within the swell range (8 to 20 s; Brander et al., 2004) at both the north-eastern and south-western sites. However, T_S at the north-eastern site oceanward margin (8.1 s) was significantly shorter than that at the south-western site (9.1 s). Similarly, significant wave heights (0.66 m) at the south-western site were found to exceed those at the north-eastern site (0.36 m).

Mandlier's (2008) field data were thus consistent with the WaveWatch III hindcast data which showed both significant wave height and dominant period to also be significantly larger at the south-western site than the north-eastern site (H_S = 2.49 m and 1.88 m; T_O = 15.53 s and 13.95 s at the south-western and north-eastern sites respectively).

However, wave heights found by Mandlier (2008) were less than half the magnitude of the values derived from WaveWatch III. This is likely given that Mandlier's instruments at the oceanward margin were deployed on top of the reef platform (i.e. on the algal rim, termed 'oceanward reef crest' zone within this thesis, section 4.3.1), while WaveWatch III data were derived 20 km off the atoll rim. Hence, pronounced attenuation of wave energy will have occurred between the open ocean and reef platform top (e.g. section 7.3.2.1). Nonetheless, all 3 datasets are consistent in demonstrating oceanward swell wave energy at the south-western site to be markedly greater than at the north-eastern site.

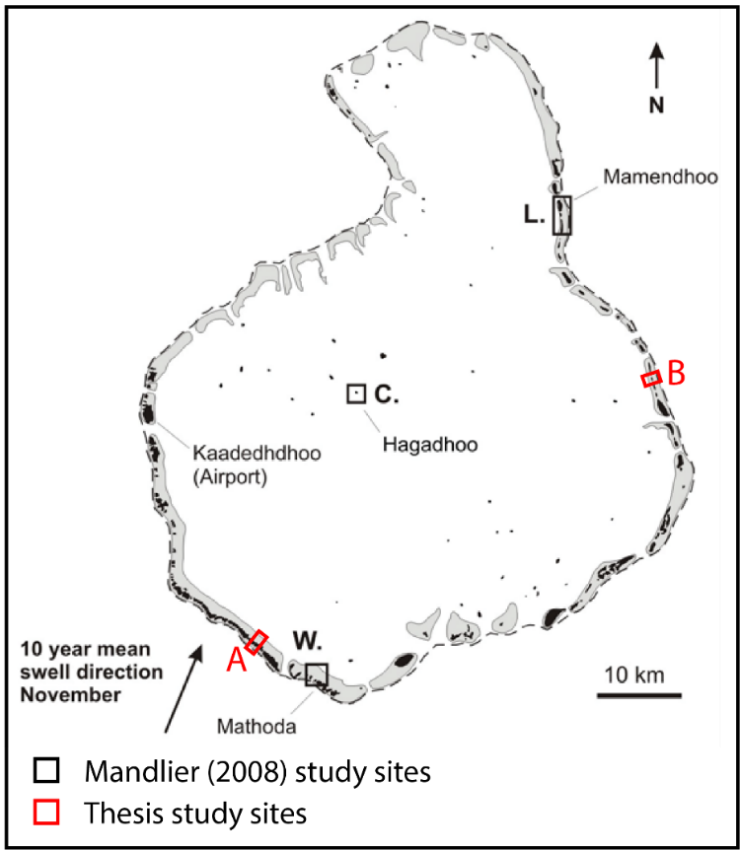

Figure 2.10 – Location of the south-western (A) and north-eastern (B) study sites within Huvadhu Atoll alongside the Mandlier's (2008) windward (W.) and leeward (L.) study sites. Mean swell direction from Young (1999). Figure adapted from Mandlier (2008).

The wave exposure modelling output also found oceanward exposure at the south-western site to markedly exceed that at the north-eastern site. However, the relative difference in wave exposure between sites was far larger in magnitude than that found by WaveWatch III and Mandlier (2008). This is because the final stage of the model

involved the multiplication of wave energies from each direction by the percentage of winds from that direction. By its nature, the model therefore effectively ascribes a far greater provenance to locally-generated wind waves, than oceanward swell wave energies. As a mere 8.4% of wind was from easterly directions (between 67.5˚ and 112.5˚), wave exposure values are relatively low off the oceanward margin of the north-eastern site, despite the fact that seas were 'fully developed'. As a consequence, oceanward wave energy at the leeward site is likely a marked underestimation of the true relative value. Nonetheless, the model illustrates that oceanward wave energy at the south-western site exceeds that at the north-eastern site.

The oceanward margin of Huvadhu Atoll is particularly exposed given that it does not form a part of the double linear chain of atolls, but is rather exposed to oceanward swell wave energy at both study sites. Indeed, there is no land mass obstructing fetch lengths for as far as Sri Lanka (~950 km) to the northeast and South Africa/Madagascar (~3,900 km) to the southwest (fetch lengths are considered 'fully developed' with a comparatively mere 650 km; Hill et al., 2010). Such unobstructed waters can mean that distal swell events have the potential to impact the study sites Indeed, distal swell events have been shown to be of significance in the Pacific. For example, swell wave energy impinges on the shorelines of Hawaii as controlled by distal storms in the North and South Pacific during winter and summer respectively (Fletcher et al., 2008). In addition, a major inundation event which impacted six Pacific island nations was attributed to the impacts of mid-latitude storms (Hoeke et al., 2013). Similarly, in the Caribbean, erosive surf in the Lesser Antilles islands, including Barbados, has been linked to swell originating from extratropical cyclones in the North Atlantic (Donn and McGuinness, 1959). An implication is that any shifts in distal storms under future climate change may have significant implications for reef island shorelines and stability.

In the Maldives, between the 15th and 17th May 2007 extensive floods covered ~30% of the island of Fares-Mathoda (southwest Huvadhu Atoll, ~8 km southeast of the windward site), which was attributed to intense storm winds on 7th May off the southern coast of South Africa (Aslam and Le Bere, 2007). Similarly, the flooding of the Maldives in April 1987 has also been attributed to swell that originated in the southern Indian Ocean (Harangozo, 1992). Indeed, the frequency of such high magnitude events was far greater at the south-western site (n = 149) than the north-

eastern site (n = 15). Due to the comparative exposure of Huvadhu, generalisations ought to be drawn with caution. Nonetheless, it is likely that parallels with other windward and leeward sites across the Archipelago may be drawn, as is likely manifest in islands of similar morphologies (with longest island axes perpendicular and parallel to the reef crest) to those in this study.

2.4.3.2 Lagoonward Rim Margins

Converse to oceanward swell wave energy, lagoonal wave energy was of greatest magnitude at the north-eastern site. This was to be anticipated as the influence of oceanward wave energy diminishes with distance from windward reefs, particularly following the rapid dissipation of oceanward wave energy at oceanward reef crests (refer to section 7.3.2.1). There is a concordant increase in the relative importance of locally generated wind wave energy across the atoll lagoon. This occurs as fetch lengths increase as wind blows from the windward to the leeward side of the atoll. Such cross-atoll gradients are evident in wave exposure modelling results (Figure 2.9) as wave exposure is at a minimum towards the west-to-south-westerly portions of the atoll lagoon (mean at the lagoonward margin of the south-western site = 18.92 ± 0.04 J m^{-3}), but increases with distance across the atoll towards the east-northeast (110.95 ± 3.26 J m^{-3}). Indeed, given the provenance that the wave exposure modelling approach attributes to wind as a variable, this model is by its nature best suited to the investigation of wind-driven waves. Wave exposure model results were supported by the relative difference between field data obtained from the lagoonward reef crests at Mandlier's atoll rim sites (2008). H_S = 0.09 m and 0.12 m at Mandlier's windward and north-eastern sites respectively.

2.4.4 Conclusion

WaveWatch III hindcast data and wave exposure modelling both confirm that on the atoll margin, wave energy at the south-western study site exceeds that at the north-eastern site. Conversely, energy received at the lagoonward rim margin is of greatest magnitude at the north-eastern site due to the longer fetch lengths and winds blow from the windward side of the atoll. Moreover, these findings are consistent with field data from Mandlier (2008). This Chapter therefore provides quantitative support for the assumption that the south-western and north-eastern sites represent windward and leeward rim environments respectively. **Hereon in the south-western and north-**

eastern study sites will be termed the 'windward' and 'leeward' sites respectively. Figure 2.11 thus illustrates several key terms employed to describe the sites within this thesis.

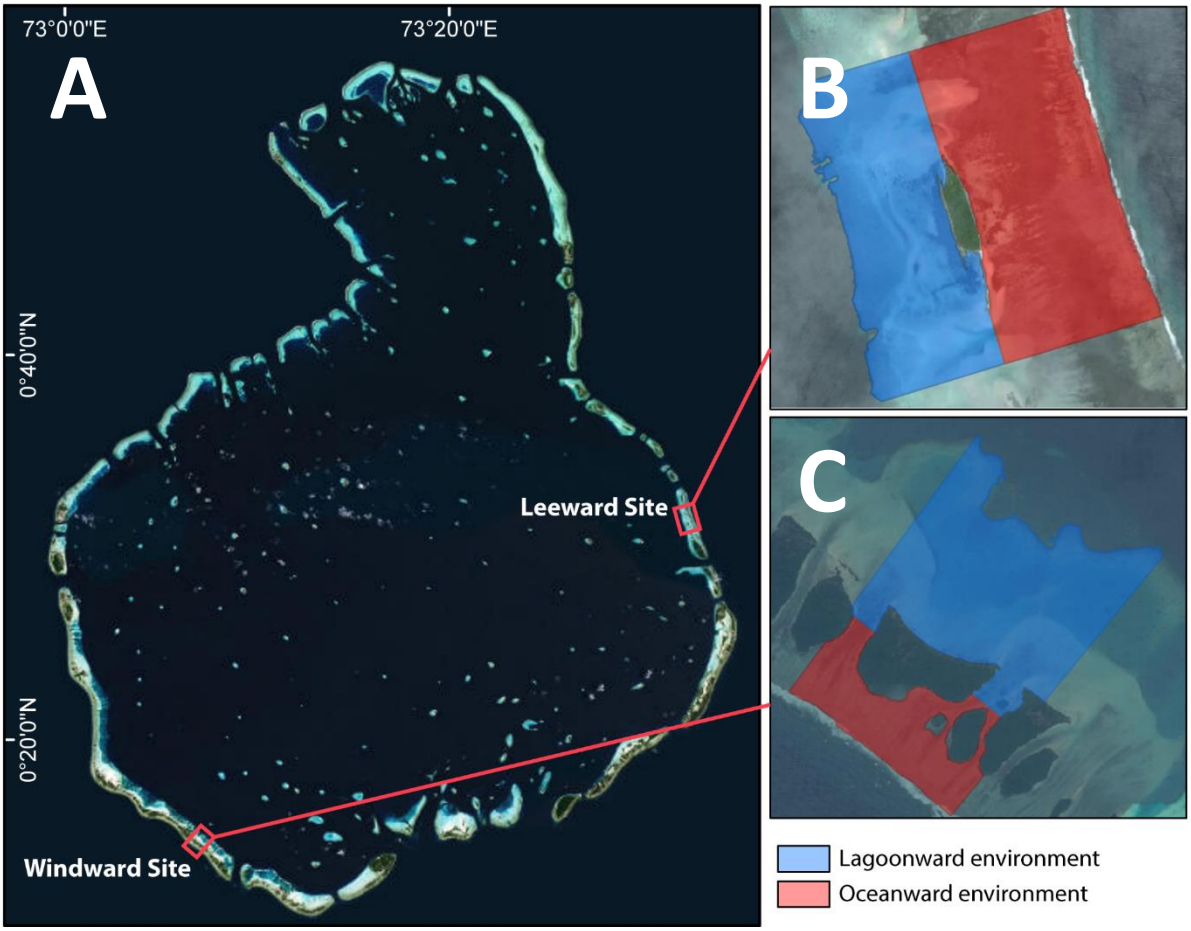

Figure 2.11 – Illustration of terminology used throughout the thesis to refer study sites (A), and the oceanward and lagoonward marine environments within the leeward (B) and windward (C) sites. (Imagery source: ESRI, 2017). N.B. within the Chapter 3, Baavanadhoo island will also be incorporated into the leeward site analyses.

Chapter 3 Island Development

3.1 Introduction

Due to their dependence upon locally generated sediment, low elevations and largely unconsolidated structure, reef islands are regarded as extremely vulnerable to environmental change, particularly to sea-level rise (Roy and Connell, 1991; Kench and Cowell, 2001; Kench and Brander, 2006a). However, assertions of vulnerability are largely made without a full understanding of how and when islands formed, the processes controlling island formation, and inter- and intra-regional variations in island-building processes (e.g. Kench et al., 2009a; Perry et al., 2011).

Understanding reef island accretionary histories and the controls on island development is crucial for assessing their morphological stability and future resilience. To date, research has focused largely upon a few discrete localities in the Pacific and within the Great Barrier Reef Shelf/Torres Strait region (e.g. Kench et al., 2014; Kench et al., 2014b; Yamano et al., 2014). In other major reef island regions such as the Maldives (a nation comprised of >1,200 reef islands inhabited by a population of 345,023; World Bank, 2013), our knowledge of island building processes is far more limited. Detailed chronostratigraphic research of reef island development in the Maldives is, to the best of the author's knowledge, restricted to two main datasets developed for interior islands within just one atoll (South Maalhosmadulu Atoll in the northern-central part of the archipelago – Kench *et al.*, 2005; Perry *et al.*, 2013). Knowledge of rim island stratigraphy is even more limited and based on qualitative descriptions of one pit in the centre of Feydhoo island, Addu Atoll (Woodroffe, 1992). However, it is the rim islands that dominate spatially (82.4% of land area), host the majority of the population (88.93%), and therefore support the nation's key infrastructure (all regional administrative capitals, hospitals, and designated 'safe islands').

The aim of this Chapter is therefore to provide the first detailed, quantitative descriptions of Maldivian rim reef island development. In the context of the windward and leeward study sites on Huvadhu Atoll rim, key research questions include:

1. What is the sedimentary composition and texture of Maldivian rim islands?

2. What is the substrate underlying (i.e. below the level of live coral growth) Maldivian rim reef islands?
3. When did the window of Maldivian rim island formation occur?
4. What are the key controls upon Maldivian reef rim island development?
5. Does variability exist in the modes and timings of Maldivian rim island development at the scale of an atoll (i.e. between windward and leeward rim aspects)?

3.2 Methodology

This study was focused upon the windward and leeward study sites on Huvadhu atoll rim (Figure 2.1). Specifically, the windward site comprised the islands of Mainadhoo, Boduhini and Kudahini; while the leeward site incorporated the islands of Galamadhoo and Baavanadhoo (Figure 3.1).

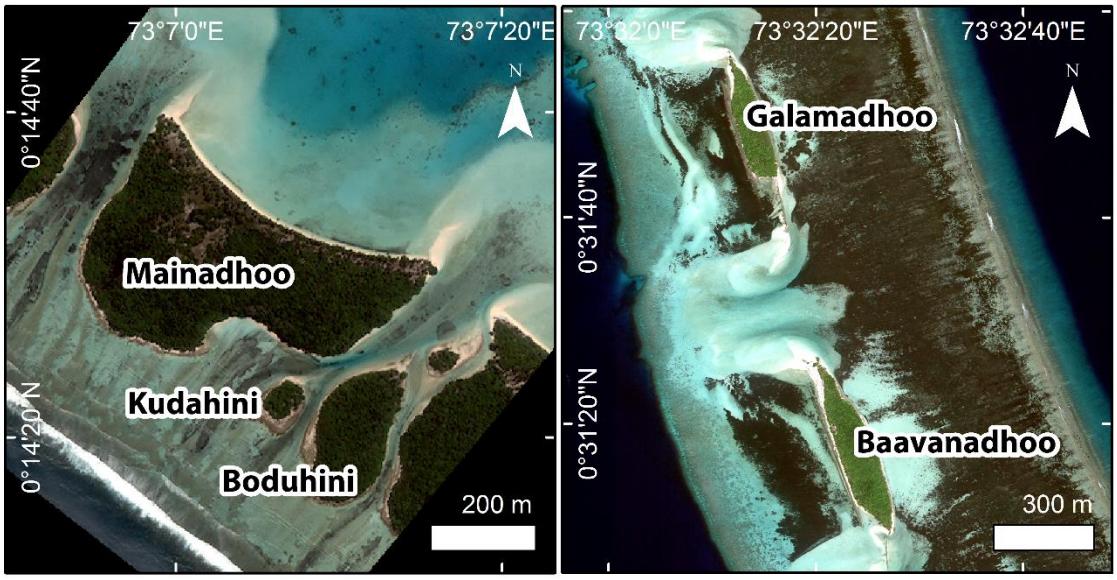

Figure 3.1 – Islands within the windward (left) and leeward (right) study sites.

Island topographic surveys were undertaken along 11 transects covering 3291 m. Each transect started and terminated on the reef flat in areas of live coral growth within the adjacent marine environments. Topographic data was corrected to height above mean sea level (MSL) using tide tables for Gan (00°41S, 73°9E) from the University of Hawaii Sea Level Centre. Island planform was surveyed using GPS to map the vegetation edge, toe of the beach, conglomerate platform and beachrock outcrops.

Subsurface stratigraphy along each traverse was determined through recovery of 28 cores, the locations of which were recorded using GPS. Core locations were selected to maximise spatial coverage of each reef island. In each case, a hole was dug through the organic soil layer, after which sand augering was used to reach the water table. Percussion coring, using aluminium piping with an internal diameter of 9 cm, then allowed for penetration to depths below the level of contemporary live coral growth. This is the only viable coring technique that allows full recovery of unconsolidated island sediment constituents without significant loss of the sediment matrix (Perry and Smithers, 2006). Island facies were determined in the field by visually assessing basicbiosedimentary facies information, including sediment colour, textural characteristics (using Udden-Wentworth nomenclature), clast-matrix ratio, coral clast size, and composition. This approach has been applied in similar studies of reef and reef island cores (e.g. Perry et al., 2017; Ryan et al., 2016). Following the delineation of basic facies units, a *c*. 100g sample was recovered for analysis from each facies within each core (n = 119).

Samples were dry sieved into 1 phi (ϕ) intervals (-1 – 4 ϕ) and analysis was undertaken within the programme GRADISTAT (Blott and Pye, 2001) to calculate sediment grain size and sorting. The percentages of gravel-sized (> 2 mm, <-1 ϕ), sand-sized (0.063 – 2 mm, -1 – 4 ϕ), and silt-sized (<0.063 mm, >4 ϕ) material were also calculated (the descriptive nomenclature of Udden-Wentworth is used throughout).

Sieve counting methods were employed to determine sediment composition whereby 100 grains were point counted under the binocular microscope from each gravel and sand-sized phi interval (i.e. >2 mm, 1-2 mm, 0.5-1 mm, 0.25-0.5 mm, 0.125-0.25 mm and 0.063-0.125 mm; a total of 600 grains per sample). Silt-sized sediments were not counted as reliable identification was not possible, however this size fraction accounted for an average of only 2.11 ± 0.57% of each sample. Likewise, the presence of organic matter precluded reliable identification of sediments within the ‘organically enriched’ horizon (facies 1). Grains were classified into one of seven compositional groups: coral, CCA, molluscs, foraminifera, echinoids, *Halimeda*, and other/unidentified. Total percentage abundance of components in each bulk sample was then calculated using the proportion of each size fraction to the bulk sample weight (e.g. Dawson and Smithers, 2014).

To further characterise facies, where possible, all coral clasts with longest axes > 1 cm were identified. In addition, an abrasive index (AI) was employed as a measure of taphonomy whereby the condition of the exterior surface of each coral clast with longest axes > 1 cm was scored on a semi-quantitative five-point scale (adapted from Pandolfi and Greenstein, 1997; Lescinsky et al., 2012; Figure 3.2). The median score was then calculated for each sample and then each facies.

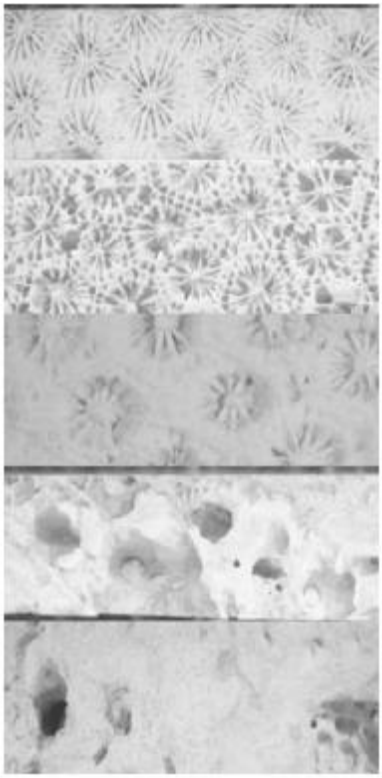

1: Pristine; detailed 3D ornamentation of septa and wall relief

2: Some 3D relief of corallites; septal ridges are preserved but lack fine detail

3: Visible internal corallite structures, but no 3D relief

4: Surface is irregular; the genus or species may be identifiable, though the fine corrallite structure is lost in some places

5: Rubble; no internal or external structures were preserved; clasts are unidentifiable in the field

Figure 3.2 – Five-point abrasive scale adapted from Pandolphi and Greenstein, 1997; Lescinsky et al., 2012 (image from Lescinsky et al., 2012)

Carbonate content of the upper organically enriched horizon was determined by loss on digestion in 2 M HCl (Palmer et al., 2010). Replicate samples (n = 12) indicated that results were reproducible within *c*. 3%.

To determine reef island chronologies, 40 samples were selected for radiocarbon dating. AMS radiometric dating is the most viable and widely used method of dating Holocene reef and reef island sequences. Dating within reef island systems is somewhat problematic as the materials have been transported from their sites of production (the adjacent reefs) and deposited to form the islands over time. There is therefore an inevitable temporal disparity between the time of death of the organism (the sediment constituent) and the time of deposition (Kench et al., 2005). However,

through careful microscopic screening of samples, and by selecting only the most pristine constituents, rapid post-mortem transport and deposition can be reliably inferred. This is because most bioclastic sediment constituents will degrade very rapidly and breakdown post-mortem if they remain in the active sedimentary environment for periods of more than a few weeks to months. Using these screening approaches, and based on component-specific dating, several previous studies have established island-building chronologies in the Pacific (Woodroffe et al., 2000; Woodroffe & Morrison, 2001; Woodroffe et al., 2007), and the Maldives (Kench et al., 2005; Perry et al., 2013).

A combination of coral samples from the underlying reef flat, as well as pristine *Acropora* sticks, *Halimeda* grains, foraminifera and gastropod shells were thus sampled from cores to constrain the timing of island building. Prior to dating, coral samples were subjected to ultrasonic agitation in distilled water to remove detrital particles, oven dried (40°C) and sealed in plastic bags. Samples of individual *Halimeda* segments, foraminifera and gastropods were soaked in distilled water for 24 hours. Radiocarbon dates were obtained from the NERC Radiocarbon Facility (East Kilbride, UK) and results were converted to calendar timescale using the Radiocarbon Calibration Curve Marine13, and a weighted mean ΔR value of 132 ± 25 (Southon et al., 2002). The ΔR value was selected to be consistent with that used by Kench et al. (2005) thus ensuring maximum comparability with existing chronologies developed for interior Maldivian islands. Kench et al. (2005) selected as the as best estimate for the central Indian Ocean reservoir effect from Southon et al. (2002).

Given the spatial limitations of core records, any quantifications of volumetric sediment storage must, at best, be considered as extremely crude. However, to allow comparison with the volumes of material presented elsewhere in this thesis, first order estimates were calculated. Total island volume (above the seafloor) was estimated by multiplying island planform area (as found from GPS planform surveys) by island height (as found from topographic surveys). Using average facies thicknesses, the volume of each facies was then calculated as a proportion of total island volume.

In order to interpolate between cores, Ground Penetrating Radar (GPR) data were collected using a Geophysical Survey Systems Inc. (GSSI) SIR2000 system with 200 mHz shielded antennae. Traces were collected along sections (where vegetation

densities allowed) of each transect on Mainadhoo (windward site), and along the entire central transect of Baavanadhoo (leeward site). Normalisation, stacking and depth conversions were undertaken within RADAN 6.5 software.

3.3 Results

3.3.1 Reef island morphology

At the windward site, topographic survey data (Figure 3.3 and 3.4) showed the mean elevations of the vegetated island surfaces (excluding marginal ridges) to be remarkably consistent between islands (0.81 ± 0.02 m, 0.81 ± 0.01 m and 0.82 ± 0.04 m above MSL at Mainadhoo, Boduhini and Kudahini respectively). At Mainadhoo, the vegetated surface was relatively uniform in elevation with the exception of a pond on the western transect (*c*. 260–330 m along the transect). Perhaps the most striking feature of Mainadhoo's topography was the steep ridge (2.00 m above MSL) found on the oceanward island margin of the western transect, which was formed of unconsolidated coral rubble and boulders (<0.8 m diameter; Figure 3.5B and D). The oceanward margin of the central transect also possessed a ridge, though this was comprised of smaller-sized rubble (<0.3 m diameter), as well as a bay of predominantly sand-sized material (Figure 3.5C). The eastern transect of Mainadhoo did not possess an oceanward ridge, likely as it is in the lee of Kudahini. On the lagoonward shoreline of Mainadhoo, the coastline was comprised of sand-sized material (Figure 3.5A). Ridges were also found, though they were lower in elevation (<0.98 m above MSL) and formed entirely of sand-sized sediments.

Boduhini and Kudahini islands possessed more variable topography with high points of 1.18 m and 1.16 m respectively (on the vegetated island surfaces). At their oceanward margins, steep rubble ridges were found (1.94 m and 1.93 m above MSL respectively), which were formed coral rubble and boulders (<0.8 m diameter). Their lagoonward margins were also characterised by rubble (<0.3 m diameter) ridges (<0.8 m above MSL). Small outcrops (*c*. <20 m^2) of beachrock were found off the lagoonward coasts of Boduhini and Kudahini. Conglomerate outcrops (*c*. 45 cm above MSL) formed headlands off the oceanward margins of Boduhini, Kudahini, and the eastern and western transects of Mainadhoo (Figure 3.5E and F). All windward islands also had sand and rubble spits which were orientated approximately perpendicular to the reef crest (Figures 3.3 and 3.4).

At the leeward site, the vegetated surfaces Galamadhoo and Baavanadhoo were also notably consistent in elevation (1.45 ± 0.02 m and 1.44 ± 0.02 m above MSL respectively; Figures 3.6 and 3.7). Galamadhoo was characterised by an asymmetrical basin-shaped morphology with higher island elevation on the lagoonward (<1.92 m above MSL) than the oceanward margin (<1.49 m). Baavanadhoo island was more uniform in elevation, though the island surface was also inclined towards the lagoonward margin. Both islands possessed seaward dipping banks of beachrock on the lagoonward margin at comparable angles to the contemporary beach (Figure 3.8C); smoother and flatter beachrock outcrops on the oceanward margin (Figure 3.8D); and stranded beachrock off the southern coasts (65 m and 230 m offshore on the lagoonward margin, and 85 m and 105 m offshore on the oceanward margin from Galamadhoo and Baavanadhoo respectively; Figure 3.8B and E). Both islands also possessed sand spits off the northern coasts, which were predominantly parallel to the reef crest (Figure 3.8A).

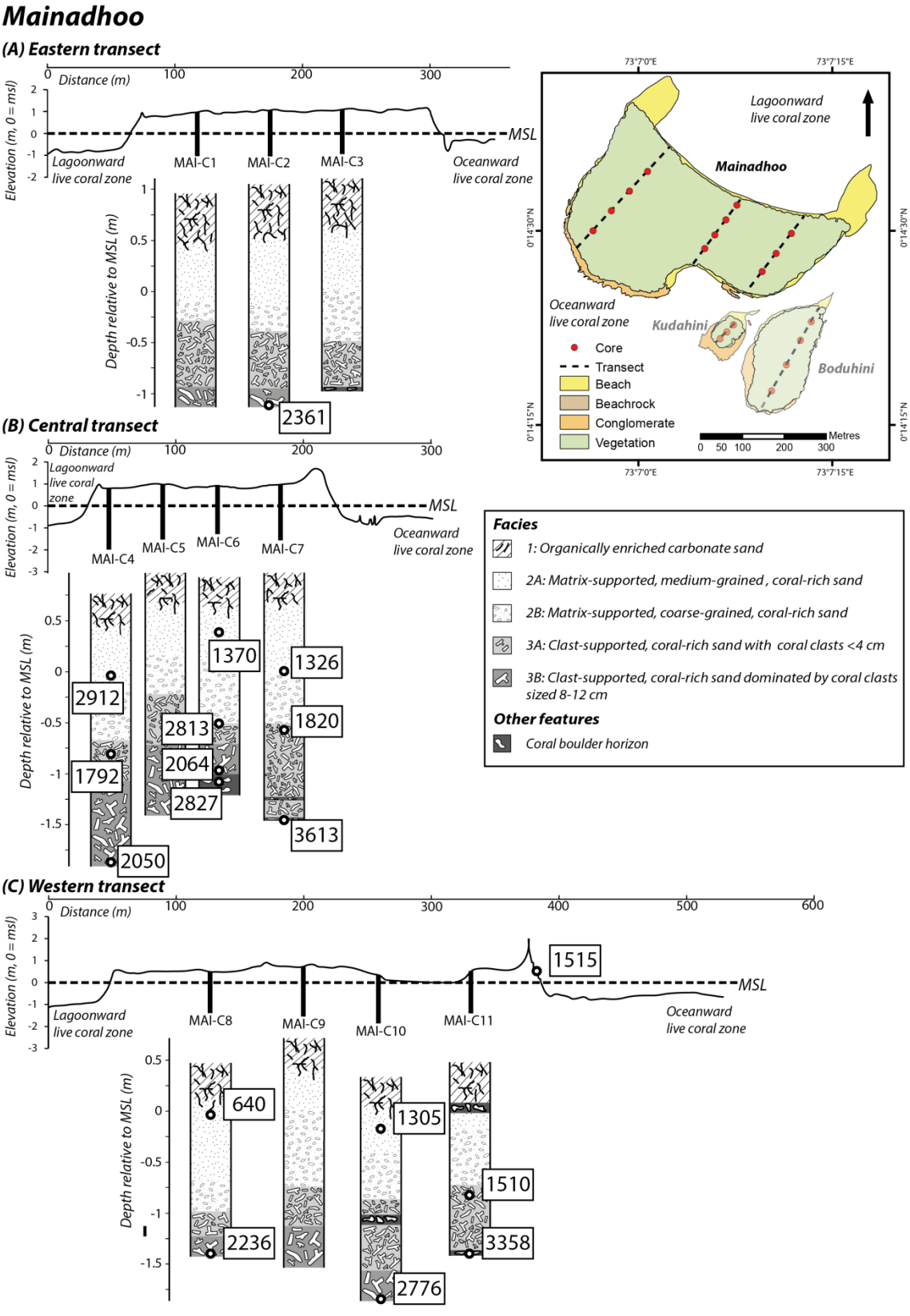

Figure 3.3 – Topographic cross-sections, planform surveys, core logs, and median radiometric dates from Mainadhoo, windward site.

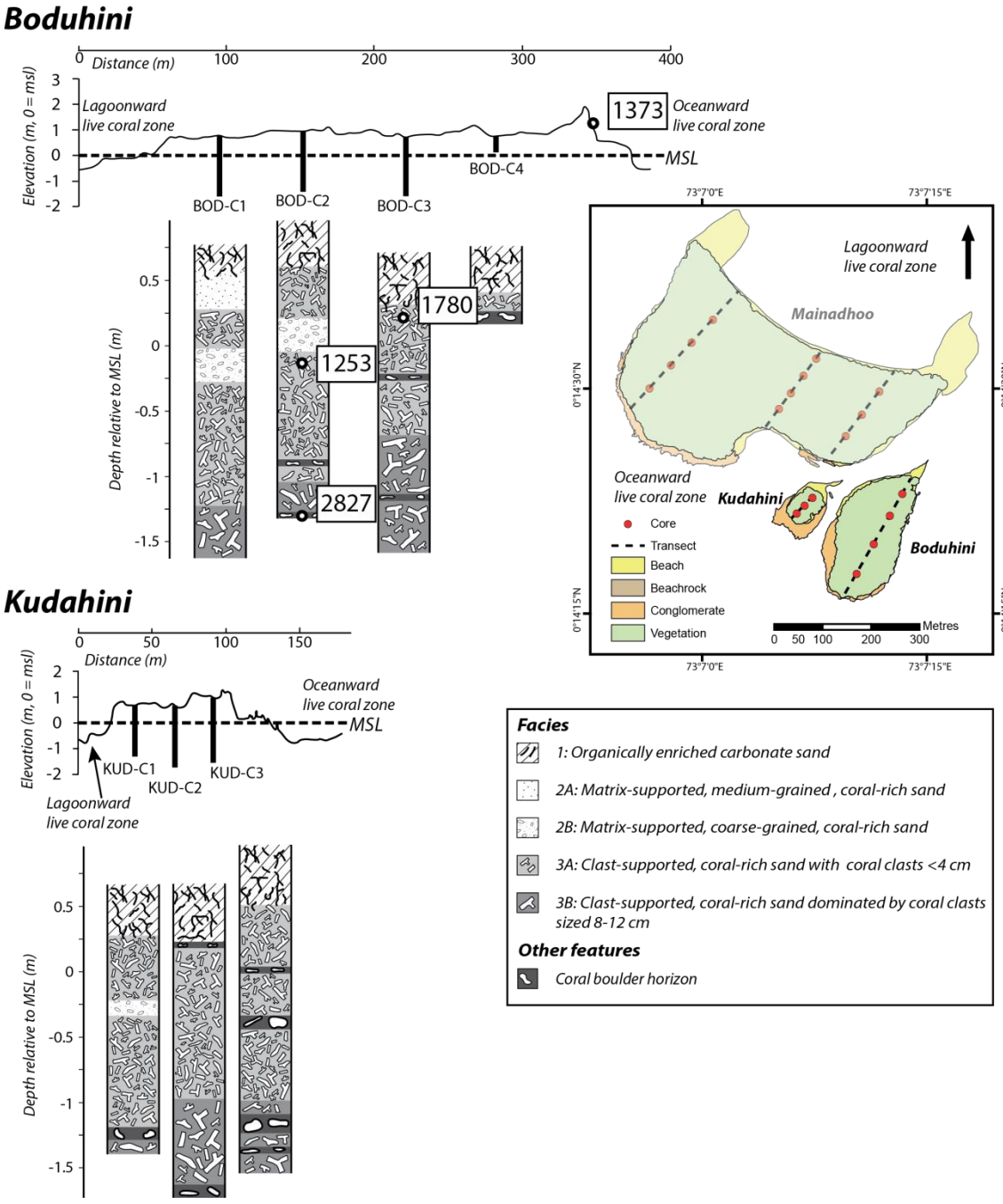

Figure 3.4 – Topographic cross-sections, planform surveys, core logs, and median radiometric dates from Boduhini and Kudahini, windward site.

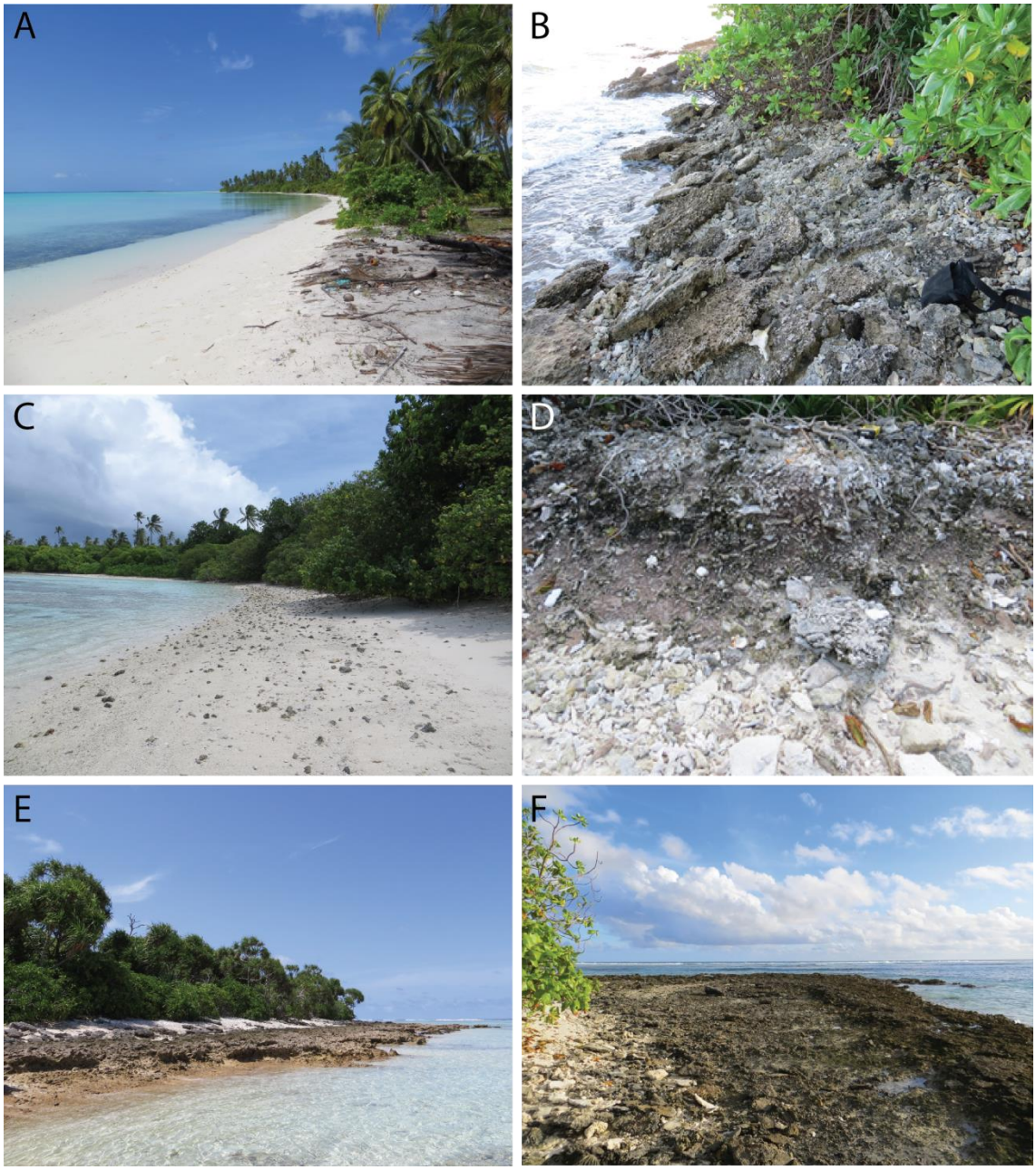

Figure 3.5 – Examples of geomorphic features at the windward study site: lagoonward island coast of Mainadhoo (A); oceanward island coast of Mainadhoo, near the western transect (B); oceanward coast of Mainadhoo, near the central transect (C); rubble ridge on the oceanward island coast of Mainadhoo, western transect (D); conglomerate platform off Boduhini (E) and Kudahini (F).

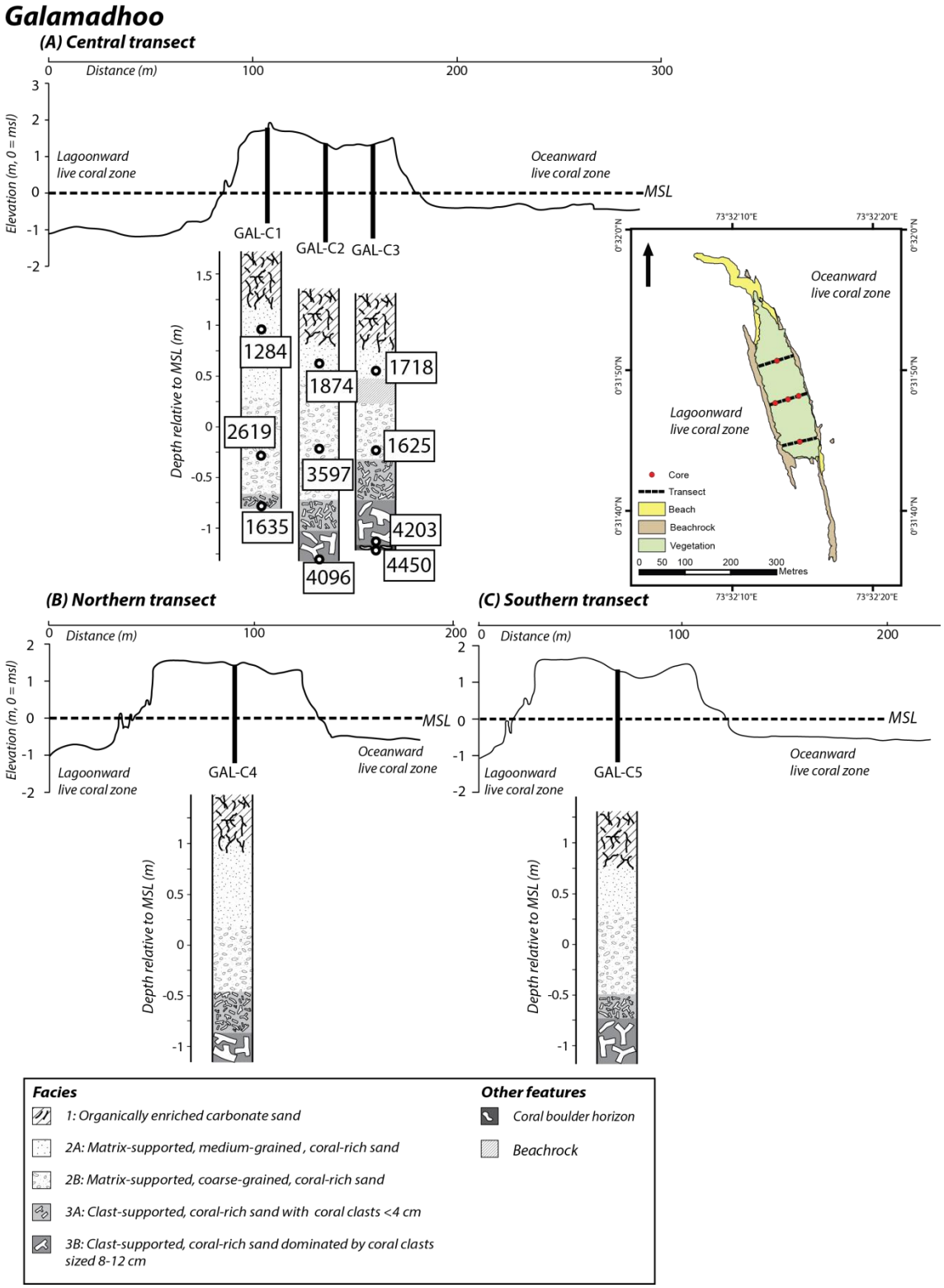

Figure 3.6 – Topographic cross-sections, planform surveys, core logs, and median radiometric dates from Galamadhoo, leeward site.

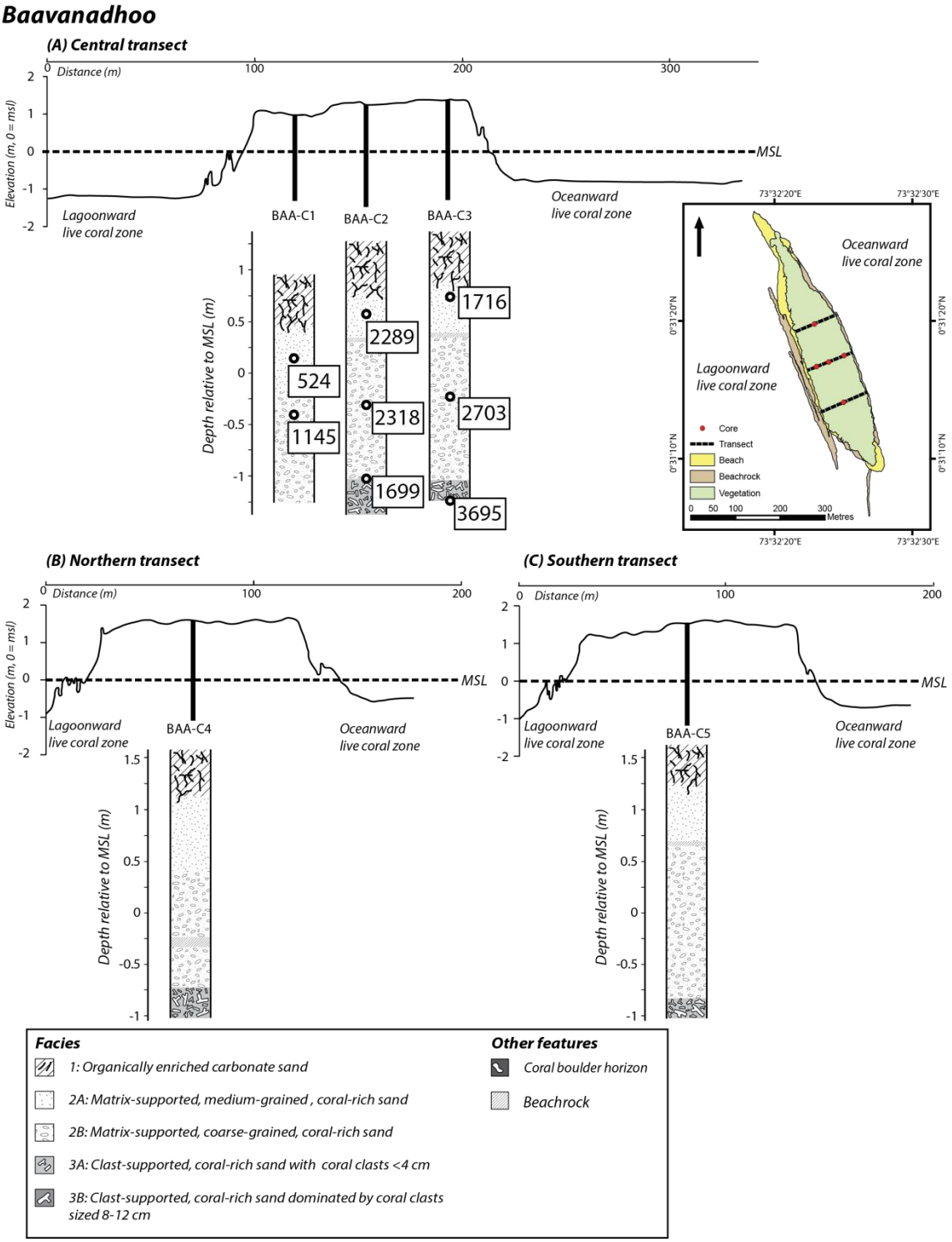

Figure 3.7 – Topographic cross-sections, planform surveys, core logs, and median radiometric dates from Galamadhoo, leeward site.

Figure 3.8 – Examples of geomorphic features at the leeward study site: northern sand spit (A); stranded beachrock off the south coast of Galamadhoo (B and E); lagoonward-dipping beachrock on the lagoonward coast of Baavanadhoo (C); and flatter beachrock on the oceanward coast of Baavanadhoo (D).

3.3.2 Reef island sedimentology and stratigraphy

At the windward site, a total of 18 reef island cores were recovered (Figures 3.3 and 3.4), 17 of which extended below the level of live coral growth on the adjacent reef flats (*c*. 0.5 m below MSL), and 6 of which terminated on a solid lithified reef surface. Cores reached a maximum depth of 1.93 m below MSL (i.e. *c*. 1.4 m below live coral growth and *c*. 2.7 m below the island surface). At the leeward site, a total of 10 reef island cores were recovered (Figures 3.6 and 3.7), all of which extended below the level of live coral growth on the adjacent reef flats (*c*. 0.5 m below MSL), and 1 of which terminated on a solid lithified reef surface. Cores reached a maximum depth of 1.45 m below MSL (i.e. *c*. 0.95 m below live coral growth and *c*. 2.9 m below the island surface).

All cores recovered an organically enriched upper horizon with varying proportions of unconsolidated carbonate sand and coral rubble (Table 3.1). Sediment composition was highly consistent between facies, islands and sites (Table 3.2; Figures 3.9 and 3.10). However, three discrete facies, and an additional two subfacies, were identified primarily on the basis of textural characteristics (Figures 3.9 to 3.11; Table 3.1).

Table 3.1 - Textural data for each facies from both windward and leeward sites, interquartile ranges (quartile 1 – quartile 3 in italics)

Site	Facies	n	Mean grain size (Φ)	Matrix mean grain size (excluding gravel, Φ)	% Gravel	% Sand	% Silt	Sorting (σ_Φ)	Gravel size	Taphonomy (median abrasive index)
Windward	1	18	0.7 ± 0.1	1.4 ± 0.1	29.4 ± 6.8	68.9 ± 6.6	1.7 ± 0.2	1.4 ± 0.1	<1 cm	3
			-0.2 - 1.5	*0.9 - 1.7*	*3.7 - 52.2*	*46.8 - 93.5*	*1.0 - 2.2*	*1.2 - 1.5*		*3-3*
	2A	12	1.2 ± 0.2	1.6 ± 0.1	15.3 ± 6.8	82.6 ± 6.7	2.1 ± 0.7	1.3 ± 0.1	< 1 cm	
			1.1 - 1.7	*1.4 - 1.9*	*2.2 - 14.5*	*83.4 - 95.3*	*0.7 - 2.3*	*1.1 - 1.6*		
	2B	14	0.8 ± 0.2	1.4 ± 0.1	21.4 ± 4.6	76.2 ± 4.4	2.4 ± 0.3	1.6 ± 0.1	< 1 cm	
			0.6 - 1.4	*1.3 - 1.7*	*9.9 - 26.1*	*72.2 - 87.7*	*1.5 - 3.0*	*1.5 - 1.7*		
	3A	18	0.6 ± 0.2	1.9 ± 0.1	40.6 ± 4.9	56.1 ± 4.8	3.3 ± 0.6	1.9 ± 0.1	< 4 cm	4
			0.2 - 1.1	*1.7 - 2.0*	*31.0 - 49.4*	*48.5 - 66.7*	*2.1 - 3.5*	*1.7 - 1.9*		*3-4*
	3B	14	0.4 ± 0.1	1.8 ± 0.1	47.7 ± 3.6	49.6 ± 3.4	2.7 ± 0.4	1.9 ± 0.1	< 12 cm	3
			0.0 - 0.6	*1.7 - 2.0*	*45.2 - 53.4*	*44.6 - 51.6*	*1.7 - 4.0*	*1.8 - 2.0*		*3-4*
Leeward	1	10	1.2 ± 0.1	1.2 ± 0.1	1.8 ± 0.6	96.6 ± 0.6	1.7 ± 0.2	1.1 ± 0.0	<1 cm	
			1.1 - 1.3	*1.1 - 1.3*	*0.4 - 2.0*	*96.2 - 97.7*	*1.4 - 2.1*	*1.1 - 1.2*		
	2A	10	1.1 ± 0.1	1.2 ± 0.1	1.8 ± 0.4	97.4 ± 0.4	0.8 ± 0.3	0.9 ± 0.1	< 1 cm	
			0.9 - 1.2	*1.0 - 1.3*	*0.9 - 2.6*	*96.7 - 98.2*	*0.3 - 0.9*	*0.8 - 1.0*		
	2B	10	0.7 ± 0.1	1.0 ± 0.1	9.4 ± 1.9	89.2 ± 1.9	1.4 ± 0.3	1.2 ± 0.1	< 1 cm	
			0.6 - 0.8	*0.8 - 1.1*	*6.2 - 13.0*	*86.0 - 92.7*	*0.8 - 1.8*	*1.1 - 1.3*		
	3A	9	0.2 ± 0.1	1.4 ± 0.0	45.6 ± 3.1	53.1 ± 3.1	1.3 ± 0.2	1.7 ± 0.0	< 4 cm	3
			0.1 - 0.3	*1.3 - 1.5*	*36.2 - 49.4*	*49.7 - 62.4*	*1.0 - 1.7*	*1.6 - 1.7*		*3-3*
	3B	4	-0.1 ± 0.2	1.7 ± 0.1	60.2 ± 6.8	38.2 ± 6.8	1.6 ± 0.4	1.7 ± 0.0	< 12 cm	4
			-0.3 - 0	*1.6 - 1.7*	*55.6 - 68.5*	*29.8 - 43.4*	*1.3 - 2.2*	*1.6 - 1.8*		*4-4*

Site	Facies	Coral	CCA	Mollusc	Foraminifera	Echinoid	*Halimeda*	Unidentified
Windward	2A	78.8 ± 0.0	12.8 ± 1.1	5.2 ± 0.8	1.4 ± 0.5	0.7 ± 0.2	0.7 ± 0.2	0.1 ± 0.0
		74.3 - 83.2	*10.3 - 15.0*	*3.3 - 6.8*	*0.1 - 1.8*	*0.3 - 0.9*	*0.1 - 1.2*	*0.0 - 0.0*
	2B	73.4 ± 1.6	12.6 ± 0.8	8.6 ± 1.0	2.6 ± 0.7	1.3 ± 0.2	1.0 ± 0.2	0.0 ± 0.0
		67.9 - 77.4	*11.8 - 14.5*	*6.4 - 10.4*	*0.9 - 3.5*	*0.9 - 1.7*	*0.4 - 1.3*	*0.0 - 0.0*
	3A	78.8 ± 1.2	10.8 ± 0.7	7.5 ± 0.7	1.3 ± 0.3	0.5 ± 0.1	1.0 ± 0.3	0.0 ± 0.0
		75.8 - 82.4	*9.7 - 11.4*	*5.3 - 8.7*	*0.4 - 1.6*	*0.1 - 0.6*	*0.3 - 1.3*	*0.0 - 0.0*
	3B	79.2 ± 1.1	10.5 ± 0.8	7.2 ± 0.6	0.8 ± 0.1	0.6 ± 0.1	1.6 ± 0.4	0.1 ± 0.0
		76.6 - 81.0	*8.7 - 11.7*	*5.8 - 8.7*	*0.4 - 1.3*	*0.3 - 0.9*	*0.6 - 2.1*	*0.0 - 0.1*
Leeward	2A	78.6 ± 1.4	12.6 ± 0.8	6.3 ± 0.8	3.0 ± 0.7	0.4 ± 0.1	0.3 ± 0.1	0.1 ± 0.1
		75.1 - 82.1	*10.6 - 14.0*	*4.5 - 7.9*	*1.2 - 4.0*	*0.0 - 0.6*	*0.0 -0.4*	*0.0 - 0.0*
	2B	73.4 ± 1.3	9.4 ± 0.8	12.7 ± 0.7	4.0 ± 0.7	0.7 ± 0.1	1.0 ± 0.1	0.0 ± 0.1
		69.6 - 76.9	*8.8 - 10.1*	*8.6 - 16.6*	*2.7 - 4.8*	*0.3 - 0.7*	*0.7 -1.2*	*0.0 - 0.0*
	3A	71.2 ± 1.2	9.3 ± 0.5	16.0 ± 1.1	2.8 ± 0.4	0.3 ± 0.1	1.0 ± 0.2	0.1 ± 0.1
		68.6 - 73.3	*8.6 - 9.7*	*14.1 - 17.7*	*1.9 - 3.7*	*0.1 - 0.5*	*0.9 - 1.4*	*0.0 - 0.0*
	3B	77.5 ± 5.3	6.1 ± 1.0	12.7 ± 4.4	1.0 ± 0.1	0.5 ± 0.4	2.6 ± 0.8	0.0 ± 0.0
		71.3 - 85.3	*4.7 - 7.5*	*6.1 - 17.4*	*0.8 - 1.1*	*0.1 - 0.5*	*1.8 - 2.8*	*0.0 - 0.0*

Table 3.2 – Compositional (%) data for each facies from both windward and leeward sites, interquartile ranges (quartile 1 – quartile 3) in italics.

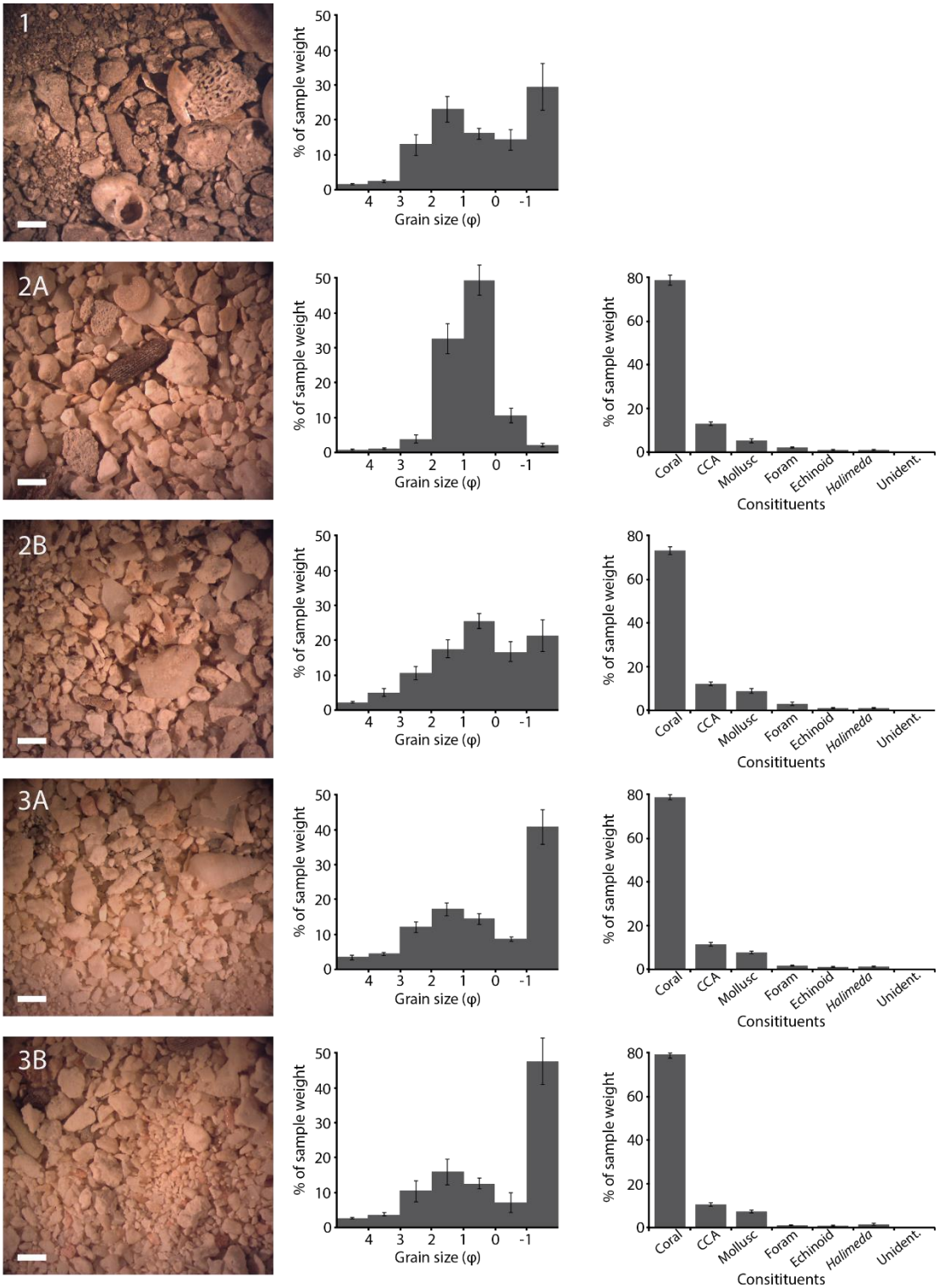

Figure 3.9 – Windward site facies: images (white bar = 1 mm), grain size distributions and compositional data.

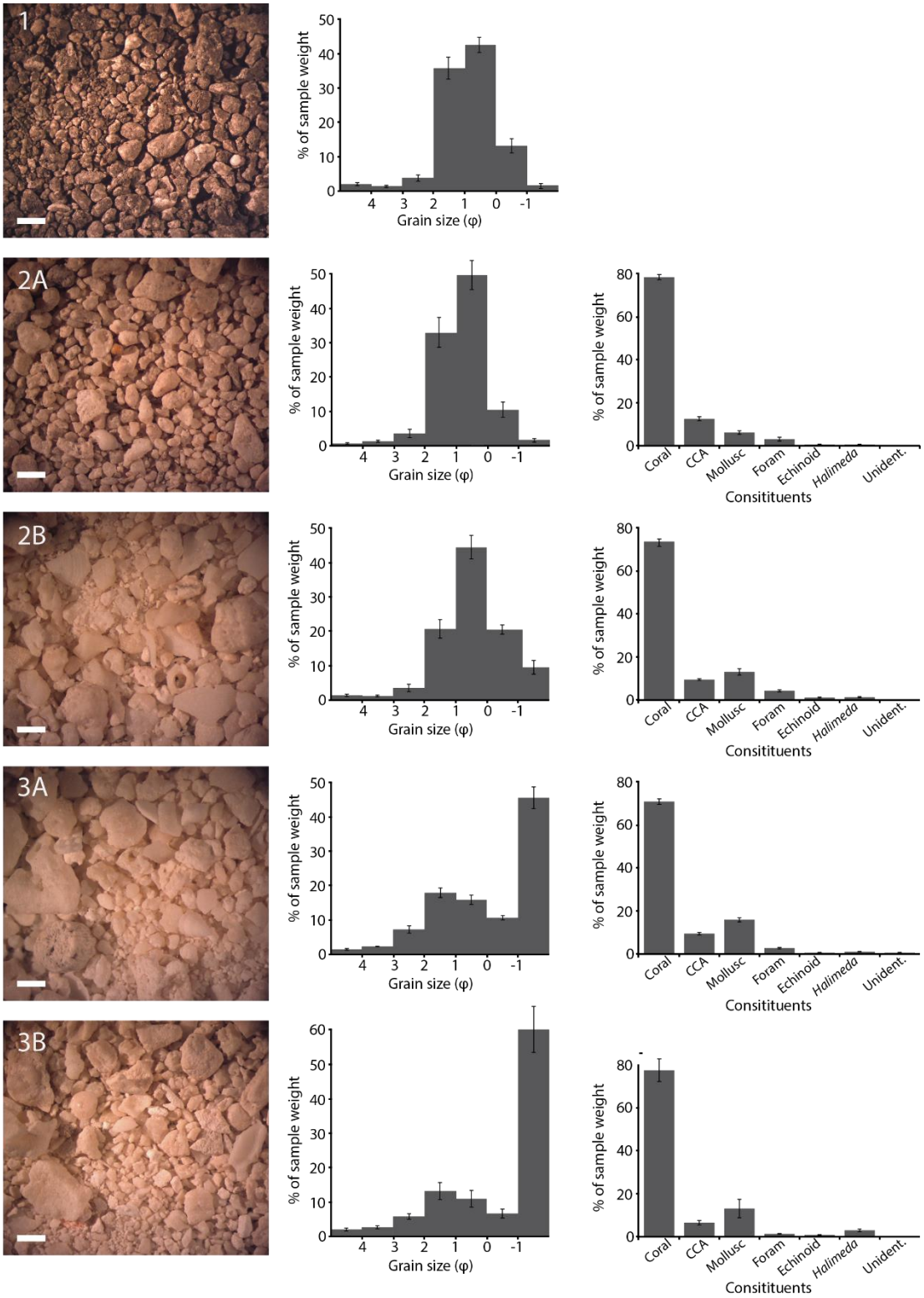

Figure 3.10 - Leeward site facies: images (white bar = 1 mm), grain size distributions and compositional data.

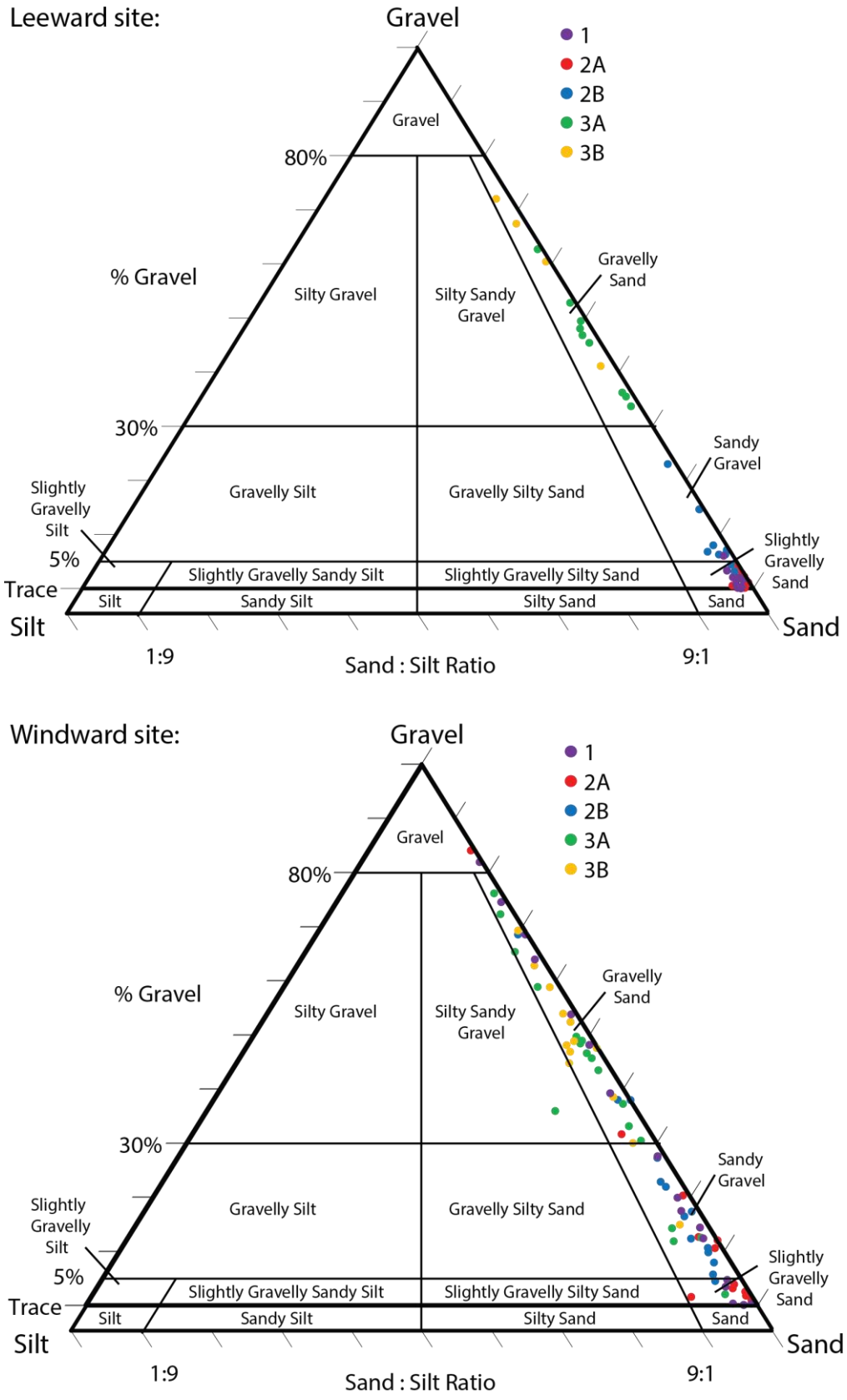

Figure 3.11 - Ternary plots of grain size data from each island sediment sample recovered from the windward and leeward sites

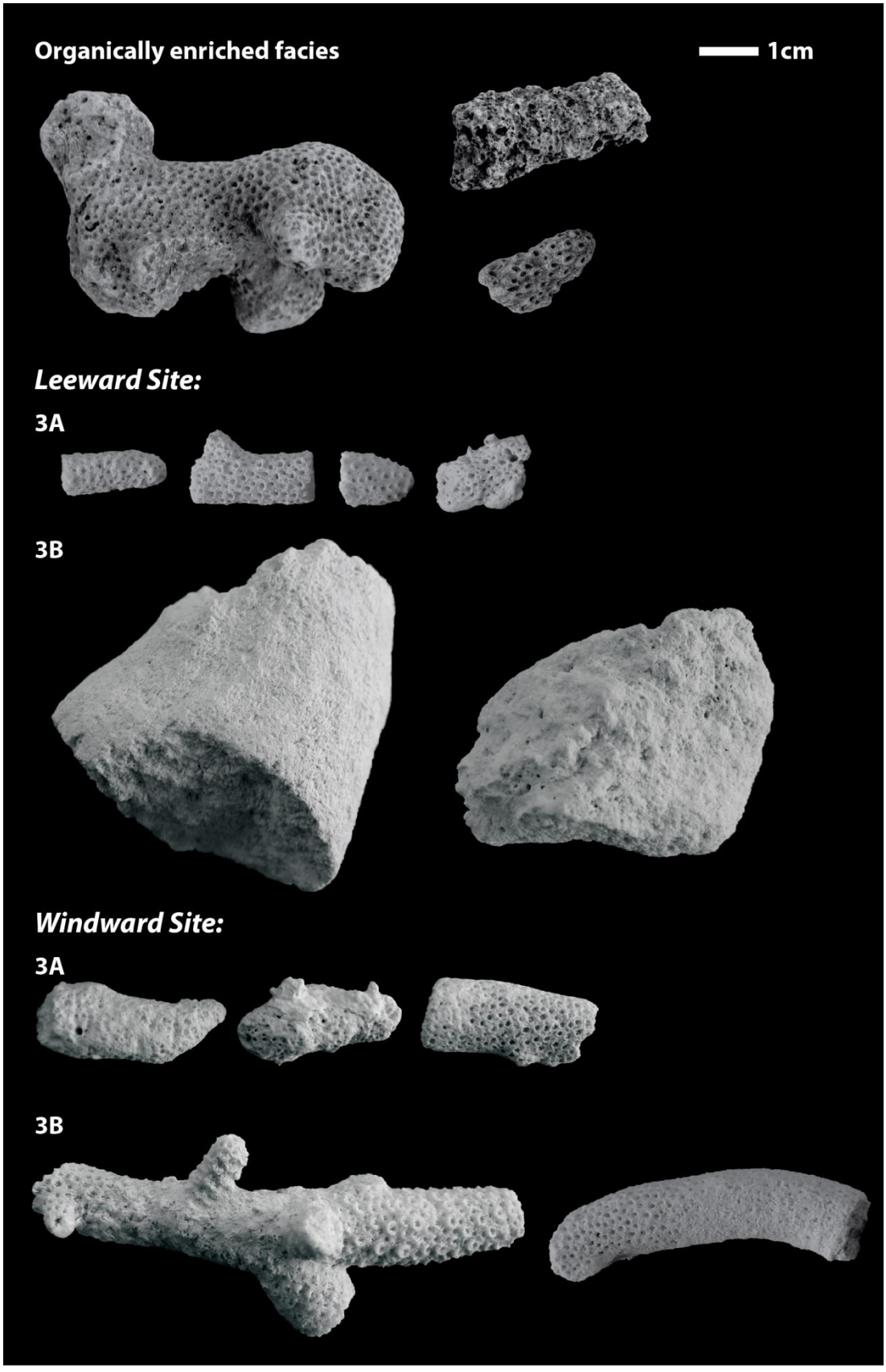

Figure 3.12 – Examples of coral clasts > 1 cm recovered from each facies

	Windward site		Leeward site	
	3A	3B	3A	3B
Unidentifiable	46.4 ± 8.94%	19.1 ± 9.1%	4.5 ± 2.7%	76.7 ± 13.9 %
Acropora spp.	70.1 ± 9.2%	83.8 ± 10.9%	82.0 ± 9.7%	100.0 ± 0.0%
Pocillopora sp.	15.2 ± 6.6%	-	5.4 ± 3.0%	-
Porites sp.	2.4 ± 2.4%	0.1 ± 0.1%	10.0 ± 10.0%	-
Fungi sp.	-	-	2.6 ± 2.6%	-
Stylophora pisti	3.1 ± 2.5%	7.7 ± 7.7%	-	-
Montipora sp.	3.3 ± 3.3%	-	-	-

Table 3.3 – Identification of coral clasts (with longest axes >1 cm) within facies 3 at the windward and leeward sites. Proportion of unidentifiable coral clasts is given as a proportion of total clast weight. Compositional data is provided as a proportion of the weight of identifiable clasts.

Facies 1: Organically enriched carbonate sand

This reef island 'soil' facies was characterised by the presence of organic matter, a well-developed root horizon and its brown-ish colour. Its thickness was relatively consistent within sites – ~0.5 m (~1.45–0.95 m above MSL) and ~0.3 m (~0.8–0.5 m above MSL) at the leeward and windward sites respectively. Samples contained 6.0 ± 0.6% organic matter at the windward site and 7.8 ± 0.9% at the leeward site. Sediment was coarse-grained (0.7 ± 0.1 Φ at both sites) and poorly sorted (1.1 ± 0.0 Φ and 1.4 ± 0.1 Φ at the leeward and windward sites respectively), and primarily sand-sized (leeward: 96.6 ± 0.6% and windward: 68.9 ± 6.6%).

At the leeward site, all gravel-sized material (18.2 ± 3.5%) was <1 cm along the longest axis (clast-matrix ratio 0:1). At the windward site, there was 31.7 ± 2.8% gravel-sized material and coral clasts were also primarily < 1 cm (clast-matrix ratio 1:9) with the exception of those from the cores nearest the oceanward reef crest – cores 10 and 11 on Mainadhoo and all organically enriched samples from Boduhini and Kudahini. Of the windward site coral clasts with longest axes >1 cm, a median AI score of 3 was found and 46.0 ± 9.5% of clasts were unidentifiable (Figure 3.12). The identifiable clasts comprised 40.3 ± 14.2% *Acropora spp.*, 36.2 ± 17.3% *Stylophora pistillata* and 23. ± 12.1% *Pocillopora sp.* (Table 3.3).

Facies 2: Matrix-supported coral-rich sand

Facies 2 was matrix-supported and divided into two subfacies primarily on the basis of mean grain size whereby 2A and 2B were characterised by medium- (leeward: 1.1

± 0.1 Φ, windward: 1.2 ± 0.2 Φ) and coarse-grained (leeward: 0.7 ± 0.1 Φ, windward: 0.8 ± 0.2 Φ) sediments respectively. Sediment was predominantly sand sized (2A: 97.4 ± 0.4%, 82.6 ± 6.7%; 2B: 89.2 ± 1.9%, 76.2 ± 4.4%) with the longest axes of all coral clasts <1 cm (clast:matrix ratio = 0:1). 2A was moderately sorted at the leeward site (0.9 ± 0.1 Φ) and poorly sorted at the windward site (1.3 ± 0.1 Φ), while 2B was poorly sorted at both sites (1.2 ± 0.1 Φ, 1.6 ± 0.1 Φ).

Coral was the dominant sedimentary constituent, accounting for ~79% and ~73% (mean values – Table 3.2) of subfacies 2A and 2B respectively. CCA was of secondary importance accounting for ~12% of facies 2, though slightly lower concentrations were found within subfacies 2B at the leeward site (9.4 ± 0.8%). Concentrations of molluscs were correspondingly relatively high within subfacies 2B at the leeward site (12.7 ± 0.7%). Proportions of molluscs within other facies 2 samples were ~5-8% (Table 3.2).

At the leeward site, 2A was identified ~1.2– -0.25 m relative to MSL (thickness = 0.35–0.95 m) and 2B was found ~0.6– -1.3 m relative to MSL (thickness = 0.55–1.5 m). This variability occured along an oceanward-lagoonward gradient with depth of penetration and thickness increasing toward the lagoonward coast. At the windward site, on Maindadhoo, 2A was 0.4–0.8 m thick and identified between ~0.65 and -0.65 m relative to MSL. Thickness and depth of penetration also increased toward the lagoon. Facies 2B (thickness = 0.2–0.75 m), terminated at relatively consistent depths within each transect on Mainadhoo (*e.g.* central transect = ~0.5 m below MSL). On Boduhini and Kudahini, facies 2 was only identified in lagoonward cores and 2A was absent from Kudahini (Figure 3.4).

Facies 3: Clast-supported coral-rich sand

Facies 3 was defined by its clast-supported character and was divided into subfacies on the basis of clast size. Subfacies 3A was characterised by coral clasts with longest axes <4 cm, whilst 3B was dominated by clasts sized between 8 and 12 cm (*i.e.* as large as could be recovered given the core width). In addition, 3A and 3B were distinguished by differences in taphonomy. Systematic variability was found between sites whereby, at the leeward site, clasts within 3A were less degraded (AI = 3) than those at the windward site (AI = 4). Conversely, clasts within 3B were more degraded at the leeward site (AI = 4) than at the windward site (AI = 3). The mean grain size of the matrix was again medium-grained (average values = 1.4–1.9 Φ; Table 3.1), though

overall mean grain-size was coarse (average values = -0.1–0.6 Φ) as the proportion of gravel-sized material increased. Proportions of gravel-sized material were larger at the windward site (3A: 45.6 ± 3.1%; 3B: 60.2 ± 6.8%) than at the leeward site (3A: 40.6 ± 4.9%; 3B: 47.7 ± 3.6%). Clast-matrix ratio was approximately 4:10 (3A) and 5.5:10 (3B) at the leeward site, and 3.5:10 (3A) and 4:10 (3B) at the windward site (Table 3.1).

Composition was largely consistent with that of facies 2 whereby coral was the dominant constituent (mean values = 71.2–79.2%; Table 3.2). Proportions of CCA (means = 9.3–12.7%) were also comparable to those found within facies 2. Mollusc concentrations at the windward site (means = 7.2–7.5%) were approximately consistent with those within facies 2. However, concentrations of molluscs were relatively higher at the leeward site (3A: 16.0 ± 1.1%; 3B: 12.7 ± 4.4%) than both those found within facies 3 at the windward site and facies 2 at either site. The majority of identifiable coral clasts (longest axes >1 cm) were *Acropora spp.* (mean values = 70.1–100.0%; Table 3.3).

At the leeward site, 3A occured ~-0.35– -1.45 m relative to MSL (thickness = 0.15–0.4 m) and 3B was found ~-0.75– -1.3 m relative to MSL (thickness = 0.3–0.45 m), but was not identified on Baavanadhoo. In contrast to facies 2, the thickness and minimum depth of facies 3 increased toward the oceanward coast (Figure 3.6). At the windward site, facies thickness varied with the greatest thicknesses on Boduhini and Kudahini (3A: 0.15–1.4 m; 3B: 0.2–0.85 m), but the 3A-3B interface was found at relatively consistent depths within each transect (*e.g.* central transect of Mainadhoo = ~1 m below MSL). The exception was the cores nearest the oceanward coast within which facies 2B was not found (Figure 3.4).

Oceanward-lagoonward gradient in reef island sedimentology

While discrete sedimentary facies were identified, a weak positive oceanward-lagoonward trend was also found whereby grain size coarsened with closer proximity to the oceanward reef crest (Figure 3.13). This relationship was significant at both study sites, though was slightly more pronounced at the windward site ($P = <0.001$, $R^2 = 0.203$) than the leeward site ($P = 0.008$, $R^2 = 0.16$).

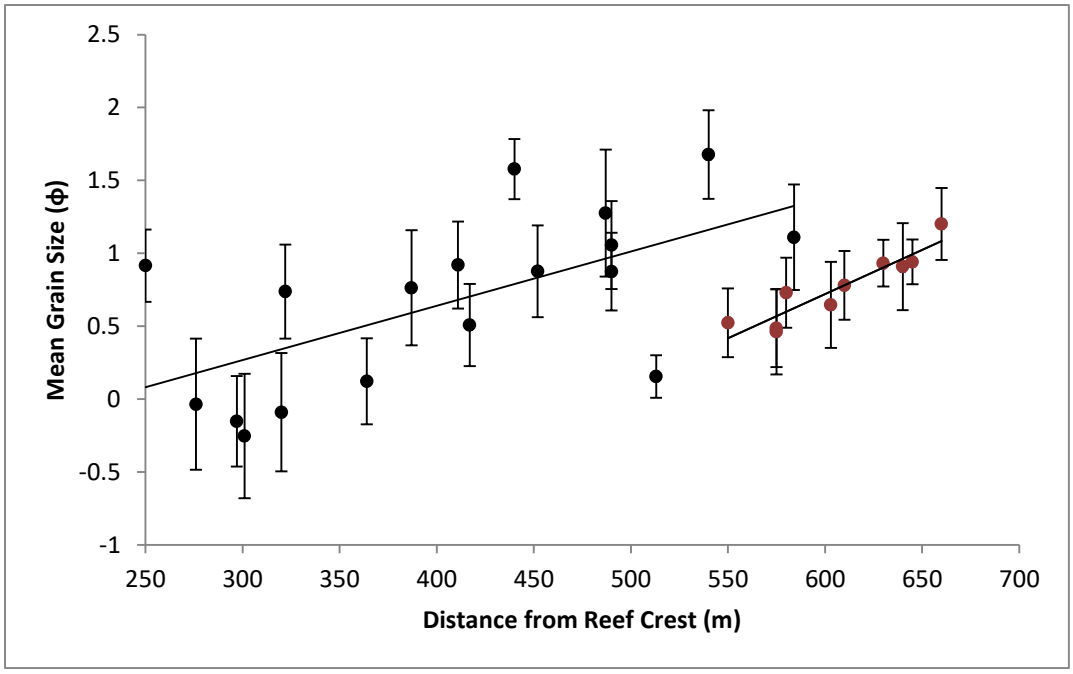

Figure 3.13 – Relationship between grain size and distance from the oceanward reef crest at windward (black) and leeward (red) sites. Regression for individual sample grain size vs. distance from reef crest: windward site, P = <0.001, R^2 = 0.203; leeward site, P = 0.008, R^2 = 0.16).

3.3.3 Reef island chronologies

The 40 AMS radiocarbon dates and their associated error terms are detailed in Table 3.4. The radiocarbon dates discussed throughout this chapter are the median of the calibrated age range, though the associated error terms must be borne in mind in the interpretation of these values. However, the average range between upper and lower estimates, with 95.4% probabilities, was 160 years. This is notably smaller than the time periods suggested for each of the stages in the conceptual models (section 4.3). A total of 22 AMS radiocarbon dates were obtained from the windward site (Figures 3.3 and 3.4). Age inversions were found within 2 cores, both of which were located on the central transect of Mainadhoo. Dates ranged from 3,613 calibrated years Before Present (cal. yr. B.P.) at the base of the oceanward core on the central transect of Mainadhoo (MAI-C7), to 640 cal. yr. B.P. within facies 2A toward the lagoonward coast (MAI-C8). Notably, dates from the interface between facies 2 and 3 (n = 4), and also from the upper surface of the conglomerate platform (n = 2) were relatively consistent (between ~1,400 and ~1,800 cal. yr. B.P.). There was one exception to this consistency, which was within core MAI-C6, which contained an age inversion.

A total of 18 AMS radiocarbon dates were obtained from the leeward site (Figures 3.6 and 3.7; Table 3.4). Age inversions were found in 3 cores. Dates ranged from 4,450 cal. yr. B.P. at the base of the oceanward core on Galamadhoo (GAL-C3), to 524 cal. yr. B.P. for the upper date from the lagoonward core of Baavanadhoo (BAA-C1). Dates from the interface between facies 2 and 3 were, again, notably consistent (~1,600 to 1,700 cal. yr. B.P., n = 3).

	Island	Lab code	Facies	Depth relative to MSL (m)	Material	Conventional age (yr. B.P.)	Calibrated age range, 63.8% probability (cal. yr. B.P.)	Calibrated age range, 95.4% probability (cal. yr. B.P.)	Median
Windward site	Mainadhoo	MAI-C2-210	3B	-1.05	*Acropora*	2797 ± 46	2301 - 2418	2207 - 2510	2361
	Mainadhoo	MAI-C4-80	2A	0.02	*Halimeda*	3265 ± 43	2844 - 2972	2786 - 3045	2912
	Mainadhoo	MAI-C4-160	2B-3A	-0.78	Gastropod	2327 ± 45	1731 - 1851	1676 - 1913	1792
	Mainadhoo	MAI-C4-270	3B	-1.88	*Acropora*	2547 ± 43	1989 - 2110	1917 - 2173	2050
	Mainadhoo	MAI-C6-60	2A	0.29	Gastropod	1960 ± 45	1303 - 1411	1282 - 1491	1370
	Mainadhoo	MAI-C6-140	2B-3A	-0.51	*Halimeda*	3177 ± 45	2753 - 2852	2728 - 2925	2813
	Mainadhoo	MAI-C6-190	3B	-1.01	*Halimeda*	2558 ± 43	1997 - 2120	1926 - 2201	2064
	Mainadhoo	MAI-C6-200	C*	-1.11	*Porites*	3192 ± 45	2761 - 2870	2736 - 2941	2827
	Mainadhoo	MAI-C7-100	2A-2B	-0.05	Gastropod	1913 ± 43	1281 - 1363	1242 - 1426	1326
	Mainadhoo	MAI-C7-155	2B-3A	-0.6	Gastropod	2351 ± 43	1762 - 1878	1701 - 1928	1820
	Mainadhoo	MAI-C7-245	C	-1.5	*Porites*	3829 ± 44	3555 - 3676	3476 - 3747	3613
	Mainadhoo	MAI-C8-50	2A	-0.02	Bivalve shell	1207 ± 43	604 - 681	547 - 710	640
	Mainadhoo	MAI-C8-195	3B	-1.47	Gastropod	2698 ± 45	2179 - 2302	2120 - 2335	2236
	Mainadhoo	MAI-C10-50	2A	-0.17	Gastropod	1887 ± 43	1264 - 1342	1224 - 1395	1305
	Mainadhoo	MAI-C10-220	3B	-1.87	Acropora	3134 ± 45	2729 - 2817	2696 - 2877	2776
	Mainadhoo	MAI-C11-130	2B-3A	-0.81	Gastropod	2089 ± 43	1440 - 1564	1383 - 1622	1510
	Mainadhoo	MAI-C11-190	C	-1.41	Coral - *Porite*	3608 ± 44	3311 - 3425	3228 - 3463	3358
	Mainadhoo	MAI-CP	CP**	0.35	Coral clast fr	2093 ± 43	1447 - 1453	1386 - 1629	1515
	Boduhini	BOD-C2-110	2B-3A	-0.16	Foraminifera	1825 ± 32	1223 - 1286	1175 - 1309	1253
	Boduhini	BOD-C2-235	C	-1.41	Coral - *Porite*	3193 ± 44	2762 - 2870	2737 - 2941	2827
	Boduhini	BOD-C3-60	3A	0.11	*Halimeda*	2317 ± 45	1717 - 1837	1654 - 1897	1780
	Boduhini	BOD-CP	CP	0.4	Coral clast fr	1963 ± 43	1306 - 1413	1285 - 1490	1373
Leeward site	Galamadhoo	GAL-C1-75	2A	0.97	Foraminifera	1863 ± 45	1243 - 1327	1185 - 1371	1284
	Galamadhoo	GAL-C1-200	2B	-0.28	*Halimeda*	2986 ± 45	2552 - 2558	2465 - 2731	2619
	Galamadhoo	GAL-C1-255	2B-3A	-0.83	Gastropod	2195 ± 45	1570 - 1691	1523 - 1761	1635
	Galamadhoo	GAL-C2-70	2A	0.66	Foraminifera	2397 ± 44	1815 - 1927	1750 - 1989	1874
	Galamadhoo	GAL-C2-160	2B	-0.23	*Halimeda*	3816 ± 43	3543 - 3665	3462 - 3716	3597
	Galamadhoo	GAL-C2-270	3B	-1.34	*Acropora*	4195 ± 45	4005 - 4158	3950 - 4240	4096
	Galamadhoo	GAL-C3-75	2A	0.56	Foraminifera	2263 ± 43	1663 - 1792	1592 - 1835	1718
	Galamadhoo	GAL-C3-155	2B-3A	-0.24	Bivalve shell	2186 ± 44	1564 - 1682	1515 - 1747	1625
	Galamadhoo	GAL-C3-250	3B	-1.19	*Halimeda*	4269 ± 43	4131 - 4277	4070 - 4357	4203
	Galamadhoo	GAL-C3-252	C	-1.21	*Porites*	4450 ± 45	4394 - 4510	4301 - 4576	4450
	Baavanadhoo	BAA-C1-80	2A	0.16	*Halimeda*	1047 ± 48	480 - 557	457 - 619	524
	Baavanadhoo	BAA-C1-130	2B	-0.34	Foraminifera	1714 ± 45	1085 - 1206	1035 - 1256	1145
	Baavanadhoo	BAA-C2-70	2A	0.56	Gastropod	2740 ± 44	2209 - 2215	2145 - 2397	2289
	Baavanadhoo	BAA-C2-160	2B	-0.34	Coral	2764 ± 43	2267 - 2381	2172 - 2444	2318
	Baavanadhoo	BAA-C2-230	2B-3A	-1.04	Gastropod	2248 ± 45	1628 - 1763	1569 - 1816	1699
	Baavanadhoo	BAA-C3-60	2A	0.76	Foraminifera	2260 ± 32	1671 - 1780	1609 - 1812	1716
	Baavanadhoo	BAA-C3-160	2B	-0.23	Foraminifera	3045 ± 35	2675 - 2737	2570 - 2571	2703
	Baavanadhoo	BAA-C3-263	3A	-1.26	Coral	3892 ± 44	3624 - 3763	3572 - 3822	3695

Table 3.4 – Radiometric dates from the windward and leeward study sites and their associated error terms. *C = Consolidated underlying substrate; **CP = Conglomerate platform.

3.3.4 Volumetric sediment storage

First order estimations of the volumes of gravel-, sand- and fine-grade sediment stored within each facies at both the windward and leeward sites are presented in Tables 3.5 and 3.6 respectively. Such estimates highlight that the proportion of gravel-sized material within the leeward site islands (17%) is substantially lower than within the windward-site islands (30%). Moreover, the volume of sediment stored within the windward site islands (~433,839 m^3) was almost twice that in the leeward site islands (~224828 m^3). This is primarily a function of island planform area as windward site island area (66,509 m^2) markedly exceeded that at the windward site (187,668 m^3).

The predominant period of island accumulation was ~3,000 and ~4,000 years at the windward and leeward sites respectively. While island accretion was likely at least partially episodic, average long-term island accumulation rates can be derived of ~63 $m^3\ yr^{-1}$ and ~17 $m^3\ yr^{-1}$ at the windward and leeward sites respectively. Long term accumulation rates of each facies can also be estimated, though such rates are only very approximate due to the uncertainties in constraining their timeframes of accumulation. At the windward site, facies 1, 2 and 3 accumulated at rates of roughly 118 $m^3\ yr^{-1}$, 206 $m^3\ yr^{-1}$ and 84 $m^3\ yr^{-1}$ respectively (assuming they accreted within timeframes of 600, 900 and 2,100 years). At the leeward site, facies 1, 2 and 3 accumulated at rates of roughly 88 $m^3\ yr^{-1}$, 128 $m^3\ yr^{-1}$ and 16 $m^3\ yr^{-1}$ respectively (assuming they accreted within timeframes of 500, 1,100 and 2,500 years).

Island	Facies	Total sediment storage (m^3)	Gravel (m^3)	Sand (m^3)	Fines (m^3)
Mainadhoo	1	62079	18251	42773	1055
	2a	99166	15172	81911	2082
	2b	82235	17598	62663	1974
	3a	91103	36988	51109	3006
	3b	50792	24228	25193	1371
Boduhini	1	7380	2170	5085	125
	2a	1581	242	1306	33
	2b	2636	564	2008	63
	3a	20031	8133	11238	661
	3b	8171	3897	4053	221
Kudahini	1	1267	372	873	22
	2a	0	0	0	0
	2b	140	30	106	3
	3a	5444	2210	3054	180
	3b	1815	866	900	49
	Total	433839	130722 *(30%)*	292271 *(67%)*	10846 *(3%)*

Table 3.5 – First order estimates of the volumes of gravel-, sand- and fine-grade sediment stored within each facies at the windward site.

Island	Facies	Total sediment storage (m^3)	Gravel (m^3)	Sand (m^3)	Fines (m^3)
Galamadhoo	1	17050	5013	11747	290
	2a	13640	2087	11266	286
	2b	28984	6203	22086	696
	3a	11935	4845	6695	394
	3b	12787	6099	6342	345
Baavanadhoo	1	27115	488	26167	460
	2a	28894	520	28142	231
	2b	69525	6535	62017	973
	3a	14898	6794	7911	194
	3b	0	0	0	0
	Total	224828	38584 *(17%)*	182374 *(81%)*	3870 *(2%)*

Table 3.6 – First order estimates of the volumes of gravel-, sand- and fine-grade sediment stored within each facies at the leeward site.

3.3.4 GPR traces

At the leeward site, a GPR trace was obtained from the central transect of Baavanadhoo (Figure 3.14). Stratigraphy from the upper c. 0.5 m appeared relatively horizontal and was congruent with facies 1 (the ‘organically enriched’ horizon). Most

notably, reflections below the upper 0.5 m were found to be lagoonward-dipping. No notable reflections were found below *c*. -1.5 m (relative to MSL).

At the windward site, dense vegetation rendered GPR surveys impossible across Bduhini, Kudahini and the majority of Mainadhoo. However, several traces were obtained (Figure 3.15) from less densely vegetated sections of the western (Figures 3.16 and 3.17) and central (Figures 3.18, 3.19 and 3.20) transects of Mainadhoo. Stratigraphy from the upper c. 0.3 m of all traces was approximately parallel to the island surface and appears concordant with facies 1. Below the upper ~0.3 m, the strongest reflections in the lagoonward, shore-normal traces (A and C; Figures 3.16 and 3.18) were lagoonward-dipping. In contrast, the strongest reflections in the shore-parallel traces (B and D; Figures 3.16 and 3.18) were approximately horizontal. No clear stratigraphy was evident below the upper ~0.3 m of the oceanward trace (E; Figure 3.20).

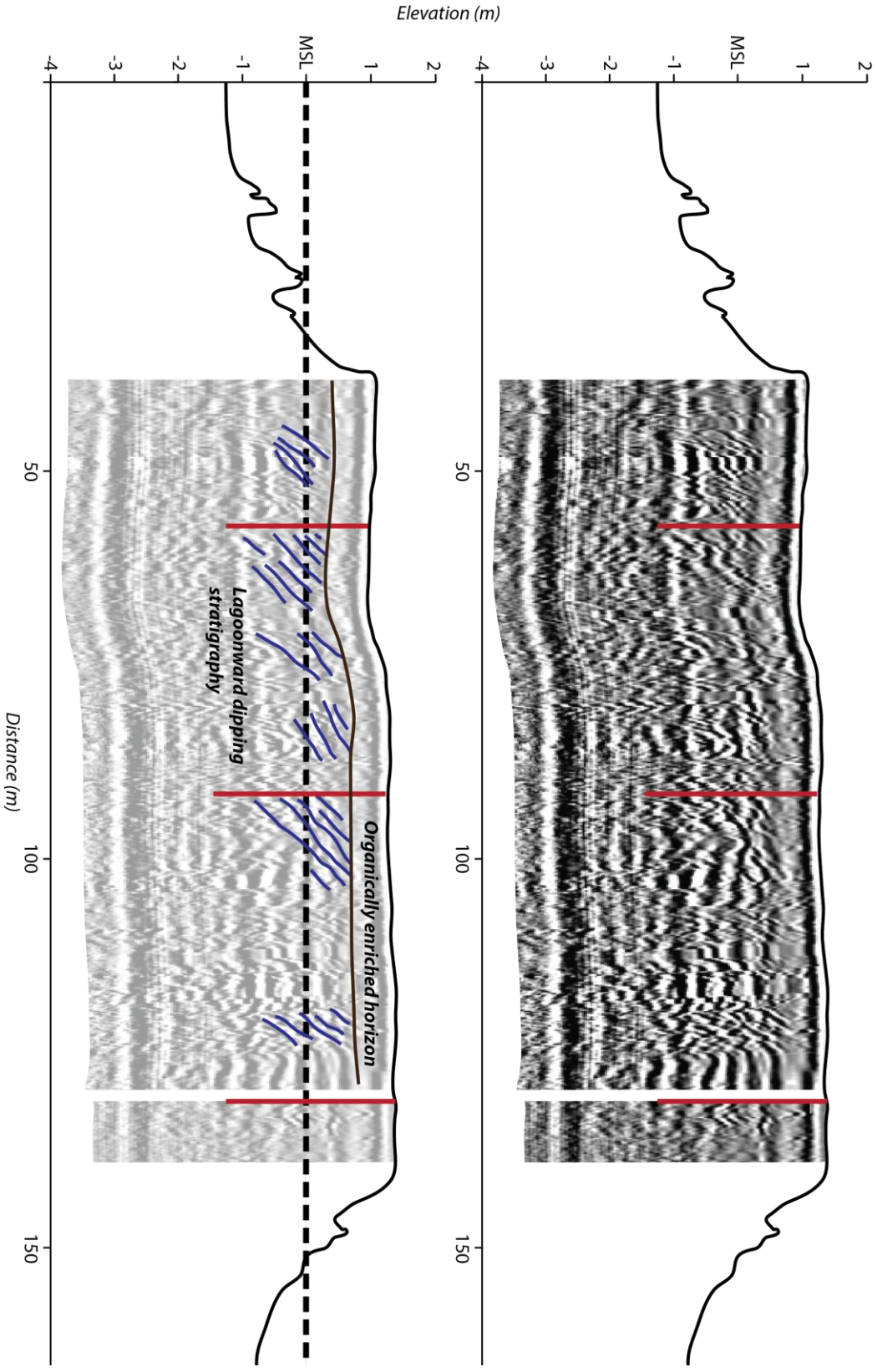

Figure 3.14 – GPR lagoonward-oceanward trace from the central transect of Baavanadhoo, leeward site. Red lines represent locations of cores.

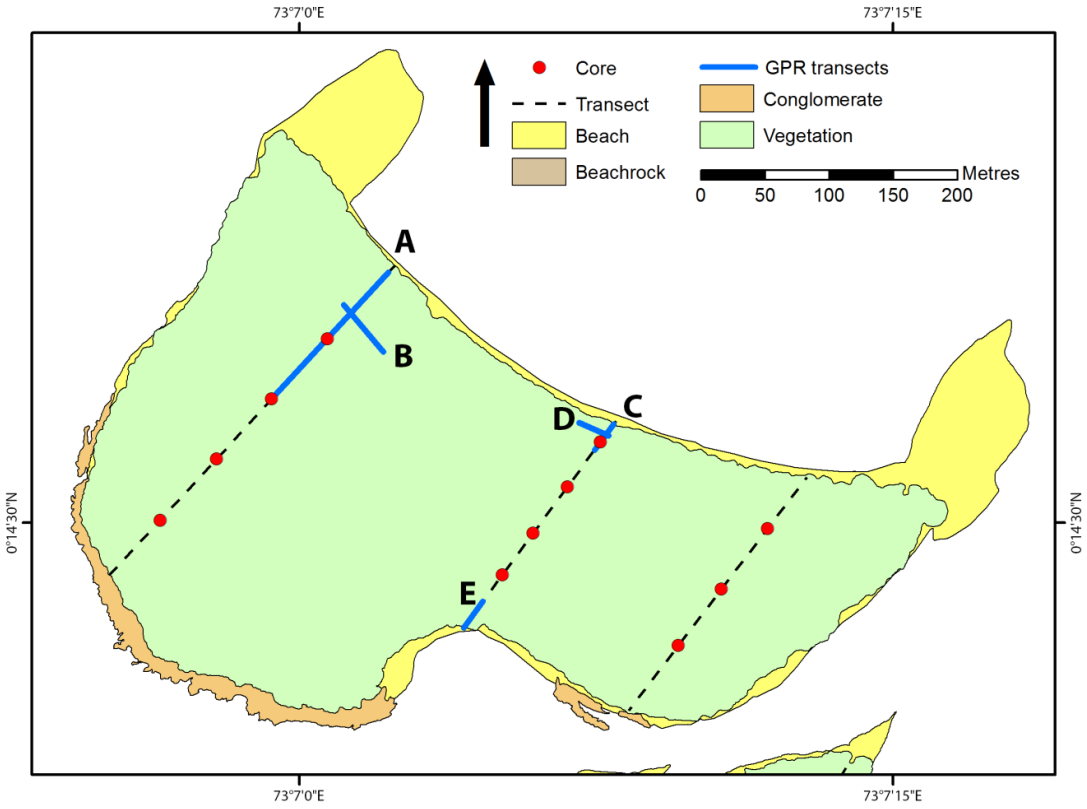

Figure 3.15 – Locations of GPR traces obtained from Mainadhoo, windward site.

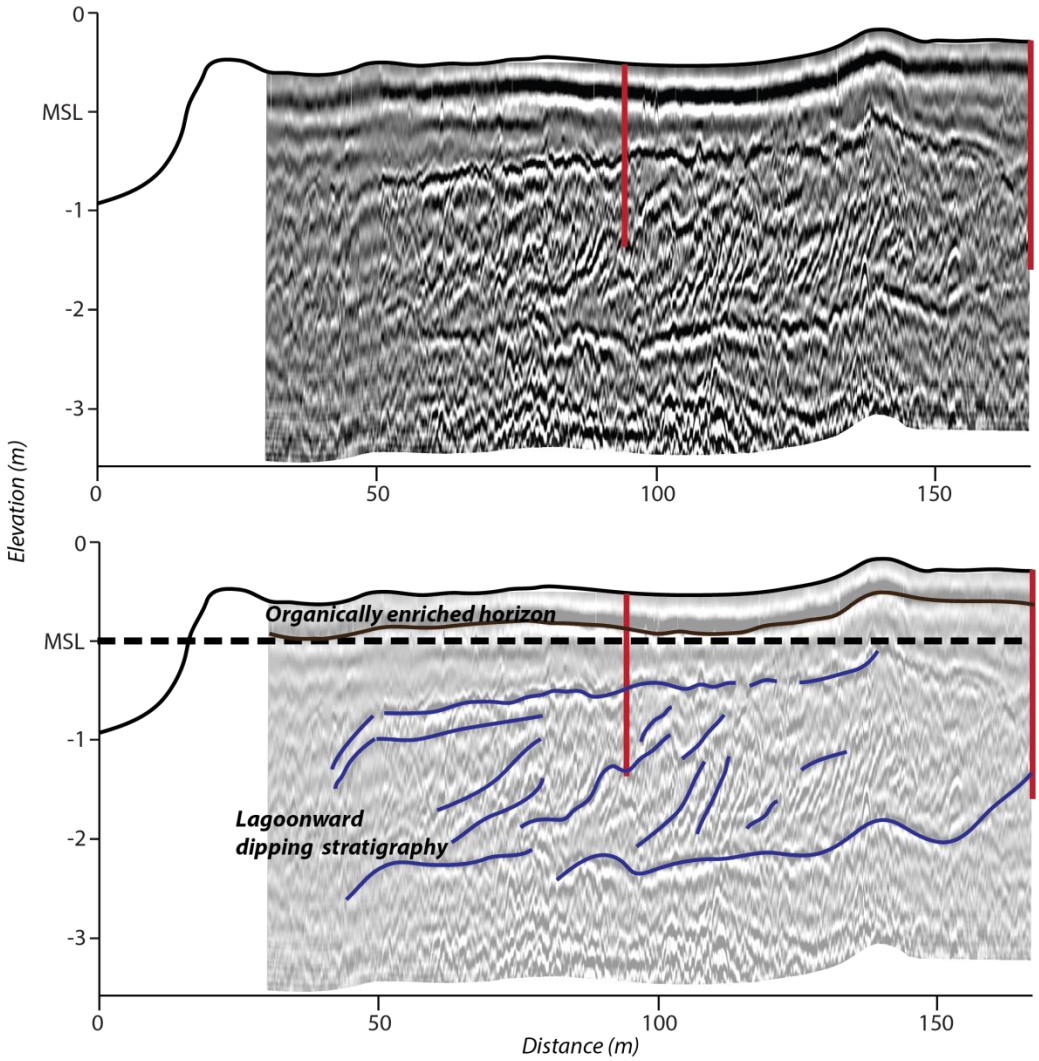

Figure 3.16 – GPR trace A, obtained from the western transect of Mainadhoo, perpendicular to the lagoonward coast. Red lines represent core locations.

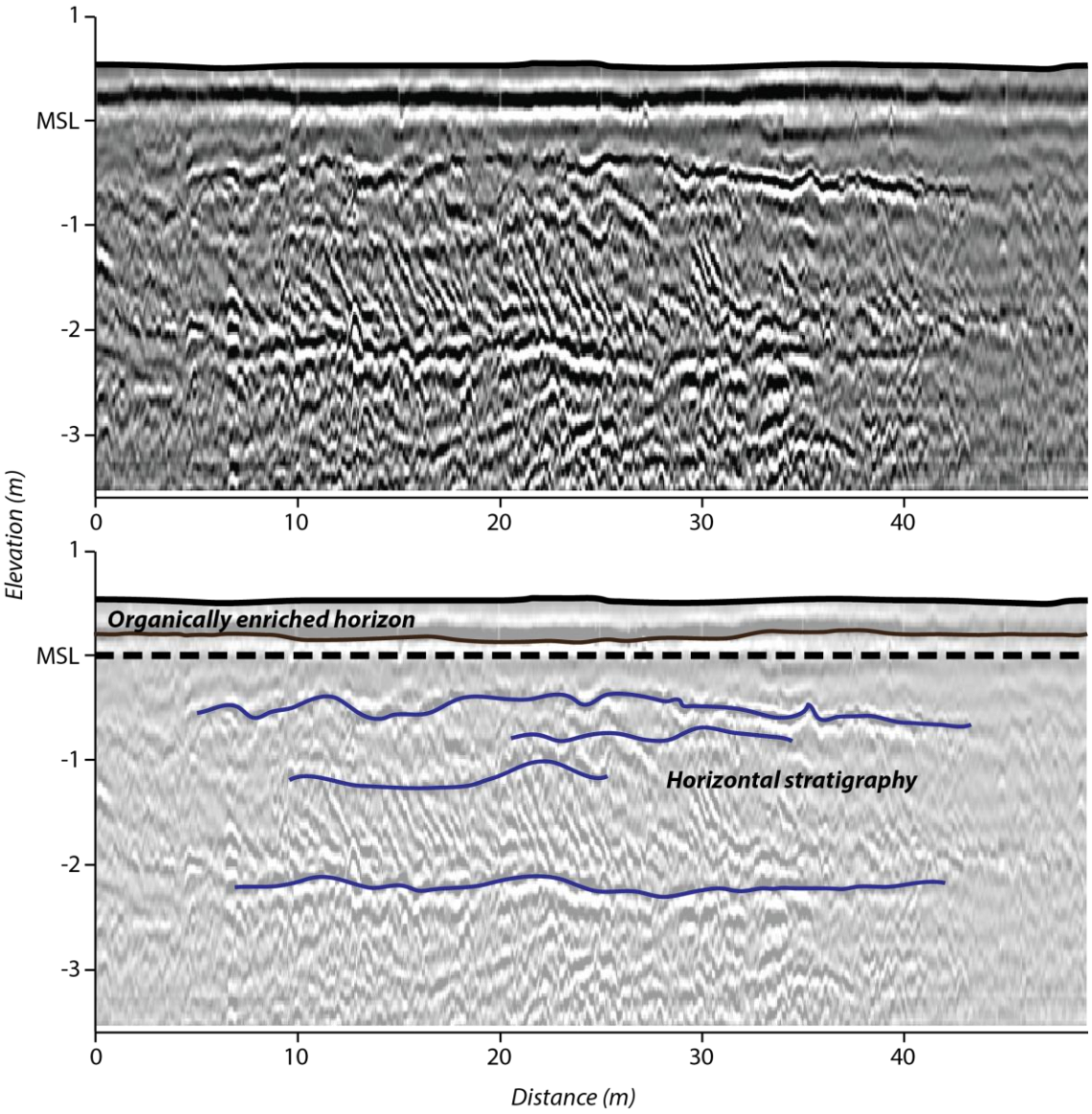

Figure 3.17 – GPR west-east trace B, obtained perpendicular to the western transect of Mainadhoo, parallel to the lagoonward coast.

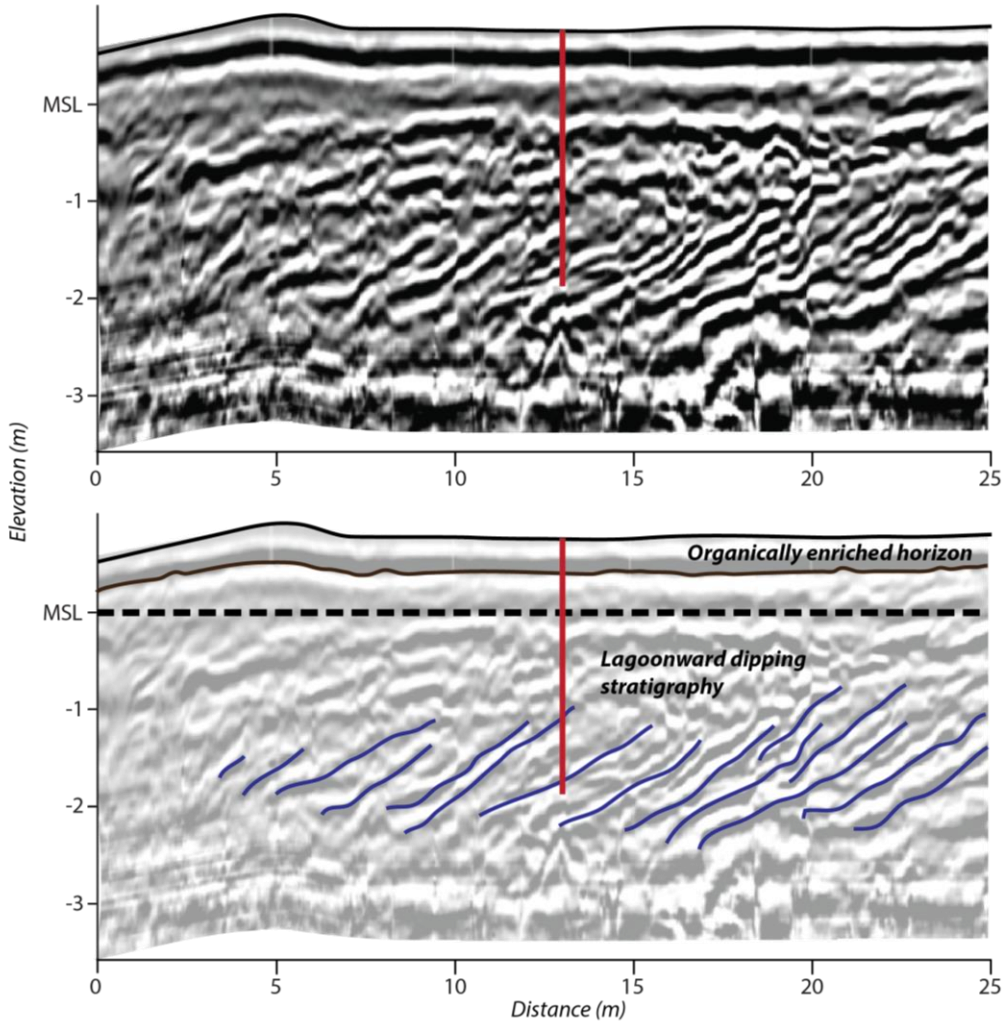

Figure 3.18 – GPR lagoonward-oceanward trace C, obtained from the central transect of Mainadhoo, perpendicular to the lagoonward coast. Red lines represent core locations.

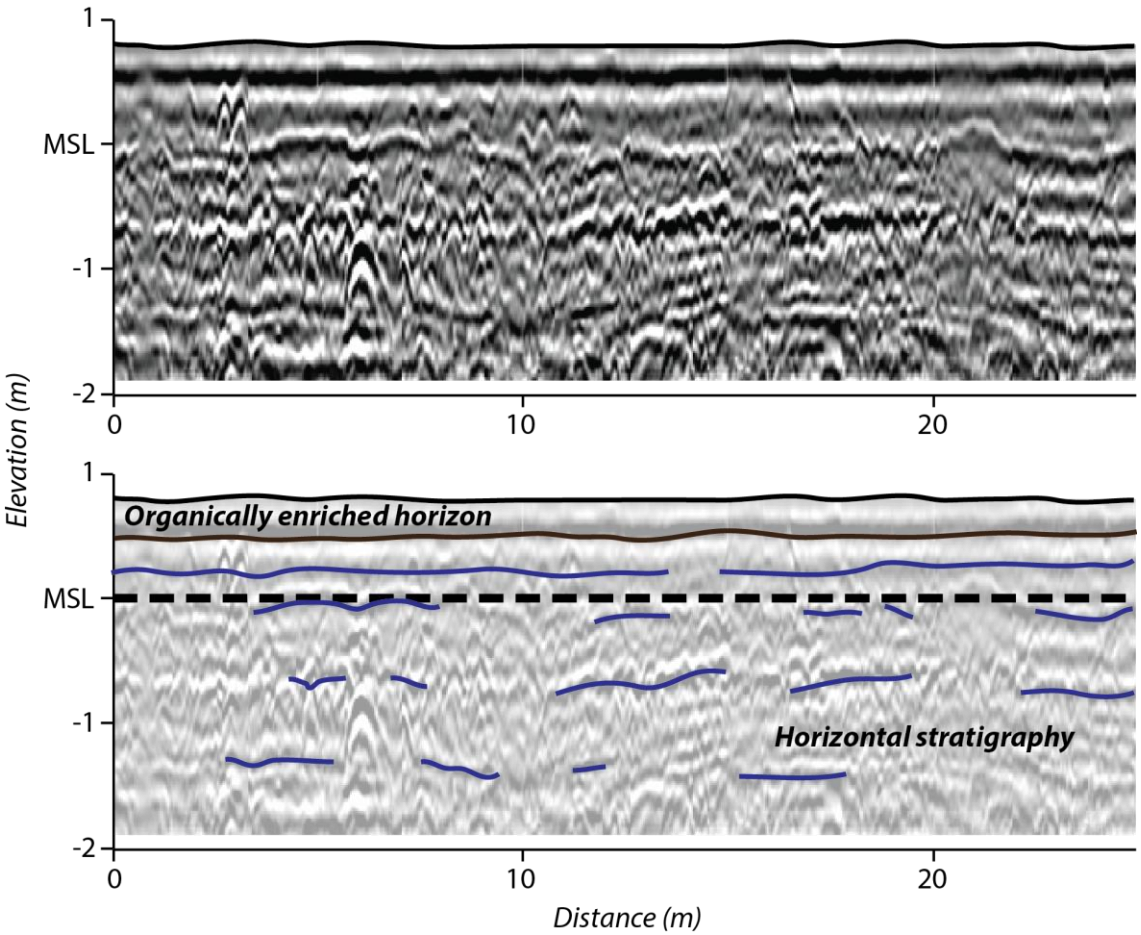

Figure 3.19 – GPR west-east trace D, obtained perpendicular to the central transect of Mainadhoo, parallel to the lagoonward coast.

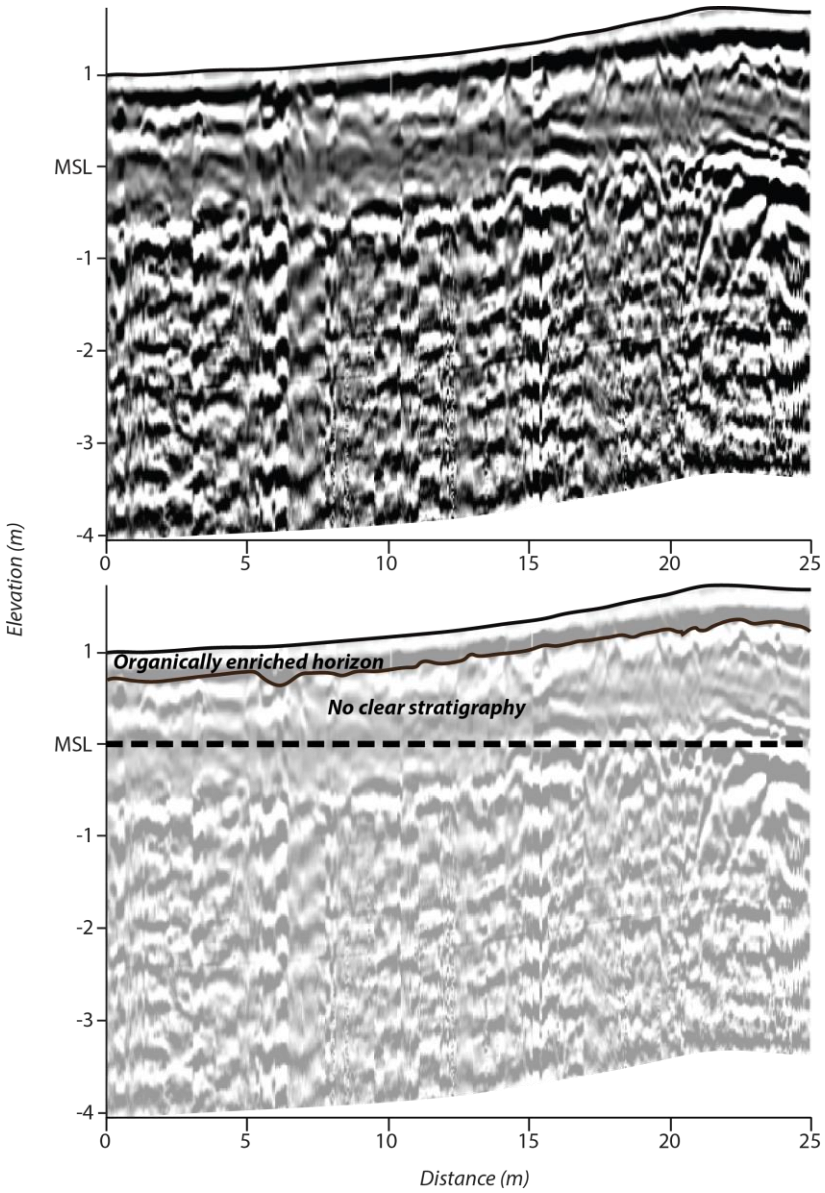

Figure 3.20 – GPR lagoonward-oceanward trace E, obtained from central transect of Mainadhoo, perpendicular to the oceanward coast.

3.4 Discussion

3.4.1 Reef island morphology: topography and planform surveys

Marked differences were found in island geomorphology between the windward and leeward study sites. For example, islands at the windward site possessed steep peripheral rubble ridges (<~2 m above MSL, 1.2 m above the island surface), which were found on the oceanward island margins. By contrast, no rubble ridges were found at the leeward site. This is interpreted as a function of the larger oceanward wave exposure at the windward site (Chapter 2). Hence, there is likely more potential for rubble generation and transport at the windward site. In addition, the wave energy received at oceanward island margins is likely to be larger at the windward site given their closer proximity to the oceanward reef crest. Indeed, the windward islands have formed nearer the oceanward reef crest (~850 m and ~250 m from the lagoonward and windward reef crests respectively), whilst the leeward islands were closest to the lagoonward reef crest (~380 m and ~540 m from the lagoonward and windward reef crests respectively). Notably, rubble ridge elevations were comparable to those found on the windward rim of Addu Atoll (0.8 – 1.1m and 2.2 – 3 m above MSL respectively – Woodroffe, 1992). This suggests that some generalisations may likely be drawn (albeit with caution) between this study and island building processes on other southern Maldivian windward rim platforms.

In contrast to the windward islands, leeward island topography was either highest (Galamadhoo) or inclined towards (Baavanadhoo) the lagoonward island margin. This may indicate a higher degree of connectivity between the leeward islands and the lagoonward marine environment. This is likely a function of wave exposure as lagoonward wave energies are higher than at the windward site due to the longer fetch lengths (Chapter 2). Alternatively, or additionally, this could be reflective of higher rates of lagoonward sediment production (Chapter 5). Furthermore, the lagoonward islands are located closer to the lagoonward, rather than the oceanward, reef crest. While island topographic profiles varied between sites, the mean island elevations were remarkably similar within each study site. This suggests that uniform processes of island evolution have operated within each site.

A further key geomorphological difference between sites was the presence of conglomerate platforms at the windward site, while the leeward site was characterised

by the prevalence of beachrock. Conglomerate formation is likely indicative of high oceanward swell wave energies, but also relative island stability. Conversely, the extensive beachrock outcrops at the leeward site suggest the associated islands have been more dynamic. Indeed, lagoonward coast outcrops are dipped at angles comparable to the contemporary beach, which suggests they mark the former beach position. Similarly, the absence of a beach on the oceanward margin is concordant with the smoother and flatter beachrock outcrops that were immediately adjacent to the island oceanward coasts. Off the southern coasts of the islands, stranded beachrock is also suggestive of relict beach deposits, which may be a result of island migration to the north, perhaps facilitated by spit elongation off the northern margin. Alternatively, or additionally, it may be that the islands have eroded as a whole. Increased dynamism of reef islands at the leeward site may be attributed to the relatively larger influence of lagoonal wind waves on the leeward rim (Chapter 2). As a result, island geomorphology is likely responsive to changes in the prevailing wind-generated wave conditions. The apparent relative stability of the windward islands may thus be given that ocean swell wave energy is less variable than lagoonal wind wave energy (Mandlier, 2008).

3.4.2 Reef island sedimentology and stratigraphy

Using a series of 28 reef island cores from contrasting rim aspects, the first detailed account of Maldivian rim island sedimentology is presented. While variability was found in island geomorphology, sediment composition was remarkably consistent between facies, islands and sites. The composition contrasts with that of Maldivian interior islands, within which a *Halimeda*-rich facies has been found within basal island sediments (Kench *et al.*, 2005). Here, the proportion of *Halimeda* averaged only 1.0 ± 0.0%. With exposure to oceanward swell wave energy on the atoll rim, the composition of the rim sediments is a reflection of the relative durabilities of the skeletal constituents. Indeed, in a comparison of foraminifera, molluscs, coral and *Halimeda*, Ford and Kench (2012) found grain durability to vary by several orders of magnitude, the most durable clast type being coral, whilst *Halimeda* was most rapidly abraded. The homogeneity of composition may also reflect the relative consistency of reef ecology both spatially (between sites) and temporally. This is in contrast to other cases, such as at Green Island, Australia, where an ecological shift was found to a foraminifera dominated reef platform (Yamano et al., 2000). Moreover, as the atoll rim

is a relatively high wave energy environment, it is likely that sediment residence times in their zones of production are low and thus the sediment reservoir is homogenised by rapid spatial dispersal.

Most notably, island composition was dominated by a restricted range of sedimentary constituents, primarily coral (mean = 76.6 ± 0.6%) highlighting its importance for Maldivian rim island formation and maintenance. Of equal importance is the process by which coral is converted from reef framework into material for reef island building. Four processes may cause this conversion, which may be inferred from sediment texture: (1) physical erosion of the reef framework produces sand-sized sediments via abrasion (though this is unlikely to be a dominant process given the high durability of coral – Ford and Kench, 2012; Perry *et al.*, 2015) or rubble grade clasts; (2) endolithic sponge bioerosion produces silt-sized (<63 μm) material, though is evidently of minimal significance for reef island building as silt-sized material accounted for only 2.11 ± 0.57% of each sample; (3) urchin grazing produces predominantly silt-sized material and is thus, likewise, unlikely to represent a dominant process (Perry et al., 2015); (4) sand-sized sediments are produced as a by-product of parrotfish grazing (Hoey and Bellwood, 2008; Perry *et al.*, 2015). The prevalence of sand- and rubble-sized coral within the rim islands is therefore likely primarily attributable to parrotfish grazing, and physical erosion of the reef framework by low-frequency high-magnitude events, respectively.

A similar provenance for coral-dominated sands has recently been suggested for Maldivian atoll interior islands and attributed to parrotfish grazing (Perry *et al.*, 2015). Similarly, Woodroffe's (1992) descriptions of Feydhoo island reported the predominance of coral sands. This contrasts with the composition of Pacific island sediment where foraminifera-rich sands have been documented (e.g. <63% - Kench et al., 2014). This is reflective of differences in reef ecology, as a function of differing sea-level histories, as the Pacific mid-Holocene sea-level highstand produced tidally-emergent reef flats favour foraminifera production (Perry et al., 2011). Conversely, in the Caribbean, *Halimeda* has been documented as a dominant sediment constituent as the shallow reef crests and lagoons that characterise the Caribbean favour *Halimeda* production (Perry et al., 2011).

The most distinct division within cores was that between facies 2 and 3 which were differentiated by the transition from clast- to matrix-support, reflecting a shift in sediment supply. The presence of coral rubble toward the base of the cores, downcore increase in rubble size, predominance of branched coral morphologies (which are more susceptible to physical erosion than other growth forms – Scoffin, 1993) and poor sorting of facies 3, are likely a function of higher wave energy associated with low-frequency high-magnitude events. It is thus likely that such events played a significant role in reef island initiation.

Given the proximity of the Maldives, and particularly Huvadhu Atoll, to the equator (*e.g.* the windward site is only 26 km north of the equator), storms are exceedingly rare. High magnitude events that contributed to island initiation may therefore comprise swell events (e.g. Hoeke et al., 2013). For instance, between the 15th and 17th May 2007 extensive floods covered ~30% of the island of Fares-Mathoda (southwest Huvadhu Atoll), which was attributed to intense storm winds on 7th May off the southern coast of South Africa. 11 m wave heights were reported at the origin, which likely had a period of 18 seconds. The result at Fares-Mathoda was groups of waves (locally known as '*Ralhe Vaali*') that were higher than the normal swells, which broke at the reef edge the surf from which washed over the island (Aslam and Le Bere, 2007). By comparison, the swell waves that flooded Malé Island between 10th and 15th of April 1987 had a peak wave period of 16 seconds with a peak wave height of 5 m (Aslam and Le Bere, 2007). In addition, there may have been higher intensity storms during the Holocene and thus we may need to reinterpret the meaning of storms in this setting.

While facies characteristics were consistent between sites, this study demonstrates that key differences in reef island development exist even at the scale of an individual atoll. For example, comparing clast taphonomy of facies 3A and 3B, the better preservation of coral clasts in facies 3B at the windward site is indicative of a shorter temporal lag between sediment production (in this instance coral erosion) and deposition. In contrast, although high energy events also likely played a role at the leeward site, island initiation may have been a more gradual process.

The most marked stratigraphic difference between sites was the increased proportion of rubble recovered at the windward site. Indeed, facies 3 was notably thicker at the

windward site than at the leeward site. Numerous coral boulder horizons were also recovered from windward cores, which were likely deposited in high energy overwash events. Facies 2 was also almost entirely absent from Boduhini and Kudahini in the windward setting. This may be due to greater exposure to wave energy given their slightly closer proximity to the reef crest than at Mainadhoo.

Higher wave exposure may also explain why textural differences between facies at the windward site were markedly less clear-cut than at the leeward site (as illustrated by the ternary plots; Figure 3.11). This could be due to the increased frequency of overwash events and greater sediment reworking. Reworking may occur through a process of rollover whereby material eroded from the oceanward shore is deposited toward the lagoonward coast facilitated by high energy events (Woodroffe *et al.*, 1999).

Intra-site diversity is also evident in the spatial and vertical distribution of facies. At the leeward site, the most striking pattern in island stratigraphy is the oceanward-lagoonward gradient in grain size. Facies 2 increased, while facies 3 concordantly decreased, in thickness and stratigraphic position toward the lagoonward coast. This suggests that, following deposition of a rubble bank, the input of sand-grade material has primarily been off the lagoonward coast. Conversely, at the windward site, the interface between facies 2 and 3 is more consistent within transects. This may be due to the combined impact of the higher wave exposure, greater frequency of high magnitude events, and the closer proximity of the islands to the oceanward reef crest. In combination, these factors have resulted in the deposition of more horizontal rubble sheets in island initiation at this site. Similarly, Woodroffe (1992) documented *Acropora* sticks at 0.5 m below MSL and under on Feydhoo island. Feydhoo is located on the south-western rim of Addu Atoll and it thus seems likely that similar processes of island formation operated to those at the windward site in this study.

Overlying facies 2 and 3 was facies 1, the organically enriched horizon. No relationship was found between island age and the organic content of the upper organically enriched ‘soil’ horizon, which is consistent with Woodroffe and Morrison’s (2001) analyses of soil development on Makin, Kiribati. The organic content of the younger windward islands was actually found to be slightly higher than on the leeward islands, though this may be a function of depth as samples were collected centrally within each facies, the windward samples from facies 1 were recovered from shallower depths.

However, facies 1 was markedly thicker within the leeward islands than within the windward islands, hence a hypothesis could be suggested that a relationship exists between island age and the thickness of the organically enriched horizon.

3.4.3 Reef island chronologies

3.4.3.1 Island initiation

A fundamental prerequisite for reef island formation is the availability of a suitable substrate, or 'foundation', upon which a reef island can develop. Of the 27 cores that extended below the level of live coral growth on the adjacent reefs, 21 did not terminate on a solid non-erodible reef surface, but rather on unconsolidated sediment and reef rubble. This unconsolidated sediment and rubble underlying the islands likely represents a part of a sequence of infilling of the atoll rim as described by 'bucket-infill'. This is a style of carbonate platform evolution in which sediment derived from the higher elevation and more carbonate productive reef crest infills the deeper and more extensive lagoon (Ladd, 1945; Schlager, 1993; Purdy and Gischler, 2005). Infilling buckets exist at cascading spatial scales across the Maldives Archipelago. The double linear chain of atolls represents the largest (3.8×10^{10} m) bucket with the Inner Sea as its internal lagoonal area. Each atoll also comprises a bucket within which the exterior reef platforms that comprise the rim represent further buckets, and the reef platforms within atoll lagoons (faro) comprise the smallest buckets (200 – 300 m^2; Schlager and Purkis, 2013). The cores that terminated on solid reef substrate were in all cases found towards the oceanward rim margin and thus the underlying reef flat likely slopes in a bucket-shaped morphology toward the lagoon.

At least some degree of infilling must occur in order to provide a 'foundation', or underlying substrate, for reef island formation. Buckets are transient features (Purdy and Gischler, 2005), which infill at variable rates as controlled by the hydrodynamic regime, sediment availability and the size of the platform (i.e. bucket). Hence, the unconsolidated sediment and reef rubble within which 21 of the cores terminated represents the 'infill' material that has been deposited on the rim platform contributing to the gradual infilling of the platform. Island formation may occur following sufficient infilling of the rim platform to enable sediment accumulation to attain elevations above MSL.

Results of radiocarbon dating within the present study suggest that differences may exist in the ages of the basal core dates and reef island initiation, even at the scale of an individual atoll. The oceanward underlying consolidated substrates were dated at (~3,600-2,800 cal. yr. B.P. and ~4,400 cal. yr. B.P. at the windward and leeward sites respectively) and, similarly, radiocarbon dates suggest that reef island initiation at the leeward site (4,200-3,600 cal. yr. B.P.) predated that at the windward site (2,800-2,000 cal. yr. B.P.). Leeward island formation may have preceded windward island formation due to faster infilling of the rim platform (i.e. bucket), which would have meant a suitable island 'foundation' would have been available earlier than at the windward site. Faster infilling may have occurred because the windward rim platform is wider (e.g. *c*. 1.7 km wide, compared to *c*. 1.1 km at the leeward site) and larger (*c*. 60 km^2, compared to *c*. 8 km^2 at the leeward site) meaning there is a greater volume (i.e. accommodation space) to infill. In addition, the sediment supply at the leeward site may be larger as it is likely supplemented by greater lagoonward inputs of sediment from the lagoonward reef crest facilitated by the higher lagoonward wave exposure than at the windward site (Chapter 2). In contrast, low lagoonal wind wave energy at the windward site may mean connectivity with the lagoonward production zones is more limited. Indeed, maximum water depths at the leeward site were *c*. 2 m below MSL, while maximum depths at the windward site were *c*. 10 m below MSL (section 7.3.1). This suggests that while the leeward platform has infilled entirely, further accommodation space remains available for infilling sediments at the windward site.

The timing of island initiation at both the windward and leeward study sites is roughly consistent with the window of formation (from 3000 yr. B.P. to present) suggested by Woodroffe (1992). However, timings of island initiation differed markedly to those of the interior reef islands in South Maalhosmadulu Atoll, northern-central Maldives (Kench et al., 2005; Perry et al., 2013). Dates were obtained from four islands, and the basal dates from the infilling facies of three of the islands were dated at ~5,500 cal. yr. B.P., while the infilling facies in the fourth island was dated at cal. 3,053 cal. yr. B.P. (Kench et al., 2005; Perry et al., 2013). The interior platforms likely host the oldest islands as they infilled first and thus were first to possess a suitable island basement. This is because the smaller platforms would require a smaller volume of sediment to fill and the entire perimeter of the interior platforms forms a reef crest meaning small platforms comprise a relatively large zone of high sediment production. Of the four

dated interior islands, the younger island formed on a larger island platform than the three older interior islands. Hence, a longer time period would be required in order to infill the larger accommodation space afforded by the larger platform meaning a suitable island foundation would not have been available until later than on the smaller platforms. Indeed, Perry et al., (2013) found the size of interior reef platforms was a key control on the extent of infilling and, in turn, reef island formation. A threshold of 500 m^2 was found below which platforms were likely to be entirely infilled and host to reef islands (Perry et al., 2013).

The different timings of island formation in different settings found in this study are of key significance to reef island research. Prior reef island research has predominantly focused on differences in the timings of reef island formation between regions (e.g. Perry et al., 2011) and has thus been underpinned by the assumption that timings are consistent within regions. However, this work demonstrates that within the Maldives Archipelago contrasting island ages may exist both between interior and rim islands and between windward and leeward sites on the atoll rim. In addition to the difference between the windward and leeward sites, timings of island formation also differed to those found for interior islands in South Maalhosmadulu atoll (Kench et al., 2005; Perry et al., 2013). Assertions of reef island vulnerability typically implicate sea-level as the sole control upon reef islands. However, examining timings of formation in relation to Kench et al.'s (2009b) sea-level curve for the region, highlights that islands are able to form under variable sea-level histories (Figure 3.21).

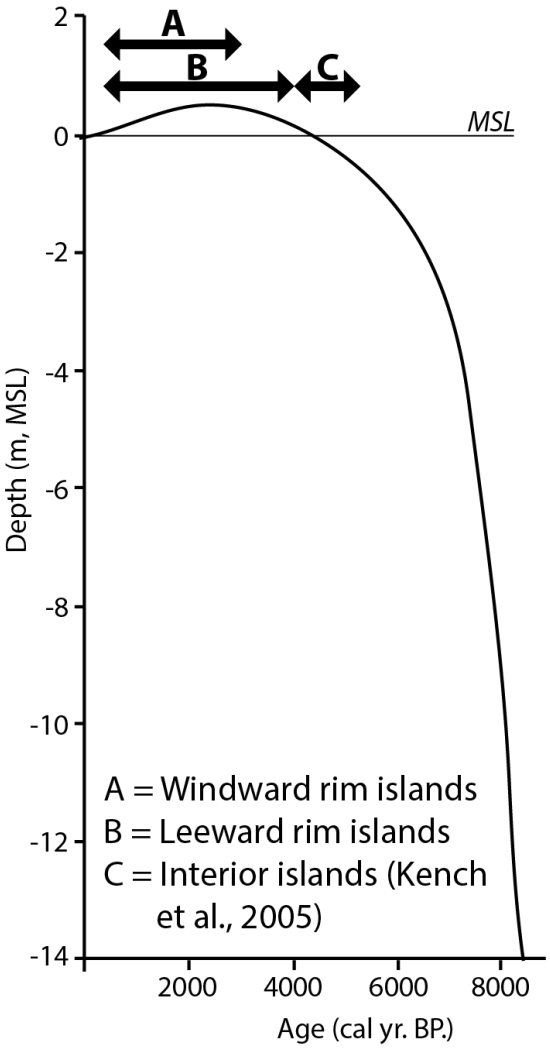

Figure 3.21 – Timings of island formation at the windward site (A), leeward site (B), and South Maalhosmadulu atoll interior islands (Kench et al., 2005), in relation to the sea-level curve for the region given in Kench et al. (2009b)

3.4.3.2 Models of reef island development

The morphological, stratigraphic, sedimentological and chronological datasets suggest that contrasting models for reef island evolution may exist for the windward (Figure 3.22) and leeward (3.23) sides of the atoll.

Stage 1, *~3,600 cal. yr B.P.*: Bucket infilling. Sea-level has reached its current level.

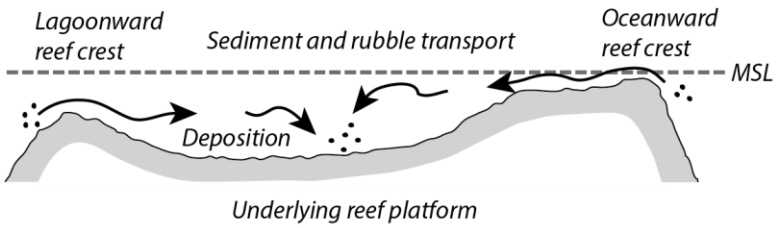

Stage 2, *~2,800 - 1,800 cal. yr B.P.*: Deposition of a series of rubble sheets and oceanward rubble ridges(?). Conglomerate bank deposited and cemented.

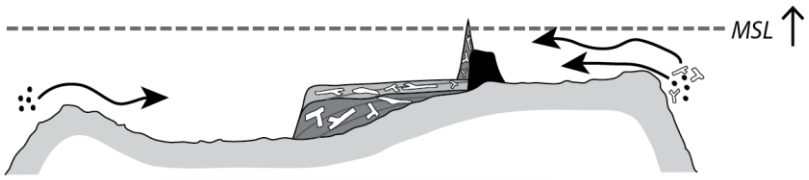

Stage 3, *~1,800 - 1,500 cal. yr B.P.*: Shift from accumulation of primarily rubble- to sand-sized material. Rollaround of older material (preferentially sand-sized) to amalgamate adjacent islands.

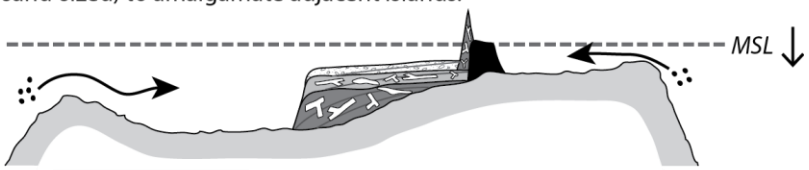

Rollaround mechanism:

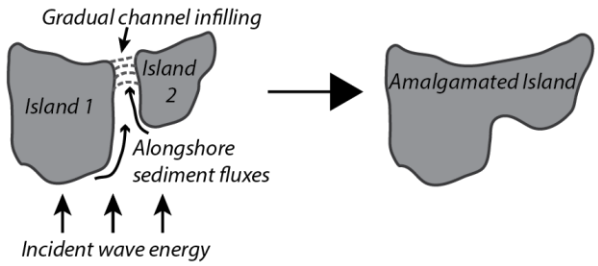

Stage 4, *~1,300 - 600 cal. yr B.P.*: Lateral lagoonward accretion of matrix-supported material

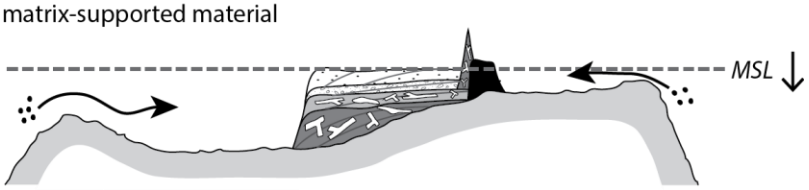

Stage 5, *~600 cal. yr B.P. - pres.*: Relative island senescence.

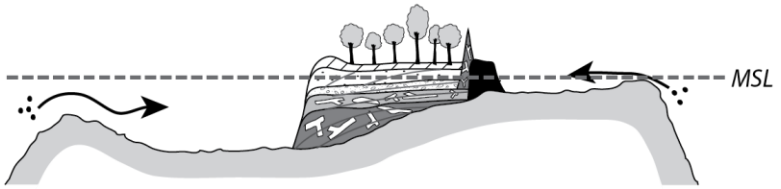

Figure 3.22 – Conceptual model of reef rim island development, windward site. Note that vertical exageration is substantial for the pupose of illustration.

Stage 1, *~4,500 cal. yr B.P.*: Bucket infilling; Sea-level has reached its current level.

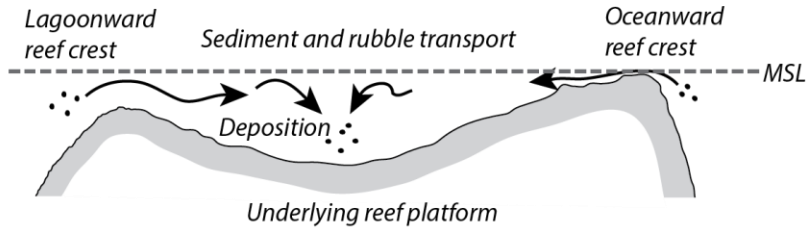

Stage 2, *~4,100 - 1600 ? cal. yr B.P.*: Deposition of a rubble bank, likely mobile and/or episodically reworked.

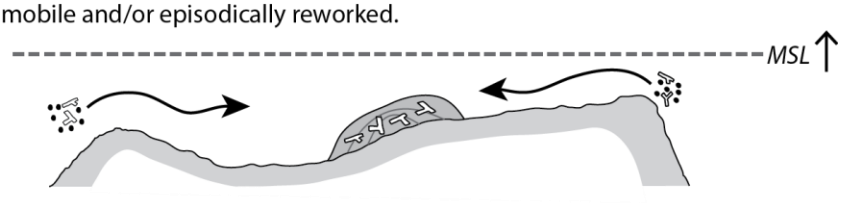

Stage 3, *~3,500 ? - 1,600 ? cal. yr B.P.*: Shift from accumulation of primarily rubble- to sand-sized material. Continued island mobility, rollover and/or episodic reworking.

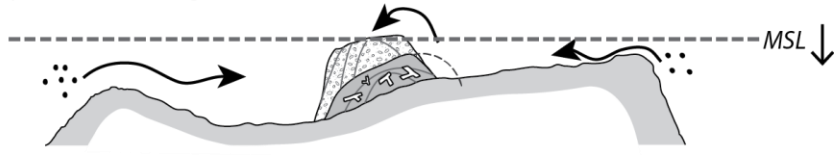

Stage 4, *~1,600 - 500 cal. yr B.P.*: Lateral lagoonward accretion of sand-sized material. Continued island mobility, rollover and/or episodic reworking.

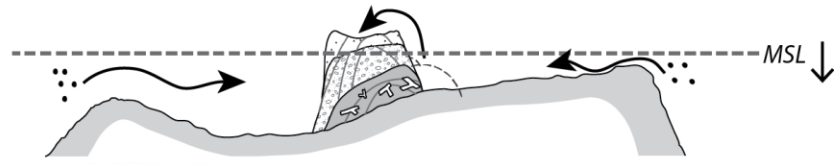

Stage 5, *~500 cal. yr B.P. - pres.*: Relative island senescence.

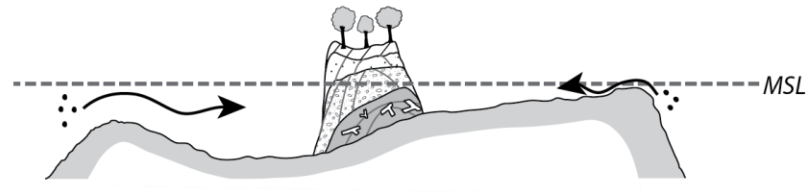

Figure 3.23 – Conceptual model of reef rim island development, leeward site. Note that vertical exageration is substantial for the pupose of illustration.

Windward site

The consolidated substrate underlying the oceanward island cores was dated between ~3,600 and ~2,800 cal. yr. B.P., which corresponds to a time when sea-level was comparable to contemporary levels (Kench et al., 2009b) and bucket infilling was likely occurring (Stage 1; Figure 3.22). Island initiation occurred (Stage 2), as a part of the continual infilling of the sand apron, from 2,800 cal. yr. B.P. with the deposition of a

series of gravel and rubble sheets by successive low-frequency high-magnitude events (e.g. storms and swell events). Indeed, WaveWatch III hindcast modelling suggested such events may be relatively frequent at the windward site (section 2.4.2.1). The three islands at this site were selected to represent different island sizes with the aim of ascertaining whether a temporal evolutionary sequence of island development (e.g. Perry et al., 2013) exists on the atoll rim. However, dates from the base of cores on Mainadho and Boduhini were relatively consistent. Rubble sheets were deposited between ~2,800 and ~1,800 cal. yr. B.P., which is congruent with the mid-Holocene sea-level highstand (Kench et al., 2009b) within which sea-level was ~ 0.5 ± 1 m higher than present levels. Higher sea-levels would have enabled higher wave energies to propagate across the reef flat, also resulting in increased rates of coral rubble generation (via physical erosion) and increased transport of rubble-sized material across the reef flat. No dates were obtained from the oceanward island ridges, but given the large size (<0.8 m) of the rubble clasts, it is plausible that they were also deposited within this time period. Similarly, the upper surface of the conglomerate platform was dated at ~1,400 yr. B.P and thus was also likely deposited and cemented at this time. Woodroffe (1992). The conglomerate platform may also have aided reef island formation as a low energy depocentre may have been created in the lee of the conglomerate allowing gravel and sand-sized material to accumulate. Indeed, the absence of western rim reef islands on South Maalhosmadulu Atoll, Maldives, has been attributed to that fact that high energy levels are too large to provide a low energy depocentre for island formation and thus sand-sized sediments are swept off the rim (Kench and Brander, 2006).

A striking feature of the radiometric dates is the relative consistency of the dates from the interface between facies 2 and 3 (i.e. the rubble-sand interface). The period from ~1,800 to 1,500 cal. yr. B.P. was thus associated with a shift from the accumulation of primarily rubble- to sand-sized material (Stage 3). During this time period, sea-levels were falling toward contemporary levels and thus the high energy window was closing (Kench et al., 2009b). Hence, there was likely a progressive reduction in the rates of rubble generation and transport over this period. It seems likely that a comparable time period (approximately ~1,800 to 1,400 cal. yr. B.P.) may also have been associated with a period of relative island mobility. Indeed, Mainadhoo may once have been two separate islands, which have coalesced along the central transect. This may have

occurred through a mechanism of ‘roll-around’ whereby older, preferentially sand-sized, material from the separate islands has been transported by alongshore sediment fluxes to fill the shallow passage between the islands. Once this material blocked the passageway, the islands may have progressively welded through subsequent embayment infilling by lagoonward-directed sediments. Indeed, this would account for the age inversions on the central transect as material of varying ages may have been washed in from the western and eastern transects. In addition, the geomorphology of the oceanward coast of the central transect differs from that of the eastern and western sections of the island in that there is an absence of conglomerate. This process of island welding through the infill of narrow inter-island passages has been documented on rim islands with a similar morphology to the windward islands (i.e. orientated, prior to welding, with their longest axes perpendicular to the reef crest) at Funafuti Atoll, Tuvalu, central Pacific (Kench et al., 2015).

Subsequent to the accumulation of predominantly rubble-sized material, the period from ~1,300 to 600 cal. yr. B.P. was associated with the accumulation of predominantly sand-sized material (Stage 4). This indicates a reduction in wave energy with the closure of the high energy window. While rubble-sized material was primarily derived from the oceanward reef crest, the sand-grade material comprising facies 2 was likely derived primarily from the lagoonward environment. This may account for the relative absence of facies 2 from Boduhini and Kudahini, given their locations further from the lagoonward environment. This process of accumulation was likely lateral lagoonward accretion, as is suggested by the radiocarbon dates which, on Boduhini and the western transect of Mainadhoo were younger toward the atoll lagoon. In addition, the lagoonward GPR traces exhibited lagoonward-dipping reflections, which likely represent a series of progradational beach faces indicating that Mainadhoo accreted towards the lagoon (Figure 3.16 and 3.18). Traces obtained perpendicular to transects (i.e. parallel to the lagoonward coastline and to the reef crest) were characterised by a horizontally stratified pattern indicating that processes were relatively uniform in an alongshore direction. Hence, island development has likely occurred primarily along an oceanward-lagoonward gradient. The oceanward trace lacked any clear reflections, which suggests that there may have been greater reworking of island sediments toward the oceanward coast. Finally, the youngest date obtained from the windward site was 600 cal. yr. B.P. and the development of an organically enriched

horizon and substantial vegetation growth have occurred (Stage 5) since this time, which appears to be a period of relative island senescence.

Leeward site

As at the windward site, sufficient infilling of the underlying reef platform is a fundamental prerequisite for island formation as the unconsolidated infilling sediments provide the basement for reef island formation. The underlying consolidated substrate was dated ~4,400 cal. yr. B.P. and so bucket infilling (Stage 1; Figure 3.23) was likely occurring from this time. Following sufficient infill, Stage 2 was characterised by reef island initiation, which was marked by the deposition of a rubble bank between ~4,200 and 3,600 cal. yr. B.P.. As at the windward site, the deposition of the rubble-dominated material (i.e. facies 3) corresponded to the mid-Holocene sea-level highstand during which higher wave energies would have been able to propagate across the reef flat. Facies 3 was thus likely generated and deposited by low-frequency high-magnitude events during this timeframe. The rubble bank would have remained below MSL and, in the absence of a conglomerate platform to somewhat anchor deposits, it is likely that the 'islands' were highly mobile.

The most striking feature of the leeward site radiocarbon dates was the relative consistency of the dates from the interface between facies 2 and 3, which was dated at ~1,625 to ~1,699 cal. yr. B.P.. The transition from the accumulation of predominantly rubble- to sand-sized material (Stage 3) at this site is may be attributed to the closure of the high energy window following the mid-Holocene sea-level highstand. Moreover, the dates are relatively consistent with the timing of the shift from predominantly rubble- to sand- accumulation at the windward site. Indeed, the interface between facies 2 and 3, and also the upper surface of the conglomerate platform at the windward site were also dated between ~1,800 and 1,400 cal. yr. B.P.. However, the presence of several dates from above the facies 2-to-3 interface (i.e. within facies 2) also pre-date this time period, which renders the development of an island model somewhat problematic at this site. The model proposed at this site therefore ought to be considered as one hypothesis for island development. An alternative model of island development could be proposed whereby islands accreted from a more central island core. However, age inversions were found in 3 of the 6 dated cores, and it thus seems likely that the islands at this site have been highly mobile throughout their

development. This is supported by the presence of extensive beachrock outcrops, the striking intra- and inter-site consistencies of the facies 2-3 interface dates, and the presence of age inversions within 3 of the 6 leeward site cores. Indeed, reworking may have occurred via a process of rollover whereby material was eroded from the oceanward island shore and deposited toward the lagoonward island coast (e.g. Woodroffe, 1999). Similarly, in an analysis of 29 islands at Funafuti Atoll, central Pacific, several of the less stable islands were formed of predominantly sand-sized material, while those with greater proportions of gravel were more stable (Kench et al., 2015). Hence, this is consistent with the greater mobility of the leeward islands (which were comprised of predominantly sand-grade material), in comparison to the more stable windward islands in this study. The notion that islands comprised of predominantly sand-sized material are more mobile than their gravel-based counterparts has implications for ongoing island resilience. This is given that the maintenance of more dynamic islands likely necessitates a more continuous sediment supply (Kench et al., 2015).

Following the transition from the accumulation of predominantly rubble to sand-sized material, islands appear to have developed through lateral accretion with progressive deposition of sand-sized material primarily derived from the lagoonward margin (Stage 4). This is supported by island topography as the elevation of the lagoonward coast of Galamadhoo island was higher than that of the oceanward coast. Likewise, the lagoonward section (~30 m) of the central transect of Baavanadhoo was inclined toward the lagoon. In addition, relatively strong lagoonward-dipping reflections were found in the GPR trace, even beyond the oceanward side of the central island core. Reflections appear to represent a series of progradational beachfaces and thus provide compelling evidence that the mode of island development has been of lateral accretion from an oceanward island core. In addition, it seems likely that island mobility, reworking and rollover continued throughout this time period. The timeframe (~1,600 – 500 cal. yr. B.P.) corresponds to the gradual closure of the high energy window meaning lower wave energies would propagate across the atoll rim. The youngest date from this site (toward the lagoonward coast of Baavanadhoo) was 524 cal. yr. B.P. and the islands since appear to have been relatively senescent. Stage 5 (~500 cal. yr. B.P. – present) has thus been characterised by the development of an organically enriched horizon and vegetation growth.

3.5 Conclusions

The first detailed study of Maldivian coral reef rim islands is presented through analyses of island core records from windward and leeward sections of Huvadhu atoll rim. Several key inter-site consistencies were found. Firstly, sedimentary composition was relatively uniform between facies, islands and rim aspects. Three distinct sedimentary facies, and an additional two subfacies, were identified on the basis of differences in facies textural characteristics. Islands were dominated by coral sand and rubble, the former most likely generated as a by-product of parrotfish grazing, and the latter by low-frequency high-magnitude events. Secondly, radiocarbon dates suggested the timing of the transition from predominantly rubble- to sand-accumulation to be consistent between islands and sites, which is congruent with the closure of the high energy window associated with the mid-Holocene sea-level highstand. Given that reef island initiation likely occurred when sea-levels were higher than present, the implication is that future sea-level rise may result in a reactivation of the process regime responsible for reef island formation. This could potentially result in further island mobilisation and formation.

Inter-site inconsistencies in reef island development were also found. For example, islands at the leeward site appear to have been more mobile than those at the windward site, likely as they are formed of predominantly sand-sized materials, as is consistent with Kench et al.'s (2015) findings from Funafuti Atoll. This could render the leeward islands more vulnerable to environmental change as a larger sediment supply may be needed to maintain current island volumes (Kench et al., 2015). In addition, inter-site differences may exist in the models of island development, specifically in the likely timings of island initiation and in the differing island morphologies. Assertions of reef island vulnerability typically implicate sea-level as the sole control upon reef islands. However, radiocarbon dates suggested that between-site differences may exist in the timings of island formation. Hence, sea-level may not be the sole control upon island development and reef islands may form at various stages of sea-level rise. In particular, wave exposure was highlighted as a likely key control upon the variability between the windward and leeward site. In the context of environmental change, this highlights the potential for significant between-site variations in reef island sensitivity to shifts in oceanographic boundary conditions. Thus, given the diversity of reef islands at the local scale, it is likely that future responses of reef islands to environmental

change may be equally diverse. The challenge then for the adaptive capacity of atoll nations is to recognise this diversity in future island management plans.

Chapter 4: Eco-geomorphic zonations and sediment storage

4.1 Introduction

While Chapter 3 provided details of reef island sedimentology and accretionary histories, Chapter 4 will focus on the adjacent contemporary marine environment, specifically eco-geomorphic zonations and sedimentology. Such data will allow inferences to be made as to the key controls acting upon Maldivian rim reef systems. This is because sedimentary facies characteristics are an expression of the key biological and physical processes that control coral reef systems (Kench, 2011a; Hamylton et al., 2016). Furthermore, as reef islands are formed solely of sediments derived from the adjacent marine environments, understanding reef sedimentology is critical for assessing reef island vulnerability and future trajectories. Understanding the eco-geomorphic zonation and sedimentology of the adjacent marine environments is thus imperative to gaining an integrated understanding of reef island systems.

Studies of benthic sedimentology within the Maldives have been comparatively limited to those undertaken within the Caribbean, Indo-Pacific and Great Barrier Reef. Several predominantly qualitative accounts of Maldivian sedimentology were provided by Gardiner and Murray (1906), Ciarapica and Passeri (1993), and Bianchi et al. (1997). Gischler (2006) undertook a quantitative study of sediment composition and texture within Ari and Rasdhoo atolls, however as this was an atoll-scale study, sampling resolution was coarse (n = 52) and included only 4 samples from rim platforms. The first detailed quantitative studies of Maldivian sedimentology at the reef platform scale were undertaken by Perry et al. (2015), and Morgan and Kench (2016b). These studies examined interior platform systems within the northern-central portion of the Maldives Archipelago (Raa and North Male Atolls respectively). The only detailed quantitative work to be undertaken in an atoll rim setting was an analysis of textural characteristics on the oceanward reef flat of Gan island, Addu Atoll (Stoddart, 1966). Stoddart's focus on the oceanward reef flat is reflective of a broader bias in studies of reefal sedimentology to analyse only reef flat environments (Yamano et al., 2001).

However, a holistic approach is required to understand both pathways of sediment production, transport and storage, and also reef-to-island connectivity.

This Chapter will therefore provide the first detailed quantitative study of sediment texture and composition to be undertaken within an atoll rim setting. This analysis will encompass the entirety of the benthic environment across the rim (from the oceanward to the lagoonward platform edge). In addition, the eco-geomorphic zonation of the marine environments at each study site were defined in order to both structure benthic sediment sampling design and to further characterise Maldivian atoll rim settings. Marine benthic sedimentology was compared to that of the reef islands (as described within Chapter 3). Beach samples were also recovered as a means of examining the interface between the marine and terrestrial environments (Hart, 2009). Specifically, research key research questions include:

1) What is the eco-geomorphic zonation of the windward and leeward study sites and what are their benthic characteristics?
2) What are the textural and compositional characteristics of sediments stored within each eco-geomorphic zone and beach deposits?
3) Does sedimentology suggest a high degree of marine-beach-island connectivity?
4) What is the spatial distribution and volume of sediment stored within the marine environment at each study site?

4.2 Methodology

4.2.1 Study Site

Marine eco-geomorphic zonations and their sedimentology were examined within the windward and leeward study sites (Figure 4.1). At the windward site, this encompassed the marine environment adjacent to Mainadhoo, Kudahini and Boduhini islands (0.84 km^2), whilst, at the leeward site, this comprised the section of rim surrounding Galamadhoo Island (1.06 km^2).

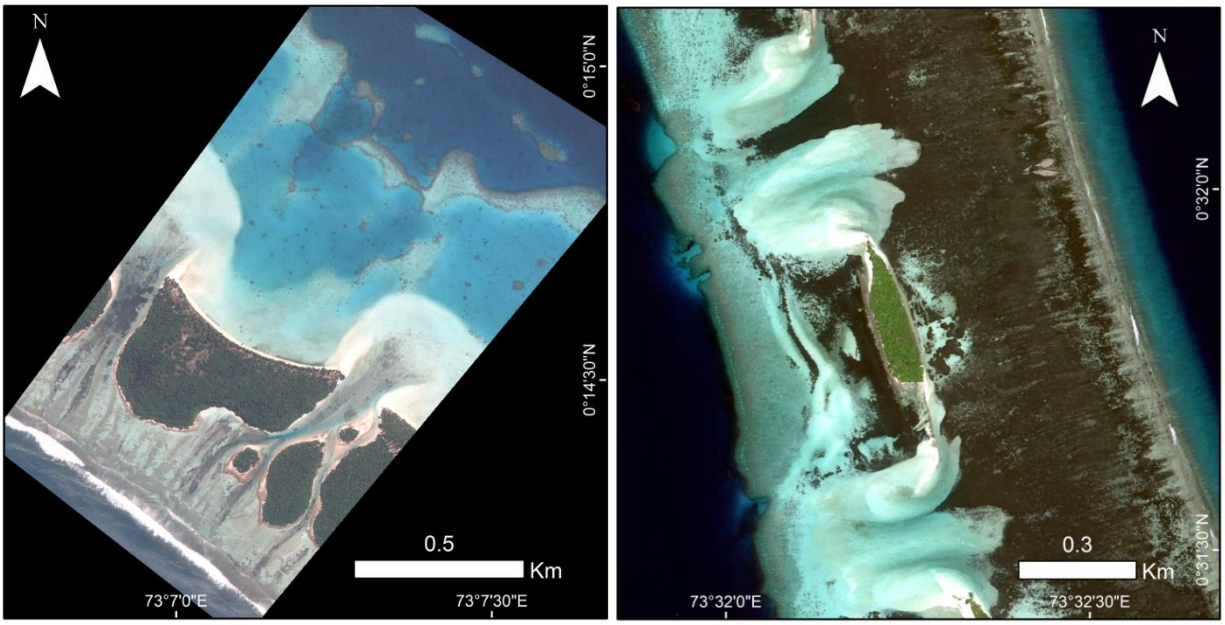

Figure 4.1 – Quickbird and WorldView-2 imagery of the windward (left) and leeward (right) study sites.

4.2.2 Eco-geomorphic Zonation

Prior to fieldwork, eco-geomorphic zones were identified at each site as a means of structuring sampling design. Zones were selected based on preliminary snorkelling and examination of satellite imagery in order to characterise the range of substrate types, hydrodynamic settings and ecological communities (e.g. Harney and Fletcher, 2003; Perry et al., 2015). At the leeward site, six distinct zones were identified: lagoonward reef crest, lagoonward patch, oceanward sand, dense seagrass, oceanward sparser seagrass, and oceanward reef crest. At the windward site, five zones were identified: lagoonward patch, lagoonward sand, oceanward patch, rubble and oceanward reef crest.

High resolution satellite imagery was employed to generate digital habitat maps of the eco-geomorphic zonation at each site. A WorldView-2 image of the leeward site was acquired on 13th April 2015, and, at the windward site, a Quickbird image was acquired on 27th May 2010. WorldView-2 and Quickbird have a spatial resolution of 1.86 m and 2.40 m in the visible optical bands, and 0.46 m and 0.60 m in the pan-chromatic band. Images were free of both sun glint on the water surface and cloud cover. The imagery was pan-sharpened using the Hyperspherical Color Space (HCS) algorithm within Erdas Imagine (Padwick et al., 2010). Pre-processing was also undertaken to correct for the effects of scattering and absorption in the atmosphere through dark object

subtraction. Water column correction was deemed unnecessary given the small areal extent, low bathymetric variability and shallow nature of the sites (Zhang et al., 2013).

A Maximum Likelihood Classification was performed within Erdas Imagine on the pan-sharpened bands (Mather, 2004). Ground truth data were obtained from each zone (n = 190 and n = 210 for the leeward and windward sites respectively; Figures 4.2 and 3). Waypoint averaging was used to reduce GPS error, which was ~5 m. The data were divided to train (20%) and validate (80%) the classifications. Error matrices were then generated comparing ground truth and classification data to validate the classification. Three complementary accuracy statistics were calculated from the matrix: overall, user's and producer's accuracies. The overall accuracy denotes the percentage of pixels assigned to the correct class. User's accuracy gives the probability that a classified pixel represents that class on the ground, while producer's accuracy is the probability that any pixel in a class has been correctly classified (Green et al., 2000).

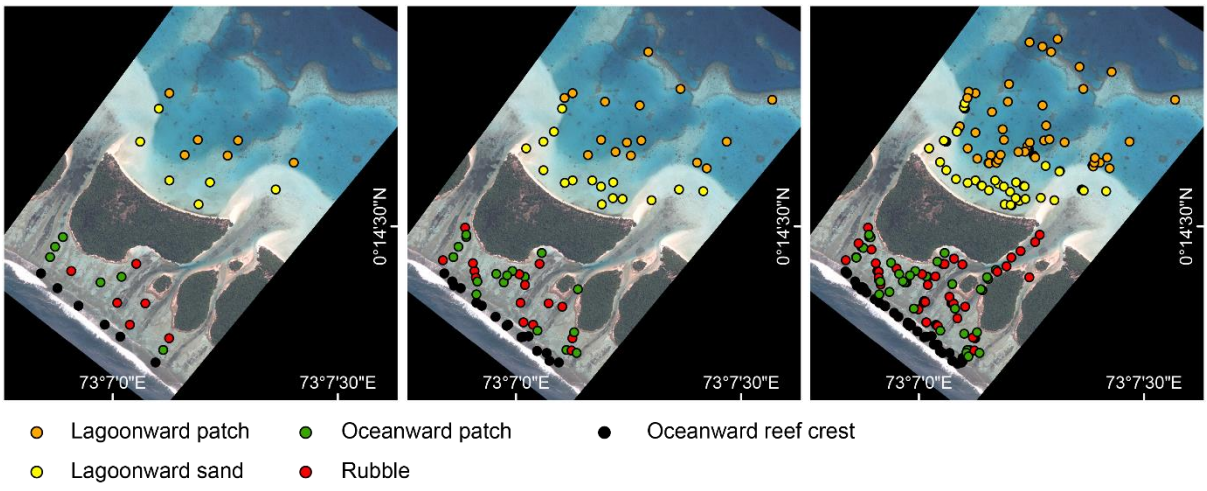

Figure 4.2 – Windward site sampling design. Locations of benthic surveys (left), sediment samples (centre), and ground-truth points (right).

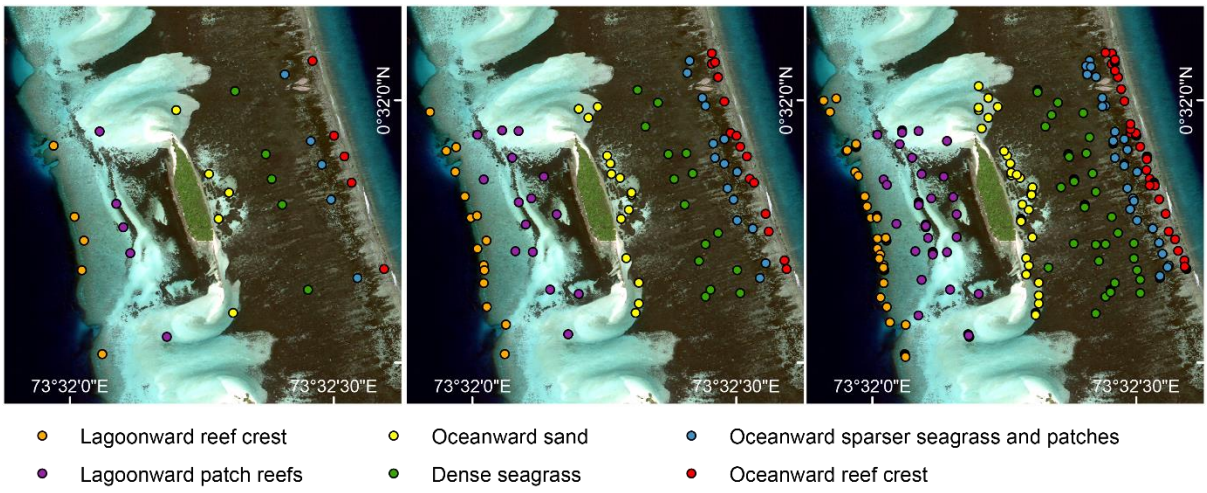

Figure 4.3 – Leeward site sampling design. Locations of benthic surveys (left), sediment samples (centre), and ground-truth points (right).

4.2.3 Marine Benthic Surveys

Marine benthic surveys were undertaken to assess eco-geomorphic characteristics of each zone. Survey stations were established along transects perpendicular to both the reef crest and reef island shorelines (Figures 4.2 and 3), which were approximate extensions of the terrestrial island transects along which cores were recovered (see Chapter 3; Figures 3.3, 3.4, 3.6 and 3.7). A total of 30 surveys were undertaken at each study site, which afforded 6 and 5 replicates within each zone at the windward and leeward sites respectively. At each survey station, a 10 m transect (running parallel to the reef crest and reef islands) was marked using a flexible tape pulled taught between two sand pegs. Survey station locations were determined by taking GPS points at 0 m, 5 m and 10 m along each transect.

Each survey site was initially characterised by assessing topographic complexity using a five-point Rugosity Index (RI) whereby each site was graded on a scale where 0 = no vertical relief, 1 = low and sparse relief, 2 = low but widespread relief, 3 = moderately complex, 4 = very complex with numerous fissures and caves, 5 = exceptionally complex with numerous caves and overhangs (Polunin and Roberts, 1993; Wilson et al., 2007). Wilson et al. (2007) found this visually assessed five-point scale to be a reliable indicator of habitat complexity. Water depths were measured using a single beam echosounder at 0 m, 5 m, and 10 m along the transect. Water depths were to heights relativeto MSL using tide tables for Gan (00°41S, 73°9E) from the University of Hawaii Sea Level Centre. Surveys of benthic substrate type were

undertaken using line intercept transects whereby the nature of the substrate below the transect tape was classified at 10 cm intervals. Benthic categories included live and dead coral, Crustose Coralline Algae (CCA), seagrass, consolidated limestone pavement, bare sediment, and rubble. Although initial categories also included soft coral, sponges, macroalgae and articulated coralline algae, none were observed in this study. The census data were then converted to percentages for each category. Seagrass densities were also calculated by placing a 50 x 50 cm quadrat 5 times along the transect at random.

4.2.4 Marine Benthic and Beach Sedimentology

Benthic surficial sediment samples analysed in order to examine the sediment stored within the identified eco-geomorphic zones. Samples were obtained from each of the survey station sites (n = 30 at each study site). This dataset was also augmented through the recovery of an additional 10 samples from locations selected at random within each zone. 90 samples were thus analysed from the windward site and 96 from the leeward site (Figure 4.2 and 3).

Sediment samples were also collected from the top and toe of beach along each of the terrestrial oceanward-lagoonward transects. At the windward site, 5 samples were thus collected from the top and toe of both the oceanward and lagoonward beaches (n = 20). At the leeward site, samples were collected both on Galamadhoo and Baavanadhoo islands, hence 6 samples were obtained from the top and toe of the oceanward and lagoonward beaches (n = 24).

Each sediment sample was hand scooped using a 500 ml sample pot, rinsed in freshwater twice for 12 hours, soaked in a 5% bleach solution for 24 hours (to neutralise organic matter), and oven dried (40°C). Samples were dry sieved into phi intervals to ascertain grain size distributions and analysis was undertaken within the programme GRADISTAT (Blott and Pye, 2001) to determine mean grain size and sorting (the descriptive nomenclature of Udden-Wentworth is used throughout). In order to assess sediment hydraulic characteristics (i.e. transport potential), sand-sized (0.063 – 2 mm) sediment (bulked) from each sample was divided using a riffle splitter to obtain a 10-15 g sub-sample, which was then settled through a McArthur Rapid Sediment Analyser (RSA) with a vertical fall of 1.75 m. The settling behaviour of the sediment was recorded to calculate the mean settling velocity (cm s^{-1}) for each sample.

While the mean grain size values calculated through sieving are used throughout this Chapter, settling velocities were also converted into mean grain sizes using the equations of Gibbs et al. (1971). Conversions were undertaken purely for comparative purposes (through use of a paired t-test and linear regression).

As in Chapter 3, sieve counting methods were employed to determine sediment composition (e.g. Dawsson and Smithers, 2014) whereby 100 grains were point counted under the binocular microscope from each gravel and sand-sized fraction (>2 mm, 1-2 mm, 0.5-1 mm, 0.25-0.5 mm, 0.125-0.25 mm and 0.063-0.125 mm; a total of 600 grains per sample). Silt-sized sediments were not counted as reliable identification was not possible, however this size fraction accounted for a mean of only 1.54 ± 0.42% of each sample. Grains were classified into one of seven categories: coral, crustose coralline algae (CCA), *Halimeda*, molluscs, foraminifera, echinoids, and other (including unidentifiable grains). Total percentage abundance of components in each bulk sample was then calculated using the proportion of each size fraction to the bulk sample weight.

In order to visualise spatial variability, sediment textural and compositional properties were interpolated using a block kriging algorithm, which was constructed within ArcMap's ModelBuilder utility. Interpolation was undertaken using Ordinary Kriging within, but not across the boundaries of, each of the eco-geomorphic zones (spatial resolution = 3.4 m). Focal statistics were employed to dampen artefacts of interpolation (e.g. Ford, 2009).

4.2.5 Volumetric Sediment Storage

Sediment storage was also examined in terms of the depths, and in turn volumes, of sediment stored within each of the eco-geomorphic zones. Sediment depth was measured at each survey station using a depth probe at metre intervals along the transect tape and also at 0.5 m on either side (n = 30 per survey station). This dataset was augmented through taking 3 measurements at each of the ground truth locations (n = 1200 and n = 1260 at the windward and leeward sites respectively). To examine spatial variability in depths of sediment storage, the block kriging algorithm was employed. Cell values of the interpolated surface were summed and multiplied by pixel dimensions in order to generate a first order estimate of the total sediment stored within each zone and across the marine study sites. First order estimates of the volume

of gravel-, sand- and fine-grade sediments were also generated by multiplying the proportion of sand-, gravel- and fine-grade material within each pixel by its sediment depth. All pixel values were then summed within each zone and multiplied by the pixel dimensions.

4.2.6 Statistical Analyses

In order to examine cross-rim trends in marine sedimentology, linear regression analyses were undertaken and regression matrices constructed incorporating sediment texture (mean grain size, % gravels, sorting, and settling velocity), sediment composition (% of coral, CCA, molluscs, foraminifera, echinoids and *Halimeda*), distance from the oceanward reef crest, and sediment depths. to examine differences between beach samples, ANOVAs and ANCOVAs were undertaken.

In addition, to enable visualisation of similarity across all sediment samples, non-metric multi-dimensional scaling (nMDS) plots were generated. The Bray-Curtis dissimilarity coefficient was used and analyses undertaken within the vegan package in R (Oksanen et al., 2007).

4.3 Results

4.3.1 Eco-geomorphic Zonation

Digital habitat maps of the eco-geomorphic zonations at the windward and leeward sites were generated with overall accuracies of 88.0% and 91.1% respectively (Figure 4.4 and 4.5). Tables 4.1 and 4.2 represent error matrices detailing the correspondence of the digital habitat maps and the validation ground truth datasets. In applications of habitat maps, user accuracies may be deemed the most pertinent as they quantify the probability that a mapped pixel class represents that category on the ground (Green et al., 2000). Notably, average user accuracies for both windward and leeward maps were particularly high (88.6 ± 3.7% and 95.7 ± 3.0% respectively).

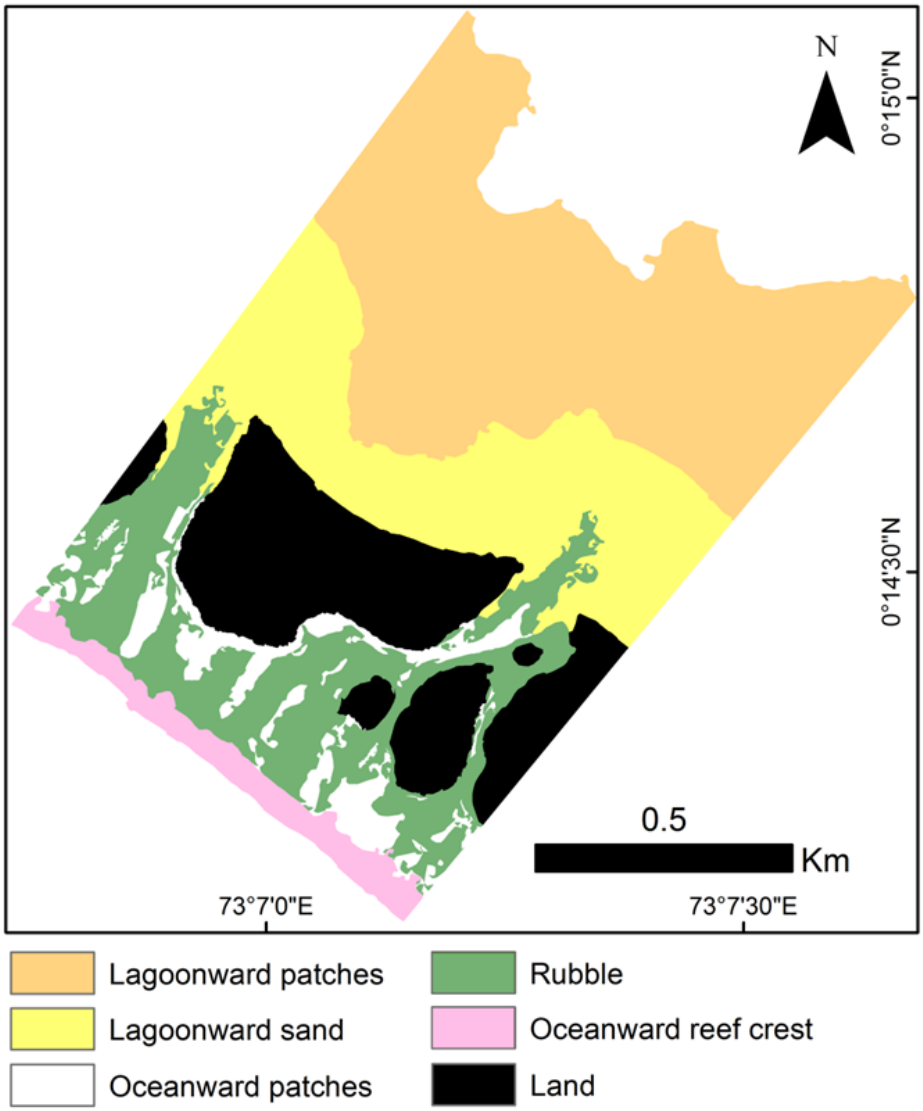

Figure 4.4 – Windward site classification of eco-geomorphic zones generated from Quickbird imagery (spatial reslution = 0.6 m).

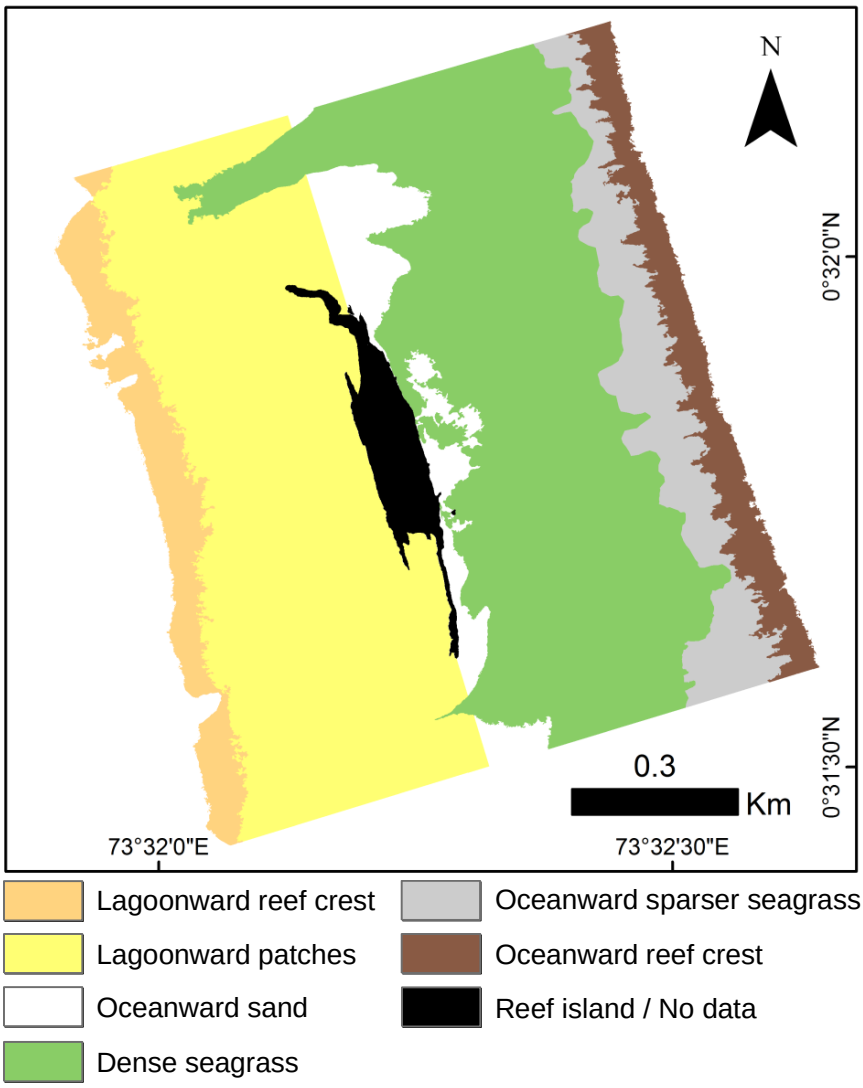

Figure 4.5 – Leeward site classification of eco-geomorphic zones generated from WorldView-2 imagery (spatial reslution = 0.46 m).

		Ground Truth Data						
		LP	LS	OP	R	ORC	Total	User Accuracy
Classification	LP	27	2				29	93%
	LS	3	28				31	90%
	OP			22	3		25	88%
	R			7	27	2	36	75%
	ORC			1		28	29	97%
	Total	30	30	30	30	30		
	Producer Accuracy	90%	93%	73%	90%	93%		

Table 4.1 - Error matrix detailing the correspondence of the marine classification and ground truth data within each of the eco-geomorphic zones at the windward site where LP = lagoonward patch, LS = lagoonward sand, OP = oceanward patch, R = rubble, and ORC = oceanward reef crest.

		Ground Truth Data							
		LRC	LP	OS	DSG	OSS	ORC	Total	User Accuracy
Classification	LRC	22						22	100%
	LP	1	30					31	97%
	OS			25				25	100%
	DSG			5	30	2		37	81%
	OSS					28	1	29	97%
	ORC						29	29	100%
	Off rim	7						7	
	Total	30	30	30	30	30	30		
	Producer Accuracy	73%	100%	83%	100%	93%	97%		

Table 4.2 - Error matrix detailing the correspondence of the marine classification and ground truth data within each of the eco-geomorphic zones at the leeward site where LRC = lagoonward reef crest, LP = lagoonward patch, OS = oceanward sand, DSG = dense seagrass, OSS = oceanward sparser seagrass, and ORC = oceanward reef crest.

The marine environments differed markedly between the windward and leeward sites and thus different eco-geomorphic zones were identified. Five distinct zones were defined at the windward site (Figure 4.6; Table 4.3): (1) the oceanward reef crest comprised an algal rim at the oceanward edge of the platform (~50 m wide; 0.04 km^2; 4.7% of the site area); (2) perpendicular to the oceanward reef crest, tongues of coral rubble extended ~300-600 m inland covering 18.2% (0.15 km^2) of the site area; (3) an oceanward patch zone comprised the remainder of the oceanward reef flat and was found within the intervening gaps between the rubble tongues with a total area of 0.06 km^2 (7.6% of the marine environment); (4) a lagoonward sand zone extended ~100-

400 m from the toe of the beach toward the atoll lagoon covering an area of 0.20 km^2 (23.6% of the marine environment); and (5) located with nearest proximity to the atoll lagoon the lagoonward patch zone was 0.39 km^2 in area (45.9% of the marine environment).

At the leeward site, six distinct zones were delineated (Figure 4.7; Table 4.4): (1) the oceanward reef crest comprised an algal rim at the oceanward edge of the platform, which was comparable to that at the windward site and formed a band (~50 m wide) of 0.06 km^2 in area (5.6%); (2) located immediately landward of the algal rim, the oceanward sparser seagrass zone formed a 30-150 m wide band covering 0.08 km^2 (7.8%) with seagrass densities of 1132.7 ± 157.1 blades per m^2; (3) the dense seagrass zone (densities = 1621.6 ± 163.4 blades m^{-2}) covered the majority of the oceanward marine environment (0.40 km^2; 37.6%) and also, in between islands, extended into the lagoon; (4) the oceanward sand zone accounted for the remainder of the marine environment on the oceanward side of Galamadhoo island (0.06 km^2, 5.9% of the marine environment) – i.e. extending from the toe of beach to the edge of the dense seagrass zone; (5) immediately lagoonward of Galamadhoo island was the lagoonward patch zone, which covered 0.39 km^2 (36.6%); and (6) a lagoonward reef crest was located in a ~60 m wide band at the lagoonward edge of the platform with an area of 0.07 km^2 (6.6%).

Given that the islands at the windward site formed closer to the oceanward reef crest than the lagoonward edge of the platform (~850 m and ~250 m from the lagoonward and windward reef crests respectively), the lagoonward zones had a greater areal extent than their oceanward counterparts. Conversely, islands at the leeward site were located closer to the lagoonward reef crest than the oceanward reef crest (~380 m and ~540 m from the lagoonward and windward reef crests respectively) and hence the oceanward zones were more extensive.

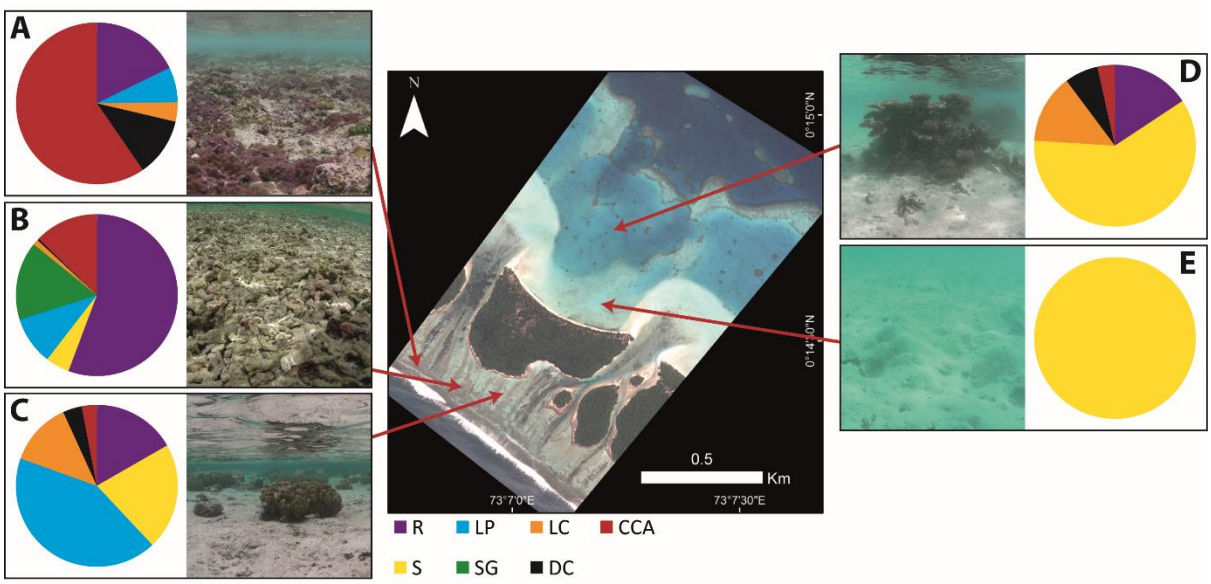

Figure 4.6 – Benthic characteristics and images of each windward site eco-geomorphic zone whereby A = oceanward reef crest, B = rubble, C = oceanward patch, D = lagoonward patch, E = lagoonward sand. Benthic classes: rubble (R), sand (S), limestone pavement (LP), seagrass (SG), live coral (LC), dead coral (DC), and CCA.

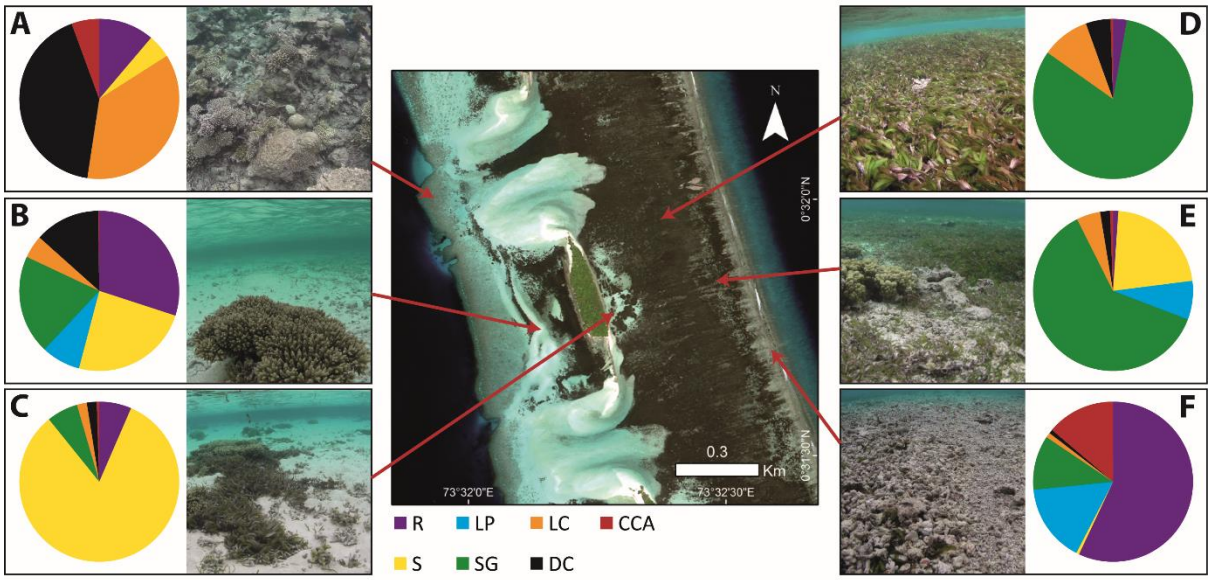

Figure 4.7 – Benthic characteristics and images of each leeward site eco-geomorphic zone whereby A = lagoonward reef crest, B = lagoonward patch, C = oceanward patch, D = dense seagrass, E = oceanward sparser seagrass, and F = oceanward reef crest. Benthic classes: rubble (R), sand (S), limestone pavement (LP), seagrass (SG), live coral (LC), dead coral (DC), and CCA.

Zone	Lagoonward Patch	Lagoonward Sand	Rubble	Oceanward Patch	Oceanward Reef Crest
% reef framework	24.0 ± 3.1	0.0 ± 0.0	14.3 ± 4.0	19.5 ± 5.7	74.2 ± 4.0
% coral rubble	15.7 ± 4.3	0.0 ± 0.0	55.7 ± 5.2	16.7 ± 8.1	18.5 ± 3.8
% sediment	60.3 ± 6.6	100 ± 0.0	4.8 ± 1.2	21.3 ± 3.5	0.0 ± 0.0
% limestone pavement	0.0 ± 0.0	0.0 ± 0.0	9.6 ± 2.1	42.5 ± 3.7	7.3 ± 1.2
% seagrass	0.0 ± 0.0	0.0 ± 0.0	15.7 ± 8.8	0.0 ± 0.0	0.0 ± 0.0
% live coral cover	13.8 ± 2.7	0.0 ± 0.0	1.1 ± 0.8	12.7 ± 3.5	4.0 ± 3.9
% dead coral cover	6.7 ± 1.8	0.0 ± 0.0	0.4 ± 0.3	3.8 ± 1.0	10.2 ± 2.2
% Coralline algal cover	3.5 ± 1.3	0.0 ± 0.0	12.7 ± 3.5	3.0 ± 1.8	60.0 ± 1.9
Substrate rugosity	3	0	1	2	2
Average water depth (m, relative to MSL)	-5.21 ± 2.95	-0.92 ± 0.59	-0.44 ± 0.17	-0.65 ± 0.31	-0.36 ± 0.12
Areal Extent (km2)	0.39 (45.9%)	0.20 (23.6%)	0.15 (18.2%)	0.06 (7.6%)	0.04 (4.7%)

Table 4.3 – Benthic cover, rugosity, depth (relative to MSL) and areal extent of eco-gomorphic zones at the windward site.

Zone	Lagoonward Reef Crest	Lagoonward Patch	Oceanward Sand	Dense Seagrass	Oceanward Sparser Seagrass	Oceanward Reef Crest
% reef framework	84.0 ± 3.0	18.0 ± 1.6	4.0 ± 1.6	15.2 ± 6.0	7.4 ± 4.7	15.6 ± 4.1
% coral rubble	11.2 ± 3.6	30.0 ± 4.8	6.5 ± 4.6	0.0 ± 0.0	1.06 ± 5.3	57.0 ± 10.2
% sediment	4.8 ± 2.5	24.1 ± 5.9	82.7 ± 5.0	0.0 ± 0.0	21.9 ± 8.2	0.6 ± 0.4
% limestone pavement	0.0 ± 0.0	7.9 ± 0.2	0.0 ± 0.0	3.5 ± 0.4	7.8 ± 0.8	15.8 ± 1.9
% seagrass	0.0 ± 0.0	20.0 ± 4.5	6.3 ± 2.1	82.0 ± 5.6	61.8 ± 10.4	11.0 ± 3.3
% live coral cover	36.4 ± 7.0	4.6 ± 0.7	2.0 ± 1.2	9.7 ± 5.1	4.8 ± 3.1	1.0 ± 0.4
% dead coral cover	42.0 ± 4.6	13.2 ± 1.9	2.0 ± 1.2	5.0 ± 3.3	2.0 ± 1.5	0.8 ± 0.8
% Coralline algal cover	5.6 ± 3.3	0.2 ± 0.2	0.5 ± 0.3	0.5 ± 0.3	0.6 ± 0.4	13.8 ± 3.4
Substrate rugosity	5	3	2	3	3	1
Average water depth (m, relative to MSL)	-1.44 ± 0.20	-1.12 ± 0.26	-0.74 ± 0.21	-0.77 ± 0.14	-0.66 ± 0.10	-0.46 ± 0.12
Areal Extent (km2)	0.07 (6.55%)	0.39 (36.6%)	0.06 (5.9%)	0.40 (37.6%)	0.08 (7.8%)	0.06 (5.6%)

Table 4.4 – Benthic cover, rugosity, depth (relative to MSL) and areal extent of eco-geomorphic zones at the leeward site.

Marked differences in benthic characteristics were found between sites and eco-geomorphic zones (Figures 4.6 and 4.7, Tables 4.3 and 4.4).

4.3.1.1 Windward Site Zonation:

Oceanward Reef Crest (ORC):

Located at the oceanward edge of the reef platform, the oceanward reef crest zone comprised an algal rim, which was exposed to the highest wave energies. Such high energy breaking waves rendered sediment accumulation minimal (0% benthic cover). With a mean depth of -0.36 ± 0.12 m (relative to MSL), the zone was relatively shallow and thus exposed at extreme low tides. At its landward edge, there was a marked shift

in elevation as the rim was raised ~0.3 m above the adjacent landward reef flat. It was primarily comprised of red and purple Crustose Coralline Algae (CCA, 60.0 ± 1.9%) and reef rubble (18.5 ± 3.8%). The surface was therefore irregular with low and sparse relief (median Rugosity Index, RI = 1).

Rubble (R):

Rubble tongues were raised slightly above the elevation of the adjacent oceanward patch zone and were exposed at extreme low tides (mean elevation = -0.44 ± 0.17 m, Figure 4.8). As on the oceanward reef crest, the surface was irregular with low and sparse relief (median RI = 1). The coral rubble primarily consisted of *Acropora* sticks (<15 cm), which appeared to be stable as the area has been colonised by CCA (12.7 ± 3.5%), seagrass (15.7 ± 8.8%; mean blade density = 492.5 ± 48.9 per m^2) and some coral recruits (1.1 ± 0.8% live coral cover; 0.4 ± 0.3% dead coral cover). The rubble itself was poorly preserved with minimal evidence of internal or external structures.

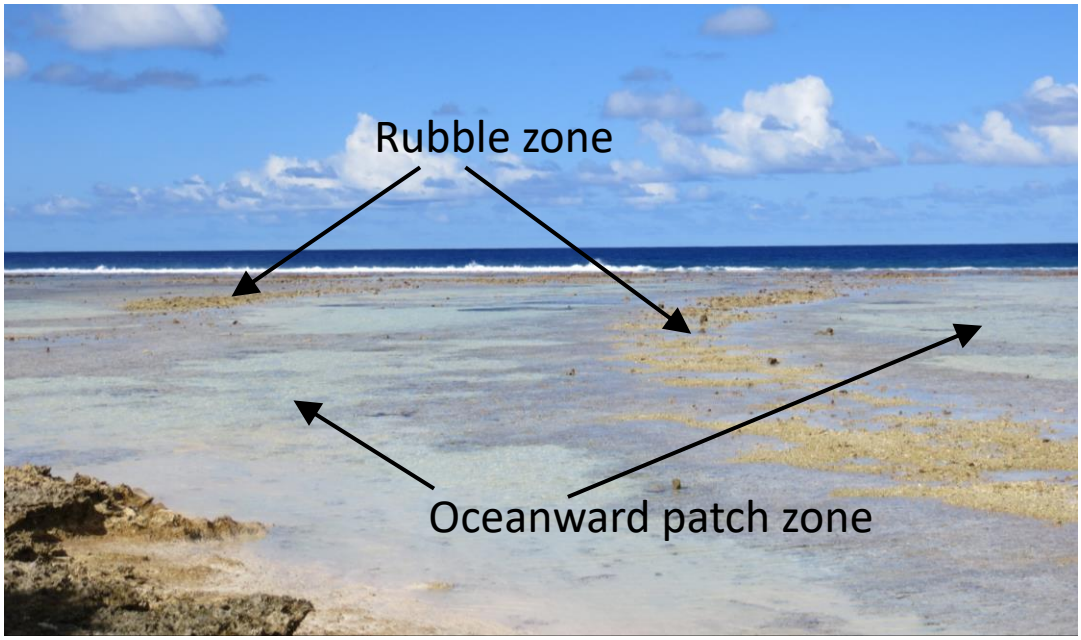

Figure 4.8 – Rubble tongues and the intervening oceanward patch zone at low tide, windward site.

Oceanward Patch (OP):

The zone was largely comprised of cemented limestone pavement (42.5 ± 3.7%), which melded into the conglomerate platforms off the oceanward island shorelines. There were occasional coral patches (overall live coral cover = 12.7 ± 3.5%), typically *Heliopora* and *Porites* microatolls (microatoll elevation = ~0.3 m above the underlying substrate). There were also thin patches of sand (21.3 ± 3.5%) and coral rubble (16.7

± 8.1%). The surface was at a lower elevation than the oceanward reef crest and rubble zones (-0.65 ± 0.31 m) and was uniform with the exception of relief afforded by coral patches (median RI = 2).

Lagoonward Sand (LS):

The LS zone consisted solely of sand cover (100 ± 0.0%) and, with the exception of sand ripples, there was an absence of any surface relief (median RI = 0). The area was gently sloped toward the atoll lagoon (mean elevation = -0.92 ± 0.59 m).

Lagoonward Patch (LP):

The division between the lagoonward sand and patch zones was marked by a relatively abrupt increase in water depth (mean elevation = -5.21 ± 2.95 m) and the presence of large and irregularly spaced coral patches. Live coral cover accounted for 13.8 ± 2.7% of the zone, while dead coral cover accounted for 6.7 ± 1.8%. The surrounding matrix was comprised of bare sand (60.3 ± 6.6%) and occasional coral rubble (15.7 ± 4.3%). The zone generally sloped toward the atoll lagoon, but also possessed a bowl-shaped morphology, shallowing slightly towards the atoll lagoon where coral patches were more frequent. Large coral patches (rising <~1 m above the substratum), typically *Porites* and *Acropora* spp., provided this zone with the greatest surface complexity of the windward site (median RI = 3).

4.3.1.2 Leeward Site Zonation:

Oceanward Reef Crest (ORC):

As at the windward site, the oceanward reef crest was elevated ~0.3 m above the adjacent landward reef flat at its landward edge. However, the zone itself was of a slightly lower elevation relative to MSL (-0.46 ± 0.12 m) than that at the windward site, as was the case for the entirety of the oceanward environment at this site. All oceanward zones therefore remained unexposed throughout the tidal cycle. The zone was largely comprised of reef rubble (57.0 ± 10.2%), hard limestone pavement (15.8 ± 1.9%) and CCA (13.8 ± 3.4%). Surface relief was therefore low and sparse (median RI = 1). There were also patches of seagrass cover (11.0 ± 3.3%; mean blade density = 557.3 ± 146.5 per m^2), which may be indicative of the relative stability of this zone and its rubble deposits.

Oceanward Sparser Seagrass (OSS):

The oceanward sparser seagrass zone was characterised by seagrass beds (*Thallasia hempricii*; 61.8 ± 10.4%), coral patches (predominantly *Acropora* spp.; 7.4 ± 4.7%) and bare sediment (21.9 ± 8.2%). Coral patches and seagrass created a degree of surface complexity (median RI = 3). Elevation (-0.66 ± 0.10 m) was lower than that of the oceanward reef crest zone, and was comparable to that of the oceanward reef flat (oceanward patch zone) at the windward site.

Dense Seagrass (DSG):

The dense seagrass zone was characterised by seagrass beds (*Thallasia hempricii*; 82.0 ± 5.6%) and coral patches (predominantly *Acropora* spp.; 9.7 ± 5.1%). It was differentiated from the OSS zone by both the higher coverage and densities of seagrass (1132.7 ± 157.1 and 1621.6 ± 163.4 blades m^{-2} in the OSS and DSG zones respectively). The zone was slightly sloped toward the atoll interior with a mean elevation of -0.77 ± 0.14 m. As in the OSS zone, surface complexity was created by the seagrass blades and coral patches (median RI = 3).

Oceanward Sand (OS):

The oceanward sand zone was primarily characterised by bare sediment (82.7 ± 5.0%), with infrequent coral patches (typically *Acropora* spp; live coral cover = 2.0 ± 1.2%) and very sparse seagrass (6.3 ± 2.1%). Relief was therefore low and sparse (RI = 2). Elevation (-0.74 ± 0.21 m) was comparable to that of the dense seagrass zone.

Lagoonward Patch (LP):

As at the windward site, elevations of the lagoonward zones were lower relative to MSL (-1.12 ± 0.26 m) than the oceanward environment. Coral patches rose further above the underlying substrate (<~0.8 m) than in the oceanward zones and, hence, there was a degree of surface complexity (median RI = 3). The zone comprised a mix of benthic cover types, including rubble (30.0 ± 4.8%), bare sediment (24.1 ± 5.9%), coral patches (live coral cover = 4.6 ± 0.7%, dead coral cover = 13.2 ± 1.9%; of which *Acropora* spp. and *Porites* spp. were particularly common) and varying densities of seagrass (cover = 20.0 ± 4.5%; mean density = 13.5 ± 7.8 blades m^{-2}).

Lagoonward Reef Crest (LRC):

The lagoonward edge of the platform was host to a defined and spatially discrete reef crest. This is in contrast to the windward site where the lagoonward edge of the platform was more gradually sloping and supported coral patches rather than a defined

reef crest. The LRC zone was largely comprised of reef framework with both live and *in situ* dead coral cover (36.4 ± 7.0% and 42.0 ± 4.6% respectively). As in the lagoonward patch zone, *Acropora* spp. and *Porites* spp. were particularly common. The large proportion of reef framework afforded the most complex relief found in this study, this variable architecture formed a complex habitat for organisms within this zone (RI = 5). The zone was slightly deeper than the adjacent patch zone with a mean elevation of -1.44 ± 0.20 m.

4.3.2 Marine Benthic Sedimentology

Tables 4.5 and 4. 6 describe the textural and compositional characteristics of marine benthic sediments within each of the eco-geomorphic zones. Sediment grain size is represented in ternary plots, constructed for both study sites (Figure 4.9). Mean grain size distributions and cross-rim characteristics are also characterised in Figures 4.10 and 4.11.

Site	Zone	n	Mean grain size (Φ)	% Gravel	% Sand	% Silt	Sorting (σ_Φ)	Settling velocity (cm/s)
Windward	Lagoonward patches	15	2.5 ± 0.3	4.1 ± 1.5	87.0 ± 3.1	12.0 ± 3.4	1.7 ± 0.1	3.2 ± 0.2
			1.6 - 3.1	*0.1 - 7.3*	*75.2 - 91.9*	*2.2 - 15.9*	*1.4 - 2.0*	*2.7 - 4.1*
	Lagoonward sand	15	1.9 ± 0.2	3.9 ± 1.7	93.8 ± 2.3	2.3 ± 0.7	1.2 ± 0.1	3.1 ± 0.3
			1.3 - 2.3	*0.6 - 3.5*	*92.2 - 98.3*	*0.4 - 3.3*	*1.1 - 1.5*	*2.0 - 3.8*
	Oceanward patches	15	0.2 ± 0.1	30.6 ± 5.5	69.3 ± 0.1	0.1 ± 0.0	1.1 ± 0.1	6.1 ± 0.3
			-0.2 - 0.6	*14.9 - 40.7*	*59.2 - 84.9*	*0.0 - 0.2*	*0.9 - 1.3*	*5.3 - 6.9*
	Rubble	15	0.5 ± 0.1	25.9 ± 4.1	73.9 ± 4.1	0.2 ± 0.1	1.2 ± 0.1	5.9 ± 0.4
			0.0 - 0.8	*12.0 - 34.0*	*65.9 - 87.8*	*0.0 - 0.5*	*1.1 - 1.3*	*4.6 - 6.6*
	Oceanward reef crest	15	-0.1 ± 0.1	38.6 ± 3.8	61.4 ± 3.8	0.0 ± 0.0	1.0 ± 0.0	7.9 ± 0.3
			-0.4 - 0.1	*29.0 - 52.7*	*47.2 - 71.1*	*0.0 - 0.0*	*1.0 - 1.1*	*7.1 - 8.6*
Leeward	Lagoonward reef crest	15	0.7 ± 0.1	13.5 ± 3.1	86.0 ± 3.1	0.5 ± 0.3	1.0 ± 0.1	6.0 ± 0.3
			0.3 - 1.0	*5.2 - 19.2*	*80.7 - 94.5*	*0.0 - 0.3*	*0.9 - 1.1*	*5.4 - 6.9*
	Lagoonward patches	15	1.3 ± 0.1	11.5 ± 1.7	88.3 ± 1.7	0.2 ± 0.1	1.2 ± 0.1	3.9 ± 0.3
			1.0 - 1.5	*7.4 - 15.2*	*84.4 - 92.4*	*0.0 - 0.4*	*1.1 - 1.4*	*3.5 - 4.0*
	Oceanward sand	15	1.2 ± 0.1	6.8 ± 2.0	93.0 ± 2.0	0.2 ± 0.1	1.1 ± 0.1	5.4 ± 0.2
			0.8 - 1.5	*0.4 - 13.2*	*86.7 - 99.5*	*0.0 - 0.3*	*1.0 - 1.2*	*4.8 - 6.2*
	Dense seagrass	15	0.8 ± 0.1	18.3 ± 1.5	81.3 ± 1.4	0.4 ± 0.2	1.3 ± 0.0	5.0 ± 0.2
			0.5 - 0.9	*15.1 - 21.5*	*77.9 - 84.8*	*0.0 - 0.4*	*1.2 - 1.5*	*4.5 - 5.4*
	Oceanward sparser seagrass	15	0.5 ± 0.1	18.8 ± 2.1	81.1 ± 2.1	0.1 ± 0.1	1.1 ± 0.0	6.3 ± 0.2
			0.2 - 0.8	*15.4 - 22.4*	*77.6 - 84.5*	*0.0 - 0.1*	*1.0 - 1.2*	*5.5 - 6.9*
	Oceanward reef crest	15	0.0 ± 0.1	35.3 ± 3.4	64.4 ± 3.4	0.3 ± 0.1	1.2 ± 0.1	7.4 ± 0.2
			-0.2 - 0.3	*24.9 - 43.2*	*55.6 - 74.7*	*0.0 - 0.2*	*1.0 - 1.2*	*6.9 - 8.0*

Table 4.5 – Textural characteristics of sediment samples recovered from each eco-geomorphic zone. Interquartile ranges in italics (*IQR1 – IQR3*).

Site	Zone	Coral	CCA	Mollusc	Foraminifera	Echinoid	*Halimeda*	Unidentified
Windward	Lagoonward patches	73.7 ± 1.9	8.2 ± 0.6	10.8 ± 1.4	1.5 ± 0.4	0.3 ± 0.1	5.1 ± 1.4	0.1 ± 0.0
		69.6 - 77.7	*6.8 - 9.9*	*7.2 - 12.8*	*0.5 - 1.9*	*0.0 - 0.6*	*1.2 - 7.0*	*0.0 - 0.2*
	Lagoonward sand	69.9 ± 2.8	6.7 ± 0.7	17.0 ± 2.5	2.2 ± 0.4	0.5 ± 0.1	3.2 ± 1.2	0.1 ± 0.0
		66.7 - 75.3	*4.8 - 7.6*	*10.9 - 18.3*	*0.8 - 3.1*	*0.1 - 0.7*	*0.8 - 3.0*	*0.0 - 0.0*
	Oceanward patches	71.8 ± 1.4	16.6 ± 1.0	6.7 ± 0.4	3.2 ± 0.8	0.4 ± 0.1	1.7 ± 0.4	0.1 ± 0.0
		69.2 - 76.6	*13.1 - 18.4*	*5.6 - 7.7*	*1.2 - 3.3*	*0.1 - 0.7*	*0.7 - 2.4*	*0.0 - 0.0*
	Rubble	73.3 ± 1.0	15.2 ± 0.7	6.1 ± 0.5	2.3 ± 0.6	0.6 ± 0.1	2.2 ± 0.5	0.1 ± 0.0
		70.2 - 76.3	*13.5 - 17.1*	*5.3 - 6.7*	*0.6 - 3.6*	*0.4 - 0.8*	*0.9 - 3.0*	*0.0 - 0.2*
	Oceanward reef crest	73.0 ± 1.0	18.4 ± 0.9	4.8 ± 0.3	0.5 ± 0.1	1.0 ± 0.2	1.2 ± 2.3	0.1 ± 0.0
		70.3 - 75.0	*16.3 - 20.7*	*3.7 - 6.0*	*0.1 - 0.7*	*0.5 - 1.5*	*1.0 - 3.7*	*0.0 - 0.1*
Leeward	Lagoonward reef crest	72.8 ± 2.0	9.7 ± 0.6	10.9 ± 1.0	3.9 ± 0.5	0.8 ± 0.2	3.0 ± 0.6	0.0 ± 0.0
		66.6 - 77.5	*9.1 - 10.6*	*8.2 - 13.1*	*2.4 - 5.8*	*0.3 - 1.0*	*0.5 - 4.7*	*0.0 - 0.1*
	Lagoonward patches	74.1 ± 2.4	6.8 ± 0.5	11.5 ± 1.5	6.3 ± 0.9	0.6 ± 0.1	1.5 ± 0.3	0.1 ± 0.0
		68.9 - 79.3	*5.8 - 8.3*	*8.0 - 15.1*	*3.3 - 8.3*	*0.2 - 1.0*	*0.8 - 2.1*	*0.0 - 0.0*
	Oceanward sand	79.0 ± 1.1	8.5 ± 0.7	9.1 ± 0.7	2.5 ± 0.4	0.4 ± 0.1	0.7 ± 0.1	0.1 ± 0.0
		76.3 - 82.8	*6.1 - 10.7*	*7.3 - 11.2*	*1.8 - 2.7*	*0.1 - 0.5*	*0.3 - 0.9*	*0.0 - 0.1*
	Dense seagrass	71.4 ± 1.4	8.3 ± 0.5	9.2 ± 0.6	9.7 ± 1.5	0.7 ± 0.1	1.1 ± 0.1	0.1 ± 0.0
		67.0 - 76.3	*7.5 - 8.9*	*7.7 - 11.3*	*4.9 - 13.2*	*0.3 - 1.0*	*0.7 - 1.6*	*0.0 - 0.1*
	Oceanward sparser seagrass	73.3 ± 1.3	9.8 ± 0.6	7.3 ± 0.4	10.5 ± 1.5	0.6 ± 0.1	0.8 ± 0.1	0.0 ± 0.0
		69.5 - 77.8	*8.3 - 10.9*	*6.2 - 8.7*	*6.7 - 12.2*	*0.3 - 0.9*	*0.4 - 1.3*	*0.0 - 0.0*
	Oceanward reef crest	72.2 ± 0.9	17.9 ± 1.0	7.0 ± 0.7	1.2 ± 0.3	0.4 ± 0.1	1.2 ± 0.2	0.2 ± 0.1
		70.5 - 74.0	*15.4 - 19.9*	*5.4 - 7.9*	*0.3 - 1.7*	*0.1 - 0.7*	*0.6 - 1.7*	*0.0 - 0.2*

Table 4.6 – Concentrations (%) of skeletal constituents within sediment samples recovered from each eco-geomorphic zone. Interquartile ranges in italics (*IQR1* – *IQR3*).

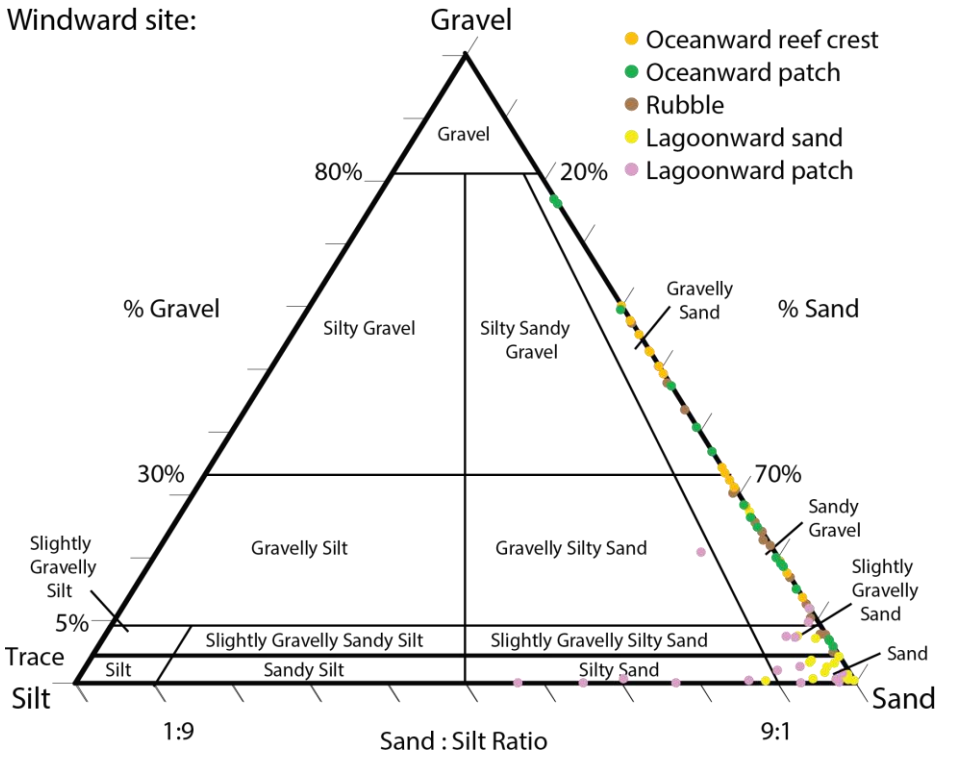

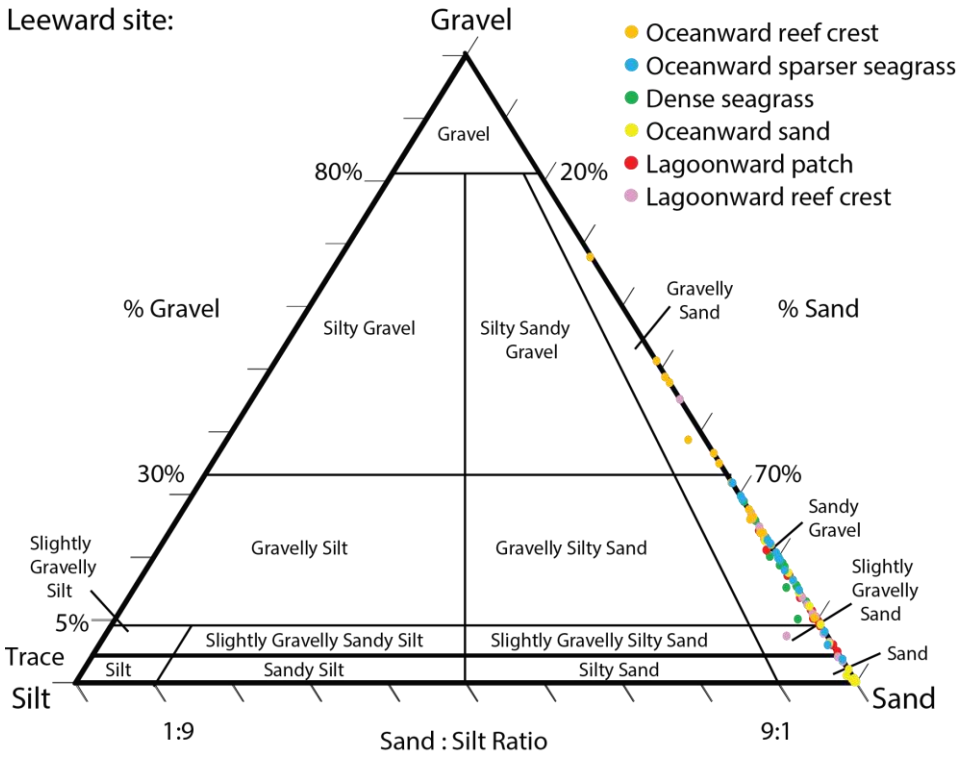

Figure 4.9 – Ternary plots of sediment texture within each eco-geomorphic zone at both the windward (upper) and leeward (lower) sites.

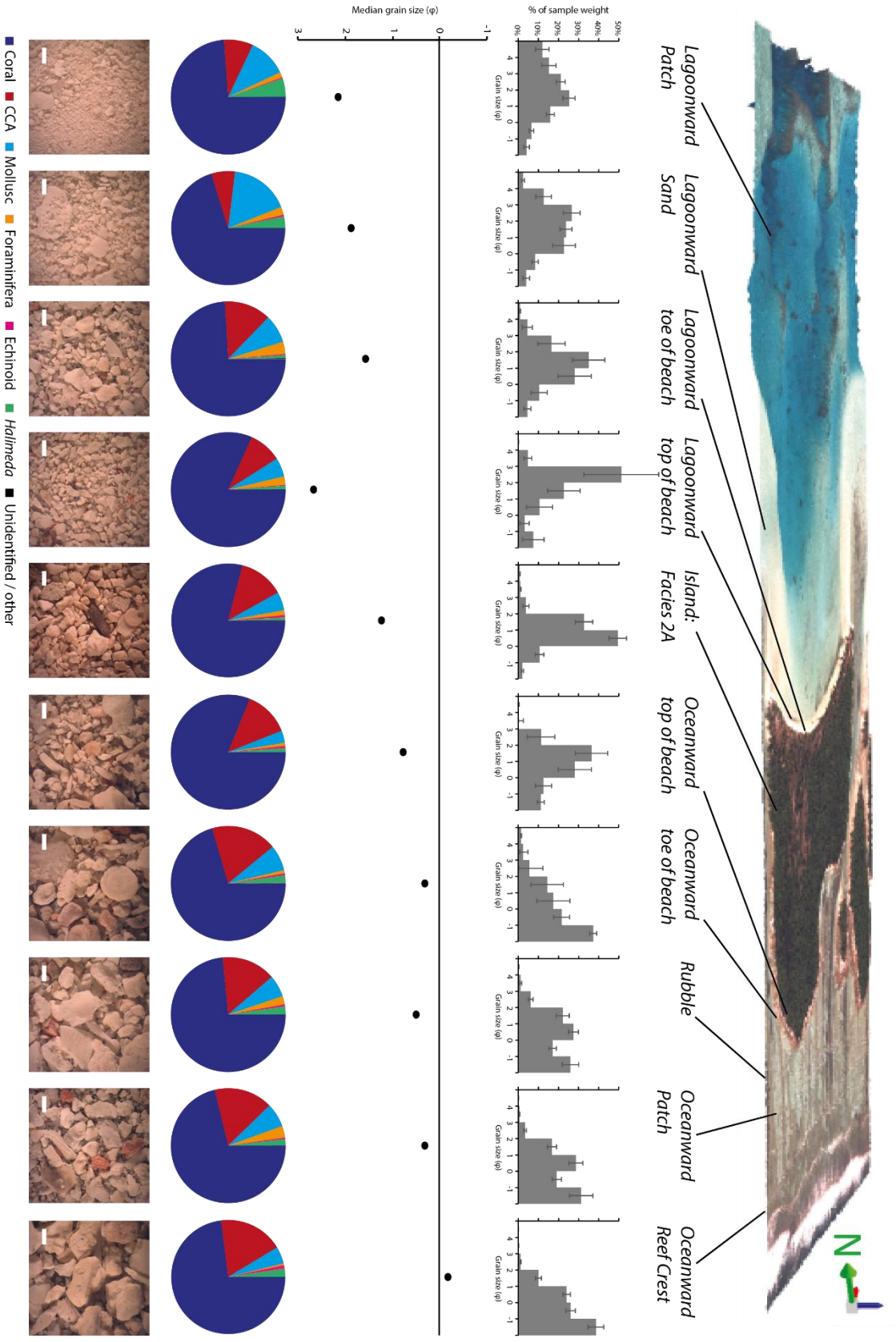

Figure 4.10 – Windward site grain size distributions, median grain sizes, composition, and images (white bar = 1 mm) from each eco-geomorphic zone, top and toe of beach samples, and island facies 2A (i.e. uppermost facies).

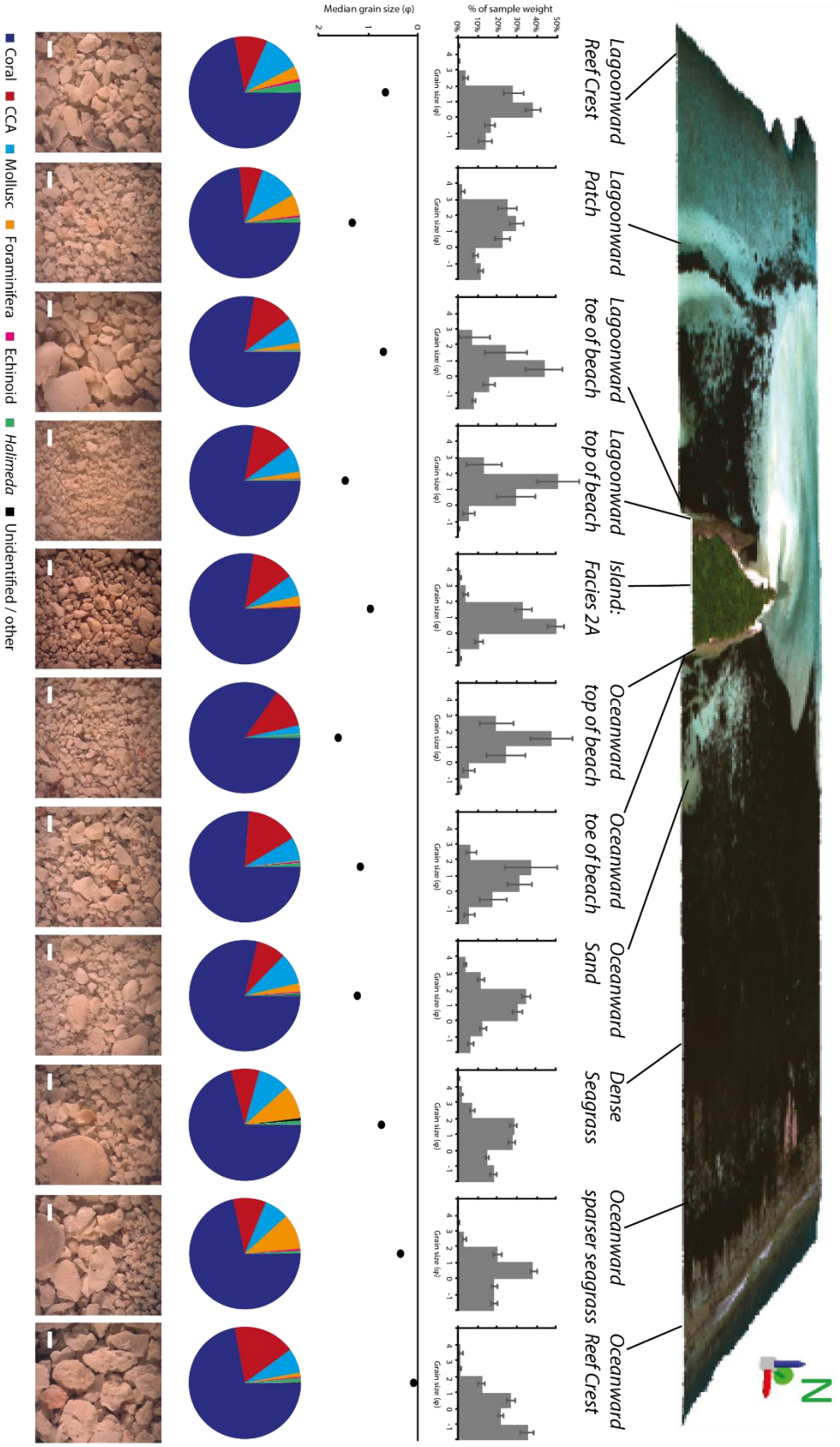

Figure 4.11 – Leeward site grain size distributions, median grain sizes, composition, and images (white bar = 1 mm) from each eco-geomorphic zone, top and toe of beach samples, and island facies 2A (i.e. uppermost facies).

4.3.2.1 Windward Site

Oceanward Reef Crest (ORC):

Oceanward reef crest samples were characterised by very coarse grain sizes (-0.1 ± 0.1 Φ) and high proportions of gravel-sized material (38.6 ± 3.8%). Grain size was thus the coarsest and the gravel proportion the highest of that found in this study. Likewise, mean settling velocity (7.9 ± 0.3 cm s^{-1}) was also the highest found within this study. Sorting was poor to very poor (1.0 ± 0.0 Φ) and the majority of sediment was sand-sized (61.4 ± 3.8%). As within all windward zone sediment samples, sediment was dominated by coral (73.0 ± 1.0%) and there were only minor contributions from foraminifera, echinoids and *Halimeda* (0.5 ± 0.1%, 1.0 ± 0.2% and 1.2 ± 2.3% respectively). Nonetheless, the proportion of echinoids was the highest of the study, albeit still marginal (1.0 ± 0.2%). The ORC samples were also characterised by the highest proportions of CCA within the site (18.4 ± 0.9%).

Rubble (R):

Sediment within the rubble zone was coarse-grained (0.5 ± 0.1 Φ) with relatively fast settling velocities (5.9 ± 0.4 cm s^{-1}) and poor sorting (1.2 ± 0.1 Φ). While sand-sized material dominated (73.9 ± 4.1%), proportions of gravel-sized material were relatively high (25.9 ± 4.1%). Coral was the dominant sediment constituent (73.3 ± 1.0%), although rubble zone sediment also possessed relatively high concentrations of CCA (15.2 ± 0.7%).

Oceanward Patch (OP):

Mean grain-size of sediment within the oceanward patch zone was slightly coarser (0.2 ± 0.1 Φ) than that found within the rubble zone. Similarly, proportions of gravels were slightly higher (30.6 ± 5.5%) and settling velocities slightly faster (6.1 ± 0.3 cm s^{-1}) than in the rubble zone. Nonetheless, samples were still predominantly comprised of sand-sized material (69.3 ± 0.1%) with poor sorting (1.1 ± 0.1 Φ). The composition of oceanward patch zone samples was comparable to the sediment of the rubble zone. Coral represented the most significant sediment contributor (71.8 ± 1.4%) and concentrations of CCA were relatively high (16.6 ± 1.0%).

Lagoonward Sand (LS):

Lagoonward sediment could be differentiated from oceanward material as it was markedly finer (medium-grained, 1.9 ± 0.1 Φ), with lower proportions of gravels (3.9 ±

1.7%) and slightly higher proportions of silts (2.3 ± 0.7%). In turn, the settling velocity of lagoonward sand zone sediment was almost half that of oceanward sediments (3.1 ± 0.3 cm s^{-1}). However, as in the oceanward zones, the vast majority of material was sand-sized (93.8 ± 2.3%) and poorly sorted (1.2 ± 0.1 Φ). The composition of lagoonward sand zone sediment was marked by the highest concentrations of molluscs (17.0 ± 2.5%) found in the entire study. Proportions of *Halimeda* were also slightly greater (3.2 ± 1.2%) than those found within the oceanward zones. The contribution of CCA was the lowest found within the study (6.7 ± 0.7%), while coral was consistently the dominant contributor to the sediment reservoir (69.9 ± 2.8%).

Lagoonward Patch (LP):

The lagoonward reef crest zone contained the finest mean grain size of the entire study (fine-grained, 2.5 ± 0.3 Φ). This is partially attributable to the proportion of silts, which was the highest of the study (12.0 ± 3.4%), and the relatively low proportion of gravel-sized material (4.1 ± 1.5%). Settling velocities of the sand-sized fractions were comparable to those in the lagoonward sand zone (3.2 ± 0.2 cm s^{-1}), though sorting was the poorest found in this study (very poor, 1.7 ± 0.1 Φ). As found throughout both sites, the majority of sediment was sand-sized (87.0 ± 3.1%) and composed of coral (73.7 ± 1.9%). As in the lagoonward patch zone, concentrations of CCA were relatively low (8.2 ± 0.6%), whereas proportions of molluscs and *Halimeda* were relatively high (10.8 ± 1.4% and 5.1 ± 1.4%).

4.3.2.2 Leeward Site

Oceanward Reef Crest (ORC):

Sediment from the oceanward reef crest was characterised by its coarse to very coarse (0.0 ± 0.1 Φ) grain size with high proportions of gravel-sized material (35.3 ± 3.4%). Indeed, mean grain size was the coarsest and, likewise, proportions of gravel were the highest of any zone within the leeward site. Similarly, samples recovered from this zone had the fastest settling velocities (7.4 ± 0.2 cm s^{-1}). As within all zones at the leeward site, sediment was predominantly sand-sized (64.4 ± 3.4%) and sorting was poor (1.2 ± 0.1 Φ). In terms of composition, sediment was dominated by coral (72.2 ± 0.9%), but was distinguishable as it contained higher proportions of CCA than found in any other zone (17.9 ± 1.0%).

Oceanward Sparser Seagrass (OSS):

Sediment of the sparser seagrass zone was coarse-grained (0.5 ± 0.1 Φ), though finer than that found on the oceanward reef crest. Proportions of gravel-sized material and settling velocities were thus lower (18.8 ± 2.1%; 6.3 ± 0.2 cm s^{-1}) than found in the ORC zone. The majority of sediment was sand-sized (81.1 ± 2.1%) and sorting was poor (1.1 ± 0.0 Φ). Compositionally, although dominated by coral (73.3 ± 1.3%), samples possessed the highest concentrations of foraminifera (10.5 ± 1.5%) found within the study site. This is likely because forams were frequently observed (and counted, refer to Chapter 6) as epibionts on seagrass blades.

Dense Seagrass (DSG):

The dense seagrass zone was host to coarse-grained sediment, (0.8 ± 0.1 Φ), which was, again, slightly finer than that within the sparser seagrass zone. Likewise, settling velocities were slightly slower than in zones closer to the oceanward reef crest (5.0 ± 0.2 cm s^{-1}). Material was predominantly sand-sized (81.3 ± 1.4%) while silts remained negligible (0.4 ± 0.2%), albeit with marginally increased concentrations. As in all zones, sorting was poor (1.3 ± 0.0 Φ) and composition was coral-dominated (71.4 ± 1.4%). However, concentrations of both molluscs and foraminifera were relatively high (9.2 ± 0.6% and 9.7 ± 1.5% respectively), which is likely attributable to the habitat they are offered by seagrass beds.

Oceanward Sand (OS):

The oceanward sand zone was distinguished by a shift in mean grain size to that of medium-grained sediment (1.2 ± 0.1 Φ). Concentrations of gravel-sized material were the lowest within the study site (6.8 ± 2.0%) and thus proportions of sand-sized fractions were the highest (93.0 ± 2.0%). Settling velocities (5.4 ± 0.2 cm s^{-1}) were slightly faster than those within the dense seagrass zone, which may be due to the lower concentrations of more plate-shaped grains, for example foraminifera concentrations were especially low (2.5 ± 0.4%). Coral concentrations were the highest of the study site (79.0 ± 1.1%).

Lagoonward Patch (LP):

Mean grain size within the lagoonward patch zone was medium-grained (1.3 ± 0.1 Φ), comprised of poorly sorted (1.2 ± 0.1 Φ), predominantly sand-sized material (88.3 ± 1.7%). While grain size was the finest within the lagoonward site, settling velocities

were, similarly, the slowest (3.9 ± 0.3 cm s^{-1}). The composition of lagoonward patch zone samples was characterised by the highest concentrations of molluscs (11.5 ± 1.5%). Proportions of foraminifera were also relatively high (6.3 ± 0.9%), which may also be attributable to the presence of varying densities of seagrass within the zone. Composition was dominated by coral (74.1 ± 2.4%), while proportions of CCA were the lowest of the study site (6.8 ± 0.5%).

Lagoonward Reef Crest (LRC):

While grain-size within all other zones decreased with distance from the reef crest, sediment of the lagoonward reef crest was characterised by a relative increase in grain size to that of coarse-grained sediment (0.7 ± 0.1 Φ). In turn, settling velocities were relatively high (6.0 ± 0.3 cm s^{-1}), although proportions of gravel-sized material were low (13.5 ± 3.1%). Indeed, samples were comprised of poor to very poorly sorted (1.0 ± 0.1 Φ) sediment with an average of 86.0 ± 3.1% sand-sized material. Samples were comprised of coral (72.8 ± 2.0%) with relatively high proportions of CCA (9.7 ± 0.6%) and molluscs (10.9 ± 1.0%).

4.3.2.3 Spatial Variability in Marine Benthic Sedimentology

Trends in the data were particularly evident when examined spatially. Figures 4.12 to 4.15 represent the results of block kriging analyses of textural (4.12 and 4.13) and compositional (4.14 and 4.15) data from the windward and leeward sites respectively. Tables 4.7 and 4.8 comprise correlation matrices for the windward and leeward sites respectively, which are depicted in Figures 4.16 and 4.17. At the windward site, several statistically significant gradients in textural data were found with increasing distance from the oceanward reef crest. For example, mean grain size decreased from coarse-grained at the oceanward reef crest (-0.1 ± 0.1 Φ) to fine-grained in the lagoonward patch zone (2.5 ± 0.3 Φ; P = <0.0005, R^2 = 0.60). Similarly, there was a significant corresponding decrease in both the proportion of gravel-sized material (from 38.6 ± 3.8% at the oceanward reef crest to 4.1 ± 1.5% in the lagoonward patch zone; P = <0.0005, R^2 = 0.38) and settling velocities (oceanward reef crest: 7.9 ± 0.3 cm s^{-1}; lagoonward patch: 3.2 ± 0.2 cm s^{-1}; P = <0.0005, R^2 = 0.52) with distance from the reef crest. This is also evident in the relatively distinct groupings in the windward site tri-plot (Figure 4.9). Likewise, a significant decrease was found in the degree of sorting with proximity to the lagoonward edge of the platform from moderate (1.0 ± 0.0

Φ) at the oceanward reef crest to poor (1.7 ± 0.1 Φ) in the lagoonward patch zone (P = <0.0005, R^2 = 0.57).

Spatial trends in textural data at the leeward site were perhaps more complex as oceanward-lagoonward gradients were evident across all zones, but with the exception of the lagoonward reef crest. While significant relationships were found with increased distance from the oceanward reef crest, correlation coefficients and R^2 values were therefore lower than those found at the windward site. Indeed, this is also evidenced in that groupings in tri-plots are less distinct than those from the windward site (Figure 4.9). For instance, mean grain size decreased from 0.0 ± 0.1 Φ on the oceanward reef crest to 1.3 ± 0.1 Φ within the lagoonward patch zone, then increased to 0.7 ± 0.1 Φ on the lagoonward reef crest (P = <0.0005, R^2 = 0.22). In turn, there was an associated decrease in the proportion of gravel-sized material (35.3 ± 3.4% to 11.5 ± 1.7%) with distance between the oceanward reef crest and lagoonward patch zones (P = <0.0005, R^2 = 0.21). However, the proportion of gravels was greater on the lagoonward reef crest than in the lagoonward patch zone (13.5 ± 3.1%). Likewise, there was a decay in settling velocities from 7.4 ± 0.2 cm s^{-1} at the oceanward reef crest to 3.9 ± 0.3 cm s^{-1} in the lagoonward patch zone, while velocities at the lagoonward reef crest increased to (6.0 ± 0.3 cm s^{-1}; P = <0.0005, R^2 = 0.17).

Similar oceanward-lagoonward gradients were also evident in sediment composition. At the windward site, there was a significant increase in concentrations of CCA with proximity to the oceanward reef crest (from averages of 18.4 ± 0.9% at the oceanward reef crest to 8.2 ± 0.6% in the lagoonward patch zone; P = <0.0005; R^2 = 0.55), and, conversely, a decrease in proportions of *Halimeda* (1.2 ± 2.3% at the oceanward reef crest to 5.1 ±1.4% in the lagoonward patch zone; P = <0.0005, R^2 = 0.11). CCA abundances also increased toward the oceanward reef crest at the leeward site (17.9 ± 1.0% at the oceanward reef crest to 6.8 ± 0.5% in the lagoonward patch zone; P = <0.0005, R^2 = 0.21), though then increased at the lagoonward reef crest (9.7 ± 0.6%). In addition, at both sites the proportion of molluscs was markedly higher in the lagoonal environments, than the oceanward environments (e.g. at the windward site, 17.0 ± 2.5% in the lagoonward sand zone; at the leeward site, 11.5 ± 1.5% in the lagoonward patch zone; P = <0.0005, R^2 = 0.21 with distance from the ORC). Similarly, at the leeward site the proportion of molluscs increased from 7.0 ± 0.7% at the oceanward reef crest to 11.5 ± 1.5% in the lagoonward patch zone (P = <0.0005, R^2 = 0.17 with

increasing distance from the ORC). Also notable were the relatively high proportions of foraminifera with the seagrass zones (9.7 ± 1.5% in the dense seagrass zone, and 10.5 ± 1.5% in the sparser seagrass zone).

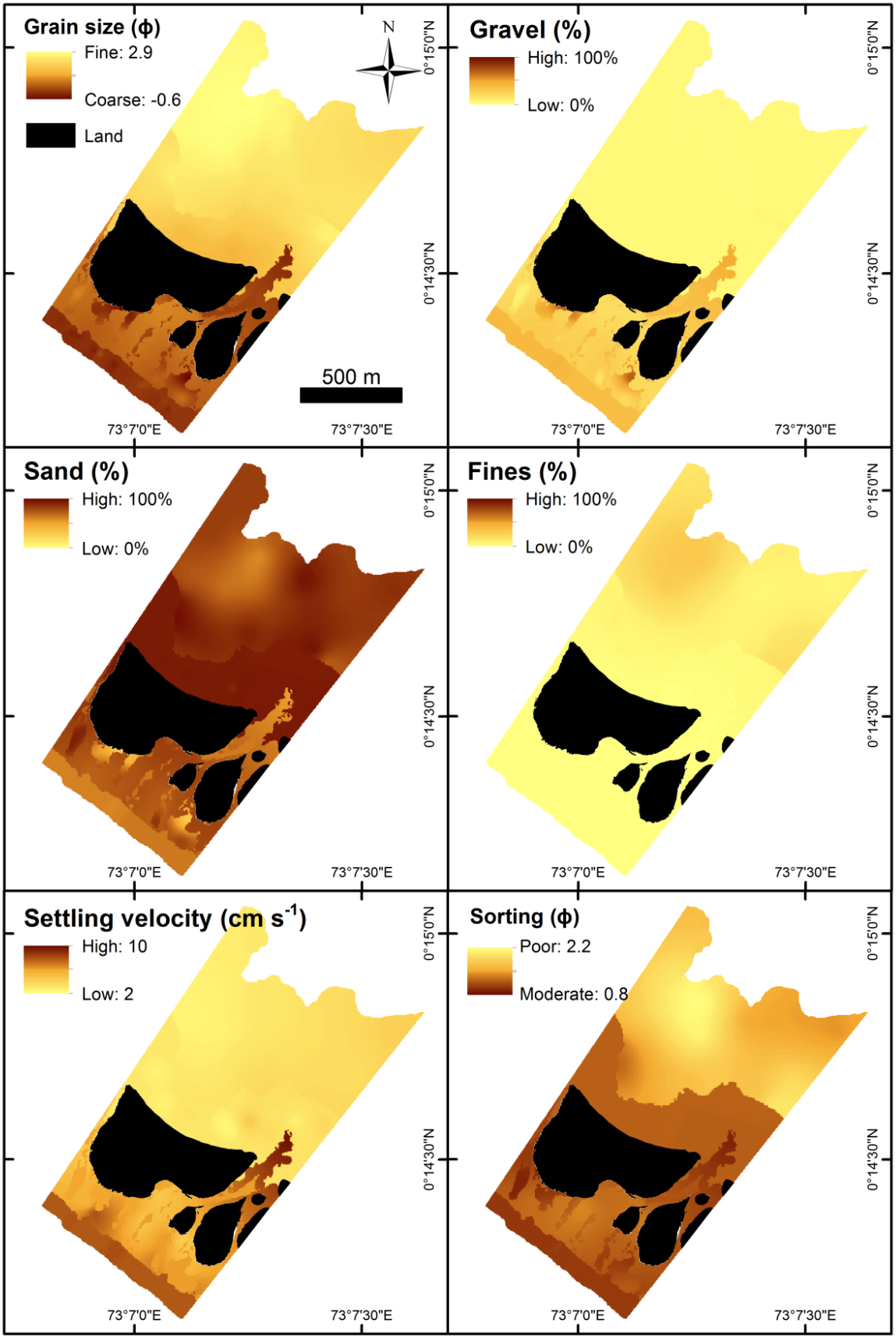

Figure 4.12 – Block kriging results of textural characteristics of windward site sediment samples.

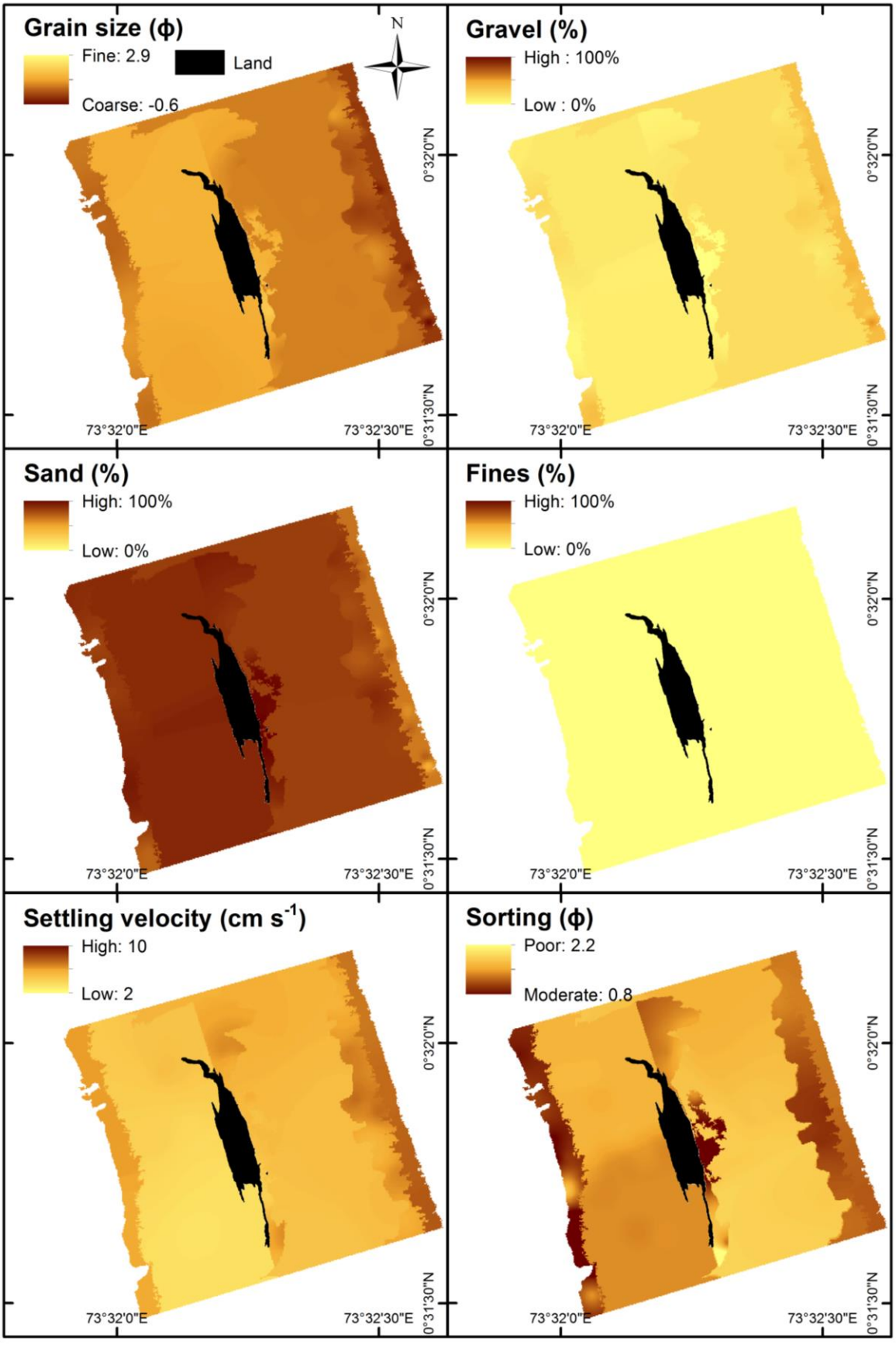

Figure 4.13 – Block kriging results of textural characteristics of leeward site sediment samples.

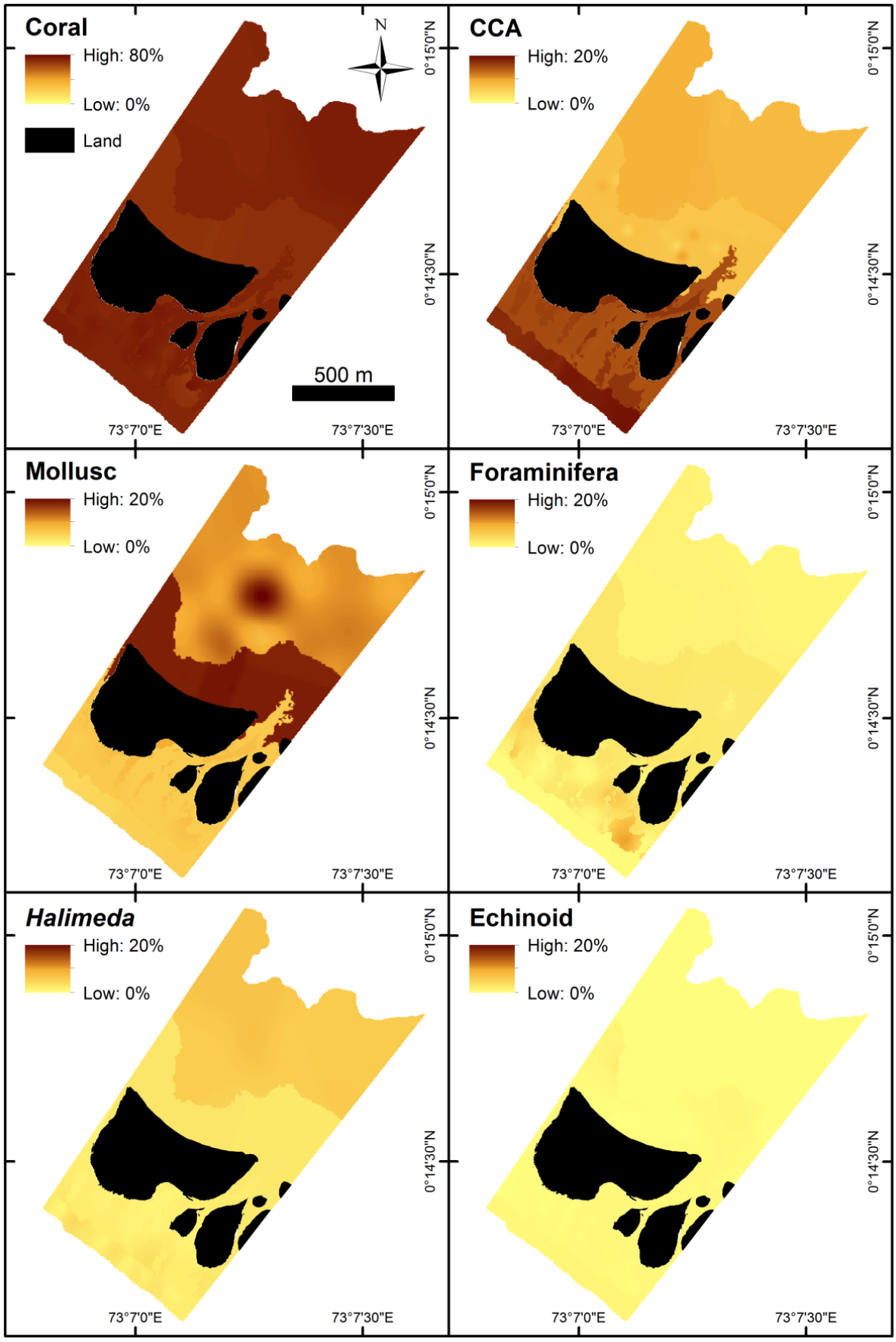

Figure 4.14 – Block kriging results of windward site sediment composition.

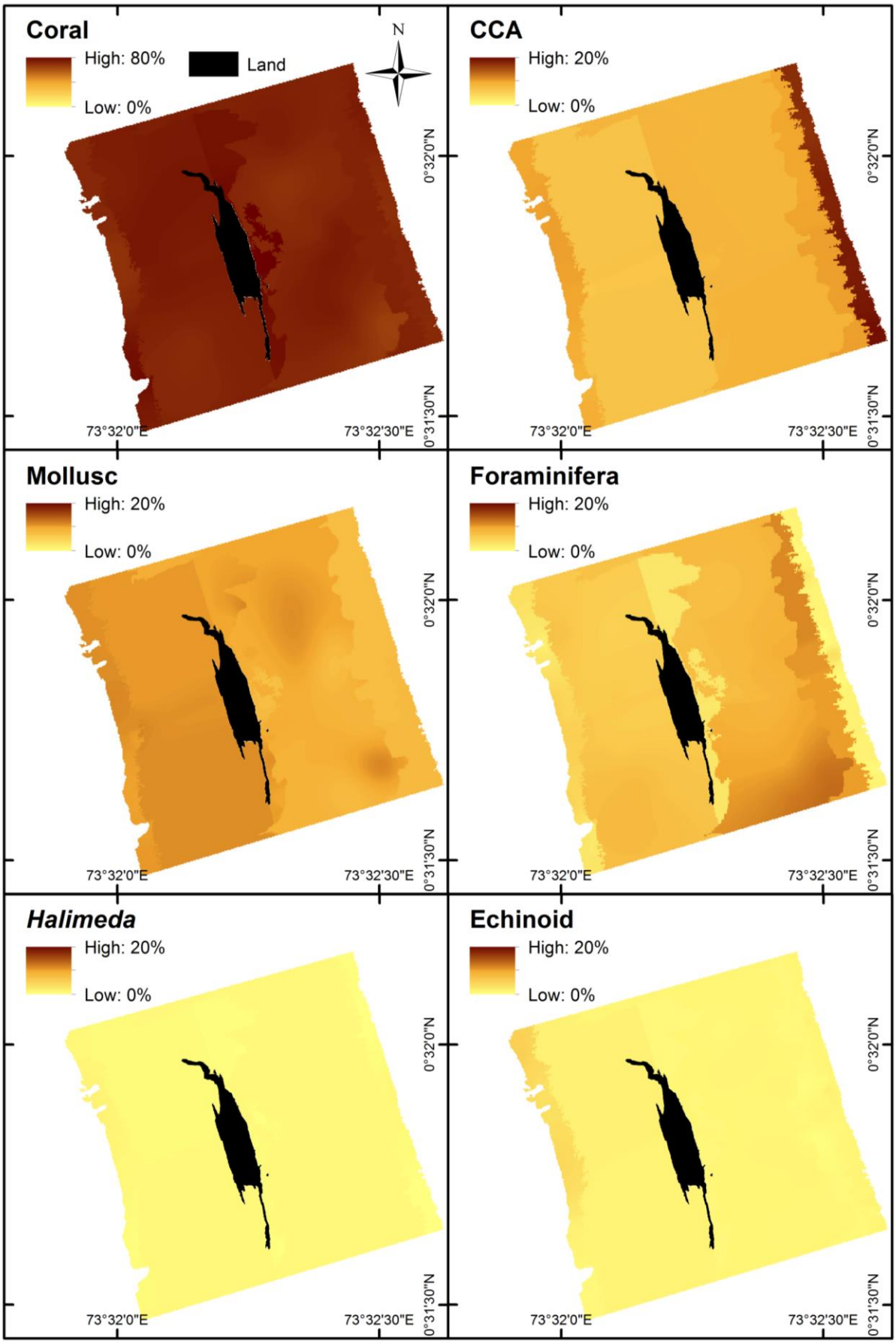

Figure 4.15 – Block kriging results of leeward site sediment composition.

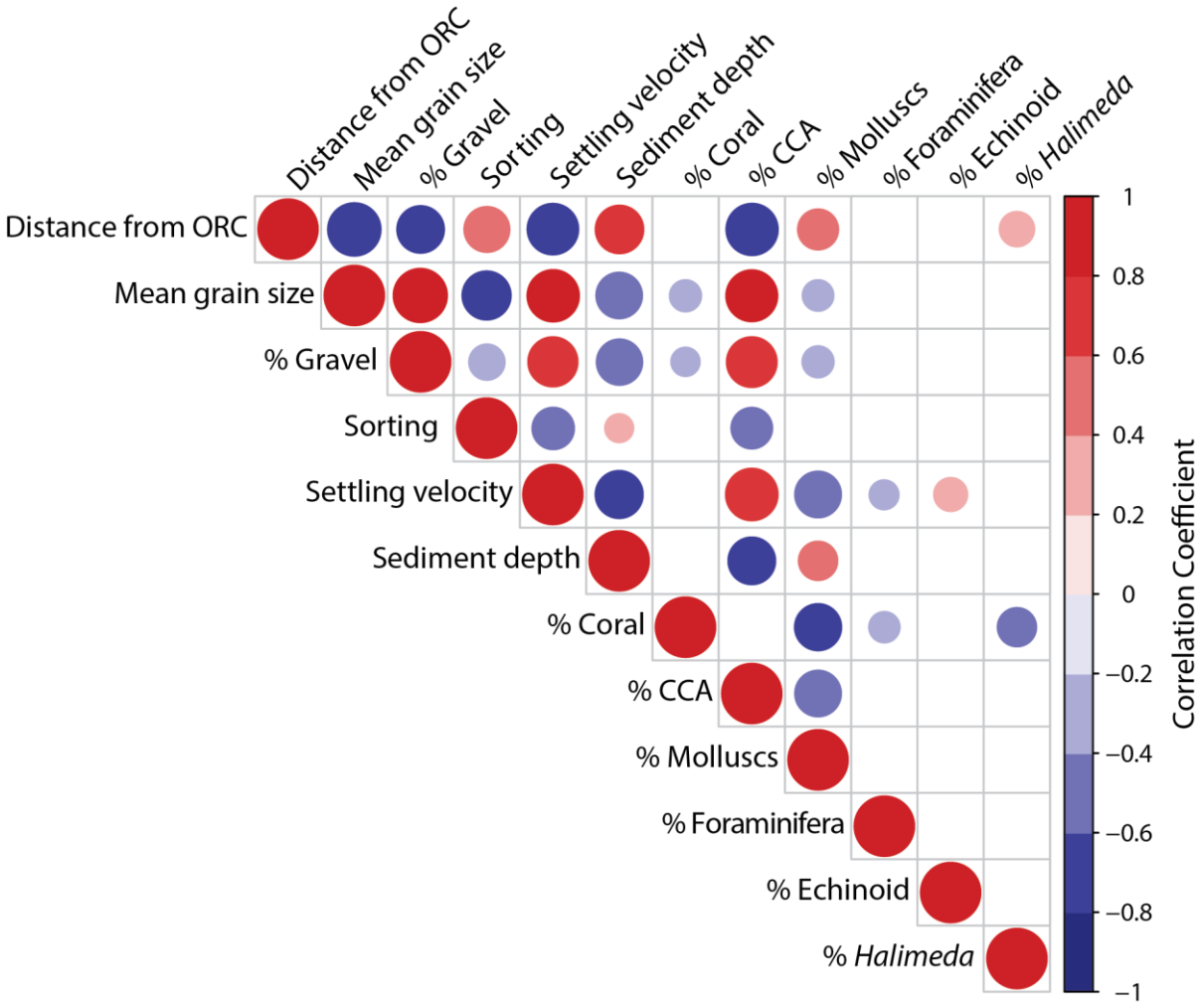

Figure 4.16 – Windward site correlation matrix showing significant relationships (only those where $P < 0.05$ are included) between sediment textural characteristics, composition, sediment depths, and distance from the oceanward reef crest. Colour intensity and circle size are proportional to the correlation coefficients.

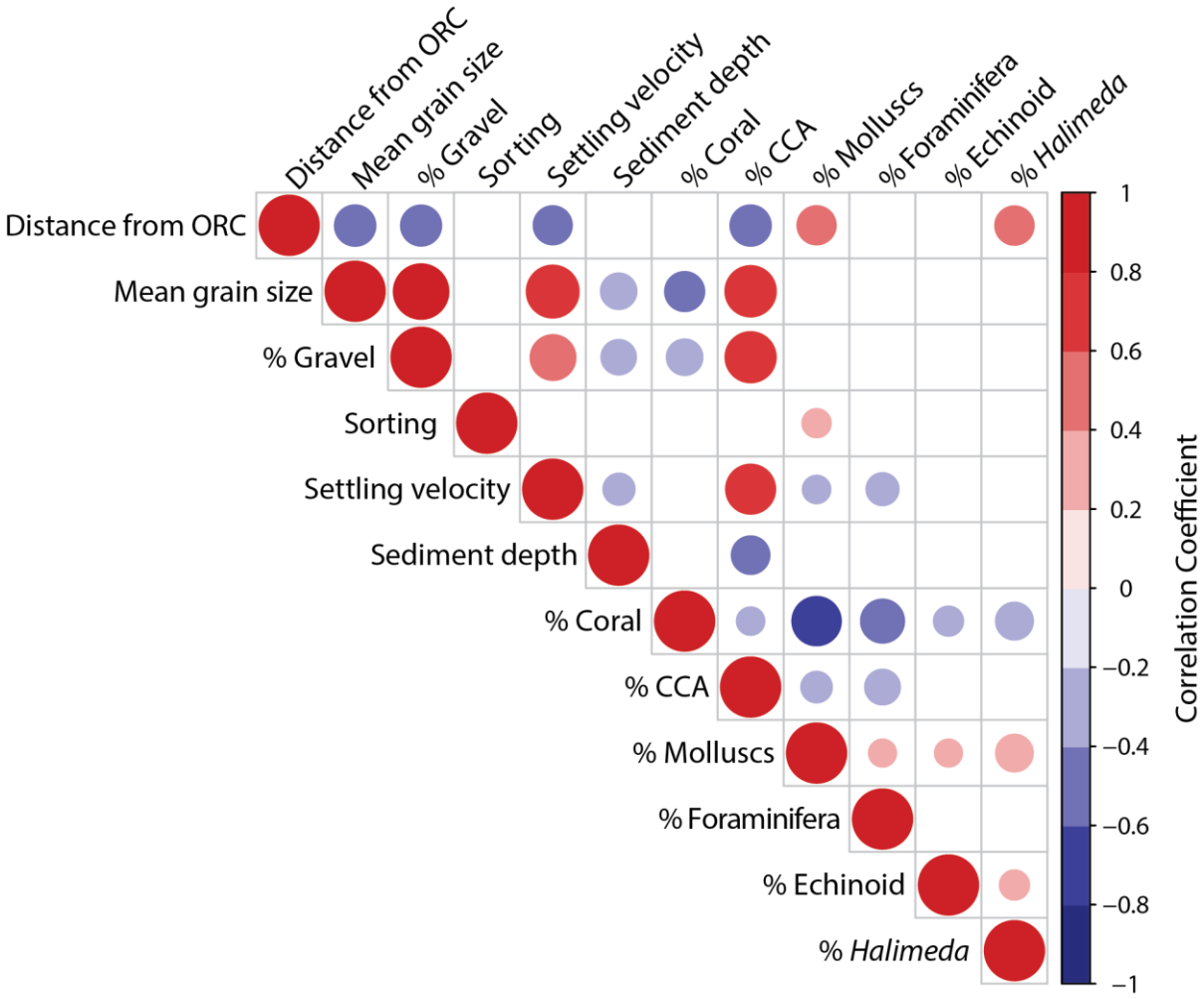

Figure 4.17 – Leeward site correlation matrix showing significant relationships (only those where P < 0.05 are displayed) between sediment textural characteristics, composition, sediment depths, and distance from the oceanward reef crest. Colour intensity and circle size are proportional to the correlation coefficients.

	Distance from ORC	Mean grain size	% Gravel	Sorting	Settling velocity	Sediment depth	% Coral	% CCA	% Molluscs	% Foraminifera	% Echinoid	% *Halimeda*
Distance from ORC		0.78	-0.62	0.57	-0.72	0.64	-0.02	-0.74	0.46	-0.04	-0.22	0.34
Mean grain size	**0.00**		0.8	-0.65	0.75	-0.59	-0.28	0.73	-0.27	-0.02	0.18	0.05
% Gravel	**0.00**	**0.00**		-0.36	0.69	-0.58	-0.23	0.7	-0.28	-0.09	0.06	-0.05
Sorting	**0.00**	**0.00**	**0.00**		-0.49	0.22	0.14	-0.47	0.2	-0.15	-0.18	0.12
Settling velocity	**0.00**	**0.00**	**0.00**	**0.00**		-0.63	0.12	0.75	-0.59	-0.24	0.31	-0.11
Sediment depth	**0.00**	**0.00**	**0.00**	**0.04**	**0.00**		-0.02	-0.62	0.42	0.03	-0.06	0.16
% Coral	0.84	**0.01**	**0.04**	0.21	0.27	0.84		-0.1	-0.6	-0.26	0.06	-0.42
% CCA	**0.00**	**0.00**	**0.00**	**0.00**	**0.00**	**0.00**	0.36		-0.59	-0.04	0.16	-0.19
% Molluscs	**0.00**	**0.02**	**0.01**	0.07	**0.00**	**0.00**	**0.00**	**0.00**		0.08	-0.19	0.1
% Foraminifera	0.71	0.85	0.43	0.19	**0.03**	0.80	**0.02**	0.72	0.47		-0.11	-0.14
% Echinoid	0.05	0.12	0.62	0.12	**0.00**	0.62	0.59	0.14	0.09	0.31		-0.04
% *Halimeda*	**0.00**	0.64	0.63	0.28	0.31	0.15	**0.00**	0.08	0.38	0.21	0.70	

Table 4.7 – Windward site correlation matrix of sediment textural characteristics, composition, sediment depths, and distance from the oceanward reef crest. Correlation coefficients and P values are in the upper right and lower left portions of the table respectively. Significant P values (<0.05) are in bold.

	Distance from ORC	Mean grain size	% Gravel	Sorting	Settling velocity	Sediment depth	% Coral	% CCA	% Molluscs	% Foraminifera	% Echinoid	% *Halimeda*
Distance from ORC		0.47	-0.46	-0.09	-0.42	-0.05	0.06	-0.46	0.42	-0.13	0.10	0.42
Mean grain size	**0.00**		0.85	0.07	0.77	-0.36	-0.44	0.72	-0.05	-0.01	0.13	0.05
% Gravel	**0.00**	**0.00**		0.18	0.57	-0.34	-0.36	0.72	-0.06	-0.10	0.10	-0.06
Sorting	0.38	0.53	0.09		-0.18	0.03	-0.16	-0.15	0.23	0.06	0.03	0.16
Settling velocity	**0.00**	**0.00**	**0.00**	0.08		-0.28	-0.11	0.69	-0.22	-0.29	0.03	0.03
Sediment depth	0.62	**0.00**	**0.00**	0.79	**0.01**		0.05	-0.40	0.09	0.20	-0.08	-0.17
% Coral	0.54	**0.00**	**0.00**	0.14	0.31	0.61		-0.22	-0.67	-0.53	-0.24	-0.39
% CCA	**0.00**	**0.00**	**0.00**	0.17	**0.00**	**0.00**	**0.04**		-0.27	-0.35	-0.10	-0.09
% Molluscs	**0.00**	0.66	0.54	**0.03**	**0.04**	0.42	**0.00**	**0.01**		0.21	0.21	0.39
% Foraminifera	0.21	0.90	0.35	0.59	**0.00**	0.05	**0.00**	**0.00**	**0.05**		0.12	-0.02
% Echinoid	0.36	0.22	0.33	0.74	0.81	0.45	**0.02**	0.36	**0.05**	0.25		0.25
% *Halimeda*	**0.00**	0.64	0.55	0.14	0.80	0.12	**0.00**	0.38	**0.00**	0.88	**0.02**	

Table 4.8 – Leeward site correlation matrix of sediment textural characteristics, composition, sediment depths, and distance from the oceanward reef crest. Correlation coefficients and P values are in the upper right and lower left portions of the table respectively. Significant P values (<0.05) are in bold.

4.3.3 Beach Sedimentology

Tables 4.9 and 4.10 describe the textural and compositional characteristics of beach sediment samples recovered from each study site. Mean sedimentary characteristics are also characterised in Figures 4.10 and 4.11.

Oceanward Toe of Beach:

Toe of beach samples from the windward site were characterised by the coarsest mean grain size (coarse-grained, 0.2 ± 0.3 Φ) and highest proportions of gravel-sized material (37.3 ± 8.1%) found within the beach sediments. At the leeward site, samples were coarse-to-medium-grained (1.0 ± 0.3 Φ) with lower proportions of gravel (5.8 ± 2.6 %). Sorting at the windward site was poor (1.4 ± 0.2 Φ), while leeward site sorting was moderate (0.9 ± 0.1 Φ). Nonetheless, material from both sites was predominantly sand-sized (61.3 ± 8.2% and 94.0 ± 2.6% at the windward and leeward sites respectively) with relatively high settling velocities (7.1 ± 1.1 cm s^{-1} and 6.2 ± 0.8 cm s^{-1} at the windward and leeward sites respectively). Sediment from both sites was comprised primarily of coral (70.4 ± 4.0% and 74.9 ± 5.3% at the windward and leeward sites respectively). Proportions of CCA were relatively high (18.5 ± 3.4% at the windward site and 9.2 ± 1.1% at the leeward site), particularly at the windward site. Likewise, there were relatively high concentrations of molluscs (7.2 ± 0.8% at the windward site and 11.4 ± 3.6% at the leeward site), particularly at the leeward site. As within all samples, sediment possessed lesser contributions from foraminifera (0.9 ± 0.3%; 3.0 ± 0.8% at the windward and leeward sites respectively), echinoids (0.6 ± 0.1%; 0.6 ± 0.2%) and *Halimeda* (2.1 ± 0.6%; 1.3 ± 0.5%).

Oceanward Top of Beach:

Oceanward top of beach samples were notably finer (1.0 ± 0.4 Φ and 1.5 ± 0.2Φ at the windward and leeward sites respectively) and possessed lower proportions of gravel (11.2 ± 6.6%, 1.3 ± 0.8%) than their counterparts at the oceanward toe of the beach. Similarly, there were increases in the proportions of sand (88.6 ± 6.6%, 98.7 ± 0.8%) and settling velocities were slower (6.2 ± 1.1 cm s^{-1}, 5.5 ± 0.7 cm s^{-1}). At both sites, sorting was moderate (0.8 ± 0.1 Φ, 0.7 ± 0.1 Φ) and coral represented the key skeletal constituent (81.4 ± 3.2%, 82.7 ± 4.3%). In comparison to the toe of beach samples, both concentrations of CCA (12.9 ± 2.3%, 8.2 ± 1.3%) and molluscs (3.4 ± 0.6%, 6.8 ± 2.3%) were lower. Contributions from foraminifera (0.9 ± 0.4%, 2.1 ±

0.8%), echinoids (0.6 ± 0.3%, 0.2 ± 0.1%) and *Halimeda* (1.1 ± 0.4%, 0.8 ± 0.2%) remained relatively low.

Lagoonward Toe of Beach:

Lagoonward toe of beach material was characterised by medium-grained sediment (1.4 ± 0.3 Φ) at the windward site and coarse-grained sediment (0.8 ± 0.1 Φ) at the leeward site. Indeed, at the leeward site, mean grain size and the proportion of gravels (7.8 ± 1.6%) were comparable to those found at the oceanward toe of beach. By contrast, samples at the windward site were markedly finer in grade and comprised lower proportions of gravels (4.6 ± 1.7%) than those on the oceanward coast. Lagoonward toe of beach samples at the leeward site thus had faster settling velocities (7.1 ± 0.3 cm s^{-1}) than those at the windward site (4.6 ± 0.7 cm s^{-1}). At both sites sorting was poor (1.1 ± 0.1 Φ, 1.0 ± 0.1 Φ at the windward and leeward sites respectively) and the majority of material was sand-sized (94.6 ± 1.6%, 92.2 ± 1.6%). Sediments were principally comprised of coral (73.8 ± 2.2%, 74.4 ± 3.2% at the windward and leeward sites respectively), although proportions of molluscs were relatively high (7.9 ± 0.7%, 11.9 ± 2.2%). CCA concentrations were comparable to those found on the oceanward coasts at the leeward site (9.7 ± 0.5%), while at the windward site concentrations of CCA were slightly lower on the lagoonward coasts (13.1 ± 0.8%).

Lagoonward Top of Beach:

The lagoonward top of beach samples at the windward site had the finest mean grain size (fine-grained, 2.0 ± 0.5 Φ) and slowest settling velocity (3.3 ± 0.5 cm s^{-1}) of the beach samples. Leeward top of beach samples were medium-grained (1.5 ± 0.2 Φ) with settling velocities of 6.3 ± 0.7 cm s^{-1}. At both sites, sediment sorting was moderate (0.7 ± 0.2 Φ, 0.6 ± 0.0 Φ at the windward and leeward sites respectively) and sand-sized material dominated (92.4 ± 5.4%, 99.6 ± 0.1%) over gravels (7.5 ± 5.4%, 0.3 ± 0.1%) and silts (0.1 ± 0.1%, 0.0 ± 0.0%). Lagoonward top of beach sediment samples were also characterised by the highest proportions of coral found within beach sediments (81.7 ± 4.5%, 83.1 ± 3.9% at the windward and leeward sites respectively), while proportions of CCA (9.2 ± 2.1%, 8.0 ± 1.3%) and molluscs (5.3 ± 0.6%, 6.7 ± 1.9%) were relatively low.

Overall, toe of beach samples were significantly coarser than those from the top of the beach (P = 0.001; paired t-test). Sorting at the toe of the beach was also significantly poorer than at the top of the beach (P = <0.001; paired t-test). Controlling for the differences between top and toe samples, sediments on the lagoonward coasts were significantly finer grained than those from the oceanward coasts ($F_{1,39}$ = 5.798, P = 0.021; ANCOVA).

Site	Sample location	Mean grain size (Φ)	% Gravel	% Sand	% Silt	Sorting (σ_Φ)	Settling velocity (cm/s)
Windward	Oceanward toe	0.2 ± 0.3	37.3 ± 8.1	61.3 ± 8.2	1.4 ± 0.9	1.4 ± 0.2	7.1 ± 1.1
		-0.2 - 0.7	*23.0 - 44.0*	*55.6 - 75.3*	*0.3 - 1.1*	*1.2 - 1.5*	*5.9 - 8.4*
	Oceanward top	1.0 ± 0.4	11.2 ± 6.6	88.6 ± 6.6	0.2 ± 0.1	0.8 ± 0.1	6.2 ± 1.1
		0.5 - 1.8	*0.0 - 14.3*	*85.6 - 99.9*	*0.0 - 0.1*	*0.5 - 1.0*	*5.5 - 7.2*
	Lagoonward toe	1.4 ± 0.3	4.6 ± 1.7	94.6 ± 1.6	0.9 ± 0.3	1.1 ± 0.1	4.6 ± 0.7
		1.0 - 1.9	*1.8 - 7.4*	*92.2 - 97.4*	*0.4 - 1.2*	*0.9 - 1.2*	*3.8 - 4.8*
	Lagoonward top	2.0 ± 0.5	7.5 ± 5.4	92.4 ± 5.4	0.1 ± 0.1	0.7 ± 0.2	3.3 ± 0.5
		1.1 - 2.7	*0.0 - 10.0*	*89.8 - 100.0*	*0.0 - 0.2*	*0.4 - 1.0*	*2.5 - 4.4*
Leeward	Oceanward toe	1.0 ± 0.3	5.8 ± 2.6	94.0 ± 2.6	0.2 ± 0.0	0.9 ± 0.1	6.2 ± 0.8
		0.5 - 1.4	*1.1 - 10.6*	*89.2 - 98.9*	*0.1 - 0.2*	*0.8 - 1.0*	*5.6 - 6.9*
	Oceanward top	1.5 ± 0.2	1.3 ± 0.8	98.7 ± 0.8	0.1 ± 0.0	0.7 ± 0.1	5.5 ± 0.7
		1.3 - 1.8	*0.1 - 1.3*	*98.6 - 99.8*	*0.0 - 0.1*	*0.5 - 0.9*	*4.4 - 6.9*
	Lagoonward toe	0.8 ± 0.1	7.8 ± 1.6	92.2 ± 1.6	0.1 ± 0.0	1.0 ± 0.1	7.1 ± 0.3
		0.7 - 0.9	*4.5 - 11.2*	*88.8 - 95.2*	*0.0 - 0.1*	*0.8 - 1.0*	*6.8 - 7.4*
	Lagoonward top	1.5 ± 0.2	0.3 ± 0.1	99.6 ± 0.1	0.0 ± 0.0	0.6 ± 0.0	6.3 ± 0.7
		1.1 - 1.9	*0.2 - 0.3*	*99.7 - 99.8*	*0.0 - 0.0*	*0.5 - 0.7*	*5.9 - 7.5*

Table 4.9 – Textural characteristics of top and toe of beach sediment samples from both the windward and leeward study sites. Interquartile ranges in italics (*IQR1 – IQR3*).

Site	Zone	Coral	CCA	Mollusc	Foraminifera	Echinoid	*Halimeda*	Unidentified
Windward	Oceanward toe	70.4 ± 4.0	18.5 ± 3.4	7.2 ± 0.8	0.9 ± 0.3	0.6 ± 0.1	2.1 ± 0.6	0.2 ± 0.2
		66.8 - 77.7	*13.3 - 23.0*	*6.0 - 8.8*	*0.2 - 1.4*	*0.4 - 0.8*	*1.0 - 3.0*	*0.0 - 0.1*
	Oceanward top	81.4 ± 3.2	12.9 ± 2.3	3.4 ± 0.6	0.9 ± 0.4	0.6 ± 0.3	1.1 ± 0.4	0.0 ± 0.0
		76.8 - 85.4	*10.4 - 14.7*	*2.2 - 4.6*	*0.2 - 1.2*	*0.0 - 0.9*	*0.9 - 1.4*	*0.0 - 0.0*
	Lagoonward toe	73.8 ± 2.2	13.1 ± 0.8	7.9 ± 0.7	3.4 ± 1.3	0.4 ± 0.1	0.8 ± 0.4	0.2 ± 0.1
		73.5 - 75.9	*11.4 - 14.8*	*7.0 - 8.8*	*1.9 - 2.5*	*0.2 - 0.5*	*0.4 - 0.5*	*0.0 - 0.3*
	Lagoonward top	81.7 ± 4.5	9.2 ± 2.1	5.3 ± 0.6	2.4 ± 1.5	0.3 ± 0.2	0.9 ± 0.6	0.1 ± 0.1
		72.1 - 88.0	*7.8 - 11.2*	*3.9 - 5.9*	*0.2 - 3.5*	*0.0 - 0.3*	*0.0 - 2.1*	*0.0 - 0.0*
Leeward	Oceanward toe	74.9 ± 5.3	9.2 ± 1.1	11.4 ± 3.6	3.0 ± 0.8	0.6 ± 0.2	1.3 ± 0.5	0.0 ± 0.0
		63.7 - 83.1	*7.5 - 11.1*	*6.5 - 18.2*	*1.5 - 4.4*	*0.1 - 1.0*	*0.4 - 2.3*	*0.0 - 0.0*
	Oceanward top	82.7 ± 4.3	8.2 ± 1.3	6.8 ± 2.3	2.1 ± 0.8	0.2 ± 0.1	0.7 ± 0.5	0.0 ± 0.0
		78.6 - 90.4	*7.1 - 10.5*	*3.2 - 8.5*	*0.7 - 2.7*	*0.0 - 0.3*	*0.0 - 0.6*	*0.0 - 0.0*
	Lagoonward toe	74.4 ± 3.2	9.7 ± 0.5	11.9 ± 2.2	4.0 ± 1.6	0.3 ± 0.1	0.8 ± 0.2	0.1 ± 0.0
		69.7 - 79.6	*8.7 - 10.3*	*9.6 - 13.9*	*0.9 - 7.3*	*0.2 - 0.5*	*0.7 - 0.8*	*0.0 - 0.2*
	Lagoonward top	83.1 ± 3.9	8.0 ± 1.3	6.7 ± 1.9	2.2 ± 1.0	0.2 ± 0.2	0.6 ± 0.4	0.0 ± 0.0
		77.2 - 90.6	*6.1 - 10.5*	*3.0 - 8.3*	*0.0 - 4.4*	*0.0 - 0.1*	*0.1 - 0.6*	*0.0 - 0.0*

Table 4.10 – Concentrations (%) of skeletal constituents within top and toe of beach sediment samples from both the windward and leeward study sites. Interquartile ranges in italics (*IQR1 – IQR3*).

4.3.4 Marine – Beach – Island Sedimentology

While linear regression analyses highlight that cross-rim trends exist in marine sedimentology, it is pertinent to note that perhaps the most striking finding was the general homogeneity of sediment texture and composition across all sediment samples. Indeed, of particular note was the dominance of both sand-sized material (76.4 ± 2.7% and 82.3 ± 1.4% at the windward and leeward sites respectively) and also coral (72.3 ± 1.1% and 73.8 ± 0.7% at the windward and leeward sites respectively). Specifically, sand-grade coral accounted for 56.9 ± 0.6% and 62.6 ± 0.5% of marine sediment; 60.6 ± 1.9% and 69.4 ± 2.7% toe of beach sediment; 66.0 ± 2.1% and 81.2 ± 2.7% of top of beach sediment; and 63.1 ± 1.7% and 75.5 ± 1.4% of sediment within upper island facies 2A (values relate to the windward and leeward site respectively in each case).

The nMDS ordinations were generated to enable visualisation of sediment similarity (textural and compositional) across all of the sediment samples. Plots (Figures 4.18 and 4.19) illustrate a high degree of overlap, and hence strong similarity, of all sediment samples at both the windward and leeward sites. Indeed, all groups overlap

except island samples within facies 3B at the leeward site, which is likely due to the large proportion of rubble-sized material within those samples (Table 3.1).

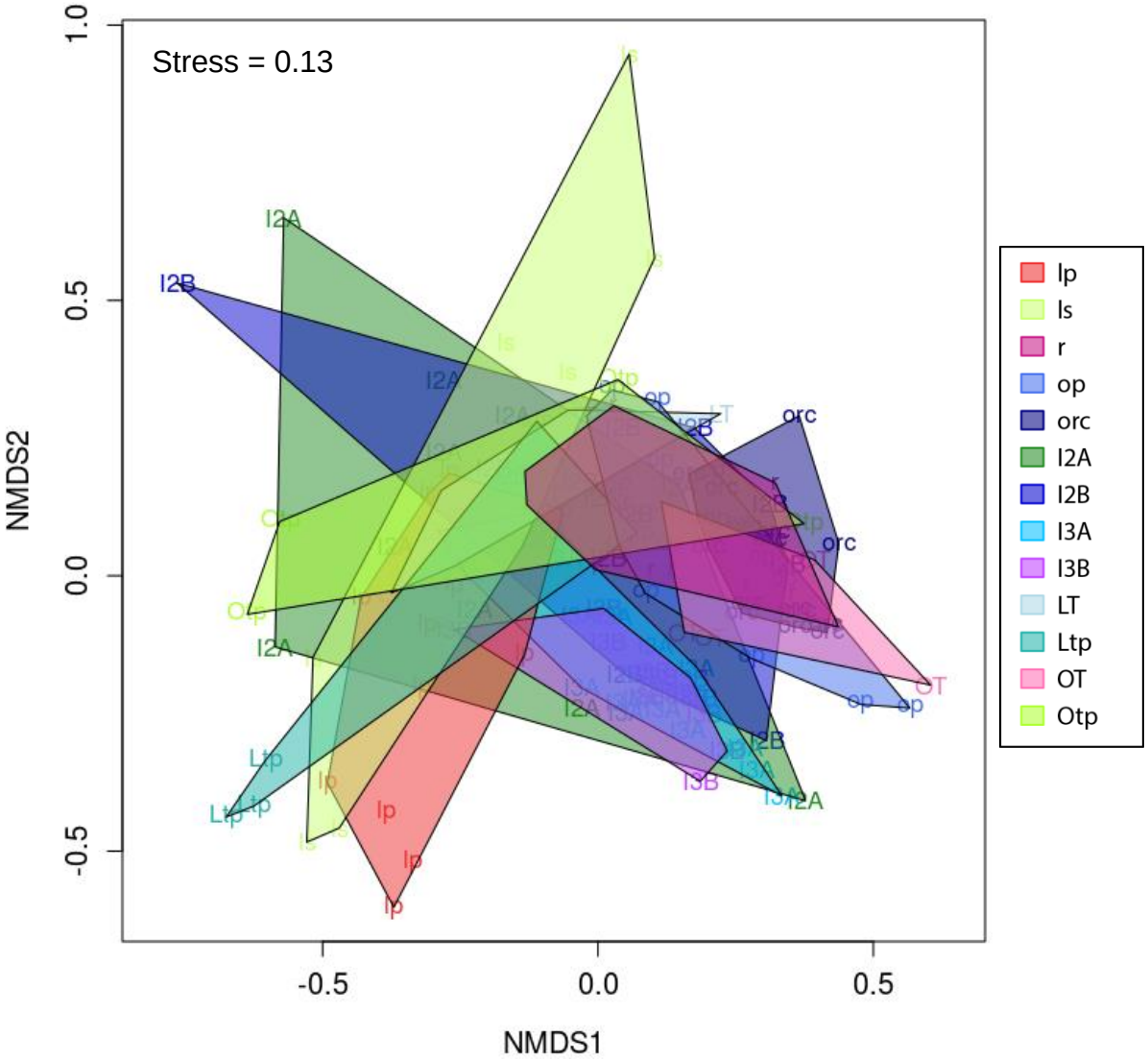

Figure 4.18 – Windward site nMDS plot including sediment tectural and compositional data from each eco-geomorphic zone (lp = lagoonward patch, ls = lagoonward sand, r = rubble, op = oceanward patch, orc = oceanward reef crest), island facies (I2A, I2B, I3A, I3B), and beach samples (LT = lagoonward toe, Ltp = lagoonward top, OT = oceanward toe, Otp = oceanward top).

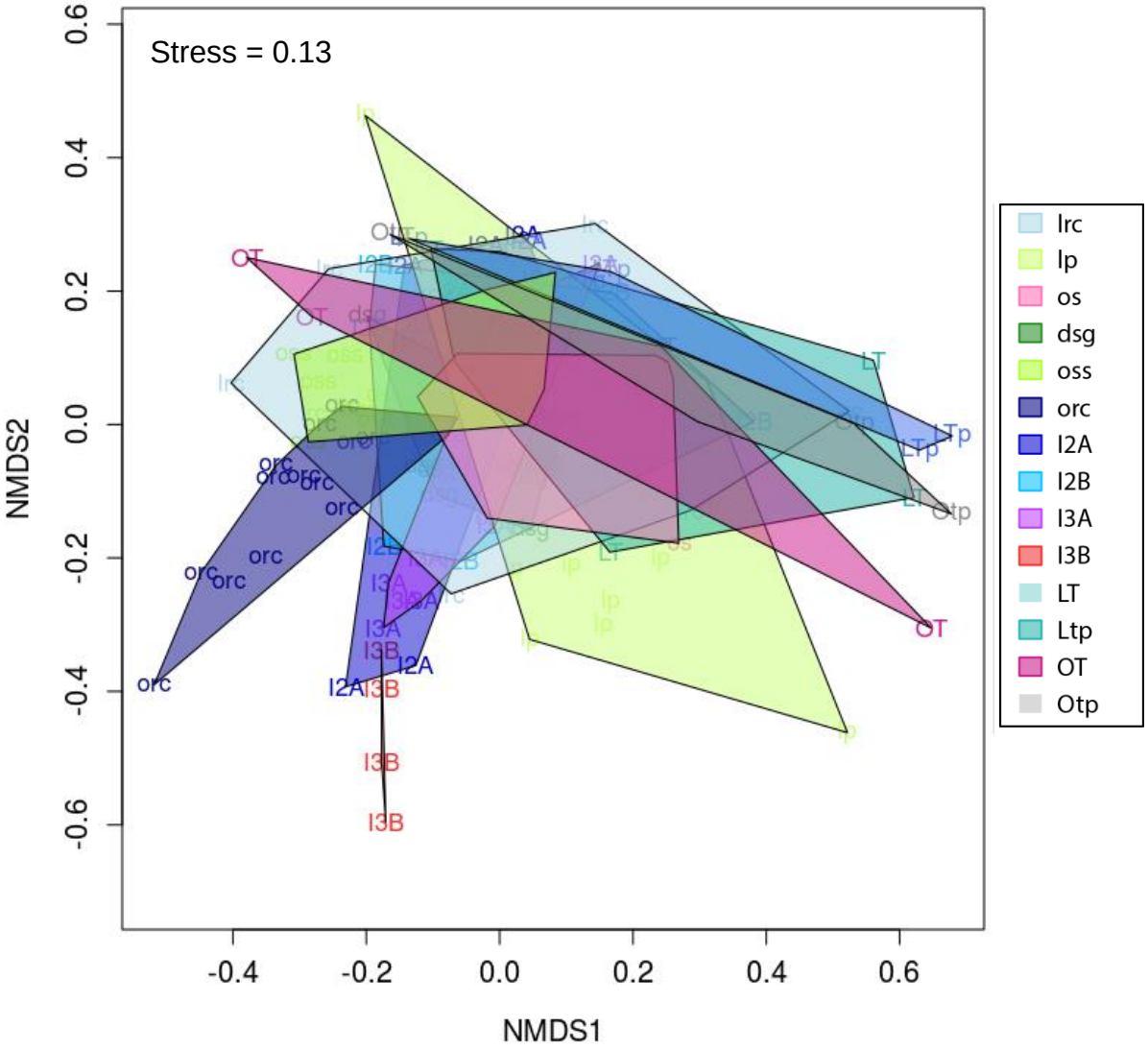

Figure 4.19 – Leeward site nMDS plot including sediment tectural and compositional data from each eco-geomorphic zone (lrc = lagoonward reef crest, lp = lagoonward patch, os = oceanward sand, dsg = dense seagrass, oss = oceanward sparser seagrass, orc = oceanward reef crest), island facies (I2A, I2B, I3A, I3B), and beach samples (LT = lagoonward toe, Ltp = lagoonward top, OT = oceanward toe, Otp = oceanward top).

4.3.5 Methodological Comparison: Sieving versus Settling

Across all sedimentological data, it is also interesting to compare methodologies for calculating mean grain size, specifically sieve and settling approaches. While a highly significant linear relationship was found between the approaches (P = <0.0005, Figure 4.20A), it was somewhat noisy (R^2 = 0.59) with sieving producing higher mean grain size data (Settling = 0.6*Sieving + 0.2). Indeed, differences were as large as 1.9 Φ.

Sieve results were found to be significantly higher than those derived via the RSA (paired t-test, P = <0.0005; Figure 4.20B). From a practical perspective, settling analyses took approximately a quarter of the time in comparison to processing the same number of samples by dry sieving.

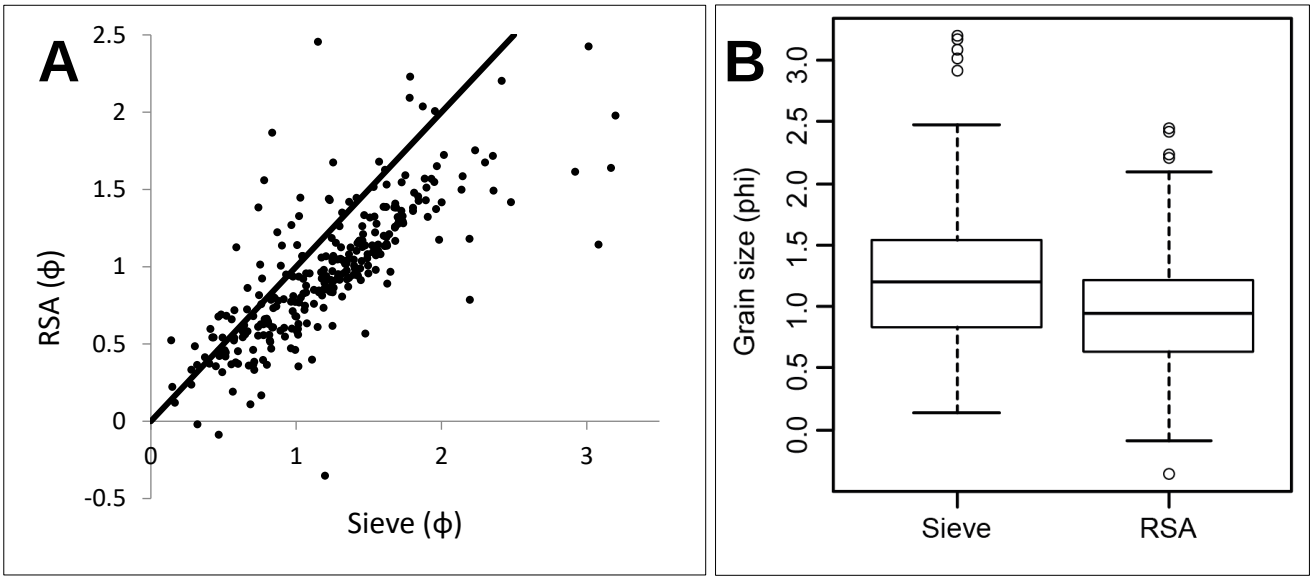

Figure 4.20 – Comparison of mean grain size (Φ) calculated using settling- (i.e. RSA) and sieve-derived approaches. For eae of comparison, the plotted line in plot B is y = x.

4.3.6 Volumetric Sediment Storage

Results from block kriging analyses of sediment probe data are depicted in Figures 4.21 and 4.22 for the windward and leeward sites respectively. First order estimates of the volume of sediment stored within each zone were then generated by summing all pixel values for each zone and multiplying by pixel dimensions (Tables 4.11 and 4.12). Total sediment storage was thus estimated as 126,940 m^3 (over an area of 0.84 km^2) within the windward site and 93,677 m^3 (over 1.06 km^2) within the leeward site. First order estimates of the volume of gravel-, sand- and fine-grade sediments were also generated. Within each pixel, the proportion of sand-, gravel- and fine-grade material (as in Figures 4.12 and 4,13) was multiplied by sediment depth (Figures 4.21 and 4.22). All pixel values were then summed within each zone and multiplied by the pixel dimensions. At both study sites, sand-grade material accounted for approximately 85% of all sediment stored. The proportion of gravel-grade material stored at the leeward site (~15%) was larger than that at the windward site (~7%). In turn, the proportion of fine-grade sediment storage was thus larger at the windward

site (~9%) than the leeward site (<1%), the majority of which (~87%) was stored within the lagoonward patch zone (~15% of sediment within that zone).

Marked variability was found in sediment storage between zones. At the windward site, sediment was primarily stored within the lagoonward environment; the largest sediment depths were found within the lagoonward sand zone (mean depth = 23.9 ± 4.5 cm), though, as a function of its larger areal extent, the largest volume of sediment was found within the lagoonward patch zone (64,709 m^3, mean depth = 16.4 ± 3.4 cm). Although vastly exceeded by lagoonward sediment storage, sediment stored within the oceanward zones was primarily within the rubble zone (11,939 m^3, 7.8 ± 3.2 cm), while the smallest volumes of sediment storage were on the oceanward reef crest (105 m^3, 0.3 ± 0.6 cm). Indeed, a significant relationship was found between sediment depths and distance from the oceanward reef crest (P = <0.0005, R^2 = 0.41).

Spatial variability in sediment storage was less pronounced at the leeward site than at the windward site and, indeed, the relationship between sediment depth and distance from the oceanward reef crest was not statistically significant (P = 0.62; R^2 = 0.003). The largest volume of sediment was stored in the dense seagrass zone (399,896 m^3, mean depth = 11.2 ± 2.2 cm). However, mean sediment depths were slightly higher within the oceanward sand zone (13.1 ± 1.6 cm), although the volume of sediment storage within this zone was relatively small (8,239 m^3) due to its smaller spatial extent. The lagoonward patch zone was host to the second largest volume of sediment (390,686 m^3), which was partially attributable to its extensive planform area (29,029 m^2, mean depth = 7.4 ± 4.2 cm). Intra-zone variability was at a maximum within the lagoonward patch zone (S.D. = 4.2 cm) and, indeed, two spatially explicit zones of high sediment storage are evident from the results of kriging analysis (Figure 4.22) toward the north and south of Galamadhoo island. Notably, these zones are leeward of Galamadhoo's northern and southern spits. On both the oceanward and lagoonward reef crests sediment storage was relatively minimal (mean depths = 2.5 ± 1.5 cm and 5.1 ± 1.8 cm respectively). Indeed, as at the windward site, the smallest volumes and mean sediment depths were found on the oceanward reef crest.

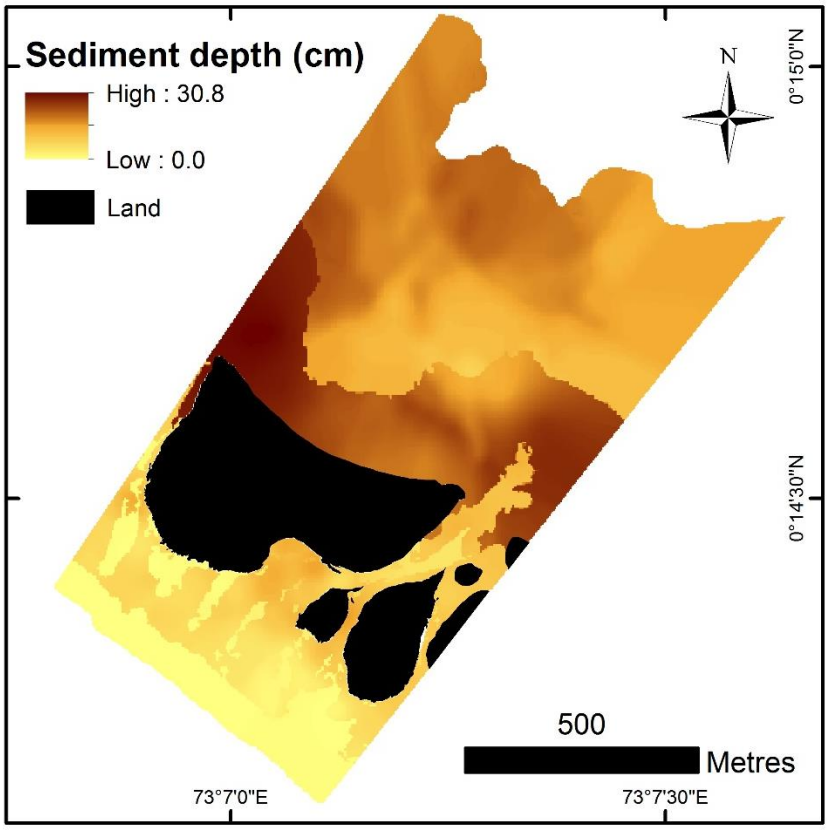

Figure 4.21 – Block kriging results of windward site benthic sediment storage.

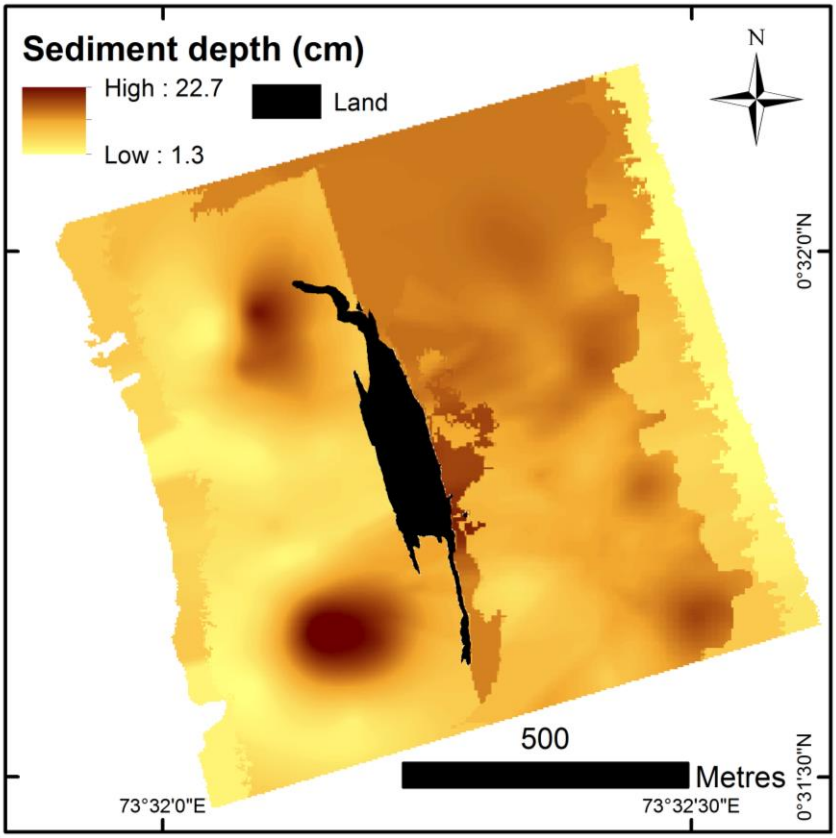

Figure 4.22 – Block kriging results of leeward site benthic sediment storage.

Zone	Area (m^2)	Total sediment storage (m^3)	Gravel storage m^3	Gravel storage %	Sand storage m^3	Sand storage %	Fines storage m^3	Fines storage %	Mean depth (cm ± 1 SD)
Oceanward Reef Crest	40068	105	36	*35%*	68	*65%*	0	*0%*	0.3 ± 0.6
Oceanward Patch	56547	1336	392	*29%*	942	*70%*	2	*0%*	2.3 ± 3.3
Rubble	153027	11939	3147	*26%*	8758	*73%*	34	*0%*	7.8 ± 3.2
Lagoonward Sand	204129	48851	2096	*4%*	45384	*93%*	1372	*3%*	23.9 ± 4.5
Lagoonward Patch	394254	64709	2722	*4%*	52551	*81%*	9436	*15%*	16.4 ± 3.4
Total	848025	126940	8393	*7%*	107703	*85%*	10844	*9%*	

Table 4.11 – Estimates of sediment storage within each of the windward site eco-geomorphic zones.

Zone	Area (m^2)	Total sediment storage (m^3)	Gravel storage m^3	Gravel storage %	Sand storage m^3	Sand storage %	Fines storage m^3	Fines storage %	Mean depth (cm ± 1 SD)
Oceanward Reef Crest	59973	1493	500	*33%*	988	*66%*	4	*0%*	2.5 ± 1.5
Oceanward Sparser Seagrass	83846	6554	1273	*19%*	5266	*80%*	15	*0%*	7.8 ± 2.3
Dense Seagrass	399896	44763	8134	*18%*	36458	*81%*	171	*0%*	11.2 ± 2.2
Oceanward Sand	62910	8239	681	*8%*	7544	*92%*	14	*0%*	13.1 ± 1.6
Lagoonward Patch	390686	29029	3142	*11%*	25829	*89%*	58	*0%*	7.4 ± 4.2
Lagoonward Reef Crest	70021	3600	496	*14%*	3084	*86%*	21	*1%*	5.1 ± 1.8
Total	1067333	93677	14226	*15%*	79169	*85%*	283	*0%*	

Table 4.12 – Estimates of sediment storage within each of the leeward site eco-geomorphic zones.

4.4 Discussion

4.4.1 Eco-geomorphic Zonation

Analysis of the benthic characteristics of a coral reef environment allows for elucidation of the key controls and processes acting upon the system. The differing characteristics of the windward and leeward reef systems are likely primarily attributable to their differing wave exposures. Most broadly, this is evident in the different reef eco-geomorphic zonations, which varied markedly between study sites. The distribution of zones was predominantly shore-parallel, indicating that wave energy is likely a key control upon reef zonation. This interaction between wave exposure and band-like reef zonations has been well documented in prior work (e.g. Roberts, 1974; Rosen, 1975; Geister, 1983).

The one exception to the band-like zonation, was the shore-normal rubble and intervening oceanward patch zone at the windward site. Rubble tongues were observed to be very approximately coincident with the spur and groove morphology of the oceanward edge of the rim platform. Their shore-normal orientation may therefore be a function of wave refraction around spurs and subsequent convergence on the reef platform. This would concentrate the deposition of reef rubble along shore- and reef-normal tongues (Etienne and Terry, 2012). Rubble was most likely generated during large swell events (e.g. section 3.4.2). Indeed, similar shore-normal rubble tongues have been documented on other reef island platforms as storm deposits (e.g. Scoffin, 1993; Etienne and Terry, 2012) and thus highlight the likely significance of low-frequency high-magnitude events at the windward site. This is consistent with WaveWatch III hindcast model results (section 2.4.2.1). There is hence a parallel between the marine and terrestrial environments given that there was a greater prevalence of rubble found within the windward islands than the leeward islands (section 3.3.2).

Overall, the eco-geomorphic zonations were comparable to those described by Stoddart (1966) on windward and leeward sections of Addu Atoll rim. On the windward rim, Stoddart documented (1) an algal platform at the oceanward platform edge; (2) rubble tongues of <50 m in length; (3) an oceanward rock reef flat within minimal sediment storage and variable seagrass growth; and (4) a lagoonward sand moat with

scattered coral patches. Stoddart's descriptions of the leeward rim were more limited as he was unable to access the platform and thus made observations from a distance. Nonetheless, he noted (1) high coral growth at the lagoonward and oceanward platform edges; and (2) in between the reef crests, coral patches surrounded by coarse sand with decreasing live coral toward the platform centre. The leeward description corroborates less readily with this study, partly as there is no mention of an algal rim, and also due to the absence of seagrass (although this is noteworthy in lieu of Chapter 6). However, the broad consistencies in the described zonations and those found in this study highlight the likely significance of wave exposure to the zonations of windward and leeward reef rim systems. The consistencies also suggest that the findings of this study may relate to other windward and leeward rim settings across the south of the Maldives Archipelago.

4.4.2 Marine Benthic Sedimentology

Key controls upon reef systems may also be discerned through examination of their sedimentology. Indeed, Maiklem (1968) defined two sedimentological end-members based on the dominance of either physical or biological processes. Firstly, 'immature' sediment possesses a grain-size distribution that is a function of the *in situ* sediment-producing biota (i.e. biological processes). The grain size distribution of immature sediment is thus inherited from the abundance, type and associated grain size properties of the organisms present. Secondly, the grain size distribution of 'mature' sediment is a product of the hydrodynamic modification of the inherited texture (i.e. physical processes). Sedimentology within the majority of reef systems is thus characterised by a continuum of sediment types that reflect differential relative roles of biological and physical processes in facies formation. The sedimentology of both the windward and leeward reef systems in this study are no exception.

4.4.2.1 Physical Processes

The provenance of unimodal, as oppose to polymodal, grain size distributions (Figures 4.10 and 4.11) suggests that physical processes dominate atoll rim systems (Kalbfleisch and Jones, 1998). Moreover, the asymmetry of grain size distributions towards the oceanward reef crests found within the present study sites is likely reflective of hydrodynamic sorting as finer grade material has been preferentially winnowed from zones with closer proximity to the oceanward reef crest and

transported towards the atoll lagoon. Indeed, coarse-grained sediment with faster settling velocities is indicative of high wave exposures and local sediment production (Kench, 1997). Hence, at both study sites, the coarsest grain sizes (-0.1 ± 0.1 Φ and 0.0 ± 0.1 Φ at the windward and leeward sites respectively) and fastest settling velocities (7.9 ± 0.3 cm s^{-1} and 7.4 ± 0.2 cm s^{-1}) were found on the oceanward reef crest, which is exposed to the highest wave energies. At the leeward site, the second highest grain sizes and settling velocities were found on the lagoonward reef crest (0.7 ± 0.1 Φ; 6.0 ± 0.3 cm s^{-1}). This is consistent with the notion that, while wave exposure is greatest at the oceanward reef crest, lagoonal wind wave energies are also high at the leeward site (Chapter 2).

Conversely, finer grained sediment with slower settling velocities is preferentially transported as lower threshold velocities are required to entrain this material. It is therefore associated with low wave energies and zones of sediment deposition (Kench, 1997). At the windward site, the lagoonal zones possessed the finest grain sizes (1.9 ± 0.2 Φ, 2.5 ± 0.3 Φ) and slowest settling velocities (3.1 ± 0.3 cm s^{-1}, 3.2 ± 0.2 cm s^{-1}), which corresponds with the lower wave exposures of these zones and suggests they represent depositional sinks. At the leeward site, the finest grain sizes and slowest settling velocities were found in the lagoonward patch (1.3 ± 0.1 Φ) and oceanward sand (1.2 ± 0.1 Φ) zones and thus they likely represent areas of preferential sediment deposition. Notably, the deposition of sediment to form Galamadhoo island has occurred between these two zones.

Similarly, sediment sorting was poorest within the lagoonward patch zone at the windward site (1.7 ± 0.1 Φ), which suggests it is exposed to the lowest wave energies as hydrodynamic energy has been insufficient to facilitate sediment sorting (Kench, 1994). However, the poorest sorting at the leeward site was found within the dense seagrass zone (1.3 ± 0.0 Φ), which is likely a result of the baffling effect of seagrass upon wave energy (e.g. Gacia et al., 1999; van Keulen and Borowitzka, 2002).

Low proportions of silt-grade material were found throughout both study sites, which suggests that either it has been preferentially transported off-rim as a result of hydrodynamic sorting, or large amounts of fine grade material are not produced. Hence, wave energies were sufficient across both reef platform to transport material of this grade. Similarly, coarse-grade sand and gravel-sized material have been found

to dominate facies in other wave-exposed environments (e.g. Rankey et al., 2011; Dawson and Smithers, 2014). The lagoonward patch zone at the windward site was the only zone to contain notable proportions of silt-grade sediment (12.0 ± 3.4%), which is indicative of very low hydrodynamic energies. This zone was also the deepest of the study (-5.21 ± 2.95 m, relative to MSL), which is consistent with the positive correlations between the abundance of silt and water depth found in Radhoo and Ari Atolls (Gischler, 2006).

4.4.2.2 Biological Processes

Physical processes evidently represent a key control upon facies characteristics. However, biological processes also exert a fundamental control over sedimentary composition. This is particularly because, in the absence of terrigenous material, sediment within atoll settings is solely produced by carbonate-producing reefal organisms. Sediment composition is therefore a function of the relative abundances and distribution of sediment producing biota. This relationship between biology (i.e. sediment-producing organisms) and sediment production is discussed in far greater detail in Chapter 5. However, the relation is immediately evidenced by the association between high CCA benthic cover in the oceanward reef crest zones and the high sedimentary concentrations within these zones (the highest of the study: 18.4 ± 0.9% and 17.9 ± 0.1% at the windward and leeward sites respectively). Likewise, zones with higher seagrass coverage (the dense seagrass, and oceanward sparser seagrass zones at the leeward site) were associated with higher concentrations of foraminifera (9.7 ± 1.5% and 10.5 ± 1.5% respectively), which is likely because foraminifera may live as epibionts upon seagrass blades (Orth, 1992; see Chapter 6).

Biology is also a key control upon the physical properties of skeletal grains, including density, shape, size, surface texture and skeletal microarchitecture (Kench, 2011a). Consequently, biology is also key in controlling the relative durabilities of skeletal constituents and, in turn, their persistence within the marine environment. The consistent predominance of coral across the sediment reservoir (74.5 ± 0.8% and 74.8 ± 0.6% across all samples at the windward and leeward sites respectively) likely, in part, reflects relative sediment durabilities. Indeed, in a comparison of foraminifera, molluscs, coral and *Halimeda*, Ford and Kench (2012) found grain durability to vary by several orders of magnitude, the most durable clast type being coral, whilst *Halimeda*

was most rapidly abraded. Hence, coral dominated sediment composition, while *Halimeda* was found in only subordinate concentrations, particularly within the most exposed oceanward environments (1.2 ± 2.3% and 1.2 ± 0.2% within the oceanward reef crest zones at the windward and leeward sites respectively). Furthermore, sediment breakdown pathways are also constituent-specific (Sorby, 1879; Folk and Robles, 1964), for example *Halimeda* rapidly disaggregates into mud-grade material (Perry et al., 2016). By contrast, the persistence of coral branches within the oceanward environment at the windward site is likely testament to their high durabilities which enable them to remain in reef flat settings over long timescales (Ford and Kench, 2012). Hence, sediment composition is, in part, a function of the exposed nature of both study sites.

Biology also represents a key control upon the hydrodynamic properties of individual grains, which vary markedly and distinctly between different skeletal constituents as mechanisms of growth and calcification are highly species-specific. Due to their associated heterogeneity, sediment transport processes in reefal environments differ to those in more terrigenous settings (e.g. Masselink and Hughes, 1998). For example, block-shaped sediment (e.g. coral, CCA) possesses a high surface-area-to-volume ratio and thus settles substantially faster than plate-shaped grains (e.g. *Halimeda*, molluscs; Maiklem, 1968; Kench and McLean, 1996). These marked differences are evidenced in this study, the significant increase in CCA concentrations with proximity to the oceanward reef crest may thus be partially due to the higher threshold velocities that would be required to initiate its entrainment. Following sediment generation, CCA grains have therefore remained *in situ* and/or been preferentially deposited. Conversely, there was significant increase in the concentrations of *Halimeda* and molluscs with increasing distance from the oceanward reef crest at both study sites. Lower wave velocities would be required to entrain this material and so such grains are more likely to be transported further than block-like grains under a comparable process regime. Increases in abundance may therefore indicate that sediment has become transport-limited and that these zones form long-term depositional sinks (Kench, 1997).

Due to the variability in hydraulic properties of sediments of the same physical grain size, settling velocities were analysed in addition to grain size. Comparing these approaches, grain sizes derived from sieving were significantly larger than those

calculated using settling approaches. Likewise, Kench and McLean (1997) also found the sieving method overestimated entrainment velocities. Hence, reef systems are more dynamic than physical grain sizes would suggest.

4.4.3 From Source to Sink: Delineation of Zones of Sediment Deposition and Transport

Through collective examination of the influence of physical and biological processes upon facies characteristics, zones of sediment production, storage and transport may be inferred. At the windward site, textural and compositional characteristics suggest the key transport pathway is from the oceanward reef crest toward the atoll lagoon, reflecting the decay in wave energy as it travels over the platform. In contrast, at the leeward site, key sediment transport vectors are likely from both the lagoonward and oceanward reef crests toward the platform interior, specifically the lagoonward patch and oceanward sand zones. Lagoonward transport vectors thus appear shorter than those from the oceanward reef crest, which reflects their relative wave exposures (i.e. greater at the oceanward reef crest than the lagoonward reef crest). Hence, wave exposure is highlighted as a key control upon reef rim systems.

Transport vectors inferred from sedimentary characteristics corroborate with spatial variability in sediment depths. Indeed, at the oceanward site, a significant oceanward-lagoonward gradient was found in the volumes of sediment stored with the greatest volumes found toward the atoll lagoon. Mean depths however, were greater within the lagoonward sand zone (23.9 ± 4.5 cm) than the lagoonward patch zone (16.4 ± 3.4%), which is likely a function of wave energy gradients given that wave velocities within the lagoonward patch zone were sufficiently low to deposit fine-grade sediment (12.0 ± 3.4%). It thus seems likely that wave velocities were sufficiently low to deposit coarse-moderate grade material within the lagoonward sand zone. In addition, this may imply that some sediment transport may occur from the lagoonward patch to the lagoonward sand zone, which may be episodic depending on wind conditions. A further key control upon sediment depths is likely to be variability in sediment production rates, which will be discussed within Chapter 5.

At the leeward site, the reduced spatial variability in sediment depths likely results from lower variability in wave exposures due to the intersection of both lagoonward and oceanward wave energies. The greatest volumes of sediment were found in the dense

seagrass zone (44,763 m^3), likely due to its large spatial extent, the habitat they provide to sediment-producing biota, the role of seagrass in baffling wave energy, and also as seagrass blades may bind and trap sediment (e.g. Gacia et al., 1999; van Keulen and Borowitzka, 2002). The greatest mean sediment depths were found within the oceanward sand zone (13.1 ± 1.6 cm). This was followed by the lagoonward patch zone (11.2 ± 2.2 cm), within which maximum sediment depths were found (<22.7 cm in the lee of the northern and southern sand spits). Hence, this supports the notion that the lagoonward patch and oceanward sand zones represent key areas of sediment storage at this site. It is notable that island formation has occurred adjacent to the key zones of sediment storage at both sites.

Sediment storage is of geomorphic importance as it contributes to the process of bucket infilling (Purdy and Gischler, 2005; section 3.4.3.1), which occurs on Huvadhu Atoll at two spatial scales. At the atoll scale, the export of (preferentially fine-grade) material off the lagoonward platform edge and its subsequent deposition in the atoll lagoon will contribute to atoll infilling over geological timescales. Secondly, at the scale of an individual reef platform, sediment storage may contribute to the infilling of the reef platform. Understanding these processes is of particular pertinence given that platform infill is a necessary prerequisite for island formation (i.e. Stage 1 of the models of island development – section 3.4.3.2; Figures 3.21 and 3.22).

4.4.4 Marine – Beach – Island Sedimentary Connectivity

In addition to marine benthic sediments, samples were also obtained from the top and toe of island beaches in order to examine reef-to-island connectivity. Top and toe of beach samples from both study sites also demonstrated the roles of physical and biological processes in determining facies characteristics. For example, toe of beach samples comprised material that would require higher entrainment threshold velocities than top of beach samples. Mean grain size, the proportion of gravel and settling velocities were thus found to be greater at the toe of beach than the top of beach. Compositionally, CCA concentrations were significantly greater in toe of beach samples than top of beach samples, which was likely to be a result of their dense and block-like structures which would necessitate high wave exposures to be entrained and transported to the top of the beach. In contrast, molluscs were found in significantly higher concentrations at the toe of the beach. This is likely due to their

more plate-like morphologies, which render them relatively buoyant and transportable (Kench and McLean, 1996). In combination with their high durabilities (Ford and Kench, 2012), mollusc grains are thus well-suited to retention within the marine environment (Hart, 2009). Comparing oceanward and lagoonward beach samples mirrors trends found within benthic marine sediment samples as coarser material with higher proportions of gravel and faster settling velocities was found on the oceanward island shorelines than on the lagoonward shorelines, particularly at the windward site.

Comparing reef island sedimentology (of the upper island horizons as reported in Chapter 3) with beach and benthic marine sediments, differences were relatively minor. Texturally, mean grain sizes of the upper reef island facies at the leeward site were 1.2 ± 0.1 Φ (organically enriched horizon) and 1.1 ± 0.1 Φ (facies 2A; Table 3.1), which is extremely comparable to the adjacent eco-geomorphic zones (1.3 ± 0.1 Φ and 1.2 ± 0.1 Φ in the lagoonward patch and oceanward sand zones respectively). At the windward site, mean grain sizes within the upper island horizons were 0.7 ± 0.1 Φ and 1.2 ± 0.2 Φ within facies 1 and 2A respectively. Greater variability in grain size was found at this site, typically with coarser grain sizes found toward the oceanward island coasts. However, as at the leeward site, mean island grain sizes were between those of the adjacent eco-geomorphic zones. Indeed, off the oceanward island coast, mean grain sizes within the rubble and oceanward patch zones were 0.5 ± 0.1 Φ and 0.2 ± 0.1 Φ respectively, while mean grain size within the lagoonward sand zone was 1.9 ± 0.2 Φ. Previously, reef islands have been described as highly selective landforms (e.g. Morgan and Kench, 2016b; Perry et al., 2015) with sedimentology that differs significantly (Morgan and Kench, 2016b) from that stored within the adjacent marine environments. However, examining reef platform systems as a whole, island grain size was not found to be particularly distinct from the sediment stored within the marine environments. Rather, island sediment characteristics were a portion of the broader oceanward-lagoonward cross-rim gradients in sediment texture.

Comparing the composition of upper island (Chapter 3), marine and beach sediments, the upper island horizons were comprised of slightly more coral (78.8 ± 0.0% and 78.6 ± 1.4% at the windward and leeward sites respectively) than the marine samples (72.3 ± 0.8% and 73.8 ± 0.7% at the windward and leeward sites respectively). The mean values are were highly consistent between study sites, which is indicative that similar processes of sediment production, transport and deposition operate within both

windward and leeward atoll rim systems. The increased proportions of coral within the islands is likely a function of its high durability (Ford and Kench, 2012). The slightly higher coral concentrations found within the islands, in comparison to the surrounding marine environment, could suggest that the rim reef islands are in fact selective landforms (Morgan and Kench, 2016b). However, this is a marginal difference and nMDS plots illustrate the substantial overlap between all upper island, beach and marine sediment characteristics at both study sites. It seems likely that, given the exposed nature of the atoll rim, sediment residence times in their zones of production are low and thus the sediment reservoir is homogenised across the system by rapid spatial dispersal.

A high degree of comparability between marine and island sedimentology is indicative of active reef-to-island linkages (McKoy et al., 2010; Morgan and Kench, 2016b; Liang et al., 2016). Hence, the high degree of comparability found in this study suggests that the islands are actively maintained by their surrounding sediment reservoirs, which has key implications for ongoing reef island resilience. If active reef-to-island linkages are maintained, it is more likely that islands will possess the adaptive capacity to morphologically adjust to shifts in environmental conditions (McKoy et al., 2010). However, given that the sedimentology within the upper island horizons is consistent (i.e. <~1,400 - 1,800 yr. B.P.), such assertions ought to be made with caution as results may also reflect temporal consistency. If the islands are in fact disconnected from their surrounding marine environments, island resilience will be contingent upon the adjustment of a finite volume of sediment (McKoy et al., 2010). Moreover, the dominance of a restricted range of sedimentary constituents across the system (predominantly sand-grade coral) may also render reef islands particularly vulnerable to change.

4.4.5 Inter- and Intra-Regional Comparisons of Marine Benthic Sedimentology

Studies of the sedimentary characteristics of Maldivian atoll rim environments are extremely limited. Indeed, Stoddart's (1966) analysis of atoll rim sedimentology was limited to the texture of oceanward reef flat sediments adjacent to Gan island, Addu Atoll (on a windward rim aspect). Mean grain size was 0.5 Φ (range = -1.3 to +1.7 Φ), which is comparable to that found on the oceanward reef flat at the windward site. The only other study to analyse atoll rim sedimentology was that of Gischler (2006) on Ari

and Rasdhoo Atolls, though only 4 samples from rim environments were analysed. A ‘coral grainstone’ facies was identified around atoll margins within which coral was the most abundant constituent (55%). Concentrations of coral, although dominant, were lower than those found in this study, which may be a function of the lower wave exposures toward the centre of the archipelago (prevailing swell is from the south – Young, 1999). Alternatively (or additionally) the lower proportions could be a function of facies extent as ‘coral grainstone’ also encompassed interior lagoonal platforms and Gischler’s (2006) low sampling density on the atoll rim (n = 8 of 24 coral grainstone samples).

Detailed work on Maldivian reef sedimentology has been undertaken recently on interior reef platforms (Perry et al., 2015; Morgan and Kench, 2016b; Liang et al., 2016). In each case, sand-grade material has dominated texturally with mean grain sizes of 0.83 to 1.34 Φ within Huvadhu Atoll (Liang et al., 2016), and 1.0 - 1.7 Φ within inner and outer reef flat zones of Vakkaru, Raa Atoll (Perry et al., 2015). Hence, mean grain sizes were comparable to those found within this study, though the range of grain sizes was more restricted, which is likely a function of smaller gradients in wave energy across island interior platforms (Chapter 2). Compositionally, coral dominated sediment composition of interior Maldivian reef platforms, which was also consistent with this study. Coral concentrations ranged from 50.2% to 67.9% on interior island platforms in Huvadhu atoll (Liang e al., 2016), and accounted for 53% and 51% of outer and inner reef flat sediments respectively at Vakkaru (Perry et al., 2015). In contrast, proportions of *Halimeda* were markedly higher with concentrations ranging from 6.9% to 19.1% at Huvadhu (Liang et al., 2016), and accounting for ~43% of sand moat sediments at Vakkaru (Perry et al., 2015). Concentrations of *Halimeda* were likely higher in interior settings due to the absence of oceanward swell wave energies within the atoll lagoon. *Halimeda* transport and breakdown may therefore occur less rapidly than on the atoll rim.

The concentrations of coral found in this study were also higher, to the best of the author’s knowledge than typically found in reef sediments of the GBR/ Torres Strait region (Dawson and Smithers, 2014; Flood and Scoffin, 1978; Frank, 2008; Maxwell et al., 1964; Yamano et al., 2000; Tudhope and Scoffin, 1984, 1988; Hart, 2009; Schueth and Frank, 2008; Hamylton et al., 2016). Proportions of coral ranged from 13% (Warraber - Hart, 2009) to 60% (Heron Island - Schueth and Frank, 2008). Reef

sediment from this study also contrasts that of the Pacific, which is characterised by foraminifera-dominated sediments, for example, the Marshall Islands (~63% - Smith and Collen, 2010), Caroline Islands (~60% - McKee et al., 1959), and Gilbert and Ellis Islands (~38-70% - Woodroffe and Morrison, 2001; Collen and Garton, 2004). The prevalence of foraminifera has been attributed Pacific sea-level history as extensive emergent reef flats (which favour high foraminifera productivity) were produced with post-highstand sea-level fall (Yamano et al., 2000). By contrast, *Halimeda* production is more prevalent in the Caribbean as the shallow reef crests and lagoons that characterise the Caribbean favour its production (Perry et al., 2011).

4.5 Conclusions

This Chapter represents the most comprehensive sedimentological study of a Maldivian reef rim island system, comprising investigation of marine, beach and island sediments. Facies characteristics reflect the roles of physical and biological processes within atoll rim environments. Specifically, wave energy is highlighted as the primary control upon both intra- and inter-site variability. This is evident in eco-geomorphic zonations and their associated sedimentology. Indeed, at the windward site, facies characteristics represent the decay in wave energy from the oceanward reef crest toward the atoll lagoon. Zones toward the oceanward reef crest were therefore characterised by the preferential transport of material, while the lagoonward zones serve as depositional sinks. By contrast, leeward site sedimentology is a function of the intersection between both lagoonward and windward wave energy. Both reef crests are characterised by facies properties that are indicative of preferential sediment transport, and thus the leeward site depositional sinks are located within the platform interior (namely, the oceanward sand and lagoonward patch zones). Notably, reef island formation at both study sites has occurred adjacent to zones of preferential deposition. While prior work has suggested rim island sedimentology to be distinct from that of the adjacent marine environments, analyses of the system as a whole reveals that island sediments vary as a function of the broader cross-rim gradients. While cross-rim gradients in sedimentology were found, perhaps the most striking finding was the relative homogeneity of the sediment reservoir across marine, beach and island sediments. Specifically, sand-grade coral was dominant across all sediment samples. This implies that the rim islands are actively maintained by their adjacent

carbonate-producing communities. Furthermore, this dominance of a restricted range of sedimentary constituents (i.e. sand-grade coral) may render reef islands particularly vulnerable to shifts any shifts reef ecology.

Chapter 5: Sediment Production

5.1 Introduction

Chapters 3 and 4 provided detailed quantified descriptions of sediment stored within both Maldivian rim reef islands (Chapter 3) and their adjacent marine environments (Chapter 4). To gain a full understanding of the controls upon sediment storage within reef settings also requires the development of datasets concerning the rates and types of reefal sediment production. Sediment production occurs either directly or indirectly (refer to section 1.2.2.2). *Direct* (i.e. primary) sediment production refers to the direct post-mortem deposition of the skeletal remains of infaunal and epifaunal calcareous taxa. For example, upon death, the skeletal remains of foraminifera, molluscs and *Halimeda* contribute directly to the sediment reservoir. Indirect (i.e. secondary) sediment production occurs due to physical and/or biological erosion of the reef framework (Perry et al., 2011). Physical erosion typically occurs episodically as a result of high energy events, and is a function of the hydrodynamic energy exceeding the strength of the coral (Madin, 2005). Biological erosion (i.e. bioerosion) is facilitated by organisms, such as parrotfish and echinoids, which break down the coral framework and subsequently excrete finer grade coral sediment. In turn, sediment properties (e.g. grain size, shape and density) are largely inherited from their parent material (Kench, 2011a; Maiklem, 1968; refer to section 4.4.2.2). For example, *Halimeda* initially disarticulates into discoid segments of 2-5 mm. By contrast, sediment production associated with parrotfish is typically coral fragments of 0.25 – 1 mm (Morgan and Kench, 2016a).

Given that reef islands are formed entirely of sediment produced by organisms within their surrounding marine environments, understanding sediment production is integral to ascertaining future reef island resilience. However, attempts to calculate sediment production rates within reef environments have been limited, with the exception of a few notable examples: Stearn and Scoffin (1977; 17.5 kg m^{-2} y^{-1}; Bellairs Reef, Barbados), Hubbard et al. (1990; 0.71 kg m^{-2} y^{-1}; Cane Bay, St. Croix), Harney and Fletcher (2003; 0.53 kg m^{-2} y^{-1}; Kailua Bay, Hawaii), and Morgan (2014; 3.5 kg m^{-2} y^{-1} in the live coral zone; Vabbinfaru, Maldives) and Perry et al., (2015; 5.71 kg m^{-2} y^{-1} and 1.90 kg m^{-2} y^{-1} on the outer and inner reef flats respectively; Vakkaru, Maldives).

By contrast, increasing reef research efforts have focused on quantifying the framework component of reef carbonate budgets (e.g. Eakin 1996, 2001; Edinger et al., 2000; Kennedy et al., 2013; Perry et al., 2013, 2014; Jones et al., 2015) and standardised methodologies have been developed, including census-based (e.g. *ReefBudget* – Perry et al., 2012) and hydrochemical (Kinsey, 1978; Gattuso et al., 1999) approaches. However, carbonate production does not equate to sediment production as carbonate is converted into sediment by biological and physical processes. Until recently, there has been an absence of any standardised approach for quantifying reefal sediment production. This renders comparison of the existing studies somewhat problematic as any sediment budget is highly sensitive to the parameters and methodologies employed. Perry et al. (2015) have thus made a first step towards a standardised methodology, which will be applied and built upon within this Chapter.

Previous work on reef island sediment budgets in the Maldives has been limited to the two aforementioned studies of interior reef island platforms in the northern-central section of the archipelago: Vakkaru reef platform in South Maalhosmadulu Atoll (Perry et al., 2015), and Vabbinfaru reef platform in North Malé Atoll (Morgan, 2014). The eco-geomorphic zonations and the prevailing process regimes differ markedly between the rim and interior platforms (e.g. Chapter 2). However, to the best of the author's knowledge, there have been no attempts to quantify sediment production within an atoll rim setting in the Maldives. The aim of this Chapter is therefore to provide the first sediment production rates within atoll rim setting in the Maldives. More specifically, research questions include:

1) What are the rates of sediment production within a windward and leeward atoll rim setting in the Maldives?
2) What are the key sediment producers within atoll rim environments?
3) What is the degree of spatial variability in sediment production across the eco-geomorphic zones on the atoll rim?
4) How does sediment production vary between the windward and leeward sites?
5) How does sediment production compare to sediment stored within the marine environment and also within reef islands?

5.2 Methodology

First order estimates of sediment production were calculated following the methodology of Perry et al. (2015). Detailed ecological surveys were undertaken in order to quantify the abundances of each of the suite of sediment producers within each eco-geomorphic zone (refer to Chapter 4 for zone descriptions). The spatial extent of the marine study sites was the same as examined in Chapter 4. This comprised the marine environment surrounding Galamadhoo at the leeward site (1.06 km^2), and Mainadhoo, Boduhini and Kudahini at the windward site (0.84 km^2; Figure 4.1). The same survey stations were employed as those in Chapter 4 (left panels of Figures 4.2 and 4.3), along transects perpendicular to both the reef crest and reef island shorelines, extending from the terrestrial island transects (Figures 3.3, 3.4, 3.6 and 3.7). 30 surveys were undertaken at each study site, which afforded 6 and 5 replicates within each zone at the windward and leeward sites respectively. Densities of each sediment producer within each zone were then multiplied by published data on species-level carbonate production rates to estimate sediment production rates within each zone (G, kg $CaCO_3$ m^{-2} yr^{-1}). In order to estimate total sediment production across each site (kg $CaCO_3$ yr^{-1}), sediment production rates (G) were multiplied by the area (m^2) of each zone as calculated using digital habitat maps derived from high-resolution (0.6 m) satellite imagery (refer to section 4.3.1).

Specifically, rates of both direct and indirect sediment production were estimated. At each survey station a 10 m transect (running parallel to the reef crest and reef islands) was marked using a flexible tape pulled taught between two sand pegs. Survey station locations were recorded by taking GPS points at each end of the 10 m transect (GPS error = ~5 m). Direct sediment production was then assessed within an area 0.5 m either side of each 10 m transect tape (i.e. total 10 m^2), including:

1. *Halimeda* spp. – counts of the number of thalli were undertaken within the 10 m^2 area. The average number of thalli per m^2 was then used to calculate an annual production rate with Mayakun et al.'s (2014) average rate of 0.006 g $CaCO_3$/thallus yr^{-1}.
2. Other plants of calcifying green algae – counts were undertaken within the 10 m^2 area, though none were observed.
3. Articulated red coralline algae – counts of plants were undertaken within the 10 m^2 area, though none were observed.

4. Molluscs – counts of epifaunal molluscs were undertaken within each 10 m^2 survey area. In addition, the number of the abundance of infaunal molluscs was assessed through collecting three bulk samples of volume 10 cm^3 (where possible) at equidistant points along each transect, which were sieved to isolate any living specimens. The average number of bivalves and gastropods per m^2 was calculated and production rates generated using Bosence's (1989) average production rates of 0.14 g $CaCO_3$/individual yr^{-1} and 2.46 g $CaCO_3$/individual yr^{-1} for gastropods and bivalves respectively.
5. Foraminifera – the methodology of Langer et al. (1997) was employed whereby calcium carbonate production was estimated as a proportion of skeletal component percentages found within the benthic sediment samples recovered from each survey station. The conversion to calcium carbonate production was undertaken using the equation

$$F_{prod} = S \frac{F_{max}}{100}$$

where; F_{prod} = foraminiferal calcium carbonate production (g $CaCO_3$ m^{-2} yr^{-1}), S = skeletal component percentage; and F_{max} = average foraminiferal carbonate production rates (g m^{-2} yr^{-1}). Langer et al. used 600 g m^{-2} yr^{-1} as F_{max} within high productivity reef areas and 120 g m^{-2} yr^{-1} within lower productivity lagoonal areas. The high productivity value (600 g m^{-2} yr^{-1}) was applied within the lagoonward reef crest zone at the leeward site as its rates of sediment generation by other producers far exceeded those of any other zone. The low productivity value (120 g m^{-2} yr−1) was applied within all other zones as their rates of sediment generation by other producers were relatively low both in comparison to those of the lagoonward reef crest zone and also other studies (e.g. Morgan, 2014; Perry et al., 2015).
6. Seagrass epiphytes – a 50 x 50 cm quadrat was placed 5 times along the transect at random within which seagrass densities were calculated. 10 blades were also collected from each site and epibiont calcium carbonate per blade was assessed using the weight loss on acidification technique (Nelsen and Ginsburg, 1986; Bosence, 1989; Perry and

Beavington-Penney, 2005). Epibiont calcium carbonate produced was calculated as

$E_{prod} = A - [B+(A \times C)]$

where; E_{prod} = epibiont calcium carbonate production (g $CaCO_3$ m^{-2} yr^{-1}), A = the weight of the encrusted dry blades, B = the weight of the acid treated blades, C = the % weight loss from unencrusted blades treated with acid. Annual epibiont production (g $CaCO_3$ m^{-2} yr^{-1}) was then calculated for each survey site by multiplying epibiont production by blade density and crops per year (refer to Chapter 6 for further details.)

Indirect sediment production, produced as a by-product of bioerosion, was assessed by surveying echinoids and parrotfish:

1. Echinoids – the number and test size of echinoids was counted and identified to genus level within the 10 m^2 area. The urchin erosion rates from Bak (1994) were employed and erosion was used as a proxy for sediment production rate as the excreted sediment then directly contributes to the sediment reservoir. The genuses identified were *Diadema* sp. and *Echinometra* sp. Erosion rates for *Diadema*, as a function of test size, were (g/individual yr^{-1}): 0-20 mm – 3.65 g, 21-40 mm – 182.5 g, 41-60 mm – 365 g, 61-80 mm – 2555g. Erosion rates by *Echinometra* were: 0-20 mm – 105.85 g, 21-40 mm – 65.7 g. In each case, sediment generation rates were calculated by multiplying the erosion rates by data for the average size frequency of urchins per m^2. Rates were then reduced by 43% as this proportion of carbonate sediment ingested is estimated to be reworked (Hunter, 1977).
2. Parrotfish – at each survey station, parrotfish were surveyed along 4 belt transects of 30 m x 4 m (i.e. 2 m either side of the transect tape, totalling 120 m^2). Parrotfish were counted, classified as scrapers or excavators following the functional differentiation of Bellwood and Choat (1990), and categorised into the following size groups (5-14 cm, 15-24 cm, 25-34 cm and >35 cm). For each size group, average abundances were calculated by taking a mean of the 4 belt transect survey counts and dividing by 120 m^2. The most abundant parrotfish observed was *Scarus psittacus*,

followed by *Chlorurus sordidus* and *Chlorurus strongylocephalus*. As for echinoids, erosion rates were used as a proxy for sediment generation as the excreted sediment contributes directly to the sediment reservoir. The sediment production rates of Perry et al. (2015) were employed (following from the work of Bellwood, 1995a; Bruggemann et al., 1996; Ong et al., 2010; Lokrantz et al., 2008). Rates were based upon species-level data concerning daily mass removal, bite rates, the proportion of bites leaving scars, and the volumes removed per bite. Rates (kg per individual yr^{-1}) for 'excavating' species of parrotfish within each size category were 5-14 cm – 0.288 kg, 15-24 cm – 39.067 kg, 25-34 cm – 90.240 kg, >35 cm –163.076 kg; while rates for 'scraping' species of parrotfish were 5-14 cm – 0.147 kg, 15-24 cm – 0.410 kg, 25-34 cm – 6.525 kg, >35 cm – 25.681 kg. Annual rates of sediment production (kg $CaCO_3$ m^{-2} yr^{-1}) were thus calculated by multiplying the aforementioned rates by the densities of parrotfish within each size category per m^2. Rates of sediment production by 'excavating' species were then reduced by 27% as this proportion (on average) of the carbonate ingested is estimated to be reworked sediment (Bellwood, 1996). Likewise, rates of production by 'scraping' species were reduced by 50% as this proportion of carbonate ingested is reported to represent reworked material (Bruggermann et al., 1996).

This methodology follows directly from that of Perry et al. (2015) with the exception of two differences. Firstly, the methodology for calculating foraminiferal production differs from that of Perry et al.'s counts of the abundance of live foraminifera on the surface of reef rubble. The decision to make this amendment was taken because the abundance on rubble did not reflect the concentrations of foraminifera within the sediment of each eco-geomorphic zone. By sampling infaunal foraminifera, Langer et al.'s (1997) approach therefore likely provides a more reliable means of ascertaining their rates of production. Secondly, the approach for estimating production by seagrass epiphytes was added to the methodology as Perry et al. found no seagrass within their study.

The approach represents a first step in the development of a standardised methodology for quantifying reefal sediment production. It is pertinent to note that

several caveats exist, which will be discussed within section 5.4.2. In particular, the methodology does not incorporate material produced by physical erosion. In addition, due to the paucity of datasets on sediment production rates at the individual constituent level, both within the Maldives and also globally, as with Perry et al. (2015), it has been necessary to use datasets from other regions to estimate *Halimeda*, foraminifera and molluscan production, though their abundances were relatively low at both the windward and leeward study sites. While this methodology is proposed as a standardised approach for estimating sediment production rates, as Perry et al. (2015) suggest, any future applications of this methodology ought to employ the most locally available published production rates.

5.3 Results

Tables 5.1 – 5.6 detail the abundances and, in turn, sediment production rates (G = kg $CaCO_3$ m^{-2} yr^{-1}) associated with each sediment producer/process within each zone at both the windward and leeward study sites. Figure 5.1 displays the relative roles of different sediment producers within each eco-geomorphic zone and at each site. Figure 5.2 illustrates the average rates of production within each eco-geomorphic zone at each study site. The rates were added to calculate the total sediment production rate for each zone and the relative contributions of each of the sediment producers/ processes (Tables 5.7 and 5.8). The sediment production rates were also multiplied by the area of each zone (as calculated from the digital habitat maps, section 4.3.1), to calculate total sediment production (kg $CaCO_3$ yr^{-1}; Tables 5.9 and 5.10). At the windward site, total sediment production was 74,825 kg yr^{-1} over an area of 0.84 km^2. At the leeward site, total production amounted 324,633 kg yr^{-1} over an area of 1.06 km^2. At both sites, sediment production was dominated by that associated with excavator parrotfish (72.8% and 68.3% at the windward and leeward sites respectively).

As a function of the eco-geomorphic variability, sediment production rates were found to vary markedly between both study sites and zones:

5.3.1 Windward site

At the windward site, sediment production rates ranged from 0.01 G in the lagoonward sand zone to 0.20 G in the oceanward reef crest zone. Sediment production was

dominated by that associated with excavator parrotfish, which accounted for 72.8% of total production (<0.13 G). The majority of sediment was produced within the lagoonward patch zone (72.7% of total production), 94.9% of which was produced by excavator parrotfish (0.13 G). Sediment production by urchins was of secondary significance accounting for 11.1% of total production. This was predominantly by *Diadema* sp. within the oceanward reef crest zone (0.17 G). Production associated with seagrass epiphytes was also relatively notable, accounting for 8.2% of total production, all of which occurred within the rubble zone (0.04 G; 6,128 kg yr^{-1}).

Production rates associated with other sediment-producing biota were minimal. The lagoonward patch zone was also the only windward zone within which *Halimeda* was found (0.73 thalli per m^2; 0.004 G; 2.1% of total production). Similarly, scraper parrotfish produced 2.5% of total sediment (<0.016 G). In combination, foraminifera, gastropods, bivalves and sponges produced 3.3% of the total sediment (i.e. <0.01 G, which was solely attributable to molluscs within the lagoonward sand zone).

5.3.2 Leeward site

At the leeward site, sediment production rates were markedly higher than those at the windward site, ranging from 0.05 G in the oceanward sand zone to 0.84 G in the lagoonward reef crest zone. Variability was largely attributable to differences in the densities of excavator parrotfish, which dominated sediment production rates in all zones except for the dense seagrass zone (97.6%, 88.6%, 58.8%, 61.3% and 85.6% in the lagoonward reef crest, lagoonward patch, oceanward sand, oceanward sparser seagrass and patch, and oceanward reef crest zones respectively). The highest rates of sediment production by excavator parrotfish were found within the lagoonward environments (0.82 G and 0.30 G in the lagoonward reef crest and lagoonward patch zones respectively). Consequently, the lagoonward zones accounted for a disproportionately large amount of sediment production (59.3%), despite accounting for the minority of the marine environment's areal extent at the leeward site (43.1%). Production rates associated with excavator parrotfish also increased with proximity to the oceanward reef crest (0.25 G and 0.18 G in the oceanward reef crest, and oceanward sparser seagrass and patch zones respectively).

Following excavator parrotfish, the second largest contribution to sediment production was from seagrass epiphytes, which accounted for 0.15 G (69.3%) of production within

the dense seagrass zone and 0.10 G (33.7%) within the sparser seagrass and patch zone. As at the windward site, sediment production rates associated with other biota at the were relatively low (<0.001 G). *Halimeda* production was negligible across all zones (<0.001 G), accounting for 0.2% of total sediment production. Similarly, scraper parrotfish accounted for 2.7% of total production (<0.018 G). In combination, foraminifera, gastropods, bivalves and sponges produced 0.2% of the total sediment (<0.001 G).

	Lagoonward Patch		Lagoonward Sand		Rubble		Oceanward Patch		Oceanward Reef Crest	
	Abundance	Production Rate (G)	Abundance	Production Rate (G)	Abundance	Production Rate (G)	Abundance	Production Rate (G)	Abundance	Production Rate (G)
Halimeda (thalli/m^2)	0.734 ± 0.242	0.004 ± 0.001	0.0 ± 0.0	0.0 ± 0.0	0.0 ± 0.0	0.0 ± 0.0	0.0 ± 0.0	0.0 ± 0.0	0.0 ± 0.0	0.0 ± 0.0
Gastropods (no./m^2)	0.1 ± 0.1	0.0 ± 0.0	0.8 ± 0.3	0.0 ± 0.0	0.4 ± 0.1	0.0 ± 0.0	0.4 ± 0.1	0.0 ± 0.0	0.3 ± 0.1	0.0 ± 0.0
Bivalves (no./m^2)	0.5 ± 0.3	0.001 ± 0.001	4.0 ± 1.4	0.01 ± 0.003	0.1 ± 0.0	0.0 ± 0.0	0.1 ± 0.0	0.0 ± 0.0	0.1 ± 0.0	0.0 ± 0.0
Foraminifera (%)	2.2 ± 1.0%	0.0 ± 0.0	2.0 ± 0.7%	0.0 ± 0.0	3.3 ± 0.9%	0.0 ± 0.0	4.3 ± 1.7%	0.0 ± 0.0	0.3 ± 0.2%	0.0 ± 0.0
Seagrass (blade density/m^2)	0.0 ± 0.0	0.0 ± 0.0	0.0 ± 0.0	0.0 ± 0.0	492.5 ± 48.9	0.04 ± 0.03	0.0 ± 0.0	0.0 ± 0.0	0.0 ± 0.0	0.0 ± 0.0
Endolithic sponges (no./m^2)	0.0 ± 0.0	0.0 ± 0.0	0.0 ± 0.0	0.0 ± 0.0	0.0 ± 0.0	0.0 ± 0.0	0.0 ± 0.0	0.0 ± 0.0	0.0 ± 0.0	0.0 ± 0.0
Total direct sediment production (G)	*0.005*		*0.010*		*0.040*		*0.000*		*0.000*	

Table 5.1 – Abundances and sediment production rates (G = kg $CaCO_3$ m^{-2} yr^{-1}) associated with direct sediment producers and endolithic sponges at the windward study site.

	Lagoonward Reef Crest		Lagoonward Patch		Oceanward Sand		Dense Seagrass		Oceanward Sparser Seagrass		Oceanward Reef Crest	
	Abundance	Production Rate (G)	Abundance	Production Rate (G)	Abundance	Production Rate (G)	Abundance	Production Rate (G)	Abundance	Production Rate (G)	Abundance	Production Rate (G)
Halimeda (thalli/m^2)	0.18 ± 0.08	0.001 ± 0.001	0.14 ± 0.09	0.001 ± 0.001	0.0 ± 0.0	0.0 ± 0.0	0.067 ± 0.034	0.0004 ± 0.00	0.14 ± 0.098	0.001 ± 0.001	0.02 ± 0.02	0.0 ± 0.0
Gastropods (no./m^2)	1.6 ± 0.7	0.0 ± 0.0	0.8 ± 0.4	0.0 ± 0.0	0.2± 0.1	0.0 ± 0.0	1.0 ± 0.5	0.0001 ± 0.00	0.3 ± 0.1	0.0 ± 0.0	0.3 ± 0.1	0.0 ± 0.0
Bivalves (no./m^2)	0.2 ± 0.1	0.001 ± 0.000	0.1 ± 0.1	0.0 ± 0.0	0.03 ± 0.03	0.0 ± 0.0	0.2 ± 0.1	0.0004 ± 0.00	0.1 ± 0.0	0.0 ± 0.0	0.04 ± 0.03	0.0 ± 0.0
Foraminifera (%)	3.5 ± 1.1%	0.0 ± 0.0	5.4 ± 0.9%	0.0 ± 0.0	2.5 ± 0.5%	0.0 ± 0.0	5.6 ± 1.9%	0.0003 ± 0.00	9.9 ± 1.5%	0.001 ± 0.000	1.1 ± 0.8%	0.0 ± 0.0
Seagrass (blade density/m^2)	0.0 ± 0.0	0.0 ± 0.0	13.5 ± 7.8	0.003 ± 0.003	145.2 ± 84.8	0.02 ± 0.01	1621.6 ± 163.4	0.15 ± 0.01	1132.7 ± 157.	0.10 ± 0.02	557.3 ± 146.5	0.03 ± 0.01
Endolithic sponges (no./m^2)	0.0 ± 0.0	0.0 ± 0.0	0.0 ± 0.0	0.0 ± 0.0	0.0 ± 0.0	0.0 ± 0.0	0.0 ± 0.0	0.0 ± 0.0	0.0 ± 0.0	0.0 ± 0.0	0.0 ± 0.0	0.0 ± 0.0
Total direct sediment production (G)	*0.002*		*0.004*		*0.020*		*0.151*		*0.102*		*0.030*	

Table 5.2 – Abundances and sediment production rates (G = kg $CaCO_3$ m^{-2} yr^{-1}) associated with direct sediment producers and endolithic sponges at the leeward study site.

Size categories	Lagoonward Patch Abundance (no./m^2)	Lagoonward Patch Erosion rate (G)	Lagoonward Sand Abundance (no./m^2)	Lagoonward Sand Erosion rate (G)	Rubble Abundance (no./m^2)	Rubble Erosion rate (G)	Oceanward Patch Abundance (no/.m^2)	Oceanward Patch Erosion rate (G)	Oceanward Reef Crest Abundance (no./m^2)	Oceanward Reef Crest Erosion rate (G)
Excavators										
5-14cm	0.0003	0.0001	0	0	0.002	0.0003	0.0003	0.0001	0.0003	0.0001
15-24cm	0.004	0.149	0	0	0	0	0.001	0.054	0.001	0.014
25-34cm	0.0003	0.031	0	0	0	0	0	0	0.0003	0.005
>35cm	0	0	0	0	0	0	0	0	0	0
Total gross rate (G)		0.180		0		0.0003		0.054		0.019
G - % reworked sediment		0.131		0		0.0002		0.039		0.014
Scrapers										
5-14cm	0.004	0.001	0	0	0.021	0.003	0.034	0.005	0.002	0.0003
15-24cm	0.002	0.001	0	0	0	0	0.001	0.001	0	0
25-34cm	0.0003	0.002	0	0	0	0	0	0	0.001	0.031
>35cm	0	0	0	0	0	0	0	0	0	0
Total gross rate (G)		0.004		0		0.003		0.006		0.031
G - % reworked sediment		0.002		0		0.002		0.003		0.016

Table 5.3 – Windward site parrotfish abundances and substrate erosion/sediment generation rates (G = kg $CaCO_3$ m^{-2} yr^{-1}) grouped by functional group and body size category.

Size categories	Lagoonward Reef Crest Abundance (no./m^2)	Lagoonward Reef Crest Erosion rate (G)	Lagoonward Patch Abundance (no./m^2)	Lagoonward Patch Erosion rate (G)	Oceanward Sand Abundance (no./m^2)	Oceanward Sand Erosion rate (G)	Dense Seagrass Abundance (no./m^2)	Dense Seagrass Erosion rate (G)	Oceanward Sparser Seagrass Abundance (no./m^2)	Oceanward Sparser Seagrass Erosion rate (G)	Oceanward Reef Crest Abundance (no./m^2)	Oceanward Reef Crest Erosion rate (G)
Excavators												
5-14cm	0.001	0.0004	0.0004	0.0001	0.002	0.0004	0.016	0.005	0.018	0.005	0.002	0.001
15-24cm	0.018	0.716	0.009	0.342	0.001	0.041	0.001	0.041	0.006	0.244	0.009	0.342
25-34cm	0.003	0.263	0.001	0.075	0	0	0	0	0	0	0	0
>35cm	0.001	0.136	0	0	0	0	0	0	0	0	0	0
Total gross rate (G)		1.116		0.417		0.041		0.046		0.249		0.342
G - % reworked sediment		0.815		0.304		0.030		0.034		0.182		0.250
Scrapers												
5-14cm	0.077	0.011	0.003	0.0004	0.013	0.002	0.141	0.021	0.166	0.024	0.014	0.002
15-24cm	0.014	0.006	0.009	0.004	0.001	0.0002	0.001	0.0004	0.005	0.002	0.006	0.002
25-34cm	0.003	0.019	0.001	0.005	0	0	0	0	0	0	0	0
>35cm	0	0	0	0	0	0	0	0	0	0	0	0
Total gross rate (G)		0.036		0.009		0.002		0.021		0.026		0.004
G - % reworked sediment		0.018		0.005		0.001		0.011		0.013		0.002

Table 5.4 – Leeward site parrotfish abundances and substrate erosion/sediment generation rates (G = kg $CaCO_3$ m^{-2} yr^{-1}) grouped by functional group and body size category.

Size categories	Lagoonward Patch Abundance (no./m^2)	Lagoonward Patch Erosion rate (G)	Lagoonward Sand Abundance (no./m^2)	Lagoonward Sand Erosion rate (G)	Rubble Abundance (no./m^2)	Rubble Erosion rate (G)	Oceanward Patch Abundance (no./m^2)	Oceanward Patch Erosion rate (G)	Oceanward Reef Crest Abundance (no./m^2)	Oceanward Reef Crest Erosion rate (G)
Diadema sp.										
0-20 mm	0	0	0	0	0	0	0	0	0.03	0.0003
21-40 mm	0	0	0	0	0	0	0	0	0	0
41-60 mm	0	0	0	0	0	0	0	0	0.07	0.07
61-80 mm	0	0	0	0	0	0	0	0	0.03	0.23
Echinometra sp.										
0-20 mm	0	0	0	0	0.02	0.01	0	0	0	0
21-40 mm	0	0	0	0	0	0	0	0	0	0
41-60 mm	0	0	0	0	0	0	0	0	0	0
61-80 mm	0	0	0	0	0	0	0	0	0	0
Total gross rate (G)		0		0		0.01		0		0.3003
G - % reworked sediment		0.00		0.00		0.01		0.00		0.17

Table 5.5 – Windward site urchin abundances and substrate erosion/sediment generation rates (G = kg $CaCO_3$ m^{-2} yr^{-1}) grouped by species and size category.

	Lagoonward Reef Crest		Lagoonward Patch		Oceanward Sand		Dense Seagrass		Oceanward Sparser Seagrass		Oceanward Reef Crest	
Size categories	Abundance (no./m^2)	Erosion rate (G)	Abundance (no./m^2)	Erosion rate (G)	Abundance (no./m^2)	Erosion rate (G)	Abundance (no./m^2)	Erosion rate (G)	Abundance (no./m^2)	Erosion rate (G)	Abundance (no./m^2)	Erosion rate (G)
Diadema sp.												
0-20 mm	0	0	0.02	0.0002	0	0	0.02	0.0002	0	0	0	0
21-40 mm	0	0	0	0	0	0	0	0	0	0	0.04	0.02
41-60 mm	0	0	0	0	0	0	0	0	0	0	0	0
61-80 mm	0	0	0	0	0	0	0	0	0	0	0	0
Echinometra sp.												
0-20 mm	0.06	0.02	0.04	0.06	0	0	0.02	0.03	0	0	0	0
21-40 mm	0	0	0	0	0	0	0	0	0	0	0	0
41-60 mm	0	0	0	0	0	0	0	0	0	0	0	0
61-80 mm	0	0	0	0	0	0	0	0	0	0	0	0
Total gross rate (G)		0		0.0602		0		0.0302		0		0.02
G - % reworked sediment		0		0.03		0		0.02		0		0.01

Table 5.6 – Leeward site urchin abundances and substrate erosion/sediment generation rates (G = kg $CaCO_3$ m^{-2} yr^{-1}) grouped by species and size category.

	Lagoonward Patch		Lagoonward Sand		Rubble		Oceanward Patch		Oceanward Reef Crest	
	Sediment production rate (G)	% of new sediment production	Sediment production rate (G)	% of new sediment production	Sediment production rate (G)	% of new sediment production	Sediment production rate (G)	% of new sediment production	Sediment production rate (G)	% of new sediment production
Excavator parrotfish	0.131	94.7%	0	0.0%	0.0002	0.0%	0.039	92.9%	0.014	7.0%
Scraper parrotfish	0.002	1.4%	0	0.0%	0.002	3.8%	0.003	7.1%	0.016	8.0%
Halimeda	0.004	2.9%	0	0.0%	0	0.0%	0	0.0%	0	0.0%
Seagrass	0	0.0%	0	0.0%	0.04	76.9%	0	0.0%	0	0.0%
Urchins	0	0.0%	0	0.0%	0.01	19.2%	0	0.0%	0.17	85.0%
Other	0.001	0.7%	0.01	100.0%	0	0.0%	0	0.0%	0	0.0%
Total new sediment (G)	0.14		0.01		0.05		0.04		0.20	

Table 5.7 – Rates (G = kg $CaCO_3$ m^{-2} yr^{-1}) and the proportional contributions (per m^2) of new sediment production associated with each of the key sediment producers at the windward site.

	Lagoonward Reef Crest		Lagoonward Patch		Oceanward Sand		Dense Seagrass		Oceanward Sparser Seagrass		Oceanward Reef Crest	
	Sediment production rate (G)	% of new sediment production	Sediment production rate (G)	% of new sediment production	Sediment production rate (G)	% of new sediment production	Sediment production rate (G)	% of new sediment production	Sediment production rate (G)	% of new sediment production	Sediment production rate (G)	% of new sediment production
Excavator parrotfish	0.815	97.6%	0.304	88.7%	0.03	58.8%	0.034	15.7%	0.182	61.5%	0.25	85.4%
Scraper parrotfish	0.018	2.2%	0.005	1.5%	0.001	2.0%	0.011	5.1%	0.013	4.4%	0.002	0.7%
Halimeda	0.001	0.1%	0.001	0.3%	0	0.0%	0.0004	0.2%	0.001	0.3%	0	0.0%
Seagrass	0	0.0%	0.003	0.9%	0.02	39.2%	0.15	69.3%	0.1	33.8%	0.03	10.2%
Urchins	0	0.0%	0.03	8.8%	0	0.0%	0.02	9.2%	0	0.0%	0.01	3.4%
Other	0.001	0.1%	0	0.0%	0	0.0%	0.001	0.5%	0.001	0.3%	0	0.0%
Total new sediment (G)	0.84		0.34		0.05		0.22		0.30		0.29	

Table 5.8 – Rates (G = kg $CaCO_3$ m^{-2} yr^{-1}) and the proportional contributions (per m^2) of new sediment production associated with each of the key sediment producers at the leeward site.

	Sediment production within each zone (kg/yr)					Sediment producer total (kg/yr)	% Sediment production by each sediment producer
	Lagoonward Patch	**Lagoonward Sand**	**Rubble**	**Oceanward Patch**	**Oceanward Reef Crest**		
Excavator parrotfish	51647	0	31	2205	561	54,444	72.8%
Scraper parrotfish	789	0	306	170	641	1,905	2.5%
Halimeda	1577	0	0	0	0	1,577	2.1%
Seagrass	0	0	6121	0	0	6,121	8.2%
Urchins	0	0	1530	0	6812	8,342	11.1%
Other	394	2041	0	0	0	2,436	3.3%
Zone total (kg/yr)	54,407	2,041	7,988	2,375	8,014		
% of total sediment production	72.7%	2.7%	10.7%	3.2%	10.7%		

Table 5.9 – Total new sediment production within each zone at the windward site (kg yr^{-1}, i.e. following multiplication by the areal extent of each eco-geomorphic zone), and proportional contributions both within each zone and by each of the key sediment producers.

	Sediment production within each zone (kg/yr)						Sediment producer total (kg/yr)	% Sediment production by each sediment producer
	Lagoonward Reef Crest	**Lagoonward Patch**	**Oceanward Sand**	**Dense Seagrass**	**Oceanward Sparser Seagrass**	**Oceanward Reef Crest**		
Excavator parrotfish	57067.115	118768.544	1887.3	13596.464	15259.972	14993.25	221573	68.3%
Scraper parrotfish	1260.378	1953.43	62.91	4398.856	1089.998	119.946	8886	2.7%
Halimeda	70.021	390.686	0	159.9584	83.846	0	705	0.2%
Seagrass	0	1172.058	1258.2	59984.4	8384.6	1799.19	72598	22.4%
Urchins	0	11720.58	0	7997.92	0	599.73	20318	6.3%
Other	70.021	0	0	399.896	83.846	0	554	0.2%
Zone total (kg/yr)	58468	134005	3208	86537	24902	17512		
% of total sediment production	18.0%	41.3%	1.0%	26.7%	7.7%	5.4%		

Table 5.10 – Total new sediment production within each zone at the leeward site (kg yr^{-1}, i.e. following multiplication by the areal extent of each eco-geomorphic zone), and proportional contributions both within each zone and by each of the key sediment producers.

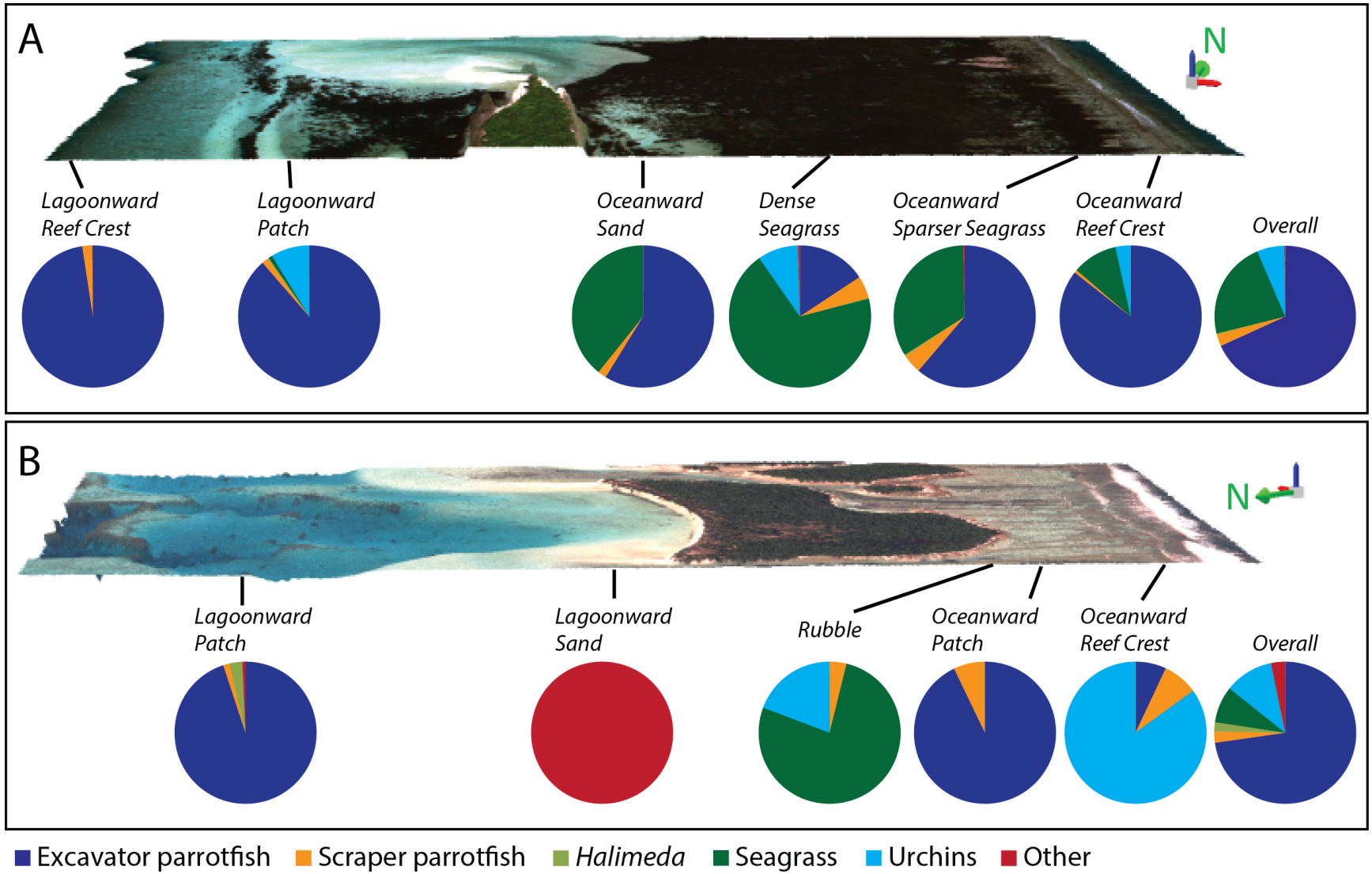

Figure 5.1 – Relative contributions of sediment producers within each of the eco-geomorphic zones and overall at the windward (A) and leeward (B) study sites.

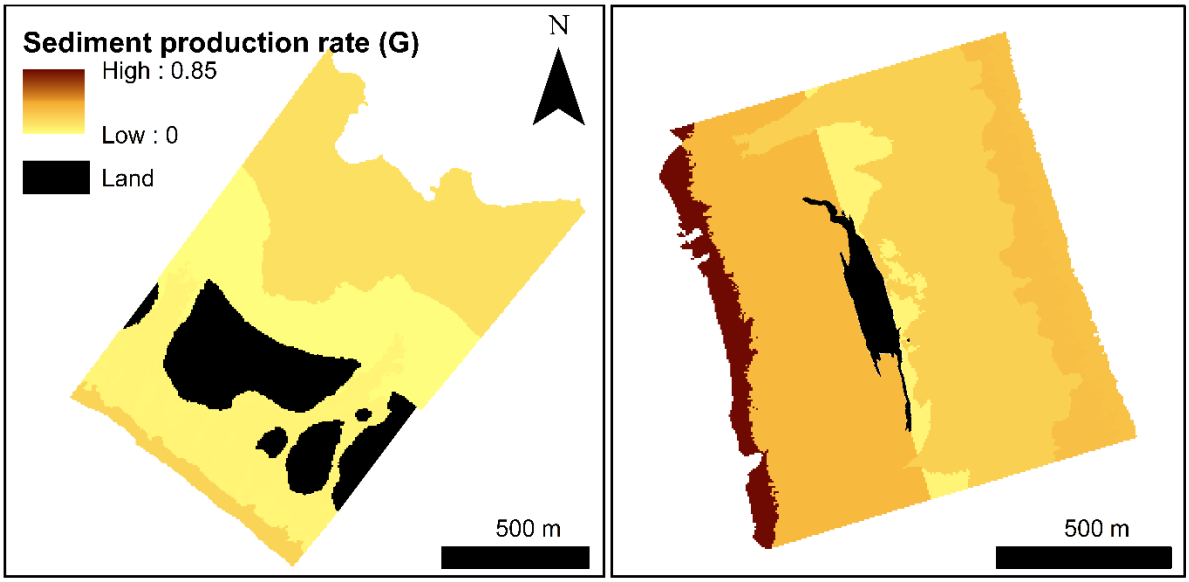

Figure 5.2 – Spatial variability (i.e. between zones) in average rates of sediment production (G) at the windward (left) and leeward (right) sites.

5.4 Discussion

5.4.1 Sediment generation

This Chapter presents the first attempt to estimate sediment production rates within a Maldivian atoll rim setting. Perhaps the most striking finding was the dominance of sediment production by excavator parrotfish (72.8% and 68.3% of total production at the windward and leeward sites; Figure 5.1). This is consistent with Perry et al.'s (2015) sediment budget on Vakkaru reef platform, Raa Atoll, which found parrotfish accounted for the vast majority of sediment production - 86.3% and 81.6% within the outer and inner reef flats, respectively. Likewise, on Vabbinfaru reef platform (an interior platform within North Malé Atoll), Morgan (2014) found 97% of sediment production was associated with parrotfish. Of secondary importance at the windward site was sediment production associated with urchin bioerosion, which attained rates of 0.17 G on the oceanward reef crest. At the leeward site, sediment production associated with seagrass epiphytes was of secondary importance, with rates of 0.15 G within the dense seagrass zone. Epiphytes principally comprised CCA, molluscs and foraminifera (refer to Chapter 6).

Seagrass epiphytes represented the only source of direct sediment production to be generated in notable quantities (e.g. 0.15 G within the dense seagrass zone). Indeed,

contributions from *Halimeda*, endolithic sponges, and non-epiphytic foraminifera, gastropods and molluscs were negligible across all eco-geomorphic zones and sites. This is consistent with sediment budget studies undertaken on Maldivian interior platforms as direct sediment production accounted for <1.5% on Vabbinfaru platform (Morgan, 2014). Likewise, on Vakkaru production by foraminifera, bivalves, gastropods and also urchin bioerosion accounted for <5% of total sediment production, while *Halimeda* contributed ~10% (Perry et al., 2015). However, direct sediment production has been found to be more notable in other regions, for example, Harney and Fletcher (2003) found direct sediment production (by *Halimeda*, branching coralgae, foraminifera and molluscs) to account for ~37.7% (0.20 ± 0.06 G) of total normalised sediment production at Kailua Bay, Hawaii. In particular, foraminifera have been highlighted as a key carbonate producer within the Pacific (Yamano et al., 2000) and *Halimeda* within the Caribbean (Stoddart et al., 1962b; Yamano et al., 2005). This is likely a function of differences in sea-level histories as the Pacific mid-Holocene sea-level highstand produced tidally-emergent reef flats that favour foraminifera production (Perry et al., 2011). Conversely, the shallow reef crests and lagoons that characterise the Caribbean favour *Halimeda* production (Perry et al., 2011).

Also striking was the substantial inter- and intra-site variability in sediment production rates. Production rates at the leeward site far exceeded those found at the windward site. Given the dominance of excavator parrotfish production, variability was largely a function of their differing abundances and sizes. Hence, the highest rates of sediment production were found in the eco-geomorphic zones that were host to the greatest densities and sizes of excavator parrotfish, namely the lagoonward reef crest and lagoonward patch zones at the leeward site. This was likely partially attributable to the high surface complexity (also the highest of the study) within these zones, which would afford shelter and food availability, (e.g. Verway et al., 2006) and also the presence of seagrass within the lagoonward patch zone. Indeed, within the leeward site lagoonward reef crest and lagoonward patch zones excavator parrotfish production accounted for 0.82 G and 0.30 G respectively. The lagoonward environments at the leeward site therefore accounted for a disproportionately large proportion of sediment production (59.3%) given their areal extent (43.1% of the marine environment).

By contrast, the lower sediment production rates found at the windward site were partially attributable to the lower densities of excavator parrotfish in comparison to the

leeward site. This may be due to the lower degree of surface complexity as there was an absence of seagrass and lower proportions of reef framework coverage in the lagoonward environments at the windward site. Indeed, at the windward site, there was an absence of any coral cover in the lagoonward sand zone and also an absence of a defined lagoonward reef crest at the windward site in comparison to the leeward site. The lagoonward sand zone at the windward site was comparable with the sand moat zone at Vakkaru, which was also solely comprised of rippled sand. Similarly, no parrotfish were found within this zone (Perry et al., 2015). In addition, the oceanward environment at the windward site was also notably shallow (mean depths were -0.36 m, -0.44 m and -0.65 m within the oceanward reef crest, rubble and oceanward patch zones respectively; Table 7.2), which may also have impacted parrotfish distribution. Yarlett (unpublished data, 2016) also found relatively low densities of parrotfish within a rubble zone on an atoll rim platform in Lhaviyani Atoll, Maldives, which was somewhat akin to the rubble zone at the windward site. While differences in the densities of excavator parrotfish were the primary reason that sediment production at the leeward site exceeded that at the windward site, of secondary importance was the higher rates of sediment production associated with seagrass epiphytes at the leeward site. This is a function of both greater densities of seagrass blades and also areal extent. Hence, seagrass habitats may contribute to sediment production both due to epiphytic carbonate production and also by providing parrotfish with shelter and food. Given that seagrass is frequently removed in the Maldives (e.g. Gillis, 2009), this study highlights the fact that the potential sedimentary, and in turn geomorphic, implications of its removal ought to be considered in the management of these environments (refer to Chapter 6 for further discussion).

While leeward site sediment production was markedly higher than windward production, sediment production found on Vakkaru platform (Raa Atoll) far exceeded that found at either study site. Indeed, Perry et al. (2015) calculated total annual sediment production to be ~685,000 kg over a marine area of ~0.27 km^2, which was far smaller than either the windward (0.84 km^2) or leeward (1.06 km^2) site marine environments in this study. This high rate of sediment production may partially be attributed to the highly productive reef crest which encircled the entire platform covering 37% of the marine environment. By contrast, the lagoonward reef crest in this study accounted for 6% of the marine environment. Nonetheless, rates of production

on Vakkaru's reef crest (5.71 G) far exceeded those found in this study (highest rate = 0.84 G at the leeward site lagoonward reef crest). The majority of production (86.3%) on the reef crest was associated with parrotfish and may hence be attributable parrotfish densities, body sizes, and also to the greater proportions of live coral cover within this zone (25.7 ± 9.6% and 19.7 ± 8.0% in the outer and inner reef flat zones respectively; Perry et al., 2015).

5.4.2 Methodological considerations

In considering the sediment production estimates of the present study, it is pertinent to note that several caveats exist. Firstly, as mentioned, is the paucity, both globally and locally, of constituent-level carbonate production rate datasets. As in Perry et al.'s (2015) Maldivian sediment budget, this study necessitated the application of data from other regions in order to estimate *Halimeda*, foraminifera and molluscan production rates. Sediment production by *Halimeda*, foraminifera and molluscs was negligible (as a function of their low abundances) and so this likely had limited impact upon the findings of this study. However, a recent study (Perry et al., 2016) has proposed a new census-based approach for estimating carbonate production by *Halimeda* based upon rates calculated within Huvadhu Atoll. Unfortunately, this approach could not be utilised within the present study as *Halimeda* identification was not undertaken, but future applications of the sediment production methodology in the Indian Ocean ought to employ Perry et al.'s (2016) approach.

Secondly, the estimates of sediment production did not incorporate material produced by physical erosion. Likewise, this was omitted from sediment budgets calculated for the interior Maldivian platforms (Morgan, 2014; Perry et al., 2015). Physical erosion may occur episodically as a result of storms, cyclones and tsunami, and is a function of hydrodynamic energy exceeding the strength of the coral (Madin, 2005). The omission of sediment production via physical breakdown is partially justifiable given that the close proximity of the Maldives to the equator renders storm events as rare (Woodroffe, 1992). In addition, a key rationale for the existing Maldivian sediment budgets (Morgan, 2014; Perry et al., 2015) and also that of this study was to employ sediment production estimates as a means of improving understanding of reef-island connectivity. However, material produced by mechanical breakdown is predominantly of rubble-grade (>2 mm; Maragos et al., 1973; Kench, 2011a), while the material in

the upper island horizons were comprised of predominantly sand-grade material (i.e. facies 1 and 2; Chapter 3). Hence, physical erosion is likely of limited importance for contemporary reef island building and maintenance.

Nonetheless, the presence of rubble within basal island sediments (Chapter 3) and in the marine environment at the windward site (section 4.3.1) suggests that low-frequency high-magnitude swell events likely result in rubble generation and its deposition on the oceanward reef flat. However, quantifying rates of generation is problematic as they are a function of several interrelated factors, including: (1) coral growth form, as sensitivity to physical erosion is dependent upon coral growth form as massive corals typically have a higher resistance than branched, tabulate and arborescent forms (Done, 1992; Madin and Connolly, 2006; Kench, 2011a); (2) the magnitude of the concerned event; (3) the recurrence interval between such high energy events; and (4) the condition of the reef prior to (i.e. extent of coral cover) the event. Several studies have documented episodic generation of storm-derived rubble (e.g. Maragos et al., 1973; Bayliss-Smith, 1988; Blanchon and Jones, 1997; Blanchon et al., 1997; Hayne and Chappell, 2001). Understanding of the interactions between the listed factors is poor and the calculation of meaningful site-specific estimates of physical breakdown is therefore problematic. It is also possible for physical erosion to generate sand-sized material via abrasion of coral branches. However, given their high durabilities (Ford and Kench, 2012) and their persistence in the marine environment, this process likely occurs over long temporal scales. Physical abrasion to produce sand-grade material therefore likely represents a subordinate contribution to the sediment reservoir (e.g. Perry et al., 2015).

An additional caveat was that it was not possible to survey beyond the oceanward algal rim at either study site due to the highly exposed nature of the sites. At both study sites, spur-and-groove features were observed beyond the oceanward algal rims both at low tide and in satellite imagery. Indeed, an underrepresentation of spur and groove research more broadly has been highlighted due to the difficulties of accessing and working within such high energy environments (Guilcher, 1988; Duce et al., 2016). Likewise, knowledge of the oceanward reef crests beyond the breaker zone is also limited and, on Indo-Pacific atolls, Wells (1957) termed this the ‘innominate’ zone (*‘mare incognitum’*). Likewise, knowledge of Maldivian oceanward reef crest ecology is limited to qualitative descriptions (Hass, 1961; Eibl-Eibesfeldt, 1964; Stoddart, 1966;

Ciarapica and Passeri, 1993; Morri et al., 1995; Bianchi et al., 1997). The omission of spur-and-groove systems from the sediment production calculations is problematic as they likely form highly productive zones (Perry et al., 2013). However, the steep gradient is described as forming a 'reef wall' (Hass, 1961; Eible-Eibesfeldt, 1964) and it is thus likely that a large proportion of sediment generated within this zone will not surmount the algal rim to be transported onto the rim platform surface. Rather, it seems more likely that sediment produced off the algal rim will be either stored on the reef slope or exported off-reef. Stoddart (1966) described continual suspension of coarse sand and fine gravel (to heights of 1.2 – 1.5 m above the substratum), though only within the bases of groove channels (at depths of ~4.5 – 6 m). However, the presence of *Acropora* rubble on the reef flat and the absence of live *Acropora* within the oceanward zones implies that material can be transported from beyond the breaker zone and onto the reef flat. It seems likely that this is an episodic process, coincident with low-frequency high-magnitude events.

A final caveat is the uncertainty associated with sediment production by parrotfish within the smallest (5-14 cm) size category. Indeed, 30.5% and 44.6% of excavator parrotfish were in the 5-14 cm size category at the windward and leeward sites respectively. However, estimations of bioerosion rates associated with this size category are somewhat ambiguous. Bioerosion rates were adopted from Perry et al. (2015). However, prior research also suggests that variability exists in the rates and volumes of bioerosion associated with parrotfish within this size category. For example, it has been suggested that there is no bioerosion associated with *Chlorurus perspicillatus* that are below 7 cm in size. In addition, only *C. perspicillatus* that were >10 cm were said to leave bite scars, hence generating greater volumes of sediment (Ong and Holland, 2010). Incorporating such variability in sediment production within this category is problematic, although the vast majority of the excavating parrotfish observed in this study were toward the upper limits of the category (i.e. >10 cm) and thus were likely of significance for sediment production. Constraining the rates of sediment production associated with small (5-14 cm) parrotfish would be a useful direction for future research.

5.4.3 Linking sediment production to sediment storage

Despite the caveats, the high degree of correspondence found between sediment production and sediment storage (see Chapters 3 and 4) lends confidence to the sediment budget approach employed in this study. Indeed, the sediment stored within the marine environment, beaches and the upper horizons of reef islands was predominantly sand-grade coral (Chapter 4). Similarly, sediment production associated with parrotfish is also dominated by sand-grade coral (Hoey and Bellwood, 2008; Morgan and Kench, 2016a). Indeed, Morgan and Kench (2016a) examined the properties of sediment produced by parrotfish on Vabbinfaru reef platform, Maldives and found sediment to be predominantly (94%) comprised of coral and sized between 0 and 2 ϕ (i.e. sand-grade). In addition to sediment production associated with parrotfish, there are three other processes by which coral framework may be converted into sand-grade material (Perry et al., 2015): (1) physical erosion of the reef framework produces sand-sized sediments via abrasion (though this is unlikely to be a dominant process given the high durability of coral – Ford and Kench, 2012; Perry *et al.*, 2015) or rubble-grade clasts; (2) endolithic sponge bioerosion produces silt-sized (<63 μm) material, though is evidently of minimal significance for reef island building as silt-sized material accounted for only 2.11 ± 0.57% of each sample and no endolithic sponges were observed in this study; (3) urchin grazing produces predominantly silt-sized material and is thus, likewise, unlikely to represent a dominant process (Hunter, 1977; Perry et al., 2015). The prevalence of sand-grade coral across all components of rim island systems is therefore most plausibly attributable to parrotfish grazing.

It is also interesting to note that there is no statistically significant relationship between depths of sediment storage (Tables 4.11 and 4.12, Chapter 4) and sediment production rates ($P = 0.23$; $R^2 = 0.14$). Indeed, the highest rate of sediment production was found within the lagoonward reef rest zone at the leeward site (0.84 G), yet, sediment depths within the lagoonward reef crest zone were relatively shallow (5.1 ± 1.8 cm). In contrast, the lowest sediment production rates of the study (0.01 G) were found in the lagoonward sand zone at the windward site, which was also the zone with the largest sediment depths of the study (23.9 ± 4.5 cm). This, in part, verifies the suggestion within Chapters 3 and 4 that sediment is transported relatively rapidly from

zones of production and hence highlights that wave exposure represents a key control upon atoll rim systems.

In considering the implications of sediment production rates for sediment storage and reef island evolution, it must be borne in mind that not all of the generated sediment would be retained on the reef platform. Rather, sediment is inevitably lost from the platform surface due to: (1) export of fine-grade material in solution (e.g. Land, 1976); (2) sediment retention within the reef framework (e.g. Hubbard et al., 1990; Perry and Hepburn, 2008); (3) biologically-mediated export (e.g. by parrotfish – Bellwood, 1995b); and (4) physical transport by currents of removal (e.g. Morgan and Kench, 2010; 2012). In addition, of the sediment produced, not all material is of a suitable grade for reef island building. Rather, islands are predominantly comprised of sand-grade material (Chapter 3; Kench et al., 2005; Perry et al., 2015; Liang et al., 2016; Morgan and Kench, 2016a, 2016b). Of the three key sediment producers found in this study: (1) sand-sized sediments are produced as a by-product of parrotfish grazing (Hoey and Bellwood, 2008; Morgan and Kench, 2016a); (2) seagrass epiphytes comprise CCA, which likely disaggregates into carbonate mud (Land, 1970), and foraminifera and molluscs, which are likely sand-grade (Scoffin, 1992); and (3) urchin grazing produces predominantly fine-grained sand and silt-sized material (Hunter, 1977; Perry et al., 2015). As such, sediment production associated with parrotfish and epiphytic molluscs and foraminifera are thus likely to be of greatest significance for reef island building.

5.4.4 Linking ecological and geomorphic temporal scales

This Chapter is primarily concerned with ecological temporal scales (Figure 1.6). However, given that reef islands are formed solely of sediment produced within the surrounding marine environments, the contemporary sediment production regime has key implications for reef island building and maintenance. Hence, there are implications that cascade from ecological to geomorphic temporal scales. The notable concurrence between the dominance of sand-grade coral within the sediment reservoir and the dominance of excavator parrotfish production suggests that a tight coupling exists between reef islands and their surrounding marine environments (McKoy et al., 2010). This study therefore highlights the inter-connected nature of reef island systems and the importance of reef ecology for reef island geomorphology. While Chapters 3

and 4 highlighted the reliance of reef island systems upon a restricted range of sedimentary constituents, data presented in this Chapter highlights that there is a corresponding reliance of reef islands upon a restricted range of sediment producers, specifically excavator parrotfish. Contemporary reef ecology is therefore well-suited to generate sediments that are appropriate for reef island construction and maintenance. Moreover, the downcore dominance of sand-grade coral also suggests that ecology has been temporally stable and that the reefs have likely maintained healthy populations of excavator parrotfish, particularly since the transition to the accumulation of facies 2 (i.e. predominantly sand-grade material) occurred at ~1,400 to 1,800 yr. B.P. (Chapter 3). This highlights the significance of any future shifts in reef ecology that may be associated with environmental change. In particular, any shifts in the abundance of excavator parrotfish could have detrimental effects on future reef island resilience.

Moreover, linkages may be drawn between sediment production (at ecological temporal scales) and modes of island building (at geomorphic temporal scales). Examining the spatial variability in sediment production rates, at both study sites, the lagoonward environments were found to contribute larger volumes of sediment (75.4% and 59.4% at the windward and leeward sites respectively) than the oceanward environments (Figure 5.2). This is an important observation in the context of AMS radiocarbon dates, island topography and GPR profiles which suggest that more recent island development has occurred via lateral lagoonward accretion (Chapter 3). Indeed, at the leeward site, the higher elevations of Galamadhoo island also imply that there are larger inputs of sediment off the island's lagoonward coast. This suggests that the modes of island building are reflective of the relative inputs of sediment from the adjacent reef environments. The evolutionary models of island development proposed by Woodroffe et al. (1999; 2002) could therefore be a function of spatial variability in the relative rates of sediment production and thus reef ecology.

Island formation occurs as a part of the continuum of platform infilling, which is a function of platform area and rates of sediment production. It could thus be hypothesised that the earlier dates of island formation found for interior islands in South Maalhosmadulu Atoll (~27 km from Vakkaru) may be a function of both the smaller platform size and higher rates of sediment production. Hence, platform infilling could occur earlier and in turn, island formation could occur earlier. Likewise, the

difference in island ages between the windward and leeward study sites may be due to slower rates of platform infill at the windward site. This is because sediment production rates were found to be markedly lower than at the windward site and the windward platform is greater in areal extent than the leeward platform.

5.5 Conclusion

This Chapter presents the first attempt to estimate rates of sediment production within an atoll rim setting in the Maldives. The study applies and builds upon the approach of Perry et al. (2015) which represents a first step in developing a standardised methodology for quantifying sediment production. It is pertinent to note that several caveats exist, including the omission of sediment production by physical erosion, the reliable quantification of which remains problematic.

New sediment production at the leeward site (324,633 kg yr^{-1} over an area of 1.06 km^2) far exceeded that found at the windward site (74,825 kg yr^{-1} over an area of 0.84 km^2), which was largely attributable to the differing densities of excavator parrotfish. Indeed, excavator parrotfish were identified as the dominant sediment producers at both sites, accounting for 72.8% and 68.2% of the total annual production at the windward and leeward sites respectively. Notably, this is consistent with the prevalence of sand-sized coral that was found stored within marine, beach and island sediments. Moreover, modes of recent island development (via lateral lagoonward accretion) are consistent with spatial variability sediment production by excavator parrotfish. This study therefore highlights the role of excavator parrotfish as major biophysical engineers in the formation and maintenance of Maldivian rim islands. Our results also emphasise the reliance of Maldivian rim islands upon a limited range of sediment producing organisms. Any shifts in their abundance could thus have a critical impact upon reef island resilience in the face of future environmental change.

Chapter 6: The distribution of Maldivian seagrass meadows and implications for sediment production

6.1 Introduction

Seagrass beds are highly productive ecosystems that provide a range of key ecological services. They sequester a globally significant quantity of carbon (Duarte et al., 2005), improve water quality through sediment stabilisation, provide protection from coastal erosion, and produce oxygen. Their habitats support both commercial fisheries valued at \$3,500 ha^{-1} yr^{-1} (McRoy, 1977) and artisanal fisheries that represent the livelihoods of millions in tropical regions (de al Torre-Castro and Ronnback, 2004; Bjork et al., 2008; Unsworth and Cullen, 2010). They also serve as a major food supply to the marine food web, including to endangered species (e.g. Green turtles, *Chelonia mydas*, are found in the Maldives and are on the IUCN Red List; IUCN, 2015). This range of services renders seagrass beds among the most valuable ecosystems per hectare with nutrient cycling alone estimated at \$3.8 trillion yr^{-1} (Costanza et al., 1997). However, it is widely acknowledged that seagrass ecosystems are facing a crisis (Orth et al., 2006), primarily as a result of both direct (e.g. dredging, runoff, foreshore development, aquaculture, eutrophication) and indirect (e.g. sea-level rise, shoreline erosion, increased seawater temperatures, food web alterations) human impacts (Duarte, 2002). As consequence, the global areal extent of seagrass beds worldwide is thus estimated to have declined by 29% since initial records in 1879 and rates of loss have accelerated in recent decades to 110 km^2 yr^{-1} since 1980 (Waycott et al., 2009).

While seagrass ecosystems face a plethora of direct and indirect threats, nutrient enrichment is frequently cited as the primary cause of seagrass loss (Short and Wyllie-Echeverria, 1996; Kenworthy et al., 2006; Kelaher et al. 2013). Indeed, seagrass growth, coverage and primary production are often employed as proxies for the degree of eutrophication (Bricker et al., 2003; Greening and Janicki, 2006). In this context, the

most important nutrients are nitrogen and phosphorous, which are primarily derived from anthropogenic sources (e.g. sewage effluent and agricultural run-off – NRC, 2000). With nutrient loading, the competitive advantage of algal species increases. Such species often have filamentous sheet-like growth forms, for example *Ulva, Cladophora* and *Chaetomorpha* (Valiela et al., 1997; NRC, 2000; Guidone and Thornber, 2013). This results in the development of thick algal mats, which reduce underwater light levels and further inhibit seagrass growth (Duarte, 2002). Within shallow coastal marine systems, seagrass loss with increased nutrient loading has thus been attributed to a shift from nutrient- to light-limitation (Harlin, 1993; Cloern, 2001; Figure 6.1). Threshold values for the point at which this shift may occur have been proposed, for example, in the Caribbean, ~1.0 μM dissolved inorganic nitrogen (DIN) and ~0.1 μM soluble reactive phosphorous (SRP; Lapointe, 1997). Similarly, for Great Barrier Reef sites, Bell (1992) found threshold values of ~1.0 μM DIN and 0.1-0.2 μM SRP.

The interactions between seagrass loss and eutrophication (i.e. light-limited settings – Figure 6.1) have been a key focus of recent research (e.g. Schmidt et al., 2012; Govers et al., 2014; Lapointe et al., 2015). However, there is a paucity of work on nutrient-limited settings (Figure 6.1) whereby seagrass primary production may increase with nutrient loading. Coral reefs thrive in low nutrient environments, for example, Kleypas et al. (1999) found the modal value of nitrate and phosphate among reef locations to be 0.0 μmol litre^{-1} (i.e. an immeasurable level; Kleypas et al., 1999). A moderate increase in nutrient input may therefore cause an expansion of seagrass beds in such low nutrient settings. To the best of the author's knowledge, this has been documented only once and over a relatively small spatial scale. Seagrass areal extent at Green Island, Great Barrier Reef, expanded from a narrow fringe in 1936 (Udy et al., 1999) to 151.6 ± 10.7 ha in 2003 (McKenzie et al., 2014). Though the cause of expansion has been debated (McKenzie et al., 2014), current flow studies suggest it was due to leakage from a sewage pipe that ran across the reef flat (van Woesik, 1989).

The impacts of seagrass expansion in a coral reef environment would be multifaceted. Firstly, there would be a shift in reef ecology, not only in terms of increase in seagrass extent, but also in the organisms that inhabit the area. For instance, parrotfish and turtles graze on seagrass, and the three-dimensional structure afforded by seagrass

blades provides a habitat for diverse resident faunal assemblages, including decapods, bivalves, gastropods, foraminifera and fishes (Orth, 1992). Seagrass blades may also host a range of epiphytes, such as foraminifera, gastropods, calcareous algae, serpulids and bryozoans. Secondly, consequent impacts upon sediment production may occur. As reefal sediment is produced by the organisms in the marine environment, a shift in ecology could therefore cause a fundamental change in the types and grades of sediment produced. Each of the organisms associated with seagrass beds (e.g. foraminifera, gastropods, calcareous algae, serpulids, bryozoans, parrotfish) could potentially contribute to the sediment reservoir (e.g. Nelsen and Ginsburg, 1986). Indeed, benthic sediment samples from seagrass beds adjacent to Inhaca Island, Mozambique, were predominantly composed of molluscs and benthic foraminifera that live on or within the seagrass sediment substrate (Perry and Beavington-Penney, 2005). In terms of grain size, CCA, serpulids and bryozoans would likely rapidly disaggregate into fine-grade material once detached from the blades. In contrast, foraminifera, gastropods and parrotfish would likely produce sand-grade material. Thirdly, seagrass expansion could increase the volume of benthic sediment stored on the reef flat as seagrass rhizome and root systems bind the sediment, effectively trapping it on the reef flat. For example, Gacia et al. (1999) found a significant positive relationship within *Posidonia* beds between the projected surface area of the plants and the total amount of trapped particles. Fourthly, expansion of dense seagrass beds may result in a shift in sediment transport pathways as seagrass may modify tidal currents and attenuate wave energy (e.g. Gacia et al., 1999; van Keulen and Borowitzka, 2002). *Thalassia* beds in Bimini Lagoon, Bahamas, were thus found to reduce water velocity from a speed sufficient to transport loose sand (30 cm s^{-1}) to zero (Scoffin, 1970).

With seagrass expansion in a coral reef environment, it may thus be hypothesised that such a compositional shift in the carbonate-producing community could, in turn, result in a shift in the rates, types and grades of sediment produced, in the volume of sediment stored on the reef flat, and in pathways and rates of sediment transport. As coral reef islands are formed entirely of sediment produced in the marine environment and deposited by waves at nodal points, sediment production and transport are two key controls on reef island development and maintenance. A change in the areal extent of seagrass meadows may therefore, fifthly, be highly significant for reef island

morphological stability and development. At Green Island, the baffling effect of seagrass upon wave energy is thought to have interrupted reef-to-island sediment exchange and starved the island of sediment, which necessitated major engineering works (Hopley et al., 2007). In addition, Yamano et al. (2000) found a high proportion (~30%) of benthic foraminifera within Green Island's beach sands, which they attributed to long-term island evolution since the mid-Holocene and to a fall in sea-level. However, Hopley et al. (2007) suggest that the high proportions of foraminifera may be a recent addition to island sedimentology as a consequence of seagrass expansion. Indeed, Yamano et al. analysed surficial samples and, in the marine environment, high densities of foraminfera were found within the seagrass zones. Moreover, no mention of high foraminfera abundances was made in earlier work, hence there may have been a recent increase in concentrations (van Woesik, 1988; Hopley et al., 2007). However, despite the wide-ranging and significant implications of seagrass expansion within coral reef systems, there is a paucity of research investigating the impacts upon sediment productivity.

As a nation comprised of ~1,200 reef islands, seagrass expansion could be of major significance for the Maldives. However, knowledge of the archipelago's seagrass is largely limited to accounts from early expeditions, such as the 1964 International Indian Ocean Expedition (Hackett, 1977) and the 1960 Addu Atoll Expedition (Stoddart, 1966). Subsequently, 2 species have been documented within Baa atoll (*Syringodium isoetifolium, Thalassia hemprichii*; Payri et al., 2012), Laamu Atoll (*Thalassia hemprichii*, dominant species, and *Thalassodendron ciliatum*; Miller and Sluka, 1999a) and adjacent to Kuda Huraa resort (*Thalassia hemprichii, Syringodium isoetifolium*; Gillis, 2009). Furthermore, the Maldives is not included in the 17 countries monitored by Seagrass-Watch, nor in the 33 countries monitored by SeagrassNet, and to the best of the author's knowledge there is currently no monitoring programme operating within the country. More broadly, the tropical Indo-Pacific has been identified as the largest seagrass data gap despite their abundance and areal extent (Waycott et al., 2009).

There have been two suggestions within academic literature that seagrass distribution in the Maldives is linked to eutrophication. Firstly, an urbanisation-seagrass association was noted on Laamu Atoll and attributed to fishing waste over generational timescales (Miller and Sluka, 1999a, 1999b). Secondly, a note in Seagrass-Watch

magazine suggests eutrophication has caused an increase in seagrass areal extent at Kua Huraa resort, Male Atoll (Gillis, 2009). In addition, a technical paper of the 'Workshop on Integrated Reef Resources Management in the Maldives' (1997) comments, with reference to resort construction, that seagrass and algae are known to grow near effluent discharge sites as a result of eutrophication.

This Chapter seeks to provide a first step in improving knowledge of seagrass systems within the Maldives by addressing the following research questions:

1) What is the evidence that eutrophication is a control on seagrass distribution?
2) Has there been a recent increase in the areal extent of seagrass beds?
3) What impact may seagrass proliferation have upon the types, rates and volumes of sediment production?

Specifically, aims of this study are thus threefold: (1) to assess the degree of association between urbanised islands and seagrass beds; (2) to examine shifts in seagrass areal extent over the last decade (i.e. between 2006 and 2015); and (3) to investigate the implications of seagrass expansion for sediment production. While Chapters 4 and 5 investigated contemporary sediment storage and production, this Chapter thus examines the capacity of (potentially anthropogenically-induced) ecological shifts to cause changes in sediment dynamics.

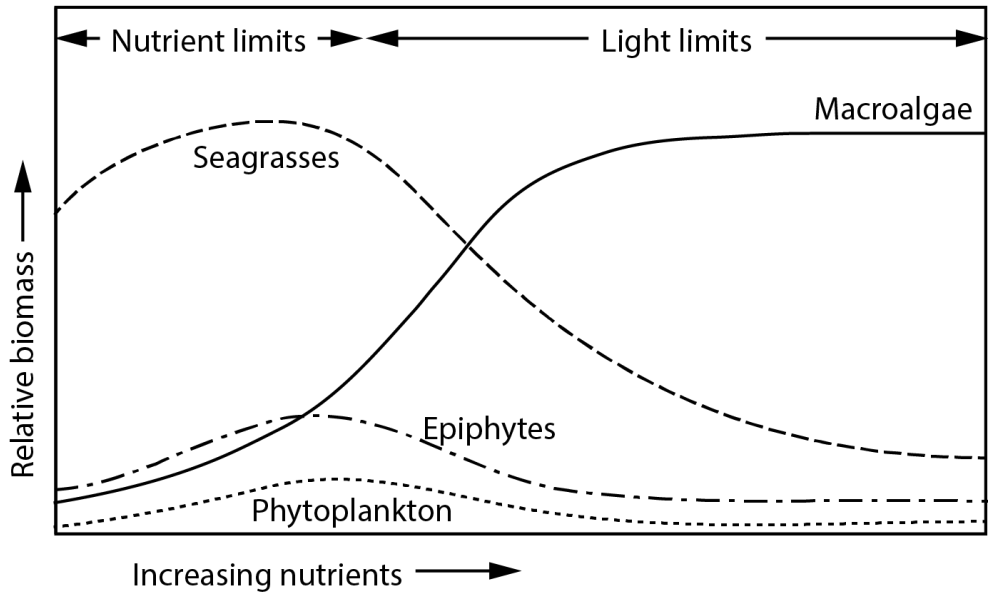

Figure 6.1 – The transition from nutrient- to light-limitation and the associated impacts upon seagrass and macroalgal biomass in shallow coastal marine ecosystems (adapted from Harlin, 1993; also in Burkholder et al., 2007)

6.2 Methodology

In order to address the three aims of the study, analyses were undertaken at three spatial scales: the archipelago-, atoll- and platform-scale.

6.2.1 Archipelago-scale: Seagrass-urbanisation association

To investigate the evidence that eutrophication is a control upon seagrass distribution, the association between anthropogenic activity (as a proxy for eutrophication) and seagrass presence was assessed. Counts of seagrass presence-absence were undertaken using Google Earth imagery for every reef platform in the Maldives with a vegetated reef island. Where seagrass presence-absence could not be identified with confidence, platforms were omitted from analysis (e.g. due to poor image resolution, cloud cover, or water glint). Reef platforms were categorised as those where island area occupied either < or > 75% of the reef platform. Reef platforms were then subcategorised as either:

(1) ‘inhabited’ if the platform was host to an inhabited island;

(2) ‘resort’ if there was a resort island on the platform, but no inhabited islands;

(3) ‘human influenced’ where a platform did not host an inhabited or resort island, but was occupied by an island that was evidently influenced by human activities, most frequently agriculture;
(4) ‘uninhabited’ if there was no observable human influence on the reef platform .

As an additional means of assessing the urbanisation-seagrass association, Google Earth imagery was also examined of the most populated Maldivian islands – i.e. those with a population above 5,000 (census data, maldives.gov.mv, 2006). Although Malé is the most populated island, it was not included as the entirety of the adjacent lagoon has been reclaimed. However, Hulamalé, to the northeast of Malé, (population = 2,866, 2006 census) was examined. The remaining five islands were Fuvahmulah (11,857; registered population figures for 2012 – planning.gov.mv/), Hithadhoo (Addu Atoll, 15,183), Thinadhoo (Huvadhu Atoll, 7,108), Naifaru (5,133), Feydhoo (Addu Atoll, 5,127).

6.2.2 Atoll-scale: Shifts in seagrass areal extent between 2006 and 2015, Huvadhu Atoll

In order to examine recent shifts seagrass areal extent, change detection analyses were undertaken using high resolution satellite imagery of 5 reef platforms with seagrass present on Huvadhu Atoll. Huvadhu Atoll was selected as it incorporates a range of reef platform morphologies that are comparable to those elsewhere in the Maldives. Platforms were selected to represent contrasting environmental settings: (i) a windward rim platform; (ii) a leeward platform; (iii) a second leeward platform was selected as it incorporated a geographical barrier (small channel); (iv) a resort platform; and (v) an atoll interior platform (Figure 6.2). Imagery was obtained for each platform from both 2006 and 2015 from either Quickbird-2, WorldView-2 or WorldView-3 satellites (Table 6.1). While ensuring minimal cloud cover, care was also taken to minimise seasonal influences (Roelfsema et al., 2015). Seagrass biomass may vary seasonally as it is primarily controlled by temperature and light (Larkum et al., 2006). The climate of the Maldives is dominated by two monsoon periods and thus image acquisition dates (5 were acquired in April and 2 in August – Table 6.1) and fieldwork (May-July 2013) were all within the *hulangu* monsoon, which occurs between April and November. Image pre-processing was undertaken to correct for the effects of scattering and absorption in the atmosphere. Water column correction was not

necessary given the shallow nature of the reef platforms (depths <1.5 m; Zhang et al., 2013). The imagery was pansharpened to a spatial resolution of 0.61 m, 0.46 m and 0.31 m for the Quickbird-2, WorldView-2 and WorldView-3 data respectively. The WorldView-2 and -3 images were then resampled to the same spatial resolution (0.61 m) as the Quickbird-2 imagery.

Unsupervised maximum likelihood classifications were performed within Erdas Imagine to assign pixels to the most likely class (Mather, 2004). It was not possible to obtain ground truth data from each of the reef platforms, however data were collected from one platform (the leeward platform host to Galamadhoo island; n = 216) and the classification of the dense seagrass zone on this platform was 100%. This is unsurprising given that seagrass is visibly and spectrally distinct from the adjacent benthic classes (sand, coral and rubble). This has been found in previous studies (e.g. Hochberg et al., 2003) and also in examination of the imagery employed in this study (Figure 6.3 – spectral data associated with the 2015 imagery of the southerly leeward rim platform was extracted from the ground truthed points and averaged).

Change detection analyses were undertaken to provide a detailed assessment of the differences on each platform between the 2006 and 2015 imagery. Classes were coded using successive powers of 2 to ensure all possible land cover transitions could be identified by a unique value, and the 2006 and 2015 classifications were then subtracted (using Raster Calculator within ArcMap) to quantify shifts in seagrass distribution.

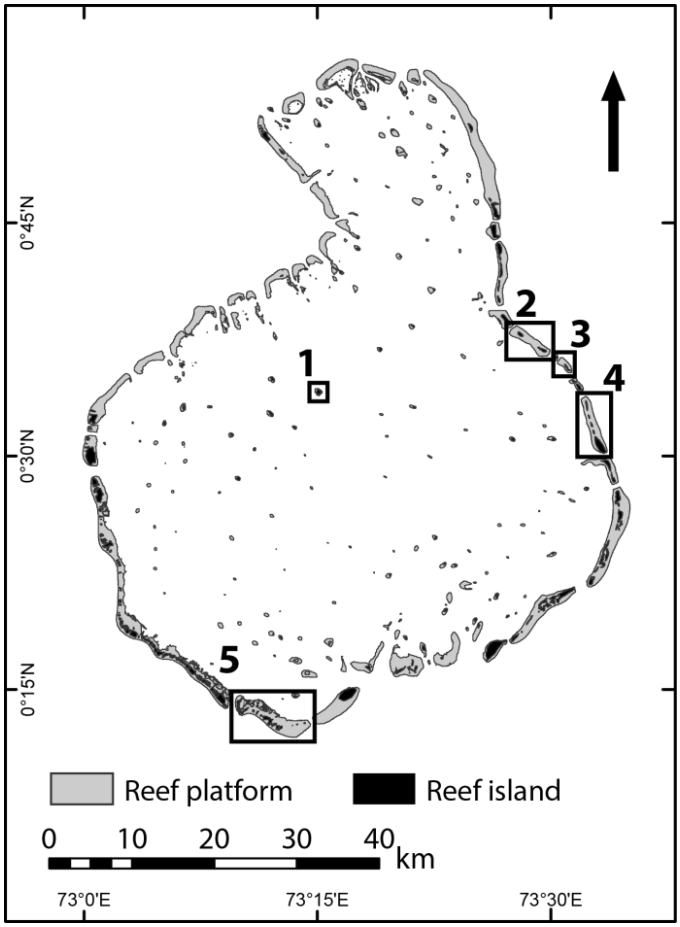

Figure 6.2 – Location of change detection reef platform sites: (1) inhabited interior; (2) northerly leeward platform incorporating a geographic barrier; (3) resort; (4) southerly leeward rim platform; and (5) windward rim.

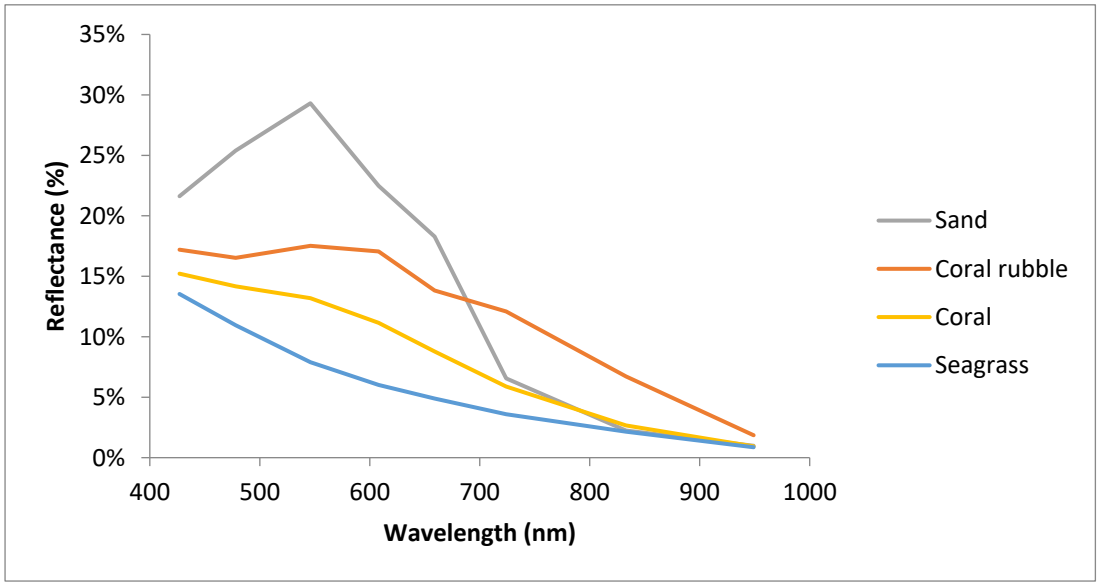

Figure 6.3 – Reflectance spectra of benthic cover types for wavelengths between 400 and 1000 nm., i.e. spectral signatures are notably distinct.

Site	Site no.s (from Figure 6.2)	Date	Satellite
Leeward rim	2, 3, 4	13/04/2006	QuickBird-2
Leeward rim	2, 3, 4	13/04/2015	WorldView-2
Leeward rim (northerly)	2	28/04/2015	WorldView-3
Interior	1	17/08/2006	QuickBird-2
Interior	1	13/04/2015	WorldView-2
Windward rim	5	04/08/2006	QuickBird-2
Windward rim	5	13/04/2015	WorldView-2

Table 6.1 – Sources of imagery and acquisition dates.

6.2.3 Platform-scale: Implications of seagrass expansion for sediment productivity

In order to examine epiphytic carbonate production and the impacts of seagrass presence upon benthic sedimentology, the marine environment off the oceanward coast of Galamadhoo was selected as a detailed study site as seagrass was most extensive within this area (of the sites surveyed for this thesis). The same survey stations and benthic datasets were employed as in Chapter 4 (left panels of Figures 4.2 and 4.3).

A reef platform is a meaningful spatial unit to examine the implications for sediment productivity as it represents an enclosed system. The leeward platform (Figure 6.2, site no. 4) was examined, though it ought to be borne in mind that this platform may not be representative of all Maldivian reef platforms. In particular, this is a rim platform and is thus likely to differ markedly from an interior platform in terms of water depth, incident wave energy and spatial extent. Nonetheless, this platform was selected due to the availability of ground truth data and also as its geomorphology is typical of leeward platforms toward the south of the Maldives archipelago (i.e. islands are orientated with their longest axes parallel to the reef crest and the platform comprises a section of a relatively continuous atoll rim).

6.2.3.1 Seagrass density and epiphytic calcium carbonate production

To assess epiphytic carbonate production on seagrass blades at each survey station (left panels of Figures 4.2 and 4.3), seagrass densities were calculated by placing a 50 x 50 cm quadrat 5 times along the transect at random. 10 mature blades (with browning tips – Nelsen and Ginsburg, 1986) were also collected from each station and epibiont calcium carbonate per blade was assessed using the weight loss on

acidification technique (n = 180; Nelsen and Ginsburg, 1986; Bosence, 1989; and Perry and Beavington-Penney, 2005). The degree of replication was thus comparable to other studies (e.g. Perry and Beavington-Penney, 2005). Each blade was rinsed in distilled water, dried, weighed, treated with 5% HCl to dissolve encrusters, re-dried and re-weighed. Natural weight loss (from unencrusted blades) averaged 39.9%. Epibiont calcium carbonate produced was calculated as

$$A - [B+(A \times C)]$$

where; *A* = the weight of the encrusted dry blades, *B* = the weight of the acid treated blades, *C* = the % weight loss from unencrusted blades treated with acid.

Annual epibiont production (g $CaCO_3$ m^{-2} $year^{-1}$) was then calculated for each survey site by multiplying epibiont production by blade density and crops per year. The average lifespan of a *Thalassia hemprichii* (the dominant seagrass species within the site) leaf is ~50 days (Stapel et al., 2001), which is calculated by multiplying the plastochrone interval (PI, i.e. the time interval between the onset of two consecutive leaves) by the number of leaves per shoot (Stapel et al., 2001). The PI of *T. hemprichii* has been found to be relatively consistent across the Indo-Pacific – 9.4 – 11.1 days in Papau New Guinea (Brouns, 1985), 9.9 ± 1.3 days and 10.1 ± 1.6 days, Indonesia (Stapel et al., 2001; Erftemeijer et al. 1993), and 10.9 ± 0.3 days in the Phillippines (Vermaat et al., 1995). The number of crops per year is thus ~7.3. In addition, the percentage coverage of composition on each blade was determined semi-quantitatively using the charts of Baccelle and Bosellini (1965) with the following categories: CCA, molluscs, foraminifera, serpulids and bryozoans.

6.2.3.2 Benthic Sedimentology

In order to examine benthic sedimentology, the same textural and compositional data as derived from sediment samples recovered the oceanward environment off Glamadhoo island were examined (i.e. data from Chapter 4). For a complete description of this methodology, refer to section 4.2.4.

6.2.3.3 Sediment productivity

The rates of sediment production associated with seagrass epiphytes were applied as estimated in Chapter 5. Rates were employed alongside change detection analysis data (section 6.2) in order to assess the implications of seagrass expansion for sediment production by seagrass epiphytes. The areal extent of each eco-geomorphic

zone in 2006 and 2015 was determined using the digital habitat classifications (generated for section 6.2). The areal extent (m^2) of each eco-geomorphic zone was then multiplied by the associated rates of sediment production associated with seagrass epiphytes (G, i.e. kg $CaCO_3$ m^{-2} yr^{-1}) to quantify sediment production in 2006 and 2015. The difference in sediment production per year was then calculated by subtracting these values.

While data were collected within the marine environment adjacent to Galamadhoo island, this is not an isolated system. Rather, the reef platform as a whole represents the enclosed system and is therefore a more meaningful spatial unit within which to examine the implications of seagrass expansion for sediment productivity. Using the change detection results for the platform (section 6.2), and the seagrass epiphyte sediment production rates derived in Chapter 3, the difference in sediment production between 2006 and 2015 was then calculated for the reef platform as a whole. It must be borne in mind that seagrass samples and density counts were only obtained from the marine environment off the oceanward coast of Galamadhoo and, likewise, census data was only obtained adjacent to Galamadhoo. Hence, in order to examine the platform-scale, an extrapolation has been made and thus results ought to be treated with some caution. Nonetheless, the platform is relatively small (6.9 km^2) and from personal observations in the field and of the satellite imagery, the eco-geomorphic zones are relatively homogeneous in their characteristics across the platform. This lends a reasonable degree of confidence to the approach, however the generated values of sediment production ought only to be treated as first order estimations.

6.3 Results

6.3.1 Archipelago-scale: Seagrass-urbanisation association

Seagrass was found on 55.9% (304) of the counted platforms (n = 539, i.e. platforms that supported a vegetated island with high quality, cloud-free Google Earth imagery; Table 6.2). Marked variability was found between seagrass presence-absence and the degree of anthropogenic activity. The greatest proportion of seagrass presence was found on urbanised reef platforms (85.7%), followed by resort platforms (71.3%) and ‘other’ human influenced platforms (52.5%, primarily industrial or agricultural; Table 6.2). Conversely, the lowest proportion of seagrass was found on uninhabited

platforms (28.4%). A chi-square test showed a highly significant association between whether a reef platform was inhabited or uninhabited and seagrass presence absence (χ^2 = 122.772, d.f. = 1, P = <0.0005). Anthropogenic activity, specifically urbanisation, is thus likely a key control upon seagrass distribution. Likewise, seagrass was found adjacent to all islands with populations >5,000 (Figure 6.4). Dense seagrass beds were found adjacent to all of the islands with the exception of Fuvahmulah island, which occupied >75% of its reef platform (Figure 6.4).

Seagrass was present on 64.5% of platforms where <75% was occupied by island area. Conversely, seagrass was present on 26.7% of platforms where island area accounted for >75% of the platform area (Table 6.2). A highly significant association was found between whether more or less than 75% of a reef platform was occupied by islands and seagrass presence-absence (χ^2 = 51.412, d.f. = 1, P = 7.5 x 10^{-13}). Hence, accommodation space likely represents an additional key control upon seagrass distribution. Seagrass was found on 99.2% (121 of 122) of urbanised platforms occupied by <75% island area. The one exception was Ukulas Island, North Ari Atoll, which is the first island in the Maldives to employ a systematic waste management scheme and was thus given the 2014 ‘Green Leaf Award’ by the Maldivian government (ukulhas.com).

Atoll	Seagrass Presence (P) / Absence (A)	Island occupies >75% of reef platform				Island occupies <75% of reef platform			
		Inhabited	Uninhabited	Other Human Influence	Resort	Inhabited	Uninhabited	Other Human Influence	Resort
Ihavandhippolhu	P	0	0	0	0	5	0	0	0
	A	0	1	0	0	0	5	0	1
Maamakunudhoo	P	0	0	0	0	1	0	0	0
	A	0	0	0	0	0	1	0	0
Thiladhunmathee	P	13	1	3	0	18	13	8	10
	A	17	20	11	1	0	7	5	2
Raa	P	4	0	0	0	7	18	1	2
	A	5	8	1	0	0	20	1	0
Baa	P	2	0	0	0	6	4	3	4
	A	1	11	1	0	0	15	1	5
Faadhippolhu	P	1	0	0	0	5	2	3	3
	A	0	1	0	0	0	6	1	1
Goidhoo	P	0	0	0	0	1	0	0	0
	A	0	0	0	0	0	0	0	0
Rasdhoo	P	0	0	0	0	1	0	0	1
	A	0	0	0	0	0	0	0	1
Thoddhoo	P	0	0	0	0	1	0	0	0
	A	0	0	0	0	0	0	0	0
Kaashidhoo	P	0	0	0	0	1	0	0	0
	A	0	0	0	0	0	0	0	0
Gaafaru	P	0	0	0	0	1	0	0	0
	A	0	0	0	0	0	0	0	0
North Male	P	1	0	0	2	7	0	1	6
	A	0	0	0	1	0	3	3	4
South Male	P	0	0	0	1	4	0	2	6
	A	0	0	0	0	0	0	0	1
Ari	P	1	0	0	0	13	3	2	20
	A	0	0	1	3	1	4	0	3
Felidhe	P	0	0	0	0	5	4	1	2
	A	0	0	0	0	0	2	0	1
Faafu	P	0	0	0	0	4	3	1	0
	A	0	0	0	0	0	5	1	1
Dhaalu	P	0	0	0	0	8	3	1	2
	A	0	1	0	0	0	8	1	0
Meemu	P	0	0	0	0	5	1	2	0
	A	0	0	0	0	0	1	0	0
Thaa	P	0	0	0	0	5	1	1	0
	A	0	0	1	0	0	5	0	0
Laamu	P	0	0	0	0	5	1	1	1
	A	0	0	0	0	0	1	0	0
Huvadhu	P	0	1	0	0	16	6	1	6
	A	0	0	0	0	0	31	0	2
Foammulha	P	1	0	0	0	0	0	0	0
	A	0	0	0	0	0	0	0	0
Addu	P	0	0	0	0	2	1	0	1
	A	0	0	0	0	0	0	0	0
Total	**P**	**23**	**2**	**3**	**3**	**121**	**60**	**28**	**64**
	A	**23**	**42**	**15**	**5**	**1**	**114**	**13**	**22**

Table 6.2 – Seagrass presence (P) – absence (A) counts of reef platforms grouped by Atoll, land use (uninhabited, inhabited, other human influence, resort), and accommodation space (where island occupy > or < 75% of the reef platform).

Figure 6.4 – The eight most populated areas in the Maldives (white bars = 1 km): (1) Hulamale (included instead of Male), (2) Fuvahmulah, (3) Hithadhoo, (4) Thinadhoo, (5) Naifaru, (6) Feydhoo, Addu Atoll.

6.3.2 Atoll-scale: Shifts in seagrass areal extent between 2006 and 2015, Huvadhu Atoll

An increase in seagrass areal extent was found between 2006 and 2015 on all five of the analysed reef platforms (Table 6.3, Figures 6.5-6.9). Variability was found in the degree of expansion with the greatest increase on the southerly leeward rim platform (240 ha, 72.3%; Table 6.3; Figure 6.8), and the smallest increase on the interior platform (1.1 ha, 6.6%; Table 6.3; Figure 6.5). Unsurprisingly, the majority of expansion occurred within lagoonal environments, rather than on reef crests. On the

rim platforms, a greater proportion of expansion occurred off the oceanward coasts of reef islands (Table 6.3).

In analysis of the northerly leeward platform (Table 6.3; Figure 6.6), an area of land has evidently been reclaimed off the western coast of the island (Figure 6.6). In the process, 0.55 ha of seagrass was removed, though this area of the image was excluded from the change detection analysis. This platform is particularly noteworthy as it incorporates a small-scale geographic barrier (channel labeled, Figure 6.6). In both 2006 and 2015, 96.5% of seagrass was distributed to the urbanised side of the channel. Moreover, of the 42 ha of seagrass expansion that occurred on the platform, 91.5% of expansion was found to the inhabited side of the barrier, while the remaining 8.5% occurred on the uninhabited side (Figure 6.6). Hence, this suggests that urbanisation is a key control upon seagrass distribution. The resort platform was also particularly notable as a stark seagrass-sand boundary is evident to the north of the island in the 2015 image. While an increase in seagrass areal extent was found (7 ha), it thus appears that seagrass was artificially removed from this area, which contained 1 ha of seagrass in 2006 (Figure 6.7).

It would be inappropriate to make generalisations from the five analysed platforms. However, observations were also made of the other reef platforms on Huvadhu Atoll where high resolution Google Earth imagery was available from both 2006 and 2015. Of the reef platforms were seagrass was present in 2015, an increase in seagrass areal extent since 2006 was found in all cases. This comprised 11 inhabited rim platforms, 4 uninhabited rim platforms, 1 agricultural rim platform and 1 resort interior platform.

Reef platform	Expansion (ha)	Expansion (%)	% Expansion within the lagoon	% Expansion on the reef crest	% Expansion off the lagoonward coast	% Expansion off the oceanward coast
1 - Interior	0.1 ha	6.60%	100.00%	0.00%	n/a	n/a
2 - Leeward rim (northerly, incorporating a barrier)	42 ha	37.60%	96.50%	3.50%	20.50%	79.50%
3 - Resort	7 ha	29.20%	93.90%	6.10%	39.80%	60.20%
4 - Leeward rim (southerly)	240 ha	72.30%	96.60%	3.40%	29.60%	70.40%
5 - Windward rim	159 ha	37.90%	99.60%	0.40%	36.40%	63.60%

Table 6.3 – Change in seagrass areal extent between 2006 and 2015 on 5 rim platforms within Huvadhu Atoll.

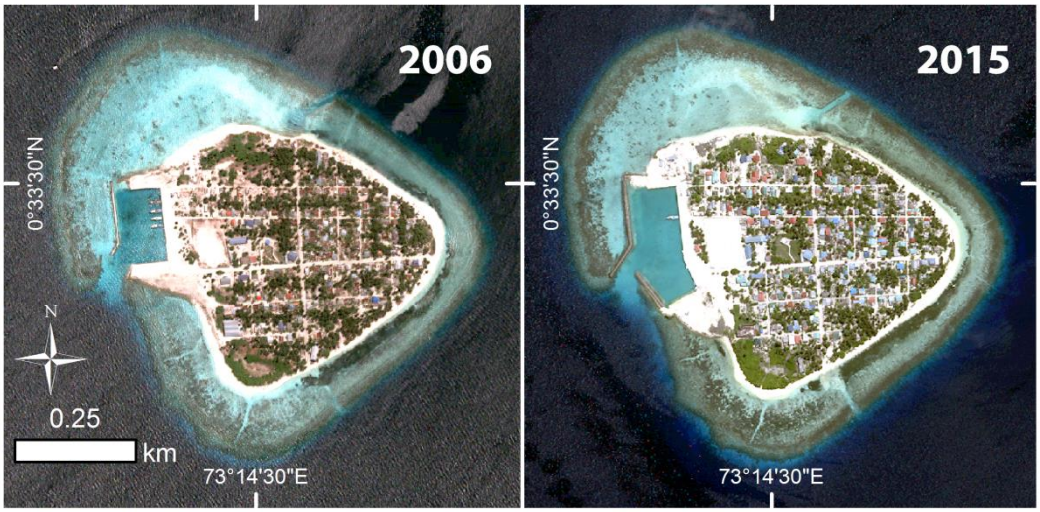

Figure 6.5 - 2006 (QuickBird-2) and 2015 (WorldView-2) imagery of the interior platform (Devvadhoo island); 6.6% (0.1 ha) increase in seagrass areal extent.

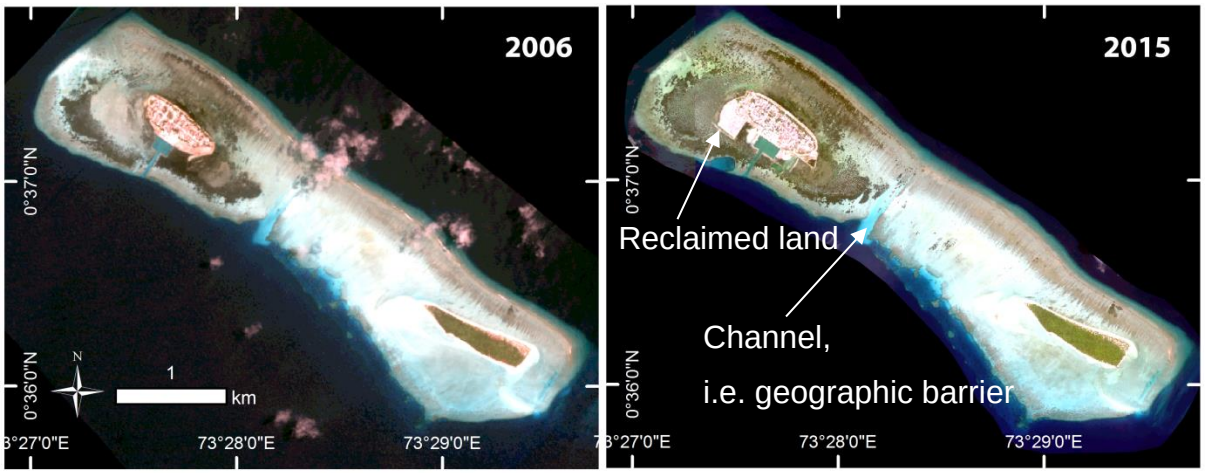

Figure 6.6 - 2006 (QuickBird-2) and 2015 (WorldView-2 and -3) imagery of the northerly leeward platform (left: Dhaandhoo island; right: Vodamulaa island); 37.6% (42 ha) increase in seagrass areal extent, 91.5% of which occurred within the inhabited side of the small channel (i.e. geographic barrier). Land has evidently been reclaimed off the island's western coast; this area was excluded from the change detection analysis.

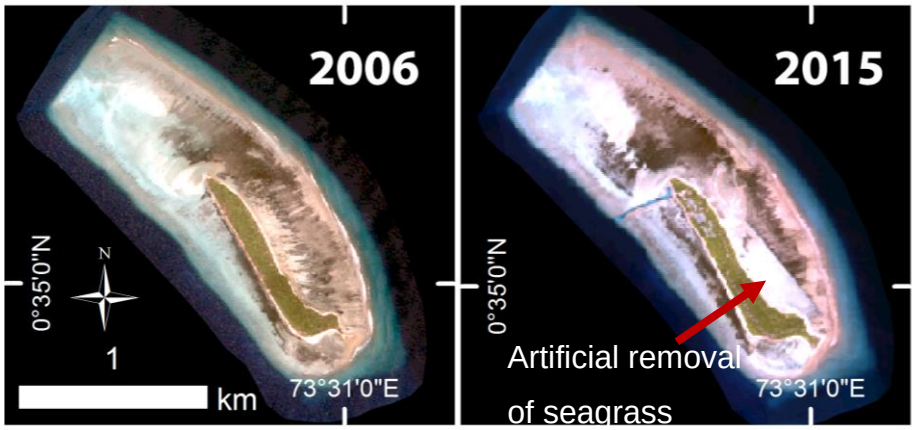

Figure 6.7 - 2006 (QuickBird-2) and 2015 (WorldView-2) imagery of the resort platform (Mahadhdhoo island); 29.2% (7 ha) increase in seagrass areal extent, 1 ha of seagrass appears to have been removed artificially.

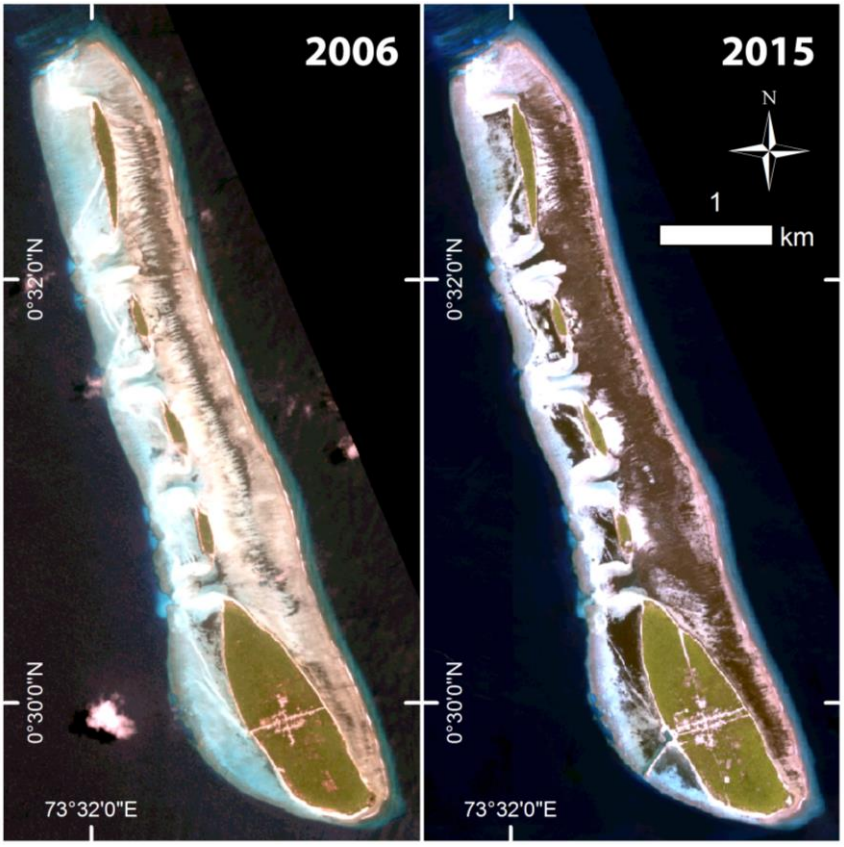

Figure 6.8 - 2006 (QuickBird-2) and 2015 (WorldView-2) imagery of the southerly leeward rim platform; 72.3% (240 ha) increase in seagrass areal extent.

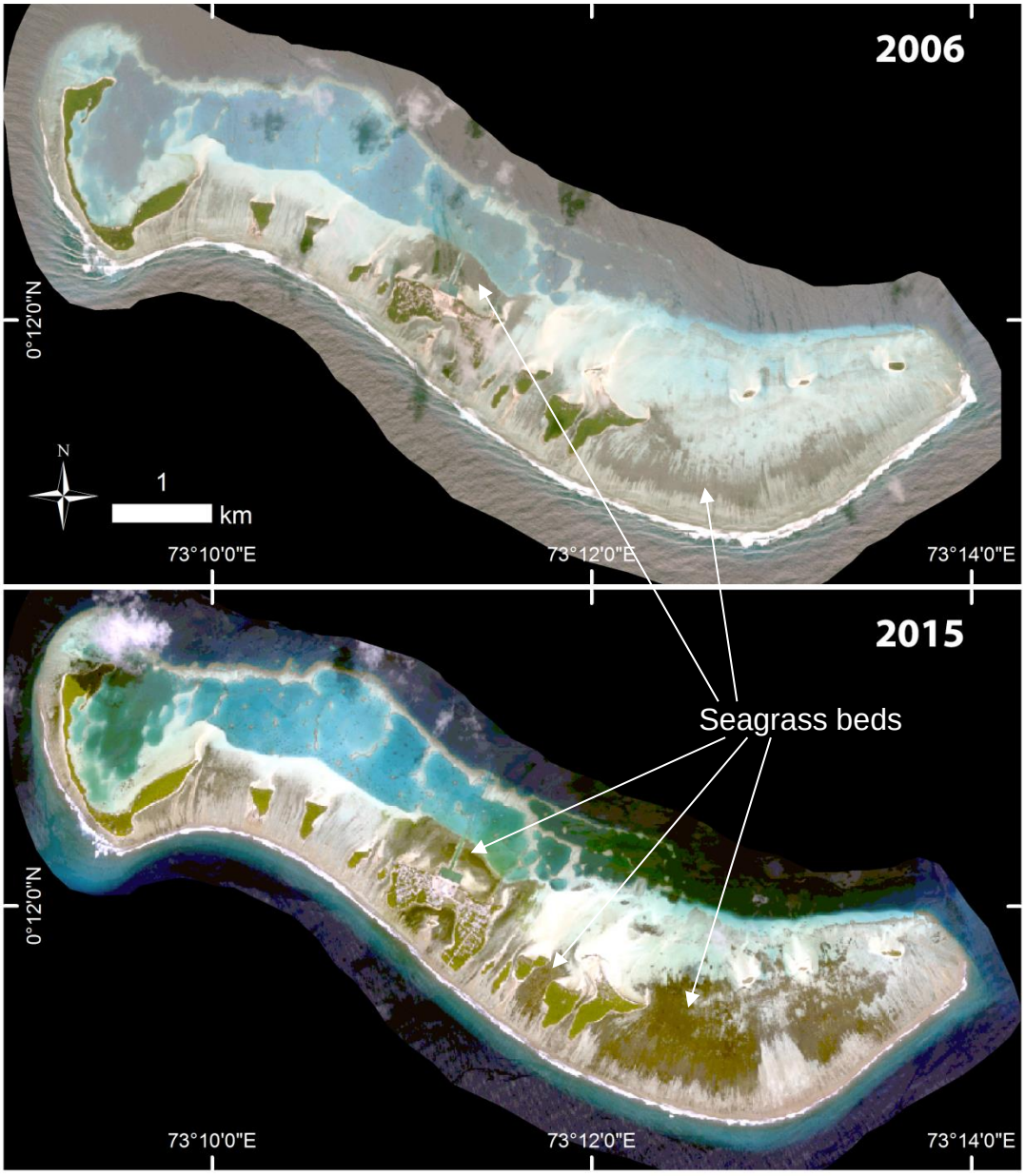

Figure 6.9 – 2006 (QuickBird-2) and 2015 (WorldView-2) imagery of the windward rim platform; 37.9% (159 ha) increase in seagrass areal extent.

6.3.3 Platform-scale: Implications of seagrass expansion for sediment productivity

6.3.3.1 Seagrass density and epiphytic calcium carbonate production

Seagrass beds were dominated by *Thallassia hemprichii* (Figure 6.10). Systematic variability in blade density was found between the eco-geomorphic zones (Table 6.4; Figure 6.11; refer to Chapter 4 for zonation descriptions). The greatest densities were in the dense seagrass zone (mean 1621 ± 163 blades m^{-2}), followed by the oceanward

sparser seagrass (1132 ± 157 blades m^{-2}), oceanward reef crest (557 ± 146 blades m^{-2}) and the oceanward sand (145 ± 85 blades m^{-2}) zones. In turn, spatial variability was thus found in estimations of epiphytic $CaCO_3$ production (Figure 6.12), whereby production rates were highest within the dense seagrass zone (108 ± 12 g $CaCO_3$ m^{-2} yr^{-1}) and lowest within the oceanward sand zone (15 ± 9 g $CaCO_3$ m^{-2} yr^{-1}). Unsurprisingly, a highly significant relationship was thus found between blade density and epibiont carbonate production (linear regression: $R^2 = 0.868$; $P = <0.0005$; Figure 6.13). Hence, blade density, rather than spatial variability in the degree of blade encrustation, is the primary control upon epibiont carbonate production.

Figure 6.10 – *Thallassia hemprichii* bed within the 'dense seagrass' zone off the oceanward coast of Galamadhoo island.

Zone	Sample	Mean blade density (m^{-2})	$CaCO_3$ production ($g\ m^{-2}\ yr^{-1}$)
DSG	NNT	1866 (±151)	136.8 (±45.7)
DSG	NT	1306 (±96)	134.9 (±38.8)
DSG	MT	2138 (±324)	192.7 (±66.7)
DSG	ST	1334 (±158)	126.7 (±42.0)
DSG	SST	1461 (±347)	165.2 (±73.7)
OSS	NNT	1452 (±225)	102.5 (±33.7)
OSS	NT	765 (±156)	63.6 (±24.2)
OSS	MT	1503 (±157)	178.1 (±42.1)
OSS	ST	1011 (±202)	82.2 (±26.3)
OSS	SST	933 (±140)	86.7 (±28.5)
ORC	NNT	471 (±168)	15.6 (±10.1)
ORC	NT	130 (±47)	5.8 (±3.7)
ORC	MT	440 (±66)	28.7 (±9.2)
ORC	ST	1086 (±398)	51.8 (±34.7)
ORC	SST	658 (±134)	33.0 (±14.9)
OS	NNT	21 (±5)	1.8 (±1.0)
OS	NT	342 (±73)	46.8 (±20.4)
OS	MT	362 (±76)	34.2 (±16.0)

Table 6.4 – Survey stations, blade densities and estimates of $CaCO_3$ production. Zones: DSG = dense seagrass, OSS = oceanward sparser seagrass, ORC = oceanward reef crest, and OS = oceanward sand.

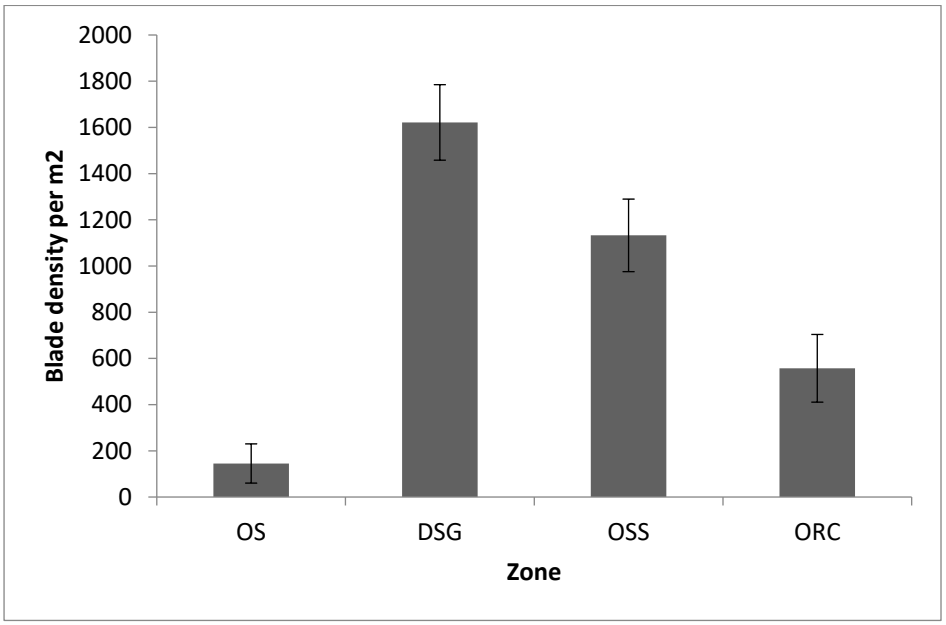

Figure 6.11 – Blade densities within each eco-geomorphic zone whereby OS = oceanward sand, DSG = dense seagrass, OSS = oceanward sparser seagrass, and ORC = oceanward reef crest.

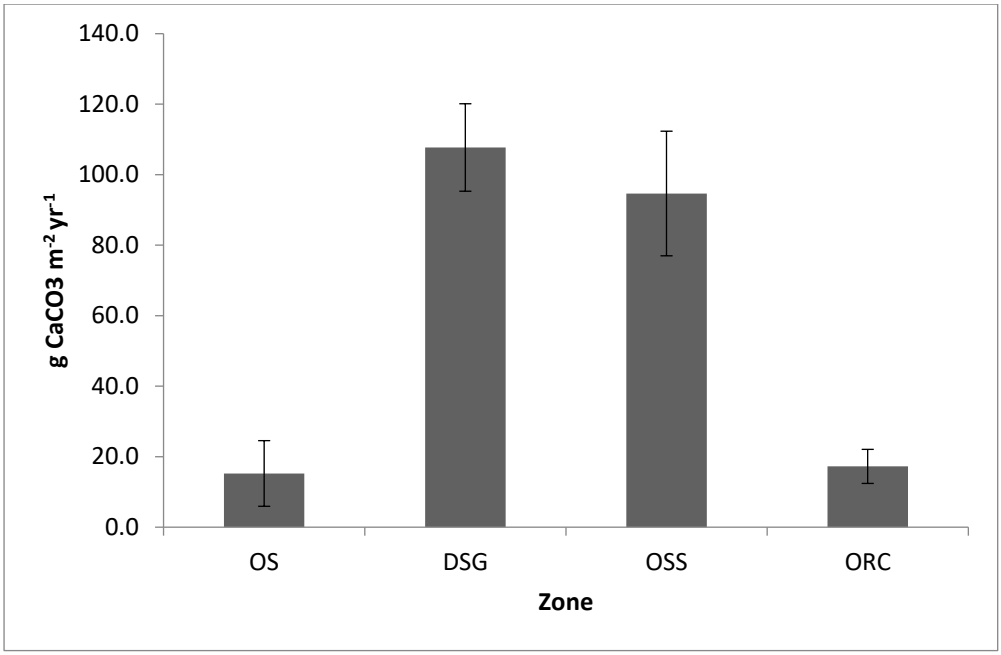

Figure 6.12 – Epiphytic $CaCO_3$ production within each eco-geomorphic zone whereby OS = oceanward sand, DSG = dense seagrass, OSS = oceanward sparser seagrass, and ORC = oceanward reef crest.

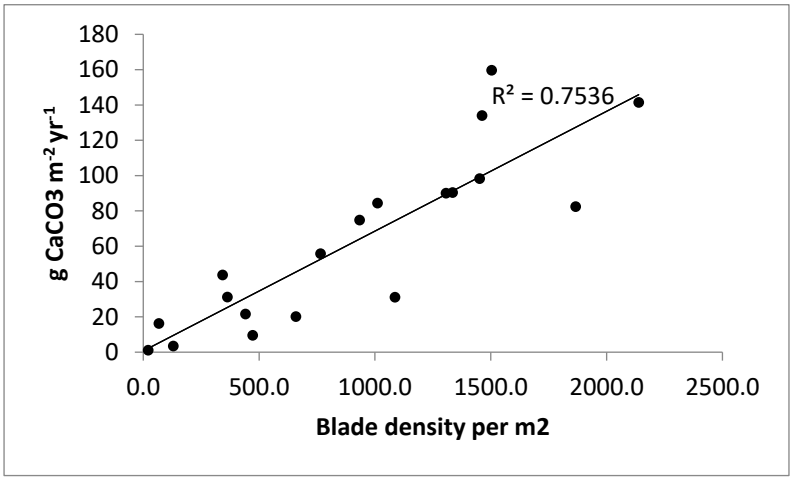

Figure 6.13 – Relationship between blade density and epiphytic $CaCO_3$ production.

The composition of epiphyte percentage cover was relatively consistent between eco-geomorphic zones. Composition was dominated by CCA (83 ± 2%), followed by bryozoans (11 ± 2%), serpulids (3 ± 1%), foraminifera (1 ± 0%), and gastropods (1 ± 0%; Figures 6.14-6.16). From examination of CCA both under the binocular microscope and in thin section, CCA typically formed thin (<75 μm) monostromatic layers (Figures 6.15 and 6.16).

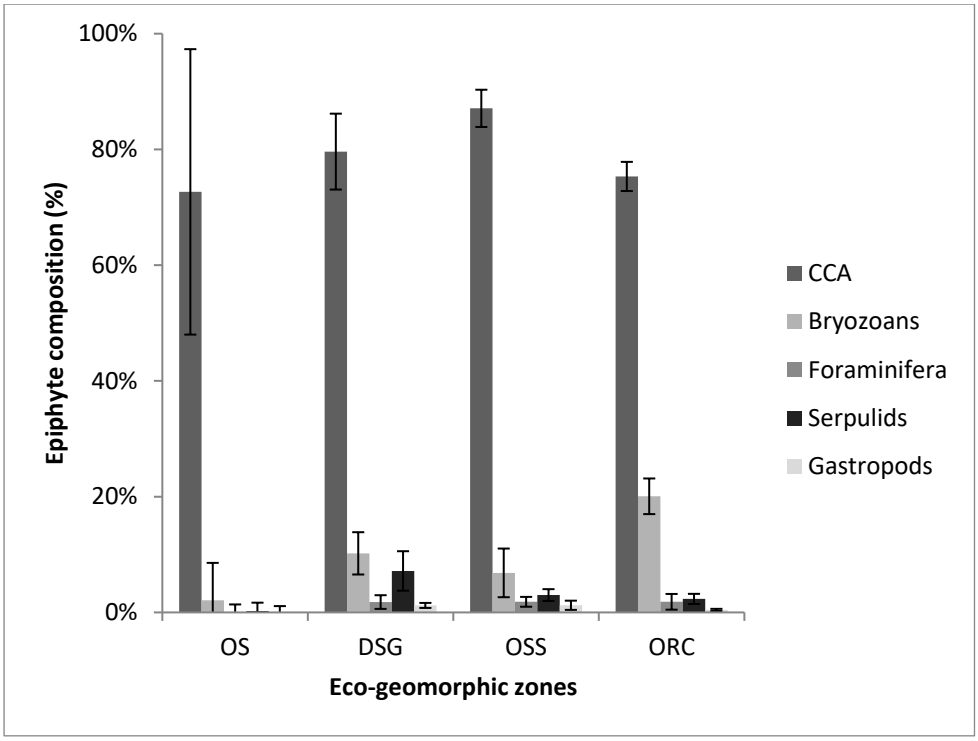

Figure 6.14 – Semi-quantitative assessments of seagrass epiphyte composition within each eco-geomorphic zone whereby OS = oceanward sand, DSG = dense seagrass, OSS = oceanward sparser seagrass, and ORC = oceanward reef crest.

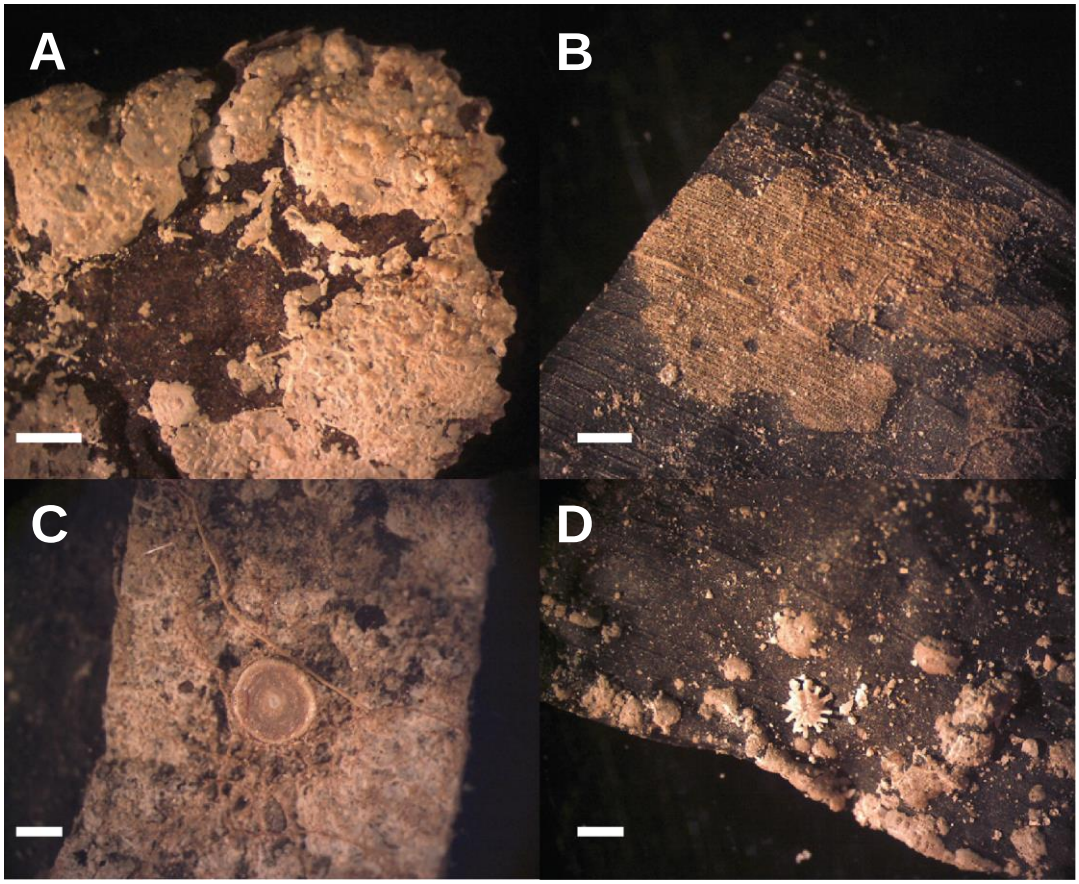

Figure 6.15 – Binocular microscope images of examples of typical seagrass epiphytes (white bar = 1 mm): CCA (A, C), serp ulids (A, C), bryozoans (B), and foraminifera (C - *Marginopora vertebralis*; D - *Calcarina spengleri*).

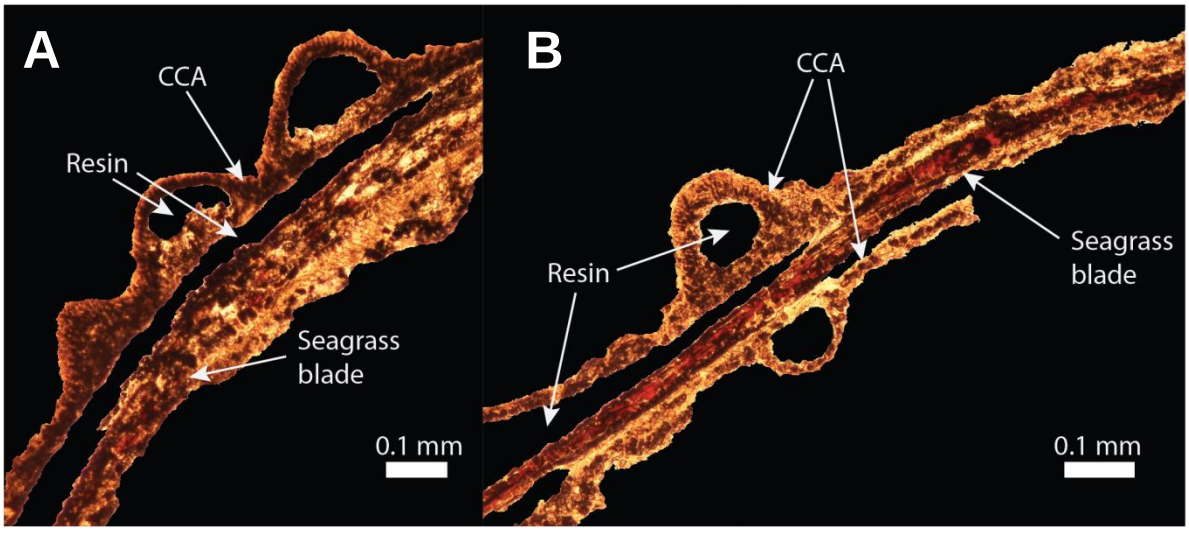

Figure 6.16 – Thin section images of cross-sections through blocks of dried seagrass blades embedded in resin. Thin (<75 μm) monostromatic layers of encrusting CCA are evident.

6.3.3.2 Benthic Sedimentology

All benthic sediment samples recovered off the oceanward coast of Galamadhoo island (n = 60) were analysed. Sediment texture was found to be relatively consistent between eco-gemorphic zones with a slight decrease in grain size with increased distance from the oceanward reef crest (as discussed in Chapter 4). Samples from the ocean reef crest zone were very coarse-grained (-0.2 ± 0.2 ϕ); dense seagrass and oceanward sparser seagrass zone samples were coarse-grained (0.8 ± 0.1 ϕ, 0.5 ± 0.1 ϕ respectively); and oceanward sand zone samples were medium-grained (1.2 ± 0.1 ϕ). The proportion of fine-grained sediment was negligible within all eco-geomorphic zones (mean values = <0.3%).

Compositionally, the samples were also relatively homogenous (Chapter 4). Coral was the dominant constituent (79.0 ± 1.1%, 71.4 ± 1.4%, 73.3 ± 1.3%, 72.2 ± 0.9% within the oceanward sand, dense seagrass, oceanward sparser seagrass and oceanward reef crest zones respectively), followed by CCA (8.5 ± 0.7%, 8.3 ± 0.5%, 9.8 ± 0.6%, 17.9 ± 1.0% respectively), and molluscs (9.1 ± 0.7%, 9.2 ± 0.6%, 7.3 ± 0.4%, 7.0 ± 0.7% respectively). However, slightly greater proportions of foraminifera were found within the seagrass zones (9.7 ± 1.5% and 10.5 ± 1.5% within the dense seagrass and oceanward sparser seagrass zones respectively, as oppose to 2.5 ± 0.4% and 1.2 ± 0.3% within the oceanward sand and oceanward reef crest zones; Figure 6.17). Moreover, in analysis of benthic sediment samples collected at the survey stations with seagrass present (n = 18), a significant relationship was found between epibiont carbonate production (g $CaCO_3$ $m^{-1}yr^{-1}$) and the percentage of foraminifera found within benthic sediment samples (linear regression: P = 0.0125, R^2 = 0.50; Figure 6.18).

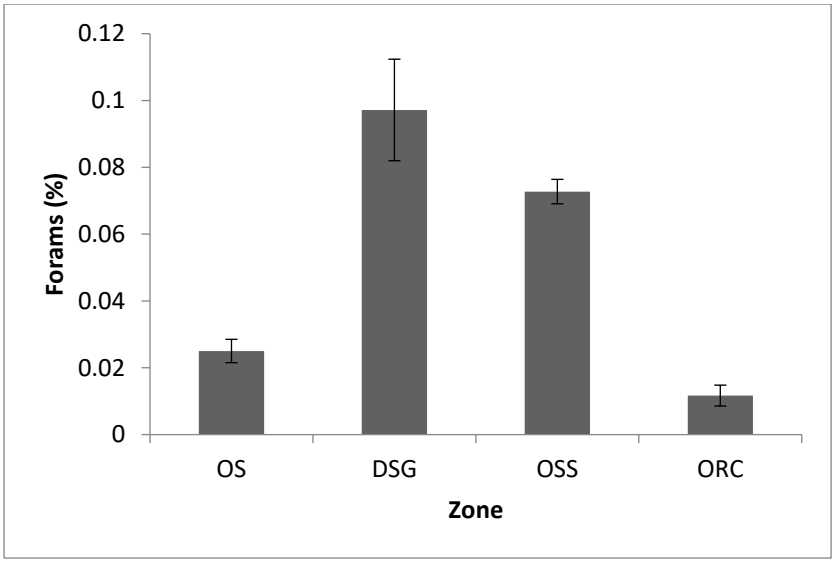

Figure 6.17 – Percentage of foraminifera found within benthic sediment from each eco-geomorphic zone whereby OS = oceanward sand, DSG = dense seagrass, OSS = oceanward sparser seagrass, and ORC = oceanward reef crest.

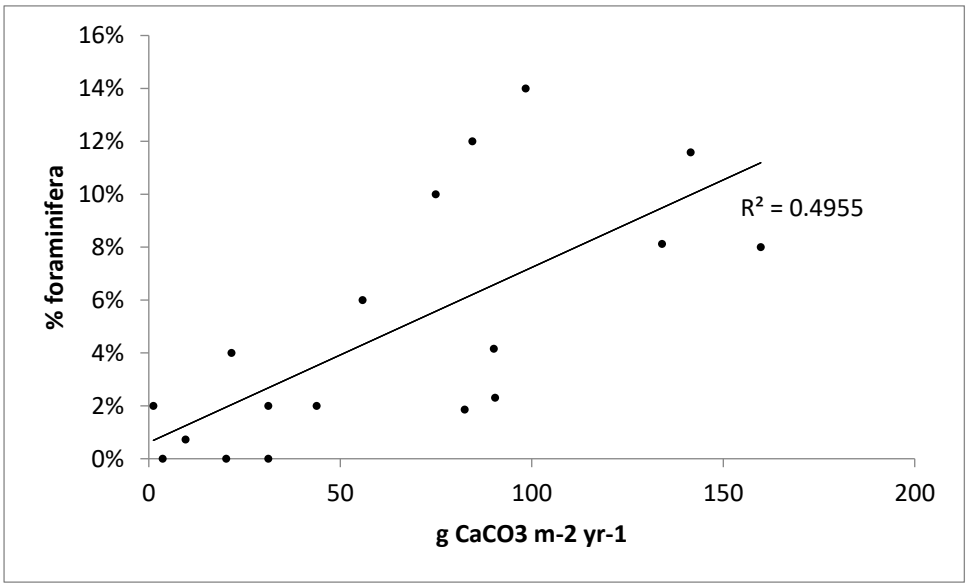

Figure 6.18 – Relationship between epibiont carbonate production (g $CaCO_3$ $m^{-1}yr^{-1}$) and the percentage of foraminifera found within benthic sediment samples.

6.3.3.3 Sediment Productivity

In order to examine the potential impact of seagrass proliferation upon sediment productivity, analysis was undertaken of the marine environment off the oceanward coast of Galamadhoo and, subsequently, extrapolations were made to the reef platform as a whole. Firstly, classifications were generated of the marine environment

off the oceanward coast of Galamadhoo island (Figure 6.19). The digital habitat maps were subtracted to generate a change matrix (Table 6.5). There was a substantial increase in the areal extent of the dense seagrass zone (20.6 ha, 46.0%). The expansion of dense seagrass into the oceanward sand zone accounted for the majority of this transition (18.1 ha), while the remainder of the expansion (4.2 ha) was into the oceanward sparser seagrass zone. Multiplying the areal extent of each eco-geomorphic zone by the associated seagrass epiphyte sediment generation rates (Table 5.2), sediment production by seagrass epiphytes was ~56,481 kg in 2006 and 80,431 kg in 2015 (Table 6.6). Hence, this suggests an increase in sediment production by seagrass epiphytes of ~24,000 kg yr^{-1}, i.e. ~24 tonne yr^{-1} (42%).

Secondly, analysis was extrapolated to the platform as a whole. The 2006 and 2015 classifications generated within Section 3.2 (Figure 6.20) were subtracted to generate a change matrix (Table 6.7). The greatest magnitude of land cover change found was from the oceanward sand zone to dense seagrass zone (89.5 ha). This was followed by the transitions to dense seagrass from the oceanward sparser seagrass (76.3 ha) and lagoonward patch (70.4 ha) zones. The areal extent of each eco-geomorphic zone was, again, multiplied by the corresponding seagrass sediment production rate (Table 5.2). Annual sediment production by seagrass epiphytes for the platform was thus estimated as 341,301 kg yr^{-1} in 2006 and 584,453 kg yr^{-1} in 2015 (Table 6.8). The difference between these values suggests a ~243,000 kg yr^{-1}, i.e. ~243 tonne yr^{-1}, (71%) increase in sediment production by seagrass epiphytes. The approximate volume of Galamadhoo island (derived from topographic and planform survey data, Chapter 3) was ~84,000 m^3 above the seafloor, which accumulated within a window of ~3,000 years. While island accumulation was likely at least partially episodic, an average long-term island accumulation rate of 28 $m^3\ yr^{-1}$ can be derived (i.e. 84,000 m^3 / 3,000 years). Taking 1840 kg m^{-3} as an approximate density of carbonate sand (Reid, 1998), the approximate mass of Galamadhoo island is 155 tonnes (i.e. 1840 kg m^{-3} x 84,000 m^3). The estimated additional sediment input attributable to seagrass expansion (i.e. ~243 tonne yr^{-1}) would be sufficient to produce this volume over approximately 0.64 years (i.e. 155 tonnes / 243 tonne yr^{-1}; 7 months and 3 weeks), hence the accumulation window may be significantly reduced. It must be borne in mind that this is a first order estimate, not all of the additional sediment would be of a suitable grade for island building, and a proportion of this would be lost due to dissolution and

off-rim transport. Nonetheless, this estimation does highlight the capacity for seagrass expansion to induce shifts in sediment production budgets.

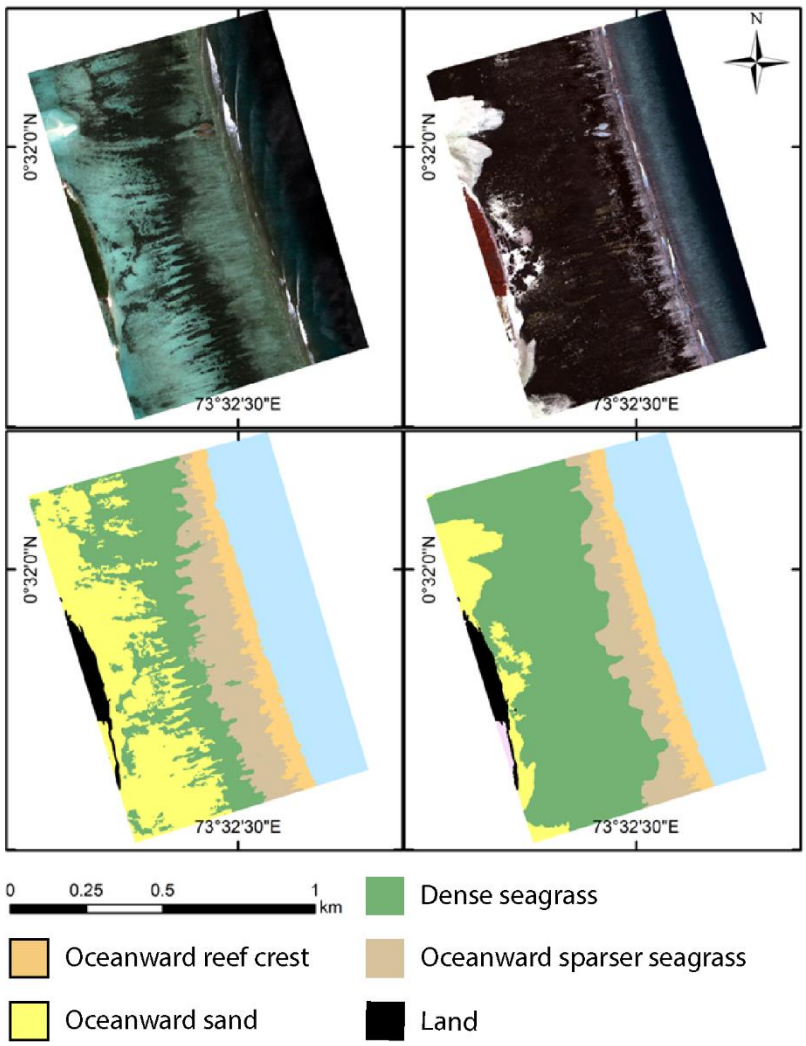

Figure 6.19 – Classifications of eco-geomorphic zones in the marine environment off the oceanward coast of Galamadhoo island generated from QuickBird-2 (2006) and WorldView-2 (2015) imagery.

		2006				
		OS	DSG	OSP	ORC	Total 2015:
2015	OS	6.4	1.0			7.5
	DSG	18.1	22.5	4.2		44.8
	OSS		0.7	9.0		9.7
	ORC				6.8	6.8
	Total 2006:	24.5	24.2	13.3	6.8	

Table 6.5 – Zonal change matrix (ha) derived by subtracting the 2006 and 2015 classifications of the marine environment off the oceanward coast of Galamadhoo (Figure 6.19).

	G	Area 2006 (m^2)	Area 2015 (m^2)	Sediment production 2006 (kg yr^{-1})	Sediment production 2015 (kg yr^{-1})
OS	0.02	245078	74552	4902	1491
DSG	0.15	241826	447980	36274	67197
OSS	0.1	132771	97145	13277	9714
ORC	0.03	67627	67627	2029	2029
			Totals:	56481	80431

Table 6.6 – Estimations of sediment production by seagrass epiphytes in 2006 and 2015 within the marine environment off the oceanward coast of Galamadhoo (Figure 6.19).

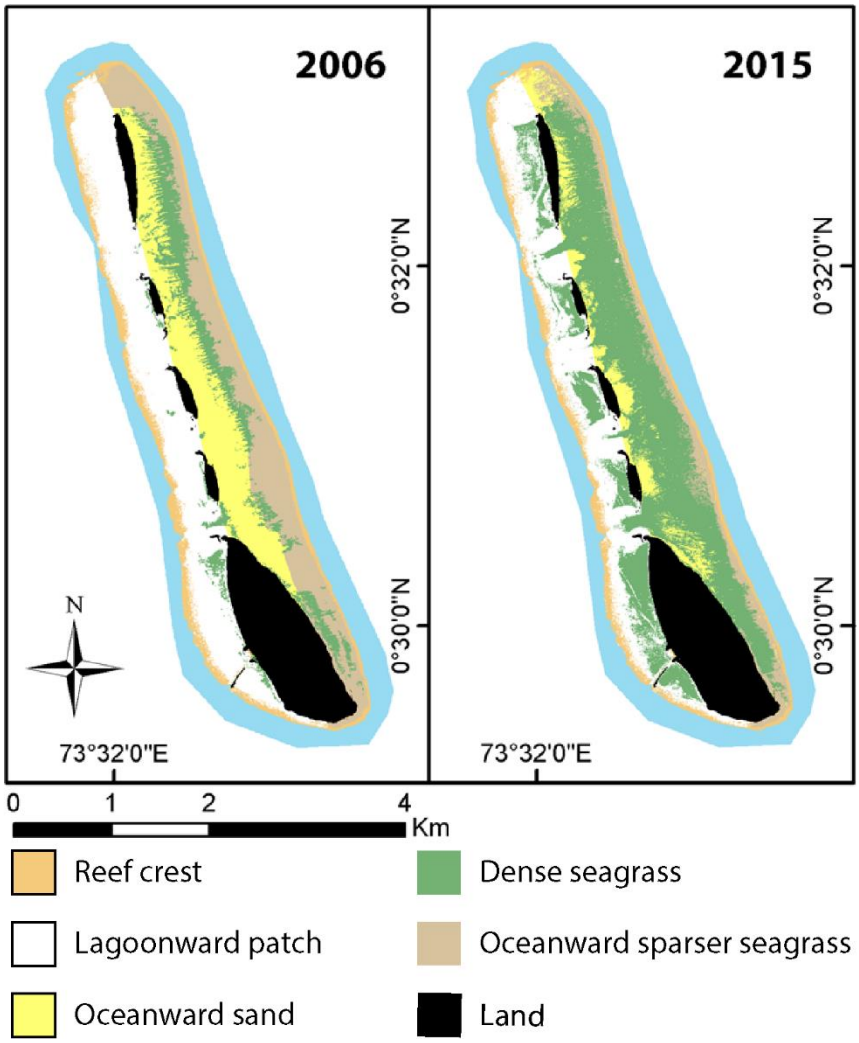

Figure 6.20 –Classifications of eco-geomorphic zones across the entirety of the leeward rim reef platform generated from QuickBird-2 (2006) and WorldView-2 (2015) imagery.

		2006						
		LRC	LP	OS	DSG	OSP	ORC	Total 2015:
2015	LRC	45.8						45.8
	LP		180.7		0.6			181.3
	OS			43.0	1.0	8.8		52.8
	DSG		70.4	89.5	86.8	76.3		323.0
	OSS				1.4	61.9		63.3
	ORC						26.4	26.4
	Total 2006:	45.8	251.1	132.5	89.8	147.0	26.4	

Table 6.7 – Zonal change matric (ha) derived by subtracting the 2006 and 2015 classifications of the leeward rim reef platform (Figure 6.20).

Zone	G	Area 2006 (m^2)	Area 2015 (m^2)	Sediment production 2006 (kg yr^{-1})	Sediment production 2015 (kg yr^{-1})
LRC	0	457549	457549	0	0
LP	0.01	2511811	1813552	25118	18136
OS	0.02	1325225	528572	26505	10571
DSG	0.15	898432	3229975	134765	484496
OSS	0.1	1469894	633263	146989	63326
ORC	0.03	264140	264140	7924	7924
			Totals:	341301	584454

Table 6.8 – Estimations of sediment production by seagrass epiphytes in 2006 and 2015 on the leeward rim reef platform (Figure 6.20).

6.4 Discussion

Through employing counts of seagrass presence-absence, change detection analyses, and field data from a case study site, this Chapter provides a first step in the study of seagrass systems within the Maldives. Specifically, the controls upon seagrass distribution, recent shifts in seagrass areal extent and the implications of seagrass expansion for sediment productivity have been examined at three spatial scales (archipelago, atoll and reef platform).

6.4.1 Archipelago-scale: Seagrass-urbanisation association

Despite the lack of existing knowledge of seagrass systems in the Maldives and also the absence of any monitoring programme, seagrass was found to be relatively widespread across the archipelago (present on all atolls and 56% of the counted reef platforms). The presence-absence counts highlight two likely key controls upon seagrass distribution: (1) anthropogenic activity, and (2) the proportion of the platform occupied by a reef island. Firstly, the proportion of platforms with seagrass presence was consistent with the degree of anthropogenic activity: the greatest proportion of seagrass presence was found on urbanised reef platforms (86%), followed by resort platforms (71%), platforms with ‘other human influence’ (53%, primarily agricultural and industrial), and finally uninhabited platforms (28%). Anthropogenic activity, as a result of eutrophication, may therefore be inferred as a likely control upon seagrass distribution in the Maldives.

The highest proportion of seagrass presence was found associated with urbanised reef islands, which are correspondingly associated with the largest degree of

anthropogenic activity. Sewage and household waste (including food, detergents and nappies) represent key sources of nitrogen (N) and phosphorous (P) on urbanised islands. With regard to sewage, 38.2% of toilets within the Maldives are connected to the sea and 50.3% are connected to septic tanks (Ministry of Environment and Energy, 2011). While toilets that are connected to the sea inherently represent an input of nutrients to the marine environment, septic tanks are also a cause for concern. Septic tanks typically comprise a small scale pre-sedimentation tank and soak pits from which sewage may migrate freely to contaminate groundwater and, in turn, the marine environment. Moreover, they often malfunction due to their poorly construction and maintenance, which is a result of the scarcity of both materials and skilled labour (Ministry of Environment and Energy, 2011). Other septic systems are connected to small-bore sea outfalls, which also frequently malfunction resulting in the direct input of raw sewage into the marine environment (Ministry of Environment and Energy, 2011). The disposal of the stools of young children represent a further issue as the 2001 census data found in the majority of cases the stool was thrown onto the beach (39.1%) or buried in the yard (23.1%; Ministry of Environment and Energy, 2011). Hence, it is likely that sewage represents a significant source of nitrogen and phosphorous into the marine environment.

Traditionally, household waste only consisted of fish bones and so its deposition in the ocean did not pose such a significant issue. However, this practice has continued despite a radical shift in lifestyle, in particular, the introduction of nappies (Aslam, pers. comm., 2013). There is no national-level waste management system as the distribution of the population over 198 islands renders the transportation of waste logistically problematic and prohibitively expensive. Individual island communities have therefore developed their own methods to address the issue. According to the 2006 census data, 74% of households used a garbage compound to dispose of waste, 10% burned their waste, 10% threw it in the bushes, and 7% in the ocean (maldives.gov.mv, 2006). However, even at garbage compounds there is no systematic sorting, segregation or recycling of waste of waste, and nor is there any system for dealing with hazardous waste, including Persistent Organic Pollutants (POPs; UNDP, 2014), asbestos, fertilisers, pesticides, healthcare waste and oil/fuel (IMF, 2008). Given the porous nature of carbonate islands and the lack of appropriate methods of waste disposal, ground water is susceptible to contamination and pollution

(UNDP, 2014). Indeed, on 162 of the nation's 198 inhabited islands, groundwater has been rendered unsuitable for drinking (UNDP, 2014). In turn, it is highly likely that the marine environment is a subsequent recipient of such pollutants. Indeed, on 90% of islands, garbage compounds are located within 100 m of the oceanward coastline (NAPA, 2006). Moreover, such issues are of particular pertinence given that they are superimposed upon a rapidly increasing population – from ~273,000 in 2005 to ~345,000 in 2013 (World Bank, 2015).

Resort platforms are also subject to a high degree of anthropogenic activity and the relatively high proportion of seagrass presence on such platforms may thus be expected. Indeed, they are continuously inhabited and thus generate substantial volumes of wastewater (an estimated 1,904,000 m^3 annually – Tourism Adaptation Project, 2015). Nonetheless, the degree of anthropogenic activity associated with resort platforms may be considered secondary in comparison to that associated with urbanised platforms. Hence, the proportion of resort platforms with seagrass presence was slightly lower than that associated with urbanised platforms (71.3% and 85.7% on resort and urbanised platforms respectively). This reduced presence may be because, firstly, the number of people on a resort island is significantly lower than on an inhabited island. The average resort capacity in 2014 was 70 people whilst the average number of staff per resort was ~50 (Ministry of Tourism, 2014), however, the average population of an inhabited island (excluding Male) in 2014 was ~950. Hence, volumes of sewage production will be correspondingly lower than on urbanised islands. Secondly, resort islands are provided with guidelines for appropriate waste disposal systems, which the government recommends specifically to avoid seagrass expansion (Hassan, 2005). The most pertinent of the regulations are those on the 'Protection and Conservation of the Environment in the Tourism Industry' which were passed in 2006 and specify that sewage must be disposed of in a manner that is 'least harmful' to the environment (Ministry and Environment and Energy, 2011). However, this document has been criticised for comprising a 'list of recommendations rather than of strict regulations' (p. 16, Tourism Adaptation Project, 2015). Unfortunately, data concerning resort waste disposal, to the best of the author's knowledge, is not available, though it is likely to be less environmentally damaging that the practices on urbanised islands so as not to impinge upon customer satisfaction. Thirdly, resorts may routinely remove seagrass beds as the governmental guidelines state the

‘presence of seagrass can affect the quality of the product provided’ (Hassan, 2005, p. 44). This is given that marketing materials are centred on white sandy beaches and thus the Maldivian government guidelines recommend smothering as a method of seagrass removal (Hassan, 2005; Gillis, 2009). Indeed, this is evident in the imagery of Mahadhdhoo island (a proposed resort; Figure 6.7) where the stark seagrass-sand boundary suggests that artificial seagrass removal has occurred.

Following resorts, islands with a form of ‘other’ human influence were associated with the next largest proportion of seagrass presence. Such islands could be considered to be subject to less anthropogenic activity than urbanised and resort platforms given the absence of continuous population pressures. Nonetheless, the majority of such islands were agricultural and thus relatively high proportions of seagrass presence may be, at least in part, a consequence of nutrient input from agricultural runoff, a significant source of both N and P. Fertilisers and pesticides are likely key to allowing crop growth given the high carbonate content of the upper organically enriched horizon (refer to Chapter 3). According to FAO data, the consumption of nitrate and phosphate fertilisers has increased dramatically between 2002 and 2013 – from 9 tonnes (t) to 264 t of nitrates, and 5 t to 262 t of phosphates (FAO, 2015). Given the highly porous nature of carbonate islands, use of fertilisers and pesticides may relatively rapidly translate into the input of nutrients to the marine environment.

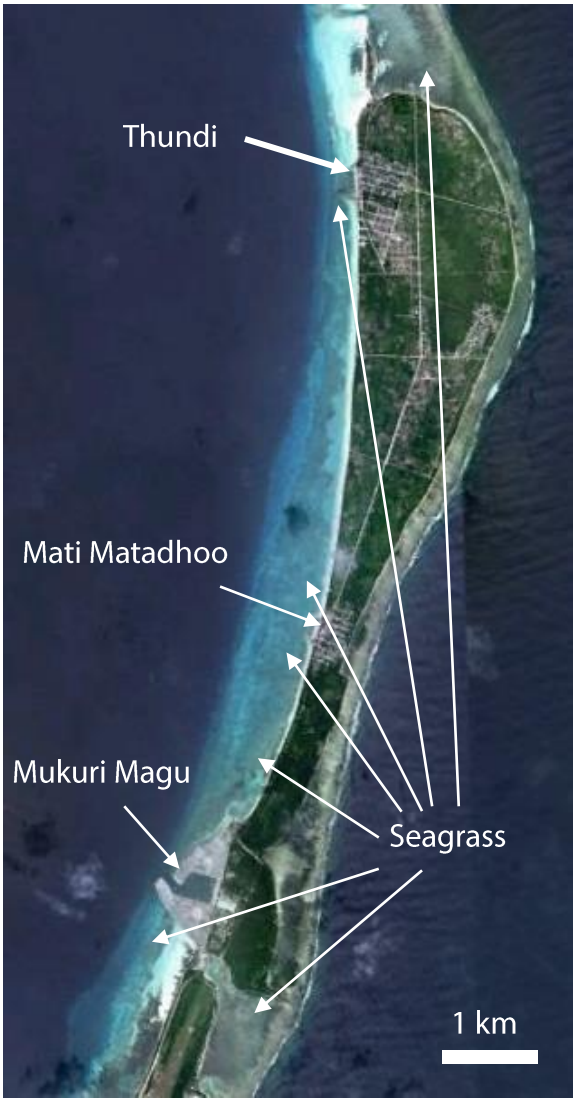

Figure 6.21 – Dense seagrass beds are evident in Google Earth (2015) imagery adjacent to the non-fishing village sites of Miller and Sluka's (1999a) study, Laamu Atoll.

The association between seagrass presence and the degree of anthropogenic activity may reflect that associated nutrient pollution is a key control upon seagrass distribution in the Maldives. Although it is not possible to infer causation from association or correlation, further supportive evidence could be gained from a comprehensive analysis of the nutrient content of seawater and sediment samples from sites with differing abundances of seagrass. Miller and Sluka's (1999a) analyses of the nutrient content of sediment samples from Laamu Atoll lend confidence to the notion that eutrophication is related to seagrass proliferation. 10 lagoonal sites were examined within Laamu Atoll – 3 fishing villages, 3 non-fishing villages and 4 uninhabited islands. Sediment samples from sites with seagrass presence were found to be significantly

enriched with phosphorus. Miller and Sluka attributed both seagrass distribution and sediment nutrient content to the chronic input of organic fishing waste. However, it may be that fishing waste represents one of multiple sources of nutrient inputs. Indeed, dense seagrass beds are now evident in Google Earth imagery (2002 and 2014) adjacent to Miller and Sluka's 'non-fishing village' sites (Figure 6.21). Such rapid rates of seagrass expansion over the last decade contrast with Miller and Sluka's (1999a) suggestions that seagrass proliferation as a result of nutrient loading occurs over generational timescales.

While the presence-absence count results suggest that seagrass distribution is at least partially controlled by nutrient loading associated with anthropogenic activity, this is not the sole control upon Maldivian seagrass distribution. Rather, seagrass distribution is a function of a myriad of controls (Greve and Binzer, 2004) and the presence-absence counts also suggest that the proportion of a platform occupied by land may represent an additional control. Where >75% of the reef platform is occupied by land, seagrass presence appears less likely (present on 26% of platforms). This may be attributable to two factors, firstly, where >75% of the reef platform is occupied by land, a larger proportion of the marine environment may comprise coral, reef framework and consolidated reef pavements as oppose to the sandy substrates which seagrasses favour (Greve and Binzer, 2004). Secondly, where a reef island occupies a larger proportion of the platform area, water flushing time is likely reduced and nutrient concentrations would therefore decrease more rapidly. Hence, substrate availability and flushing time, as a function of the proportion of a platform area occupied by land area, are likely additional controls upon seagrass distribution in the Maldives. Although presence-absence count results indicate that seagrass is most likely to be associated with rim platforms (present on 66% of platforms) than interior platforms (41%), this is likely a function of both urbanisation and substrate availability. This is given the concentration of the majority of anthropogenic activity on atoll rims (88.93% of the population). In addition, interior islands appear to more frequently almost entirely fill their reef platforms (likely as interior platforms are smaller than rim platforms) and thus, as discussed, appropriate substrates for seagrass colonisation may be more limited and flushing times reduced.

In combination, urbanisation and the proportion of a platform occupied by land area, appear to be key controls on seagrass distribution. Indeed, of the 122 urbanised

platforms upon which land occupies under 75% of the platform area, seagrass was present on all except one cases. The one exception was Ukulas Island, North Ari Atoll, which is the first island in the Maldives to employ a systematic waste management system, which was established in November 2011 having been facilitated by a UNDP grant. Household waste is segregated into recyclables, organic material, and waste to be burnt. In particular, organic waste is composted to produce fertiliser, which is both used by the island community and also sold on neighbouring islands. The island has the capacity to manage hazardous wastes and is a one of the first not to use a landfill site. The community also host 'clean up' events and several waste management awareness programs each year. Ukulhas was thus gained the 'Green Leaf Award' from the Maldivian government in 2014 (ukulhas.com; 2015).

Presence-absence counts preclude any information concerning the density or extensiveness of seagrass beds. However, as a means of illustration, the marine environments adjacent to the most populated islands within the archipelago were examined (where population >5,000). Dense seagrass beds were found adjacent to all except one of the most populated reef islands, which provides further suggestion for the relationship between urbanisation, and likely eutrophication, and seagrass distribution. The exception was Fuvahmulah island as although seagrass was present in the lagoon, seagrass beds were less extensive. Given that the island also fills almost the entirety of the reef platform (>75%), this is likely a result of the limited suitable substrate availability and shorter flushing times. Flushing times are likely particularly short on Fuvahmulah's platform as it is exposed to oceanward swell wave energies around the entirety of the platform perimeter.

6.4.2 Atoll-scale: Shifts in seagrass areal extent between 2006 and 2015, Huvadhu Atoll

Expansion in seagrass areal extent was found to have occurred on all five reef platforms over the last decade in contrasting environmental settings within Huvadhu Atoll. Variability in the proportion and areal extent of the expansion was found with the greatest expansion on rim platforms (72.3%, 37.6%, 29.2%, 37.9%), while the least expansion occurred on the interior platform (6.6%). This corroborates with results of the presence-absence counts as island area occupied a smaller percentage of the analysed rim platforms than the interior platform. Hence, as discussed, the proportion

of a platform area occupied by land area is a likely control upon seagrass distribution in the Maldives due to substrate availability and flushing time.

The role of urbanisation as a potential control upon seagrass distribution was also highlighted. In particular, the northern leeward rim platform (Figure 6.6) was selected as there is a small-scale geographic barrier afforded by a channel toward the centre of the platform at either side of which is an inhabited and uninhabited island. Seagrass distribution (96.5%) and expansion (91.5%) both occurred almost entirely on the urbanised side of the channel (Figure 6.6). Hence, while a multitude of parameters control seagrass distribution, this highlights the likely association between anthropogenic activity and both seagrass distribution and expansion.

The change detection analyses also highlighted the issue that seagrass presence and expansion poses to the tourist industry. In analysis of the resort platform, a section of seagrass has evidently been removed as a part its construction (Figure 6.7). Nonetheless, there has still been an increase in the areal extent of seagrass beds on the platform. As discussed, seagrass presence and expansion poses a threat to the tourist industry as it is regarded as an aesthetic deterrent by both tourists (Tripadvisor, 2013) and the government (Hassan, 2005). In addition to the direct aesthetic issues, alterations to seagrass extent could have indirect implications, for example for the distribution of turtles – a major tourist attraction – as they graze on seagrass beds. Given that the industry generates ~20% of the nation's GDP, this is of great significance for the Maldivian economy. On a larger scale, seagrass expansion is somewhat mirrored in the Caribbean where the economies of tourist-dependant nations are presently threatened by the sudden beaching of banks of seaweed which have been linked to eutrophication (Smetacek and Zingore, 2013).

Unsurprisingly, seagrass expansion was primarily found within lagoonal environments, rather than on reef crests. In some instances, particularly at the windward site, imagery captured waves beaking around the platform perimeters, which may have obscured the classification of additional seagrass on the reef crest. Nonetheless, the predominance of lagoonal expansion is unsurprising given their sandy substrates, which seagrass favours, and the far greater spatial extent of lagoonal areas. Lagoonal environments in the Maldives host coral patch reefs (e.g. Chapter 4) and it is unclear whether seagrass may have any detrimental impacts upon coral (Miller and Sluka,

1999b). In addition, the majority of expansion occurred on the oceanward side of reef platforms, which is partially due to the greater areal extent of the oceanward areas. This may also be a function of light availability as the oceanward marine environments are shallower than the lagoonward areas.

While it would be inappropriate to make generalisations from the five platforms, observations were made of Google Earth imagery of Huvadhu Atoll from 2006 and 2015. Of the 17 platforms with seagrass presence and available imagery, seagrass areal extent was noted to have increased in all cases. In addition to 11 inhabited platforms, this comprised 4 uninhabited platforms and thus while presence-absence counts found seagrass presence less likely on uninhabited platforms, seagrass expansion may be equally likely regardless of anthropogenic activity. This may reflect the fact that seagrass growth is a function of a myriad of controls of which anthropogenic activity, and associated nutrient input, is just one. For example, a further control upon seagrass expansion could be platform infilling as a sequence of platform-scale 'bucket-infilling' and, in turn, the shallowing of the platform. In addition, given that each of the concerned platforms neighbours an inhabited platform, this expansion may suggest that nutrient inputs may not be restricted to the concerned platform, but may also cause increases in nutrient concentrations, to a lesser extent, on adjacent platforms. Additional suggestion of seagrass expansion beyond Huvadhu Atoll may be gained with reference to Miller and Sluka's (1999a) study of Laamu Atoll. In 1999, they found that seagrass was absent from the marine environment adjacent to Mati Matadhoo and Thundi villages. However, dense seagrass beds are evident in both 2006 and 2015 Google Earth imagery (Figure 6.21). Hence, this provides further evidence for rapid and recent seagrass expansion.

6.4.3 Platform-scale: Implications of seagrass expansion for sediment productivity

6.4.3.1 Seagrass density and epiphytic calcium carbonate production

Seagrass beds were found to be dominated by *Thalassia hemprichii*, which was also found as the dominant seagrass type at Laamu Atoll (Miller and Sluka, 1999a) and has been identified within Baa (Payri et al., 2012) and North Malé (Gillis, 2009) Atolls. The presence of *T. hemprichii* lends further confidence to the likely link between

eutrophication and seagrass proliferation. This is because responses of seagrass to moderate nutrient enrichment can be species-specific (Birkholder et al., 2007), and in other settings *T. hemprichii* has been found to be phosphorous limited (Agawin et al., 1996). Hence with moderate nutrient inputs, it would be expected to increase in extent.

With regards to blade density, marked variability was found (range: 21 ± 5 m^{-2} to 2138 ± 324 m^{-2}) and also, in turn, in the preliminary estimates of epiphytic production in seagrass beds (range: 1.8 ± 1.0 g m^{-2} yr^{-1} to 192.7 ± 66.7 g m^{-2} yr^{-1}). A significant positive correlation was found between blade density and carbonate production rates, which implies that bade density, rather than spatial variability in the degree of blade encrustation, was the primary control upon epibiont carbonate production. This is consistent with Perry and Beavington-Penney's (2005) study of *Thalassia hemprichii* and *Thalassodendron ciliatum* at Inhaca Island, Mozambique. Blade density and estimates of $CaCO_3$ production were also significantly correlated (R^2 = 0.7106 for *T. hemprichii*; Perry and Beavington-Penney ,2005).

It is pertinent to note that the production rates must be regarded as estimations as there are several caveats in their calculation. For example, data (satellite imagery and field data) were collected within one monsoon season. A further investigation during the second monsoon season would be beneficial to consider any seasonal fluctuation in blade density and, in turn, epibiont production rates. In addition, it would be preferable to have obtained both density and $CaCO_3$ production data from different types of seagrass collected across the reef platform in its entirety. That said, the number of samples, $CaCO_3$ production estimates and error margins are comparable to those calculated by Perry and Beavington-Penney (2005; blade density: 625 ± 109 to 2375 ± 222 per m^2; epibiont production: 8.0 ± 5.5 to 85.7 ± 43.8 g $CaCO_3$ m^{-2} yr^{-1}). Likewise, shoot densities (Frankovich and Zieman, 1994 – 47 ± 25 to 1475 ± 207 per m^2) and estimates of $CaCO_3$ production calculated for *Thalassia* at Florida Bay were comparable to the values calculated in this study (Nelsen and Ginsburg, 1986). Hence, a reasonable degree of confidence can be gained for the epibiont production rates estimated in this study.

6.4.3.2 Benthic Sedimentology

Marked differences were found between eco-geomorphic zones in the textural characteristics of benthic sediment samples. However, the differences appear to be

primarily controlled by distance from the oceanward reef crest (with grain size decreasing with distance), rather than seagrass presence (as discussed in Chapter 4). Indeed, low proportions (range: 0.0-2.5%) of fine-grade sediment were found within the benthic samples from seagrass beds. This contrasts with previous work which has found benthic sediments within seagrass beds to be rich in fine-grade material, due to the ability of seagrass to attenuate wave energy and trap suspended sediment (e.g. Scoffin, 1970). That said, the findings of this study are consistent with those from Inhaca Island, Mozambique where 0.6-1% fines were found within sediment samples recovered from *T. hemprichii* beds (Perry and Beavington-Penney, 2005). Perry and Beavington-Penney attributed the unexpectedly low proportions of fine-grade material to low levels of epiphytic and benthic algal carbonate mud production and also the preferential resuspension of fine-grained sediment by flood tide-enhanced flow. It seems likely that given the exposed nature of Huvadhu atoll rim and the associated incident high-magnitude oceanward swell energy, that fine-grade material is also preferentially and rapidly winnowed away from the seagrass beds upon disaggregation (refer to Chapter 7).

Compositionally, the lack of any discernable differences in the concentrations of CCA within seagrass zone sediment samples may also be supportive of the notion that fine-grained sediments are rapidly winnowed away from the seagrass zone. Indeed, semi-quantitative assessments of the composition of epiphytes on seagrass blades were dominated by CCA (Figure 6.14). CCA was observed to form thin, fragile, monostromatic layers upon seagrass blades (Figures 6.15 and 6.16), which would rapidly disaggregate into fine-grade material once detached from the blades (Perry and Beavington-Penney, 2005). Hence, it seems likely that the residence time of fine-grade material (including CCA) within the seagrass zones is low as it is rapidly winnowed away given the high energy nature of the setting. Although CCA dominated blade coverage (83 ± 2%; Figure 6.14), this does not necessarily equate to the proportion of epiphytic mass given that is was found to form thin monostromatic layers. In contrast, foraminifera and gastropods possess higher densities and with greater 3-dimensional complexity, which is not considered in 2-dimensional counts of blade coverage.

While no discernible difference in concentrations of CCA was found within the seagrass zone benthic sediment samples, an epiphytic carbonate signature was

evident in foraminifera abundances. Greater proportions of foraminifera were found within benthic sediment samples from within the seagrass zones (9.7 ± 1.5% and 10.5 ± 1.5% within the dense seagrass and oceanward sparser seagrass zones respectively). As anticipated, a significant positive relationship was found between estimations of $CaCO_3$ production and the percentage of foraminifera in benthic samples. The most common foraminifera identified both on the seagrass blades and within sediment samples were *Marginopora vertebralis, Calcarina spengleri, Amphistegina lesson,* and *Sphaerogypsina globules.* While these may live upon the seagrass blades, the higher proportions of foraminifera within the sediment may also be attributable to greater proportions of forams living on or within the seagrass substrate, particularly given that predominantly benthic forams were identified. While the greater proportions of foraminifera within the sediment may appear marginal, this is a marked difference given the compositional homogeneity of the remainder of the system. Indeed, there was an average of 3.5 ± 0.0% foraminifera within the other marine samples; 3.0 ± 0.0% within Galamadhoo and Baavanadhoo island sediments; and 2.8 ± 0.0% within beach sediments. Moreover, given that the higher concentrations of foraminifera appear to be restricted to the seagrass zones rather than rather than being transported across the system. This could suggest that the seagrass beds are trapping sand-sized sediments. If this is the case, the seagrass beds could be interrupting reef-to-island sediment transport, which could result in significant implications for island maintenance and shoreline stability.

6.4.3.3 Sediment Productivity

Using census data, estimates of sediment production and change detection analyses, seagrass expansion was found to have a significant impact upon sediment productivity within the case study site. While first order estimates of sediment production have been generated, several caveats must be borne in mind. Firstly, as discussed, there are several issues concerned with the calculations of estimates of epiphytic production (refer to section 6.4.3.1). Secondly, calculations of the shift in sediment production are likely conservative as they do not incorporate any changes in seagrass blade density. It is highly likely that blade density increased as well as areal extent. From observations of imagery (Figure 6.8), this appears particularly to be the case within the oceanward sparser seagrass zone (between the dense seagrass and oceanward reef crest zones), which looks significantly less dense in 2006 than in 2015. Given that

density was found to be the primary control upon epiphytic carbonate production, and that epiphytic carbonate production was the primary sediment source in estimates of 2015 production, it is likely that the calculations are highly conservative.

A third caveat is that only sediment production by seagrass epiphytes was considered, however seagrass proliferation will likely impact the distribution of other sediment producers. For example, there may be an increase in parrotfish abundances, which is of particular significance given that parrotfish produce sediment of the appropriate grade for reef island construction and maintenance (refer to Chapter 5; Perry et al., 2015). Indeed, following epiphytic carbonate production (62%), the second largest input of sediment within the dense seagrass zone was attributable to excavator parrotfish grazing (19%, predominantly *Chlorurus strongylocephalus*).

The magnitude of the shift in sediment production (243 tonnes yr^{-1}) estimated at the scale of an individual reef platform at a decadal timescale, represents a significant and rapid shift in the platform sediment budget. Moreover, the rate of sediment accumulation (~170 m^3 yr^{-1}) is markedly greater than that which would have been required to construct Galamadhoo island (averaged long-term rate = 24 m^3 yr^{-1}). If seagrass areal extent continues to increase, this rate of sediment accumulation may also continue to concordantly increase. However, reef islands are unlikely to be the sole recipient of such additional sediment, rather several potential destinations exist, for example, sediment may be exported off the platform, reincorporated into the reef structure, transported to infill lagoonal areas, or stored on the reef surface (Morgan and Kench, 2014). Quantifying the proportion of material that may contribute to reef island construction and maintenance is problematic, although a likely indicator is grain size. The vast majority of island sediment was found to be sand-sized (leeward island average: 80.5 ± 3.5%; Chapter 1). As such, gastropods and foraminifera are likely suitable island-building constituents, while CCA, serpulids and bryozoans are less likely to be suitable given that they may disaggregate into fine-grade material. Nonetheless fine-grade may still contribute toward island building as it may contribute to platform (or 'bucket') infilling. Indeed, sediment samples collected from the 'empty bucket' portion of the rim at the windward site comprised up to 43% fine-grade material. With bucket-infilling, such fine-grade material could thus provide the substrate for further reef island accumulation as described in Chapter 3.

Seagrass expansion thus appears to be associated with numerous benefits for marine ecology and reef island maintenance. However, seagrass primary production may only increase with at best moderate levels of nutrient loading (Borum and Sand-Jensen,1996; Duarte, 2002). If an environmental threshold is crossed whereby a shift from nutrient- to light-limitation occurs (Figure 6.1), there could be an associated phase shift to a macroalgal-dominated community. High-biomass algal growth is the primary reason for seagrass loss with over-enrichment (Shepherd et al., 1989). While seagrass-coral competitive interactions are unclear, macroalgal blooms are known to have severe detrimental effects within coral reef systems. For example, macroalgae may overgrow both seagrass and adult corals, inhibit recruitment of juvenile corals, cause hypoxia and/or anoxia, and significantly reduce fisheries and biodiversity. Accounts of the transition to a macroalgal dominated system as a result of eutrophication are far more numerous than those of seagrass expansion (NRC, 2000; Howarth et al., 2000, Lapointe et al., 2004). For example, in the Florida Reef Tract, eutrophication has resulted in the rapid expansion of macroalgae and corresponding losses of hard coral cover (Porter and Meier, 1992; Chiappone and Sullivan, 1997; Porter et al., 2002; Lapointe et al., 2004). It is unclear whether this could occur in the Maldives given that Maldivian reef flats are particularly shallow (e.g. live coral occurred 0.5 m below MSL off the oceanward coast of Galamadhoo). However, macroalgal growth has been documented around Malé, Furana Fushi, Kura Bandos, Kurumathi, and Ihuru islands and attributed to in to nutrient fertilisation from sewage (Goreau, 1998). Such longer term trajectories of the transition to macroalgal-dominated systems could have catastrophic implications for the nation’s ecology, geomorphology and economy.

6.5 Conclusion

This Chapter seeks to provide a first step in attempting to understand the controls on Maldivian seagrass distribution, recent shifts in seagrass areal extent, and the implications for sediment production. At the archipelago-scale, presence-absence counts suggest that urbanisation-induced eutrophication and the proportion of a reef platform occupied by land area are key controls upon Maldivian seagrass distribution. At the atoll-scale, change detection analyses indicate that there has been a marked increase over the last decade in seagrass areal extent. At the platform-scale, first order

estimates of sediment production associated with seagrass epiphytes highlight that seagrass expansion may be associated with a marked shift in the rates and types of sediment production. It is hoped that future research may be undertaken to ascertain links between nutrient loading and seagrass proliferation. The implications of such research could be highly significant for a nation that is dependent upon its physical and ecological environment. More broadly, the expansion of seagrass may be considered a ‘bright spot’ (e.g. Cinner et al., 2016) against the bleaker backdrop of global declines in seagrass areal extent. Moreover, this work is highlights that any future shifts in reef ecology, which may be associated with environmental change, have potential to impact sediment budgets and, in turn, ongoing reef landform trajectories.

Chapter 7: Sediment transport

7.1 Introduction

Despite the importance of sediment transport for reef island location, evolution and contemporary stability, few studies have attempted to elucidate sediment transport pathways (Kench, 2011a). The majority of studies have focused on inner shelf or fringing reef systems in the Caribbean (e.g. Land, 1979; Hoskin et al., 1986; Hubbard, 1986; Hubbard et al., 1990; Li et al., 1998), and Hawaii (e.g. Ogston et al., 2004; Storlazzi et al., 2004; Presto et al., 2006). There is a greater paucity of work in the Indian Ocean (e.g. Kench, 1998a; Kench and McLean, 2004), and on reef island systems (e.g. Flood, 1974; Hopley, 1981; Gourlay and Jell, 1993). Assessments of sediment transport within the Maldives have been limited to one interior platform system (Vabbinfaru, North Malé Atoll – Morgan and Kench, 2012, 2014). To date, there have been no attempts to quantify sediment transport within Maldivian atoll rim systems. Such knowledge is key to developing a holistic understanding of the inherently integrated nature of reef island systems.

While studies quantifying contemporary sediment transport are thus limited, there is a near-absence of research examining potential shifts in sediment transport associated with projected sea level rise. This is despite the fact that such processes are fundamental to understanding future reef island landform trajectories. This contrasts the plethora of studies that have examined reef responses to other shifts associated with climate change, such as in sea surface temperatures and ocean acidification (e.g. Hoegh-Guldberg et al., 2007; Carpenter et al., 2008; De'ath et al., 2009; Pandolfi et al., 2011; Fabricius et al., 2011). Of the existing studies of future sediment transport, Ogden and Field (2010) undertook one-dimensional modelling of Molokai, Hawaii, and showed that sea level rise will increase wave heights and suspended sediment concentrations. Likewise, Storlazzi et al. (2011) employed two-dimensional modelling at the same location and demonstrated that sea-level rise would increase wave height and, in turn, the volume of sediment transport.

There is also a poor understanding of the impact of sea-level rise upon wave transformation processes within reef environments. Phase-resolving model work in

reef environments has largely focused on continental fringing reefs, rather than atoll reef island settings (Nwogu and Demirbilek, 2010; Shimozono et al., 2015; Yao et al., 2012; Zijelma, 2012), with the notable exception of Beetham and Kench's (2016) study in Tuvalu. Similarly, the majority of research on reef hydrodynamics has been focussed solely upon the reef edge, rather than wave transformation across the entirety of reef platform surfaces (exceptions include Kench, 1998b; Kench and Brander, 2006; Kench et al., 2006; Kench et al., 2009c; Beetham and Kench, 2014, 2016). Likewise, few studies of sediment transport examine hydrodynamics, but rather the majority of studies employ sedimentology as a proxy for sediment transport (e.g. Chapter 4; Rankey et al., 2011; Dawson and Smithers, 2014; Hamylton et al., 2016).

The aim of this chapter is to provide the first quantitative study of sediment transport potential within Maldivian rim island systems. In addition, sediment potential mobility under scenarios of future sea-level rise will be examined. Specific key research questions are:

1) What is the contemporary hydrodynamic environment within the windward and leeward study sites?
2) What is the potential mobility of sediment stored within each of the eco-geomorphic zones?
3) To what extent will (1) and (2) change under sea-level rise scenarios?

7.2 Methodology

7.2.1 Bathymetry

In order to model wave processes, bathymetric models were derived from Quickbird and WorldView-2 imagery (for the windward and leeward sites respectively, as in Chapter 4) using the methodology of Stumpf et al. (2003). Water depths were obtained in the field using a single beam echosounder at the locations displayed on the right-hand plots in Figures 4.2 and 4.3. (n = 210 and n = 190 at the windward and leeward sites respectively). Depths were corrected relative to MSL using the tide tables for Gan (00°41S, 73°9E) from the University of Hawaii Sea Level Centre. The field datasets were then divided to calibrate (50%) and validate (50%) the model. At each study site, a band ratio transformation was applied whereby the green and blue bands were extracted from the pre-processed (i.e. atmospherically corrected) images. A ratio layer

was generated by dividing the natural log of the green band by the natural log of the blue band. Ratio values were plotted against the calibration data and a second-order polynomial relationship was fitted. The regression equations were applied to the ratio layers to estimate bathymetry across the entirety of each study site (spatial resolution = 2.4 m and 1.86 m at the windward and leeward sites respectively). To validate the models, the field-derived depths of the validation dataset were compared to the model-derived depths and R^2 values were generated (Hamylton et al., 2015).

7.2.2 Wave processes

7.2.2.1 Approach

Two-dimensional wave modelling was undertaken in collaboration with Dr. Eddie Beetham (University of Auckland) using a Green-Naghdi (GN) free-surface solver from the open source model Basilisk (Popinet, 2015). For a full description of the model refer to Popinet (2014), the Basilisk website for source code (Popinet, 2014), Beetham and Kench (2016), and Beetham (2016). The approach uses a weakly dispersive source term for wave propagation and shoaling, extending upon the nonlinear shallow water solver from Popinet (2011). This has been demonstrated to be effective in simulating wave dispersion, wave breaking, and wet-dry interaction in shallow coastal environments (Bonneton et al, 2011; Lannes and Marche, 2015; Tissier et al., 2012). Basilisk GN is particularly effective in reef environments as it can simulate the behaviour of relatively large amplitude waves across variable bathymetry (Beetham, 2016). Hence, it is able to handle the sudden change in bathymetry at a reef crest, which is a challenge for traditional models (Roeber and Cheung, 2012). Few phase-resolving models have been validated with field data from atoll or fringing reef settings and, indeed, Beetham (2016) and Beetham and Kench (2016) were the first to validate the Basilisk GN solver in a reef setting. Beetham (2016) demonstrated the approach to be effective in representing surf-zone processes, water-level variations, and velocity dynamics within coral reef environments (refer to Beetham, 2016, for comprehensive validation of the Basilisk GN solver).

7.2.2.2 Model inputs

Bathymetric models derived in section 7.2.1 were used as inputs. At the platform edges, wave breaking in the satellite imagery precluded the ability to derive depths

beyond the platform surface. Artificial slopes were therefore added to the lagoonward and oceanward edges of the platform using depths from UK Hydrographic Office (1992) charts of Huvadhu Atoll.

Wave height and period were required as inputs (Table 7.1) to both the lagoonward and oceanward edges of the sites. A caveat of this chapter is the absence of *in situ* wave measurements. Lagoonward wave data for the windward site were thus obtained from an 8-day experiment undertaken by Mandlier (2008) between 8th and 16th November 2007 over 16 successive high tidal stages. Also with the aim of examining a windward rim setting, Mandlier placed instruments at Mathoda (Figure 2.10). Mathoda is located ~8 km to the east of the windward site, and the platform has a similar aspect relative to incident swell. There can thus be reasonable confidence that lagoonward wave conditions would be comparable. At the leeward site, given the high significance of wind-generated waves (as highlighted in Chapter 2) and thus the likely sensitivity of this site to shifts in wind speeds, linear wave theory was employed to calculate *Hs* and *Ts*. This approach was selected, rather than Mandlier's data so as to consider the upper range of wind speeds, which would likely be of most significance in inducing geomorphic change and would be unlikely to be represented within an 8-day experiment. The JONSWAP approach (Hasselmann et al., 1973) was thus used with the revisions suggested by the Shore Protection Manual (1984). This enabled a windspeed of 10 knots to be used to represent the upper range of westerly winds (Chapter 2).

Oceanward wave data were obtained from the NOAA WaveWatch III model (Tolman, 2009). A 30 year hindcast of wave conditions was generated off the oceanward edge of the atoll rim at both the windward and leeward sites. Wave period and significant wave height were extracted and the average taken (Table 7.1). Averages, rather than maximum values, were used in order to investigate fair-weather conditions, as oppose to high magnitude events. Fair weather conditions were selected so as to contribute to a currently growing body of research on reefal sediment transport under fair weather conditions. Such studies have found sediment transport to be relatively high (Kench et al., 2017; Morgan and Kench, 2014; Hubbard et al., 1981) and to have implications for reef island shoreline morphology (Beetham and Kench, 2014).

A combined approach using field data from Mandlier (2008), linear wave theory, and WaveWatch III was employed for several additional reasons: (1) Mandlier's measurements from the oceanward platform edges were not obtained in deep water; (2) a longer-term average would generate more reliable data than an 8 day 'snapshot'; and (3) the field data (Mandlier, 2008) were used for the lagoonward inputs at the windward site as abrupt changes in bathymetry are known to challenge the WaveWatch III model (Ford, pers. comm., 2014). In each case, an irregular wave field was imported into both the lagoonward and oceanward fields. The model ran with a spatial resolution of 5.8 m for 1024 s. Wave output statistics were calculated after the wave field was fully developed across the domain (t > 400 s).

	Oceanward inputs		Lagoonward inputs	
Site	*Hs* (m)	*Ts* (s)	*Hs* (m)	*Ts* (s)
Windward	1.55	10.1	0.12	8.5
Leeward	1.35	8.8	0.6	6

Table 7.1 – Wave data employed as model inputs from the oceanward and lagoonward margins for both the windward and leeward study sites. H_s = significant wave height (m), T_s = significant wave period (s).

7.2.2.3 Model outputs

In order to quantify sediment potential mobility, both mean (V_{mean}) and maximum velocities (V_{max}) were extracted from the model outputs. The mean velocity (V_{mean}) was calculated for each cell as the average velocity value between t = 400 s and t = 1024 s (i.e. the period during which the wave field was fully developed). Similarly V_{max}, is the maximum value within each cell between t = 400 s and t = 1024 s. To further understand the process regime, root mean square wave height (H_{rms}) and setup were also extracted from the model. H_{rms} is the wave height that is equivalent to the height of a sinusoidal wave with the same energy. Setup refers to the positive change in mean water level produced as waves shoal and break. To investigate the impact of sea-level rise (SLR), the model was run three times whereby SLR = 0.0, 0.5 and 1.0. An increment of 0.5 m was selected as this is consistent with (1) regional estimates of sea-level rise for the central Indian Ocean presented in IPCC AR5 report under RCP 4.5 scenario by 2081-2100 (Church et al., 2013); and also (2) the mid-Holocene sea-level highstand in the Maldives (Kench et al., 2009b).

7.2.3 Sediment Potential Mobility

The Potential Mobility (PM) of each sediment sample was calculated using the methodology proposed and validated by Kench (1998a). PM is the proportion (%) of a sample that can be mobilised under normal (i.e. 'fair-weather') conditions. Firstly, wave velocities at each sediment sample (n = 90 and 96 and the windward and leeward sites respectively) location were extracted from the wave process model outputs. Wave velocity values were used to calculate the mean threshold settling velocity (chi) for each sediment sample using the experimentally-derived entrainment threshold relationship for bioclastic sediments reported by Kench and McLean (1996, $R^2 = 0.93$, Figure 7.1). Secondly, settling velocity curves for each sediment sample were converted into chi units:

$$chi = log_2\left(\frac{s}{s_o}\right)$$

where s = settling speed (m s^{-1}), and s_o = stand settling speed of 1 m s^{-1} (May, 1981). Hence, chi increases with decreasing settling velocity. The settling velocity threshold (chi) at each sample location was then found on each settling velocity curve of the concerned sediment sample. PM is thus the proportion of the sample with equal or slower settling velocity than the threshold value (Kench, 1998a).

This approach was employed 6 times at each study site: for both mean (V_{mean}) and maximum (V_{max}) velocities under each of the 3 sea-level scenarios. In order to visualise spatial variability, PM results were interpolated using the block kriging algorithm employed in Chapter 4 (spatial resolution = 6 m).

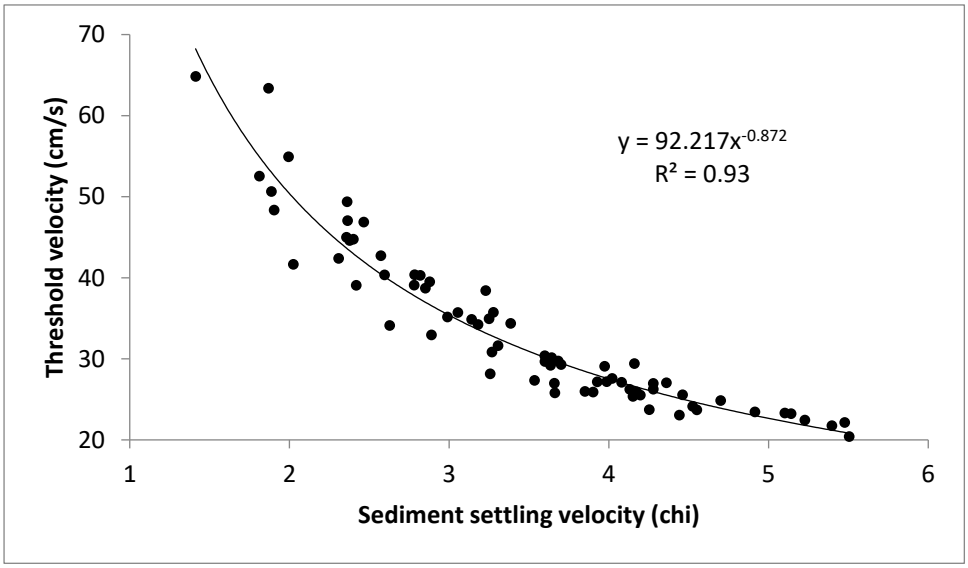

Figure 7.1 – Experimentally-derived threshold entrainment relationship digitsed from Kench and McLean (1996). This relationship was used to calculate the threshold sediment settling velocity (chi) associated with the model-derived velocities extracted from each sample location.

7.3 Results

7.3.1 Bathymetric modelling

Bathymetric DEMs of the windward and leeward study sites were derived from Quickbird and WorldView-2 imagery respectively. Strong calibration relationships were found between echosounder-derived and model-derived water depths at both study sites (R^2 = 0.86 and 0.83 at the windward and leeward sites respectively, Figures 7.2 and 7.3).

At the windward site, the model (Figures 7.4 and 7.5; Table 7.2) revealed a shallow oceanward reef flat whereby the oceanward reef crest was at the shallowest depths relative to MSL (-0.36 ± 0.12 m). The rubble tongues were slightly elevated (at depths of -0.44 ± 0.17 m) above the intervening oceanward patch zone (-0.65 ± 0.31 m). Water depths were found to increase with closer proximity to the atoll lagoon. Indeed, the lagoonward sand zone was at -0.92 ± 0.59 m relative to MSL and the lagoonward patch zone was characterised by a marked increase in depth (-5.21 ± 2.95 m) with the exception of coral patches (<-0.65 m).

The leeward site was characterised by greater consistency in water depths across the study site (range 0 - -2.03 m, Figures 7.6 and 7.7; Table 7.2). The oceanward reef crest was the shallowest eco-geomorphic zone (-0.46 ± 0.12 m) and was comparable in elevation to the windward site oceanward reef crest. The remainder of the oceanward environment was at relatively consistent depths (-0.66 ± 0.1 m, -0.77 ± 0.14 m and -0.74 ± 0.21 m of the oceanward sparser seagrass, dense seagrass and oceanward sand zones respectively). As at the windward site, the lagoonward environment was deeper than the oceanward environment: the lagoonward patch zone was at -1.12 ± 0.26 m, and the lagoonward reef crest at -1.44 ± 0.20 m.

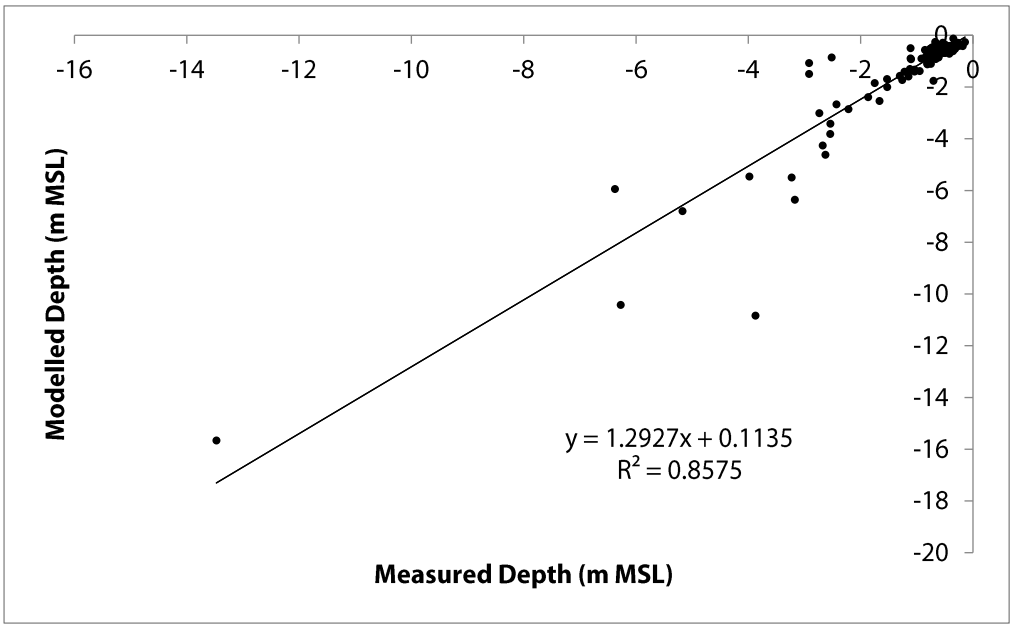

Figure 7.2 – Windward site validation plots of the relation between echosounder-derived (i.e. measured) and model-derived water depths relative to MSL.

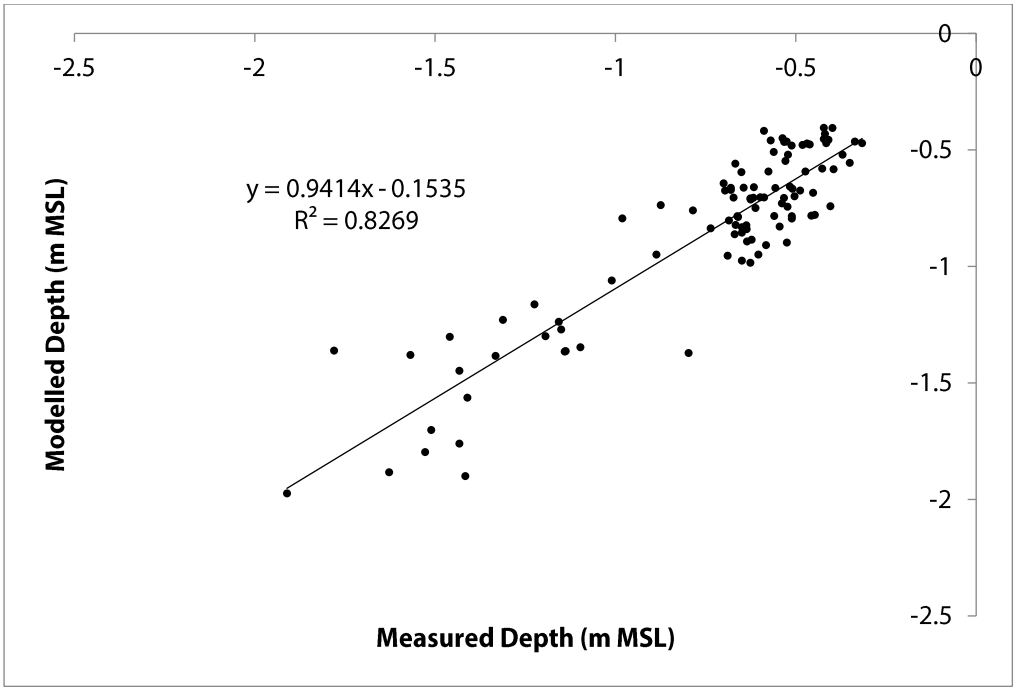

Figure 7.3 – Leeward site validation plots of the relation between echosounder-derived (i.e. measured) and model-derived water depths relative to MSL.

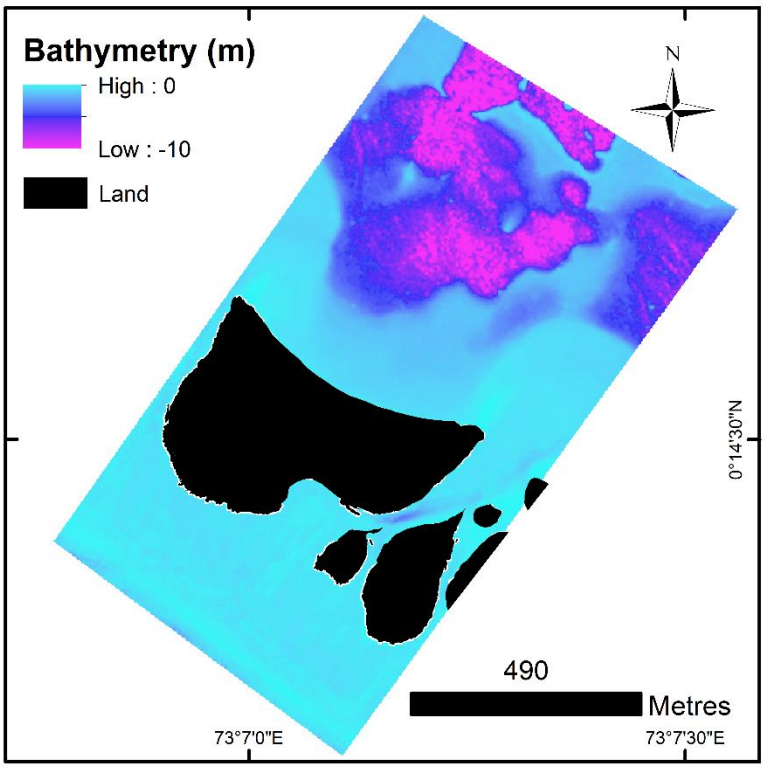

Figure 7.4 – Windward site bathymetric model derived from Quickbird imagery.

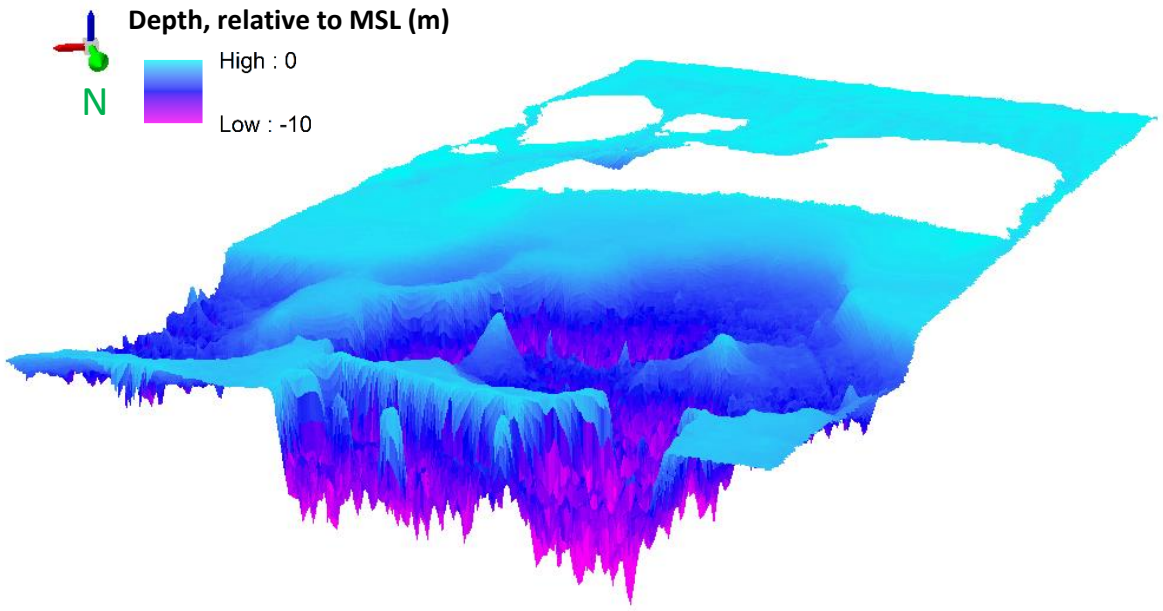

Figure 7.5 – 3-dimensional perspective view of windward site bathymetric model (vertical exaggeration = x10).

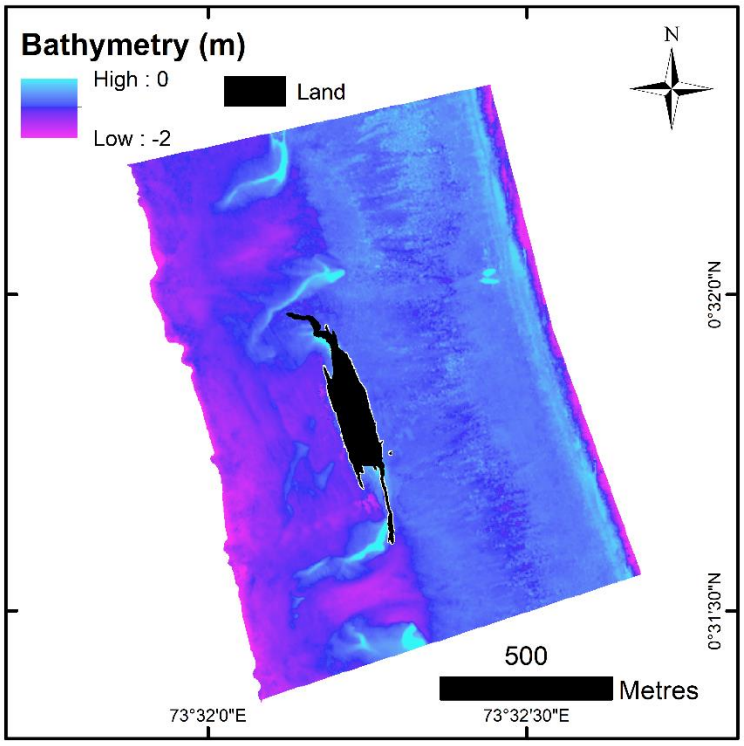

Figure 7.6 – Leeward site bathymetric model derived from WorldVIew-2 imagery.

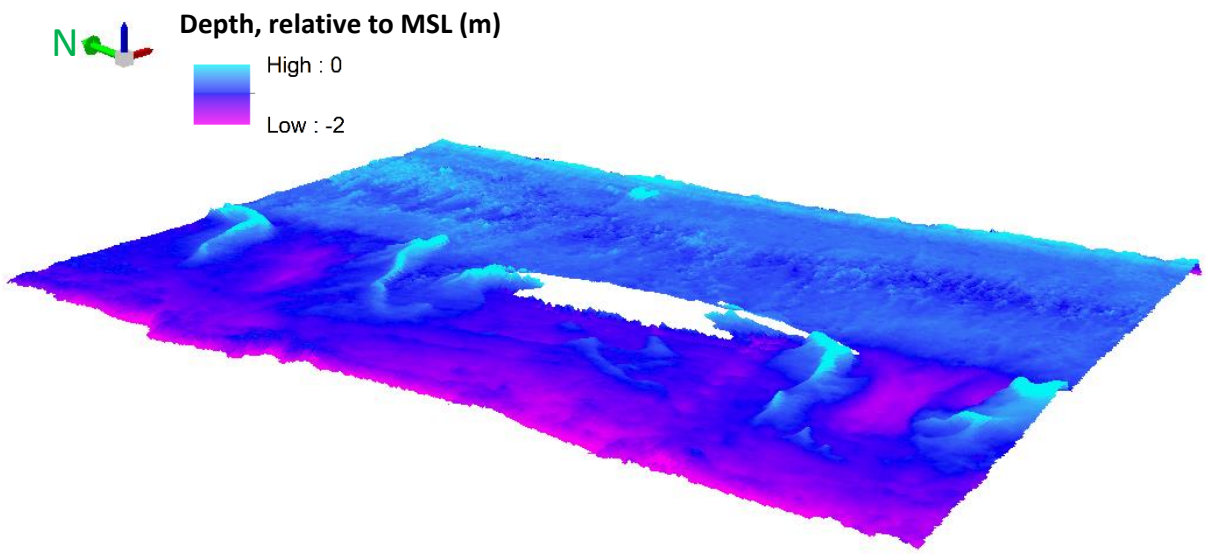

Figure 7.7 – 3-dimensional perspective view of windward site bathymetric model (vertical exaggeration = x20).

		Depth (m, relative to MSL)			
	Zone	Mean	SD	Minimum	Maximum
Windward Site	Lagoonward Patch	-5.21	2.95	-17.75	-0.65
	Lagoonward Sand	-0.92	0.59	-3.90	0.00
	Oceanward Patch	-0.65	0.31	-3.73	0.00
	Rubble	-0.44	0.17	-3.12	0.00
	Oceanward Reef Crest	-0.36	0.12	-0.79	-0.04
Leeward Site	Lagoonward Reef Crest	-1.44	0.20	-2.03	-0.95
	Lagoonward Patch	-1.12	0.26	-1.86	0.00
	Oceanward Sand	-0.74	0.21	-1.32	0.00
	Dense Seagrass	-0.77	0.14	-1.58	-0.21
	Oceanward Sparser Seagrass	-0.66	0.10	-0.89	0.00
	Oceanward Reef Crest	-0.46	0.12	-0.80	-0.12

Table 7.2 – Depths of each eco-geomorphic zone relative to MSL as derived from bathymetric models.

7.3.2 Wave processes

7.3.2.1 Contemporary wave processes

Wave modelling results for both the windward and leeward study sites are presented in Figures 7.8 to 7.17, and Tables 7.3 and 7.4.

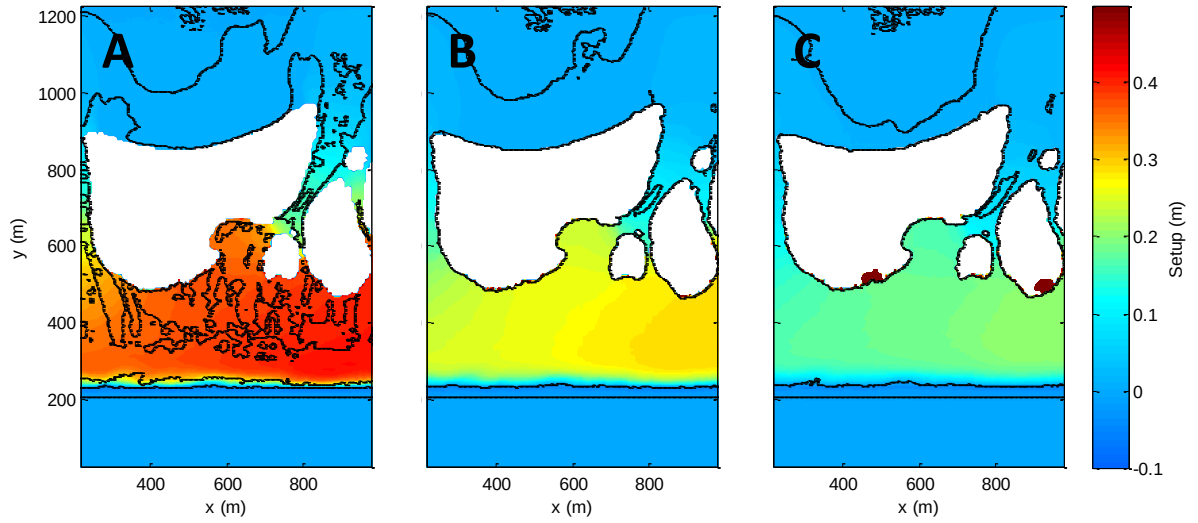

Figure 7.8 – Windward site wave setup (i.e. mean water level, m) where SLR = 0.0 m (A), 0.5 m (B) and 1.0 m (C).

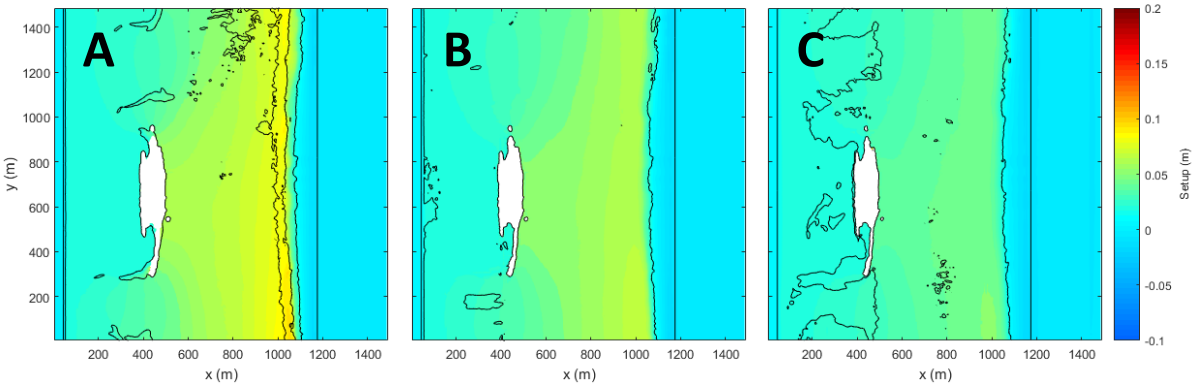

Figure 7.9 – Leeward site wave setup (i.e. mean water level, m) where SLR = 0.0 m (A), 0.5 m (B) and 1.0 m (C).

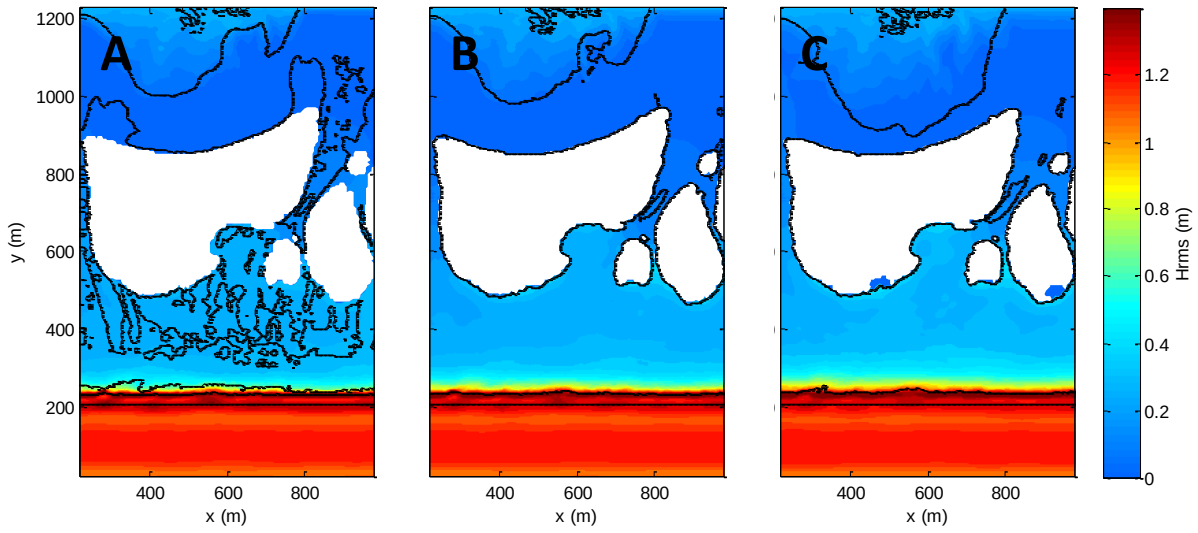

Figure 7.10 – Root mean square wave height (H_{rms}, m) across the windward site where SLR = 0.0 m (A), 0.5 m (B), and 1.0 m (C).

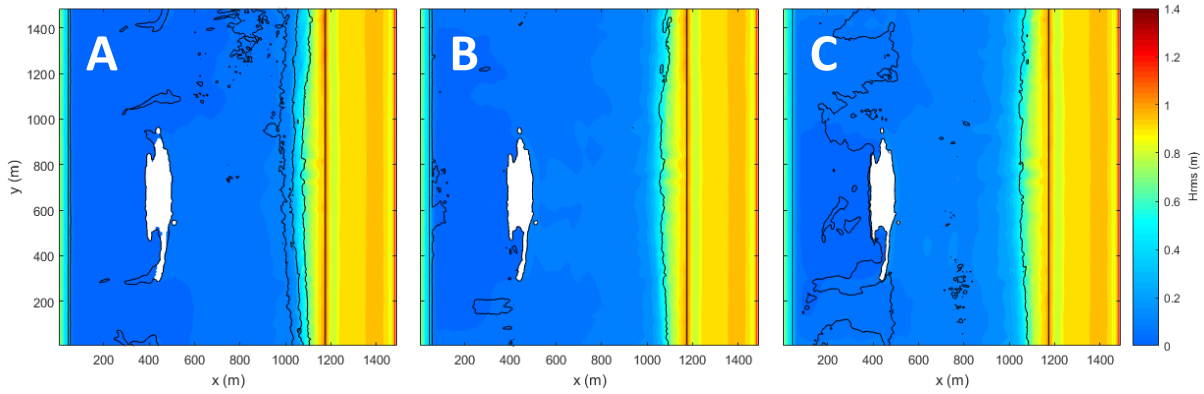

Figure 7.11 – Root mean square wave height (H_{rms}, m) across the leeward site where SLR = 0.0 m (A), 0.5 m (B), and 1.0 m (C).

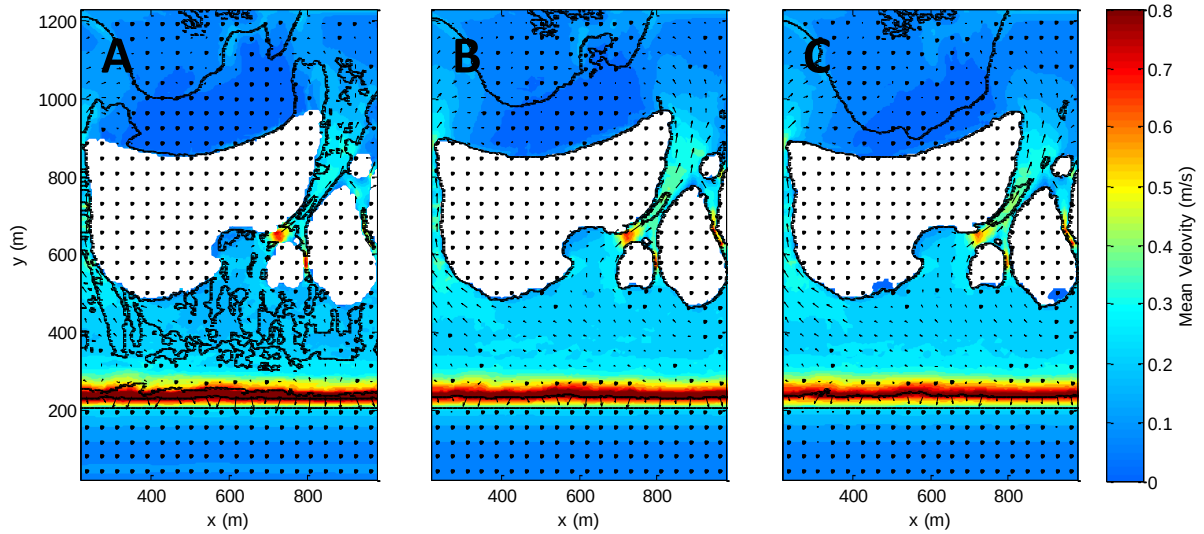

Figure 7.12 – Mean wave velocity (V_{mean}, m s^{-1}) across the windward site where SLR = 0.0 m (A), 0.5 m (B), and 1.0 m (C).

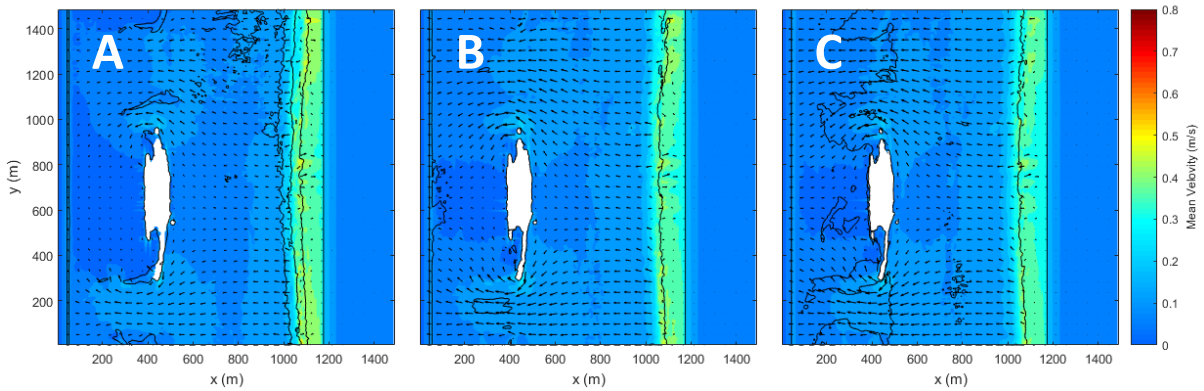

Figure 7.13 – Mean wave velocity (V_{mean}, m s^{-1}) across the leeward site where SLR = 0.0 m (A), 0.5 m (B), and 1.0 m (C).

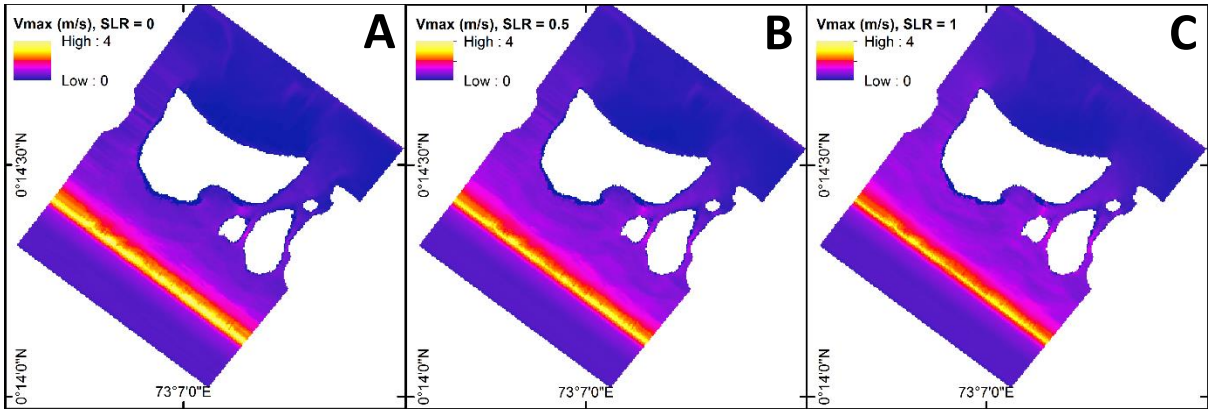

Figure 7.14 – Maximum wave velocity (V_{max}, m s^{-1}) across the windward site where SLR = 0.0 m (A), 0.5 m (B), and 1.0 m (C).

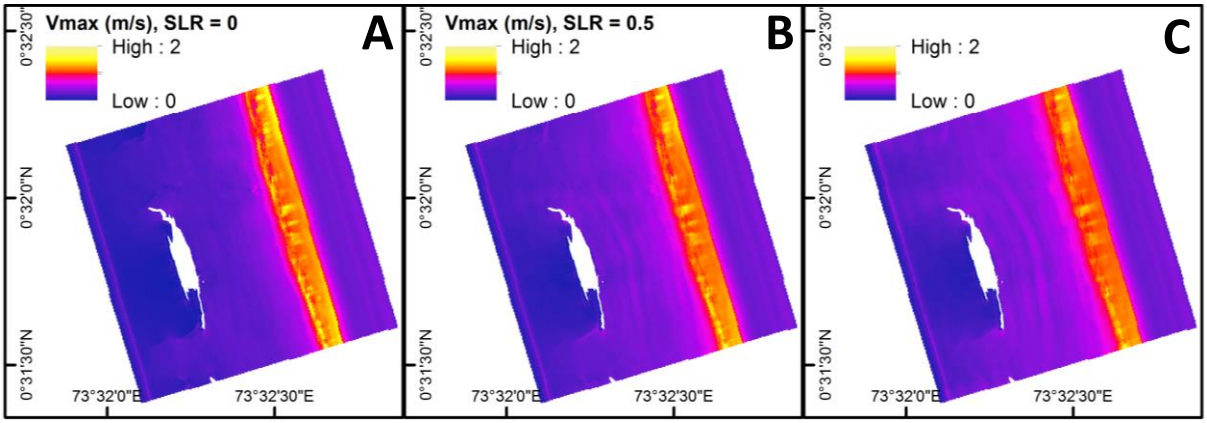

Figure 7.15 – Maximum wave velocity (V_{max}, m s^{-1}) across the leeward site where SLR = 0.0 m (A), 0.5 m (B), and 1.0 m (C). To allow visualisation of trends, note the scale differs to that in Figure 7.14.

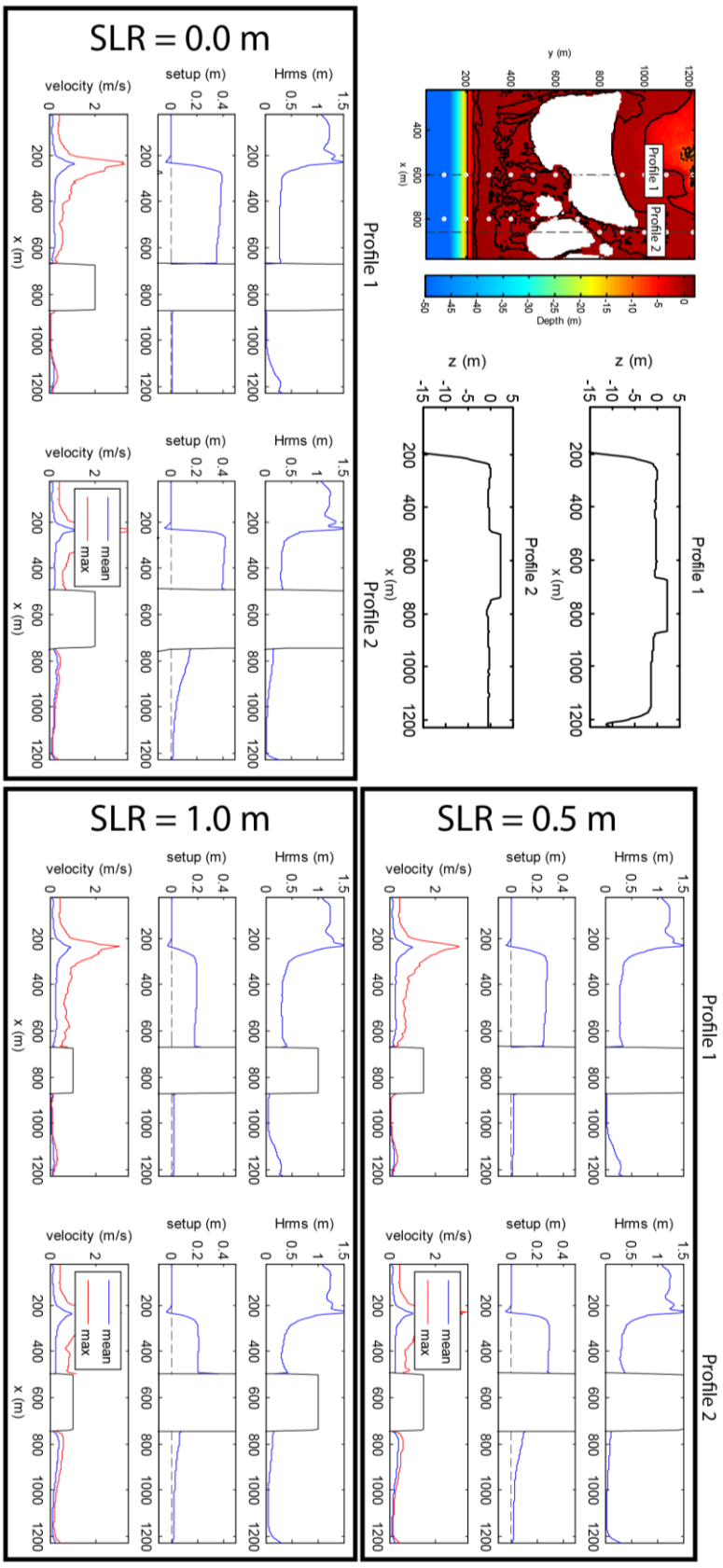

Figure 7.16 – Wave processes along oceanward-lagoonward cross-rim transects at the windward site under 0.0 m, 0.5 m and 1.0 m SLR.

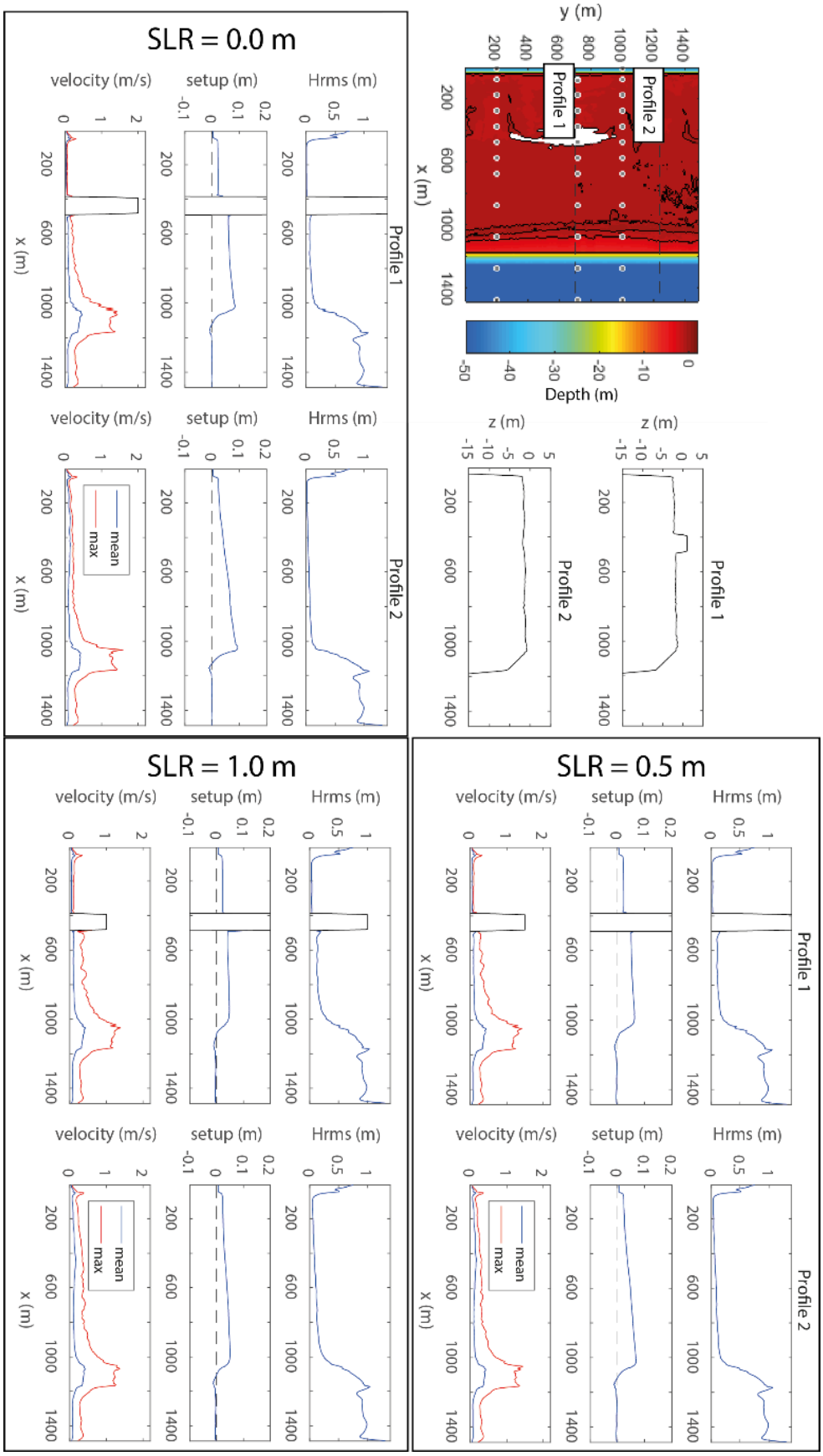

Figure 7.17 – Wave processes along oceanward-lagoonward transects at the leeward site under 0.0 m, 0.5 m and 1.0 m SLR.

		SLR = 0.0		SLR = 0.5		SLR = 1.0	
	Zone	Mean ± 1 S.D.	Range	Mean ± 1 S.D.	Range	Mean ± 1 S.D.	Range
V_{mean} (m/s)	ORC	0.28 ± 0.05	*0.17 - 0.52*	0.29 ± 0.05	*0.21 - 0.53*	0.31 ± 0.05	*0.22 - 0.56*
	R	0.22 ± 0.08	*0 - 0.78*	0.25 ± 0.08	*0 - 0.77*	0.24 ± 0.07	*0 - 0.71*
	OP	0.19 ± 0.09	*0 - 0.61*	0.21 ± 0.1	*0 - 0.72*	0.22 ± 0.09	*0 - 0.67*
	LS	0.1 ± 0.07	*0 - 0.54*	0.11 ± 0.08	*0 - 0.45*	0.11 ± 0.08	*0 - 0.49*
	LP	0.08 ± 0.03	*0.03 - 0.2*	0.08 ± 0.03	*0.04 - 0.19*	0.08 ± 0.02	*0.04 - 0.18*
V_{max} (m/s)	ORC	1.36 ± 0.28	*0.7 - 2.55*	1.33 ± 0.25	*0.85 - 2.29*	1.24 ± 0.22	*0.81 - 2.17*
	R	0.52 ± 0.22	*0 - 1.37*	0.64 ± 0.23	*0 - 1.57*	0.7 ± 0.22	*0 - 1.51*
	OP	0.51 ± 0.25	*0 - 1.22*	0.63 ± 0.28	*0 - 1.26*	0.67 ± 0.27	*0 - 1.25*
	LS	0.14 ± 0.11	*0 - 0.71*	0.18 ± 0.12	*0 - 0.68*	0.22 ± 0.13	*0 - 0.77*
	LP	0.14 ± 0.05	*0.04 - 0.36*	0.15 ± 0.04	*0.08 - 0.32*	0.17 ± 0.04	*0.1 - 0.35*
H_{rms} (m)	ORC	0.33 ± 0.04	*0.26 - 0.54*	0.36 ± 0.05	*0.25 - 0.55*	0.42 ± 0.07	*0.29 - 0.67*
	R	0.22 ± 0.09	*0 - 0.35*	0.21 ± 0.1	*0 - 0.42*	0.24 ± 0.1	*0 - 0.45*
	OP	0.23 ± 0.09	*0 - 0.35*	0.23 ± 0.1	*0 - 0.47*	0.26 ± 0.1	*0 - 0.56*
	LS	0.03 ± 0.05	*0 - 0.3*	0.04 ± 0.05	*0 - 0.3*	0.07 ± 0.05	*0 - 0.3*
	LP	0.16 ± 0.08	*0.01 - 0.33*	0.17 ± 0.07	*0.02 - 0.33*	0.18 ± 0.07	*0.04 - 0.33*
Setup (m)	ORC	0.39 ± 0.02	*0.34 - 0.42*	0.27 ± 0.02	*0.23 - 0.3*	0.19 ± 0.01	*0.15 - 0.21*
	R	0.29 ± 0.13	*0 - 0.53*	0.2 ± 0.09	*0 - 0.87*	0.15 ± 0.07	*0 - 0.88*
	OP	0.31 ± 0.13	*0 - 0.42*	0.22 ± 0.1	*0 - 1.02*	0.17 ± 0.11	*0 - 1*
	LS	0.02 ± 0.02	*0 - 0.21*	0.02 ± 0.02	*0 - 0.14*	0.02 ± 0.01	*0 - 0.14*
	LP	0.01 ± 0	*0 - 0.01*	0.01 ± 0	*0.01 - 0.01*	0.01 ± 0	*0.01 - 0.01*

Table 7.3 – Windward site V_{mean}, V_{max}, H_{rms} and setup within each of eco-geomorphic zones where SLR = 0.0, 0.5 and 1.0. Note that marked spatial variability exists within each zone.

		SLR = 0.0		SLR = 0.5		SLR = 1.0	
	Zone	Mean ± 1 S.D.	Range	Mean ± 1 S.D.	Range	Mean ± 1 S.D.	Range
V_{mean} (m/s)	ORC	0.22 ± 0.07	*0.11 - 0.47*	0.23 ± 0.07	*0.12 - 0.46*	0.25 ± 0.07	*0.13 - 0.44*
	OSS	0.12 ± 0.01	*0.06 - 0.21*	0.12 ± 0.01	*0.1 - 0.23*	0.13 ± 0.02	*0.11 - 0.26*
	DSG	0.1 ± 0.02	*0 - 0.45*	0.11 ± 0.01	*0.04 - 0.34*	0.11 ± 0.01	*0.05 - 0.19*
	OS	0.11 ± 0.03	*0 - 0.31*	0.12 ± 0.03	*0 - 0.29*	0.12 ± 0.03	*0 - 0.25*
	LP	0.06 ± 0.04	*0 - 0.33*	0.08 ± 0.04	*0 - 0.43*	0.07 ± 0.03	*0 - 0.29*
	LRC	0.07 ± 0.03	*0.02 - 0.16*	0.07 ± 0.03	*0.04 - 0.16*	0.08 ± 0.03	*0.04 - 0.15*
V_{max} (m/s)	ORC	0.94 ± 0.26	*0.45 - 1.66*	0.96 ± 0.21	*0.54 - 1.6*	0.94 ± 0.17	*0.57 - 1.49*
	OSS	0.46 ± 0.09	*0.22 - 0.97*	0.55 ± 0.08	*0.38 - 1*	0.58 ± 0.08	*0.42 - 0.96*
	DSG	0.24 ± 0.06	*0 - 0.54*	0.34 ± 0.07	*0.13 - 0.58*	0.38 ± 0.06	*0.18 - 0.61*
	OS	0.2 ± 0.04	*0 - 0.4*	0.29 ± 0.05	*0 - 0.59*	0.34 ± 0.05	*0 - 0.62*
	LP	0.1 ± 0.06	*0 - 0.4*	0.15 ± 0.07	*0 - 0.62*	0.18 ± 0.08	*0 - 0.66*
	LRC	0.13 ± 0.07	*0.05 - 0.33*	0.15 ± 0.08	*0.06 - 0.39*	0.16 ± 0.09	*0.07 - 0.42*
H_{rms} (m)	ORC	0.17 ± 0.06	*0.09 - 0.47*	0.24 ± 0.08	*0.13 - 0.55*	0.33 ± 0.09	*0.18 - 0.61*
	OSS	0.1 ± 0.01	*0.07 - 0.18*	0.14 ± 0.02	*0.11 - 0.26*	0.18 ± 0.03	*0.13 - 0.35*
	DSG	0.06 ± 0.02	*0 - 0.1*	0.1 ± 0.02	*0.01 - 0.15*	0.13 ± 0.02	*0.06 - 0.21*
	OS	0.05 ± 0.02	*0 - 0.1*	0.08 ± 0.02	*0 - 0.16*	0.11 ± 0.03	*0 - 0.2*
	LP	0.03 ± 0.09	*0 - 0.78*	0.05 ± 0.09	*0 - 0.78*	0.07 ± 0.09	*0 - 0.79*
	LRC	0.43 ± 0.25	*0.01 - 0.78*	0.44 ± 0.24	*0.02 - 0.78*	0.45 ± 0.23	*0.03 - 0.79*
Setup (m)	ORC	0.08 ± 0.01	*0.05 - 0.1*	0.06 ± 0.01	*0.03 - 0.07*	0.04 ± 0.01	*0.01 - 0.05*
	OSS	0.08 ± 0	*0.07 - 0.09*	0.06 ± 0	*0.06 - 0.07*	0.05 ± 0	*0.04 - 0.05*
	DSG	0.06 ± 0.01	*0 - 0.08*	0.05 ± 0.01	*0.03 - 0.13*	0.04 ± 0	*0.03 - 0.06*
	OS	0.05 ± 0.01	*0 - 0.09*	0.04 ± 0.01	*0 - 0.1*	0.04 ± 0.01	*0 - 0.13*
	LP	0.02 ± 0.01	*0 - 0.07*	0.02 ± 0.01	*0 - 0.08*	0.02 ± 0	*0 - 0.07*
	LRC	0.01 ± 0.01	*0 - 0.02*	0.01 ± 0.01	*0 - 0.02*	0.01 ± 0.01	*0 - 0.02*

Table 7.4 – Leeward site V_{mean}, V_{max}, H_{rms} and setup within each of eco-geomorphic zones where SLR = 0.0, 0.5 and 1.0. Note that marked spatial variability exists within each zone.

Setup

At the windward site, setup values off the oceanward rim were low (~0 m) and rapidly increased at the oceanward reef crest to 0.39 ± 0.02 m (Figures 7.8 and 7.16; Table 7.3). The magnitude of wave setup decayed across the oceanward reef flat (0.31 ± 0.13 m and 0.29 ± 0.13 m within the oceanward patch and rubble zones respectively) towards the atoll lagoon. Setup was only 0.02 ± 0.02 m within the lagoonward sand zone and 0.01 ± 0.0 m in the lagoonward patch zone.

At the leeward site, a decay in wave setup with distance from the oceanward reef crest was also found, albeit of lower gradient (Figures 7.9 and 7.17; Table 7.4). Indeed, setup was at a maximum at the oceanward reef crest with values of <0.1 m (0.08 ±

0.01 m). Setup gradually decayed across the oceanward environment to 0.06 ± 0.01 m within the dense seagrass zone and 0.05 ± 0.01 m within the oceanward sand zone. This approximate rate of decrease continued toward the lagoonward reef crest where wave setup was ~0.01 ± 0.01 m. If waves were unobstructed, i.e. in the absence of an island, the rate of decrease in wave setup was more rapid (e.g. transect 2; Figure 7.16).

H_{rms}

Converse to the cross-rim gradients in setup, oceanward-lagoonward attenuation of wave height was found at both study sites (Figures 7.10, 7.11, 7.16, 7.17; Table 7.3). The largest wave heights were found at the windward site off the oceanward reef crest (H_{rms} = <1.68 m). H_{rms} decreased rapidly to 0.33 ± 0.04 m within the oceanward reef crest zone, and 0.23 ± 0.09 m and 0.22 ± 0.09 m within the oceanward patch and rubble zones respectively. At the oceanward island shorelines H_{rms} was between ~0.15 m (within the inter-island passages) and 0.35 m. Within the lagoonward environment, H_{rms} was at a maximum at the lagoonward edge of the platform (<0.33 m) and decayed to ~0 m at the lagoonward island shorelines.

At the leeward site, H_{rms} was also at a maximum (<1.31 m) off the oceanward reef crest. H_{rms} similarly decayed with increased distance from the oceanward reef crest (Figure 7.11; Table 7.4): from 0.17 ± 0.06 m within the oceanward reef crest zone, to 0.10 ± 0.01 m, 0.06 ± 0.02 m, and 0.05 ± 0.02 m within the oceanward sparser seagrass, dense seagrass and oceanward sand zones respectively. H_{rms} was lowest within the lagoonward patch zone, albeit with relatively high variability (0.03 ± 0.09 m). However, converse to the oceanward-lagoonward trend, H_{rms} was relatively high within the lagoonward reef crest zone (0.43 ± 0.25 m).

V_{mean}

At the windward site, mean velocity was at a maximum of 1.18 m s^{-1} off the oceanward reef crest (Figures 7.12 and 7.16; Table 7.3). Velocities attenuated rapidly to 0.28 ± 0.05 m s^{-1} (<0.52 m s^{-1}) within the oceanward reef crest zone. Velocities were relatively high across the oceanward reef flat (0.22 ± 0.08 m s^{-1} and 0.19 ± 0.09 m s^{-1} within the rubble and oceanward patch zones respectively) and attenuated toward the atoll lagoon to 0.10 ± 0.07 m s^{-1} in the lagoonward sand zone and 0.08 ± 0.03 m s^{-1} within

the lagoonward patch zone. Velocity increased (<~ 0.75 m s^{-1}) in the passages between islands. The lowest velocities were found off Mainadhoo's lagoonward shoreline (>~0.01 m s^{-1}).

Such trends were largely consistent with those at the leeward site (Figures 7.13 and 7.17; Table 7.4). Indeed, mean velocities were at a maximum on the oceanward reef crest (<47 m s^{-1}) and decreased toward the atoll lagoon, initially rapidly (from 0.22 ± 0.07 m s^{-1} within the oceanward reef crest zone to 0.12 ± 0.01 m s^{-1} within the oceanward sparser seagrass zone) and then more gradually (to 0.11 ± 0.03 m s^{-1} within the oceanward sand zone). The lowest velocities (>~0.01 m s^{-1}) were found off Galamadhoo's lagoonward shoreline. Simiarly, V_{mean} was lowest within the lagoonward patch zone (0.06 ± 0.04 m s^{-1}). Converse to the oceanward-lagoonward trend, a marginal increase in V_{mean} was found in the lagoonward reef crest zone (0.07 ± 0.03 m s^{-1}). An increase in mean velocity was found in the passages between islands (<~0.11 m s^{-1}), albeit less marked than that found at the windward site.

V_{max}

Where maximum velocities were extracted, windward site values were markedly higher comparative to V_{mean} within the oceanward environment at the windward site (Figures 7.14 and 7.16; Table 7.3). Indeed, V_{max} was more than twice that of V_{mean} within both the rubble (0.52 ± 0.22 m s^{-1}) and oceanward patch (0.51 ± 0.25 m s^{-1}) zones. However, the difference between V_{mean} and V_{max} was most pronounced within the oceanward reef crest zone (V_{max} = 1.36 ± 0.28 m s^{-1}). Within the lagoonward environment, V_{max} remained relatively low (0.14 ± 0.11 m s^{-1} and 0.14 ± 0.05 m s^{-1} within the lagoonward sand and patch zones respectively).

At the leeward site, the difference between V_{mean} and V_{max} was, similarly, most pronounced within the oceanward environment (Figures 7.15 and 7.17; Table 7.4). Increases were most marked with closer proximity to the oceanward platform margin, for example, V_{max} = 0.94 ± 0.26 m s^{-1} and 0.46 ± 0.09 m s^{-1} within the oceanward reef crest and oceanward sparser seagrass zones respectively. While, velocities within the lagoonward environment were comparatively low, Vmax was still almost double those of V_{mean}. Consistent with V_{mean}, V_{max} was higher in the lagoonward reef crest zone (0.13 ± 0.07 m s^{-1}) than in the lagoonward patch zone (0.10 ± 0.06 m s^{-1}).

7.3.2.2 Sea-level rise projections

Setup

A decrease in wave setup was found with sea-level rise at the windward and leeward sites (Figures 7.8, 7.9, 7.16 and 7.17; Tables 7.3 and 7.4). Indeed, at the windward site, wave setup was at a maximum toward the oceanward reef crest at 0.27 ± 0.02 m and 0.19 ± 0.01 m with 0.5 m and 1.0 m SLR respectively. Similarly, mean setup was 0.20 ± 0.09 m and 0.15 ± 0.07 m within the rubble zone, and 0.22 ± 0.10 m and 0.17 ± 0.11 m within the oceanward patch zone with 0.5 m and 1.0 m SLR respectively. Within the lagoonward environment, setup remained consistent with mean values of 0.02 m in the lagoonward sand zone and 0.01 m in the lagoonward patch zone.

At the leeward site, setup decreased at relatively consistent rates between sea-level rise scenarios within the oceanward environment. For example, within the oceanward reef crest zone, setup decreased (from 0.08 ± 0.01 m where SLR = 0) to 0.06 ± 0.01 m and 0.04 ± 0.01 m where SLR = 0.5 m and 1.0 m respectively. Likewise, within the dense seagrass zone setup decreased (from 0.06 ± 0.01 m where SLR = 0) to 0.05 ± 0.01 m and 0.04 ± 0.00 m where SLR = 0.5 m and 1.0 m respectively. As at the windward site, setup remained consistent across all SLR scenarios in the lagoonward zones (0.02 ± 0.01 m and 0.01 ± 0.01 m within the lagoonward patch and lagoonward reef crest zones respectively).

H_{rms}

At both study sites, there was a general increase in H_{rms} with sea-level rise (Figures 7.10, 7.11, 7.16 and 7.17; Tables 7.3 and 7.4). At the windward site, maximum wave heights were found within the oceanward reef crest zone and increased in approximately equal increments with sea-level rise (to 0.36 ± 0.05 m and 0.42 ± 0.07 m with 0.5 and 1.0 m of SLR respectively). By contrast, in the remainder of the oceanward environment with 0.5 m SLR, H_{rms} remained broadly consistent within the oceanward patch zone (0.23 ± 0.10 m) and decreased within the rubble zone (0.21 ± 0.1 m). However, slight increases were found where SLR = 1.0: to 0.26 ± 0.10 m within the oceanward patch zone and 0.24 ± 0.10 m within the rubble zone. Converse to the mean trend however, H_{rms} increased with proximity to the oceanward island shorelines by ~0.05 m and ~0.10 m (with 0.5 and 1 m of SLR respectively). Marginal increases

in H_{rms} were also found within the lagoonward environment: to 0.04 ± 0.05 m and 0.07 ± 0.05 m within the lagoonward sand zone, and 0.17 ± 0.07 m and 0.18 ± 0.07 m within the lagoonward patch zone with 0.5 m and 1.0 m SLR respectively.

At the leeward site, the greatest magnitude of change under SLR scenarios was in the oceanward reef crest zone (H_{rms} increased to 0.24 ± 0.08 m and 0.33 ± 0.09 m where SLR = 0.5 and 1.0 respectively). H_{rms} similarly increased across the remainder of the oceanward environment, but the magnitude of increase was less pronounced with increased distance from the oceanward reef crest. For example, within the oceanward sand zone, H_{rms} = 0.08 ± 0.02 m and 0.11 ± 0.03 m where SLR = 0.5 and 1.0 respectively. As at the windward site, the increase in H_{rms} toward island oceanward coasts was more pronounced with sea-level rise (H_{rms} at <~0.11 m and <~0.14 m at Galamadhoo's oceanward shore with 0.5 and 1.0 m SLR respectively). H_{rms} also increased within the lagoonward zones, though the magnitude of increase was less pronounced. Indeed, the average increase was 0.02 m and 0.01 m between SLR scenarios within the lagoonward patch and lagoonward reef crest zones respectively.

V_{mean}

Marginal increases in V_{mean} were found with sea-level rise (Figures 7.12, 7.13, 7.16 and 7.17; Tables 7.3 and 7.4). At the windward site, within the oceanward reef crest zone, V_{mean} increased to 0.29 ± 0.05 m s^{-1} and 0.31 ± 0.05 m s^{-1} with 0.5 and 1.0 m SLR. Similarly, V_{mean} increased by 0.01 m s^{-1} in the oceanward patch zone with each SLR increment. Within the rubble zone a marginal (0.02 m s^{-1}) decrease in V_{mean} was found between 0.5 and 1.0 m SLR. Similarly, V_{mean} increased by 0.01 m s^{-1} (between 0.0 and 0.5 m SLR) within the lagoonward sand zone, but otherwise mean values remained constant.

At the leeward site, V_{mean} generally increased under SLR scenarios. The most pronounced increases were in the oceanward reef crest zone where, on average, V_{mean} increased by 0.02 m s^{-1} with each SLR increment. However, trends were nonlinear and nonuniform. For example, within the OSS zone, average V_{mean} values remained consistent between SLR = 0.0 m and 0.5 m, though increased by 0.01 m s^{-1} where SLR = 1.0. Conversely, within the dense seagrass zone, V_{mean} increased by 0.01 m s^{-1} between SLR = 0.0 m and 0.5 m, though remained consistent where SLR = 1.0. Marginal and variable increases were also found within the lagoonward

environments, for example, within the lagoonward reef crest zone V_{mean} values remained consistent between SLR = 0.0 m and 0.5 m, though increased by 0.01 m s^{-1} where SLR = 1.0.

V_{max}

Differences in V_{max} with SLR were more pronounced, though also notably nonlinear and nonuniform (Figures 7.14, 7.15, 7.16 and 7.17; Tables 7.3 and 7.4). Indeed, at the windward site, V_{max} decreased on the oceanward reef crest to 1.33 ± 0.25 m s^{-1} and 1.24 ± 0.22 m s^{-1} with 0.5 and 1.0 SLR respectively. Conversely, marked increases in V_{max} were found across the remainder of the oceanward environment: to 0.64 ± 0.23 m s^{-1} and 0.70 ± 0.22 m s^{-1} within the rubble zone, and 0.63 ± 0.28 m s^{-1} and 0.67 ± 0.27 m s^{-1} within the oceanward patch zone (with 0.5 and 1.0 m SLR respectively). In the lagoonward environment, increases were also found, but were of greater magnitude within the lagoonward sand zone (0.18 ± 0.12 m s^{-1} and 0.22 ± 0.13 m s^{-1}) than within the lagoonward patch zone (0.15 ± 0.04 m s^{-1} and 0.17 ± 0.04 m s^{-1}). The largest increases within the lagoonward environment were found in the lee of the inter-island passages (<~0.08 m s^{-1} increments).

At the leeward site, the most pronounced increases in V_{max} were found within the platform interior zones (as oppose to reef crest zones). Within the oceanward reef crest zone, average V_{max} values remained consistent between SLR = 0 m and 1.0 m (at 0.94 m s^{-1}). However, where SLR = 0.5, V_{max} increased by 0.02 m s^{-1}, albeit in all cases variability was relatively high. By contrast within the remainder of the oceanward environment, average V_{max} values increased by ~0.09-0.10 m s^{-1} between SLR = 0 and 0.5 m, and ~0.03-0.04 m s^{-1} between SLR = 0.5 and 1 m. In the lagoonward environment, while V_{max} increased within both zones and all SLR scenarios, the average magnitude of increase was largest within the lagoonward patch zone. Consequently, there is a shift in V_{max} gradients: under SLR = 0, V_{max} in the lagoonward reef crest zone (0.13 ± 0.07 m s^{-1}) exceeds that in the lagoonward patch zone (0.10 ± 0.06 m s^{-1}); where SLR = 0.5 m average V_{max} values are approximately equal in the two zones (~0.15 m s^{-1}); and, where SLR = 1.0 m, V_{max} within the lagoonward patch zone (0.18 ± 0.08 m s^{-1}) exceeds that within the lagoonward reef crest zone (0.16 ± 0.09 m s^{-1}).

7.3.3 Sediment Potential Mobility

7.3.3.1 Contemporary process regime

Under contemporary conditions (SLR = 0) with V_{mean}, sediment Potential Mobility (PM) at the windward site was highest on the oceanward reef crest (20.4 ± 13.7%), followed by the rubble (10.3 ± 20.7%) and oceanward patch zones (11.0 ± 23.7%; Figures 7.18 and 7.19; Table 7.5). The high variability was largely due to the high PM values found within the inter-island passages (<100%). Potential mobility was lower in the lagoonward environment with almost no potential mobility (1.5 ± 6.0% and 0.3 ± 0.7% for lagoonward sand and lagoonward patch samples respectively). One exception was in the lee of the passage between Boduhini and Mainadhoo where potential mobility of lagoonward sand was <24%. With V_{max}, potential mobility was 100% across the oceanward reef crest and the majority of the oceanward environment (99.9 ± 0.2% and 99.9 ± 0.2% within the oceanward patch and rubble zones respectively). An exception was the embayment area off the central island transect where PM was ~48%. PM remained low in the lagoonward sand zone (mode = 0%, mean = 8.3 ± 24.7%), but increased in the lee of the inter-island passages to 99% in one instance. Potential mobility of the lagoonward patch zone was greater (23.5 ± 30.2%), albeit markedly lower than that in the oceanward environments.

Texturally, under V_{mean} at the windward site, mobilisable material was of up to medium-coarse grained sand (>~1 ϕ). Across the remainder of the oceanward environment, the largest (potentially) mobilised material was medium-grained sand (>~1-2 ϕ; Figure 7.20). Within the lagoonward zones, only silt-sized sediment could be mobilised. Under V_{max}, very coarse sand could be mobilised across the oceanward zones (>-1 ϕ). In lagoonward environment, up to fine to very fine sand could be mobilised in the lagoonward sand zone (>~3 ϕ) and fine grade sand (>~2.5 ϕ) could be potentially mobilised in the lagoonward patch zone.

At the leeward site, PM was generally lower than that on the windward rim (Figures 7.21 and 7.22; Table 7.6). Indeed, under mean velocities (SLR = 0), PM was 0% across all zones except the oceanward and lagoonward reef crest zones where PM was 1.51 ± 1.27% and 1.73 ± 4.15% respectively. Maximum PM (under SLR = 0 and V_{mean}) was found in the lagoonward reef crest zone where PM attained 15%. With maximum wave velocities, there was a marginal increase in PM within the lagoonward

reef crest zone (to 2.8 ± 5.31%) and maximum PM within the zone remained at 15%. By contrast, there was a marked increase in PM of oceanward sediments. Indeed, PM was 100% across all oceanward reef crest sediments and decreased with distance from the oceanward reef crest zone: from 97.33 ± 8.23% in the oceanward sparser seagrass zone, to 38.27 ± 26.34% in the dense seagrass zone, and finally to 7.67 ± 7.75% within the oceanward sand zone.

Under V_{mean} at the leeward site, only fine sand (>~2.5 ϕ) was potentially mobile in the reef crest zones (Figure 7.23). Under V_{max}, very coarse sand (>~-0.7 ϕ) could be mobilised on the oceanward reef crest. With increased distance from the oceanward reef crest a reduction in the grain size of mobilisable material was found across the oceanward environment. Indeed, in the oceanward sand zone material of up to medium-fine sand (>~2 ϕ) could be mobilised. Within the lagoonward environment, only fine grained material (>~1.8 ϕ) could be mobilised.

Significant relationships were found between benthic sedimentology and contemporary mean wave velocity at each sample location (V_{mean}, SLR = 0.0 m). At the both sites, significant relationships were found between V_{mean} and sediment texture (Figure 7.24), specifically with mean grain size (P = <0.0005, R^2 = 0.51; P = <0.0005, R^2 = 0.38 at the windward and leeward sites respectively) and settling velocity (P = <0.0005, R^2 = 0.63; P = <0.0005, R^2 = 0.33). Compositionally a significant relationship was also found between V_{mean} and CCA concentrations (P = <0.0005, R^2 = 0.56; P = <0.0005, R^2 = 0.33).

7.3.3.2 Sea-level rise projections

At the windward site, with V_{mean}, sediment PM on the oceanward reef crest increased with sea-level rise (27.4 ± 14.6% where SLR = 0.5; 37.9 ± 20.8% where SLR = 1.0; Figure 7.18 to 7.20; Table 7.5). Increased mobility was found with sea-level rise across the remainder of the oceanward environment, however, this was not consistent in magnitude. Indeed, increases in PM were marked between 0.0 and 0.5 m SLR (to 19.2 ± 20.8% and 16.2 ± 22.9% within the rubble and oceanward patch zones), but only marginal between 0.5 and 1.0 m SLR (to 20.4 ± 21.3% and 16.8 ± 23.2%). Conversely, in the lagoonward sand zone, PM decreased marginally to 1.2 ± 4.5% and 0.8 ± 2.1% with 0.5 and 1.0 m SLR. Within the lagoonward patch zone, PM remained at 0% in all cases. Paired t-tests showed increases in PM under V_{mean} to be significant between

both SL-rise increments (between 0 and 0.5 m SLR, P = <0.0005; between 0.5 and 1 m SLR, P = <0.001).

With V_{max}, sediment across the entirety of the oceanward environment attained 100% PM under both sea-level rise scenarios (SLR = 0.5 and SLR = 1.0). Converse to PM under mean velocities, PM in the lagoonward patch zone (22.4 ± 26.4% and 30.6 ± 33.8%) exceeded that in the lagoonward sand (15.0 ± 29.5% and 22.7 ± 38.6%) zone. However, variability remained high largely due to high PM values within the lee of the inter-island passages (<100% in the lagoonward sand zone where SLR = 1.0). Under V_{max}, significant increases were found in PM between both SLR increments (0 to 0.5 m and 0.5 to 1 m, P = 0.025 and P = 0.011 respectively; paired t-tests).

At the leeward site, with V_{mean}, the only sediment to be potentially mobilised under sea-level rise scenarios was in the reef crest zones (Figures 7.21 to 7.23; Table 7.6). Within the lagoonward reef crest zone PM remained consistent with that where SLR = 0 (at 1.73 ± 4.15%, maximum = 15%). Within the oceanward reef crest zone, increases in PM were found, albeit only marginal (1.81 ± 1.69% and 4.31 ± 4.50% where SLR = 0.5 and 1.0 respectively). Under V_{mean}, paired t-tests showed the increase in PM between 0 and 0.5 m SLR not to be significant (P = 0.18). However, increases in PM were highly significant between 0.5 and 1.0 m SLR (P = <0.0005).

By contrast, with V_{max}, the increase in sediment velocities with sea-level rise was substantially more marked than that found at the windward site, particularly within the oceanward environment. PM was 100% with 0.5 and 1.0 m SLR in both the oceanward reef crest and sparser seagrass zones. As under contemporary sea-level scenarios (SLR = 0), PM decreased with increased distance from the oceanward margin. Indeed where SLR = 0.5, PM increased to 81.73 ± 19.90% and 44.87 ± 23.13% within the dense seagrass and oceanward sand zones respectively. Likewise, where SLR = 1.0, PM in the dense seagrass zone attained mean values of 95.27 ± 7.53%, while in the oceanward sand zone mean PM was 86.2 ± 12.15%. By contrast, increases in PM within the lagoonward zones under V_{max} were only marginal. Where SLR = 0.5, PM was 0.64 ± 1.47% and 3.13 ± 6.21% within the lagoonward patch and reef crest zones respectively. Where SLR = 1.0, mean PM within the lagoonward patch zone (5.33 ± 15.38%) exceeded that within the lagoonward reef crest zone (3.83 ± 8.31%), albeit increases were only marginal. More pronounced were the increases in maximum PM

values, the highest of which (60%) was found within the lagoonward patch zone where SLR = 1.0. Under V_{max}, highly significant increases were found in PM between both SLR increments (0 to 0.5 m and 0.5 to 1 m; P = <0.0005 in both cases; paired t-tests).

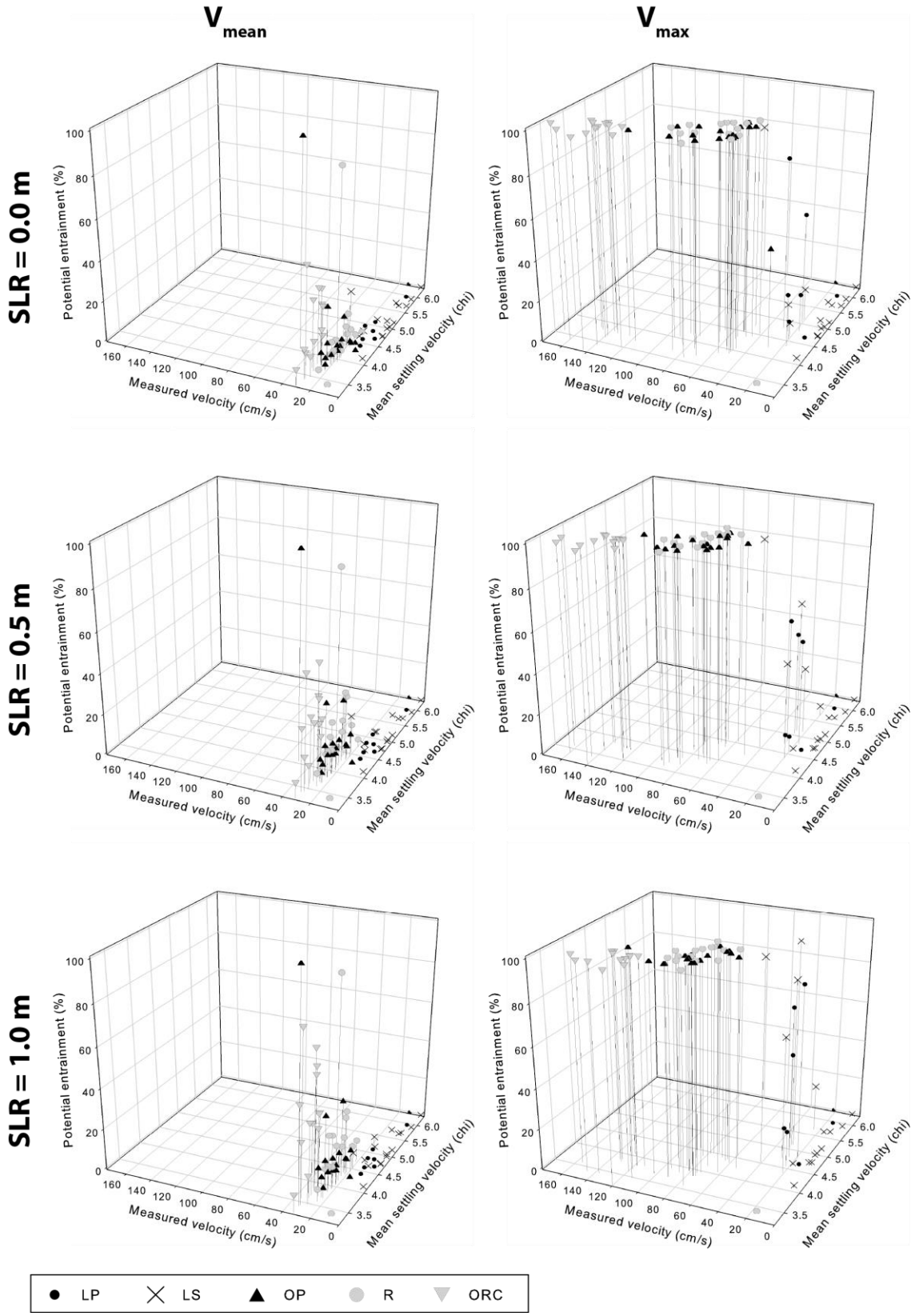

Figure 7.18 – The potential mobility (PM) of windward site sediment samples with both mean (V_{mean}) and maximum (V_{max}) velocities under scenarios of 0.0 m, 0.5 m and 1.0 m SLR where LP = lagoonward patch, LS = lagoonward sand, OP = oceanward patch, R = rubble, and ORC = oceanward reef crest.

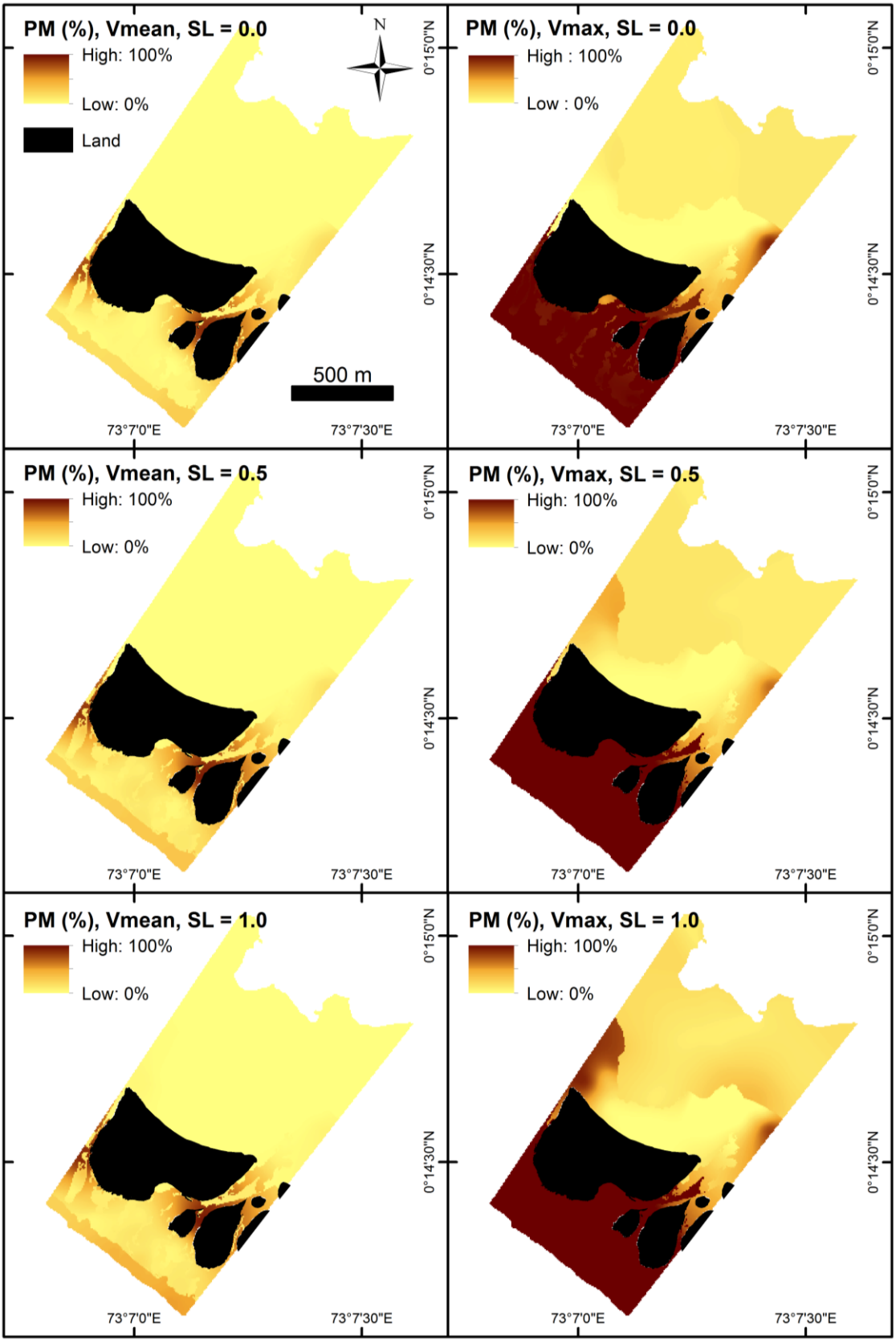

Figure 7.19 – Windward site block kriging results of sediment potential mobility (PM, %) with both mean (V_{mean}) and maximum (V_{max}) velocities under scenarios of 0.0 m, 0.5 m and 1.0 m SLR.

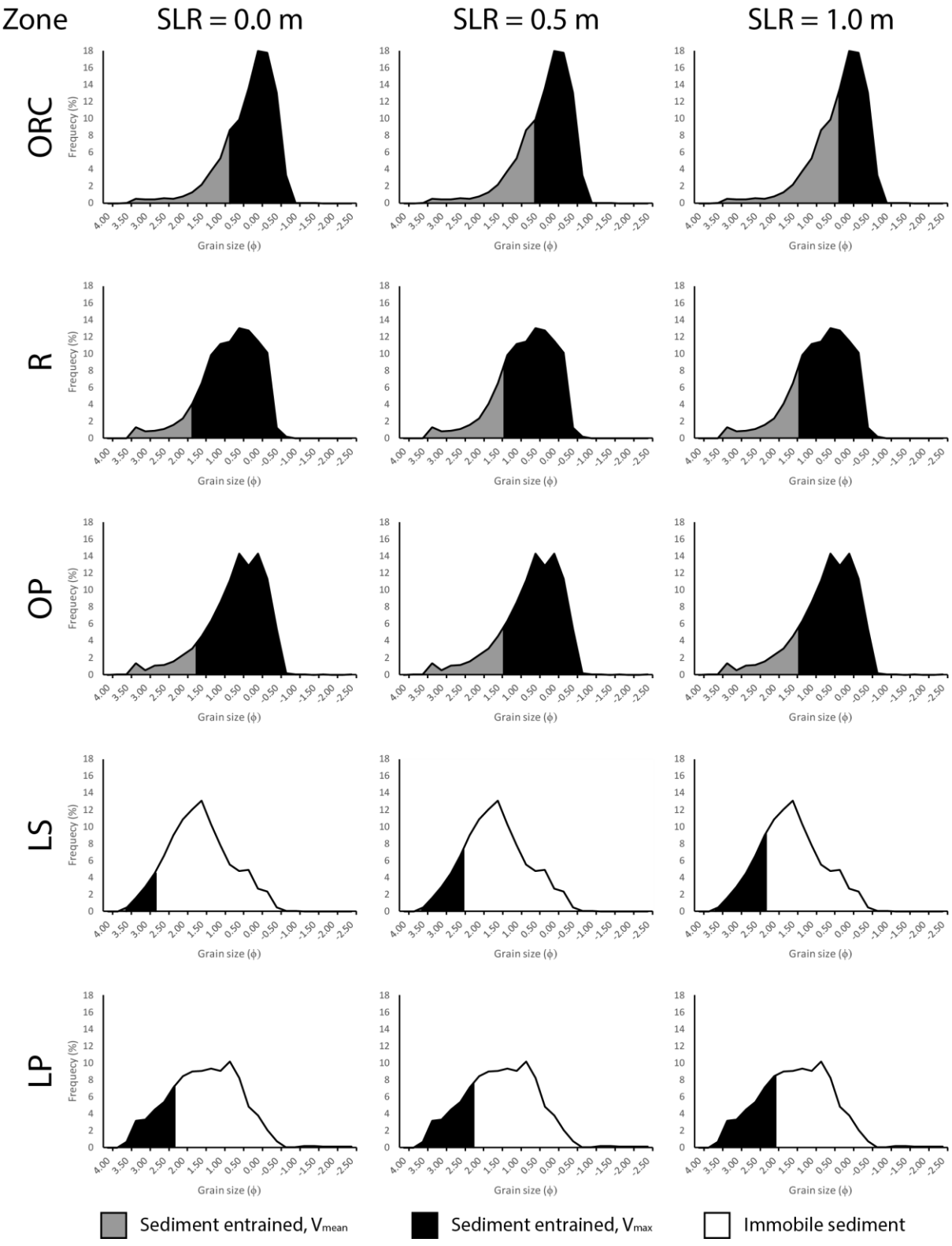

Figure 7.20 – Windward site average grain size distributions of sediment from each eco-geomorphic zone (derived via settling techniques) and average mobilised fractions under V_{mean} and V_{max} where SLR = 0.0 m, 0.5 m and 1.0 m. Note that average values are presented, but there is substantial variability within each zone (Figure 7.20).

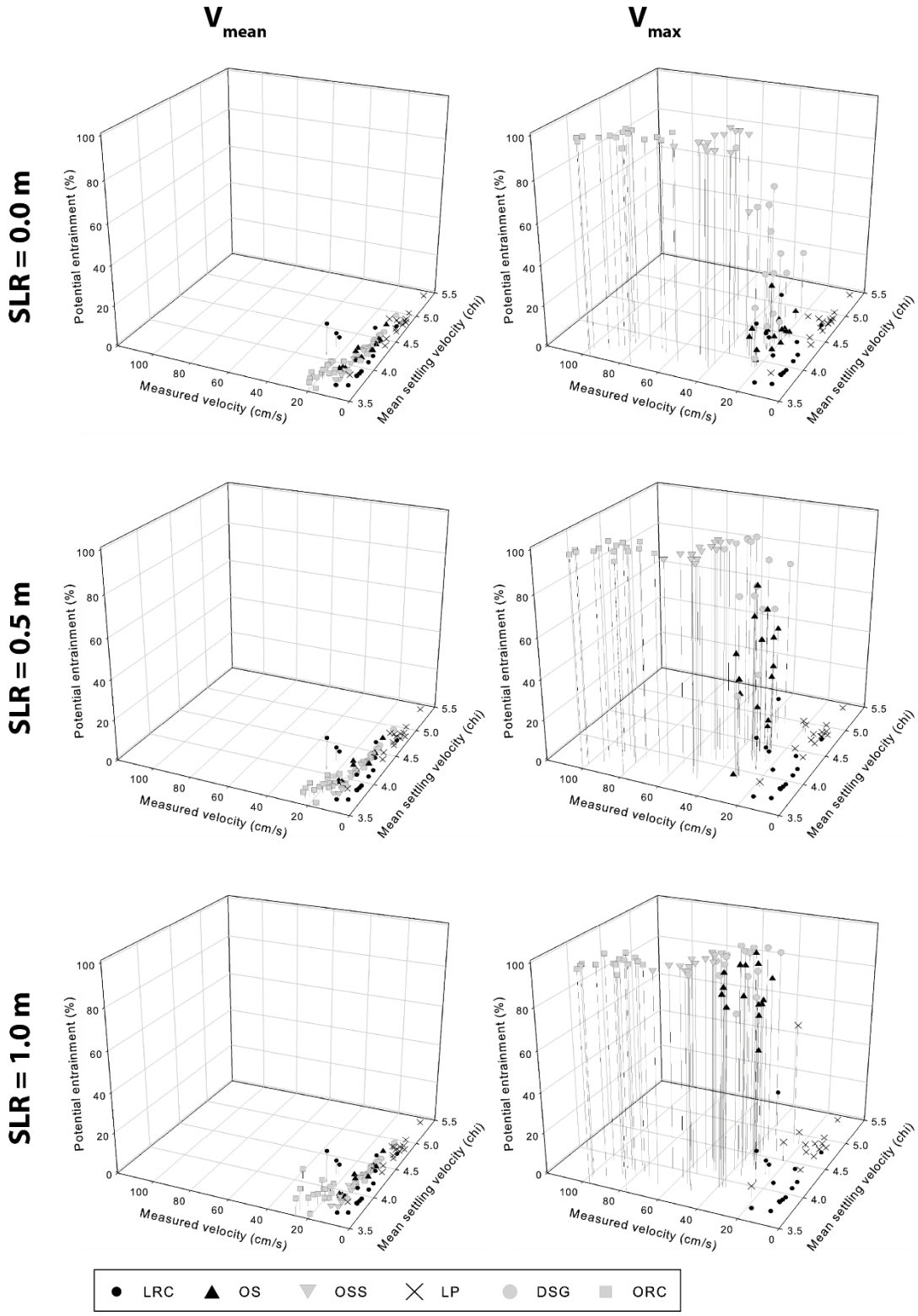

Figure 7.21 –The potential mobility (PM) of leeward site sediment samples with both mean (V_{mean}) and maximum (V_{max}) velocities under scenarios of 0.0 m, 0.5 m and 1.0 m SLR where LRC = lagoonward reef crest, LP = lagoonward patch, OS = oceanward sand, DSG = dense seagrass, OSS = oceanward sparser seagrass, and ORC = oceanward reef crest. Note that axes scales differ to those within Figure 7.18.

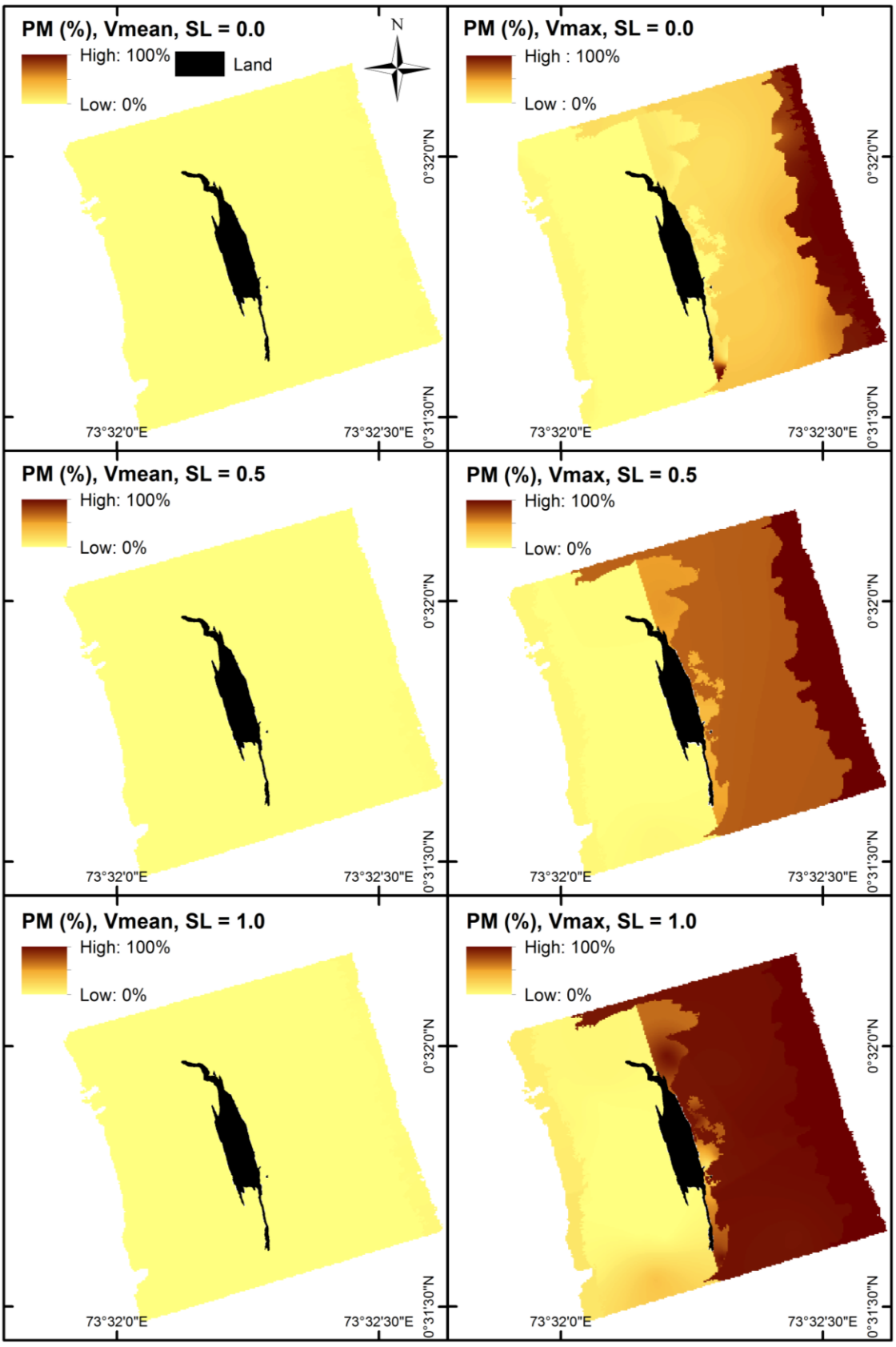

Figure 7.22 – Leeward site block kriging results of sediment potential mobility (PM, %) with both mean (V_{mean}) and maximum (V_{max}) velocities under scenarios of 0.0 m, 0.5 m and 1.0 m SLR.

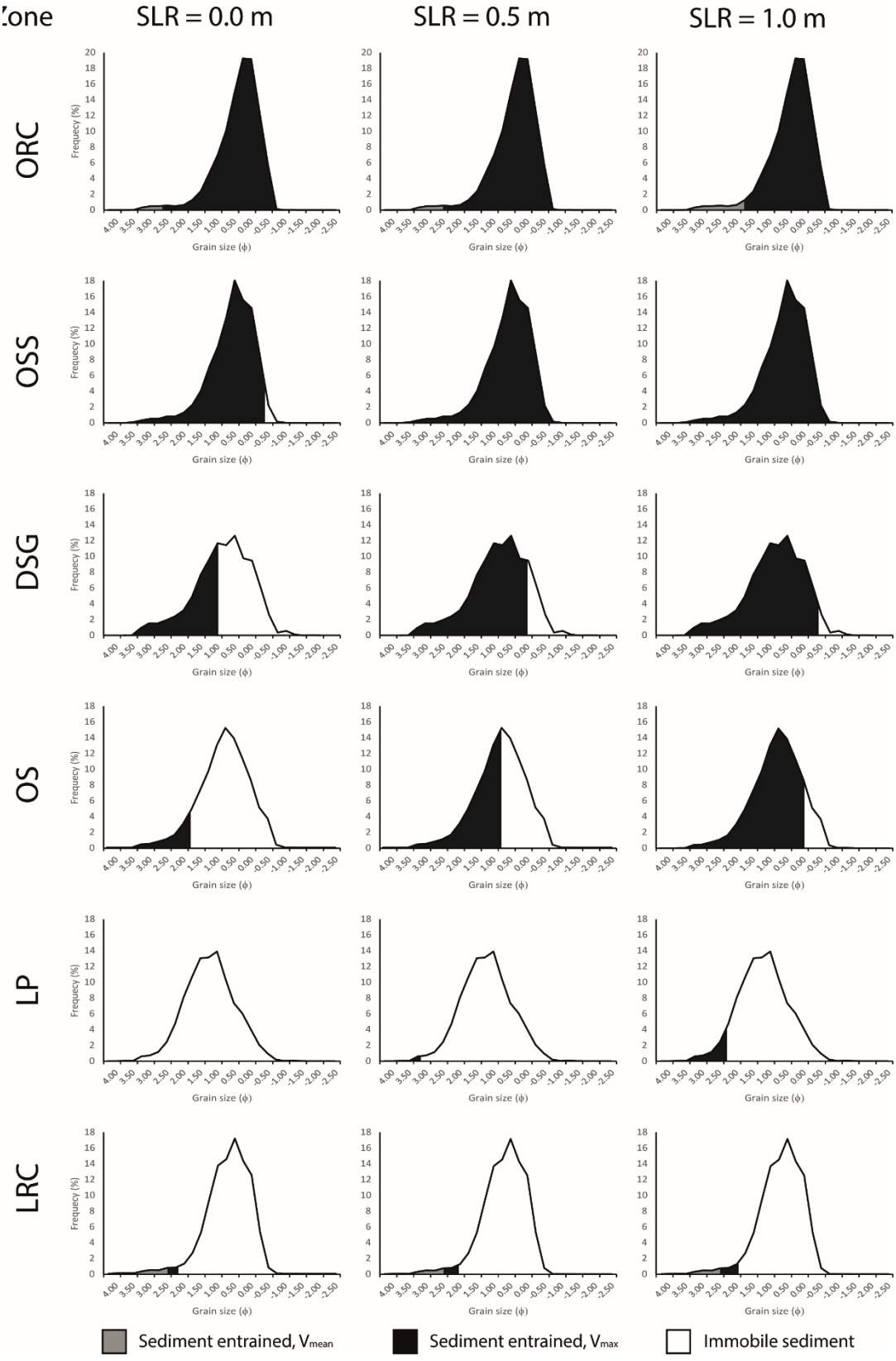

Figure 7.23 – Leeward site average grain size distributions of sediment from each eco-geomorphic zone (derived via settling techniques) and the mobilised fractions under V_{mean} and V_{max} where SLR = 0.0 m, 0.5 m and 1.0 m.

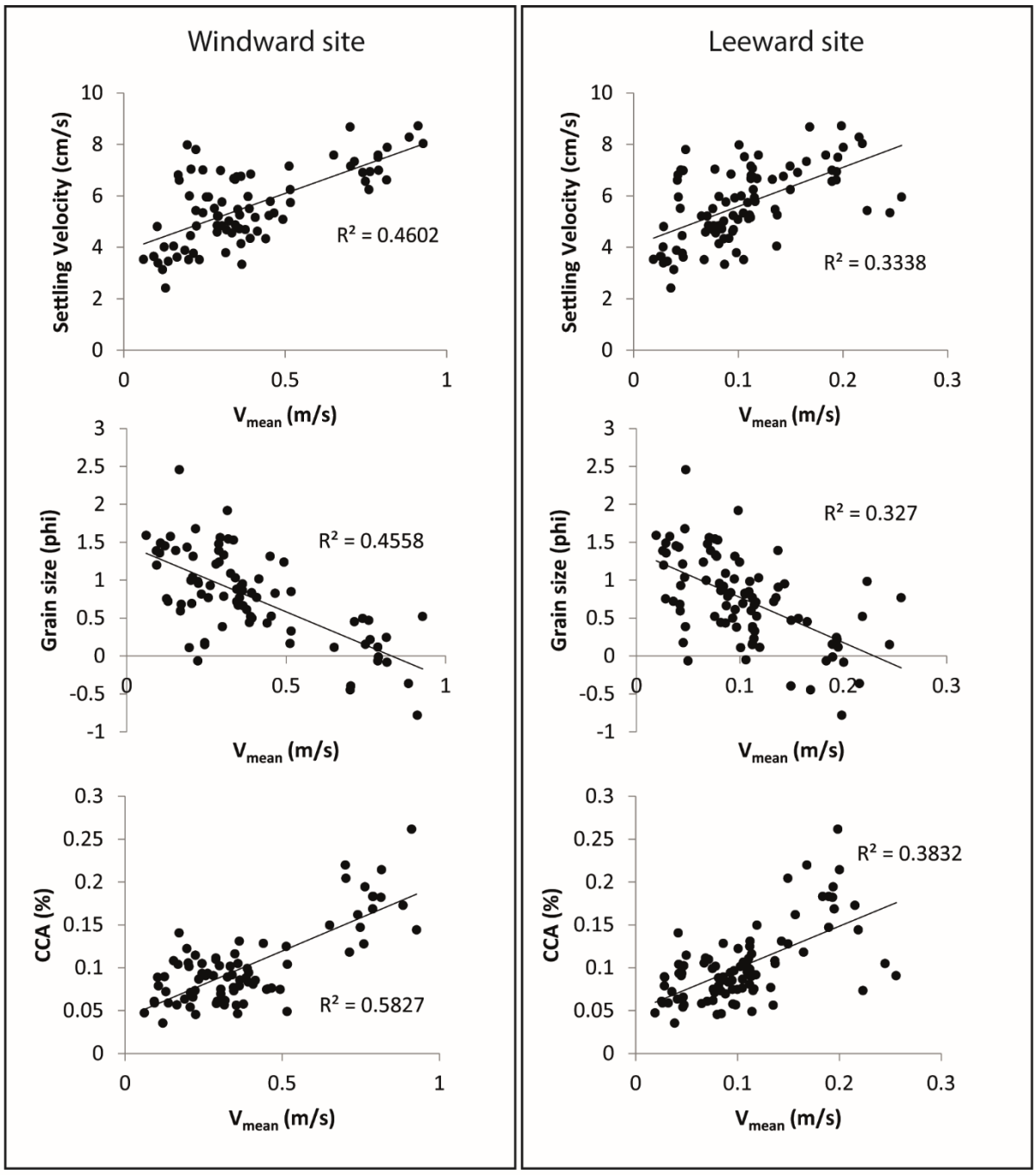

Figure 7.24 – Relationships between benthic sedimentology and contemporary mean velocities (SLR = 0).

	SLR = 0.0		SLR = 0.5		SLR = 1.0	
Zone	V_{mean}	V_{max}	V_{mean}	V_{max}	V_{mean}	V_{max}
ORC	20.4 ± 13.7	100 ± 0	27.4 ± 14.6	100 ± 0	37.9 ± 20.8	100 ± 0
	2 - 51	*100 - 100*	*7 - 54*	*100 - 100*	*8 - 80*	*100 - 100*
R	10.3 ± 20.7	99.9 ± 0.2	19.2 ± 20.8	100 ± 0	20.4 ± 21.3	100 ± 0
	0.5 - 84	*99.5 - 100*	*3 - 89*	*100 - 100*	*5 - 93*	*100 - 100*
OP	11 ± 23.7	96.9 ± 12.6	16.2 ± 22.9	100 ± 0	16.8 ± 23.2	100 ± 0
	0 - 100	*48 - 100*	*0 - 100*	*100 - 100*	*0 - 100*	*100 - 100*
LS	1.5 ± 6	8.3 ± 24.7	1.2 ± 4.5	15 ± 29.5	0.8 ± 2.1	22.7 ± 38.6
	0 - 24	*0 - 99*	*0 - 18*	*0 - 99.5*	*0 - 7*	*0 - 100*
LP	0.3 ± 0.7	23.5 ± 30.2	0 ± 0	22.4 ± 26.4	0 ± 0	30.6 ± 33.8
	0 - 2	*0 - 83*	*0 - 0*	*0 - 60*	*0 - 0*	*0 - 85*

Table 7.5 – Potential Mobility (PM, % – mean ± 1 S.D., ranges in italics) of sediment from each eco-geomorphic zone at the windward site.

	SLR = 0.0		SLR = 0.5		SLR = 1.0	
Zone	V_{mean}	V_{max}	V_{mean}	V_{max}	V_{mean}	V_{max}
ORC	1.51 ± 1.27	100 ± 0	1.81 ± 1.69	100 ± 0	4.31 ± 4.5	100 ± 0
	0 - 4	*100 - 100*	*0.5 - 5.5*	*100 - 100*	*0.5 - 18*	*100 - 100*
OSS	0 ± 0	97.33 ± 8.23	0 ± 0	100 ± 0	0 ± 0	100 ± 0
	0 - 0	*68 - 100*	*0 - 0*	*100 - 100*	*0 - 0*	*100 - 100*
DSG	0 ± 0	38.27 ± 26.34	0 ± 0	81.73 ± 19.9	0 ± 0	95.27 ± 7.53
	0 - 0	*4 - 95*	*0 - 0*	*40 - 100*	*0 - 0*	*76 - 100*
OS	0 ± 0	7.67 ± 7.75	0 ± 0	44.87 ± 23.13	0 ± 0	86.2 ± 12.15
	0 - 0	*1.5 - 30*	*0 - 0*	*0 - 83*	*0 - 0*	*54 - 100*
LP	0 ± 0	0 ± 0	0 ± 0	0.64 ± 1.47	0 ± 0	5.33 ± 15.38
	0 - 0	*0 - 0*	*0 - 0*	*0 - 5*	*0 - 0*	*0 - 60*
LRC	1.73 ± 4.15	2.8 ± 5.31	1.73 ± 4.15	3.13 ± 6.21	1.73 ± 4.15	3.83 ± 8.31
	0 - 15	*0 - 15*	*0 - 15*	*0 - 20*	*0 - 15*	*0 - 30*

Table 7.6 – Potential Mobility (PM, % – mean ± 1 S.D., ranges in italics) of sediment from each eco-geomorphic zone at the leeward site.

7.4 Discussion

7.4.1 Wave processes

7.4.1.1 Contemporary process regime

Coral reefs are among the best submerged breakwaters provided by the natural world (von Arx, 1948). This is evidenced at both study sites by the marked dissipation of wave energy at the oceanward reef crest, and broad cross-rim attenuation of wave

energy. Wave heights may be employed to calculate wave energy (WE, J) using the equation:

$$WE = \frac{1}{16}\,\rho g H_{m0}^2$$

where ρ = the density of seawater (1030 kg m^{-3}), g = gravitational acceleration (9.81 ms^{-2}), H_{m0} = significant wave height, which is approximately 1.4 times H_{rms} (Holthuijsen, 2007). Hence, at the windward site, wave energy decreased by ~96% between the ocean (off-rim) and the oceanward reef crest zone. Between the oceanward reef crest zone and the remainder of the oceanward environment, wave energy decreased by ~51% and was a further ~50% lower within the lagoonward sand zone. Similarly, at the leeward site, wave energy decreased by ~98% between the ocean (off-rim) and oceanward reef crest zone. Wave energy then reduced by an additional ~91% between the oceanward reef crest and oceanward sand zones. Such spatial gradients are consistent with prior studies, which have reported that 72-97% of incident wave energy is dissipated at the reef crest (Roberts et al., 1992; Lee and Black, 1978; Gourlay, 1994; Hardy and Young, 1996; Brander et al., 2004). Dissipation of wave energy results from both bottom friction and wave breaking (Gerritson, 1981) whereby the relative importance of wave breaking (as oppose to bottom friction) in wave energy dissipation increases with larger waves (Gourlay, 2011). The abrupt change in depth found at the oceanward perimeters of oceanic atolls is associated with a concentrated zone of energetic wave breaking.

Similarly, there was an oceanward-lagoonward cross rim decrease in wave setup, V_{mean} and V_{max} across the rim, which decreased by ~95%, ~64% and ~90% between the oceanward reef crest and lagoonward sand zones respectively at the windward site. Likewise, between the oceanward reef crest and lagoonward patch zone at the leeward site, wave setup, V_{mean} and V_{max} decreased by ~75%, ~72% and ~89%. The leeward site differs from the windward site in that parameters increase between the lagoonward patch and lagoonward reef crest zones, which is likely due to the greater significance of lagoonward wind-driven waves at this site (Chapter 2). Nonetheless, this study highlights the role of the atoll rim as an effective dissipater of oceanward wave energy.

The cross-rim gradients found in this study are consistent with the wave pump analogy (e.g. Bruun and Viggoson, 1977). At the scale of an atoll rim platform, the analogy

regards the waves breaking at the oceanward reef crest as a pump that lifts water from the ocean and discharges it across the reef flat. The water then drains into the lagoonward environment, creating a water level gradient and gravity driven flow across the platform (Callaghan et al., 2006). Water thus flows over the leeward reef edge and into the atoll lagoon. Field surveys and models have shown the process to intensify with greater inputs of wave energy (Callaghan et al., 2006). Hence, the analogy is particularly useful in exposed settings such as atoll rim environments. Furthermore, the analogy is most effective on steep-faced reefs with elevations close to MSL, as is the case at both the windward and leeward study sites (Gourlay, 2011.; Nielsen, 2009). The larger waves within the oceanward environment are also mirrored in platform bathymetry as the oceanward platform elevation is higher than that of the lagoonward environment at both study sites (Samosorn and Woodroffe, 2008). This was particularly notable at the windward site where cross-rim oceanward-lagoonward gradients were more pronounced.

In addition to the examination of cross-platform gradients, two-dimensional model-based approaches allow elucidation of the spatial variability in wave transformation across the entirety of each study site. Such data (Figures 7.8 to 7.17; Tables 7.3 and 7.4) highlight the nonuniformity of wave processes. In particular, wave diffraction and refraction around reef islands is evident with the orientation of wave vectors toward lagoonward island shorelines. The area immediately leeward of islands is thus highlighted as a zone of wave convergence and in turn, potentially, sediment deposition. Such focal points have been invoked as fundamental to reef island existence, location and stability (Gourlay, 1988; Mandlier and Kench, 2012). Notably, this convergence was most pronounced at the leeward site, which corroborates with more recent lateral lagoonward island accretion (Chapter 3, section 3.4.3.2). Chapter 5 invoked the assumption that the more recent lateral lagoonward accretion of reef islands was derived from lagoonward sediment sources. However, model outputs suggest that this is not necessarily the case and that oceanward environments may also contribute to lagoonward accretion.

7.4.1.2 Sea-level rise projections

Sea-level rise (SLR) was generally associated with a decrease in wave setup, and increases in both wave heights and velocities. This is consistent with prior work which

has suggests SLR on reef flats will result in increased wave heights (Lugo-Fernandez et al., 1998; Brander et al., 2004; Kench and Brander, 2006; Ogden and Field, 2010; Péquignet et al., 2011; Storlazzi et al., 2011). Likewise, as a function of wave attenuation, prior research has projected setup to decrease with SLR (Gourlay, 1994; Vetter et al., 2010; Becker et al., 2014), with the exception of Storlazzi's (2011) study. This is because greater water depths enable a larger proportion of incident wave energy to propagate onto reef flats. In some instances, this may allow larger waves to cross the reef crest without breaking and greater energies to leak onto the reef platform surface (Brander et al., 2004; Kench et al., 2009c). In addition, SLR would decrease hydrodynamic roughness relative to water depth and thus rates of H_{rms} and velocity attenuation would also reduce (Storlazzi et al., 2011).

Reductions in wave setup could suggest that SLR may be offset on reef platforms. However, the decrease in setup has previously been demonstrated, using field data from the Marshall Islands, to be smaller than the magnitude of sea-level rise (e.g. Quataert et al., 2015). Indeed, setup has been found to decrease at approximately half the rate of sea-level rise (Becker et al., 2014). While variability in the decrease in setup was found in this study, in all cases its reduction was of a smaller magnitude than that of SLR (e.g. reductions were of <~0.2 m with SLR of 1.0 m). Hence, the relative magnitude of this negative feedback is insufficient to offset sea-level rise on reef platforms, though it will serve to reduce rates of sea-level rise in such settings.

Although broad trends exist in the data, changes in wave processes with SLR were notably nonuniform and nonlinear. That is, the magnitude of change varied both spatially and between SLR projections (Figures 7.8 to 7.17; Tables 7.3 and 7.4). For example, while intra-zone variability was high, between 0.0 m and 1.0 m SLR at the windward site, mean V_{max} increased by ~0.18 m s^{-1} within the oceanward patch zone, but decreased by ~0.12 m s^{-1} within the oceanward reef crest zone. In addition, the increase in mean V_{max} was three times greater between 0.0 and 0.5 m SLR (0.51 to 0.63 m s^{-1}) than that from 0.5 to 1.0 m SLR (to 0.67 m s^{-1}). Similarly, at the leeward site, increases in V_{max} were marginal on the reef crests (between 0.0 m and 1.0 m SLR, mean V_{max} was remained consistent on the oceanward reef crest and increased by 0.03 m s^{-1} on the lagoonward reef crest). However, increases were most pronounced within the remainder of the oceanward environment, for example in the oceanward sand and dense seagrass zones, V_{max} increased by ~0.14 m s^{-1} between

0.0 and 1.0 m SLR. This contrasts with widely-held assumptions that wave energy will increase linearly with SLR (e.g. Ferrario et al., 2014; Quataert et al., 2015). Rather, this chapter highlights the nonlinear and complex nature of atoll rim process regimes.

7.4.2 Sediment Potential Mobility

Under the contemporary process regime (SLR = 0.0), there was minimal potential for sediment mobility where mean velocities were considered. Indeed, at the leeward site, maximum PM was 15% and average PM was 0.54 ± 1.89%. At the windward site, PM was slightly higher, particularly at the oceanward reef crest (20.4 ± 3.4%) and maximum values were found in the inter-island passages (<100%). Nonetheless, mean PM across the windward site was also relatively low at 9.5 ± 2.0%. Extracting the maximum velocities reveals active sediment transport occurs at both sites, even under fair-weather scenarios. Notably, mobilised material comprised predominantly sand-sized sediments (Figures 7.20 and 7.23), which are of an appropriate grade to contribute to reef island building (Chapter 3). Hence, the dynamic nature of reef island systems is highlighted. This is consistent with prior work on PM at Vabbinfaru (interior) reef platform (North Malé Atoll, Maldives; Morgan and Kench, 2016b) and Cocos Keeling (Kench, 1998a).

Examining spatial variability in PM enables the delineation of contemporary sediment transport pathways along gradients from high to low PM (Kench, 1998a). Gradients are reflective of shifts in both wave velocity and sediment texture. At the windward site under mean velocities, benthic sediment remains predominantly immobile. However, transport occurs from the oceanward reef crest (20.4 ± 13.7%) into the remainder of the oceanward environment. Material is then transported from the oceanward environment (10.3 ± 20.7% and 11.0 ± 23.7% PM in the rubble and oceanward patch zones respectively), through inter-island passages (<100%) and into the lagoonward environment where sediment is transported in the lee of the inter-island passages (<24%).

Under maximum velocities, there is greater potential for sediment mobility. Sediment is transported from the oceanward environment (PM = ~100%), along inter-island passages (PM = ~100%), and into the lagoonward sand zone (PM = 8.3 ± 24.7%). The lagoonward sand zone remains predominantly immobile and thus represents a depositional sink. However, in the lee of the inter-island passages, sediment is

transported from the lagoonward send zone into the lagoonward patch zone (PM = <99%). There is also evidence that material may also be transported (along gradients of higher to lower PM) from the lagoonward patch to the lagoonward sand zone, particularly in the lee of Mainadhoo island (e.g. profile 1, Figure 7.16). Additional evidence of lagoonward patch to lagoonward sand zone transport includes the higher PM within the lagoonward patch zone (23.5 ± 30.2%), sediment mobilised within the lagoonward patch zone is of a larger grain size than that mobilised in the lagoonward sand zone (Figure 7.23), and wave energy vectors within the central component of the zone (albeit short) are orientated towards Mainadhoo island (Figure 7.12). This also this supports the suggestions within Chapter 3 that the lagoonward patch zone represents a sediment source for island building and maintenance.

The one exception to the near-unanimously high PM values across the oceanward environment, is in the embayment area off the central transect where PM = 48%. This is consistent with shoreline geomorphology as this is the only portion of the oceanward coastline to be composed of sand-sized sediments, while the remainder of the oceanward island margins were comprised reef rubble and coral boulders (section 3.3.1). Lower PM suggests sediment deposition may occur within the embayment areas. Hence, sediment PM analysis provides support for the process of embayment infilling within the windward site model of island development (section 3.4.3.2) and also observed in other regions with similar island geomorphology (Kench et al., 2015). However, the key sediment transport pathway at the windward site is evidently from the oceanward reef crest toward the atoll lagoon and, hence, while potential mobility analysis is able to shed additional light on the nature of sediment transport, the findings of this Chapter this corroborates with those inferred from sedimentology (Chapter 4).

Under mean velocities at the leeward site, the only potentially mobilised sediment was found within the reef crest zones. This suggests sediment may be transported towards the platform interior, though mean values were low in both cases (PM = 1.51 ± 1.27%, 1.73 ± 4.15% on the oceanward and lagoonward reef crests respectively). Notably, maximum PM was markedly higher at the lagoonward (<15%) than the oceanward reef crest (<4%), which was primarily a function of wave energy, rather than grain size. Indeed, wave energies at the mobilised sample locations were also at a maximum (<0.26 m s^{-1}). Hence, results are consistent with the evidence presented within

Chapter 4 that the leeward site is characterised by the intersection of lagoonward and oceanward wave energies.

As at the windward site, sediment PM was also higher under V_{max} at the leeward site. Interestingly, while sediments within the lagoonward reef crest zone attained the highest PM values under V_{mean}, mean PM remained low (2.80 ± 5.31%) and maximum values remained consistent at 15% under V_{max}. By contrast, increases in PM were far more pronounced within the oceanward environment (<100%). Within the oceanward environment, proportions of mobilisable sediment decrease with increased distance from the oceanward reef crest. Sediment transport thus likely occurs (along gradients of high to low PM) from the oceanward reef crest towards the oceanward sand zone. No mobilisable material was found within the lagoonward sand zone and PM was relatively low within the oceanward sand zone (7.67 ± 7.75%), which is consistent with the suggestions within Chapter 4 that these zones are characterised by preferential deposition. Similarly, this is consistent with sediment storage data as depths were greatest within these zones (Table 4.12).

The overriding trend is of increased sediment mobility with SLR and significant increases in PM were found in all cases. However, the nonlinearity and nonuniformity of the shifts in wave processes with SLR, are mirrored in changes in sediment PM. Indeed, marked inter- and intra-site variability was found in the magnitude of change. For example, within the lagoonward sand zone at the windward site, PM remained low (under V_{max} where SLR = 1.0 m, mode = 0%), with the exception of the areas in the lee of the inter-island passages whereby, in one instance PM increased from 0% (SLR = 0.0) to 100% (SLR = 1.0). Moreover, in 4 cases, there was a decrease in PM between SLR = 0.0 and SLR = 1.0 at the windward site (<32%). Likewise, at the leeward site, PM within the lagoonward reef crest zone remained relatively low across all SLR scenarios (<3.83 ± 8.31%). By contrast, increases in PM within the oceanward were sufficient to shift the zone from one of preferential deposition (under V_{max} SLR = 0.0, PM = 7.67 ± 7.75%) to preferential sediment transport (under V_{max} SLR = 1.0, PM = 86.20 ± 12.15%). Furthermore, the increase in sediment PM at the leeward site was substantially more marked than at the windward site. This is likely given the highly exposed nature of the windward setting means that PM is already almost uniformly at 100% (under V_{max} where SLR = 0.0 m) across the oceanward environment and there is therefore minimal potential for further increases. Hence, this highlights that reef

island responses to future environmental change are likely to be diverse even at the scale of an individual atoll.

7.4.3 Geomorphic implications

A crucial consequence of increases in wave velocity and height is the associated increase in wave energy received at island shorelines, which is consistent with the findings of Ogston and Field (2010), Storlazzi et al., (2011), and Beetham et al. (2016). Conceptually, this is expressed in Kench and Brander's (2006b) reef energy window index which is calculated by dividing mean reef flat water depth at high tide by reef flat width. The temporal window within which sediment entrainment and geomorphic activity occurs is thus invariably lengthened with increased water depths.

The approach presented focuses solely on benthic sediments and thus, so as not to invoke a 'bathtub' approach, assumes that no changes will occur in island morphologies. However, reef islands are not morphologically passive entities, but are dynamic landforms that will continually adjust with the shifts in the process regime (e.g. Beetham and Kench, 2014). SLR, and associated shifts in hydrodynamics and sediment mobility, will move reef islands out of their current dynamic equilibrium with the contemporary process regime. Indeed, data in Chapter 4 showed that island sediment characteristics represented a part of the oceanward-lagoonward continuum in sediment characteristics. With increased sediment potential mobility, this continuum will likely change and a new equilibrial continuum may develop. Alternatively, if an equilibrium, does not develop, SLR may mark a shift to a period of heightened island mobility and instability.

Higher wave energies are likely to increase rates of coastal erosion and therefore provide an input of sediment to the marine environment. Indeed, Storlazzi et al. (2011) suggest that increased wave heights and velocities would increase rates of coastal erosion at Molokai, Hawaii. Conversely, with increases in benthic PM, islands may be recipients of increased volumes of sediment meaning that shoreline accretion may occur. Notably, the mobilised sediment was predominantly sand-sized material (Figures 7.20 and 7.23) and thus of an appropriate grade to contribute to island building (Chapter 3). Indeed, Sheppard et al. (2005) examined fringing reefs in the Seychelles following mortality (<95%) associated with the 1998 bleaching event. Disintegration of coral framework increased water depths creating conditions of

pseudo-SLR. In this case, complex patterns of both accretion and erosion were found on island shorelines.

While island sediment movement was not investigated directly, by examining results from benthic sediment samples, a conceptual model of reef island trajectories may be proposed (Figure 7.25). Indeed, benthic areas of preferential sediment storage may evidently shift to preferential transport (such as found within the oceanward sand zone at the leeward site). Areas where PM remains low may thus become the recipients of greater volumes of sediment. This shift in the benthic environment may also apply to reef island sediment storage whereby areas of current island sediment storage may become areas of preferential transport, hence erosion will likely occur along such shorelines. Island erosion will provide an input of sediment into the marine environment, which (along with mobilised benthic sediments) may either be exported off-rim or be stored on the platform surface in areas where PM remains low. This deposited material may either remain below MSL as a benthic deposit, or it may attain elevations above MSL hence contributing either to new island formation and/or accretion of the existing islands.

Potential island accretion may occur via two key mechanisms. Firstly, roll-around as areas immediately oceanward of reef islands become areas of increased sediment mobility (i.e. preferential transport) and areas immediately lagoonward of the island shorelines remain areas of low sediment mobility (i.e. preferential deposition). Hence, as material is removed from the oceanward areas and deposited at lagoonward shorelines, island lagoonward migration will likely occur. Secondly, island accretion may be facilitated by the process of rollover whereby material from the oceanward coast is eroded and deposited towards the lagoon (Woodroffe et al.,1999). This may result in both horizontal and vertical accretion and also contribute to island lagoonward migration.

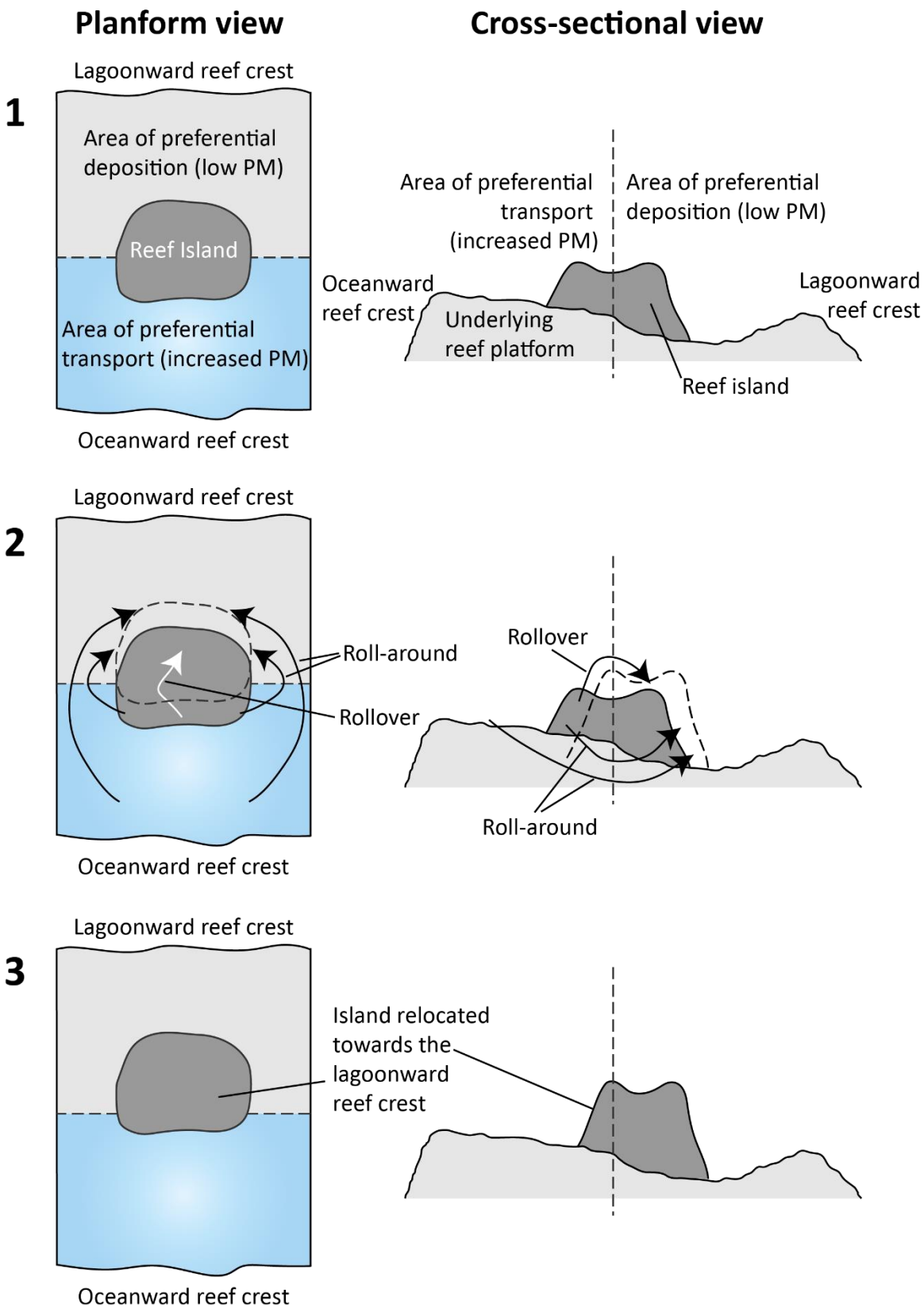

Figure 7.25 – Conceptual model of potential rim reef island morphological response to shifts in sediment potential mobility. For illustrative purposes, cross-sectional diagrams are substantially vertically exaggerated.

Processes of island roll-around and rollover would likely be most prevalent at the leeward site. This is because the increase in PM at the leeward site is of greater magnitude with shifts from characteristically low PM (SLR = 0.0 m) to high PM found within the dense seagrass and oceanward sand zones under conditions of SLR. By contrast, at the windward site, PM is already close to 100% across the oceanward environment, with the exception of the embayment area off the island's central transect from which sand-sized material would likely be removed. Hence, leeward islands may become more mobile under conditions of SLR than their windward counterparts. However, at the windward site, mean island elevations of Mainadhoo, Boduhini and Kudahini were 0.81 ± 0.02 m, 0.81 ± 0.01 m and 0.82 ± 0.04 m above MSL respectively. Under scenarios of 0.5 m SLR, island inundation would occur at hightide (+~0.5 m). Vertical island accretion, likely via rollover, would therefore be necessary to sustain future reef island existence at this site.

Prior research on reef island morphological responses to sea-level rise provides support for the conceptual island rollover and roll-around model. In early reef island research, Stoddart and Steers (1977) suggested lagoonward migration, and concurrent oceanward erosion, may be a universal feature of reef islands. Stoddart et al. (1982) also reported lagoonward migration of islands in response to sea-level rise in Belize. Subsequent analyses of reef island evolution, have demonstrated a suite of possible morphological shifts in island shorelines (e.g. Webb and Kench, 2010; Kench et al., 2015). However, Kench and Cowell (2001a; 2001b) simulated island responses to sea-level rise and found that in all scenarios islands receded from the reef edge. While a variety of other morphological responses were found, rollover was prevalent particularly where islands were of low elevation and narrow. Rollover in this instance comprised both vertical accretion with deposition on the island surface and also lateral transfer of material to the lagoonward shoreline (i.e. termed roll-around in this thesis).

Remote analyses of island shorelines also provide support for projections of island lagoonward migration under sea-level rise scenarios. For example, at Funafuti Atoll, which has experienced some of the highest rates of sea-level rise (~5.1 ± 0.7 mm yr^{-1}), the predominant direction of island migration was toward the atoll lagoon (n = 29; Kench et al., 2015). However, in some cases, on leeward rim aspects, islands

migrated oceanward. Furthermore, under conditions of sea-level rise in the central Pacific, net island lagoonward migration was found in >65% of cases (n = 27; Webb and Kench, 2010). In addition, the long-term adjustments of reef islands at Nadikdik Atoll, Marshall Islands, following a typhoon in 1905 (i.e. following higher wave energies) were examined and island lagoonward migration was found in 10 cases (of <100 m; Ford and Kench, 2014).

Notably, there are striking parallels between the suggestions of both former (Chapter 3, section 3.4.3.2) and future island rollover and roll-around. Indeed, roll-around and rollover were identified as key mechanisms in reef island development at the present study sites, as primarily controlled by higher than present sea-levels associated with the mid-Holocene sea-level highstand (Kench et al., 2009b). Likewise, it was suggested that in island formation, the leeward islands were more mobile than their windward counterparts (section 3.4.3.2). This is echoed in the suggestion that, with future sea-level rise, leeward islands may experience greater rollover and roll-around than windward islands. Hence, results of sediment PM analysis provide support for the suggestion that sea-level rise could lead to a reactivation of the process regime responsible for reef island formation with the reopening of the high energy window.

7.4.4 Methodological considerations and further work

This Chapter presents a first step in developing an approach to project future sediment mobility across reef platforms. However, it is pertinent to note that there are caveats that must be borne in mind and, in turn, there are several ways in which this work could be developed in future research. For example, the approach is predominantly focused upon the physical process regime, but biological processes may also alter sediment transport pathways. In particular, the role of seagrass in reducing wave energies was not included in wave energy modelling (as in the majority of reef top wave modelling studies) and it is therefore likely wave velocities and, in turn, sediment PM have been overestimated. In addition, as seagrass roots can bind and trap sediment, sediment PM within seagrass zones may be further reduced.

In considering rollover and roll-around as possible landform trajectories, it is pertinent to note that PM estimations relate to the material currently stored on the in the system. However, with increased mobility, the grade of sediment storage will change (e.g. Figures 7.20 and 7.23). The projected heightened levels of sediment mobility material

will only continue if there is continual production of sediment of that grade. If sediment storage is not replenished, island resilience will be contingent upon the adjustment of a finite volume of sediment, which could render reef islands more vulnerable to environmental change (McKoy et al., 2010).

Another caveat to the approach is that sea-level (i.e. bathymetry) was the sole variable altered in investigation of SLR scenarios. There was thus no consideration of possible shifts in boundary conditions as a consequence of future environmental change. However, climate change may alter both H_S and T_S. Indeed, both H_S and mean wave period (T_M) have been projected to decrease within the central Indian Ocean (Hemer et al., 2013). Moreover, the largest increases in wave activity have been projected within the Southern Ocean. This of significance for the Maldives as a larger contribution of Southern Ocean swell was found to propagate north. Propagation of this swell into the Indian Ocean could increase the frequency of high magnitude swell events (Chapter 2).

A further variable omitted from investigation of SLR scenarios was shifts in the characteristics of the reef platform itself. Just as islands are not morphologically passive, it is crucial to stress that reef morphology may also change with sea-level rise. Three broad modes of reef response to Holocene sea-level rise have been identified: keep-up, give-up and catch-up (Neuman and Macintyre, 1985). Keep-up reefs are those that accrete at a rate comparable to SLR; catch-up reefs accrete at a slower rate than SLR and thus ‘catch-up’ when SLR slows or stabilises; give-up reefs effectively drown as they are unable to keep pace with SLR. In addition to reef accretion potential, it must also be noted that an increase in water depth will create new accommodation space for calcifying organisms and, in turn, may create new sediment stores, which could have implications for reef island sediment supply regimes. There will most likely be variability in sea-level rise responses between eco-geomorphic zones. For example, Hopley and Kinsey (1988) suggest that, under sea-level rise scenarios, the high energy nature of algal rims will render such zones largely unmodified, except for some encroachment by corals at the outer edge. In contrast, reef flat zones may experience the most immediate impacts of sea-level rise as sand may be removed more efficiently (see Chapter 7), and coral growth may become more prolific with increased growth of branching forms. Such responses are evidently

ignored within the approach employed in this chapter, which assumes no change in reef morphology with sea-level rise.

The approach represents a single snapshot in time, yet wave transformation occurs under constantly changing conditions. As such, seasonality was not considered which, in the Maldives Archipelago, constitutes monsoonal reversals in wave direction. The reversals have been shown to impact hydrodynamics and sediment transport on interior reef platforms within the Maldives (Morgan and Kench, 2012; Beetham and Kench, 2016). Kench et al. (2006) highlight seasonal differences in wave energies at the atoll-scale. However, such reversals are of greatest significance for lagoonal wind-wave energies (Kench et al., 2006), rather than oceanward swell wave energy and thus are likely of less significance within the highly exposed settings on Huvadhu Atoll rim. The seasonal shifts would likely be of most importance to incident lagoonward energy at the leeward site (due to the longer fetch lengths over the atoll lagoon (Chapter 2).

Another facet of the 'snapshot' approach, is that the presented results relate only to 'fair-weather' conditions and thus the implications of low-frequency high-magnitude events, such as storms (although rare with such close proximity to the equator) and swell events (e.g. Hoeke et al., 2013, refer also to Chapter 3) were not considered. The geomorphic implications of such events may be exacerbated by increases in MSL as the likelihood of this energy leaking onto the reef platform surface is increased. This could result in episodic inputs of reef rubble material, such as likely occurred during island initiation (see Chapter 3).

The snapshot approach also neglects the influence of tidal cycles, which represent a key control upon wave processes (e.g. Brander et al., 2004; Kench and Brander, 2006; Jago et al., 2007; Becker et al., 2014; Beetham and Kench, 2016; Quataert et al., 2015). Tides serve to modulate the transmission of wave energy whereby greater energies are able to propagate across reef flats at high tide, as is the case with SLR. Studies of wave processes at high tide have thus been employed to implicate the impacts of future SLR on wave processes (e.g. Brander, et al., 2004, Kench and Brander, 2006). Hence, in his setting, the SLR = 0.5 m effectively represents the contemporary process regime at high tide.

A further caveat of the approach employed within this Chapter is the assumption that sediment transport will occur along gradients from high to low PM. This assumption is inherent in Kench's (1998a) methodology and, in turn, that of this study. However, this is a simplistic assumption which fails to acknowledge, for example, the direction of the currents, which may be oscillatory, and also the role of shear stresses. Bed shear stress relates to the tangential component of stress that occurs on the fluid plane in contact with the bed. Entrainment of a sediment grain occurs when bed shear stress exceeds the critical shear stress, which can be predicted using a modified Shields (1936) diagram (Masselink et al., 2014). Hence, computing bed sheer stresses would provide a more robust means of quantifying sediment transport. However, it must also be acknowledged that the Shields diagram is in part a function of grain diameter. Such an approach may therefore be less applicable in analyses of reefal sediments, as oppose to siliclastic sediments, given the heterogeneity of grain morphologies and densities.

There are thus several avenues which could be investigated in future work. For example, it would be interesting to run the model with projected future shifts in T_s and H_s, for 'keep up', 'catch up' and 'give up' scenarios, with integration of differing sea-level rise responses within different zones (e.g. Hopley and Kinsey, 1988), and at different tidal stages (low tide, high tide and MSL). In addition, rather than adopting a snapshot approach, the development of an iterative model would enable the investigation of a range of changes through time (e.g. in island morphology, reef ecology, sediment production, and sediment storage). Moreover, a further direction for future work would be to develop an approach for modelling reefal sediment transport incorporating the calculation of bed sheer stresses while also acknowledging the heterogeneous nature of reefal sediments.

It is also pertinent to note that, again, the oceanward reef crests beyond the algal rim at each site were not included in the study. However, they may increase in importance as an input of sediment. With increased depths over the algal rim, it seems likely that sediment inputs from this source may become more likely to surmount the rim and be transported onto the platform surface.

While the sole focus of this chapter was to investigate sediment transport, it is pertinent to note that a myriad of contemporaneously occurring processes may also change

with shifts in wave processes and SLR. For example, with increases in wave velocities, water residence times on the reef platform will also decrease, which may cause changes in the physical and chemical properties of the water column (Storlazzi et al., 2011). Indeed, hydrodynamic processes are a fundamental control upon a series of chemical and biological processes, including photosynthesis, nutrient uptake, species distribution, coral bleaching and prey capture (Storlazzi et al., 2011 and references therein). In particular, with increased sediment mobility, concentrations of suspended sediment may increase and act to reduce light availability for corals and seagrass (Storlazzi, 2008). Shifts may thus occur in the sediment-producing communities causing changes in the grade and composition of sediment produced and consequently stored within Maldivian atoll rim systems.

7.5 Conclusion

This Chapter highlights that active sediment transport occurs under the fair-weather contemporary process regime. Hence, this demonstrates the dynamic nature of Maldivian rim reef island systems. Potential benthic sediment mobility was higher at the windward site than the leeward site under contemporary conditions, particularly within the oceanward environment. This reflects the diversity of rim island systems at the scale of an individual atoll. Under conditions of sea-level rise, shifts in wave processes, and in turn sediment potential mobility, were found to be both nonlinear and nonuniform. This is converse to general assumptions that reef islands will respond linearly to environmental change. Broadly, shifts were of a greater magnitude at the leeward than the windward site. Hence, it is suggested that environmental change will invoke diverse reef island responses, even at the atoll scale. Although island sediments were not examined directly within this Chapter, a conceptual model of reef island response to sea-level rise is suggested on the basis of the shifts in the mobility of the adjacent benthic sediments. This suggests that the processes of rollover and roll-around may result in island (horizontal and vertical) lagoonward migration. It is likely that these processes will become most prevalent at the leeward site as it was associated with the largest increases in sediment potential mobility. Notably, striking parallels may be drawn between the suggestions of both former (under conditions of higher sea-levels than present, Chapter 3) and future island rollover and roll-around.

This supports the notion that future sea-level rise could reactivate the process regime responsible for island development.

Chapter 8: Conclusion

8.1 Research Rationale

Despite widespread recognition of the integrated nature of reef island systems (e.g. Woodroffe, 2008; Kench et al., 2009a; Perry et al., 2011), there is currently no study of a reef island system that integrates reef island chronostratigraphy, with datasets on marine sediment storage, production and transport. Indeed, there is an absence of any standardised integrated approach for investigating reef island vulnerabilities. Hence, the primary aim of this thesis was to provide the first such integrated study of a reef island system, and thus propose an approach for understanding the controls upon, and in turn vulnerabilities of, reef island systems.

The Maldives was selected as a study site as, despite comprising the most populated atoll nation (World Bank, 2013), it has remained one of the world's least known groups of coral reef islands (Kench, 2011b). There has been a recent increase in the development of datasets obtained from this Archipelago, relating to models of island development (Kench et al., 2005; Perry et al., 2013), sediment storage (Perry et al., 2015; Morgan and Kench, 2016b), and sediment production (Perry and Morgan, 2017; Perry et al., 2015, 2016; Morgan and Kench, 2016a). Such detailed datasets have been solely obtained from interior islands (i.e. those formed upon platforms within the atoll lagoon) and thus our knowledge of rim island systems is far more limited. However, rim islands are of greater physical and socioeconomic significance: the rim islands dominate spatially (accounting for 82.43% of the nation's land area; Andréfouët et al., 2006), host the majority of the population (88.93%), and thus support a large proportion of the nation's infrastructure (all regional administrative capitals, hospitals and designated 'safe islands'). The secondary aim of this thesis was therefore to advance our understanding of Maldivian reef rim island evolution, specifically reef island development and the degree of reef-to-island connectivity within atoll rim settings. To this end, two study sites with contrasting process regimes were selected on windward and leeward rim aspects of Huvadhu Atoll. This thesis therefore also represents the first study to examine whether variability exists in reef island development at the scale of an individual atoll.

8.2 Key Findings

Through the collective fulfilment of the primary and secondary thesis aims, it is possible to contribute towards our understanding of the six broad research questions posed within Chapter 1 (Section 1.4). Within this section, each of these questions will be re-addressed in relation to windward and leeward settings on Huvadhu Atoll rim thereby summarising the key findings of this thesis.

Q. 1) What are the key controls upon, and modes of, Maldivian reef rim island development?

Through an integrated approach to reef island research, it is possible to elucidate the key controls upon, and in turn modes of, Maldivian reef rim island development. Firstly, sea-level was evidently a key control upon island formation. Radiocarbon dates obtained from the base of reef island cores (Chapter 3) suggest that the timing of island initiation was consistent with that of the mid-Holocene sea-level highstand (Kench et al., 2009b). The basal facies (i.e. facies 3) was characterised by the prevalence of coral rubble, which suggests that low-frequency high-magnitude events, such as swell events (e.g. Hoeke et al., 2013), likely played a key role in island formation. Further investigation of rubble generation by physical erosion is highlighted as an area for future work (see Q.3, and sections 5.4.2 and 8.3). Nonetheless, the significance of such events was likely exacerbated by the higher sea-levels, which would have enabled higher wave energies to propagate across the reef flat. This would result in increased rates of coral rubble generation (via physical erosion), and also increased transport of rubble-sized material across the reef flat. This is consistent with evidence presented in the results of Chapter 7, which showed that wave velocities typically increased (albeit in a nonuniform and nonlinear manner) under conditions of sea-level rise. In turn, increased potential mobility of material with larger grain sizes was found under sea-level rise conditions (Figures 7.20 and 7.23).

While the models of reef island development differed between sites (Figures 3.22 and 3.23), two broad predominant modes of island building may be identified through the amalgamation of results from Chapters 3, 4, 5 and 7. At all times, both island building modes (A and B) will operate in tandem, but the relative importance of A and B may vary through time. The first of the mode of island building (A) is characterised by the

facilitation of reef island building under conditions of higher than present sea (Figure 8.1A). Sea-level also represents the most likely control upon the relative reduction in the significance of island building mode A, i.e. the transition from predominantly rubble to sand accumulation. Interestingly, this study suggests that this timeframe (~1,800 to 1,400 yr. B.P.) was notably consistent between islands and sites. During this period, sea-level was falling toward contemporary levels and thus the high energy window was closing (Kench et al., 2009b). Hence, there was likely a progressive reduction in the rates of rubble generation and transport over this period.

A second key control upon reef island development was reef ecology. Following the reduction in the significance of island building mode A, there was a transition to the increased relative significance of island building mode B (Figure 8.1B) within which reef ecology represented the key control upon reef island development. Island building mode B was characterised by the accumulation of predominantly sand-grade material. Specifically, facies 2 was dominated by sand-grade coral, which, for example, comprised 63.1 ± 1.7% and 75.5 ± 1.4% of sediment within subfacies 2A at the windward and leeward sites respectively (Chapter 3). The most likely source of this sand-grade coral is excavator parrotfish (Perry et al., 2015; Morgan and Kench, 2016a), which is consistent with ecological survey-based estimates of contemporary sediment production (Chapter 5). Indeed, first-order estimates of sediment production were found to be dominated by that associated with excavator parrotfish (72.8% and 68.2% of sediment production at the windward and leeward sites respectively). Moreover, as a function of spatial variability in excavator parrotfish densities, the highest rates of sediment production were found within the lagoonward eco-geomorphic zones. Indeed, 59.4% and 75.4% of sediment was produced within the lagoonward environments at the windward and leeward sites respectively. This is an important observation in the context of AMS radiocarbon dates, island topography and GPR traces, which suggest that more recent island development has occurred via lateral lagoonward accretion (Chapter 3) Hence, this is the first study to link contemporary reef ecology with longer term island accretionary histories (to ~1,800 - 1,400 yr. B.P.).

In addition to sea level and reef ecology, wave exposure represents a third key control upon Maldivian reef rim island development. Several key between-site differences in reef island geomorphology were likely controlled by differences in wave exposure.

Indeed, numerous geomorphic differences are the result of a greater prevalence of rubble at the windward site, which was likely generated and transported across the reef flat by higher wave energies. For example, the windward site was characterised by the greater prevalence of facies 3 within island cores, the presence of rubble ridges and conglomerate outcrops on oceanward island margins, and the rubble eco-geomorphic zone within the marine environment (Chapter 4). In addition, evidence from radiocarbon dates (i.e. age inversions) and island geomorphology (e.g. beachrock outcrops) is indicative that the leeward islands have been more mobile than those at the windward site. This is likely because the leeward islands are more sand- (as oppose to rubble-) dominated (e.g. Kench et al., 2015). The leeward islands are also exposed to higher magnitudes of lagoonal wind-driven wave energy (Chapter 2) and may thus be more susceptible to shifts in wind conditions (e.g. Kench and Brander, 2006). Finally, island formation at both study sites has notably occurred adjacent to zones of preferential deposition. Specifically, adjacent to the lagoonward sand zone at the windward site; and between the lagoonward patch and oceanward sand zones at the leeward site (Chapter 4). Hence, island location is also likely in part a product of wave exposure.

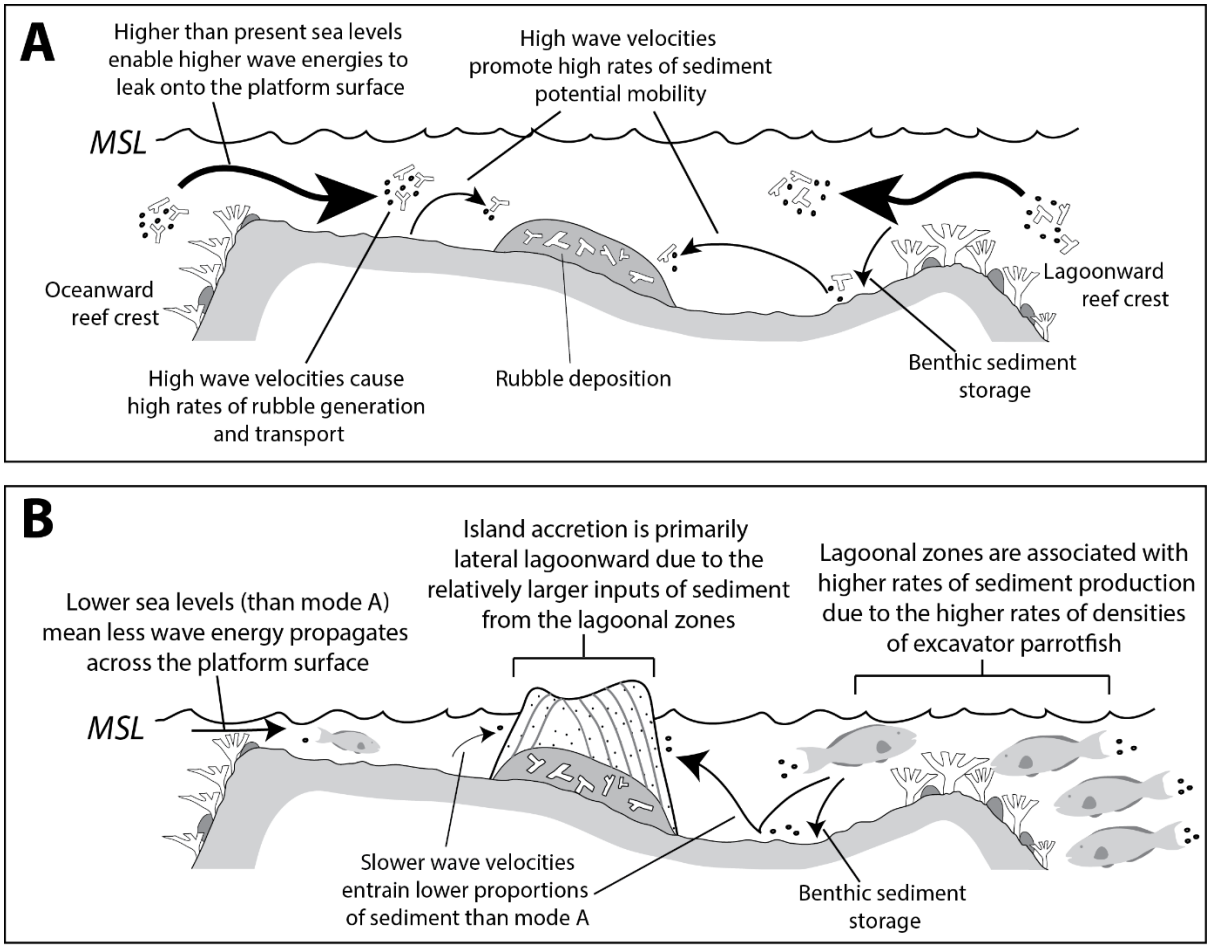

Figure 8.1 – Conceptual model characterising the predominant island building processes within modes A and B. Models were informed by datasets from Chapters 3, 4, 5 and 7. Note that for illustrative purposes, vertical (and fish) exaggeration is substantial.

Q. 2) To what extent does variability exist in reef island development at the scale of an individual atoll?

While the focus of prior work on reef island development has predominantly been upon the variability that exists between regions (e.g. Perry et al, 2011), this thesis investigated whether variability in island development exists at the scale of an atoll. The preceding discussion (i.e. under Q.1) has highlighted several of the key intra-site consistencies and inconsistencies. Specifically, key consistencies include the roles of sea-level and reef ecology as key controls upon island building, as illustrated by island building modes A and B (Figure 8.1). While there are evident parallels between sites, there are also notable differences which highlight the diversity of reef island systems, even at the atoll-scale. Indeed, between-site differences in island geomorphology were

also discussed under Q.1, as likely primarily controlled by differences in wave exposure. A further key difference in the contemporary environment was in the rates of sediment production calculated at the windward and leeward sites. Sediment production at the leeward site far exceeded that at the windward site (mean = 0.089 G and 0.306 G at the windward and leeward sites respectively), which was primarily a function of the differences in densities and sizes of excavator parrotfish. Results in Chapter 7 also suggested that shifts in sediment potential mobility under sea-level rise scenarios may be far more pronounced at the leeward than the windward site.

An additional fundamental difference between both the windward and leeward sites, and also Maldivian interior islands, was found in the timings of island initiation (Chapter 3). Island initiation at the leeward site (4,200-3,600 cal. yr. B.P.) markedly predated that at the windward site (2,800-2,000 cal. yr. B.P.). In addition, timings of island initiation at both rim sites were markedly later (i.e. more recent) than found at interior islands (~5,500 yr. B.P.). It could be hypothesised that the earlier dates of island formation found for interior islands in South Maalhosmadulu Atoll (~27 km from Vakkaru) may be a function of both the smaller platform size and higher rates of sediment production. Hence, platform infilling could occur earlier and in turn, island formation could occur earlier. Likewise, the difference in island ages between the windward and leeward study sites may be due to slower rates of platform infill at the windward site. This is likely because sediment production rates were found to be markedly lower than at the windward site and the windward platform is greater in areal extent than the leeward platform.

Atoll-scale diversity in reef island systems is also evident in comparing Maldivian rim and interior island systems. A key parallel between rim and interior island systems is the significance of excavator parrotfish for sediment production and, in turn, reef island building (Perry et al., 2015; Morgan and Kench, 2016a). Similarly, the corresponding dominance of sand-grade coral within interior platform systems has been highlighted in prior work (Perry et al., 2015; Morgan and Kench, 2016b). However, in addition to differences in the timings of island initiation, there are further key differences between Maldivian rim and interior island systems. Compositional and textural differences are evident, for example, neither Kench et al. (2005) nor Perry et al. (2013) found rubble within interior island cores. Higher proportions of *Halimeda* were found within both interior island cores (Kench et al., 2015) and marine benthic samples (e.g. Perry et al.,

2016; Morgan and Kench, 2016b; Liang et al., 2016). This is likely a reflection of differences in reef ecology, but also the of the lower energy depositional environments within interior settings, which enable such comparatively fragile grains (Murray and Ford, 2012) to persist within the marine environment. Island planform and topographical surveys also highlight differences between rim and interior island geomorphology. Topographically, interior islands exhibit the typical basin morphology and lack any rubble ridges (Kench et al., 2005), as is comparable to the leeward islands, but contrasts with steep rubble ridges and relative uniformity of the windward island platform surfaces. Similarly, in contrast to the windward site, no conglomerate outcrops were surveyed within interior settings. Such distinctions are a likely function of the differences in wave exposure between these settings.

Q. 3) Can a sediment budget be constructed linking sediment production to both island and marine benthic sediment storage?

Through linking the findings of Chapters 3 (reef island sediment storage), 4 (marine benthic sediment storage) and 5 (sediment production), a first step can be made in constructing a sediment budget. While this thesis provides data on inputs and storage, an inherent requirement of a budget is to also quantify outputs from the system and, to this end, values were obtained from the literature. Published data from Morgan and Kench (2014) were applied to calculate off-rim export rates of sand- and gravel-sized material. It is pertinent to note that this data is somewhat problematic as it was collected on an interior, as oppose to a rim, reef platform. Nonetheless, it is the most applicable data available, particularly as rates were applied to the lagoonward margin within the present study. Indeed, given the high magnitude of oceanward wave energy and the cross-platform gradients in wave energy found in Chapter 7, it is most likely that off-rim export would occur from the zones within closest proximity to the lagoonward platform edge (i.e. the lagoonward patch zone at the windward site, and the lagoonward patch and lagoonward reef crest zones at the leeward site). Sand- and gravel-sized export rates of 0.15 kg m^{-2} y^{-1} and 0.02 kg m^{-2} yr^{-1} were applied respectively. Sediment export was then subtracted from sediment production (Chapter 5) to give an estimation of rates of sediment storage at each site (Figures 8.2 and 8.3). For comparison, storage rates are displayed alongside sediment storage totals

estimated within both the terrestrial (Tables 3.5 and 3.6) and marine (Tables 4.11 and 4.12) environments.

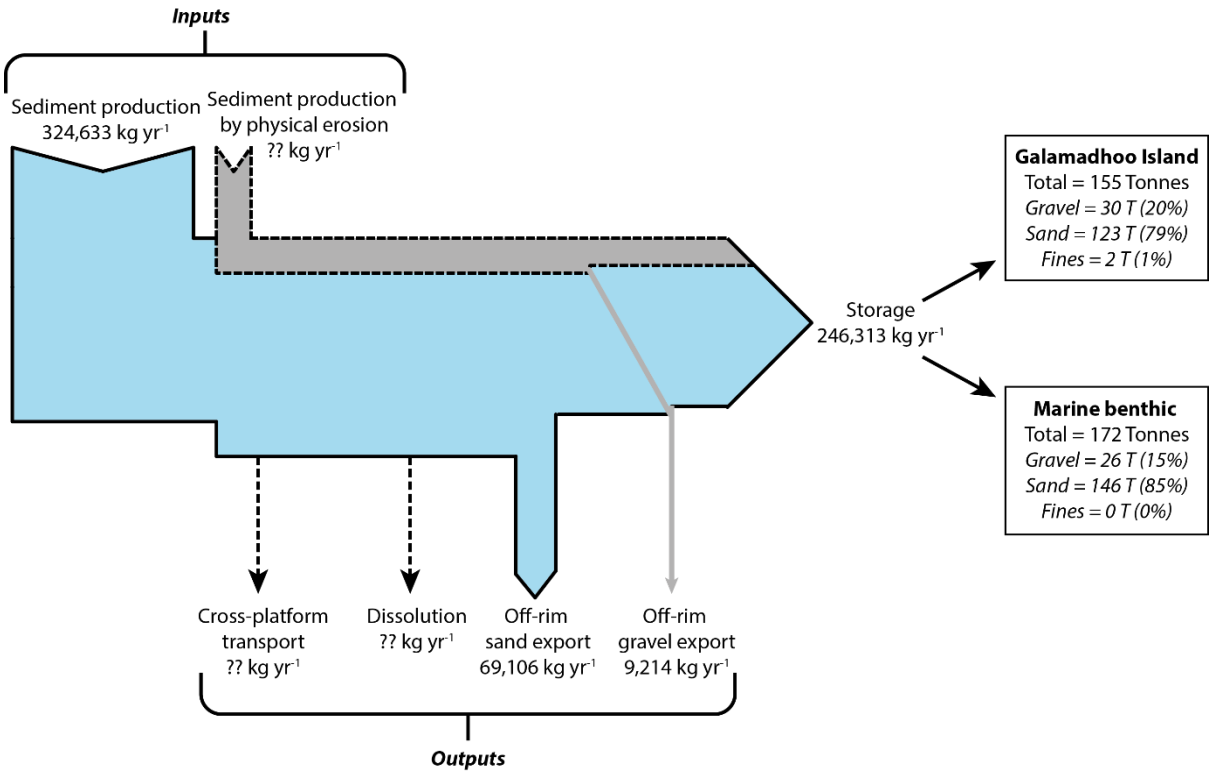

Figure 8.2 – Leeward site sediment budget diagram linking rim system inputs, outputs and storage. Arrow size is approximately proportional to the associated value. Dashed lines represent unquantified processes. Data from Chapters 3 (Galamadhoo island storage), 4 (marine benthic storage) and 5 (inputs).

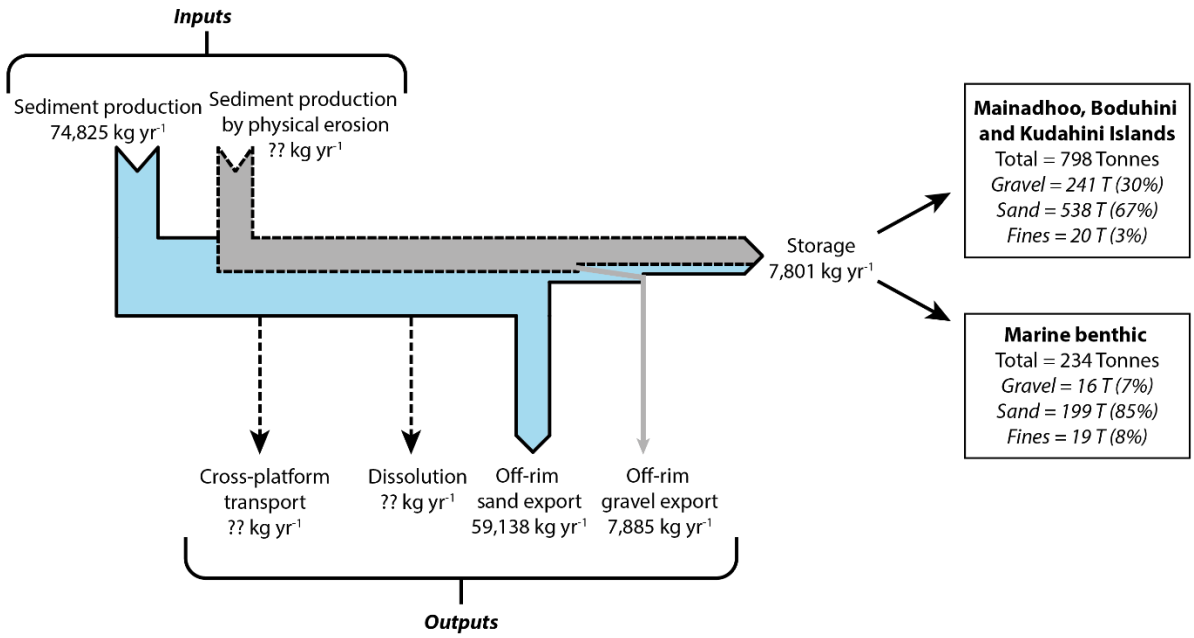

Figure 8.3 – Windward site sediment budget diagram linking rim system inputs, outputs and storage. Arrow size is approximately proportional to the associated value. Dashed lines represent unquantified processes. Data from Chapters 3 (Mainadhoo, Boduhini and Kudahini island storage), 4 (marine benthic storage) and 5 (inputs).

In addition to illustrating the linkages between sediment inputs, outputs and storage, the proposed sediment budgets (Figures 8.2 and 8.3) serve to highlight knowledge gaps in the field and, in turn, areas for future work. Two key knowledge gaps are of particular significance. Firstly, rates of sediment production, especially of reef rubble, by physical erosion are poorly constrained (refer to section 5.4.2). Calculation of meaningful site-specific estimates is problematic due to a poor understanding of the interacting controls upon physical breakdown, including the magnitude and frequency of high energy events, the condition of the reef prior to such events, and abundance of different types of coral growth forms. Secondly, loss of sediment by dissolution likely represents a significant (e.g. Eyre et al., 2014) output from the system. Ascribing a value from the literature is difficult given the variability in estimations, typically from 0.09 to 3.50 kg m^{-2} yr^{-1} (Andersson and Gledhill, 2013). Moreover, the majority of existing studies were undertaken at night or under dark conditions and thus do not account for the full diel cycle of $CaCO_3$ precipitation and dissolution (Eyre et al., 2014). Dissolution has frequently been omitted from reef carbonate budget studies (e.g.

Hubbard et al., 1990; Harney and Fletcher, 2003; Morgan, 2014), though it is a topic receiving increasing recognition (e.g. Andersson, 2015; Cryonak and Eyre, 2016).

In addition to highlighting knowledge gaps, the sediment budgets also illustrate the rates of sediment storage at both sites. Due to the marked difference in sediment production between sites, the budget for the leeward site was strongly positive (net storage of 246,313 kg yr^{-1}) in comparison to the windward site budget, which was only weakly positive (7,801 kg yr^{-1}). Moreover, unquantified outputs from the system, dissolution in particular, ought also to have been subtracted from these values and so it may be that the windward site budget is negative with net sediment loss from the system. However, given the higher energy conditions at the windward site (Chapters 2 and 7), it is likely that rates of sediment production by physical erosion are higher than those at the leeward sites. Hence, the importance of constraining rates of sediment production by physical erosion is, again, highlighted. Nonetheless, the net storage rates have implications for ongoing rim reef island maintenance and stability in the face of future environmental change. Indeed, the values suggest that the leeward site rim islands may possess a greater future resilience as the additional sediment retained on the rim (246,313 kg yr^{-1}) may enable the system to adjust to changing conditions. By contrast, windward site island resilience may be contingent upon the adjustment of a more finite volume of material (McKoy et al., 2010).

Sediment budget construction also allows for comparison between the rates of sediment storage, and the mass of marine and island sediments currently stored on the platform. At the leeward site, contemporary rates of sediment storage (246,313 kg yr^{-1}) would produce the mass of sediment within Galamadhoo island and the marine benthic environment over ~629 years (i.e. 155 T / 0.25 T yr^{-1}) and ~698 years (i.e. 172 T / 0.25 T yr^{-1}) respectively. Hence, over a period of ~1,327 years. The predominant period of island building occurred over ~4,000 years (Chapter 3) and so, considering additional unquantified losses through dissolution, the timeframes are very broadly comparable. This could suggest there has been relative consistency in the sediment production regime, and thus reef ecology, through time.

While the sediment storage rates and timeframes of island formation at the leeward site were broadly comparable, this was not the case at the windward site. Indeed, the windward site contemporary rates of sediment storage (7,801 kg yr^{-1}) would produce

the mass of sediment within Mainadhoo, Boduhini and Kudahini islands over some 102,294 years (i.e. 798 T / 0.008 T yr^{-1}). Likewise, the mass of sediment in the marine environment would be produced over 29,996 years. The collective production period would thus be a substantial 132,290 years (i.e. 234 T / 0.008 T yr^{-1}). Evidently such timeframes are not at all comparable with the timeframe of island formation (~3,000 years). This could be attributed to the unquantified input of sediment production by physical erosion. Indeed, due to the greater exposure of this site and the shorter recurrence intervals between high magnitude events (Chapter 2), it is likely that sediment production by physical erosion represents a far larger input of material than at the leeward site. Hence, there was a far greater provenance of reef rubble in both the terrestrial (Chapter 3) and marine (Chapter 4) environments at this site. Material produced via physical erosion is most likely to be of gravel-grade and so it can be, extremely crudely, discounted by focussing solely on sand- and fine-grade sediments. To suggest that all gravel-sized material was produced by physical erosion is, of course, a substantial over simplification as such gravel-grade sediment may also comprise, for example, foraminifera and molluscs. Nonetheless, the timeframe for sand- and fine-grade sediment storage, according to the sediment budget, is equally incomparable to that of island formation. Indeed, sand- and fine-grade material within the islands and marine environment would have taken some 71,529 and 27,945 years respectively (i.e. 558 T / 0.008 T yr^{-1}; 218 T / 0.008 T yr^{-1}).

There thus remains a substantial discrepancy between rates of sediment storage and that stored on that platform. This could be due to one of several reasons, including: (1) that the contemporary sediment production regime has changed since the predominant period of island formation; (2) there are errors in the quantification of sediment production rates; and/or (3) there are inputs of sediment to the system that are unquantified in the methodology of this study. While the discrepancy is likely caused by a combination of these factors, it seems most plausible that a substantial cause is an unquantified input of sediment, likely from the oceanward reef crest, beyond the algal rim (see section 5.4.2). Moreover, it is likely that sediment from the zone represented a larger input of sediment when sea-level was higher than present (Figure 3.21). This is because with increased depths over the algal rim, it seems likely that sediment may become more likely to surmount the rim and be transported onto the platform surface. Hence, this highlights a further knowledge gap in the sediment

productivity and transport within the eco-geomorphic zone beyond the oceanward algal rim (section 8.3).

Q. 4) What is the degree of contemporary reef-to-island connectivity?

There was a striking consistency between ecological survey-based estimates of sediment production (Chapter 5); benthic marine, beach and island sedimentology (Chapter 4); and lateral lagoonward modes of more recent island accretion (Chapter 3). As discussed under Q.s 1 and 2, and as illustrated by reef island building mode B, the results of this thesis highlight that reef ecology is a key control upon island geomorphology. Such reef-to-island connections necessitate sediment transport by waves. Potential mobility analyses (Chapter 7) provide further evidence for active linkages between reefs and reef islands as results demonstrated that active sediment transport may occur even under fair-weather conditions (PM <100%). This thesis therefore highlights the interconnected nature of reef island systems and the intrinsic relationship between reef ecology and island building processes.

Additional evidence for active reef-to-island connectivity may be gained from reef rim sedimentological data. Within the broad homogeneity of the Maldivian rim sediment reservoirs (predominantly sand-grade coral), some variability in texture and composition was found within each study site. The majority of this variability was evident across oceanward-lagoonward gradients, likely primarily controlled by wave energy. This variability may be conceptualised within facies models (Figures 8.4 and 8.5), which represent the compilation of datasets from Chapters 3, 4, 5, and 7. While wave exposure represents the primary control upon variability, the roles of both physical and biological processes are evident. For example, grain size was significantly related to wave velocity whereby finer grade material is winnowed away from areas with high wave velocities and deposited within lower energy conditions. An example of the role of biological processes is evident in the higher proportions of CCA found within the oceanward reef crest zones, which is consistent with the higher benthic CCA coverage found on the algal rims.

Reef islands have previously been described as highly selective landforms, comprised of sediment that is significantly different from that in the adjacent marine environments (e.g. Morgan and Kench, 2016b). However, the conceptual models demonstrate that rather than being particularly distinctive, island sedimentology represents a portion of

the broader cross-rim gradients in rim platform sediment properties. Hence, this suggests that reef rim islands are in a dynamic equilibrium with the contemporary process regime and are actively linked to their adjacent marine environments.

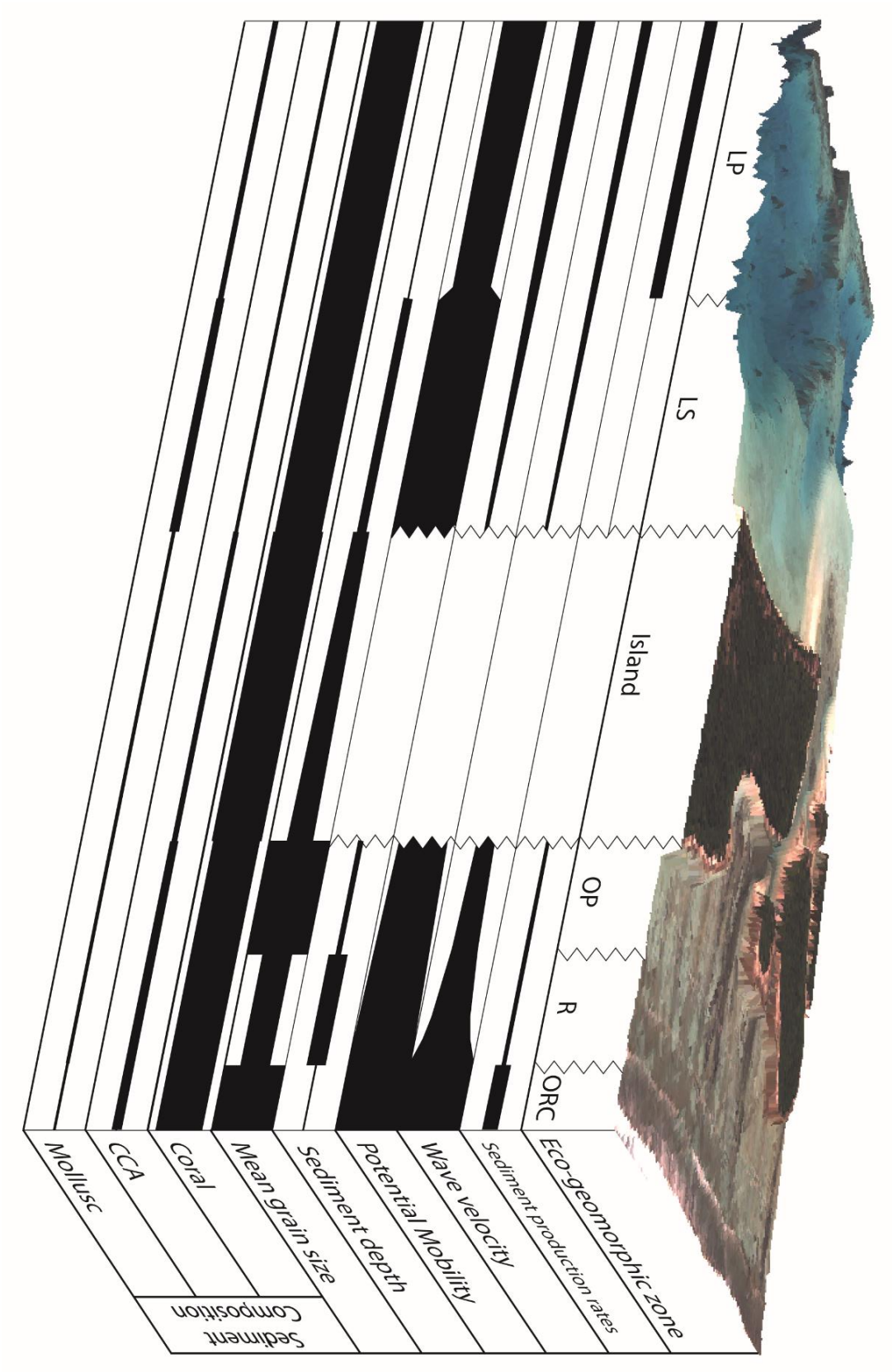

Figure 8.4 – Conceptual model of cross-rim trends at the windward site. This incorporates datasets from Chapters 3, 4, 5 and 7. LP = lagoonward patch, LS = lagoonward sand, OP = oceanward patch, R = rubble, ORC = oceanward reef crest.

Figure 8.5 – Conceptual model of cross-rim trends at the leeward site. This incorporates datasets from Chapters 3, 4, 5 and 7. LRC = lagoonward reef crest, LP = lagoonward patch, OS = oceanward sand, DSG = dense seagrass, OSS = oceanward sparser seagrass, ORC = oceanward reef crest.

Q. 5) What are the implications of research findings for the future of Maldivian reef rim island systems and their management under conditions of environmental change?

A central purpose of seeking to develop our knowledge of past and contemporary processes within reef island systems, is to further our understanding of future reef island trajectories, particularly in an era of environmental change. Indeed, through the application of an integrated approach and, in turn, the preceding discussion, several inferences may be made. Firstly, using the past as an analogue for the future, the findings of Chapter 3 highlight the role of sea level in reef island formation: the period of island initiation and heightened mobility occurred during the mid-Holocene sea-level highstand, when sea-levels were higher than present. The implication is that future sea-level rise may reactivate the process regime responsible for reef island initiation. Hence, further island building and/or heightened island mobilisation may occur. This suggestion is supported by the results of Chapter 7 which suggest sea-level rise may be associated with increases in both benthic sediment and reef island mobility.

Data presented in both Chapters 3 and 7 suggest that islands at the leeward site have exhibited greater mobility than their windward counterparts (refer to Q. 1). Similarly, the results of Chapter 7 found increases in sediment potential mobility under sea-level rise scenarios to be markedly greater at the leeward site than at the windward site. In terms of the implications for future island resilience, a more mobile island may be indicative of an ability to shift in response to changes in boundary conditions. Island mobility could thus result in greater resilience in the face of environmental change. By contrast, the windward islands appear to have been more stable (Chapter 3) and increases in sediment mobility under sea-level rise scenarios were less marked (Chapter 7). However, as the windward islands are lower in elevation (Mainadhoo, Boduhini and Kudahini were at 0.81 ± 0.02 m, 0.81 ± 0.01 m and 0.82 ± 0.04 m respectively, relative to MSL) than the leeward islands, their future resilience necessitates reworking and/or the input of additional sediment to maintain supratidal elevations. While island mobility and vertical accretion may be necessary processes for future island persistence, such processes pose a challenge for the management of inhabited reef islands. This is particularly given that contemporary island infrastructure

was constructed with cement and concrete – presumably with the hope for permanence in mind. Designing more easily mobilised structures could provide a more adaptive approach to the construction of buildings on reef islands.

The extent to which an island has the ability to adjust to changing environmental conditions is also in part a product of sediment supply. That is, in the absence of a sediment supply, island resilience is contingent upon the adjustment of a finite volume of material (McKoy et al., 2010). Sediment production rates were markedly higher at the leeward site than at the windward site (mean = 0.089 G and 0.306 G at the windward and leeward sites respectively), which may render the windward islands less resilient to environmental change. However, rates of sediment production at both sites were low in comparison to those found with the same methodology on interior Maldivian platforms (Perry et al., 2015). Hence, interior reef islands may be more resilient to future change than rim islands. Even where sediment production rates remain high, in order to contribute to reef island building, sediment production must be of a suitable type (grade and composition). In particular, fine-grade material is less likely to contribute to reef island building (2.11 ± 0.57% of reef island sediments were fine-grade) as its grade would render it susceptible to rapid winnowing off-rim (Chapter 7). Presently, reef ecology is well-suited to generate sediments that are appropriate for reef island construction and maintenance. This is indicated by the consistency between sediment production (which was dominated by that associated with excavator parrotfish) and sediment stored within the upper island facies (predominantly sand-grade coral). As parrotfish are the most likely source of sand-grade coral, the consistency is indicative of active reef-to-island linkages. However, these results also emphasise the reliance of Maldivian rim islands upon a limited range of sediment producing organisms, specifically excavator parrotfish. Any shifts in their abundance could thus have a critical impact upon reef island resilience in the face of future environmental change. To attempt to conserve reef island geomorphology, it thus seems imperative to conserve both excavator parrotfish populations and live coral cover. Hence, management strategies ought to ensure the acknowledgement of such ecological-geomorphological linkages.

In light of the intrinsic ecological-geomorphological linkages, the geomorphic implications of any shifts in ecology ought to be considered in reef island management. The recent areal expansion of seagrass beds is demonstrative of the relative rapidity

with which ecological shifts can occur, and also the impact that ecological change can have upon sediment production budgets. In a sense, the apparent expansion of Maldivian seagrass beds is perhaps an ecological ‘bright spot’ (e.g. Cinner et al., 2016) against a backdrop of decline. Indeed, Chapter 6 suggests that the expansion of seagrass on the leeward rim platform could result in a 243 tonne increase in sediment production per year. For reef islands, this could be particularly fortuitous if their associated carbonate producing communities are able contribute material of an appropriate grade for island building, for example by increasing excavator parrotfish populations. However, the extent to which expansion is detrimental (or not) to coral cover is unclear. Far more concerning, would be if a threshold in nutrient levels was crossed sufficient to induce a coral-algal phase shift. Ascertaining whether such a threshold exists ought to represent a priority for management agendas. The implications of such a phase shift could be catastrophic for the Maldives as a nation that is so dependent upon its physical and ecological environment.

In addition to sea level and ecology, wave exposure was highlighted as the third key control upon rim island systems (refer to Q. 1). Indeed, between-site differences in island geomorphology (e.g. topography, presence of conglomerate, rubble ridges) were attributed to the differing wave exposures of the two sites. This highlights both the sensitivity of rim islands to shifts in oceanographic boundary conditions, and the potential for significant between-site variations in future reef island geomorphic change. Indeed, this corroborates with the results of Chapter 7 as marked between-site differences were found in shifts in sediment potential mobility under conditions of sea-level rise. Moreover, Chapter 7 highlights the nonlinear and nonuniform nature of wave processes on reef platforms. Hence, in turn, it is likely that shifts in island geomorphology will also be nonuniform and nonlinear.

Through highlighting the roles of both reef ecology and wave exposure as key controls upon rim islands, this research highlights that sea-level is not the sole control upon reef islands, as is frequently implicated by assertions of island vulnerability. Rather, such suggestions are an oversimplification of the series of controls that interact to produce a diverse range of island systems. Indeed, this work highlights that island formation is possible at a range of stages of sea-level rise. Moreover, given the local scale diversity in reef island responses to past environmental change (i.e. the differing models of reef island development - Figures 3.22 and 3.23), the implication is that

geomorphic responses to future change may be equally diverse, even at the local scale. A challenge then for the adaptive capacity of atoll nations is thus to acknowledge this diversity in any future management strategies.

Q. 6) Does an integrated methodology provide an effective means of understanding reef rim island systems?

In the absence of any standardised methodologies for the investigation of reef island systems, a secondary aim of this thesis was to develop an integrated approach for understanding the evolution of reef island systems and, in turn, their potential vulnerability to future change. Specifically, this approach comprised the integration of several datasets (Figure 8.6), including reef island chronostratigraphic data (including cores that attained depths below contemporary live coral growth in the adjacent marine environment), marine ecological surveys, beach and marine benthic sedimentology, and wave process modelling. This thesis represented the first study of any reef island system to examine both chronostratigraphic data alongside reef ecological survey data. The research thus sought to provide a holistic approach with reference to both spatial and temporal scales. Spatially, previous reef island studies have typically focused predominantly on either the marine (e.g. Perry et al., 2015; Morgan and Kench, 2016b) or the terrestrial (e.g. Kench et al., 2005) environments. Furthermore, even within the marine environment, there is typically a bias towards the reef flat, rather than lagoonal environments (Yamano et al., 2001). However, this study found lagoonal environments to be of disproportionate importance for reef island building. For example, at the leeward site the lagoonward zones comprised 43.1% of the marine environment, but accounted for 59.3% of sediment production. Temporally, this study has transcended cascading temporal scales from millennial, to contemporary, and towards the future (Figure 1.6). Through this approach, this study has highlighted, for the first time within reef island research, the linkages between contemporary reef ecology and long-term modes of island accretion.

Through integrating this series of datasets, it is possible to highlight the integrated nature of reef island systems: just as no Chapter within this thesis stands entirely alone, no component of a reef island systems exists in isolation from the remainder of the system. In turn, this thesis proposes, and advocates the merits of, a holistic approach to examining reef island systems and their potential vulnerabilities. Perhaps

most notably, this approach transcends the fields of reef ecology and geomorphology. This contrasts the traditional dichotomy that exists in coral reef science between these fields. However, this work highlights that through eco-geomorphic approach we are able to best understand reef systems, the controls upon them and their potential future vulnerabilities. As we attempt to best understand and manage reef environments under conditions of environmental change, such a bridging of disciplines seems ever more vital.

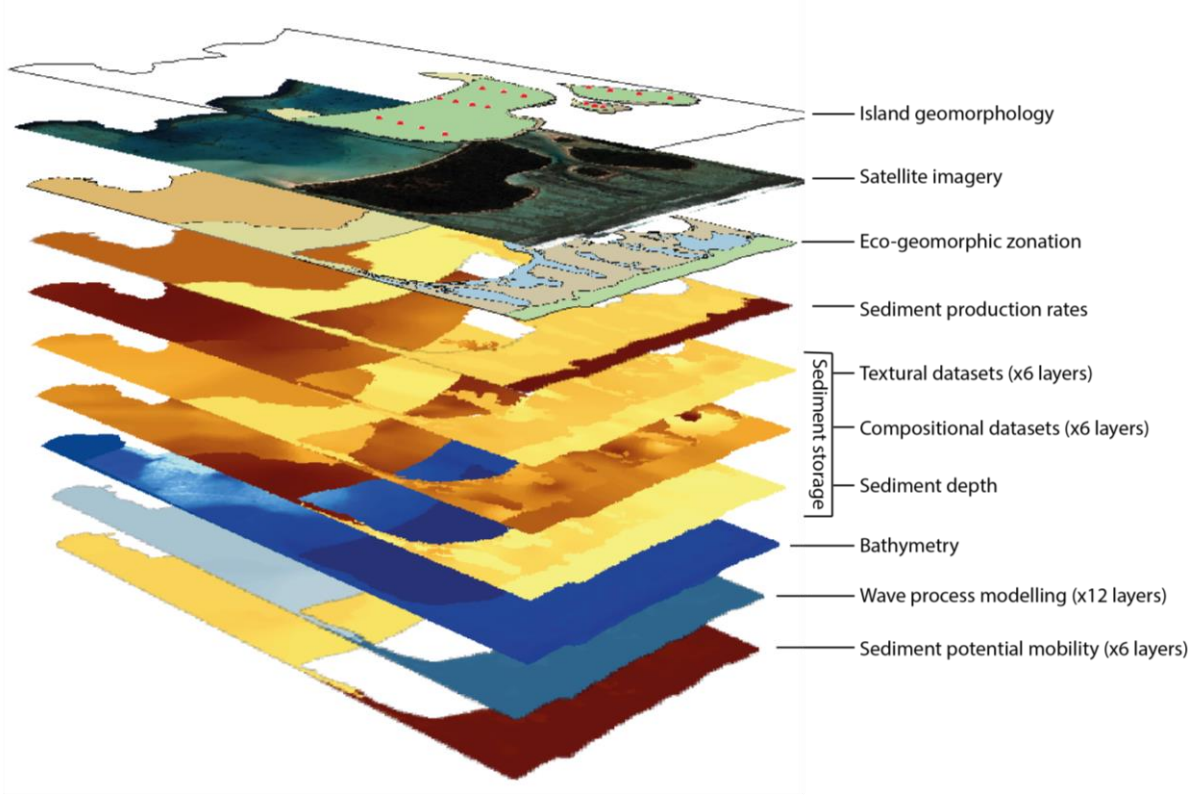

Figure 8.6 – Illustration of the integrated approach employed within this thesis in order to improve understanding of the evolution of reef island systems and, in turn, their potential vulnerability to future change.

8.3 Limitations and Further Work

A limitation of this study was the inability to gain any understanding – be it areal extent (from satellite imagery), sediment samples or benthic survey data – of the oceanward reef crest beyond the oceanward algal rim. Undoubtedly, these areas ought to represent additional eco-geomorphic zones with contrasting ecological and geomorphic characteristics to those analysed within Chapters 4 and 5. Just as Stoddart (1966) was unable to access these zones, they remain ‘innominate’ (Wells,

1957). A direction for future research would therefore be to increase our knowledge of these areas, which would be feasible with the aid of SCUBA and careful planning (i.e. selecting the calmest possible conditions, and perhaps hiring a more substantial vessel). More challenging, would be the assessment of the degree of connectivity between these zones, the platform surface (i.e. other eco-geomorphic zones), and the reef islands. These zones likely represent highly productive areas that generate large volumes of sediment. However, the ease with which this material is able to surmount the comparatively shallow edge of the algal rim is questionable. Securing sediment traps on the oceanward edge of the algal ridge (a challenge!) could provide rates of transport (e.g. Morgan and Kench, 2012). However, as suggested (Chapter 5), it may be that sediment transport of oceanward material onto the platform surface occurs only episodically, such as facilitated by swell events. To gain more meaningful data, a longitudinal sediment trapping study would provide a very informative dataset. Similarly, obtaining sediment trap data from across the platform systems would be an effective means of quantifying the rates and types of sediment transport. Under fair-weather conditions, it would be interesting to compare the findings of such a study with those of the potential mobility analyses (within Chapter 7). In addition, obtaining, and re-running the wave model with *in situ* wave data would increase the reliability of wave model outputs. Such data would further aid our understanding of the linkages between reef ecology and reef island building.

A further caveat was the omission of sediment production via physical erosion. Given the low proportions of rubble-grade material within upper island horizons, physical erosion is likely of limited importance for contemporary reef island building within the study sites of this thesis. However, better constraining our knowledge of physical erosion on reefs would be a useful direction for future research. In addition, developing regional constituent-level carbonate production rate datasets would also aid the development of a more robust approach for the calculation of sediment production budgets.

With the generation of each additional reef island dataset, we are able to better understand the controls upon reef island systems. We then move closer to the development of a holistic model of reef island development. While some attempts at numerical reef island modelling have been made (e.g. Kench and Cowell. 2001a; 2001b), they typically focus upon shifts in a single process, as was the case in Chapter

7 which focused on sediment transport. However, as in any natural system, there are a whole series of contemporaneously occurring processes. Just as this thesis advocates for a holistic approach to understanding reef island systems, a realistic model of reef island futures ought also to integrate all aspects of the system, including the ecological and geomorphological processes, specifically reef ecology, sediment production, transport and deposition, and reef island accretion/erosion. In order to understand these processes, this thesis also incorporates a series of cascading temporal scales. However, incorporating this range of temporal scales (seconds, years, decades and millennia) would pose a challenge for numerical modelling. Nonetheless, developing such a model would represent a major step for reef island research and management.

References

Agawin, N.S.R., Duarte, C.M. and Fortes, M.D. (1996) Nutrient limitation of Philippine seagrasses (Cape Bolinao, NW Philippines): In situ experimental evidence, *Marine Ecology Progress Series. Oldendorf*, *138*(1): 233-243.

Allen, J.R.L. (1984) Experiments on the settling, overturning and entrainment of bivalve shells and related models, *Sedimentology,* 31: 227-250.

Andersson, A.J. (2015) A fundamental paradigm for coral reef carbonate sediment dissolution. *Frontiers in Marine Science*, 2: 52.

Andersson, A.J. and Gledhill, D. (2013) Ocean acidification and coral reefs: effects on breakdown, dissolution, and net ecosystem calcification, *Annual Review of Marine Science*, 5:321-348.

Andréfouët, S. and Payri, C. (2001) Scaling-up carbon and carbonate metabolism of coral reefs using in-situ data and remote sensing, *Coral Reefs,* 19(3): 259-269.

Andréfouët, S., Muller-Karger, F.E., Robinson, J.A., Kranenburg, C.J., Torres-Pulliza, D., Spraggins, S.A. and Murch, B. (2006) Global assessment of modern coral reef extent and diversity for regional science and management applications: a view from space, *Proceedings of the 10th International Coral Reef Symposium,* 1: 1732-1745.

Aronson, R.B., Precht, W.F., Macintyre, I.G. and Toth, L.T. (2012) Catastrophe and the life span of coral reefs, *Ecology,* 93(2): 303-313.

Aslam, M. (2013) *Personal communication*. Director of LaMer, former Minister of Housing and Environment, Maldives

Aslam, M. and Berre, T. (2007) *Causes of the Severe Flooding of Fares Mathoda, Huvadhu Atoll – Maldives,* Report for the Maldivian Democratic Party (MDP).

Aslam, M. and Kench, P.S. (2017) Reef Island Dynamics and Mechanisms of Change in Huvadhoo Atoll, Republic of Maldives, Indian Ocean, *Anthropocene*, 18: 57-68.

Baccelle, L. and Bosellini, A. (1965) Diagrammi per la stima visiva della composizione percentuale nelle rocce sedimentary, *Università di Ferrara.; Annali. Nuova ser. Sez. IX: Scienze geologiche e paleontologiche*, 59–62

Bak, R.P.M. (1994) Sea urchin bioerosion on coral reefs: place in the carbonate budget and relevant variables, *Coral Reefs,* 13: 99-103.

Bayliss-Smith, T.P. (1988) The role of hurricanes in the development of reef islands, Ontong Java Atoll, Solomon Islands, *Geographical Journal,* 154:377-391.

Becker, J., Merrifield, M. and Ford, M. (2014) Water level effects on breaking wave setup for Pacific Island fringing reefs, *Journal of Geophysical Research: Oceans*, 119: 914- 932.

Beetham, E., Kench, P.S., O'Callaghan, J. and Popinet, S. (2016) Wave transformation and shoreline water level on Funafuti Atoll, Tuvalu, *Journal of Geophysical Research: Oceans*, 121(1): 311-326.

Beetham, E.P. (2016) *Field and numerical investigations of wave transformation and inundation on atoll islands* (Doctoral dissertation, ResearchSpace@Auckland).

Beetham, E.P. and Kench, P.S. (2014) Wave energy gradients and shoreline change on Vabbinfaru platform, Maldives, *Geomorphology*, 209: 98-110.

Bell, P.R.F. (1992) Eutrophication and coral reefs: some examples in the Great Barrier Reef lagoon, *Water Research*, *26*(5): 553-568.

Bellwood, D.R. (1995a) Direct estimate of bioerosion by two parrotfish species, Chlorurus gibbus and C. sordidus, on the Great Barrier Reef, *Australia. Marine Biology*, 121(3): 419-429.

Bellwood, D.R. (1995b). Carbonate transport and within-reef patterns of bioerosion and sediment release by parrotfishes (family Scaridae) on the Great Barrier Reef, *Oceanographic Literature Review*, *9*(42): 740.

Bellwood, D.R. and Choat, J.H. (1990) A functional analysis of grazing in parrotfishes (family Scaridae): the ecological implications, *Environmental Biology of Fishes*, 28: 189-214.

Bianchi, M., Feliatra, F., Tréguer, P., Vincendeau, M-A. and Morvan, J. (1997) Nitrification rates, ammonium and nitrate distribution in upper layers of the water column and in sediments of the Indian sector of the Southern Ocean, *Deep Sea Research Part II: Topical Studies in Oceanography,* 44(5):1017-1032.

Björk, M., Short, F., Mcleod, E. and Beer, S. (2008) *Managing seagrasses for resilience to climate change*, IUCN, Gland, Switzerland.

Blanchon, P. and Jones, B. (1997) Hurricane control on shelf-edge-reef architecture around Grand Cayman, *Sedimentology*, 44(3): 479-506.

Blanchon, P., Jones, B. and Kalbfleisch, W. (1997) Anatomy of a fringing reef around Grand Cayman; storm rubble, not coral framework, *Journal of Sedimentary Research*, 67(1): 1-16.

Blott, S.J. and Pye, K. (2001) GRADISTAT: a grain size distribution and statistics package for the analysis of unconsolidated sediments, *Earth surface processes and Landforms*, 26(11): 1237-1248.

Bonneton, P., Chazel, F., Lannes, D., Marche, F. and Tissier, M. (2011) A splitting approach for the fully nonlinear and weakly dispersive Green–Naghdi model, *Journal of Computational Physics,* 230(4): 1479-1498.

Borum, J. and Sand-Jensen, K. (1996) Is total primary production in shallow coastal marine waters stimulated by nitrogen loading?. *Oikos*, 76(2): 406-410.

Bosence, D (1989) Biogenic carbonate production in Florida Bay, *Bulletin of Marine Sciences*, 44: 419-433.

Boss, S.K. and Liddell, W.D. (1987) Patterns of sediment composition of Jamaican fringing reef facies, *Sedimentology*, 34(1): 77-87.

Braithwaite, C.J.R. (1973) Settling behaviour related to sieve analysis of skeletal sands, *Sedimentology,* 20: 251-262.

Brander, R.W., Kench, P.S. and Hart, D. (2004) Spatial and temporal variations in wave characteristics across a reef platform, Warraber Island, Torres Strait, Australia. *Marine Geology*, 207(1): 169-184.

Bricker, S.B., Ferreira, J.G. and Simas, T. (2003) An integrated methodology for assessment of estuarine trophic status, *Ecological modelling*, 169(1): 39-60.

Brouns, J.J.W.M. (1985) A comparison of the annual production and biomass in three monospecific stands of the seagrass Thalassia hemprichii (Ehrenb.) aschers, *Aquatic Botany*, 23(2): 149-175.

Brown, H. (2005) Lost innocence: the tsunami in the Maldives. *Forced Migration Review*.

Bruggemann, J.H., Van Kessel, A.M., Van Rooij, J.M. and Breeman, A.M. (1996) Bioerosion and sediment ingestion by the Caribbean parrotfish Scarus vetula and Sparisoma viride: implications of fish size, feeding mode and habitat use, *Marine Ecology Progress Series*, 134: 59-71.

Bruun, P. F., and Viggoson, G. (1977) The wave pump: conversion of wave energy to current energy, *American Society of Civil Engineers, Waterway, Port, Coastal and Ocean Division Journal,* 103: 449-469.

Buckley, R. (2003) *Case Studies in Ecotourism*, CABI Publishing, Cambridge, MA, USA.

Burkholder, J.M., Tomasko, D.A. and Touchette, B.W. (2007) Seagrasses and eutrophication, *Journal of Experimental Marine Biology and Ecology*, *350*(1): 46-72.

Callaghan, D.P., Nielsen, P., Cartwright, N., Gourlay, M.R., and Baldock, T.E. (2006) Atoll lagoon flushing forced by waves, *Coastal Engineering*, 53(8): 691-704.

Camoin, G.F., Montaggioni, L.F. and Braithwaite, C.J.R. (2004) Late glacial to post glacial sea levels in the Western Indian Ocean, *Marine Geology,* 206(1): 119-146.

Carpenter, K.E., Abrar, M., Aeby, G., Aronson, R.B., Banks, S., Bruckner, A., Chiriboga, A., Cortés, J., Delbeek, J.C., DeVantier, L. and Edgar, G.J. (2008) One-third of reef-building corals face elevated extinction risk from climate change and local impacts, *Science*, 321(5888): 560-563.

Caterall, C. (1998) Molluscs on coral reefs. In Beesley, P.L., Ross, G.J.B., and Wells, A. (eds.), *Mollusca: The Southern Synthesis. Fauna of Australia, Vol. 5*. CSIRO Publishing, Melbourne, pp33-36.

Chiappone, M. and Sullivan, K.M. (1997) Rapid assessment of reefs in the Florida Keys: Results from a synoptic survey. In *Proceedings of the 8th International Coral Reef Symposium, Volume 2*, pp1509-1514.

Chollett, I. and Mumby, P.J. (2012) Predicting the distribution of Montastraea reefs using wave exposure, *Coral Reefs*, *31*(2): 493-503.

Church, J.A. and Clark, P.U. *et al.* (2013) Sea Level Change, In Climate Change 2013: The Physical Science Basis. Contribution of Working Group I to the Fifth Assessment Report of the Intergovernmental Panel on Climate Change. (eds Stocker T.F. *et al.*). Cambridge University Press, Cambridge, United Kingdom and New York, NY, USA, pp1137-1216.

Ciarapica, G. and Passeri, L. (1993) An overview of the Maldivian coral reefs in Felidu and North Malé Atoll (Indian Ocean): Platform drowning by ecological crises. *Facies,* 28: 33-65.

Cloern, J.E. (2001) Our evolving conceptual model of the coastal eutrophication problem, *Marine Ecology Progress Series*, 210: 223-253.

Collen, J.D and Garton, D.W. (2004) Larger foraminifera and sedimentation around Fongafale Island, Funafuti Atoll, Tuvalu, *Coral Reefs,* 23:445-454.

Congalton, R.G. and Green, K. (1999) *Assessing the accuracy of remotely sensed data: principles and practices.* Lewis Publishers, Boca Raton, FL.

Costanza, R., d'Arge, R., de Groot, R., Farber, S., Grasso, M., Hannon, B., Limburg, K., Naeem, S., O'Neill, R.V., Paruelo, J., Raskin, R.G., Sutton, P. and van den Belt, M. (1997) The value of the world's ecosystem services and natural capital, *Nature*, 387: 253-260.

Courtillot, V., Feraud, G., Maluski, H., Vandamme, D., Moreau, M.G., and Besse, J. (1988) Deccan flood basalts and the Cretaceous/Tertiary boundary. *Nature*, 333(6176):843-846.

Cowell, P.J. and Kench, P.S. (2001) The morphological response of atoll islands to sea-level rise. Part 1: modifications to the shoreface translation model, *Journal of Coastal Research*, 34: 633-644.

Cowell, P.J. and Thom, B.G. (1994) Morphodynamics of coastal evolution. In Carter, R.W.G. and Woodroffe, C.D. (Eds.), *Coastal Evolution: late quaternary shoreline morphodynamics*. Cambridge University Press, Cambridge, United Kingdom and New York, NY, USA, pp33-86.

Cyronak, T. and Eyre, B.D. (2016) The synergistic effects of ocean acidification and organic metabolism on calcium carbonate (CaCO 3) dissolution in coral reef sediments, *Marine Chemistry*, 183: 1-12.

Cyronak, T., Santos, I.R. and Eyre, B.D. (2013) Permeable coral reef sediment dissolution driven by elevated pCO2 and pore water advection, *Geophysical Research Letters*, *40*(18), 4876-4881.

Darwin, C.R. (1842) *The structure and distribution of coral reefs.* Smith Elder and Co, London.

Dawson, J.L. and Smithers, S.G. (2014) Carbonate sediment production, transport, and supply to a coral cay at Raine Reef, Northern Great Barrier Reef, Australia: a facies approach, *Journal of Sedimentary Research*, 84(11): 1120-1138.

Dawson, J.L., and Smithers, S.G. (2010) Shoreline and beach volume change between 1967 and 2007 at Raine Island, Great Barrier Reef, Australia, *Global and Planetary Change*, 72:141–154.

de la Torre-Castro, M. and Rönnbäck, P. (2004) Links between humans and seagrasses: an example from tropical East Africa, *Ocean & Coastal Management*, 47(7): 361-387.

De'ath, G., Lough, J.M. and Fabricius, K.E. (2009) Declining coral calcification on the Great Barrier Reef, *Science*, 323(5910): 116-119.

Denny M.W. (1988) *Biology and the mechanics of the waveswept environment.* Princeton University Press, Princeton, NJ.

Dickinson, W.R. (1999) Holocene sea-level record on Funafuti and potential impact of global warming on central Pacific atolls, *Quaternary Research*, 51(2): 124-132.

Dollar, S.J. (1982) Wave stress and coral community structure in Hawaii, *Coral Reefs*, 1(2): 71-81.

Done, T.J. (1982) Patterns in the distribution of coral communities across the central Great Barrier Reef, *Coral Reefs*, 1(2): 95-107.

Done, T.J. (1983) Coral zonation, its nature and significance. In *Perspectives on coral reefs*. Australian Institute of Marine Science (AIMS), pp107-147.

Done, T.J. (1992) Phase shifts in coral reef communities and their ecological significance. In *The Ecology of Mangrove and Related Ecosystems*, Springer, Netherlands, pp121-132.

Donn, W.L. and McGuinness, W.T. (1959) Barbados storm swell, *Journal of Geophysical Research*, 64(12): 2341-2349.

Dorenbosch, M., Grol, M.G.G., Nagelkerken, I. and Van der Velde, G. (2006) Seagrass beds and mangroves as potential nurseries for the threatened Indo-Pacific humphead

wrasse, Cheilinus undulatus and Caribbean rainbow parrotfish, Scarus guacamaia, *Biological Conservation*, *129*(2): 277-282.

Drew, E. (2011) Halimeda. In Hopley, D. (ed.) *Encyclopaedia of Modern Coral Reefs: Structure, Form and Process.* Springer, Dordrecht, The Netherlands, pp535-539.

Duarte, C.M. (2002) The future of seagrass meadows, *Environmental conservation*, 29(02): 192-206.

Duarte, C.M., Middelburg, J.J. and Caraco, N.F. (2005) Major role of marine vegetation on the oceanic carbon cycle, *Eco-geosciences*, *2*(1): 1-8.

Duce, S., Vila-Concejo, A., Hamylton, S.M., Webster, J.M., Bruce, E. and Beaman, R.J. (2016) A morphometric assessment and classification of coral reef spur and groove morphology, *Geomorphology*, 265: 68-83.

Duncan, R.A. and Hargraves, R.B. (1990) 40Ar/39Ar geochronology of basement rocks from the Mascarene Plateau, the Chagos Bank, and the Maldives Ridge. In *Proceedings of the Ocean Drilling Program, scientific results* (Vol. 115, pp. 43-51) College Station, TX: Ocean Drilling Program.

Durrant, T., Hemer, M., Trenham, C. and Greenslade, D. (2013) CAWCR Wave Hindcast 1979-2010, v5. CSIRO. *Data Collection*, doi:10.4225/08/523168703DCC5.

Duvat, V.K. and Pillet, V. (2017) Shoreline changes in reef islands of the Central Pacific: Takapoto Atoll, Northern Tuamotu, French Polynesia, *Geomorphology*, 272: 96-118.

Eakin, C.M. (1996) Where have all the carbonates gone? A model comparison of calcium carbonate budgets before and after the 1982–1983 El Nino at Uva Island in the eastern Pacific, *Coral Reefs*, 15(2): 109-119.

Eakin, C.M. (2001) A tale of two ENSO events: carbonate budgets and the influence of two warming disturbances and intervening variability, Uva Island, Panama, *Bulletin of Marine Science*, 69: 171-186.

Edinger, E.N., Limmon, G.V., Jompa, J., Widjatmoko, W., Heikoop, J.M. and Risk, M.J. (2000) Normal coral growth rates on dying reefs: are coral growth rates good indicators of reef health? *Marine Pollution Bulletin* 40: 404-425.

Eibl-Eibesfeldt, I. (1964) *Land of a thousand atolls: a study of marine life in the Maldive and Nicobar Islands*, World Publishing Company, Cleveland.

Ekebom, J., Laihonen, P. and Suominen, T. (2003) A GIS-based step-wise procedure for assessing physical exposure in fragmented archipelagos, *Estuarine, Coastal and Shelf Science*, 57(5): 887-898.

Emery, K.O., Tracey, J.I. Jr. and Ladd, H.S. (1954) Geology of Bikini and nearby atolls, *US Geological Survey Professional Paper*, 260(A): 1-265.

Erftemeijer, P.L., Osinga, R. and Mars, A.E. (1993) Primary production of seagrass beds in South Sulawesi (Indonesia): a comparison of habitats, methods and species, *Aquatic Botany*, 46(1): 67-90.

Etienne, S. and Terry, J.P. (2012) Coral boulders, gravel tongues and sand sheets: features of coastal accretion and sediment nourishment by Cyclone Tomas (March 2010) on Taveuni Island, Fiji, *Geomorphology*, 175: 54-65.

Eyre, B.D., Andersson, A.J. and Cyronak, T. (2014) Benthic coral reef calcium carbonate dissolution in an acidifying ocean, *Nature climate change*, 4(11): 969.

Fabricius, K.E., Langdon, C., Uthicke, S., Humphrey, C., Noonan, S., De'ath, G., Okazaki, R., Muehllehner, N., Glas, M.S. and Lough, J.M. (2011) Losers and winners in coral reefs acclimatized to elevated carbon dioxide concentrations, *Nature Climate Change*, 1(3): 165-169.

FAO, 2015. http://faostat3.fao.org/compare/E

Finlayson, D.P. (2005) Puget Sound Fetch. School of Oceanography, University of Washington, Seattle, WA. Available at: http://david.p.finlayson.googlepages.com/pugetsoundfetch

Fletcher, C.H., Bochicchio, C., Conger, C.L., Engels, M.S., Feirstein, E.J., Frazer, N., Glenn, C.R., Grigg, R.W., Grossman, E.E., Harney, J.N. and Isoun, E. (2008) Geology of Hawaii reefs, *Coral Reefs of the USA*, 435-487.

Flood, P. G. (1974) Sand movements on Heron Island a vegetated sand cay Great Barrier Reef province, Australia. *Proceedings Second International Coral Reef Symposium, Brisbane*, Vol. 2: 387–394.

Folk, R.L. and Robles, R. (1964) Carbonate sands of Isla Perez, Alacran Reef complex, Yucatán. *Journal of Geology*, 72:255–292.

Ford, M.R. (2010) *Sedimentological implications of durability and physical taphonomic processes on a fringing reef, Lizard Island, Australia*, Doctoral dissertation, ResearchSpace@Auckland.

Ford, M.R. (2014) *Personal Communication*, University of Auckland.

Ford, M.R. and Kench, P.S. (2012) The durability of bioclastic sediments and implications for coral reef deposit formation, *Sedimentology*, *59*(3): 830-842.

Ford, M.R. and Kench, P.S. (2015) Multi-decadal shoreline changes in response to sea level rise in the Marshall Islands, *Anthropocene*, 11: 14-24.

Frank, T.D. (2008) Late Holocene island reef development on the inner zone of the northern Great Barrier Reef: insights from Low Isles Reef, *Australian Journal of Earth Sciences*, 55(5): 669-683.

Frankovich, T.A. and Zieman, J.C. (1994) Total epiphyte and epiphytic carbonate production on Thalassia testudinum across Florida Bay, *Bulletin of Marine Science*, 54(3): 679-695.

Fuentes, M.M.P.B., Dawson, J., Smithers, S., Limpus, C.J. and Hamann, M. (2010) Sedimentological characteristics of key sea turtle rookeries: potential implications under projected climate change, *Journal of Marine and Freshwater Research*, 61: 464-473.

Fujita, K., Osawa, Y., Kayanne, H., Ide, Y. and Yamano, H. (2009) Distribution and sediment production of large benthic foraminifers on reef flats of the Majuro Atoll, Marshall Islands, *Coral Reefs*, 28(1): 29-45.

Gacia, E., Granata, T.C. and Duarte, C.M. (1999) An approach to measurement of particle flux and sediment retention within seagrass (Posidonia oceanica) meadows, *Aquatic Botany*, 65(1): 255-268.

Gardiner, J.S. and Murray, J. (1906) Lagoon deposits, *The fauna and geography of the Maldive and Laccadive Archipelagoes*, 2: 581-588.

Gattuso, J.P., Frankignoulle, M. and Smith, S.V. (1999) Measurement of community metabolism and significance in the coral reef CO2 source-sink debate, *Proceedings of the National Academy of Sciences*, 96(23): 13017-13022.

Geister, J. (1983) Holozäne westindische Korallenriffe: Geomorphologie, Ökologie und Fazies. *Facies*, 9(1): 173-283.

Gerritsen, F. (1981) Wave attenuation and wave set-up on a coastal reef. In *Technical Report*. Look Lab, University of Hawaii: Honolulu.

Gibbs, R.J., Matthews, M.D. and Link, D.A. (1971) The relationship between sphere size and settling velocity, *Journal of Sedimentary Research*, 41: 7-18.

Gillis, L.G. (2009) Kuda Huraa, Republic of Maldives, Raising Awareness, *Seagrass-Watch*, 36: 10. (Available at: http://www.seagrasswatch.org/Newsletters/SW_News_36_low.pdf).

Gischler, E. (2006) Sedimentation on Rasdhoo and Ari Atolls, Maldives, Indian Ocean, *Facies*, 52(3): 341-360.

Gischler, E., Hudson, J.H., and Pisera, A. (2008) Late Quaternary reef growth and sea level in the Maldives (Indian Ocean), *Marine Geology*, 250(1): 104-113.

Glynn, P.W. (1990) Feeding ecology of selected coral-reef macroconsumers: patterns and effects on coral community structure, *Ecosystems of the world*, 25: 365-400.

Godfrey, T. (2004) *Atlas of the Maldives*, Atoll Editions.

Goreau, T.J. (1998) *Damage to Maldivian Reefs from Mining, sea Level Rise, Sewage and Global Warming: Recommendations for Coral and Shore Protection; Report to Maldives Department of Fisheries*. Global Coral Reef Alliance: Chappaqua, NY, USA.

Gourlay, M.R. (1988) Coral cays: products of wave action and geological processes in a biogenic environment, *Proceedings of the 6th International Coral Reef Symposium, Townsville,* 2: 491-496.

Gourlay, M.R. (1994) Wave transformation on a coral reef, *Coastal engineering*, 23(1-2): 17-42.

Gourlay, M.R. (2011) Waves and wave-driven currents. In Hopley, D. (ed.) *Encyclopaedia of Modern Coral Reefs: Structure, Form and Process*. Springer, Dordrecht, The Netherlands, pp1154-1170.

Gourlay, M.R.and Jell, J.S. (1993) *Heron Island Spoil Dump*. Research Publication No. 28, Great Barrier Reef Marine Park Authority, Townsville, Australia.

Govers, L.L., de Brouwer, J.H., Suykerbuyk, W., Bouma, T.J., Lamers, L.P., Smolders, A.J. and van Katwijk, M.M. (2014) Toxic effects of increased sediment nutrient and organic matter loading on the seagrass Zostera noltii, *Aquatic Toxicology*, 155: 253-260.

Graham, N.A., Jennings, S., MacNeil, M.A., Mouillot, D. and Wilson, S.K. (2015) Predicting climate-driven regime shifts versus rebound potential in coral reefs, *Nature*, 518(7537): 94-97.

Green, E.P., Mumby, P.J., Edwards, A.J., Clark, C.D. and Edwards, J. (2000) Remote Sensing Handbook for Tropical Coastal Management, UNESCO.

Greening, H. and Janicki, A., (2006) Toward reversal of eutrophic conditions in a subtropical estuary: water quality and seagrass response to nitrogen loading reductions in Tampa Bay, Florida, USA. *Environmental Management*, 38(2): 163-178.

Greve, T.M. and Binzer, T. (2004) Which factors regulate seagrass growth and distribution. In Borum, J., Duarte, C.M., Krause-Jensen, D. and Greve, T.M. (Eds), *European seagrasses: an introduction to monitoring and management*, EU Project Monitoring and Managing of European Seagrasses, pp19-23.

Guidone, M. and Thornber, C.S. (2013) Examination of ulva bloom species richness and relative abundance reveals two cryptically co-occurring bloom species in Narragansett Bay, Rhode Island, *Harmful Algae*, 24: 1-9.

Guilcher, A. (1988) Coral Reef Geomorphology. Coastal Morphology and Research, John Wiley and Sons, New York.

Hackett, H.E. (1977) Marine algae known from the Maldive Islands, *Atoll Research Bulletin*, 210: 1-30.

Haining, R.P. (2003) *Spatial data analysis: theory and practice*. Cambridge University Press.

Hamylton, S. (2011) The use of remote sensing and linear wave theory to model local wave energy around Alphonse Atoll, Seychelles, *Estuarine, Coastal and Shelf Science*, 95(4): 349-358.

Hamylton, S.M., Carvalho, R.C., Duce, S., Roelfsema, C.M. and Vila-Concejo, A. (2016) Linking pattern to process in reef sediment dynamics at Lady Musgrave Island, southern Great Barrier Reef, *Sedimentology*, 63(6): 1634-1650.

Hamylton, S.M., Hedley, J.D. and Beaman, R.J. (2015) Derivation of high-resolution bathymetry from multispectral satellite imagery: a comparison of empirical and optimisation methods through geographical error analysis, *Remote Sensing*, 7(12): 16257-16273.

Harangozo, S.A. (1992) Flooding in the Maldives and its implications for the global sea level rise debate, *Sea Level Changes: Determination and Effects*, 69: 95.

Harborne, A.R., Mumby, P.J., ZŻychaluk, K., Hedley, J.D. and Blackwell, P.G. (2006) Modeling the beta diversity of coral reefs, *Ecology*, 87(11): 2871-2881.

Hardy, T.A. and Young, I.R. (1996) Field study of wave attenuation on an offshore coral reef, *Journal of Geophysical Research*, C101: 14311-14326.

Harlin, M.M. (1993) Changes in major plant groups following nutrient enrichment. In: McComb, J. (Ed.), Eutrophic Shallow Estuaries and Lagoons. CRC Press, Inc., Boca Raton (FL), pp173-187.

Harney, J.N. and Fletcher, C.H. (2003) A budget of carbonate framework and sediment production, Kailua Bay, Oahu, Hawaii. *Journal of Sedimentary Research,* 73(6): 856-868.

Hart, D.E. (2009) The maintenance of reef islands*, Proceedings of the 11th International Coral Reef Symposium, Fort Lauderdale, FL, USA,* 409-413.

Hart, D.E., and Kench, P.S. (2007) Carbonate production of an emergent reef platform, Warraber Island, Torres Strait, Australia, *Coral reefs*, 26(1): 53-68.

Hass, H. (1961) Expedition ins Unbekannte. Ein Bericht uber die Expedition des Forschungsschiffes Xarifa zu den Malediven und Nikoharen. Berlin, Frankfurt, Wien, pp167.

Hassan, M.Z. (2005) *Environmental Guidelines for Tourist Resort Development & Operation in the Maldives.* Available at: http://www.tourism.gov.mv/pubs/Enviromental_guidelines_Resorts.pdf

Hasselmann, K., Barnett, T.P., Bouws, E., Carlson, H., Cartwright, D.E., Enke, K., Ewing, J.A., Gienapp, H., Hasselmann, D.E., Kruseman, P. and Meerburg, A. (1973) *Measurements of wind-wave growth and swell decay during the Joint North Sea Wave Project (JONSWAP)*. Deutches Hydrographisches Institut.

Hayne, M. and Chappell, J. (2001) Cyclone frequency during the last 5000 years at Curacoa Island, north Queensland, Australia. *Palaeogeography, Palaeoclimatology, Palaeoecology*, 168(3): 207-219.

Hemer, M.A., Fan, Y., Mori, N., Semedo, A. and Wang, X. L. (2013) Projected changes in wave climate from a multi-model ensemble, *Nature climate change*, 3(5): 471.

Hochberg, E.J., Atkinson, M.J. and Andréfouët, S. (2003) Spectral reflectance of coral reef bottom-types worldwide and implications for coral reef remote sensing, *Remote Sensing of Environment*, *85*(2): 159-173.

Hoegh-Guldberg, O., Mumby, P.J., Hooten, A.J., Steneck, R.S., Greenfield, P., Gomez, E., Harvell, C.D., Sale, P.F., Edwards, A.J., Caldeira, K. and Knowlton, N. (2007) Coral reefs under rapid climate change and ocean acidification, *Science*, 318(5857): 1737-1742.

Hoeke, R.K., McInnes, K.L., Kruger, J.C., McNaught, R.J., Hunter, J.R. and Smithers, S.G. (2013) Widespread inundation of Pacific islands triggered by distant-source wind-waves, *Global and Planetary Change*, 108: 128-138.

Hoey, A.S., and Bellwood, D.R. (2008) Cross-shelf variation in the role of parrotfishes on the Great Barrier Reef, *Coral Reefs*, 27(1): 37-47.

Holthuijsen, L.H. (2007). *Waves in Oceanic And Coastal Waters*. Cambridge University Press. pp 70. ISBN 978-0-521-86028-4.

Hopley, D. (1981) Sediment movement around a coral cay, Great Barrier Reef, Australia, *Pacific Geology*, 15: 17–36.

Hopley, D. and Kinsey, D. W. (1988) The effects of a rapid short-term sea-level rise on the Great Barrier Reef, *Greenhouse: Planning for climate change*, 189-201.

Hopley, D., Smithers, S.G. and Parnell, K. (2007) *The geomorphology of the Great Barrier Reef: development, diversity and change*. Cambridge University Press.

Hoskin, C.M., Reed, J.K. and Mook, D.H. (1986) Production and off-bank transport of carbonate sediment, Black Rock, southwest Little Bahama Bank, *Marine Geology*, *73*(1), 125-144.

Howarth, R., Anderson, D., Cloern, J., Elfring, C., Hopkinson, C., Lapointe, B., Malone, T., Marcus, N., McGlathery, K., Sharpley, A. and Walker, D. (2000) Nutrient pollution of coastal rivers, bays, and seas, *Issues in Ecology*, 7(7): 1-14.

Hubbard, D.K. (1986) Sedimentation as a control of reef development: St. Croix, USVI, *Coral reefs*, 5(3): 117-125.

Hubbard, D.K., Miller, A.I. and Scaturo, D. (1990) Production and cycling of calcium carbonate in a shelf-edge reef system (St. Croix, US Virgin Islands): applications to the nature of reef systems in the fossil record, *Journal of Sedimentary Research,* 60(3).

Hubbard, D.K., Sadd, J.L. and Roberts, H.H. (1981) The role of physical processes in controlling sediment transport patterns on the insular shelf of St. Croix, US Virgin Islands. In: Gomez, et al. (Eds.), *The Reef and Man: Proceedings of the Fourth International Coral Reef Symposium*, 18-22.

Hunter, I.G. (1977) Sediment production by Diadema antillarum on a Barbados fringing reef, *Proceedings, Third International Coral Reef Symposium*, Vol.2: 105–109.

Hunter, J. (2012) A simple technique for estimating an allowance for uncertain sea-level rise, *Climatic Change*, 113(2), 239-252.

IMF (2008) *Maldives: Poverty Reduction Strategy Paper*. International Monetary Fund, Washington, USA.

IPCC (2013) *Working Group I Contribution to the IPCC Fifth Assessment Report Climate Change 2013: The Physical Science Basis Summary for Policymakers*, http://www.climatechange2013.org/images/uploads/WGIAR5-SPM_Approved27Sep2013.pdf

IUCN (2015) *The IUCN Red List of Threatened Species.* Version 2015-4 Available at: www.iucnredlist.org

Jago, O.K., Kench, P.S. and Brander, R.W. (2007) Field observations of wave-driven water-level gradients across a coral reef flat, *Journal of Geophysical Research-Oceans,* 112(C6).

Johansen, H.W. (1969) *Morphology and systematics of coralline algae with special reference to Calliarthron*. University of California Press.

Jones, N.S., Ridgwell, A. and Hendy, E.J. (2015) Evaluation of coral reef carbonate production models at a global scale, *Biogeosciences*, *12*(5): 1339-1356.

Kalbfleisch, W.B. and Jones, B. (1998) Sedimentology of shallow, hurricane-affected lagoons: grand Cayman, British West Indies, *Journal of Coastal Research*, 140-161.

Kayanne, H., Yasukochi, T., Yamaguchi, T., Yamano, H. and Yoneda, M. (2011) Rapid settlement of Majuro Atoll, central Pacific, following its emergence at 2000 years CalBP, *Geophysical Research Letters*, 38(20).

Kelaher, B.P., Van Den Broek, J., York, P.H., Bishop, M.J. and Booth, D.J. (2013) Positive responses of a seagrass ecosystem to experimental nutrient enrichment, *Marine Ecology Progress Series*, 487: 15-25.

Kench, P.S. (1997) Contemporary sedimentation in the Cocos (Keeling) Islands, Indian Ocean: interpretation using settling velocity analysis, *Sedimentary Geology*, 114(1-4): 109-130.

Kench, P.S. (1998a) A currents of removal approach for interpreting carbonate sedimentary processes, *Marine Geology*, 145(3-4): 197-223.

Kench, P.S. (1998b) Physical processes in an Indian Ocean atoll, *Coral Reefs*, 17(2): 155-168.

Kench, P.S. (2011a) Sediment dynamics. In Hopley, D. (ed.) *Encyclopaedia of Modern Coral Reefs: Structure, Form and Process.* Springer, Dordrecht, The Netherlands, pp 994-1005.

Kench, P.S. (2011b) Maldives. In Hopley, D. (ed.) *Encyclopaedia of Modern Coral Reefs: Structure, Form and Process.* Springer, Dordrecht, The Netherlands, pp 648-652.

Kench, P.S. (2012) The Geomorphology of Baa (South Maalhosmadulu) Atoll and Its Reef Islands, *Atoll Research Bulletin*, 590: 1-29.

Kench, P.S. and Brander, R.W. (2006a) Wave processes on coral reef flats: implications for reef geomorphology using Australian case studies, *Journal of Coastal Research*, 209-223.

Kench, P.S. and Brander, R.W. (2006b) Response of reef island shorelines to seasonal climate oscillations: South Maalhosmadulu atoll, Maldives, *Journal of Geophysical Research*, 111: F1.

Kench, P.S., Brander, R.W., Parnell, K.E. and McLean, R.F. (2006) Wave energy gradients across a Maldivian atoll: Implications for island geomorphology, *Geomorphology*, 81(1): 1-17.

Kench, P.S., Brander, R.W., Parnell, K.E. and O'Callaghan, J.M. (2009c) Seasonal variations in wave characteristics around a coral reef island, South Maalhosmadulu atoll, Maldives, *Marine Geology*, *262*(1): 116-129.

Kench, P.S., Beetham, E., Bosserelle, C., Kruger, J., Pohler, S.M.L., Coco, G. and Ryan, E.J. (2017) Nearshore hydrodynamics, beachface cobble transport and morphodynamics on a Pacific atoll motu, *Marine Geology*, 389: 17-31.

Kench, P.S., Chan, J., Owen, S.D., and McLean, R.F. (2014) The geomorphology, development and temporal dynamics of Tepuka Island, Funafuti atoll, Tuvalu, *Geomorphology*, 222: 46-58.

Kench, P.S. and Cowell, P.J. (2001) The morphological response of atoll islands to sea-level rise: Part 2: application of the Modified Shoreface Translation Model (STM), *Journal of Coastal Research Special Issue*, 34: 645-656.

Kench, P.S. and Cowell, P.J. (2002) Variations in sediment production and implications for atoll island stability under rising sea level, *Proceedings of 9th International Coral Reef Symposium, Bali*, *October 2000*, Vol 2: 1181-1186.

Kench, P.S. and McLean, R.F. (1996) Hydraulic characteristics of bioclastic deposits: new possibilities for environmental interpretation using settling velocity fractions, *Sedimentology*, 43: 561-570.

Kench, P.S. and McLean, R.F. (2004) Hydrodynamics and sediment flux of hoa in an Indian Ocean atoll, *Earth Surface Processes and Landforms*, 29(8): 933-953.

Kench, P.S., McLean, R.F., and Nichol, S.L. (2005) New model of reef-island evolution: Maldives, Indian Ocean. *Geology*, 33:145–148.

Kench, P.S., McLean, R.F., Brander, R.W., Nichol, S.L., Smithers, S.G., Ford, M.R., Parnell, K.E., and Aslam, M. (2006) Geological effects of tsunami on mid-ocean atoll islands: the Maldives before and after the Sumatran tsunami, *Geology,* 34(3): 177-180.

Kench, P., Perry, C. and Spencer, T. (2009a) Coral reefs. In Slaymaker, O., Spencer, T. and Embleton-Hamann, C. (Eds.) *Geomorphology and Global Environmental Change.* Cambridge University Press, Cambridge, pp180-213.

Kench, P.S., Smithers, S.G., McLean, R.F., and Nichol, S.L. (2009b) Holocene reef growth in the Maldives: Evidence of a mid-Holocene sea-level highstand in the central Indian Ocean, *Geology*, 37(5): 455-458.

Kench, P.S., Smithers, S.G., and McLean, R.F. (2012) Rapid reef island formation and stability over an emerging reef flat: Bewick Cay, northern Great Barrier Reef, Australia, *Geology*, 40(4): 347-350.

Kench, P.S., Thompson, D., Ford, M.R., Ogawa, H. and McLean, R.F. (2015). Coral islands defy sea-level rise over the past century: Records from a central Pacific atoll, *Geology*, 43(6): 515-518.

Kennedy, E.V., Perry, C.T., Halloran, P.R., Iglesias-Prieto, R., Schönberg, C.H., Wisshak, M., Form, A.U., Carricart-Ganivet, J.P., Fine, M., Eakin, C.M. and Mumby, P.J. (2013) Avoiding coral reef functional collapse requires local and global action, *Current Biology*, *23*(10): 912-918.

Kenworthy, W.J., Wyllie-Echeverria, S., Coles, R.G., Pergent, G. and Pergent-Martini, C. (2006) Seagrass conservation biology: an interdisciplinary science for protection of the seagrass biome. In *Seagrasses: Biology, Ecologyand Conservation*, Springer, Netherlands, pp595-623.

Kinsey, D.W. (1978) Alkalinity changes and coral reef calcification, *Limnology and Oceanography*, 23.5: 989-991.

Kleypas, J.A., McManus, J.W. and Meñez, L.A., (1999) Environmental limits to coral reef development: where do we draw the line? *American Zoologist*, 39(1), pp.146-159.

Ladd, H.S. (1945) Physical Geology, pp 487-488.

Land, L.S. (1970) Carbonate Mud: Production by Epibiont Growth on Thalassia Testudinum: NOTES, *Journal of Sedimentary Research*, 40(4).

Land, L.S. (1976) Early dissolution of sponge spicules from reef sediments, North Jamaica, *Journal of Sedimentary Research*, 46(4): 967-969.

Land, L.S. (1979) The fate of reef-derived sediment on the north Jamaican island slope, *Marine Geology*, 29: 55-71.

Langer, M.R., and Hottinger, L. (2000) Biogeography of selected “larger" foraminifera, *Micropaleontology*, 46: 105-126.

Langer, M.R., Silk, M.T. and Lipps, J.H. (1997) Global ocean carbonate and carbon dioxide production; the role of reef Foraminifera, *Journal of Foraminiferal Research*, 27(4): 271-277.

Lannes, D. and Marche, F. (2015) A new class of fully nonlinear and weakly dispersive 631 Green-Naghdi models for efficient 2D simulations*, Journal of Computational Physics,* 282: 238-268.

Lapointe, B.E. (1997) Nutrient thresholds for bottom-up control of macroalgal blooms on coral reefs in Jamaica and southeast Florida, *Limnology and Oceanography*, 44: 1586-1592.

Lapointe, B.E., Barile, P.J. and Matzie, W.R. (2004) Anthropogenic nutrient enrichment of seagrass and coral reef communities in the Lower Florida Keys: discrimination of local versus regional nitrogen sources, *Journal of Experimental Marine Biology and Ecology*, 308(1): 23-58.

Lapointe, B.E., Herren, L.W., Debortoli, D.D. and Vogel, M.A. (2015) Evidence of sewage-driven eutrophication and harmful algal blooms in Florida's Indian River Lagoon, *Harmful Algae*, 43: 82-102.

Larcombe, P., Carter, R.M., Dye, J., Gagan, M.K. and Johnson, D.P. (1995) New evidence for episodic post glacial sea level rise, central Great Barrier Reef, Australia, *Marine Geology*, 127: 1-44.

Larkum, A.W., Drew, E.A. and Ralph, P.J. (2006) *Photosynthesis and metabolism in seagrasses at the cellular level*. Springer, Netherlands, pp 323-345.

Lee, T.T. and Black, K.P. (1978) The energy spectra of surf waves on a coral reef. In *Coastal Engineering,* 588-608.

Lescinsky, H., Titus, B. and Hubbard, D. (2012). Live coral cover in the fossil record: an example from Holocene reefs of the Dominican Republic, *Coral reefs*, 31(2): 335-346.

Lewis, S.E., Wüst, R.A.J., Webster, J.M. and Shields, G. A. (2008) Mid-late Holocene sea-level variability in eastern Australia, *Terra Nova,* 20.1: 74-81.

Li, C., Jones, B. and Kalbfleisch, W. B. (1998) Carbonate sediment transport pathways based on foraminifera: case study from Frank Sound, Grand Cayman, British West Indies, *Sedimentology*, *45*(1): 109-120.

Liang, Y., Kench, P.S., Ford, M.R. and East, H.K. (2016) Lagoonal reef sediment supply and island connectivity, Huvadhu Atoll, Maldives, *Journal of Coastal Research*, 75(sp1): 587-591.

Lokrantz, J., Nyström, M., Thyresson, M. and Johansson, C. (2008) The non-linear relationship between body size and function in parrotfishes, *Coral Reefs*, 27: 967-974.

Lugo-Fernandez, A., Roberts, H.H. and Wiseman, W.J. (1998) Tide effects on wave attenuation and wave set-up on a Caribbean coral reef, *Estuarine Coastal and Shelf Science,* 47: 385-393.

Lunn, D.J., Thomas, A., Best, N. and Spiegelhalter, D. (2000) WinBUGS-a Bayesian modelling framework: concepts, structure, and extensibility, *Statistics and Computing*, 10(4): 325-337.

Lyzenga, D.R. (1981) Remote sensing of bottom reflectance and water attenuation parameters in shallow water using aircraft and Landsat data, *International Journal of Remote Sensing,* 2: 71-82.

Ma, Z. and Redmond, R.L. (1995) Tau coefficients for accuracy assessment of classification of remote sensing data, *Photogrammetric Engineering and Remote Sensing*, 61: 435-439.

Madin, J.S. and Connolly, S.R. (2006) Ecological consequences of major hydrodynamic disturbances on coral reefs, *Nature*, 444(7118): 477-480.

Maiklem, W.R. (1968) Some hydraulic properties of bioclastic carbonate grains, *Sedimentology*, 10(2): 101-109.

Maldivian Census, (2006) Available at maldives.gov.mv

Mandlier, P. (2008) Wave Processes in Huvadhoo Atoll: Maldives, Indian Ocean, *Masters of Science Thesis*, University of Auckland.

Mandlier, P.G., and Kench, P.S. (2012) Analytical modelling of wave refraction and convergence on coral reef platforms: Implications for island formation and stability, *Geomorphology*, 159*:* 84-92.

Mann, T. and Westphal, H. (2014) Assessing long-term changes in the beach width of reef islands based on temporally fragmented remote sensing data *Remote Sensing*, *6*(8): 6961-6987.

Maragos, J.E., Baines, G.B. and Beveridge, P.J. (1973) Tropical cyclone Bebe creates a new land formation on Funafuti Atoll, *Science*, 181(4105): 1161-1164.

Masselink, G., and Hughes, M. (1998) Field investigation of sediment transport in the swash zone. *Continental Shelf Research*, *18*(10): 1179-1199.

Masselink, G., Hughes, M. and Knight, J (2014) *Introduction to coastal processes and geomorphology*. Routledge.

Mather, P.M. 2004 *Computer Processing of Remotely Sensed Images: An Introduction.* John Willey and Sons Ltd., West Sussex, England.

Maxwell, W.G.H., Jell, J.S. and McKellar, R.G. (1964) Differentiation of carbonate sediments in the Heron Island reef, *Journal of Sedimentary Research*, 34(2), 294-308.

May, J.P. (1981) CHI (X): a proposed standard parameter for settling tube analysis of sediments, *Journal of Sedimentary Research*, *51*(2).

Mayakun, J., Bunruk, P. and Kongsaenget, R. (2014) Growth rate and calcium carbonate accumulation of Halimeda macroloba Decaisne (Chlorophyta: Halimedaceae) in Thai waters, *Songklanakarin Journal of Science and Technology* 36: 419-423.

McKee, E.D., Chronic, J. and Leopold, E.B. (1959) Sedimentary belts in lagoon of Kapingamarangi Atoll, *AAPG Bulletin*, 43: 501–562.

McKenzie, L.J., Yoshida, R.L. and Unsworth, R.K. (2014) Disturbance influences the invasion of a seagrass into an existing meadow, *Marine pollution bulletin*, *86*(1):186-196.

McKoy, H., Kennedy D.M. and Kench P.S. (2010) Sand cay evolution on reef platforms, Mamanuca Islands, Fiji, *Marine Geology*, 269: 61–73.

McLean, R.F. (2011) Atoll Islands. In Hopley, D. (ed.) *Encyclopaedia of Modern Coral Reefs: Structure, Form and Process.* Springer, Dordrecht, The Netherlands pp 47-51.

McLean, R.F. and Hosking, P.L. (1991) Geomorphology of reef islands and atoll motu in Tuvalu, *South Pacific Journal of Natural Science*, 11: 167-189.

McLean, R. and Kench, P. (2015) Destruction or persistence of coral atoll islands in the face of 20th and 21st century sea-level rise?, *Wiley Interdisciplinary Reviews: Climate Change*, 6(5): 445-463.

McLean, R.F., and Woodroffe, C.D. (1994) Coral atolls. In: Carter, R.W.G., and Woodroffe, C.D. (eds.) *Coastal Evolution: Late Quaternary Shoreline Morphodynamics*, Cambridge University Press, Cambridge, pp 267-302.

McRoy, C.P. and Helfferich, C. (1977) Seagrass ecosystems, *Marine Science (USA)*.

Miller, M.W. and Sluka, R.D. (1999) Patterns of seagrass and sediment nutrient distribution suggest anthropogenic enrichment in Laamu Atoll, Republic of Maldives, *Marine Pollution Bulletin*, 38(12): 1152-1156.

Milliman, J.D. (1967) Carbonate sedimentation on Hogsty Reef, a Bahamian Atoll, *Journal of Sedimentary Petrology*, 37: 658-676.

Ministry of Environment and Energy (2011) *State of the Environment Report*. Available at: http://apps.unep.org/publications/pmtdocuments/-State_of_the_Environment_Report__-_Maldives-2011Maldives_SoER_2011.pdf.pdf

Ministry of Environment Water and Energy (2006) *National Adaptation Plan of Action Republic of Maldives*. Available at: http://www.uncsd2012.org/content/documents/Maldives%20National%20Adaptation%20Plan%20of%20Action.pdf

Ministry of Tourism (2014) http://www.tourism.gov.mv/

Morgan, K. (2014) *A calcium carbonate budget of a Maldivian reef platform*, Doctoral dissertation, ResearchSpace@ Auckland.

Morgan, K.M. and Kench, P.S. (2012) Export of reef-derived sediments on Vabbinfaru reef platform, Maldives. In *Proceedings of the 12th International Coral Reef Symposium, Cairns, Australia,* 9-13.

Morgan, K.M. and Kench, P.S. (2014) A detrital sediment budget of a Maldivian reef platform, *Geomorphology*, 222: 122-131.

Morgan, K.M. and Kench, P.S. (2016a) Parrotfish erosion underpins reef growth, sand talus development and island building in the Maldives, *Sedimentary Geology*, 341: 50-57.

Morgan, K.M. and Kench, P.S. (2016b) Reef to island sediment connections on a Maldivian carbonate platform: using benthic ecology and biosedimentary depositional facies to examine island-building potential, *Earth Surface Processes and Landforms*, 41(13): 1815-1825.

Morri, C., Bianchi, C.N. and Aliani, S. (1995) Coral reefs at Gangehi (North Ari Atoll, Maldive Islands), *Publ Serv Géol Luxemb*, 29: 3-12.

Moses, C.S., Andréfouët, S., Kranenburg, C.J. and Muller-Karger, F.E. (2009) Regional estimates of reef carbonate dynamics and productivity using Landsat 7 ETM+, and potential impacts from ocean acidification, *Marine Ecology Progress Series,* 380:103-115.

Murray, J.W. (1991) *Ecology and Paleoecology of Benthic Foraminifera.* John Wiley & Sons Inc., New York.

Nair, N., Anand, S.P. and Rajaram, M. (2013) Tectonic framework of Laccadive Ridge in western Continental margin of India, *Marine Geology*, 346: 79-90.

Naseer, A. (2003) *The integrated growth response of coral reefs to environmental forcing: Morphometric analysis of coral reefs of the Maldives*, Doctoral dissertation, Dalhousie University, Nova Scotia.

Naseer, A. and Hatcher, B.G. (2004) Inventory of the Maldives' coral reefs using morphometrics generated from Landsat ETM+ imagery, *Coral Reefs*, 23(1): 161-168.

Nelsen Jr, J.E. and Ginsburg, R.N. (1986) Calcium carbonate production by epibionts on Thalassia in Florida Bay, *Journal of Sedimentary Research*, 56(5).

Neuman, A.C. (1985) Reef response to sea level rise: keep-up, catch-up or give-up. In *Proceedings of the Fifth International Coral Reef Congress, Tahiti,* Vol 3: 105–110.

Neumann, A.C. and Land, L.S. (1975) Lime mud deposition and calcareous algae in the Bight of Abaco, Bahamas: a budget, *Journal of Sedimentary Petrology*, 45: 763-786.

Nielsen, P. (2009) *Advanced Series on Ocean Engineering Vol 29: Coastal and Estuarine Processes*. World Scientific, Singapore.

Norton, I.O. and Sclater, J.G. (1979) A model for the evolution of the Indian Ocean and the breakup of Gondwanaland, *Journal of Geophysical Research: Solid Earth*, 84(B12): 6803-6830.

NRC (2000) *Clean Coastal Waters: Understanding and Reducing the Effects of Nutrient Pollution.* National Academy Press, Washington, DC. (available at http://www.nap.edu/catalog/9812.html)

Nwogu, O. and Demirbilek, Z. (2010) Infragravity wave motions and runup over shallow fringing reefs, *Journal of Waterway, Port, Coastal, and Ocean Engineering*, 136(6): 295-305.

Ogston, A.S. and Field, M.E. (2010) Predictions of turbidity due to enhanced sediment resuspension resulting from sea-level rise on a fringing coral reef: evidence from Molokai, Hawaii, *Journal of Coastal Research*, 26(6): 1027-1037.

Ogston, A.S., Storlazzi, C.D., Field, M.E. and Presto, M.K. (2004) Sediment resuspension and transport patterns on a fringing reef flat, Molokai, Hawaii, *Coral Reefs*, 23(4): 559-569.

Oksanen, J., Kindt, R., Legendre, P., O'Hara, B., Stevens, M.H.H., Oksanen, M.J. and Suggests, M.A.S.S. (2007) The vegan package, *Community Ecology Package*, 10: 631-637.

Ong, L. and Holland, K.N. (2010) Bioerosion of coral reefs by two Hawaiian parrotfishes: species, size differences and fishery implications, *Marine Biology*, 157(6): 1313-1323.

Orth, R.J. (1992) A perspective on plant-animal interactions in seagrasses: physical and biological determinants influencing plant and animal abundance, *Plant–animal interactions in the marine benthos. Clarendon Press, Oxford*, pp 147-164.

Orth, R.J., Carruthers, T.J., Dennison, W.C., Duarte, C.M., Fourqurean, J.W., Heck, K.L., Hughes, A.R., Kendrick, G.A., Kenworthy, W.J., Olyarnik, S. and Short, F.T. (2006) A global crisis for seagrass ecosystems, *Bioscience*, 56(12): 987-996.

Padwick, C., Deskevich, M., Pacifici, F. and Smallwood, S. (2010). WorldView-2 pan-sharpening, *Proceedings of the ASPRS 2010 Annual Conference, San Diego, CA, USA* (Vol. 2630).

Palmer, S.E., Perry, C.T., Smithers, S.G. and Gulliver, P. (2010) Internal structure and accretionary history of a nearshore, turbid-zone coral reef: Paluma Shoals, central Great Barrier Reef, Australia, *Marine Geology*, *276*(1), 14-29.

Pandolfi, J.M. and Greenstein, B.J. (1997) Taphonomic alteration of reef corals: effects of reef environment and coral growth form. I. The Great Barrier Reef, *Palaios*, pp 27-42.

Pandolfi, J.M., Connolly, S.R., Marshall, D.J. and Cohen, A.L. (2011) Projecting coral reef futures under global warming and ocean acidification, *Science*, *333*(6041): 418-422.

Parker, J.H., and Gischler, E. (2011) Modern foraminiferal distribution and diversity in two atolls from the Maldives, Indian Ocean, *Marine Micropaleontology*, 78(1): 30-49.

Parry, M.L., Canziani, O.F., Palutikof, J.P., van der Linden, P.J., and Hanson, C.E. (2007) *Contribution of Working Group II to the Fourth Assessment Report of the Intergovernmental Panel on Climate Change, 2007*. Cambridge University Press, Cambridge, UK.

Parson, L.M. and Evans, A.J. (2005) Seafloor topography and tectonic elements of the Western Indian Ocean. *Philosophical Transactions of the Royal Society of London A: Mathematical, Physical and Engineering Sciences*, 363(1826): 15-24.

Paulay, G. (1997) Diversity and distribution of reef organisms. In Birkeland, C.E. (ed.) *Life and death of coral reefs*. Chapman and Hall, New York, pp 298-353.

Payri, C.E., N'Yeurt, A.D.R. and Mattio, L. (2012) Benthic algal and seagrass communities in Baa atoll, Maldives, *Atoll Research Bulletin*, 590:31-66.

Péquignet, A.C., Becker, J.M., Merrifield, M.A. and, Boc, S.J. (2011) The dissipation of wind wave energy across a fringing reef at Ipan, Guam, *Coral Reefs* 30: 71-82.

Perry, C.T. (1998) Grain susceptibility to the effects of microboring: implications for the preservation of skeletal carbonates, *Sedimentology*, 45(1):39-51.

Perry, C.T. (2007) Tropical Coastal Environments – coral reefs and mangroves. In Perry, C.T. and Taylor, K.G. (eds.) *Environmental Sedimentology*, Blackwells, Oxford, pp 302-350.

Perry, C.T. and Beavington-Penney, S.J. (2005) Epiphytic calcium carbonate production and facies development within sub-tropical seagrass beds, Inhaca Island, Mozambique, *Sedimentary Geology*, *174*(3):161-176.

Perry, C.T., Edinger, E.N., Kench, P.S., Murphy, G.N., Smithers, S.G., Steneck, R.S. and Mumby, P.J. (2012) Estimating rates of biologically driven coral reef framework production and erosion: a new census-based carbonate budget methodology and applications to the reefs of Bonaire, *Coral reefs*, 31(3): 853-868.

Perry, C.T. and Hepburn, L. (2008) Syn-depositional alteration of coral reef framework through bioerosion, encrustation and cementation: taphonomic signatures of reef accretion and reef depositional events, *Earth-Science Reviews,* 86: 106-144.

Perry, C.T., Kench, P.S., O'Leary, M.J., Morgan, K.M. and Januchowski-Hartley, F. (2015) Linking reef ecology to island building: Parrotfish identified as major producers of island-building sediment in the Maldives, *Geology*, 43(6): 503-506.

Perry, C.T., Kench, P.S., O'Leary, M.J., Morgan, K.M. and Januchowski-Hartley, F. (2015) Linking reef ecology to island building: Parrotfish identified as major producers of island-building sediment in the Maldives, *Geology*,*43*(6): 503-506.

Perry, C.T., Kench, P.S., Smithers, S.G., Riegl, B.R., Gulliver, P. and Daniells, J.J. (2017) Terrigenous sediment-dominated reef platform infilling: an unexpected precursor to reef island formation and a test of the reef platform size–island age model in the Pacific, *Coral Reefs*, 1-9.

Perry, C.T., Kench, P.S., Smithers, S.G., Riegl, B., Yamano, H. and O'Leary, M.J. (2011) Implications of reef ecosystem change for the stability and maintenance of coral reef islands, *Global Change Biology*, 17: 3679-3696.

Perry, C.T., Kench, P.S., Smithers, S.G., Yamano, H., O'Leary, M. and Gulliver, P. (2013) Time scales and modes of reef lagoon infilling in the Maldives and controls on the onset of reef island formation, *Geology*, 41(10): 1111-1114.

Perry, C.T., Morgan, K.M. and Salter, M.A. (2016) Sediment generation by Halimeda on atoll interior coral reefs of the southern Maldives: A census-based approach for estimating carbonate production by calcareous green algae, *Sedimentary Geology*, 346: 17-24.

Perry, C.T., Murphy, G.N., Kench, P.S., Edinger, E.N., Smithers, S.G., Steneck, R. S. and Mumby, P.J. (2014) Changing dynamics of Caribbean reef carbonate budgets: emergence of reef bioeroders as critical controls on present and future reef growth potential, *Proceedings of the Royal Society B,* Vol. 281, No. 1796: 20142018.

Perry, C.T., Murphy, G.N., Kench, P.S., Smithers, S.G., Edinger, E.N., Steneck, R.S. and Mumby, P. J. (2013) Caribbean-wide decline in carbonate production threatens coral reef growth, *Nature communications*, 4: 1402.

Perry, C.T. and Smithers, S.G. (2006). Taphonomic signatures of turbid-zone reef development: examples from Paluma Shoals and Lugger Shoal, inshore central Great Barrier Reef, Australia, *Palaeogeography, Palaeoclimatology, Palaeoecology*, *242*(1): 1-20.

Perry, C.T., Spencer, T. and Kench, P.S. (2008) Carbonate budgets and reef production states: a geomorphic perspective on the ecological phase-shift concept, *Coral Reefs*, 27(4): 853-866.

Phinn, S.R., Roelfsema, C.M. and Mumby, P.J. (2012) Multiscale, object-based image analysis for mapping geomorphic and ecological zones on coral reefs, *International Journal of Remote Sensing*, *33*(12): 3768-3797.

planning.gov.mv, 2015.

Polunin, N.V.C. and Roberts, C.M. (1993) Greater biomass and value of target coral-reef fishes in two small Caribbean marine reserves, *Marine Ecology-Progress Series*, 100: 167-167.

Popinet, S. (2011) Quadtree-adaptive tsunami modelling, *Ocean Dynamics***,** 61: 1261-1285.

Popinet, S. (2014) A solver for the Green-Naghdi equations, http://www.basilisk.fr/src/green-naghdi.h.

Popinet, S. (2015) A quadtree-adaptive multigrid solver for the Serre–Green–Naghdi equations, *Journal of Computational Physics,* 302: 336-358.

Porter, J.W. and Meier, O.W. (1992) Quantification of loss and change in Floridian reef coral populations, *American Zoologist*, *32*(6): 625-640.

Porter, J.W., Kosmynin, V., Patterson, K.L., Porter, K.G., Jaap, W.C., Wheaton, J.L., Hackett, K., Lybolt, M., Tsokos, C.P., Yanev, G., Marcinek, D.M., Dotten, J., Eaken, D., Patterson, M., Meyer, O., Brill, M. and Dustan, P. (2002) Detection of coral reef change by the Florida Keys coral reef monitoring project. In Porter, J.W. and Porter, K.G. (Eds.), *The Everglades, Florida Bay, and Coral Reefs of the Florida Keys: An Ecosystem Sourcebook*. CRC Press, Boca Raton, FL, pp 749-769.

Presto, M.K., Ogston, A.S., Storlazzi, C.D. and Field, M.E. (2006) Temporal and spatial variability in the flow and dispersal of suspended-sediment on a fringing reef flat, Molokai, Hawaii, *Estuarine, Coastal and Shelf Science*, 67(1): 67-81.

Purdy, E.G. and Bertram, G.T. (1993) *Carbonate concepts from the Maldives, Indian Ocean*. American Association of Petroleum Geologists.

Purdy, E.G. and Gischler, E. (2005) The transient nature of the empty bucket model of reef sedimentation, *Sedimentary Geology*, 175(1): 35-47.

Purdy, E.G. and Winterer, E.L. (2001) Origin of atoll lagoons. *Geological Society of America Bulletin*, 113(7): 837-854.

Pushcharovskiy, Y.M. (1995) Tectonics of the Indian Ocean, *Geotectonics C/C Of Geotektonika*, 29:336-354.

Pushcharovsky, Y.M. (2011) First-order linear tectonovolcanic ridges in ocean, *Geotectonics*, 45(2): 101.

Quataert,E., Storlazzi, C., van Rooijen, A., Cheriton, O. and van Dongeren, A. (2015) The influence of coral reefs and climate change on wave-driven flooding of tropical coastlines, *Geophysical Research Letters,* 42(15): 6407-6415.

Rankey, E.C. and Reeder, S.L. (2011) Holocene oolitic marine sand complexes of the Bahamas, *Journal of Sedimentary Research*, 81(2): 97-117.

Rankey, E.C., Reeder, S.L. and Garza-Pérez, J R. (2011) Controls on links between geomorphical and surface sedimentological variability: Aitutaki and Maupiti atolls, South Pacific Ocean, *Journal of Sedimentary Research*, 81(12): 885-900.

ReefBase (2012) http://www.reefbase.org

Reid, R.P. (2003) *Composition, texture and diagenesis of carbonate sediments: Effects on benthic optical properties*. Rosenstiel School Of Marine And Atmospheric Science Miami, FL.

Resio, D.T., Bratos, S.M. and Thompson, E.F. (2003) Meteorology and Wave Climate, Chapter II-2. *Coastal Engineering Manual. US Army Corps of Engineers,. Washington DC, 72pp*.

Roberts, H.H. (1974) Variability of reefs with regard to changes in wave power around an island. In *Proceedings of the Second International Symposium on Coral Reefs,* Vol. 2.

Roberts, H.H., Wilson, P.A. and Lugo-Fernandez, A. (1992) Biologic and geologic responses to physical processes: examples from modern reef systems of the Caribbean–Atlantic region, *Continental Shelf Research*, 12: 809-834.

Roeber, V. and K.F. Cheung (2012) Boussinesq-type model for energetic breaking waves in 672 fringing reef environments, *Coastal Engineering*, 70: 1-20.

Roelfsema, C.M., Kovacs, E.M. and Phinn, S.R. (2015) Field data sets for seagrass biophysical properties for the Eastern Banks, Moreton Bay, Australia, 2004–2014, *Scientific Data*, 2.

Rohweder, J., Rogala, J.T., Johnson, B.L., Anderson, D., Clark, S., Chamberlin, F., Potter, D. and Runyon, K. (2012) Application of wind fetch and wave models for habitat rehabilitation and enhancement projects – 2012 update, *US Army Corps of Engineers, Contract Report.* http://www.umesc.usgs.gov/management/dss/wind_fetch_wave_models_2012update.html

Rosen, B.R. (1975) The distribution of reef corals, *Report of the Underwater Association*, 1: 1-16.

Roy, P.S. and Connell, J. (1991) Climate change and the future of atoll states. *Journal of Coastal Research*, 7: 1057-1075.

Ryan, E.J., Smithers, S.G., Lewis, S.E., Clark, T.R., and Zhao, J.X. (2016) Chronostratigraphy of Bramston Reef reveals a long-term record of fringing reef growth under muddy conditions in the central Great Barrier Reef, *Palaeogeography, Palaeoclimatology, Palaeoecology*, 441: 734-747.

Schlager, W. (1993) Accommodation and supply—a dual control on stratigraphic sequences, *Sedimentary Geology*, 86(1-2): 111-136.

Schlager, W. and Purkis, S.J. (2013) Bucket structure in carbonate accumulations of the Maldive, Chagos and Laccadive archipelagos, *International Journal of Earth Sciences*, 102(8): 2225-2238.

Schmidt, A.L., Wysmyk, J.K., Craig, S.E. and Lotze, H.K. (2012) Regional-scale effects of eutrophication on ecosystem structure and services of seagrass beds, *Limnology and Oceanography*, 57(5): 1389-1402.

Schofield, J.C. (1977) Effect of Late Holocene sea-level fall on atoll development, *New Zealand Journal of Geology and Geophysics*, 20: 531-536.

Schueth, J.D. and Frank, T.D. (2008) Reef foraminifera as bioindicators of coral reef health: Low Isles Reef, northern Great Barrier Reef, Australia, *Journal of Foraminiferal Research*, 38(1): 11-22.

Scoffin, T.P. (1970) The trapping and binding of subtidal carbonate sediments by marine vegetation in Bimini Lagoon, Bahamas, *Journal of Sedimentary Research*, *40*(1).

Scoffin, T.P. (1987*) Introduction to Carbonate Sediments and Rocks,* Blackie and Sons, Glasgow.

Scoffin, T.P. (1992) Taphonomy of coral reefs: a review, *Coral Reefs*, 11(2): 57-77.

Scoffin, T.P. (1993) The geological effects of hurricanes on coral reefs and the interpretation of storm deposits, *Coral Reefs*, 12(3): 203-221.

Shephard, S.A., McComb, A.J., Bulthuis, D.A., Neverauskas, V., Steffensen, D.A. and West, R. (1989) Decline of seagrasses. Elsevier Science Publishing.

Sheppard, C., Dixon, D.J., Gourlay, M., Sheppard, A. and Payet, R. (2005) Coral mortality increases wave energy reaching shores protected by reef flats: examples from the Seychelles, *Estuarine, Coastal and Shelf Science*, 64(2): 223-234.

Shields, A. (1936) Application of similarity principles ai1d turbulence research to bed-load movement. Mitteilungen der Preussischen Versuchsanstalt fur Wasserbau und Schifbau, Berlin. In: Ott, W.P. and van Uchelen, J.C. (translators), California Inst. Tech., W.M. Keck Lab. of Hydraulics and Water Resources, Rept. No. 167

Shimozono, T., Tajima, Y., Kennedy, A.B., Nobuoka, H., Sasaki, J. and Sato, S. (2015) Combined infragravity wave and sea-swell runup over fringing reefs by super typhoon Haiyan, *Journal of Geophysical Research: Oceans*, 120(6): 4463-4486.

Short, F.T. and Wyllie-Echeverria, S. (1996) Natural and human-induced disturbance of seagrasses, *Environmental conservation*, 23(01): 17-27.

Siljander, M., Venäläinen, E., Goerlandt, F. and Pellikka, P. (2015) GIS-based cost distance modelling to support strategic maritime search and rescue planning: a feasibility study, *Applied Geography*, 57: 54-70.

Smetacek, V. and Zingone, A. (2013) Green and golden seaweed tides on the rise, *Nature*, 504(7478): 84-88.

Smith, R. and Collen, J. (2010) *Sand and gravel resources of Majuro Atoll, Marshall Islands, Technical report 360*. South Pacific Applied Geoscience Commission, Victoria University of Wellington, pp 1-127.

Solomon, S.M. and Forbes, D.L. (1999) Coastal hazards and associated management issues on South Pacific Islands, *Ocean & Coastal Management*, 42(6): 523-554.

Sorby, H.C. (1879) The Structure and Origin of Limestones, *Proceedings of the Geological Society, London*, 35: 56-95.

Southon, J., Kashgarian, M., Fontugne, M., Metivier, B. and Yim, W.W. (2002) Marine reservoir corrections for the Indian Ocean and Southeast Asia, *Radiocarbon*, 44(01): 167-180.

Spencer, T. (1992) Bioerosion and biogeomorphology. In John, D.M., Hawkins, S.J., and Price, J.H. (eds.) *Plant-animal interactions in the marine benthos. Systematic Association Special Volume, No. 46.* Oxford: Clarendon Press, pp 493-509.

Stapel, J., Hemminga, M.A., Bogert, C.G. and Maas, Y.E. (2001) Nitrogen (15N) retention in small Thalassia hemprichii seagrass plots in an offshore meadow in South Sulawesi, Indonesia, *Limnology and oceanography*, 46(1): 24-37.

Stearn, C., Scoffin, T. and Martindale, W. (1977) Calcium Carbonate Budget of a Fringing Reef on the West Coast of Barbados Part I Zonation and Productivity, *Bulletin of Marine Science,* 27: 479-510

Stoddart, D.R. (1962) Catastrophic storm effects on the British Honduras reefs and cays, *Nature,* 196: 512-515.

Stoddart, D.R. (1962) Three Caribbean atolls: Turneff Islands, Lighthouse Reef, and Glover's Reef, British Honduras. *Atoll Research Bulletin*, 87: 1-140.

Stoddart, D.R. (ed) (1966) Reef studies at Addu Atoll, Maldive Islands: preliminary results of an expedition to Addu Atoll in 1964, *Atoll Research Bulletin,* 116: 1-122.

Stoddart, D.R. (1985) Hurricane effects on coral reefs, *Proceedings of the fifth international coral reef congress, Tahiti,* 3: 349-350.

Stoddart, D.R. and Steers, J.A. (1977) The nature and origin of coral reef islands. In: Jones, O.A., and Endean, R. (eds.) *Biology and Geology of Coral Reefs*, *Vol. IV*, Academic Press, New York, pp 59-105.

Storlazzi, C.D. (2011) The influence of sea level rise on fringing reef sediment dynamics: field observations and numerical modelling, *The Proceedings of the Coastal Sediments 2011: In 3 Volumes*. World Scientific, 2011, pp 244-257.

Storlazzi, C.D. and Jaffe, B.E. (2008) The relative contribution of processes driving variability in flow, shear, and turbidity over a fringing coral reef: West Maui, Hawaii, *Estuarine, Coastal and Shelf Science*, 77(4): 549-564.

Storlazzi, C.D., Brown, E.K., Field, M.E., Rodgers, K. and Jokiel, P.L. (2005) A model for wave control on coral breakage and species distribution in the Hawaiian Islands, *Coral Reefs*, 24(1): 43-55.

Storlazzi, C.D., Elias, E., Field, M.E. and Presto, M.K. (2011) Numerical modelling of the impact of sea-level rise on fringing coral reef hydrodynamics and sediment transport, *Coral Reefs*, 30(1): 83-96.

Storlazzi, C.D., Ogston, A.S., Bothner, M.H., Field, M.E. and Presto, M.K. (2004) Wave-and tidally-driven flow and sediment flux across a fringing coral reef: Southern Molokai, Hawaii, *Continental Shelf Research*, 24(12): 1397-1419.

Stumpf, R.P., Holderied, K., and Sinclair, M. (2003) Determination of water depth with high-resolution satellite imagery over variable bottom types, *Limnology and Oceanography*, 48(1; NUMB 2): 547-556.

Tissier, M., Bonneton, P., Marche, F., Chazel, F. and Lannes, D. (2012) A new approach to handle wave breaking in fully non-linear Boussinesq models, *Coastal Engineering,* 67: 54-66.

Todd, R. (1960) Some observations on the distribution of *Calcarina* and *Baculogypsina* in the Pacific, *Science Reports, Tohoku University, Sendai, Japan, 2nd Series (Geology) Special Volume*, 4: 100-107.

Tolman, H.L. (2009) User manual and system documentation of WAVEWATCH III TM version 3.14, *Technical note, MMAB Contribution*, 276: 220.

Toscano, M.A., and Macintyre, I.G. (2003) Corrected western Atlantic sea-level curve for the last 11,000 years based on calibrated ^{14}C dates from *Acropora palmata* framework and intertidal mangrove peats, *Coral Reefs*, 22: 257-270.

Tourism Adaptation Project (TAP) (2015) Addressing Barriers to Effective Climate Change Adaptation in the Water And Wastewater Services in Resorts and Dependent Communities. Available at: http://www.tourism.gov.mv/wp-content/uploads/2015/05/WasteWater.pdf

Tripadvisor (2013) http://www.tripadvisor.co.uk/ShowTopic-g293953-i7445-k6637507-Meeru_Big_problem_with_seagrass_on_the_beaches-Maldives.html

Tudhope, A.W. and Scoffin, T.P. (1984) The effects of Callianassa bioturbation on the preservation of carbonate grains in Davies Reef Lagoon, Great Barrier Reef, Australia, *Journal of Sedimentary Research* 54(4).

Tudhope, A.W. and Scoffin, T.P. (1988) The relative importance of benthic foraminiferans in the production of carbonate sediment on the central Queensland shelf, *Proceedings of the 6th International Coral Reef Symposium,* Vol. 2: 583-588.

Tudhope, A.W., Scoffin, T.P., Stoddart, D.R. and Woodroffe, C.D. (1985) Sediments of Suwarrow Atoll, *Proceedings of the 5th International Coral Reef Congress*, 6: 611-616.

U.S. Army Corps of Engineers (1984) Shore Protection Manual, Coastal Engineering Research Center, Fort Belvoir, Virginia.

Udden, J.A. (1914) Mechanical composition of clastic sediments, *Bulletin of the Geological Society of America*, 25: 655-744.

Udy, J.W., Dennison, W.C., Lee Long, W.J. and McKenzie, L.J. (1999) Responses of seagrass to nutrients in the Great Barrier Reef, Australia, *Marine Ecology Progress Series*, 185: 257-271.

UKHO (1992) Hydrographic Charts. Taunton, UK.

ukulhas.com, 2015

UNDP (2014) CBA Country Programme Strategy Maldives. Available at: http://www.mv.undp.org/content/dam/maldives/docs/Environment%20and%20Energy/GEF/CBA_CPS%20Maldives.pdf

Unsworth, R.K. and Cullen, L.C. (2010) Recognising the necessity for Indo-Pacific seagrass conservation, *Conservation Letters*, 3(2): 63-73.

Valiela, I., McClelland, J., Hauxwell, J., Behr, P.J., Hersh, D. and Foreman, K. (1997) Macroalgal blooms in shallow estuaries: controls and ecophysiological and ecosystem consequences, *Limnology and oceanography*, *42*(5): 1105-1118.

Van Alphen, K., van Sark W.G. and Hekkert M.P. (2007) Renewable energy technologies in the Maldives—determining the potential, *Renewable and Sustainable Energy Reviews*, 11(8):1650-1674.

Van Keulen, M. and Borowitzka, M.A. (2002) Comparison of water velocity profiles through morphologically dissimilar seagrasses measured with a simple and inexpensive current meter, *Bulletin of Marine Science*, 71(3): 1257-1267.

Van Woesik, R. (1989) A preliminary examination of the sedimentology, reef growth and hydrography of Green Island, *Draft report to Great Barrier Reef Marine Park Authority, Townsville*.

Vermaat, J.E., Agawin, N.S.R., Duarte, C.M., Fortes, M.D., Marba, N. and Uri, J.S. (1995) Meadow maintenance, growth and productivity of a mixed Philippine seagrass bed, *Marine ecology progress series. Oldendorf*, 124(1): 215-225.

Verwey, M.C., Nagelkerken, I., Graaff, D.D., Peeters, M., Bakker, E.J. and Velde, G. (2006) Structure, food and shade attract juvenile coral reef fish to mangrove and seagrass habitats: a field experiment, *Marine Ecology Progress Series*, 306: 257-268.

Vetter, O., Becker, J.M., Merrifield, M.A., Pequignet, A.C., Aucan, J., Boc, S.J. and Pollock, C.E. (2010) Wave setup over a Pacific Island fringing reef. *Journal of Geophysical Research-Oceans,* 115(C12).

von Arx, W.S. (1948) The circulation systems of Bikini and Rongelap lagoons, *Transactions of the American Geophysical Union*, 29(6): 861-870.

Waycott, M., Duarte, C.M., Carruthers, T.J., Orth, R.J., Dennison, W.C., Olyarnik, S., Calladine, A., Fourqurean, J.W., Heck, K.L., Hughes, A.R. and Kendrick, G.A. (2009) Accelerating loss of seagrasses across the globe threatens coastal ecosystems, *Proceedings of the National Academy of Sciences*, 106(30):12377-12381.

Weather Underground: wunderground.com

Webb, A.P. and Kench, P.S. (2010) The dynamic response of reef islands to sea-level rise: evidence from multi-decadal analysis of island change in the Central Pacific, *Global and Planetary Change*, 72:234-246.

Wells, J.W. (1957) Coral reefs, Treatise on marine ecology and paleoecology, v.1, Mem. *Geological Society of America* 67, 1: 609-631.

White, R. and McKenzie, D. (1989) Magmatism at rift zones: the generation of volcanic continental margins and flood basalts, *Journal of Geophysical Research: Solid Earth*, 94(B6): 7685-7729.

Wilson, S.K., Graham, N.A.J. and Polunin, N.V.C. (2007) Appraisal of visual assessments of habitat complexity and benthic composition on coral reefs. *Marine Biology*, 151(3): 1069-1076.

Woodroffe, C.D. (2003) *Coasts, form, process and evolution.* Cambridge University Press.

Woodroffe, C.D. and McLean, R.F. (1994) Reef Islands of the Cocos (Keeling) Islands, *Atoll Research Bulletin*, 403: 1-36.

Woodroffe, C.D. and Morrison, R.J. (2001) Reef-island accretion and soil development on Makin, Kiribati, central Pacific, *Catena*, 44: 245-261.

Woodroffe, C.D. (1992) Morphology and evolution of reef islands in the Maldives, *Proceedings of 7th International Coral Reef Symposium, Guam*, 2: 1217-1226.

Woodroffe, C.D. (2008) Reef-island topography and the vulnerability of atolls to sea-level rise, *Global and Planetary Change*, 62: 77-96.

Woodroffe, C.D., Kennedy, D.M., Hopley, D., Rasmussen, C.E., and Smithers, S.G. (2000) Holocene reef growth in Torres Strait, *Marine Geology*, 170: 331-346.

Woodroffe, C.D., McLean, R.F., Smithers, S.G., and Lawson, E.M. (1999) Atoll reef-island formation and response to sea-level change: West Island, Cocos (Keeling) Islands, *Marine Geology*, 160: 85-104.

Woodroffe, C.D., Samosorn, B., Hua, Q. and Hart, D.E. (2007) Incremental accretion of a sandy reef island over the past 3000 years indicated by component-specific radiocarbon dating, *Geophysical Research Letters*, 34(3).

Workshop on Integrated Reef Resources Management in the Maldives, 1997. Available at: http://www.nzdl.org/gsdlmod?e=d-00000-00---off-0aginfo--00-0----0-10-0---0---0direct-10---4-------0-1l--11-en-50---20-about---00-0-1-00-0--4----0-0-11-10-0utfZz-8-00&cl=CL2.6&d=HASH013e6c0decb1dccda406838f.7.3&gc=1

World Bank, 2013. http://data.worldbank.org/indicator/SP.POP.TOTL

World Bank, 2015. http://www.worldbank.org/en/country/maldives

Yamano, H., Abe, O., Matsumoto, E., Kayanne, H., Yonekura, N. and Blanchon, P. (2003) Influence of wave energy on Holocene coral reef development: an example from Ishigaki Island, Ryukyu Islands, Japan, *Sedimentary Geology*, 159(1):27-41.

Yamano, H., Cabioch, G., Chevillon, C., and Join, J.L. (2014) Late Holocene sea-level change and reef-island evolution in New Caledonia, *Geomorphology*, 222: 39-45

Yamano, H., Miyajima, T. and Koike, I. (2000) Importance of foraminifera for the formation and maintenance of a coral sand cay: Green Island, Australia,*Coral Reefs*, 19(1): 51-58.

Yamano, H., Kayanne, H. and Chikamori, M. (2005) An overview of the nature and dynamics of reef islands, *Global Environmental Research*, 9: 9-20.

Yamano, H., Kayanne, H. and Yonekura, N. (2001) Anatomy of a modern coral reef flat: a recorder of storms and uplift in the late Holocene,.*Journal of Sedimentary Research*, 71: 295-304.

Yamano, H., Miyajima, T., and Koike, I. (2000) Importance of foraminifera for the formation and maintenance of a coral sand cay: Green Island, Australia, *Coral Reefs*, 19: 51-58.

Yao, Y., Huang, Z., Monismith, S.G. and Lo, E.Y. (2012) 1DH Boussinesq modeling of wave transformation over fringing reefs, *Ocean Engineering*, 47: 30-42.

Yarlett, R. (2017) *Personal Communication*, unpublished PhD (in progress) data, University of Exeter.

Yates, M.L., Le Cozannet, G., Garcin, M., Salaï, E. and Walker, P. (2013) Multidecadal atoll shoreline change on Manihi and Manuae, French Polynesia, *Journal of Coastal Research*, 29(4): 870-882.

Young, I.R. (1999) Seasonal variability of the global ocean wind and wave climate, *International Journal of Climatology*, 19(9): 931-950.

Zhang, C., Selch, D., Xie, Z., Roberts, C., Cooper, H. and Chen, G. (2013) Object-based benthic habitat mapping in the Florida Keys from hyperspectral imagery, *Estuarine, Coastal and Shelf Science*, 134: 88-97.

Zijlema, M. (2012) Modelling wave transformation across a fringing reef using swash, *Proceedings of the 33rd International Conference on Coastal Engineering*, 33.